VOL. 595 NOS. 1 + 2 MARCH 20, 1992

COMPLETE IN ONE ISSUE

JOURNAL OF CHROMATOGRAPHY

INCLUDING ELECTROPHORESIS AND OTHER SEPARATION METHODS

ELSEVIER

JOURNAL OF CHROMATOGRAPHY

INCLUDING ELECTROPHORESIS AND OTHER SEPARATION METHODS

Scope. The *Journal of Chromatography* publishes papers on all aspects of chromatography, electrophoresis and related methods. Contributions consist mainly of research papers dealing with chromatographic theory, instrumental development and their applications. The section *Biomedical Applications*, which is under separate editorship, deals with the following aspects: developments in and applications of chromatographic and electrophoretic techniques related to clinical diagnosis or alterations during medical treatment; screening and profiling of body fluids or tissues with special reference to metabolic disorders; results from basic medical research with direct consequences in clinical practice; drug level monitoring and pharmacokinetic studies; clinical toxicology; analytical studies in occupational medicine.

Submission of Papers. Manuscripts (in English; *four* copies are required) should be submitted to: Editorial Office of *Journal of Chromatography*, P.O. Box 681, 1000 AR Amsterdam, Netherlands, Telefax (+31-20) 5862 304, or to: The Editor of *Journal of Chromatography, Biomedical Applications*, P.O. Box 681, 1000 AR Amsterdam, Netherlands. Review articles are invited or proposed by letter to the Editors. An outline of the proposed review should first be forwarded to the Editors for preliminary discussion prior to preparation. Submission of an article is understood to imply that the article is original and unpublished and is not being considered for publication elsewhere. For copyright regulations, see below.

Publication. The *Journal of Chromatography* (incl. *Biomedical Applications*) has 39 volumes in 1992. The subscription prices for 1992 are:

J. Chromatogr. (incl. *Cum. Indexes, Vols. 551–600*) + *Biomed. Appl.* (Vols. 573–611):
Dfl. 7722.00 plus Dfl. 1209.00 (p.p.h.) (total *ca.* US$ 4880.25)

J. Chromatogr. (incl. *Cum. Indexes, Vols. 551–600*) only (Vols. 585–611):
Dfl. 6210.00 plus Dfl. 837.00 (p.p.h.) (total *ca.* US$ 3850.75)

Biomed. Appl. only (Vols. 573–584):
Dfl. 2760.00 plus Dfl. 372.00 (p.p.h.) (total *ca.* US$ 1711.50).

Subscription Orders. The Dutch guilder price is definitive. The US$ price is subject to exchange-rate fluctuations and is given as a guide. Subscriptions are accepted on a prepaid basis only, unless different terms have been previously agreed upon. Subscriptions orders can be entered only by calender year (Jan.–Dec.) and should be sent to Elsevier Science Publishers, Journal Department, P.O. Box 211, 1000 AE Amsterdam, Netherlands, Tel. (+31-20) 5803 642, Telefax (+31-20) 5803 598, or to your usual subscription agent. Postage and handling charges include surface delivery except to the following countries where air delivery via SAL (Surface Air Lift) mail is ensured: Argentina, Australia, Brazil, Canada, China, Hong Kong, India, Israel, Japan*, Malaysia, Mexico, New Zealand, Pakistan, Singapore, South Africa, South Korea, Taiwan, Thailand, USA. *For Japan air delivery (SAL) requires 25% additional charge of the normal postage and handling charge. For all other countries airmail rates are available upon request. Claims for missing issues must be made within three months of our publication (mailing) date, otherwise such claims cannot be honoured free of charge. Back volumes of the *Journal of Chromatography* (Vols. 1–572) are available at Dfl. 217.00 (plus postage). Customers in the USA and Canada wishing information on this and other Elsevier journals, please contact Journal Information Center, Elsevier Science Publishing Co. Inc., 655 Avenue of the Americas, New York, NY 10010, USA, Tel. (+1-212) 633 3750, Telefax (+1-212) 633 3990.

Abstracts/Contents Lists published in Analytical Abstracts, Biochemical Abstracts, Biological Abstracts, Chemical Abstracts, Chemical Titles, Chromatography Abstracts, Clinical Chemistry Lookout, Current Contents/Life Sciences, Current Contents/Physical, Chemical & Earth Sciences, Deep-Sea Research/Part B: Oceanographic Literature Review, Excerpta Medica, Index Medicus, Mass Spectrometry Bulletin, PASCAL-CNRS, Pharmaceutical Abstracts, Referativnyi Zhurnal, Research Alert, Science Citation Index and Trends in Biotechnology.

See inside back cover for Publication Schedule, Information for Authors and information on Advertisements.

0021-9673/92/$05.00

Printed in the Netherlands

VOL. 595, NOS. 1+2 JOURNAL OF CHROMATOGRAPHY MARCH 20, 1992

CONTENTS

(Abstracts/Contents Lists published in Analytical Abstracts, Biochemical Abstracts, Biological Abstracts, Chemical Abstracts, Chemical Titles, Chromatography Abstracts, Current Contents/Life Sciences, Current Contents/Physical, Chemical & Earth Sciences, Deep-Sea Research/Part B: Oceanographic Literature Review, Excerpta Medica, Index Medicus, Mass Spectrometry Bulletin, PASCAL-CRNS, Referativnyi Zhurnal, Research Alert and Science Citation Index)

(Continued overleaf)

Contents (continued)

Gas Chromatography

Supercritical Fluid Chromatogaphy

Electrophoresis

SHORT COMMUNICATIONS

Column Liquid Chromatography

Gas Chromatography

Planar Chromatography

BOOK REVIEW

In articles with more than one author, the name of the author to whom correspondence should be addressed is indicated in the article heading by a 6-pointed asterisk (*).

JOURNAL OF CHROMATOGRAPHY

VOL. 595 (1992)

JOURNAL of CHROMATOGRAPHY

INCLUDING ELECTROPHORESIS AND OTHER SEPARATION METHODS

ELSEVIER

AMSTERDAM — LONDON — NEW YORK — TOKYO

0021-9673/92/$05.00

Printed in the Netherlands

Journal of Chromatography, 595 (1992) 1–43
Elsevier Science Publishers B.V., Amsterdam

CHROM. 23 880

Review

Polychlorinated biphenyls in the environment

Vít Lang

Institute of Analytical Chemistry, Czechoslovak Academy of Sciences, Veveří 97, 611 42 Brno (Czechoslovakia)

(First received July 22nd, 1991; revised manuscript received November 7th, 1991)

ABSTRACT

This review surveys the problems arising from the release of PCBs into the environment from the point of view of the analytical chemist. These problems are very complex and interdependent and so it is essential to recognize their mutual links rather than to separate one problem from another (sources of contamination, fate in the environment, toxic properties and particular capabilities, limitations and purposes of analytical methods). Prominent attention should be paid in the future to congener-specific analyses of "toxic" congeners using high-resolution gas chromatography and to toxicity-assessing biological methods.

CONTENTS

0021-9673/92/$05.00

1. INTRODUCTION

Polychlorinated biphenyls (PCBs) are prominent environmental contaminants. They can be found in diverse areas of environment all over the world and their properties indicate that they are a probable threat to health.

Many analyses of PCBs have been reported and there is a vast literature, including several books [1–3]. This review is intended to survey the current status of various aspects of PCB analysis and related problems, their mutual links and trends. It is believed that for good experimental planning, proper analyses and effective interpretation of the data obtained, it is important to have an adequate knowledge both of suitable methods for PCB analyses and of the environmental and toxicological aspects of PCBs.

2. FUNDAMENTAL TERMS

PCBs are a group of compounds derived from biphenyl by substitution of one to ten atoms of hydrogen with atoms of chlorine. PCBs are also commonly called chlorinated byphenyls, chlorobiphenyls and polychlorobiphenyls.

The following terms are used in connection with PCBs. Homologues differ one from another in the numbers of chlorine atoms; there are ten PCB homologues. Isomers differ one from another in the substitution pattern of the chlorine atoms. Each homologue has a particular number of isomers: monochlorobiphenyl 3, di- 12, tri- 24, tetra- 42, penta- 46, hexa- 42, hepta- 24, octa- 12, nona- 3 and decachlorobiphenyl 1. Congener denotes each individual polychlorinated biphenyl, on other words, any isomer of any homologue. There are 209 different PCB congeners. However, sometimes the term "isomer" is used in the sense of congener in the literature.

In order to simplify the nomenclature of PCBs, systematic numbering has been introduced [4]. Each of the congeners has been designated with a number from 1 to 209. This systematic numbering is shown in Table 1.

3. PRODUCTION AND APPLICATION

PCBs were first synthesized in 1881 by Schmidt and Schulz [5] and their commercial production began in 1929 in the USA [6,7]. PCBs were produced by numerous manufacturers throughout the world. The prominent producers include Monsanto (St. Louis, MO, USA) (products sold under the tradename Aroclor), Kanegafuchi Chemical (Tokyo, Japan) (trademark Kanechlor) and Bayer (Leverkusen, Nordrhein-Westfalen, Germany) (tradename Clophen) [8]. In Czechoslovakia, Chemko (Strážske, East Slovakia) marketed products under the trade-name Delor and the PCBs with small amounts of additives as Delotherm and Hydelor [9]. The trademark is usually followed by a number that indicates an average degree of chlorination of the product. For example, Aroclor is followed by a four-digit number, the first two (12) indicating the type of compound (biphenyl) and the other two the average percentage of chlorine. The only exception is Aroclor 1016, which contains about 40% of chlorine and is similar to Aroclor 1242 [7]. Delors are designated with a three-digit number, the first two (10) indicating the type of the molecule and the third the average number of chlorine atoms in the molecule. Delors 103 and 106 were produced in the largest amounts [9].

Because of their properties (*e.g.*, chemical and thermal stability, low or no flammability, high permittivity, low vapour pressure at ambient temperature [8,10]), PCBs have extensive applications. They are utilized (alone or in mixtures) as heat-transfer fluids, dielectrics for capacitors and transformers, hydraulic fluids, lubricants, additives in plastics and dyes, etc. [8,10]. Since the hazardous properties and widespread environmental occurrence of PCBs have been discovered, their production has substantially decreased because many manufacturers have ceased production [8,11]. In 1984 the total cumulative world's production was estimated to $1.2 \cdot 10^9$ kg [11]. In Czechoslovakia $1.89 \cdot 10^7$ kg were produced and production ceased in 1984 [12].

4. CHARACTERIZATION OF PCB MIXTURES AND PCB-RELATED COMPOUNDS

Commercial products of PCBs are mixtures of a large number of congeners. During the manufacture of PCBs by reaction of gaseous chlorine with molten biphenyl under given conditions, the chlorination is controlled by the laws of thermodynam-

TABLE 1

SYSTEMATIC NUMBERING OF PCB CONGENERS INTRODUCED BY BALLSCHMITER AND ZELL [4] AND ACCEPTED BY IUPAC

No.	Substitution pattern	No.	Substitution pattern	No.	Substitution pattern	No.	Substitution pattern
1	2	53	2,2′,5,6′	105	2,3,3′,4,4′	157	2,3,3′,4,4′,5′
2	3	54	2,2′,6,6′	106	2,3,3′,4,5	158	2,3,3′,4,4′,6
3	4	55	2,3,3′,4	107	2,3,3′,4′,5	159	2,3,3′,4,5,5′
4	2,2′	56	2,3,3′,4′	108	2,3,3′,4,5′	160	2,3,3′,4,5,6
5	2,3	57	2,3,3′,5	109	2,3,3′,4,6	161	2,3,3′.4.5′.6
6	2,3′	58	2,3,3′,5′	110	2,3,3′,4′,6	162	2,3,3′,4′,5,5′
7	2,4	59	2,3,3′,6	111	2,3,3′,5,5′	163	2,3,3′,4′,5,6
8	2,4′	60	2,3,4,4′	112	2,3,3′,5,6	164	2,3,3′,4′,5′,6
9	2,5	61	2,3,4,5	113	2,3,3′,5′,6	165	2,3,3′,5,5′,6
10	2,6	62	2,3,4,6	114	2,3,4,4′,5	166	2,3,4,4′,5,6
11	3,3′	63	2,3,4′,5	115	2,3,4,4′,6	167	2,3′,4,4′,5,5′
12	3,4	64	2,3,4′,6	116	2,3,4,5,6	168	2,3′,4,4′,5′,6
13	3,4′	65	2,3,5,6	117	2,3,4′,5,6	169	3,3′,4,4′,5,5′
14	3,5	66	2,3′,4,4′	118	2,3′,4,4′,5	170	2,2′,3,3′,4,4′,5
15	4,4′	67	2,3′,4,5	119	2,3′,4,4′,6	171	2,2′,3,3′,4,4′,6
16	2,2′,3	68	2,3′,4,5′	120	2,3′,4,5,5′	172	2,2′,3,3′,4,5,5′
17	2,2′,4	69	2,3′,4,6	121	2,3′,4,5′,6	173	2,2′,3,3′,4,5,6
18	2,2′,5	70	2,3′,4′,5	122	2′,3,3′,4,5	174	2,2′,3,3′,4,5,6′
19	2,2′,6	71	2,3′,4′,6	123	2′,3,4,4′,5	175	2,2′,3,3′,4,5′,6
20	2,3,3′	72	2,3′,5,5′	124	2′,3,4,5,5′	176	2,2′,3,3′,4,6,6′
21	2,3,4	73	2,3′,5′,6	125	2′,3,4,5,6′	177	2,2′,3,3′,4′,5,6
22	2,3,4′	74	2,4,4′,5	126	3,3′,4,4′,5	178	2,2′,3,3′,5,5′,6
23	2,3,5	75	2,4,4′,6	127	3,3′,4,5,5′	179	2,2′,3,3′,5,6,6′
24	2,3,6	76	2′,3,4,5	128	2,2′,3,3′,4,4′	180	2,2′,3,4,4′,5,5′
25	2,3′,4	77	3,3′,4,4′	129	2,2′,3,3′,4,5	181	2,2′,3,4,4′,5,6
26	2,3′,5	78	3,3′,4,5	130	2,2′,3,3′,4,5′	182	2,2′,3,4,4′,5,6′
27	2,3′,6	79	3,3′,4,5′	131	2,2′,3,3′,4,6	183	2,2′,3,4,4′,5′,6
28	2,4,4′	80	3,3′,5,5′	132	2,2′,3,3′,4,6′	184	2,2′,3,4,4′,6,6′
29	2,4,5	81	3,4,4′,5	133	2,2′,3,3′,5,5′	185	2,2′,3,4,5,5′,6
30	2,4,6	82	2,2′,3,3′,4	134	2,2′,3,3′,5,6	186	2,2′,3,4,5,6,6′
31	2,4′,5	83	2,2′,3,3′,5	135	2,2′,3,3′,5,6′	187	2,2′,3,4′,5,5′,6
32	2,4′,6	84	2,2′,3,3′,6	136	2,2′,3,3′,6,6′	188	2,2′,3,4′,5,6,6′
33	2′,3,4	85	2,2′,3,4,4′	137	2,2′,3,4,4′,5	189	2,3,3′,4,4′,5,5′
34	2′,3,5	86	2,2′,3,4,5	138	2,2′,3,4,4′,5′	190	2,3,3′,4,4′,5,6
35	3,3′,4	87	2,2′,3,4,5′	139	2,2′,3,4,4′,6	191	2,3,3′,4,4′,5′,6
36	3,3′,5	88	2,2′,3,4,6	140	2,2′,3,4,4′,6′	192	2,3,3′,4,5,5′,6
37	3,4,4′	89	2,2′,3,4,6′	141	2,2′,3,4,5,5′	193	2,3,3′,4′,5,5′,6
38	3,4,5	90	2,2′,3,4′,5	142	2,2′,3,4,5,6	194	2,2′,3,3′,4,4′,5,5′
39	3,4′,5	91	2,2′,3,4′,6	143	2,2′,3,4,5,6′	195	2,2′,3,3′,4.4′.5.6
40	2,2′,3,3′	92	2,2′,3,5,5′	144	2,2′,3,4,5′,6	196	2,2′,3,3′,4,4′,5′,6
41	2,2′,3,4	93	2,2′,3,5,6	145	2,2′,3,4,6,6′	197	2,2′,3,3′,4,4′,6,6′
42	2,2′,3,4′	94	2,2′,3,5,6′	146	2,2′,3,4′,5,5′	198	2,2′,3,3′,4,5,5′,6
43	2,2′,3,5	95	2,2′,3,5′,6	147	2,2′,3,4′,5,6	199	2,2′,3,3′,4,5,6,6′
44	2,2′,3,5′	96	2,2′,3,6,6′	148	2,2′,3,4′,5,6′	200	2,2′,3,3′,4,5′,6,6′
45	2,2′,3,6	97	2,2′,3′,4,5	149	2,2′,3,4′,5′,6	201	2,2′,3,3 ′,4′,5,5′,6
46	2,2′,3,6′	98	2,2′,3′,4,6	150	2,2′,3,4′,6,6′	202	2,2′,3,3′,5,5′,6,6′
47	2,2′,4,4′	99	2,2′,4,4′,5	151	2,2′,3,5,5′,6	203	2,2′,3,4,4′,5,5′,6
48	2,2′,4,5	100	2,2′,4,4′,6	152	2,2′,3,5,6,6′	204	2,2′,3,4,4′,5,6,6′
49	2,2′,4,5′	101	2,2′,4,5,5′	153	2,2′,4,4′,5,5′	205	2,3,3′,4,4′,5,5′,6
50	2,2′,4,6	102	2,2′,4,5,6′	154	2,2′,4,4′,5,6′	206	2,2′,3,3′,4,4′,5,5′,6
51	2,2′,4,6′	103	2,2′,4,5′,6	155	2,2′,4,4′,6,6′	207	2,2′,3,3′,4,4′,5,6,6′
52	2,2′,5,5′	104	2,2′,4,6,6′	156	2,3.3′.4.4′.5	208	2,2′,3,3′,4,5,5′,6,6′
						209	2,2′,3,3′,4,4′,5,5′,6,6′

ics. As a result, certain substitution patterns are favoured and, consequently, some congeners are more abundant than the others [13]. Owing to the varied reaction conditions for different lots and variations in other technical operations (*e.g.*, distillation of raw products), the composition of the commercial products also varies [8,9]. Hence published data on compositions of commercial PCB mixtures [14–19], giving valuable information on the abundance of congeners, should not be considered as the exact composition of all lots of the same product marketed under the same name. Published results are also partly affected by more or less inaccurate determinations.

Congener compositions of samples from different areas of the environment and biological materials are influenced by the fact that each congener differs from the others in its properties such as water solubility [20–22], Henry's law constant [23], standard reduction potential [24], ability to undergo microbial transformation [25,26], partitioning between different compartments of the environment [27–29], accumulation, distribution and elimination by various organisms [30–38], including humans [39–41]. Consequently, the abundances of individual congeners in environmental and biological samples differ from those in the products from which the contamination originated [42,43]. Moreover, contamination may originate from more than one source and it has also been shown that a number of PCB congeners are produced unintentionally, *e.g.*, during combustion of chloride-containing wastes in incinerators [44] or during syntheses of azo dyes [45], phthalocyanine pigments, chlorinated paraffins, phenolic resins, etc. [46]. Some physico-chemical characteristics (melting point, water solubility and vapour pressure) and differences between them for different congeners can be seen in Table 2. The abundances of some congeners in two lots of Aroclor 1260 and in three biological samples (human milk and bird's eggs) are given in Table 3.

Environmental samples contaminated by PCBs and commercial PCB products may also contain other groups of chlorinated compounds which have

TABLE 2

MELTING POINTS, WATER SOLUBILITIES AND VAPOUR PRESSURES OF SOME PCB CONGENERS

Congener No.	Melting point (°C)[a]	Water solubility (μg/l)[a]	Vapour pressure at 25°C (mPa)[b]
1	34	6000	1120
2	25	2400	200
3	78	1200	612
4	61	1100	133
7	24	1100	239
15	149	56	2.53
18	44	410	12.0
29	78	130	43.9
30	63	200	117
40	121	29	9.71
47	83	92	11.4
52	87	29	4.92
66	124	4.6	6.12
77	180	9.2	0.306
86	100	21	0.0771
87	114	4.1	2.13
101	77	10	1.20
105	125[c]	2.1[c]	0.904
116	124	5.2	–
118	105	2.1[c]	1.20
126	125[c]	1.0[c]	–
128	150	0.57	0.346
138	79	1.8[c]	0.532
153	103	0.91	0.692
156	141[c]	0.36[c]	0.213
171	122	2.0	0.239
180	99[c]	0.63[c]	0.129
194	159	0.22	–
208	183	0.018	–
209	306	0.0013	–

[a] Adapted from ref. 21.
[b] Adapted from ref. 6.
[c] Estimates.

TABLE 3

ABUNDANCES OF SOME PCB CONGENERS IN TWO LOTS OF AROCLOR 126 IN HUMAN MILK AND IN EGGS OF TWO SPECIES OF BIRDS

Weight %, $\sum$PCBs = 100.

PCB No.	Aroclor 1260 [17]	Aroclor 1260 [47]	Human milk [17]	Eggs of black-winged stilt [48]	Eggs of gull-billed tern [48]
52	0.25	0.56	1.9	4.4	0.4
101	2.5	5.02	0.97	4.4	1.3
118	0.49	0.57	6.5	8.9	2.2
138	6.5	6.13	10.0	9.7	9.5
153	9.6	10.80	12.0	12.6	17.1
156	0.45	0.88	4.87	1.7	2.2
180	9.1	7.12	5.3	8.0	15.3

some properties in common with PCBs. Each group of these compounds may be a complex mixture containing many individual compounds cumulated by organisms, more or less persistent, having toxicological importance, some of them having the same mechanisms of action as the "toxic" PCBs congeners and some of them able to interfere in the determination of PCBs. The presence of these compounds may affect both chemical and biological assays of PCBs and thus lead to misinterpretation of the results. Basic information on such compounds is summarized in Table 4.

In addition to chlorinated compounds, there are also bromochlorinated and brominated compounds derived from PCBs, PCDFs and PCDDs [49,50]. All these groups of the compounds can be determined using gas chromatography.

5. PCB POLLUTION: A VIEW INTO THE FUTURE

PCBs have been used for more than 60 years, but their presence in the environmental was not apparent until the electron-capture detector was extensively applied in gas chromatographic analyses [122]. In 1966 PCBs were first identified as pollutants [123] and subsequent investigations showed that they are ubiquitous [124]. Currently found concentrations are usually given in pg/m^3 in the atmosphere, ng/kg in surface waters, $\mu g/kg$ in sediments and soils and mg/kg in eggs of aquatic birds, fat of fishes, human adipose tissue and human milk fat. The amount of PCBs in the global environment has been estimated to be about $3.7 \cdot 10^8$ kg [11], and further $7.8 \cdot 10^8$ kg were estimated to be still available for utilization or deposited in different ways [11]. Hence it is of great importance for assessing the prospects for contamination to know what the fate of the non-utilized and deposited PCBs will be [11].

Generally, PCBs are very persistent compounds. There are three natural processes of degradation of environmentally dispersed PCBs: combustion, photolysis and biodegradation [125]. Natural combustion is very rare and photolysis needs access of light for a sufficiently long period of time. Moreover, during PCB photolysis (and also combustion) PCDFs and other related toxic compounds can be formed from the PCBs [126,127]. The crucial role in the clearance of the environment is played by microbial biodegradation processes. These processes are highly congener dependent. There are two basic types of microbial degradation: aerobic degradation, affecting especially the lightly chlorinated PCBs (as a result the highly chlorinated PCBs become more abundant) [128–131], and anaerobic degradation, occurring in sediments and causing reductive dechlorination of highly chlorinated PCBs (as a result the lightly chlorinated PCBs become more abundant). It is of particular interest that anaerobic dechlorination selectively removes *meta*- and *para*-chlorines and thus affects the "toxic" congeners (see Section 6.3.). The less chlorinated congeners that arise by anaerobic degradation can be then subjected to aerobic degradation [128, 129, 132]. Hence it seems that nature may have the potential to remove PCBs from the environment. These processes, however, occur under specific conditions and anaerobic degradation also needs relatively high concentrations of PCBs (on decreasing the concentration of Aroclor 1242 from 140 to 14 ppm the dechlorination becomes unobservable) [133]. This is unfortunate because the environmental concentrations are usually much lower and the higher (and potentially dangerous) concentrations usually occur in higher animals and humans owing to bioaccumulation.

Assessment of time trends is complicated owing to the difficulty of obtaining true values for PCB concentrations, to changes in analytical methods over the years and also due to seasonal variations in PCB levels (*e.g.*, [134]). Moreover, the trends may differ for different compartments of the environment. For these reasons, mere comparisons of results from various time periods (and from various locations) may in some instances be misleading and the time trends can hardly be determined exactly. However, the results obtained so far indicate that after a significant drop in PCB levels in heavily polluted areas during the 1970s (mainly as a result of decreases in leakage and of diffusion to less contaminated areas), from the early 1980s the PCB levels have been fluctuating or declining much more slowly in the samples used for monitoring environmental pollution and in humans [107,135–139] (e.g., see Table 5 and Fig. 1). Hence it seems likely that the end of PCB pollution can hardly be expected in the near future.

TABLE 4

IMPORTANT PCB-RELATED COMPOUNDS

Compound	Structure	Sources	Comments
Polychlorinated dibenzo-*p*-dioxins (PCDDs) Polychlorinated dibenzoforans (PCDFs)	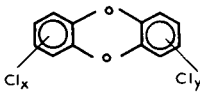 PCDDS 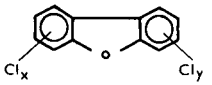 PCDFs	Heating and espescially combustion of PCBs and other chlorine-containing compounds [51–63], unwanted by-products in several chemicals (including in PCBs). PCDDs formed also in enzyme-mediated reactions [64,65]. Never produced intentionally	Extremely persistent and some congeners (2,3,7,8-TCDD) extremely toxic. Found in numerous environmental and biological samples all over the world [66–84]. PCDDs include 75 congeners and PCDFs include 135 congeners [67,68]. PCDDs and PCDFs may co-elute with PCBs when common GC stationary phases are used [85].
Polychlorinated terphenyls (PCTs)	Three types of skeletal structures: 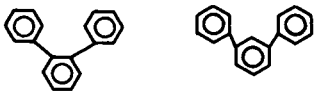 *ortho* *meta* 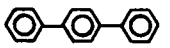 *para*	Produced, marketed and used for similar purposes to PCBs, sometimes in mixtures with PCBs [8,86,87]	High concentrations of PCTs have been recently found in US water sediments and biota [88]. Little information is available on the distribution, fate and effects of the PCTs [88]. The number of congeners is enormous. PCTs, particularly the lower chlorinated ones, may co-elute with PCBs when common GC stationary phases are used [89]
Polychlorinated quaterphenyls (PCQs)	Six skeletal structures: 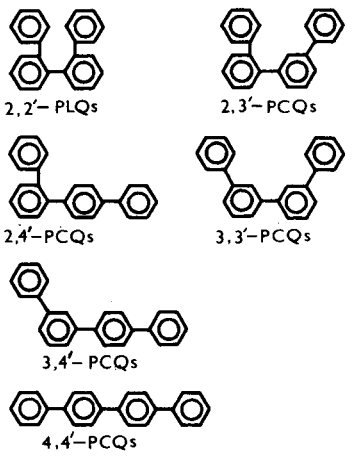 2,2′– PLQs 2,3′–PCQs 2,4′–PCQs 3,3′–PCQs 3,4′– PCQs 4,4′–PCQs	Dimerization of PCBs	All six skeletal structures of PCQs have been identified in human adipose tissue and blood [90,91]. The number of congeners is enormous (more than 100 000) [90]

Polychlorinated biphenylenes (PCBPs)	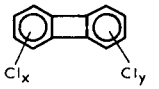	Combustion of PCBs [92]	2,3,6,7-Tetrachlorobiphenylene was found to be equipotent with 2,3,7,8-TCDD in inducing microsomal enzymes [93]. There are 75 possible congeners
Polychlorinated naphthalenes (PCNs)	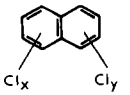	Produced commercially (under the trademark Halowax) and used mainly in the electrical industry and to impregnate wood, paper and textiles [94]	PCNs have been found in various parts of environment [95–97]. Some of them are potent AHH and EROD inducers [98]. There are 75 congeners [94]. PCNs may co-elute with PCBs when common GC stationary phases are used [99]
Polychlorinated camphenes (PCCs), also called polychlorinated bornanes (Toxaphene, Campheclor)	One of the skeletal structures of the main components is 	Produced commercially and used as pesticides [100]	Global pollutant [100–102]. Extremely complex mixture of more than 600 individual components, only a few of which have been identified [100,103]. PCCs may co-elute with PCBs when common GC stationary phases are used [100]
Technical chlordane (polychlorinated methanoindenes and indanes)	Basic tricyclic structure: 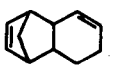	Produced commercially and used as pesticides [104]	Global pollutant [105–108]. In addition to 48 congeners derived from the basic tricyclic chlordene structure, it also contains a number of other chlorinated compounds [109,110]. Technical chlordane may co-elute with PCBs when common GC stationary phases are used [105]
Tetrachlorobenzyltoluenes (TCBTs), also called monomethyl-substituted diphenylmethanes (MePCDMs)	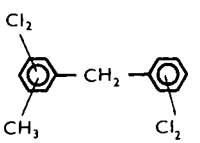	Produced commercially and used in several cases as PCBs substitutes [111–114]	Found in fish and sediment samples [115,116]. There are 96 congeners (in this instance the same as isomers) [117]. TCBTs may co-elute with PCBs when common GC stationary phases are used [118]
PCB metabolites: Oxygenated PCBs (PCB-ols) Methylsulphonyl PCBs (MSF-PCBs) Hydroxymethylsulphonyl PCBs (HMS-PCBs)	Some chlorines are substituted with –OH Substituted with $-SO_2CH_3$ Substituted with $-SO_2CH_3$ and –OH	Biological modifications of PCBs	MSF-PCBs have been found in human tissues [119] and the same is true for HMS-PCBs [120]. PCB-ols have been found also in marine sediments and biota [121]. MSF-PCBs are very persistent and are suspected to cause some distress in PCBs-affected humans [119]

TABLE 5

TIME TREND OF PCB LEVELS IN THE LIZARD GOBY FISH (RHINOGOBIUS FLUMINEUS) FROM THE RIVER NAGARAGAWA, JAPAN (ACCORDING TO REF. 107)

Year	Total PCBs (mg/kg wet weight basis)	Year	Total PCBs (mg/kg wet weight basis)
1968	14	1979	0.37
1969	15	1980	0.20
1970	13	1981	0.21
1971	2.7	1982	0.12
1972	3.1	1983	0.10
1973	2.6	1984	0.11
1974	0.58	1985	0.16
1977	0.38	1986	0.15
1978	0.34		

6. BIOLOGICAL ASPECTS OF PCBs

6.1. Effects of high doses on laboratory animals

Effects on animals by high doses of PCBs include body weight loss and lesions and dysfunctions of the skin (chloracne), liver (hepatomegaly, haemorrhage, porphyria) bile duct, gall bladder, urinary tract, endocrine system and reproductive system and also teratogenesis and carcinogenesis. There are large differences in sensitivity and types of effects between species. These effects are preceded by induction of xenobiotic metabolizing enzymes [140–147]. On the other hand, there are also antagonistic relationships between PCBs and some other toxic chemicals (*e.g.*, inhibition of aflatoxin B_1-mediated carcinogenesis by PCBs) [146,148–152].

Acute toxicity testing of commercial mixtures has not revealed a dependence of toxicity merely on the degree of chlorination. Of the Aroclors, the most toxic in rats (oral application) were Aroclor 1254 (LD_{50} 1.295 g/kg) and Aroclor 1260 (LD_{50} 1.315 g/kg) and the least toxic were Aroclor 1248 (LD_{50} 11 g/kg), 1262 (LD_{50} 11.3 g/kg) and 1268 (LD_{50} 10.9 g/kg) [153]. As will be discussed in Section 6.3., however, there are vast differences in toxicity between individual congeners.

Mutagenicity testing by the most commonly applied Ames test has shown that none of the PCBs gives positive results, either with metabolic activation or without it [146].

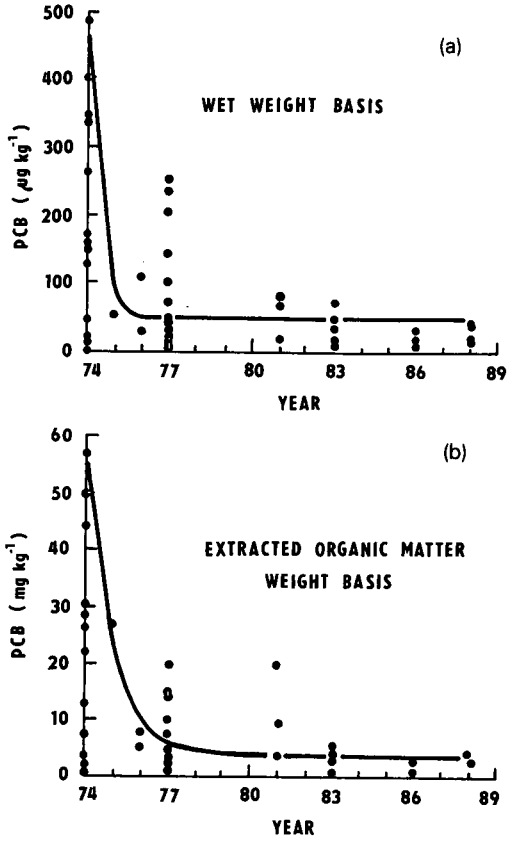

Fig. 1. Time trend of PCBs levels in mussels from the Rijeka Bay (Adriatic Sea), Croatia. Monitoring was carried out by a single analytical group (mostly by the same analyst) using uniform methodology for 14 years. Reprinted from ref. 138.

6.2. Effects of high doses on humans

The effects of high doses on humans can be investigated in individuals exposed to PCBs either occupationally or due to poisoning. There have been two accidents of mass PCB poisoning caused by ingestion of edible oil. The first, called "Yusho" , happened in 1968 in Japan [154] and the second, called "Yucheng" happened in 1979 in Taiwan [39,155]. In the poisoned humans many effects were observed such as liver damage, dermal lesions, respiratory disorders, severe ocular signs, various neurological symptoms, damage to the endocrine system, immunodeficiency and reproduction disorders [154,156]. The most common symptom in occupationally exposed humans is chloracne. Liver injury and changes in liver-related serum analytes (bi-

lirubin, transferases, β-glucoronidase, etc.) have also been observed. Other responses are more rare [156–159].

More serious problem may be the effects of PCBs on children, even in cases of non-professional (environmental) exposure. They may be exposed to PCBs during foetal development and after birth they may be fed with breast milk which may contain significant levels of PCBs [160,161]. It has been found that infants from mothers with higher PCBs concentrations in the blood had significantly decreased weights and gestational ages [162] and women with miscarriages had higher average PCBs levels in the blood than control women [163]. It has been also proposed that late haemorrhagic disease, which is an important cause of morbidity and mortality in infants older than 1 month, is caused by PCBs and related compounds given to the infants in the breast milk [164,165]. It has been observed that children who had been breast fed with milk containing higher levels of PCBs for longer periods (1 year) were less active than the less exposed children, which suggests a possible vulnerability of certain behavioural systems to PCBs (and related compounds) [166].

Carcinogenity of PCBs in humans has not been proved reliably so far. However, significantly increased levels of some oncogene proteins [167] and chromosomal aberrations of human peripheral blood lymphocytes [168] have been found in workers exposed to PCBs.

Correct interpretations of the effects of PCBs on humans are difficult owing to the possible presence of PCB-related compounds together with PCBs (*e.g.*, the contaminated Yusho oil also contained PCDFs, PCDDs and PCQs [154,169] and it is probable that the largest part of toxicity in this case arose from PCDFs and PCDDs [170], and the Yucheng oil contained PCDFs, PCQs and PCTs [155,171]) and also because an important role is played by other factors such as exposure to various chemicals, way of life and genetic differences, which are specific to individuals and which are very difficult to assess.

6.3. Biochemical insight: cytochrome P-450, its induction by PCBs and links with toxicity

Most lipophilic foreign compounds (xenobiotics) undergo in organisms enzyme-mediated biotransformation reactions, the purpose of which is elimination of these xenobiotics. The detoxification has two phases. During the first phase the polarity of a xenobiotic increases and during the second phase conjugation occurs, which means that the metabolite is combined with a product of normal metabolism (endogenous product). Such a conjugate can usually be easily excreted. However, metabolism does not lead inevitably to detoxification of a xenobiotic, as conversion into more toxic product(s) that are not conjugated and thus not excreted may also occur.

A critical role in the metabolism of many xenobiotics (and also endogenous compounds) is played by a family of enzymes named cytochrome P-450 [172]. The enzymes belonging to such a family are generally called isozymes. P-450 is a constituent of enzymatic complexes called P-450-mediated monooxygenases or mixed function oxidases (MFO). The term "P-450" arises from the fact that the reduced form of cytochrome P-450 bound to carbon monoxide exhibits an absorption maximum at about 450 nm. Various isozymes of cytochrome P-450 exist in plant and in bacterial and animal organisms including man [173–177], and there are indications that cytochrome P-450 is ubiquitous in all living organisms [172]. It is not known how many isozymes of cytochrome P-450 exist, but the data imply that there may be up to 100 enzymes [173]. The main effort has been exerted to investigate P-450 in mammals (particularly in rats and mice and in humans) and in chick embryos.

The important feature of the P-450 is its inductibility, which means that its production by cells in the organism can be increased by various xenobiotics. These xenobiotics are called inducers. Each inducer exerts a characteristic impact both on the induction of the total amount of the cytochrome P-450 and on the levels of individual cytochrome P-450 isozymes [178,179]. The isozymes have their own, but overlapping, substrate specificities [180]. Higher amounts of these isozymes in organisms are manifested by changes in the metabolism of the corresponding xenobiotics. Such stimulated metabolical modifications have been observed both in various species of laboratory animals and in humans [180]. The following cytochrome P-450 isozymes appear to be important for investigation of the effects of PCBs: P-450IA1 (also called in rats P-450c,

in mice P_1-450 or P-448 and in humans P_1-450), P-450IA2 (also called in rats P-450d and in mice and humans P_3-450), P-450IIB1 (also called in rats P-450b) and P-450IIB2 (also called in rats P-450e) [181].

Inducers are classified into groups according to the cytochrome P-450 isozymes that they induce. For the study of PCB toxicology there are two important groups of inducers. A typical representative of the first group is phenobarbital (PB) and of the second group the polycyclic aromatic hydrocarbon 3-methylcholanthrene (3-MC). Accordingly, a chemical inducing a spectrum of cytochrome P-450 isozymes similar to that induced by PB (or 3-MC) is classified as a PB-type inducer (or a 3-MC-type inducer). PB-type inducers typically significantly increase the levels of P-450IIB1 and P-450IIB2 and 3-MC-type inducers the levels of P-450IA1 and P-450IA2 isozymes. Induction of a particular cytochrome results in increasing activity of enzymatic complexes in which the particular cytochrome is involved. Such enzymatic complexes of special interest are aryl hydrocarbon hydroxylase (AHH) responsible for the metabolism of polycyclic aromatic hydrocarbons and exthoxyresorufin-*o*-deethylase (EROD). The catalytic activities of both AHH and EROD are associated with 3-MC-type inducers, or strictly, with isozyme P-450IA1 [173,178,179,182, 183].

The influence of cytochrome P-450 as such on the toxicity of xenobiotics in organisms is complicated. The P-450 activities may lead, on the one hand, to inactivation and elimination of toxic xenobiotics or, on the other, to conversion of other (or even the same) foreign compounds to more toxic or carcinogenic intermediates, and as a result, the P-450 may prevent intoxication or cause intoxication, and may protect against chemical carcinogenesis or increase the risk of cancer. The results depends on many factors, such as the nature of the foreign compound, the route into the organism, specific tissue susceptibility, the isozymal spectrum of induced P-450, and the ratio between P-450 and other related enzymes and compounds [179,180,184]. The influence of these factors on the metabolism of a xenobiotic has been most extensively investigated in benzo[*a*]pyrene [185–191].

Some time ago, it was revealed that 2,3,7,8-tetrachlorodibenzo-*p*-dioxin (2,3,7,8-TCDD), an extremely toxic and carcinogenic compound related to PCBs, is also an extremely potent inducer of AHH activity. It was also found that the biological activity is structure dependent and that the pattern of pathological changes caused by certain PCB congeners is identical with that caused by 2,3,7,8-TCDD [192–200].

After an effort to find the relationships between structure, AHH (or P-450IA1 or EROD or 3-MC type) induction activity and toxicity [201–207], a classification of PCBs into categories has been proposed [208]. The congeners having two *para*-chlorines and at least one *meta*-chlorine (according to similarity with 2,3,7,8-TCDD) have been considered. The first category, "coplanar" PCBs (having no *ortho*-chlorine), has two subcategories (the term "coplanar" is commonly applied to them because of the absence of *ortho*- and the presence of *meta*- and *para*-chlorine atoms make a coplanar conformation more probable [209]). The first subcategory contains congeners 77, 126 and 169. These are the most potent inducers of P-450IA1 and P-450IA2 (and hence AHH and EROD activity) both *in vivo* (male Wistar rats) and *in vitro* (rat hepatoma H-4-II E cells), they are "pure" 3-MC-type inducers and are the most toxic PCB congeners known. The second subcategory contains congeners 37 and 81. These are less potent AHH inducers than congeners in the first subcategory and they are mixed-type inducers, *i.e.*, they induce P-450 isozymes typical for both 3-MC and PB. PCB 37 is the least active congener in the first category and does not cause typical toxic responses. The second category comprises mono-*ortho* "coplanar" PCBs having one *ortho*-chlorine (congeners 105,114,118,123,156,157,167 and 189). They are also potent inducers of AHH activity, they are mixed-type inducers and in many of them toxic effects similar to those of 2,3,7,8-TCDD have been proved. The next category contains di-*ortho* "coplanar" PCBs (congeners 128, 137, 138, 153, 158, 166, 168, 170, 180, 190, 191, 194 and 205). Their AHH-inducing potency *in vivo* is significantly diminished (*in vitro* they are inactive) and another shift to a PB-type induction pattern is apparent [206–208,210,211].

Congeners belonging to groups other than those above (mono-*ortho* "coplanar" congeners without one *para*-chlorine or tri-*ortho* "coplanar" congeners) can also to some extent induce in high doses

(tens and hundreds of mg/kg) AHH and EROD activities *in vivo* (in mice) [212], but their inducing potencies are considerably lower in comparison with AHH-type inducers between PCBs or 2,3,7,8-TCDD.

It is noticeable that in fish only the non-*ortho* "coplanar" congeners induce EROD activity; other congeners did not cause such effects at the concentrations tested (1 and 5 mg/kg) [213].

Systematic tests in rats have revealed that there are very good correlations (in terms of orders of magnitude) between AHH- and EROD-inducing potencies *in vivo* and *in vitro* and between the inducing potencies and typical acute toxic effects (body weight loss, thymic atrophy). Such correlations have been demonstrated in selected PCB congeners [208,210,214,215] and in PCDD and PCDF congeners [216–218]. Certain PCB congeners, namely 77 and 105, however, have shown some deviations from these correlations, probably owing to their easier metabolizability *in vivo* [207]. The results also show that there are vast differences in inducing potencies and toxicities between various individual congeners. The above-mentioned correlations imply that a congener which is a potent inducer of P450IA1 is expected to also be considerably toxic (and *vice versa*). This is why the non-*ortho* and mono-*ortho* "coplanar" congeners have begun to be called "toxic" congeners. Consequently, there are thirteen or, when congener 37 is not included, twelve "toxic" congeners. The term "toxic" currently used for the twelve (or thirteen) PCB congeners does not mean that the other PCB congeners are harmless [212,219], but is reflects the very large differences in toxic potencies between the congeners.

In a search for the mechanism of P450IA1 induction and toxic effects, the ability of P450IA1-inducing chemicals to bind as ligands to an intracellular protein exhibiting typical properties of a receptor has been discovered [220–222]. This receptor is called Ah-receptor (aryl hydrocarbon or aromatic hydrocarbon receptor) or, sometimes, 2,3,7,8-TCDD receptor. There is evidence that the complex of the Ah-receptor with the ligand is the mediator of both the P-450IA1 induction and the typical toxic effects [208,221–224]. The Ah-receptors are widely distributed in many animal tissues and species and in humans [172,179,225–230] and their nature is still an object of investigation. It has recently been proposed that the toxic effects may be caused by certain products of the metabolism of arachidonic acid, namely epoxyeicosatrienoic acid and monohydroxyeicosatetranoic acid. The metabolism is P-450 dependent and highly inducible by 2,3,7,8-TCDD [231]. Nevertheless, it is probable that although Ah-receptor plays a critical role in the toxicity, it is not a mediator of all the toxic responses of P450IA1-inducing compounds [232].

It is characteristic for receptor-mediated biological process (because of limited binding sites per cell) that only certain maximum induced enzymatic activity can be reached (at doses associated with acute toxicity so-called "super-maximum" induction of hepatic EROD (but not AHH) activity has been also observed in mice [233,234], which is not considered in the following text). The dose or concentration of a congener that just induces half of the maximum value, ED_{50} (effective dose) or EC_{50} (effective concentration), is called the biological potency and serves as a measure of the biological activity of the congener. Owing to the similarity of toxic responses and mechanisms of the "toxic" PCB congeners and 2,3,7,8-TCDD, the biological potency is often expressed relative to that of 2,3,7,8-TCDD and is then termed relative biological potency [210,220] or toxic equivalent factor (TEF) [235]. The relative biological potencies of the "toxic" congeners for EROD and AHH induction are shown in Table 6 [210]. The corresponding TEFs are also available for toxic PCDDs and PCDFs [236].

Several more or less different systems of "composite" TEFs have been developed for PCDD and PCDF congeners. In addition to P450IA1 induction potency, the composite TEFs should also reflect various toxic effects including carcinogenity in different animals [235,237,238]. Recently, "international TEFs" have been introduced in order to replace the other composite TEFs systems used for PCDDs and PCDFs [239]. Composite TEFs have recently been proposed also for PCBs. These are 0.1 for congener 126, 0.05 for 169, 0.01 for 77, $1 \cdot 10^{-3}$ for mono-*ortho* "coplanar" PCBs and $2 \cdot 10^{-5}$ for di-*ortho* "coplanar" PCBs [49]. The application of TEFs enables the data on chemical composition for a sample containing PCBs (and PCB-like chemicals) to be converted into a number that indicates

TABLE 6

TOXIC EQUIVALENT FACTORS OF THE "TOXIC" PCB CONGENERS BASED ON INDUCTION OF AHH AND EROD ACTIVITY IN RAT HEPATOMA H-4-II E CELLS IN CULTURE

The values are given in the form of fraction $1/x$, where x is the molar concentration of the particular congener in solution that would cause the same biological response as a solution of 2,3,7,8-TCDD having unit concentration. TEF = EC_{50} (2,3,7,8-TCDD)/EC_{50}(PCB congener). EC_{50} (2,3,7,8-TCDD) for AHH induction is $9.6 \cdot 10^{-11}$ *M* and for EROD induction $8.02 \cdot 10^{-11}$ *M*. Modified from ref. 210.

PCB No.	AHH	EROD
77	1/370	1/1100
81	1/120 000	1/24 000
105	1/910	1/1500
114	1/41 000	1/14 000
118	1/120 000	1/110 000
123	1/10 000	1/7000
126	1/2.5	1/3
156	1/22 000	1/11 000
157	1/7400	1/16 000
167	1/140 000	1/112 000
169	1/630	1/300
189	1/120 000	1/98 000
(3-MC	1/13 000	1/7900)

how much 2,3,7,8-TCDD would cause the same biological effects as PCBs (and PCB-like compounds) contained in the sample. This value is called the 2,3,7,8-TCDD toxic equivalent [236] or toxic equivalent quantity (TEQ) [235], and it seems to be extremely useful for risk assessment. It can be obtained by congener-specific chemical analysis and calculation or, when the TEQs are derived only from enzyme induction, also by biological assay.

Vast differences between the toxicities of congeners can be illustrated by the results of a study of the mortality of chick embryos. The results have shown that a dose of 2 μg/kg of congener 126 in an egg caused mortality in 90% of the embryos 14 days after injection and 100 μg/kg congener 169 caused 80% mortality, whereas a dose of $5 \cdot 10^4$ μg/kg of congener 153 did not cause any mortality or even any abnormalities in the embryos. Corresponding results were also obtained when the inducing potencies of EROD in the chick embryos were tested [240]. It is of interest that in another similar test congener 70, belonging to the group of mono-*ortho* "coplanar" congeners without one *para*-chlorine atom (this group contains congeners 55, 56, 61, 63, 67, 68, 70, 76, 106, 107, 108, 120, 122, 124, 159 and 162) caused certain embryonic mortality, namely a dose of 5 mg/kg caused mortality of 40% of chick embryos. For the tested mono-*ortho* "coplanar" congeners with *para*-chlorines, the corresponding values were 5 mg/kg of congener 118, 45%; 5 mg/kg of congener 167, 0%; 2.5 mg/kg of congener 105, 85%; 2.5 mg/kg of congener 157, 90%; and 2.5 mg/kg of congener 156, 95% embryonic mortality [241].

An important question is whether there are any additive, synergistic or antagonistic effects both mutually between PCB congeners and between PCBs and other chemicals that may be present together in environmental and biological samples. Owing to the extreme complexity of such environmental mixtures, this question can hardly be answered definitively. The concept of toxicity equivalent factors requires additivity of the toxic effects. This seems to be generally fulfilled, but the results published so far are sometimes contradictory and they show that besides additive effects antagonisms also exist, *e.g.*, between 2,3,7,8-TCDD and technical mixtures and some congeners of PCBs, between 2,3,7,8-TCDD and some of its derivatives and between 2,3,7,8-TCDD and hexachlorobenzene [149–151,212,242–247]. A recent study, on the other hand, shows considerable synergistic effects of a combination of PCB 52 and 77 (*in vivo*) in rats [248]. The antagonistic and/or synergistic effects can be covered only by biological assays.

The considerations in this section can lead to the conclusion that there may be several PCB congeners which cause the toxic effects observed in living organisms and which represent the risk to humans of exposure to PCBs. The question is, which congeners contribute to the toxicity of PCB mixtures to such an extent that the possible effects of the other congeners in some sample (or environment) can be assumed to be negligible? It seems very likely that the congeners should have high potency of Ah-receptor-mediated induction of cytochrome P450IA1 and should bind to Ah-receptor preferentially to other binding sites that may occur in cells because of the generally very low concentrations of PCBs in cells.

The values of toxic equivalent quantities of commercial mixtures of PCBs obtained both by chemical analysis and calculation using TEFs based on

AHH and EROD induction potencies and by a biological assay using rat hepatoma H-4-II E cells in culture have been compared considering six PCB congeners (77, 105, 118, 126, 156 en 169) and eleven PCDFs congeners. The results were comparable. Interestingly, the PCDFs did not contribute significantly to the overall toxicity [249].

It is probable that the twelve "toxic" congeners contribute essentially to the overall PCBs toxicity in environmental and biological samples. Some other congeners, however, namely those belonging to the groups of di-*ortho* "coplanars" and also mono-*ortho* "coplanars" without one *para*-chlorine, could be of some importance. Steps towards a firmly based determination of toxic equivalent factors of the toxic congeners and assessement of toxicological properties of the congeners belonging to the suspected groups are of utmost importance. Results of toxicological research can guide analytical chemists in targetting their analyses effectively.

The limit concentrations of PCBs used for regulatory purposes are based either on the "total PCB" level or, more recently, on "standard" individual congeners (28, 52, 101, 138, 153 and 180) chosen in order to cover a wide range of chlorination (from 3 to 7 chlorine atoms) and taking into consideration their relatively high levels in samples. For example, the limits set by the US Food and Drug Administration (FDA) (in 1972) are for milk and milk products 1.5 mg "total PCBs"/kg milk fat, for poultry 3.0 mg/kg fat, fish (the limit was set in 1978) 5.0 mg/kg edible fraction and foodstuffs for infants 0.2 mg/kg [250]. The limits set in Germany in 1988 are for milk and milk products 40 and 50 μg/kg milk fat for congeners 28, 52, 101 and 180, and 138 and 153, respectively, and for edible animal fat 80 and 100 μg/kg for congeners 28, 52, 101 and 180, and 138 and 153, respectively [251].

7. ANALYTICAL CHEMISTRY OF PCBs

7.1. Analytical procedure in general

Considering the properties of PCBs and their distribution and concentrations in the environment (see also Table 10), the general analytical procedure is similar to that for the trace analysis of other lipophilic organic substances, *e.g.*, halogenated pesticides. The procedure in most instances consists in the following basic steps: (1) sampling; (2) extraction; (3) clean-up; and (4) determination and evaluation. Concentration steps usually follow steps 2 and 3. The particular execution of the procedure depends above all on the type of sample to be analysed and on the expected range of PCB levels.

The sample types can be divided as follows: (a) gaseous matrices (mostly air); (b) water and aqueous solutions; (c) solid matrices with no or negligible fat content (soils, water sediments); and (d) matrices containing fat (human and animal tissues, blood, milk and milk products, etc.).

A vast number of particular procedures and their various modifications (especially as for steps 2 and 3) have been described. The recoveries mentioned are mostly comparable. With respect to the differences that always exist between analytical laboratories (*e.g.*, differences between the same types of matrices, lots of chemicals used, individual styles of work of analytical chemists) it can be hardly decided which method will be the best for a specific laboratory with its own particular conditions.

7.2. Sampling and sample extraction

There is comprehensive specialized literature dealing with methods to take appropriate samples [252–254]; only sampling from air and water will be mentioned here.

For the sampling of PCBs in air, polyurethane foam is commonly used [255–259]. Chromosorb [260], Florisil [260], silica gel [108], Tenax GC [260–262], XAD-2 resin [260] and glass beads [263] have also been applied. Air particles are usually captured using glass-fibre filtration [256,261–263]. The amounts of the air pumped through the sorbent are commonly hundreds to thousand(s) of cubic metres [255,256,262]. PCBs are then extracted with various organic solvents, commonly with light petroleum [255,256] or hexane [261,262] using a Soxhlet extractor, or with dichloromethane [263] or a mixture of organic solvents, *e.g.*, acetone and hexane [258]. A recent approach is to use supercritical fluid extraction [257,264].

Water sampling is made difficult by the usually very low concentrations of PCBs in environmental waters. This makes effects such as adsorption a serious problem with a potentially substantial effect on the results [265]. Owing to adsorption, the use of polymers other than PTFE should generally be avoided during any PCB analysis, as demonstrated

by following adsorption experiment: 90 ml of a solution of 100 mg/l of Aroclor 1254 in deionized water (pH 6.9) with addition of 0.25% (w/v) of Triton X-100 (added because it increases the solubility of Aroclor) was mixed and shaken at 34°C with various polymers of approximately equal surface areas (216 cm^2). The amounts of the Aroclor 1254 adsorbed by the tested polymers were red vacuum rubber 99.0, latex 97.8, norprene 97.7, polypropylene 96.7, Tygon 96.2, polyethylene 95.7, Monosil (silicone) 93.6, phenoxyresin 33.0, nylon 22.9 and PTFE 3.4 mg/l [266].

Water samples are either extracted directly with water-immiscible organic solvents, commonly with hexane [267,268] or dichloromethane [256,263,269], or the PCBs in water are first captured on a solid sorbent (XAD-2 resin [270,271], Tenax [272] or polyurethane foam [258]) and then solvent extracted. The amounts of environmental waters taken for analysis are usually from a litre up to hundreds of litres [263,267,271,273,274].

The results of the analyses may also be substantially affected by pH. It has been shown that acidic or neutral extraction may lead to an underestimation of PCB concentrations in fresh water [275]. A promising method of sampling PCBs (and other lipophilic pollutants) in environmental waters is to use solvent-filled dialysis membranes. The sampling and extraction are carried out in one step and, what is important, the samples obtained normally do not need clean-up [276].

Samples of sediments are usually extracted (after homogenization and conditionally drying) with a mixture of acetone and a light aliphatic hydrocarbon [267,277–282] in a Soxhlet apparatus [267, 277,281], a separating funnel [279] or an ultrasonic bath [280]. Other media used are hexane [283], acetone [281] or ethyl acetate [284] applied individually or isopropyl alcohol and dichloromethane [256] or methanol and dichloromethane [285] used consecutively. Steam distillation [259,281] and supercritical fluid extraction [286] techniques have been also utilized. Dichloromethane [224,287] and ethyl acetate [288] have been applied to extract PCBs from soils.

Fat-containing samples are commonly extracted in such a way that the fat is obtained together with PCBs and removed in the following step.

Animal and human tissues are extracted, after homogenization and drying (frequently with anhydrous sodium sulphate), commonly with hexane [35,105,250,289–294] or light petroleum [137,277, 279]. Dichloromethane [284,295,296], cyclohexane [297], ethyl acetate [298] and benzene [299] have also been used. Often mixtures of solvents, are applied, *e.g.*, a small amount of diethyl ether in light petroleum [300–302] or mixtures of benzene and acetone [303,304], hexane and acetone [28,100, 267,305–308] and toluene and ethyl acetate [309]. Several extraction steps, each with a different extraction medium [102] and using more complicated solvent mixtures [310], have also been reported. A generally applied method is also to saponify the fat first and then use a light aliphatic hydrocarbon for extraction [33,169,311]. Comparison of different extraction methods has shown large differences between extraction efficiences of various solvents for different types of fish species and congeners and the necessity for a sufficiently long duration of Soxhlet extraction (at least 6 h) [312]. Plant tissues have been extracted with hexane [313,314].

Important fat-containing liquid matrices are blood and milk. PCBs in blood are determined either in whole blood or in serum. In both instances the usual organic solvents are used (*e.g.*, hexane [39,40,315,316], hexane–diethyl ether [35,317–320], acetone–hexane [321] and acetone–benzene [303]). For whole blood, saponification is often employed [39,40,316]. For milk, in addition to extraction methods similar to those used for blood [321–325], adsorption on a solid sorbent has been utilized. Milk was first mixed with fibrous cellulose and Florisil and, after evaporation of water, the mixture was extracted with hexane [326]; alternatively, the milk was mixed with Lipidex 5000 gel and the chemicals of interest (in addition PCBs also some pesticides and PCDFs and PCDDs) were successively eluted with a series of solvent mixtures [327] and then cleaned up.

To reduce the amount of extracts after extraction and to increase the concentration of PCBs prior to determination, evaporation steps are usually carried out. Common methods are to use a rotary vacuum evaporator for rough concentration and a Kuderna–Danish evaporator or a gentle stream of nitrogen for fine concentration.

7.3. Clean-up

The point of clean-up is to remove the substances that could interfere in a determination. For clean-up the methods commonly used are liquid–solid adsorption chromatography, gel permeation chromatography and chemical methods. Other techniques, such as liquid–liquid partitioning or removing fat by low-temperature precipitation, are much less frequent.

Clean-up procedures are often modifications of older procedures applied for the determination of organochlorine pesticides (*e.g.*, DDT) and they are empirical. In many instances PCBs are determined in one sample together with these pesticides.

For clean-up utilizing liquid–solid adsorption chromatography, the use of most common adsorbents and many organic solvents and their mixtures as eluents has been described. Both very different clean-up systems for nearly identical extracts and, on the other hand, identical clean-up systems for very different extracts have appeared in the literature, probably because in liquid–solid chromatography successful results can frequently be obtained under conditions which may be far from optimum for the system [328]. When fatty samples are cleaned up, fat is retained and PCBs are eluted.

The common adsorbents and eluents and their applications are as follows:

Florisil: elution with hexane [36,288,303,314,329, 330], hexane or light petroleum with small amounts of diethyl ether [7,300,331,332] or benzene [333] or stepwise elution to obtain fractions with various pesticides in addition to PCBs [279,323,334]. Florisil chromatography has been utilized for analyses of air [255], paper [335], sewage sludge [329], soils [288], sediments [7,279], various building materials [332], human and animal tissues [36,291,300,303, 304,333], plant tissues [314], milk [323,334] and blood [36,303].

Silica gel: elution with hexane [39,250,317,336, 337], benzene–hexane [338], stepwise elution using hexane and dichloromethane [269,339] or more complicated solvent systems [340]. Silica gel is sometimes impregnated with concentrated sulphuric acid [267,284] (and sodium hydroxide [341]) or oleum [45]. In these instances hexane [267,341] or small amounts of benzene in hexane [284] or cyclohexane [45] are applied. By means of silica gel extracts of water [267,269], sediments [267,284], pigments [45], wood [339], various oils [336], plant tissues [338], animal tissues [102,250,288,340,342], blood [39] and blood serum [317–319,337] have been cleaned up, in some instances after saponification [39,169,316].

Alumina: elution with light aliphatic hydrocarbons (light petroleum [255], pentane [288,322], hexane [33], isooctane [281]) or with a small amount of dichloromethane in hexane [321]. Extracts may be from air [255], sediments [281], animal tissues [33,288,308], milk [321,322] or blood [321], sometimes after saponification [33,288].

Activated carbon is special adsorbent for PCB clean-up because it is used in combination with other clean-up methods for the separation of coplanar PCBs and/or PCDDs and PCDFs. Elution is always stepwise and several eluents and their mixtures (hexane, dichloromethane, ethyl acetate, benzene, toluene) are applied successively [277,284,304, 311,342–346]. The possibility of separating PCBs according to planarity (and hence toxicity) is very useful and it can be expected that with increasing numbers of analyses for toxicity evaluation in the future, activated carbon might be widely applied. Figs. 2 and 3 show an example of the application of

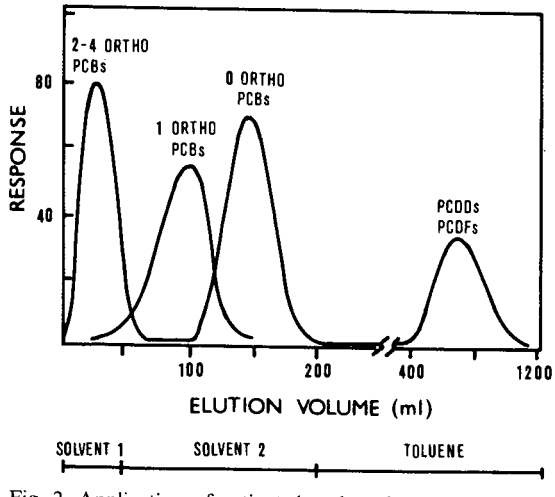

Fig. 2. Application of activated carbon for the separation of PCB congeners according to the number of *ortho*-chlorine atoms: elution profile of a PCB mixture. Sorbent, 750 g of a 1:12 mixture of activated carbon AX-21 (obtained from Anderson Development, Adrian, MI, USA) and LPS-2 silica gel (obtained from Whatman, Hillsboro, OR, USA), placed between two layers of silica gel; chromatographic column, 8 cm × 8 mm I.D.; solvent 1, dichloromethane–hexane (20:80); solvent 2, benzene–ethyl acetate (50:50). Reprinted from ref. 346.

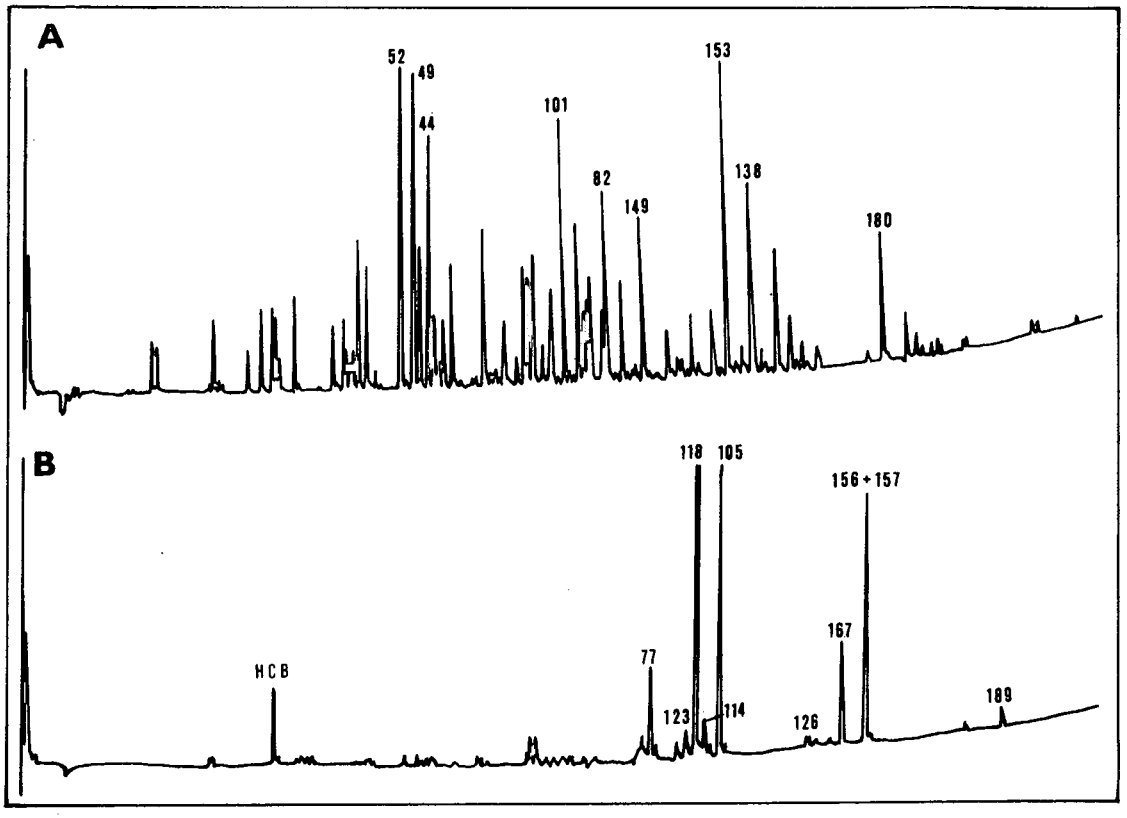

Fig. 3. Gas chromatograms of extracts from a Hudson River fish preseparated using activated carbon chromatography as shown in Fig. 2 into two fractions, the first fraction (A) containing di-to tetra-*ortho*-chlorine-substituted PCBs and the second fraction (B) containing mono- and non-*ortho*-chlorine substituted PCBs. Chromatographic conditions: 60-m glass capillary column coated with Apiezon L; temperature programme, 60°C for 2 min, increased at 10°C/min to 120°C, then at 1°C/min to 250°C; carrier gas, helium at 172 kPa (25 p.s.i.); make-up gas, argon–methane (5:95) at 40 ml/min; injector temperature, 250°C; electron-capture detector temperature 250°C. Reprinted from ref. 346.

active carbon to separate toxic congeners in fish samples [346].

Sometimes two sorbents are used for clean-up of one extract. Silica and alumina have been applied to clean up extracts from air [259], water [271], sediments [256,283], rice bran oil [155] and animal and human tissues [137,289]. Silica and Florisil have been employed to clean up extracts from sediments [249] and human and animal tissues [107,249,347]. For clean-up of extracts from fish, combinations of alumina and Florisil [100] and also alumina and silica gel have been used [267].

Another important clean-up technique is gel permeation chromatography (GPC), which is utilized for removing fat from extracts. The most widely applied gel is BioBeads S-X3 [298,301,302,344,348–350], but other gels, such as BioBeads S-X4 [297], S-X8 [297] and S-X12 [298], Sephadex LH-20 [351] and PLRP-S [326], have also been applied.

Eluents are mostly mixtures, *e.g.*, cyclohexane–ethyl acetate [298], cyclohexane–dichloromethane [302,306,348,349], toluene–ethyl acetate [301,309] and 2-propanol–heptane [326]. Because the fat removal is not so complete as when, for example, Florisil is used, it has been recommended [349] either to use GPC only when the PCB levels are high enough (more than 0.1 μg/kg) or to use GPC and then apply other clean-up technique, *e.g.*, Florisil [301,302] or silica gel [306,348] chromatography.

The point of clean-up by chemical methods is to eliminate possible interferences by means of chemical changes. Elimination of interfering substances,

particularly fat, with sulphuric acid is a commonly applied clean-up method. The sulphuric acid applied is either concentrated [95,102,258,259,267, 278,293,319,320,352–356] or fuming [169,311,357]. Sometimes the application of sulphuric acid is the only clean-up step [258,293,352–355,357,358] and sometimes it is used together with other clean-up steps [102,169,250,259,267,278,311,319,320,343, 356].

In some instances, particularly when determination is done by gas chromatography using packed columns, *p,p'*-DDE, which is often present particularly in extracts from biological samples, interferes with PCBs. This problem was solved by oxidizing the *p,p'*-DDE to 4,4'-dichlorobenzophenone using chromium trioxide or sodium dichromate [343]. The benzophenone was then removed using liquid–solid adsorption chromatography [290,343].

Saponification is also a chemical method of clean-up, but as in practice it precedes extraction, it has already been mentioned in that context.

Methods such as liquid–liquid partitioning (*e.g.*, between hexane and acetonitrile [292] or dimethylformamide and hexane [100]) and low-temperature precipitation [359], which are both utilized to remove mainly fatty substances, have relatively low efficiency and have to be used together with other clean-up methods.

When sediments or related matrices are analysed, it is often necessary to remove sulphur. In this instance either TBA–sulphite reagent (hexane-extracted tetrabutylammonium hydrogensulphate saturated with sodium sulphite) [283,352] or acid-activated fine copper [256,282,284,308,338] or mercury [28] can be applied.

It is very difficult to say in advance which particular clean-up method and technique would be the best or at least sufficient in a particular case.

Liquid–solid adsorption chromatographic (LSC) techniques are efficient and can be substantially modified. A serious problem may be reproducibility and hence standardization. The same sorbents made by different manufacturers or even from the same source but originating from different lots can show different properties. Hence the suitability of a particular adsorbent should be properly tested. Attention should be paid also to the capacity of the selected sorbent with regard to sample amount. It has been shown that the capacity of a 10 cm × 0.2 cm I.D. silica gel column to retain fat was 25 mg for elution with hexane, 20 mg for dichloromethane–hexane (5:95) and 2.5 mg for 2-propanol–hexane

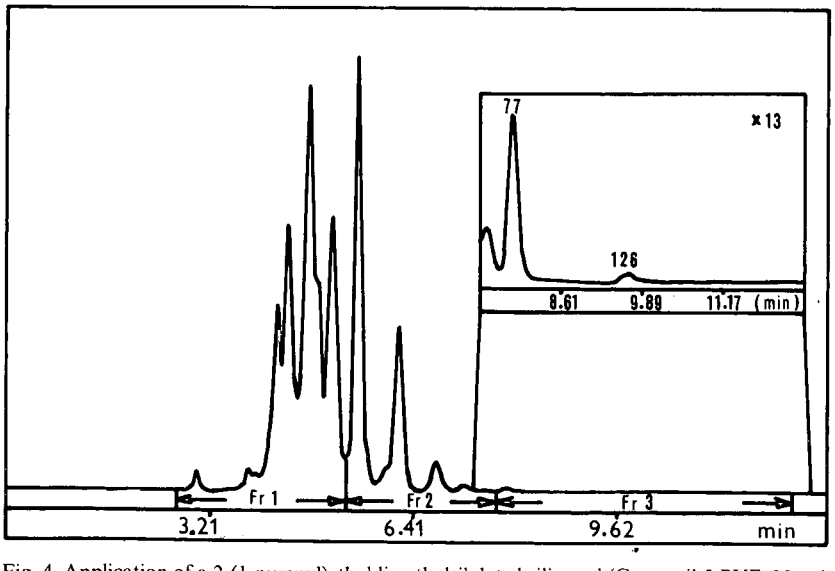

Fig. 4. Application of a 2-(1-pyrenyl)ethyldimethylsilylated silica gel (Cosmosil 5-PYE, Nacalai Tesque, Kyoto, Japan) column for the separation of PCB congeners according to number of *ortho*-chlorine atoms: HPLC of Clophen A 50. Column, 150 × 4.6 mm I.D., particle size 5μm; mobile phase, *n*-hexane; flow-rate, 0.7 ml/min; UV detection at 254 nm. Reprinted from ref. 361.

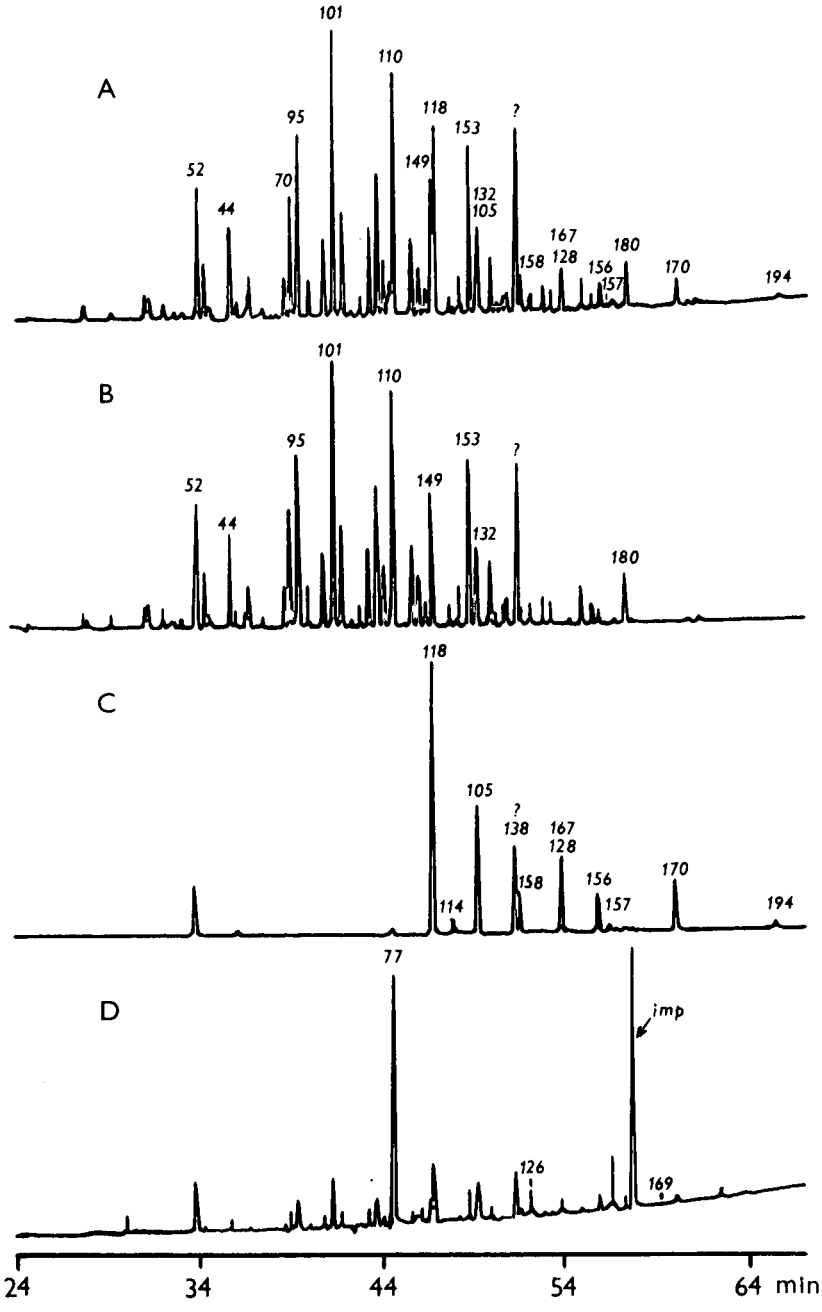

Fig. 5. Gas chromatograms of (A) Clophen A 50 and (B, C and D) the three fractions 1, 2 and 3 of Clophen A 50 obtained by HPLC as shown in Fig. 4. Chromatographic conditions: fused-silica capillary column, 50 m × 0.2 mm I.D.; stationary phase, 5% polymethylsiloxane (Ultra 2, Hewlett-Packard); film thickness, 0.33 μm; temperature programme, 70°C for 4 min, increased at 30°C/min to 180°C, held at 180°C for 2 min, then increased at 2°C/min to 300°C, and held at 300°C for 10 min; carrier gas, helium; flow-rate, 0.3 ml/min; splitless injection (90 s); electron-capture detector. The peak labelled "?" is suspected to contain two different PCB congeners; "imp" means impurity. Reprinted from ref. 361.

(0.5:99.5). Nevertheless, all the capacity cannot be fully exploited. It has also been shown that the more fat is loaded on a column, the lower are the retention volumes of eluted (separated) compounds [360].

Perhaps the most progressive modification of LSC is high-performance liquid chromatography (HPLC), *e.g.*, Nucleosil 100-5 (Machery–Nagel) stationary phase and pentane–dichloromethane as mobile phase [305], especially coupled on-line with gas chromatography [283]. However, another clean-up step is usually necessary, at least when the matrices contain fat or sulphur.

HPLC with a special stationary phase [2-(1-pyrenyl)ethyldimethylsilylated silica gel Cosmosil 5-PYE column, particle size 5 μm] and hexane as mobile phase has been shown very useful for the preseparation of PCBs according to planarity. The column separates PCBs in almost the same way as activated carbon, but this HPLC method seems to have several advantages. A high efficiency (*ca.* 45 000 theoretical plates/m) resulting in sharp peaks with good symmetry permits the accurate isolation of the mono-*ortho* "coplanar" congeners and the use of only one solvent (hexane) and small volumes of fractions, about 2–3 ml (with activated carbon stepwise elution is necessary and the volumes of fractions are commonly hundreds of ml) make reduction of the sample volume before gas chromatographic analysis very easy [361]. Fig. 4 shows the HPLC preseparation of Clophen A 50 into three fractions and Fig. 5 the gas chromatographic separation of Clophen A 50 (A) and its three fractions (B–D) [361].

GPC techniques are not as efficient as LSC and they are limited to the elimination of large molecules. However, it may be automated and made easy to operate and in comparison with LSC there is a significantly lower consumption of clean-up medium.

Sulphuric acid is an efficient clean-up agent. Problems may be caused by the fact that sulphuric acid may affect other compounds (halogenated pesticides) that are sometimes determined together with PCBs in one extract. There is also significantly slower reaction rate with decrease in the concentrations of the removed substances. Moreover, it is not desirable to handle concentrated or fuming sulphuric acid, the amounts of which can be relatively high.

Application of alkali digestion (saponification), which is limited to fat, facilitates another clean-up carried out mostly by LSC and may also increase the efficiency of extraction [312].

7.4. Determination and data evaluation

The dominant position is held by gas chromatography (GC) and other chromatographic techniques are rarely used. The development of biochemical and especially biological methods is in progress. There are also special methods that are used in particular cases, *e.g.*, determination of PCBs as total organic chlorine in transformer oils.

7.4.1. Gas chromatography. GC has several advantages over other techniques, *e.g.*, very sensitive detectors and the possibility of coupling the gas chromatograph with a device permitting identification (*e.g.*, a mass spectrometer), very efficient separation and good reproducibility. GC is therefore extremely useful for the determination of PCBs and related compounds.

Each GC process includes injection, separation and detection. Injection is not a special problem when packed columns are used. When capillary columns are used, it is mostly necessary (owing to the trace amounts present) to use either splitless injection or on-column injection. Splitless injection may cause significant discrimination [362] owing to the wide range of boiling points of PCB mixtures. The presence of dirt may substantially increase this discrimination. On-column injection yields better results [362], but it is much more sensitive to dirt than splitless injection. This can be improved by means of a retention gap. A retention gap also enables relatively large sample volumes to be injected.

The most frequently used detection system for PCBs is electron-capture detection (ECD). This is the most sensitive detection method available for GC in routine use and it is selective towards halogenated compounds. Its extreme sensitivity, on the other hand, makes ECD vulnerable to dirt and overloading. The ECD response is variable and it varies from one detector to another; in one detector it also varies with particular conditions such as detector temperature, quality of gas passing through the detector, flow-rate of the gas and cleanliness of the detector, etc. Despite the selectivity, many non-halogenated compounds may substantially interfere (*e.g.*, fatty substances, phthalate esters, elemental

sulphur). Hence careful clean-up is necessary. The linearity of an electron-capture detector working in the pulse modulated mode is approximately four orders of magnitude.

The response of a chlorinated compound depends significantly on both the number of chlorine atoms and their positions in the molecule and, consequently, there is a wide range of response factors

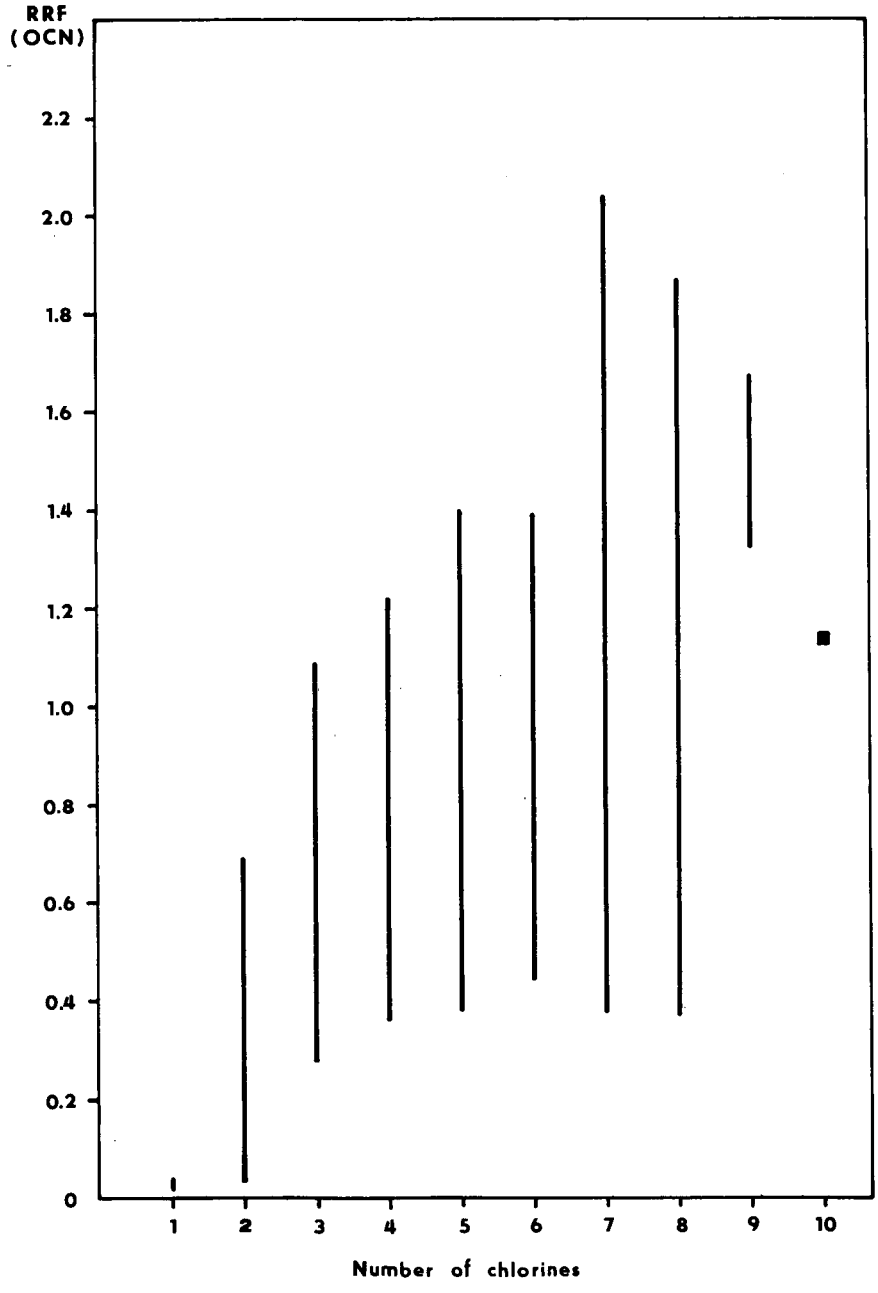

Fig. 6. Relative response factors of PCBs (relative to octachloronaphthalene) for an electron-capture detector. Vertical bars show the ranges of the RRFs within isomer groups. Horizontally can be seen differences between various isomer groups (homologues). According to ref. 363.

of PCB congeners. The relative response factors (RRFs) (relative to octachloronaphthalene) of all the PCB congeners were first reported by Mullin *et al.* [363]. Fig. 6 shows the ranges of RRFs within the isomer groups and differences between the isomer groups. The RRFs vary from one detector to another and are also dependent on the particular conditions, hence the tabulated values cannot be applied generally. These variations can be seen in RRFs published by different workers [363–365]. These significant differences in responses make determinations ambiguous unless all the congeners determined are separated and compared with the appropriate individual standards. Methods for simplifying the wide range of RRFs have been suggested, *e.g.*, grouping of congeners according to their RRFs into 31 groups. Each group is then represented by one surrogate standard [366].

The second most frequently used detection system is mass spectrometry (MS). The system provides another data dimension from which information on structure and/or molecular masses of analyte substances can be derived. It permits confirmation of identification and also the use of labelled compounds as recovery surrogates. The mass spectrometer is also very useful when the matrices contain large amounts of chlorinated organic compounds, as when determining by-product PCBs in certain commercial products (*e.g.*, in azo dyes [45], phthalocyanine pigments or chlorinated paraffins [46]) and in wastes. There are two modes in which the mass spectrometer is employed to detect PCBs: electron impact (EI) ionization and chemical ionization with negative-ion detection (NICI).

EI mass spectra are fairly reproducible, they show relatively intense molecular ions and the natural isotopic distribution of chlorine gives rise to typical clusters, which are easily recognizable (see Table 7) [367]. Nevertheless, except for the "*ortho*-effect", which allows one to distinguish several congeners having three *ortho*-chlorines and congener 52, it is impossible to distinguish between the spectra of isomers [368]. A major disadvantage of this mode is the relatively high minimum detectability, which is 2–3 orders of magnitude higher than that of ECD [369]. In order to improve the minimum detectability, limited mass scanning (LMS) over a certain mass range of interest or selected ion monitoring (SIM) are employed. On the other hand, these techniques increase the uncertainty of identification [368]. For quantification a suitable ion(s) in each isomer group is (are) chosen and the masses of these ions are monitored [326,370–372]. Ion(s) other than those used for quantification must be monitored in order to prevent misidentification and thus incorrect determination, *e.g.*, because of the tendency of PCBs to lose two chlorines [46,326,373]. Such an ion detection programme is shown in Table 8. The response factors in EI-MS differ between isomers by no more than about twofold [365], which is much less than in ECD. It is therefore possible to use one surrogate standard within each isomer group [371,374]. The surrogate standards should be those congeners whose response factors are nearest to the average response factors of corresponding isomer groups [46,371].

The response mechanism of NICI-MS is in some respects similar to that of ECD [364]. The major advantage of NICI in comparison with EI is the lower minimum detectability, particularly for highly chlorinated species [375]. Similarly to ECD, there are large differences in response factors between congeners [364]. The NICI mass spectra are considerably dependent on particular conditions such as pressure and composition of the reagent gas and source temperature [364,375]. The spectra also give less information on the structure of compounds [364]. Lightly chlorinated PCBs have a tendency to exhibit fragments (*e.g.*, chlorine atoms) and only the higher chlorinated PCBs exhibit pronounced molecular ions [364,368]. The high dependence on the conditions make it possible, however, that the optimum NICI-MS conditions have not yet been found. NICI is not currently routinely used in PCB analyses.

The impossibility of distinguishing between PCB congeners is a challenge. Distinguishing between five hexachlorobyphenyl isomers by ion–molecule reactions using ammonia in a triple-quadrupole instrument has recently been reported [376].

Other detector systems are not frequently employed for PCB analyses. The hall electrolytic conductivity detector working in the reductive mode is selective to halogens and has been employed to determine the chlorine content in peaks representing parts of Aroclor mixtures [377]. Although generally its response depends only on the chlorine content, a dependence on structure for some chlorinated com-

TABLE 7

MOLECULAR ION CLUSTER OF PCB HOMOLOGUES (ACCORDING TO REF. 367)

m/z	Relative abundance (%)	m/z	Relative abundance (%)	m/z	Relative abundance (%)
Monochlorobiphenyls		*Hexachlorobiphenyls*		*Nonachlorobiphenyls*	
188	100.00	358	51.12	460	25.89
189	13.53	359	6.83	461	3.48
190	33.86	360	100.00	462	75.55
191	4.34	361	13.32	463	10.01
Dichlorobiphenyls		362	80.95	464	100.00
222	100.00	363	10.35	465	13.27
223	13.28	364	35.61	466	72.07
224	64.84	365	4.65	467	9.69
225	8.59	366	8.71	468	35.93
226	10.54	367	1.21	469	4.95
227	1.95	368	1.17	470	11.59
Trichlorobiphenyls		369	0.15	471	1.42
256	100.00	*Heptachlorobiphenyls*		472	2.43
257	13.45	392	43.78	473	0.25
258	92.61	393	5.90	474	0.33
259	12.13	394	100.00	*Decachlorobiphenyl*	
260	29.81	395	13.02	494	25.59
261	3.43	396	96.09	495	3.34
262	3.16	397	13.08	496	78.55
263	0.26	398	53.02	497	9.84
Tetrachlorobiphenyls		399	6.51	498	100.00
290	77.14	400	16.51	499	14.28
291	10.44	401	2.12	500	92.42
292	100.00	402	3.18	501	11.64
293	13.67	403	0.45	502	51.69
294	48.84	404	0.30	503	6.86
295	6.82	*Octachlorobiphenyls*		504	20.28
296	10.84	426	34.36	505	2.71
297	1.50	427	4.56	506	5.42
298	0.96	428	88.10	507	0.75
Pentachlorobiphenyls		429	11.53	508	1.04
324	61.84	430	100.00	509	0.14
325	7.85	431	13.43		
326	100.00	432	65.33		
327	12.96	433	8.73		
328	66.33	434	26.11		
329	8.72	435	3.39		
330	21.94	436	6.99		
331	2.99	437	0.87		
332	3.86	438	1.16		
333	0.37	439	0.11		
334	0.24	440	0.11		

pounds has been mentioned [378]. The minimum detectability is too high and the detector is also difficult to operate. The Coulson conductivity detector is an older modification of the Hall electrolytic conductivity detector [379].

The recently developed helium discharge detector

TABLE 8

ION DETECTION PROGRAMME FOR EI-MS DESIGNED IN ORDER TO INCREASE THE LIMIT OF DETECTION AND TO DECREASE THE UNCERTAINTY

This programme is (with various slight modifications) currently used for EI-MS of PCBs. (According to ref. 373).

PCBs	Mass range scanned	Ion for identification	Ions for quantification
Monochloro-	186 – 190	188, 190	188, 190
Dichloro-	220 – 226	222, 224, 226	222, 224
Trichloro-	254 – 260	256, 258, 260	258
Tetrachloro-	288 – 294	290, 292, 294	292, 294
Pentachloro-	322 – 328	324, 326, 328	326, 328
Hexachloro-	356 – 364	358, 360, 362	360, 364
Heptachloro-	386 – 400	394, 396, 398	394, 398
Octachloro-	426 – 434	428, 430, 432	430, 432
Nonachloro-	460 – 468	462, 464, 466, 468	464, 468
Decachloro-	494 – 504	496, 498, 500, 502	498

has been employed to determine PCBs in model samples. The response of the detector applied to the element-selective detection of chlorine emission is based solely on the number of chlorine atoms present. Its minimum detectability (the reported limit of detection is 10–35 pg) may limit its application in some instances [380].

The flame ionization detector is not selective and has too high a minimum detectability to be used for trace environmental analyses of PCBs. It has been employed to characterize the composition of commercial PCB products [381].

Fourier transform infrared (FT-IR) spectrometry is a unique detection technique available for GC. It provides, like mass spectrometry, another data dimension but these data (infrared spectra) are, unlike mass spectrometric data, intrinsic to a particular compound. The results obtained so far indicate that each of PCB congeners has its own specific infrared spectrum [382]. It would therefore be possible to identify unambiguously any congener without a standard by comparison with a library of the spectra of the PCB congeners. The main drawback is very high minimum detectability of FT-IR detectors. When a cryogenic matrix isolation sample collector was utilized as an interface between a gas chromatograph and an IR spectrometer, the limit of detection for PCB congeners ranged from 1 to 10 ng [383]. This is why (apart from high price of the instrumentation) GC–FT-IR spectrometry, although from many points of view an extremely powerful tool, could be employed only in very limited cases.

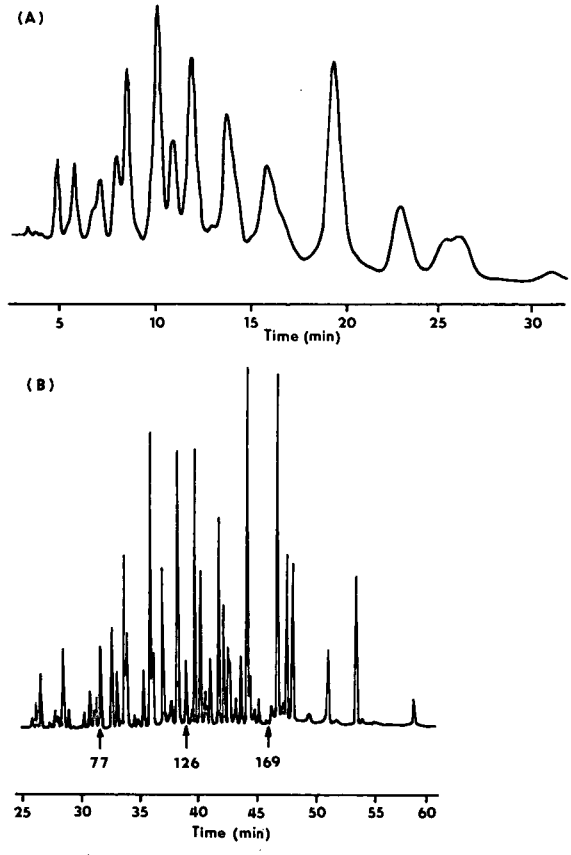

Fig. 7. Chromatograms of hazardous waste extract using (A) packed and (B) capillary columns. (A) Column, 6 ft. (183 cm) × 1/8 in. (3.2 mm) I.D. with 3% SP-2100 liquid stationary phase on 100–120-mesh Supelcoport; carrier gas, nitrogen; flow-rate, 30 ml/min; temperatures, injector 225°C, electron-capture detector 300°C, column 190°C. (B) Column, 30 m × 0.25 mm I.D. fused silica with DB-5 liquid stationary phase (J&W Scientific); carrier gas, helium; constant head pressure, 21 p.s.i. (145 kPa); 27 cm/s at 235°C; injector purge, 12 ml/min; make-up gas, nitrogen at 60 ml/min; temperatures, on-column injector at room temperature, electron-capture detector 280°C, column temperature programmed from 100 to 150°C at 10°C/min and from 150 to 235°C at 2°C/min. Reprinted from ref. 355.

For separation, either packed columns or, for high-resolution GC, capillary columns are employed. Stationary phases are commonly non-polar or slightly polar.

When packed columns are used, the chromato-

gram of a commercial product or of a mixture of PCBs in an environmental sample shows a few peaks (about 10–15, see Fig. 7A). Each of the peaks usually represents several congeners.

There are several methods of quantification using packed column gas chromatography:

"Method of selected peaks" ("method of peak comparison"): one, a few or all resolved peaks are selected to represent the total mixture. Commercial products (*e.g.*, Aroclors) are employed as standards. Areas (or heights) of the corresponding selected peaks in chromatograms of samples and standards are compared [7,292,309,329]. The results are reported as, *e.g.*, "Aroclor 1254" [292] or "total Aroclor" [329].

Webb–McCall method: in 1973, Webb and McCall [384] worked out a method of quantification using packed column GC. They chromatographed (under the same conditions) Aroclors using a Coulson conductivity detector, an electron-capture detector and a mass spectrometer. From the findings they determined the weight percent which each resolved peak of Aroclors 1221, 1232, 1242, 1248, 1254 and 1260 represents in the chromatogram and summarized the results in tables. Use of these tables and the standards enables response factors to be calculated for other electron-capture detectors and to be employed to quantify the samples. The method should give better results than the method of selected peaks but it is necessary to use the same chromatographic conditions and exactly the same standards, which the authors did. A similar paper was published in 1978 by Sawyer [377].

The congeneric compositions of PCBs in real samples are more or less different from those of commercial products employed as standards, which is why the results obtained using the above-mentioned methods should be considered only as estimates because the methods are based on conventions [288].

Perchlorination: another possibility is to convert all the PCB congeners in cleaned-up extracts to decachlorobiphenyl using a chlorination agent (*e.g.*, antimony pentachloride) and to determine the decachlorobiphenyl [385–387]. The method represents a real quantification from a chromatographic point of view because the determined compound and the standard are unambiguously defined chemical individuals. Another advantage is lower limit of detection in comparison with above-mentioned methods.

The method nevertheless has several considerable disadvantages: perchlorination causes loss of information about the congeneric composition of PCBs in the sample and the yield of the reaction may be significantly affected by small changes in the reaction conditions, especially temperature [387]. The major drawback is that several other groups of compounds may be converted into decachlorobiphenyl and cause gross errors [388]. The results obtained using perchlorination may be up to several ten times higher than those using the method of selected peaks. This is especially true for sewage sludges, paper and paper board. Although biological samples generally do not give such erroneous results, in some instances (*e.g.*, brains and livers of herons) the errors are extremely large. It has been shown that the most important interfering role is played by hydrogenated terphenyls (having one of three rings hydrogenated) which yield decachlorobiphenyl during perchlorination of PCBs. Biphenyl, hydrogenated biphenyls, polybrominated biphenyls and to a small extent polychlorinated naphthalenes may also be converted to some extent into decachlorobiphenyl and to contribute to erroneous results, but in much less extent than hydrogenated terphenyls [388].

Dechlorination: dechlorination involves the conversion of all PCB congeners to an unambiguously defined compound, biphenyl. The reducing agent may be, *e.g.*, hydrogen in the presence of palladium catalyst [389] or solution of lithium aluminium hydride ($LiAlH_4$) in diethyl ether [390]. Interfering compounds may be polybrominated biphenyls, hydroxylated PCBs and biphenyl, which in practice do not cause such large errors as hydrogenated terphenyls in the case of perchlorination [390]. Determination is carried out by GC with flame ionization detection [389]. Application of HPLC with UV detection has also been suggested for determining both decachlorobiphenyl and biphenyl [388,390,391] (see Section 7.4.2.).

When PCBs are chromatographed using a high-resolution capillary column, a mixture is separated into much more components than when using packed columns (see Fig. 7B). Nevertheless, a single capillary column is not able to separate all the 209 PCB congeners [392]. Consequently, another separation or a simplification has to be applied. The

TABLE 9

RELATIVE RETENTION TIMES (WITH RESPECT TO OCTACHLORONAPHTHALENE) FOR ALL PCB CONGENERS

Conditions: fused-silica capillary column (50 m × 0.2 mm I.D.), SE-54, programmed from 100 to 240°C at 1.0°C/min; carrier gas, hydrogen, constant pressure 221 kPa (2.25 kg/cm^2), linear velocity 45 cm/s at 100°C; injector temperature, 270°C; detector temperature, 330°C; splitting ratio, 1:10. Retention time of octachloronaphthalene was 124.9 min. (According to ref. 363).

PCB No.	Relative retention time	PCB No.	Relative retention time	PCB No.	Relative retention time	PCB No.	Relative retention time	PCB No.	Relative retention time	PCB No.	Relative retention time
1	0.1544	35	0.4738	70	0.5407	105	0.7049	140	0.6707	175	0.7611
2	0.1937	36	0.4375	71	0.4989	106	0.668	141	0.7203	176	0.7305
3	0.1975	37	0.4858	72	0.4984	107	0.6628	142	0.6848	177	0.8031
4	0.2245	38	0.4593	73	0.4554	108	0.6626	143	0.6789	178	0.7537
5	0.2785	39	0.4488	74	0.5341	109	0.6016	144	0.6563	179	0.7205
6	0.2709	40	0.5102	75	0.4643	110	0.6314	145	0.6149	180	0.8362
7	0.2566	41	0.499	76	0.5408	111	0.6183	146	0.6955	181	0.7968
8	0.2783	42	0.487	77	0.6295	112	0.5986	147	0.6608	182	0.7653
9	0.257	43	0.4587	78	0.6024	113	0.5862	148	0.6243	183	0.772
10	0.2243	44	0.4832	79	0.5894	114	0.6828	149	0.6672	184	0.7016
11	0.3238	45	0.4334	80	0.5464	115	0.6171	150	0.5969	185	0.7848
12	0.3298	46	0.445	81	0.6149	116	0.6132	151	0.6499	186	0.7416
13	0.3315	47	0.4639	82	0.6453	117	0.615	152	0.6062	187	0.7654
14	0.2973	48	0.4651	83	0.6029	118	0.6693	153	0.7036	188	0.692
15	0.3387	49	0.461	84	0.5744	119	0.5968	154	0.6349	189	0.9142
16	0.3625	50	0.4007	85	0.6224	120	0.6256	155	0.5666	190	0.874
17	0.3398	51	0.4242	86	0.6105	121	0.5518	156	0.8105	191	0.8447
18	0.3378	52	0.4557	87	0.6175	122	0.6871	157	0.8184	192	0.8269
19	0.3045	53	0.4187	88	0.5486	123	0.6658	158	0.7429	193	0.8397
20	0.417	54	0.38	89	0.5779	124	0.6584	159	0.7655	194	0.962
21	0.4135	55	0.5562	90	0.5814	125	0.6142	160	0.7396	195	0.9321
22	0.4267	56	0.5676	91	0.5549	126	0.7512	161	0.6968	196	0.8938
23	0.377	57	0.5155	92	0.5742	127	0.7078	162	0.7737	197	0.8293
24	0.3508	58	0.5267	93	0.5437	128	0.7761	163	0.7396	198	0.8845
25	0.3937	59	0.486	94	0.5331	129	0.7501	164	0.7399	199	0.8494
26	0.3911	60	0.5676	95	0.5464	130	0.7284	165	0.692	200	0.8197
27	0.3521	61	0.5331	96	0.5057	131	0.6853	166	0.7572	201	0.8875
28	0.4031	62	0.4685	97	0.61	132	0.7035	167	0.7814	202	0.8089
29	0.382	63	0.529	98	0.5415	133	0.6871	168	0.7068	203	0.8938
30	0.3165	64	0.4999	99	0.588	134	0.6796	169	0.8625	204	0.8217
31	0.4024	65	0.4671	100	0.5212	135	0.6563	170	0.874	205	0.9678
32	0.3636	66	0.5447	101	0.5816	136	0.6257	171	0.8089	206	1.0103
33	0.4163	67	0.5214	102	0.5431	137	0.7329	172	0.8278	207	0.9423
34	0.3782	68	0.504	103	0.5142	138	0.7403	173	0.8152	208	0.932
		69	0.451	104	0.4757	139	0.6707	174	0.7965	209	1.0496

rigorous determination of all congeners in a sample requires their complete separation and also the application of pure standards of all the congeners. The complete separation can be achieved using a multidimensional gas chromatograph with two capillary columns with different stationary phases. This system enables the parts of a sample which were not resolved in the first column to be transferred to the other column where their separation can be completed [18,47,392–394]. The system allows the complete and rigorous characterization of PCB mixtures.

Unfortunately, the rigorous determination of all components is extremely expensive and time consuming and, therefore, exceptional. A single capillary column is usually used, some congeners are left

TABLE 10

REPORTED CONCENTRATIONS OF "TOXIC" (T) AND "STANDARD" (S) PCB CONGENERS IN VARIOUS MATRICES AND COUNTRIES

PCB No.	Source[a]																							
	1	2	3	4	5	6	7	8	9	10	11	12	13	14	15	16	17	18	19	20	21	22	23	24
28 S	–	–	–	–	–	–	–	–	–	0.79	0.13	3.70	–	–	–	–	–	–	–	2.39	0.65	–	6.3	13.6
52 S	62	ND[b]	1.7	ND	0.44	0.75	84.3	1.6	79.1	0.60	0.17	4.80	15	2.4	62	–	–	–	–	1.60	1.05	–	3.2	20.7
77 T	–	–	–	–	–	–	–	–	–	–	–	9.10	–	–	–	18	22.5	<5	<0.5	–	0.0165	–	–	–
81 T	–	–	–	–	–	–	–	–	–	–	–	–	–	–	–	90	–	17	<0.5	–	–	–	–	–
101 S	49	14	0.97	2.3	0.84	0.39	76.4	0.9	50.0	0.46	0.16	5.03	19	3.8	270	–	–	–	–	1.16	–	–	0.3	3.6
105 T	–	–	–	–	–	–	–	–	–	–	–	–	12	0.8	–	181	486	427	5.8	–	1.55	–	162.3	65.7
114 T	–	–	–	–	–	–	–	–	–	–	–	14.10	–	–	–	–		57	1.0	–	–	–	–	–
118 T	11	10	0.3	ND	0.63	0.15	17.7	0.6	26.7	0.17	0.08	71.70	21	1.7	250	443	–	1350	11	–	3.05	40.61	30.9	5.4
123 T	–	–	–	–	–	–	–	–	–	–	–	–	–	–	–	–	–	109	1.4	–	–	–	–	–
126 T	–	–	–	–	–	–	–	–	–	–	–	–	–	–	–	19	6.96	<5	<0.5	–	0.072	–	–	–
138 S	8.1	3.6	0.14	0.67	0.25	0.23	31.0	2.0	94.5	0.55	0.26	146.00	15	1.2	260	–	–	826	6.2	2.72	14.75	107.31	5.4	3.6
153 S	–	–	–	–	–	–	33.7	1.5	70.8	0.34	0.15	129.70	23	2.2	430	723	–	–	–	2.47	19.9	150.36	36.0	33.6
156 T	–	–	–	–	–	–	–	–	–	–	–	18.20	2.3	0.2	34	78	–	79	1.7	–	1.95	–	12.4	4.3
157 T	–	–	–	–	–	–	–	–	–	–	–	4.08	–	–	–	–	–	76	<0.5	–	–	–	–	–
167 T	–	–	–	–	–	–	–	–	–	–	–	–	–	–	–	–	–	77	<0.5	–	–	–	–	–
169 T	–	–	–	–	–	–	–	–	–	–	–	–	–	–	–	ND	0.62	<5	<0.5	–	0.049	–	–	–
180 S	ND	ND	0.16	0.82	0.23	ND	4.5	0.5	21.7	0.30	0.13	67.20	13	0.8	200	–	–	–	–	1.74	15.6	77.13	0.7	4.5
189 T	–	–	–	–	–	–	–	–	–	–	–	–	–	–	–	–	–	29	<0.5	–	–	–	–	–

[a] Sources:

1 = Air vapour, Siskiwit Lake, Isle Royale, Lake Superior, MI, USA, summer concentrations, average of 13 samples (pg/m^3).
2 = Air vapour, Siskiwit Lake, Isle Royale, Lake Superior, MI, USA, winter concentrations, average of 7 samples (pg/m^3).
3 = Air particles, Siskiwit Lake, Isle Royale, Lake Superior, MI, USA, summer concentrations, average of 13 samples (pg/m^3).
4 = Air particles, Siskiwit Lake, Isle Royale, Lake Superior, MI, USA, winter concentrations, average of 7 samples, (pg/m^3).
5 = Rain, Siskiwit Lake, Isle Royale, Lake Superior, MI, USA, average of 12 samples (ng/l).
6 = Snow, Siskiwit Lake, Isle Royale, Lake Superior, MI, USA, one sample (ng/l).
7 = Air vapour, city of Kiel, Schleswig-Holstein, Germany, one sample (pg/m^3).
8 = Air particles, city of Kiel, Schleswig-Holstein, Germany, one sample (pg/m^3).
9 = Rain, city of Kiel, Schleswig-Holstein, Germany, one sample (pg/l).
10 = Water in the North Atlantic, depth 10 m, June 1987, one sample (pg/l).
11 = Water in the North Atlantic, depth 4000 m, June 1986, one sample (pg/l).
12 = Adipose tissue of birds (female razorbills), Isle of May, the Firth of Forth, Scotland, 6 samples obtained between 1978 and 1984 (mg/kg wet weight adipose tissue).
13 = Suspended sediments, Lake Ontario, average of 10 samples (μg/kg dry weight).
14 = Plankton, Lake Ontario, average of 3 samples (μg/kg wet weight).
15 = Fish, Lake Ontario, average of 60 samples (μg/kg wet weight).
16 = Fish (lake trout), Lake Ontario, composite sample of 3 fish (μg/kg whole fish).
17 = Fish (lake trout), Lake Ontario, composite sample of 50 fish (μg/kg fish lipid).
18 = Fish (whole carp), Saginaw Bay, Lake Huron, MI, USA (μg/kg).
19 = Sediment, Green Bay, Lake Michigan, USA (μg/kg).
20 = Cow milk, Bayern, Germany, average of 556 samples (μg/kg fat).
21 = Human milk, Stockholm, Sweden, average of two analyses of one sample (μg/kg fat).
22 = Human milk, city of Certaldo, Tuscany, Italy, average of 31 samples (μg/kg dry weight).
23 = Human adipose tissue, North America, one sample (μg/kg fat).
24 = Human liver, North America, one sample (the same man as in 23) (μg/kg fat).

References: 1–6 [256], 7–9 [263], 10,11 [270], 12 [405], 13–15 [28], 16 [235], 17 [406], 18,19 [345], 20 [407], 21 [408], 22 [409], 23,24 [299].

[b] ND = Not detected.

unresolved and only certain congeners are determined [48,319,324,356,362,395,396]. The columns commonly employed are 25–60 m long with I.D. 0.2–0.32 mm. The temperature is programmed, often with an extremely slow programming rate. Quantification is sometimes also done using secondary standards instead of individual congeners, which are PCB mixtures (often commercial) of known composition. Computer assistance is utilized [28,296] and retention data have to be employed. Very useful is a list of the retention data of all the 209 congeners relative to octachloronaphthalene, measured by Mullin *et al.* [363] using a column coated with SE-54 stationary phase (Table 9). There are also papers dealing with predictions of retention times from experimental data for several congeners and descriptors derived from molecular structures [44,397,398]. Metals (metal columns, metal GC–MS interface) may cause catalytic dechlorination and/or redistribution of the chlorine atoms [399,400] and, therefore, any contact of PCBs with metal should be avoided in the gas chromatograph.

Determination of only a few particularly selected congeners facilitates the use of individual congeners as standards and makes identification more certain and quantification more accurate. There is a problem as to which congeners should be selected for determination so that the analyses will provide the most useful information. There are two main approaches: either to determine the congeners that are usually present in relatively high concentrations and considering their amounts to be related to the total amount of PCBs present, or to determine the congeners most important from the toxicological point of view.

In the former instance, congeners 28, 52, 101, 138, 153 and 180 (and sometimes also 118) are most commonly determined. These "standard" congeners (PCB 118 belongs to the "toxic" congeners) cover a wide range of chlorine numbers and some of them are usually present in most samples. Determination of these congeners is now widely performed in many laboratories. Nevertheless, recent publications demonstrate that some other congeners (*e.g.*, 84, 90 and 163) may also interfere [394,401–404].

It is assumed that the principal toxic effects of PCBs are connected with interaction with Ah-receptors, it may be considered that it would be possible to determine only the congeners showing significant activity in this respect and to utilize the toxicity equivalent factors and in such a way obtain results showing the toxic potency of PCBs in a sample. This means determining the "toxic" congeners (see Section 6.3.).

The chief problems with their analyses arise from the usually very low levels of the toxic congeners in samples (reported samples and countries are shown in Table 10). It follows that very good separation is necessary (otherwise the small peaks belonging to the toxic congeners could easily be missed, see Fig. 7B), detection systems are limited to ECD and MS and effects such as adsorption become much more significant. The difficulty of such analyses can be documented, *e.g.*, by comparison of results obtained using ECD and MS detection. The median concentrations of PCBs 77, 126 and 169 was 50, 177 and 28 ng/kg, respectively, using ECD and 10, 55 and 7.7 ng/kg, respectively, using MS detection for the same samples (ten samples of horse fat) [350].

The above-mentioned carbon liquid chromatographic preseparation or similar preseparations are very useful in this instance and satisfactory separations can be achieved using multi-dimensional GC [18]. Methods for the determination of the three [311] or more [232,284,293,346] most toxic PCB congeners in environmental samples (sediments [284], fish [284,346], blubber of a marine mammal [311], eggs of snapping turtle [293], of fish and of birds [232]) have been developed and described and the problems of the analysis of the "coplanar" and mono- and di-*ortho* "coplanar" PCB congeners have recently been reviewed [410].

Special stationary phases can facilitate the determination of the "toxic" congeners. For example, *n*-octyl-(50%)–methylpolysiloxane stationary phase (SB Octyl 50; Lee Scientific) is normally used in supercritical fluid chromatography, in which the order of elution depends considerably on the degree of coplanarity of the congeners [411,412]. The application of liquid crystals as stationary phases is very interesting; the retention is highly dependent on the geometry of the molecules. Retention data for some PCB congeners on SB Octyl 50 [411] and the nematic liquid crystal N,N′-bis(*p*-methoxybenzylidene)-α,α′-bi-*p*-toluidine [413] are given in Table 11. The results show that the application of liquid crystalline stationary phases for the separation of "toxic" congeners (and not only those of PCBs) is

TABLE 11

RELATIVE RETENTION TIMES (RRT) (RELATIVE TO PCB 1) OF SELECTED PCB CONGENERS ON SPECIAL STATIONARY PHASES: SB OCTYL 50 AND BMBT LIQUID CRYSTAL

Conditions: (A) stationary phase SB-Octyl 50 (Lee Scientific), capillary column 50 m × 0.2 mm I.D., film thickness 0.25 μm, carrier gas helium, column head pressure 207 kPa (30 psi), temperature programme 100°C for 3 min, increased at 20°C/min to 160°C, then at 1.5°C/min to 268°C, 15 min isothermal, injector temperature 250°C, splitless injection (adapted from ref. 411); (B) stationary phase N,N′-bis(*p*-methoxybenzylidene)α,α′-bi-*p*-toluidine (BMBT), glass packed column 183 cm (6 ft.) × 2 mm I.D., 1.5% BMBT on 100–120-mesh Chromosorb W HP, carrier gas helium, flow-rate 30 ml/min, column temperature (isothermal) 150°C (according to ref. 413).

Congener No.	Conditions (A): RRT SB-Octyl-50	Conditions (B): corrected RRT BMBT	Congener No.	Conditions (A): RRT SB-Octyl-50	Conditions (B): corrected RRT BMBT
4	1.23	1.28	112	2.98	43.68
8	1.50	3.32	114	3.44	–
15	1.80	19.64	115	3.11	30.54
21	2.10	8.36	116	3.08	20.08
28	2.08	–	118	3.38	–
30	1.71	2.72	121	2.80	8.16
50	2.02	3.64	123	3.64	–
52	2.26	4.60	126	–	–
54	1.84	3.00	128	3.81	88.86
69	2.28	5.76	153	3.56	4.30
70	2.72	12.34	156	4.08	10.52
77	3.19	55.54	157	4.09	–
81	3.11	–	167	3.96	–
93	2.66	8.16	169	4.34	–
101	2.90	9.62	171	4.00	58.54
104	2.36	4.26	180	4.21	–
105	3.50	–	183	3.87	31.52
			209	–	126.84

very promising [414,415]. The purpose of the application of such phases is to introduce another type of separation mechanism and thus another type of elution order than with commonly used stationary phases, to improve the separation (also of multidimensional GC) and also to facilitate the identification of the "toxic" congeners by MS because they often elute between congeners having a different (smaller) number of chlorines. Chromatograms of a mixture of 51 PCB congeners on three stationary phases, low-polarity CP-Sil 8 (95% methyl–5% phenyl siloxane), moderately polar CP-Sil 19 (85% methyl–7% methyl–7% cyanopropyl–1% vinyl polysiloxane) and liquid crystalline polysiloxane SB-Smectic (Lee Scientific), are shown in Figs. 8–10. The liquid crystalline stationary phases, however, suffer from thermal and chemical instability, *e.g.*, with SB-Smectic some compounds such as octachloronaphthalene are affected, hydrogen cannot be used as the carrier gas because of its adverse effect on the phase and at higher temperatures regular significant bleeding occurs [414].

7.4.2. Other methods. In addition to the widely used GC, other methods can be employed to determine PCBs. Among these, methods utilizing biochemical and biological processes seem to be the most progressive.

HPLC. HPLC with UV detection has been used to detemine PCBs, especially in order to characterize commercial mixtures [416–418] and to determine decachlorobiphenyl (after perchlorination of PCBs) [391] or biphenyl (after dechlorination of PCBs) [390].

The retention times of PCBs decrease with increasing number of chlorine atoms in the molecules (generally opposite to the GC retention order) when a column packed with 5-μm LiChrosorb Si 60 silica gel (Merck) as stationary phase and *n*-hexane as mobile phase is used [416,417]. The "normal" elution order gives a reversed-phase system with microparticulate silica (μBondapak C_{18}; Waters Assoc.) as stationary phase and water–acetonitrile as mobile phase [418]. The system silica gel–*n*-hexane has also been employed for the determination of both decachlorobiphenyl and biphenyl [390,391]. Decachlorobiphenyl showed maximum absorbance

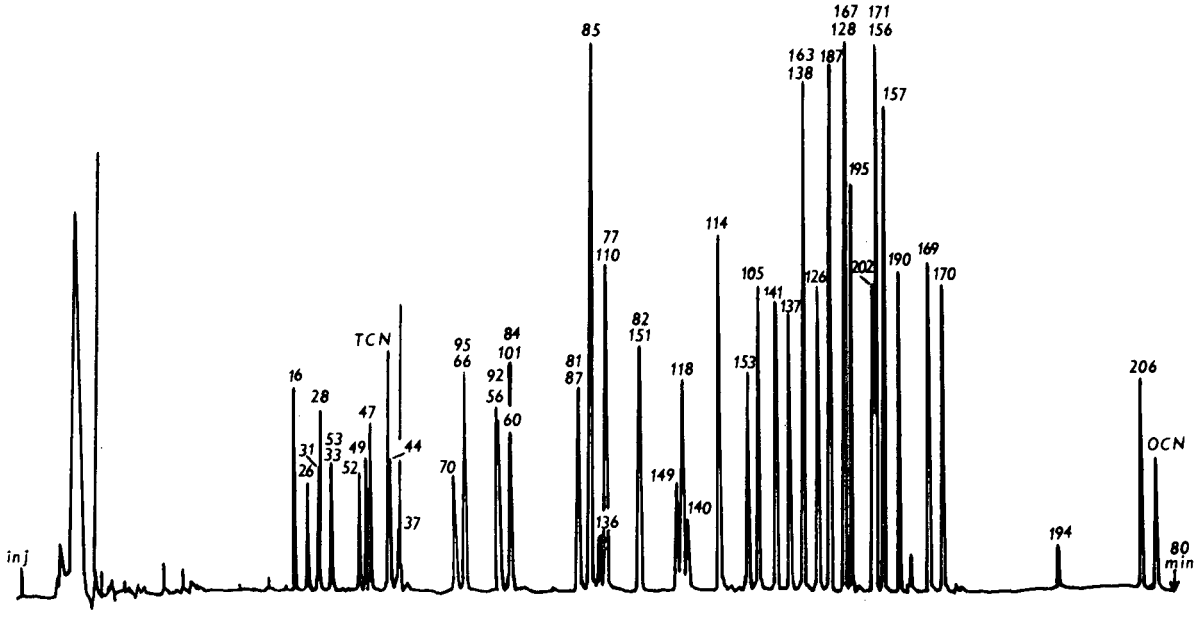

Fig. 8. Gas chromatogram of a mixture of 51 PCB congeners. Chromatographic conditions: splitless injection (2 min); injector temperature, 270°C; electron-capture detector temperature, 360°C; purge gas, nitrogen at 60 ml/min. Columns: WCOT CP-Sil 8 CB fused-silica, 95% methyl–5% phenyl polysiloxane (Chrompack, Middelburg, Netherlands), 50 m × 0.15 mm I.D.; film thickness, 0.30 μm; carrier gas, hydrogen at 310 kPa (0.31 ml/min, 27 cm/s); temperature programme, 90°C for 3 min, increased at 30°C/min to 215°C, held at 215°C for 40 min then increased at 5°C/min to 270°C and held at 270°C for 22 min. Reprinted from ref. 414.

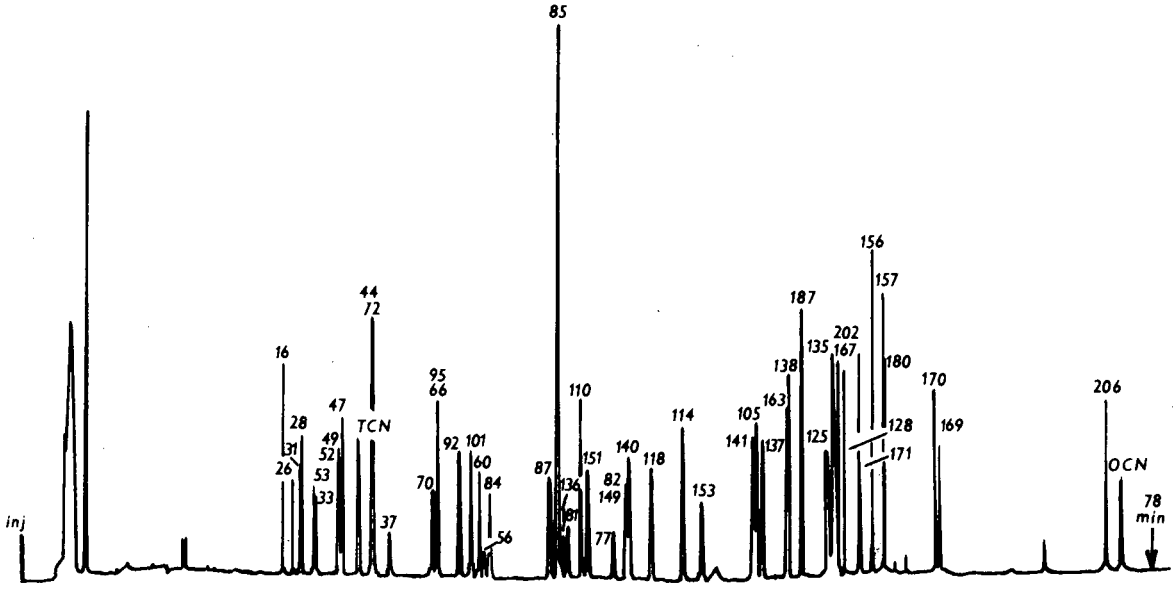

Fig. 9. As Fig. 8 except for column: WCOT CP-Sil 19 CB fused-silica, 85% methyl–7% phenyl–7% cyanopropyl–1% vinyl polysiloxane (Chrompack, Middelburg, Netherlands), 60 m × 0.15 mm I.D.; film thickness, 0.20 μm; carrier gas, hydrogen at 345 kPa (0.32 ml/min, 30 cm/s); temperature programme, 90°C for 3 min, increased at 30°C/min to 215°C, held at 215°C for 40 min, then increased at 5°C/min to 270°C and held at 270°C for 20 min. Reprinted from ref. 414.

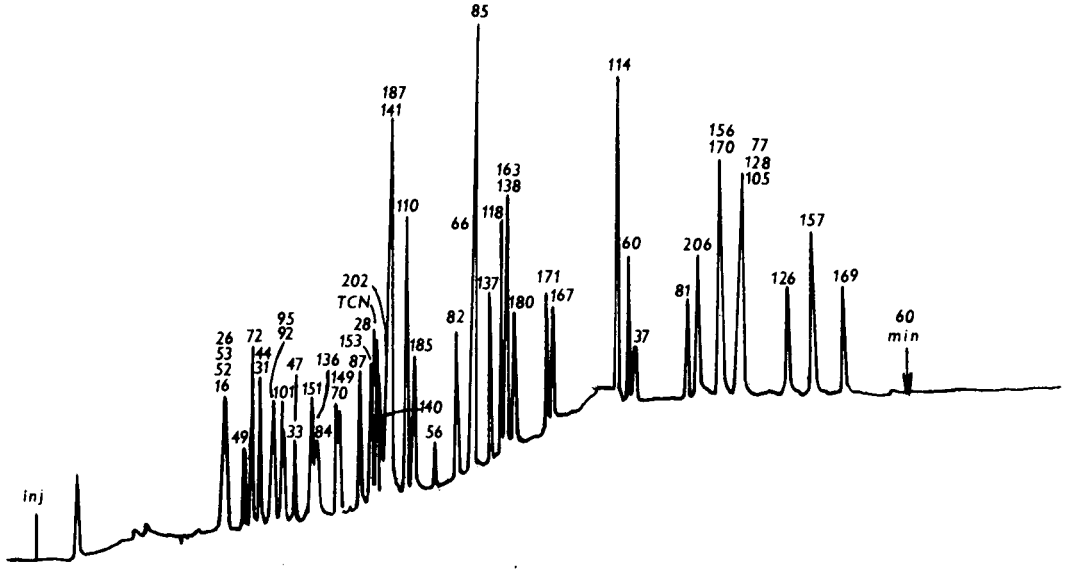

Fig. 10. As Fig. 8 except for column: SB-Smectic fused-silica liquid crystalline polysiloxane (Lee Scientific, Salt Lake City, UT, USA), 50 m × 0.20 mm I.D.; film thickness, 0.15 μm; carrier gas, nitrogen at 290 kPa (0.33 ml/min, 28 cm/s); temperature programme, 90°C for 3 min, increased at 30°C/min to 170°C, held at 170°C for 1 min, then increased at 1.5°C/min to 215°C and held at 215°C for 17 min. Reprinted from ref. 414.

at 215 nm [391] and biphenyl showed two maxima at 205 and 248 nm [390].

The decisive drawback of HPLC systems is the high limit of detection. The reported limit of detection for biphenyl is *ca.* 0.5 ng [390] and is correspondingly higher for a mixture of many congeners. For example, in a study of the characterization of commercial PCB mixtures, it has been reported that the amounts of Aroclors for each analysis could be reduced to 3 μg without markedly reducing the accuracy of the analysis [418]. Also, the resolution is lower than in high-resolution GC. HPLC may be very useful for the clean-up or preseparation of extracts before GC analysis.

Radioimmunoassay (RIA). The basis of RIA is the competition between an analyte compounds (which acts as a ligand) and a radioligand for binding sites in antiserum, which is a substance particularly prepared for the purpose employing the responses of immunity systems of animals, mostly rabbits. Sample preparation is the same as or similar to that in GC, *i.e.*, extraction and clean-up. The solvent is then evaporated to dryness and the residue is dissolved in dimethyl sulphoxide. Known amounts of antiserum and radioligand are added. After incubation, the bound and unbound ligands are separated. The amount of unbound radioligands is determined by measuring radioactivity and the amount of the ligands (*i.e.*, PCBs) in the sample is calculated. The results, expressed as "total" PCBs, are comparable to those obtained by using packed column GC. The binding affinity of PCBs to antiserum is fairly selective, but not specific, and this makes congener-specific analyses using RIA impracticable (the binding affinity is not related to toxicity). However, RIA is a relatively rapid method applicable to wide range of samples [321,419].

H-4-II E rat hepatoma cell bioassay. As discussed in Section 6.3, some PCB congeners, and also some other compounds, can significantly induce particular enzymatic systems (AHH, EROD) in animal cells. The induction potency of a congener *in vitro* generally correlates with the potency to cause toxic effects in living organisms. It is therefore possible to utilize cultured cells for the assessment of the overall Ah-receptor-related toxic potency of compounds in extracts from environmental samples. AHH and EROD induction in cultured H-4-II E rat hepatoma cells is very suitable for such an assay [236,420,421].

The sample extract dissolved in an appropriate solvent (dimethyl sulphoxide, isooctane) is added to the cells cultured in a Petri dish. After incubation (usually for 72 h [210,421,422]) the cells are harvested and the rate of conversion of benzo[*a*]pyrene to 3-hydroxybenzo[*a*]pyrene (AHH activity) [423] and/or the rate of conversion of ethoxyresorufin to resorufin (EROD activity) [424] is assessed using spectrofluorimetry. The rate of these conversions is a measure of the enzymatic complexes and hence a measure of inducing potency of the sample tested. The data obtained are compared with those obtained using a set of 2,3,7,8-TCDD standards of appropriate concentrations. The results are expressed as 2,3,7,8-TCDD toxicity equivalents. The limit of detection is 10 pg of 2,3,7,8-TCDD equivalent per plate [421]. The results include influences of all the AHH- and/or EROD-inducing compounds present, and also synergistic, antagonistic and additive effects between them. The assay does not, of course, provide information about which compounds are responsible for the induction. The assay has been successfully utilized to analyse extracts from environmental samples [421,422,425]. Although this method has not so far been used routinely, it seems that it has the potential to become (particularly together with high-resolution GC) a widely used tool in environmental studies and monitoring.

Competitive binding assay for ligands of the Ah-receptor. This method allows the calculation of the binding affinity of components in a sample to the Ah-receptor. The assay is based on competition between radioligand (2-[^{125}I]iodo-7,8-dibromodibenzo-*p*-dioxin) and components in the sample extract for binding to Ah-receptor prepared from livers of mice. The minimum detectable concentration is 0.8 pg of 2,3,7,8-TCDD in 0.25 ml [426,427]. This bioassay, which was described in 1988 and has certain features in common with H-4-II E rat hepatoma cell bioassay, is still awaiting application in environmental analyses.

In addition to the above-mentioned methods, there are several others that can be utilized in particular cases, *e.g.*, determination of chlorine in transformer oils using neutron activation and γ-ray spectrometry [428]. Conversion of chlorines in PCBs into chloride ions by metallic sodium [429,430] and their determination either using spec-

trophotometry [429] or by means of a chloride ion-selective electrode [430] have been also described. This method is limited to relatively high concentrations of PCBs and does not provide any qualitative information on the PCBs present. Its advantage is simplicity.

7.5. Interlaboratory tests

The results of interlaboratory tests provide information on the comparability of the results produced by different laboratories. The objective of such tests is especially to evaluate a proposed analytical method. The results are usually compared using relative standard deviations (R.S.D.). It is difficult to evaluate the accuracy in addition to the precision, because the determination methods are sometimes (and with packed columns always) conventional and the PCBs added may behave differently to PCBs naturally integrated into matrices. Moreover, these studies cannot give any information on problems of sampling, which may substantially affect the results of analyses. The tests indicate the present state of the routine analytical chemistry of the compounds in question.

On the basis of more than 150 interlaboratory studies, an equation has been proposed that relates R.S.D. and concentration:

$$\text{R.S.D.} = 2^{(1-0.5\log c)}$$

where c is the concentration expressed as the weight of the analyte in a sample divided by the weight of the sample [431]. It can be seen that according to this equation, for a concentration of, *e.g.*, 1 ppm the R.S.D. should be 16% and for 1 ppb the R.S.D. should be 45.3%. On the basis of theoretical considerations, another equation providing very similar results has been proposed [432]:

$$\text{R.S.D.} = c^{-0.15}/50$$

It is possible to consider that the lower the concentrations are, the more phenomena are capable of affecting the results (*e.g.*, adsorption, electronic noise, interferences) and the greater is the effort required to overcome these problems. These aspects

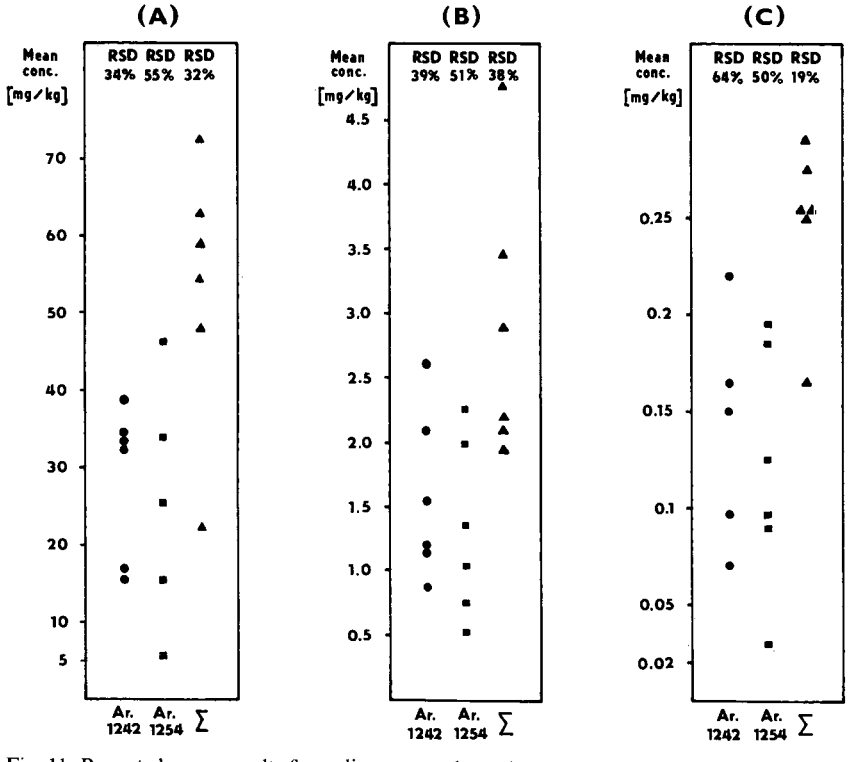

Fig. 11. Reported mean results for sediment sample analyses in an interlaboratory study [7]. For details, see text.

are very difficult to assess and hence the results obtained using the above equations should be treated with caution. The values can, however, indicate what results can be achieved in interlaboratory studies.

To illustrate the situation in the analysis of PCBs, some results from several recent interlaboratory tests using GC are presented below.

(1) Analyses of three series of contaminated marine sediment samples. Dried samples were Soxhlet extracted for 16 h with hexane–acetone (1:1), the extracts were concentrated in a Kuderna–Danish apparatus and then cleaned up by Florisil column chromatography and eluted with diethyl ether–hexane (6:94). Sulphur was removed with a tetrabutylammonium reagent. GC determinations were performed using a packed column containing methylsilicone stationary phase (SE-30, OV-1) with EC. The quantifications were made using the Webb–McCall procedure [384] and Aroclors 1242 and 1254 as standards. The real PCB concentrations were not known. From the measured data it can be seen that the concentrations in the three series of samples differed by about one and two orders of magnitude, respectively [7]. The mean measured PCB concentrations obtained by six participating laboratories are shown in Fig. 11. Interestingly, there was no apparent relation between concentration and RSD.

(2) Analyses of two series of water samples spiked with a mixture of Aroclors 1221, 1242, 1254, 1260 and 1268 so that the concentrations were 37 and 148 μg/l. The samples were extracted with dichloromethane in a separating funnel. GC determinations were performed using a 30 m × 0.25 or 0.32 mm I.D. fused-silica capillary column coated with dimethyldiphenylsiloxane (SE-54 or DB-5) with EI-MS detection. The response factors for each isomer group (except nonachlorobiphenyls) were determined using congeners 1, 5, 29, 50, 87, 154, 187, 200 and 209 and chrysene was used as an internal standard. Raw data were processed using special software. The results as mean percentage recovery reported by five participating laboratories are shown in Fig. 12 [371].

(3) Analysis of herring oil spiked with individual congeners 52 (82 μg/kg), 86 (77 μg/kg), 101 (63 μg/kg) and 153 (85 μg/kg). Clean-up was effected using chromatography on Florisil. Each of thirty participating laboratories used its own GC conditions. The results, expressed as percentage recoveries, were in the ranges 30–127%, 28–178%, 44–283% and 41–294% for PCBs 52, 86, 101 and 153, respectively. In addition to the common clean-up method, each laboratory also used its own method. The results did not show that the common clean-up gave more precise results than the laboratories' own methods [433].

The results from these three interlaboratory studies show that when current techniques and methods are employed, the differences between results obtained by various laboratories may be nearly one order of magnitude and R.S.D.s are higher than would be expected. If it is taken into consideration that the precision of routine analyses may be significantly worse than that of interlaboratory studies, it seems necessary to be cautious when comparing data on PCB pollution in various locations at various times and in various matrices. The only confirmed way to achieve R.S.D.s comparable to expected values is to introduce a learning programme covering

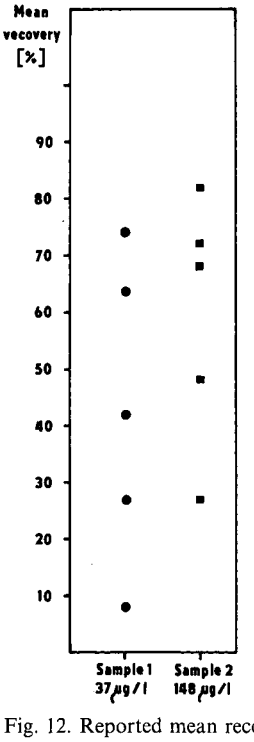

Fig. 12. Reported mean recoveries for two fortified water samples in an interlaboratory study [371]. For details, see text.

thoroughly all steps of the analytical procedure for all participants before a multi-laboratory test is carried out [434].

8. CONCLUSIONS

PCBs are amongst the most prominent environmental contaminants spread all over the world (Northern Europe [435,436], Southern Europe [437–440], Western Europe [274,441–443], Central Europe [444–446], Russia including Siberia [446], Vietnam [446], Hong Kong [447,448], Japan [449], Israel [450], Indonesia [273], North America [451–457] including Arctic regions [296], South America [458,459], Antarctica [271], oceans [270,460,461], etc.). The impact of their low-level presence in the environment, foodstuffs, humans, etc., is very difficult to assess. As discussed in Section 6, many studies show significant adverse effects of PCBs and PCBs-like compounds on living organisms; these effects, however, should be assessed realistically with respect to other environmental risks [462–464]. Interestingly, it has been shown that taking into consideration the environmental concentrations and toxicity equivalent factors, the overall toxicity of PCBs might be, owing to the "toxic" congeners, significantly greater than that of PCDDs and PCDFs together in environmental samples [235,345,465]. Moreover, it seems that an end to PCB environmental pollution cannot be expected in the near future. Therefore, the analytical chemistry of PCBs will be expected to provide not only other data, but also more valuable information.

The choice of analytical methods depends on the particular conditions and the purpose of the analysis. Conventional methods using packed column GC may be suitable for rapid screening and also for searching for sources of contamination. These methods are also used for regulatory purposes (*e.g.*, in the USA).

The perchlorination method is also relatively simple. Because the compound determined is an individual, the possibility of interference in minimized and confirmation is facilitated. There is, nevertheless, the above-mentioned possibility of gross errors [388]. The method is also included in US EPA methods.

Nevertheless, it seems obvious that in order to obtain real (not conventional) values of PCB concentrations, which could be readily comparable between laboratories, it is necessary to employ congener-specific analyses using individual standards.

Determination of the several (six or seven) "standard" congeners occurring in relatively high concentrations is now used for regulatory purposes in Western Europe (Germany, Netherlands).

Determination of the "toxic" congeners is the most progressive approach. The methods are, nevertheless, far from routine at present and represent a field for future research and development.

To assess a sample from the hygienic point of view, the best way would be, in general, to perform a simple biological test and in such a way to establish whether or not the sample may be dangerous. When this test gives positive results, then chemical analysis using high-resolution GC should be carried out to find the toxic compounds responsible. Such a biological test for PCBs and related compounds may be the H-4-II E rat hepatoma cell bioassay. However, it seems necessary to continue to work on the method in order to establish it firmly.

In general, for the future, there is a need to improve the methods for congener-specific analyses and short-term toxicity testing. These analytical approaches together with more extensive clinical and experimental data on the toxicity of PCBs will permit a real assessment of the risk that PCBs represent both in particular samples and in the global environment.

9. ACKNOWLEDGEMENTS

The author thanks Dr. M. Dressler and Dr. J. Drozd for enabling him to work on this topic, Dr. M. Dressler for helpful discussions and Mrs. Z. Bednářová for careful typing of the manuscript.

REFERENCES

1 M. D. Erickson, *Analytical Chemistry of PCBs*, Butterworth, Stoneham, MA, 1986.
2 S. H. Safe (Editor), *Polychlorinated Biphenyls (PCBs): Mammalian and Environmental Toxicology*, Springer, Berlin, 1987.
3 R. D. Kimbrough and A. A. Jensen (Editors), *Halogenated Biphenyls, Terphenyls, Naphthalenes, Dibenzodioxins and Related Products*, Elsevier, Amsterdam, 2nd ed., 1989.
4 K. Ballschmiter and M. Zell, *Fresenius' Z. Anal. Chem.*, 302 (1980) 20.

5 H. Schmidt and G. Schulz, *Justus Liebigs Ann. Chem.*, 207 (1881) 320.
6 M. D. Erickson, *Analytical Chemistry of PCBs*, Butterworth, Stoneham, MA, 1986, Ch. 2, p. 5.
7 A. L. Alford-Stevens, W. L. Budde and T. A. Bellar, *Anal. Chem.*, 57 (1985) 2452.
8 U. A. Th. Brinkman and A. de Kok, in R. D. Kimbrough (Editor), *Halogenated Biphenyls, Terphenyls, Naphthalenes, Dibenzodioxins and Related Products*, Elsevier, Amsterdam, 1980, Ch. 1, p. 1.
9 J. Lišhák (Chemko Strážske), personal communication.
10 J. W. Moore and S. Ramamorthy, *Organic Chemicals in Natural Waters*, Springer, New York, 1984, Ch. 9, p. 168.
11 S. Tanabe, *Environ. Pollut.*, 50 (1988) 5.
12 C. Mikeš, *Thesis*, University of Agriculture in Prague, Institute of Applied Ecology and Ecotechnology, Kostelec nad Černými lesy, 1988.
13 P. Lišhák, *Thesis*, Slovak Institute of Technology, Bratislava, 1981.
14 P. W. Albro and C. E. Parker, *J. Chromatogr.*, 169 (1979) 161.
15 P. W. Albro, J. T. Corbett and J. L. Schroeder, *J. Chromatogr.*, 205 (1981) 103.
16 J. C. Duinker and M. T. J. Hillebrand, *Environ. Sci. Technol.*, 17 (1983) 449.
17 S. H. Safe, L. Safe and M. Mullin, *J. Agric. Food Chem.*, 33 (1985) 24.
18 J. C. Duinker, D. E. Schulz and G. Petrick, *Anal. Chem.*, 60 (1988) 478.
19 M. R. Driss, S. Sabbah and M. L. Bouguerra, *Analusis*, 17 (1989) 252.
20 J. Brodsky and K. Ballschmiter, *Fresenius' Z. Anal. Chem.*, 331 (1988) 295.
21 R. Abramowitz and S. H. Yalkowsky, *Chemosphere*, 21 (1990) 1221.
22 J. M. Lin and S. S. Que Hee, *Am. Ind. Hyg. Assoc. J.*, 48 (1987) 599.
23 F. M. Dunnivant, J. T. Coates and A. W. Elzerman, *Environ. Sci. Technol.*, 22 (1988) 448.
24 J. F. Rusling and L. M. Chang, *Environ. Sci. Technol.*, 23 (1989) 476.
25 J. R. Parson and D. T. H. M. Sijm, *Chemosphere*, 17 (1988) 1755.
26 S. Dmochewitz and K. Ballschmiter, *Chemosphere*, 17 (1988) 111.
27 H. E. Evans, *Chemosphere*, 17 (1988) 2325.
28 B. G. Oliver and A. J. Niimi, *Environ. Sci. Technol.*, 22 (1988) 388.
29 E. K. Duursma, J. Nieuwenhuize and J. M. van Liere, *Sci. Total Environ.*, 79 (1989) 141.
30 L. G. Hansen and M. E. Welborn, *J. Pharm. Sci.*, 66 (1977) 497.
31 L. G. Hansen, *Ann. N. Y. Acad. Sci.*, 320 (1979) 238.
32 T. Mitzutani, K. Hidaka, T. Ohe, M. Matsumoto, K. Yamamoto and K. Tajima, *Bull. Environ. Contam. Toxicol.*, 25 (1980) 181.
33 A. C. de Kock and D. A. Lord, *Chemosphere*, 17 (1988) 2381.
34 J. T. Borlakoglu, V. A. Welch, C. H. Walker and R. R. Dils, *Mar. Environ. Res.*, 28 (1989) 235.
35 J. T. Borlakoglu and C. H. Walker, *Eur. J. Drug Metab. Pharmacokinet.*, 14 (1989) 127.
36 J. Mes, D. L. Arnold, F. Bryce, D. J. Davies and K. Karpinski, *Arch. Environ. Contam. Toxicol.*, 18 (1989) 858.
37 K. Kypke-Hutter and R. Malisch, *Z. Lebensm.-Unters.-Forsch.*, 188 (1989) 127.
38 S. P. Ferraro, H. Lee, II, L. M. Smith, R. J. Ozretich and D. T. Specht, *Bull. Environ. Contam. Toxicol.*, 46 (1991) 276.
39 P. H. Chen, J. M. Gaw, C. K. Wong and C. J. Chen, *Bull. Environ. Contam. Toxicol.*, 25 (1980) 325.
40 P. H. Chen, M. L. Luo, C. K. Wong and C. J. Chen, *Food Chem. Toxicol.*, 20 (1982) 417.
41 M. S. Wolff, J. Thornton, A. Fischbein, R. Lilis and I. J. Selikoff, *Toxicol. Appl. Pharmacol.*, 62 (1982) 294.
42 D. L. Stalling, T. R. Schwartz, W. J. Dunn, III, and S. Wold, *Anal. Chem.*, 59 (1987) 1853.
43 T. R. Schwartz, D. L. Stalling and C. L. Rice, *Environ. Sci. Technol.*, 21 (1987) 72.
44 A. Robbat, Jr., G. Xyrafas and D. Marshall, *Anal. Chem.*, 60 (1988) 982.
45 N. Sistovaris, U. Donges and B. Dudek, *J. High. Resolut. Chromatogr.*, 13 (1990) 547.
46 M. D. Erickson, J. S. Stanley, J. K. Turman, J. E. Going, D. P. Redford and D. T. Heggem, *Environ. Sci. Technol.*, 22 (1988) 71.
47 D. E. Schulz, G. Petrick and J. C. Duinker, *Environ. Sci. Technol.*, 23 (1989) 852.
48 S. Focardi, C. Leonzio and C. Fossi, *Environ. Pollut.*, 52 (1988) 243.
49 S. H. Safe, *CRC Crit. Rev. Toxicol.*, 21 (1990) 51.
50 J. R. Donnelli, A. H. Grange, N. J. Nunn, G. W. Sovocool and J. J. Breen, *Chemosphere*, 20 (1990) 1423.
51 A. Kanetoshi, H. Ogawa, E. Katsura and H. Kaneshima, *J. Chromatogr.*, 389 (1987) 139.
52 L. C. Dickson and F. W. Karasek, *J. Chromatogr.*, 389 (1987) 127.
53 H. Hagenmaier, M. Kraft, H. Brunner and R. Haag, *Environ. Sci. Technol.*, 21 (1987) 1080.
54 M. Berlincioni and A. di Domenico, *Environ. Sci. Technol.*, 21 (1987) 1063.
55 L. Stieglitz and H. Vogg, *Chemosphere*, 16 (1987) 1917.
56 H. C. Thompson, Jr., D. C. Kendall, W. A. Korfmacher, J. R. Kominsky, L. G. Rushing, K. L. Rowland, L. M. Smith and D. L. Stalling, in C. Rappe, G. Choudhary and L. H. Keith (Editors), *Chlorinated Dioxins and Dibenzofurans in Perspective*, Lewis, Chelsea, MI, 1986, Ch. 9, p. 121.
57 R. S. Narang, K. Swami, T. A. Amin, G. Eadon, C. Vernoy, R. Briggs and A. S. Narang, *Chemosphere*, 17 (1988) 2151.
58 A. Kanetoshi, H. Ogawa, E. Katsura and H. Kaneshima, *J. Chromatogr.*, 442 (1988) 289.
59 L. Stieglitz and H. Vogg, *Umweltanal. Umweltschutz, Suppl.*, 2/88 (1988) 4.
60 L. Stieglitz and H. Vogg, *Formation and Decomposition of Polychlorodibenzodioxins and -furans in Municipal Waste Incineration*, Kernforschungszentrum Karlsruhe, Karlsruhe, 1988.
61 T. D. Goldfarb, *Chemosphere*, 18 (1989) 1051.
62 M. D. Erickson, S. E. Swanson, J. D. Flora and G. D. Hinshaw, *Environ. Sci. Technol.*, 23 (1989) 462.

63 S. Marklund, R. Andersson, M. Tysklind, C. Rappe, K. E. Egebäck, E. Björkman and V. Grigoriadis, *Chemosphere*, 20 (1990) 553.
64 A. Svenson, L. O. Kjeller and C. Rappe, *Environ. Sci. Technol.*, 23 (1989) 900.
65 L. G. Öberg, B. Glas, S. E. Swanson, C. Rappe and K. G. Paul, *Arch. Environ. Contam. Toxicol.*, 19 (1990) 930.
66 G. Mason and S. H. Safe, *Toxicology*, 41 (1986) 153.
67 C. Rappe, M. Nygren, G. Lindström, H. R. Buser, O. Blaser and C. Wüthrich, *Environ. Sci. Technol.*, 21 (1987) 964.
68 A. Kočan and J. Garaj, *Chem. Listy*, 81 (1987) 983.
69 M. Holcomb, C. Yao and S. H. Safe, *Biochem. Pharmacol.*, 37 (1988) 1535.
70 M. Nygren, M. Hansson, M. Sjöström, C. Rappe, P. Kahn, M. Gochfeld, H. Velez, T. Ghent-Guenther and W. P. Wilson, *Chemosphere*, 17 (1988) 1663.
71 S. Tanabe, *Mar. Pollut. Bull.*, 19 (1988) 347.
72 D. E. Lilienfeld and M. A. Gallo, *Epidemiol. Rev.*, 11 (1989) 28.
73 S. A. Skene, I. C. Dewhurst and M. Greenberg, *Hum. Toxicol.*, 8 (1989) 173.
74 T. Zacharewski, L. Safe, S. H. Safe, B. Chittim, D. DeVault, K. Wiberg, P. A. Bergqvist and C. Rappe, *Environ. Sci. Technol.*, 23 (1989) 730.
75 M. Oehme, S. Manø, E. M. Brevik and J. Knutzen, *Fresenius' Z. Anal. Chem.*, 335 (1989) 987.
76 D. DeVault, W. Dunn, P. A. Bergqvist, K. Wiberg and C. Rappe, *Environ. Toxicol. Chem.*, 8 (1989) 1013.
77 A. Schecter, P. Fürst, C. Krüger, H. A. Meemken, W. Groebel and J. D. Constable, *Chemosphere*, 18 (1989) 445.
78 M. Eriksson, L. Hardell, H. O. Adami, *J. Natl. Cancer Inst.*, 82 (1990) 486.
79 A. Opperhuizen and D. T. H. M. Sijm, *Environ. Toxicol. Chem.*, 9 (1990) 175.
80 R. Gotz, E. Schumacher, L. O. Kjeller, P. A. Bergqvist and C. Rappe, *Chemosphere*, 20 (1990) 51.
81 G. D. Bellward, R. J. Norstrom, P. E. Whitehead, J. E. Elliott, S. M. Bandiera, C. Dworschak, T. Chang, S. Forbes, B. Cadario, L. E. Hart and K. M. Cheng, *J. Toxicol. Environ. Health*, 30 (1990) 33.
82 R. Frommberger, *Chemosphere*, 20 (1990) 333.
83 D. Firestone, *J. Assoc. Off. Anal. Chem.*, 74 (1991) 375.
84 R. Frommberger, *Chemosphere*, 22 (1991) 29.
85 L. M. Smith, D. L. Stalling and J. L. Johnson, *Anal. Chem.*, 56 (1984) 1830.
86 D. C. Villeneuve, L. M. Reynolds, G. H. Thomas and W. E. J. Phillips, *J. Assoc. Off. Anal. Chem.*, 56 (1973) 999.
87 G. F. Fries and G. S. Marrow, *J. Assoc. Off. Anal. Chem.*, 56 (1973) 1002.
88 R. C. Hale, J. Greaves, K. Gallagher and G. G. Vadas, *Environ. Sci. Technol.*, 24 (1990) 1727.
89 R. C. Hale, E. Bush, K. Gallagher, J. L. Gundersen and R. F. Mothershead, II, *J. Chromatogr.*, 539 (1991) 149.
90 S. Takenaka, T. Iida, K. Fukamachi, A. Mori, R. Nakagawa and K. Takahashi, *Chemosphere*, 16 (1987) 1419.
91 T. Iida, K. Fukamachi, S. Takenaka, R. Nakagawa and K. Takahashi, *Bunseki Kagaku*, 37 (1988) 230.
92 E.R. Barnhart, D. G. Patterson, Jr., J. A. H. MacBride, L. R. Alexander, C. A. Alley and W. E. Turner, in C. Rappe, G. Choundhary and L. H. Keith (Editors), *Chlorinated Dioxins and Dibenzofurans in Perspective*, Lewis, Chelsea, MI, 1986, Ch. 33, p. 501.
93 A. Poland and E. Glover, *Mol. Pharmacol.*, 13 (1977) 924.
94 U. A. Th. Brinkman and H. G. M. Reymer, *J. Chromatogr.*, 127 (1976) 203.
95 C. L. Stratton and J. B. Sosebee, Jr., *Environ. Sci. Technol.*, 10 (1976) 1229.
96 M. Doguchi, *Ecotoxicol. Environ. Safety*, 1 (1977) 239.
97 J. Jan, S. Malnersič and L. Županič, *Arh. Hig. Rada Toksikol.*, 29 (1978) 133.
98 A. Hanberg, F. Wern, L. Asplund, E. Haglund and S. H. Safe, *Chemosphere*, 20 (1990) 1161.
99 C. Rappe and H. R. Buser, in R. D. Kimbrough (Editor), *Halogenated Biphenyls, Terphenyls, Naphthalenes, Dibenzodioxins and Related Products*, Elsevier, Amsterdam, 1980, Ch. 2, p. 41.
100 M. Zell and K. Ballschmiter, *Fresenius' Z. Anal. Chem.*, 300 (1980) 387.
101 D. H. White, C. A. Mitchell, H. D. Kennedy, A. J. Krynitsky and M. A. Ribick, *Southwest. Nat.*, 28 (1983) 325.
102 Ö. Andersson, C. E. Linder, M. Olsson, L. Reutergårdh, U. B. Vemo and U. Wideqvist, *Arch. Environ. Contam. Toxicol.*, 17 (1988) 755.
103 A. B. Mohammed, *Acta Univ. Ups.*, 45 (1988) 1.
104 C.R. Worthing (Editor), *Pesticide Manual*, British Crop Protection Council, Thornton Heath, 8th ed., 1987.
105 R. J. Norstrom, M. Simon, D.C. G. Muir and R. E. Schweinsburg, *Environ. Sci. Technol.*, 22 (1988) 1063.
106 D. C. G. Muir, R. J. Norstrom and M. Simon, *Environ. Sci. Technol.*, 22 (1988) 1071.
107 B. G. Loganathan, S. Tanabe, M. Goto and R. Tatsukawa, *Environ. Pollut.*, 62 (1989) 237.
108 R. Wittlinger and K. Ballschmiter, *Fresenius' J. Anal. Chem.*, 336 (1990) 193.
109 H. Buchert, T. Class and K. Ballschmiter, *Fresenius' Z. Anal. Chem.*, 333 (1989) 211.
110 M. A. Dearth and R. A. Hites. *J. Am. Soc. Mass Spectrom.*, 1 (1990) 99.
111 V. Leoni, I. Mastroeni, N. Vescia, L. Fabiani and R. Giuliani, *Bull. Environ. Contam. Toxicol.*, 41 (1988) 523.
112 M. Friege and A. Poppe, *Chemosphere*, 18 (1989) 1359.
113 H. Friege, W. Stock, J. Alberti, A. Poppe, I. Juhnke, J. Knie and W. Schiller, *Chemosphere*, 18 (1989) 1367.
114 L. von Meyerinck, B. Hufnagel, A. Schmoldt and H. F. Benthe, *Toxicol. Lett.*, 51 (1990) 163.
115 P. G. Wester and F. van der Valk, *Bull. Environ. Contam. Toxicol.*, 45 (1990) 69.
116 R. Jaffe and R. Hites, *J. Great Lakes Res.*, 10 (1984) 440.
117 J. Ehnmann and K. Ballschmiter, *Fresenius' Z. Anal. Chem.*, 332 (1989) 904.
118 P. Fürst, C. Krüger, H. A. Meemken and W. Groebel, *J. Chromatogr.*, 405 (1987) 311.
119 K. Haraguchi, H. Kuroki and Y. Masuda, *J. Chromatogr.*, 361 (1986) 239.
120 K. Haraguchi, H. Kuroki and Y. Masuda, *Chemosphere*, 16 (1987) 2033.
121 R. W. Gossett, *Mar. Environ. Res.*, 26 (1988) 155.
122 R. B. Maybury, in A. Zlatkis and C. F. Poole (Editors),

Electron Capture, Elsevier, Amsterdam, 1981, Ch. 10.3, p. 219.
123 S. Jensen, *New Sci.*, 32 (1966) 612.
124 M. Wassermann, D. Wassermann, S. Cucos and H. J. Miller, *Ann. N. Y. Acad. Sci.*, 320 (1979) 69.
125 S. W. Hooper, C. A. Pettigrew and G. S. Sayler, *Environ. Toxicol. Chem.*, 9 (1990) 655.
126 D. G. Crosby and K. W. Moilamen, *Bull. Environ. Contam. Toxicol.*, 10 (1973) 372.
127 O. Hutzinger, S. Safe, B. R. Wentzell and V. Zitko, *Environ. Health Perspect.*, 5 (1973) 267.
128 D. A. Abramowicz, *CRC Crit. Rev. Biotechnol.*, 10 (1990) 241.
129 D. L. Bedard, in D. Kamely, A. Chakrabarty and G. S. Omenn (Editors), *Advances in Applied Biotechnology Series*, Vol. 4, Portfolio, Woodlands TX, 1990, p. 369.
130 D. L. Bedard and M. L. Haberl, *Microb. Ecol.*, 20 (1990) 87.
131 F. Fava, S. Zappoli, L. Marchetti and L. Morselli, *Chemosphere*, 22 (1991) 3.
132 J. F. Brown, Jr., and R. E. Wagner, *Environ. Toxicol. Chem.*, 9 (1990) 1215.
133 J. F. Quensen, III, J. M. Tiedje and S. A. Boyd, *Science*, 242 (1988) 752.
134 B. Pavoni, C. Calvo, A. Sfriso and A. A. Orio, *Sci. Total Environ.*, 91 (1990) 13.
135 P. C. Baumann and D. M. Whittle, *Aquat. Toxicol.*, 11 (1988) 241.
136 P. H. Becker, *Helgol. Meeresunters.*, 43 (1989) 395.
137 P. A. Greve and P. van Zoonen, *Int. J. Environ. Anal. Chem.*, 38 (1990) 265.
138 N. Picer and M. Picer, *Chemosphere*, 21 (1990) 153.
139 B.G. Loganathan, S. Tanabe, H. Tanaka, S. Watanabe, N. Miyzaki, M. Amano and R. Tatsukawa, *Mar. Pollut. Bull.*, 21 (1990) 435.
140 F. L. Mayer, P. M. Mehrle and H. O. Sanders, *Arch. Environ. Contam. Toxicol.*, 5 (1977) 501.
141 W. L. Mauck, P. M. Mehrle and F. L. Mayer, *J. Fish. Res. Board Can.*, 35 (1978) 1084.
142 E. E. McConnell, in R. D. Kimbrough (Editor), *Halogenated Biphenyls, Terphenyls, Naphthalenes, Dibenzodioxins and Related Products*, Elsevier, Amsterdam, 1980, Ch. 5, p. 109.
143 J. J. T. W. A. Stirk, F. M. H. Debets and G. Koss, in R. D. Kimbrough (Editor), *Halogenated Biphenyls, Terphenyls, Naphthalenes, Dibenzodioxins and Related Products*, Elsevier, Amsterdam, 1980, Ch. 7, p. 191.
144 R. E. Faith and M. I. Luster, in R. D. Kimbrough (Editor), *Halogenated Biphenyls, Terphenyls, Naphthalenes, Dibenzodioxins and Related Products*, Elsevier, Amsterdam, 1980, Ch. 8, p. 241.
145 A. Parkinson and S. H. Safe, in S. H. Safe (Editor), *Polychlorinated Biphenyls (PCBs): Mammalian and Environmental Toxicology*, Springer, Berlin, 1987, p. 49.
146 S. H. Safe, *Mutat. Res.*, 220 (1989) 31.
147 U. Lundkvist, *Toxicology*, 61 (1990) 249.
148 D. L. Berry, T. J. Slaga, J. diGiovanni and M. R. Juchau, *Ann. N. Y. Acad. Sci.*, 320 (1979) 405.
149 J. M. Haake, S. H. Safe, K. Mayura and T. D. Phillips, *Toxicol. Lett.*, 38 (1987) 299.
150 C. Yao and S. H. Safe, *Toxicol. Appl. Pharmacol.*, 100 (1989) 208.
151 I. Biegel, M. Harris, D. Davis, R. Rosengren, L. Safe and S. H. Safe, *Toxicol. Appl. Pharmacol.*, 97 (1989) 561.
152 M. A. Hayes, in S. H. Safe (Editor), *Polychlorinated Biphenyls (PCBs): Mammalian and Environmental Toxicology*, Springer, Berlin, 1987, p. 77.
153 E. J. Fairchild (Editor), *Registry of Toxic Effects of Chemical Substances*, US DHEW Publ. No. 78-104, NIOSH, Cincinnati, OH, 1977.
154 N. Kuratsune, in R. D. Kimbrough (Editor), *Halogenated Biphenyls, Terphenyls, Naphthalenes, Dibenzodioxins and Related Products*, Elsevier, Amsterdam, 1980, Ch. 9.B.1, p. 187.
155 P. H. Chen, K. T. Chang and Y. D. Lu, *Bull. Environ. Contam. Toxicol.*, 26 (1981) 489.
156 G. R. N. Jones, *Lancet*, ii (1989) 791.
157 R. D. Kimbrough, in R. D. Kimbrough (Editor), *Halogenated Biphenyls, Terphenyls, Naphthalenes, Dibenzodioxins and Related Products*, Elsevier, Amsterdam, 1988, Ch. 9.C, p. 373.
158 A. B. Smith, J. Schloemer, L. K. Lowry, A. W. Smallwood, R. N. Ligo, S. Tanaka, W. Stringer, M. Jones, R. Hervin and C. J. Glueck, *Br. J. Ind. Med.*, 39 (1982) 361.
159 K. K. Steinberg, L. W. J. Freni-Titulaer, T. N. Rogers, V. W. Burse, P. W. Mueller, P. A. Stehr and D. T. Miller, *J. Toxicol. Environ. Health*, 19 (1986) 369.
160 T. Yakushiji, I. Watanabe, K. Kuwabara, R. Tanaka, T. Kashimoto, N. Kunita and I. Hara, *Arch. Environ. Health*, 39 (1984) 368.
161 T. Yakushiji, *Rev. Environ. Contam. Toxicol.*, 101 (1988) 139.
162 P. R. Taylor, J. N. Stelma and C. E. Lawrence, *Am. J. Epidemiol.*, 129 (1989) 395.
163 V. Leoni, L. Fabiani, G. Marinelli, G. Puccetti, G. F. Tarsitani, A. De Carolis, N. Vescia, A. Morini, V. Aleandri, V. Pozzi, F. Cappa and D. Barbati, *Ecotoxicol. Environ. Safety*, 17 (1989) 1.
164 J. G. Koppe, E. Pluim and K. Olie, *J. R. Soc. Med.*, 82 (1989) 416.
165 J. G. Koppe, *Acta Paediatr. Scand., Suppl.*, 360 (1989) 1.
166 J. L. Jacobson, S. W. Jacobson and H. E. B. Humphrey, *Neurotoxicol. Teratol.*, 12 (1990) 319.
167 P. W. Brandt-Rauf and H. L. Niman, *Br. J. Ind. Med.*, 45 (1988) 689.
168 H. Konečná and I. Kalina, in *Proceedings of the Spring Toxicological Symposium of the Group for Toxicological Chemistry*, Luhačovice, Czechoslovakia, 1987, published in the supplementary volume of *Acta Hyg. Epidemiol. Microbiol.*, Institute of Hygiene and Epidemiology, Prague, and Research Institute of Preventive Medicine, Bratislava, No. 5, 1987, p. 89.
169 S. Tanabe, N. Kannan, T. Wakimoto, R. Tatsukawa, T. Okamoto and Y. Masuda, *Toxicol. Environ. Chem.*, 24 (1989) 215.
170 K. Takayama, H. Miyata, M. Mimura, S. Ohta and T. Kashimoto, *Chemosphere*, 22 (1991) 537.
171 P. H. Chen, Y. D. Lu, M. H. Yang and J. S. Chen, *Clin. Med.*, 7 (1981) 77.
172 C. Ioannides and D. V. Parke, *Drug. Metabol. Rev.*, 22 (1990) 1.

173 J. P. Whitlock, Jr., *Annu. Rev. Pharmacol. Toxicol.*, 26 (1986) 333.
174 P. Honkakoski and M. A. Lang, *Arch. Biochem. Biophys.*, 273 (1989) 42.
175 M. A. Pham, J. Magdalou, M. Totis, S. Fournel-Gigleux, G. Sięst and B. D. Hammock, *Biochem. Pharmacol.*, 38 (1989) 2187.
176 I. de Waziers, P. H. Cugnenc, C. S. Yang, J. P. Leroux and P. H. Beaune, *J. Pharmacol. Exp. Ther.*, 253 (1990) 387.
177 P. B. Watkins, S. A. Murray, P. E. Thomas and S. A. Wrighton, *Biochem. Pharmacol.*, 39 (1990) 471.
178 D. E. Ryan and W. Levin, *Pharmacol. Ther.*, 45 (1990) 153.
179 A. B. Okey, *Pharmacol. Ther.*, 45 (1990) 241.
180 A. H. Conney, *Cancer Res.*, 42 (1982) 4875.
181 D. W. Nebert, H. Adesnik, M. J. Coon, R. W. Estabrook, F. J. Gonzales, F. P. Guengerich, I. C. Gunsalus, E. F. Johnson, B. Kemper, W. Levin, I. R. Phillips, R. Sato and M. R. Waterman, *DNA*, 6 (1987) 1.
182 W. Levin, *Drug Metabol. Dispos.*, 18 (1990) 824.
183 M. R. Juchau, *Life Sci.*, 47 (1990) 2385.
184 G. C. Farrell and M. Murray, *Gastroenterology*, 99 (1990) 885.
185 J. M. Haake, J. C. Merrill and S. H. Safe, *Can. J. Physiol. Pharmacol.*, 63 (1985) 1096.
186 T. Shimada, M. Iwasaki, M. V. Martin and F. P. Guengerich, *Cancer Res.*, 49 (1989) 3218.
187 P. Grolier, P. Cassand, E. Antignac, J. F. Narbonne, R. Albrecht, V. Azais, L. W. Robertson and F. Oesch, *Mutat. Res.*, 211 (1989) 139.
188 J. Z. Byczkowski and T. Gessner, *Int. J. Biochem.*, 21 (1989) 525.
189 M. Hall, L. M. Forrester, D. K. Parker, P. L. Grover and C. R. Wolf, *Carcinogenesis*, 10 (1989) 1815.
190 E. L. Cavalieri, E. G. Rogan, P. D. Devanesan, P. Cremonesi, R. L. Cerny, M. L. Gross and W. J. Bodell, *Biochemistry*, 29 (1990) 4820.
191 M. E. McManus, W. M. Burgess, M. E. Veronese, A. Hugget, L. C. Quattrochi and R. H. Tukey, *Cancer Res.*, 50 (1990) 3367.
192 J. G. Vos, J. J. T. W. A. Stirk, C. W. M. van Holsteyn and J. H. Pennings, *Toxicol. Appl. Pharmacol.*, 20 (1971) 232.
193 A. Poland and E. Glover, *Mol. Pharmacol.*, 9 (1973) 736.
194 G. S. Lucier, O. S. McDaniel and G. E. R. Hook, *Pharmacology*, 10 (1974) 349.
195 A. Poland and E. Glover, *Mol. Pharmacol.*, 10 (1974) 349.
196 G. J. Johnstone, D. J. Ecobichon and O. Hutzinger, *Toxicol. Appl. Pharmacol.*, 28 (1974) 66.
197 D. J. Ecobichon and A. M. Comeau, *Toxicol. Appl. Pharmacol.*, 33 (1975) 94.
198 J. D. McKinney, K. Chae, B. N. Gupta, J. A. Moore and J. A. Goldstein, *Toxicol. Appl. Pharmacol.*, 36 (1976) 65.
199 J. A. Goldstein, J.D. McKinney, G. S. Lucier, P. Hickman, H. Bergman and J. A. Moore, *Toxicol. Appl. Pharmacol.*, 36 (1976) 81.
200 R. L. Ax and L. G. Hansen, *Poult. Sci.*, 54 (1975) 895.
201 J. A. Goldstein, *Ann. N. Y. Acad. Sci.*, 320 (1979) 164.
202 H. Yoshimura, S. Yoshikara, N. Ozawa and M. Miki, *Ann. N. Y. Acad. Sci.*, 320 (1979) 179.
203 A. Parkinson, R. Cockerline and S. H. Safe, *Chem. Biol. Interact.*, 29 (1980) 277.
204 A. Parkinson, L. Robertson, L. Safe and S. H. Safe, *Chem. Biol. Interact.*, 30 (1980) 271.
205 J. D. McKinney and P. Singh, *Chem. Biol. Interact.*, 33 (1981) 271.
206 A. Parkinson, S. H. Safe, L. W. Robertson, P. E. Thomas, D. E. Ryan, L. M. Reik and W. Levin, *J. Biol. Chem.*, 258 (1983) 5967.
207 B. Leece, M. A. Denomme, R. Towner, S. M. A. Li and S. H. Safe, *J. Toxicol. Environ. Health*, 16 (1985) 379.
208 S. H. Safe, S. Bandiera, T. Sawyer, L. Robertson, L. Safe, A. Parkinson, P. E. Thomas, D. E. Ryan, L. M. Reik, W. Levin, M. A. Denomme and T. Fujita, *Environ. Health Perspect.*, 60 (1985) 47.
209 J. J. Dynes, F. J. Baudais and R. K. Boyd, *Can. J. Chem.*, 63 (1985) 1292.
210 T. Sawyer and S. H. Safe, *Toxicol. Lett.*, 13 (1982) 87.
211 S. H. Safe, *CRC Crit. Rev. Toxicol.*, 13 (1984) 319.
212 D. Davis and S. H. Safe, *Toxicology*, 63 (1990) 97.
213 J. W. Gooch, A. A. Elskus, P. J. Kloeper-Sams, M. E. Hahn and J. J. Stegeman, *Toxicol. Appl. Pharmacol.*, 98 (1989) 422.
214 T. W. Sawyer, A. D. Vatcher and S. H. Safe, *Chemosphere*, 13 (1984) 695.
215 S. H. Safe, S. Bandiera, T. Sawyer, B. Zmudzka, G. Mason, M. Romkes, M. A. Denomme, J. Sparling, A. B. Okey and T. Fujita, *Environ. Health Perspect.*, 61 (1985) 21.
216 G. Mason, T. Sawyer, B. Keys, S. Bandiera, M. Romkes, J. Piskorska-Pliszczynska, B. Zmudzka and S. H. Safe, *Toxicology*, 37 (1985) 1.
217 G. Mason, K. Farrell, B. Keys, J. Piskorska-Pliszczynska, L. Safe and S. H. Safe, *Toxicology*, 41 (1986) 21.
218 S. H. Safe, *Annu. Rev. Pharmacol. Toxicol*, 26 (1986) 371.
219 L. W. Robertson, E. M. Silberhorn, H. P. Glavert, M. Schwartz and A. Buchmann, *Environ. Toxicol. Chem.*, 10 (1991) 715.
220 A. Poland, E. Glover and A. S. Kende, *J. Biol. Chem.*, 251 (1976) 4936.
221 A. Poland, W. F. Greenlee and A. S. Kende, *Ann. N. Y. Acad. Sci.*, 320 (1979) 214.
222 R. A. Neal, P. W. Beatty and T. A. Gasiewicz, *Ann. N. Y. Acad. Sci.*, 320 (1979) 204.
223 A. Poland and E. Glover, *Mol. Pharmacol.*, 17 (1980) 86.
224 S. H. Safe, *ISI Atlas Sci. Pharmacol.*, 2 (1988) 78.
225 E. A. Roberts, N. H. Shear, A. B. Okey and D. K. Manchester, *Chemosphere*, 14 (1985) 661.
226 P. Labruzzo, X. F. Yu and M. J. Dufresne, *Biochem. Pharmacol.*, 38 (1989) 2339.
227 C. Kiyohara, N. Mohri, J. Nagayama and T. Hirohata, *Bull. Environ. Contam. Toxicol.*, 43 (1989) 185.
228 M. S. Denison and L. M. Vella, *Arch. Biochem. Biophys.*, 277 (1990) 382.
229 A. Lorenzen and A. B. Okey, *Chemosphere*, 20 (1990) 1215.
230 W. I. Waithe, M. Michaud, P. A. Harper, A. B. Okey and A. Anderson, *Biochem. Pharmacol.*, 41 (1991) 85.
231 A. B. Rifkind, M. Gannon and S. S. Gross, *Biochem. Biophys. Res. Commun.*, 172 (1990) 1180.
232 N. I. Kerkvliet, L. B. Steppan, J. A. Brauner, J. A. Deyo, M. C. Henderson, R. S. Tomar and D. R. Buhler, *Toxicol. Appl. Pharmacol.*, 105 (1990) 26.

233 E. S. Chen, S. I. Gutman and J. R. Olson, *Toxicologist*, 7 (1987) 160.
234 J. R. Olson, S. I. Gutman and E. S. Shen, *Chemosphere*, 18 (1989) 363.
235 A. J. Niimi and B. C. Oliver, *Chemosphere*, 18 (1989) 1413.
236 S. H. Safe, *Chemosphere*, 16 (1987) 791.
237 J. R. Olson, J. S. Bellin and D. G. Barnes, *Chemosphere*, 18 (1989) 371.
238 J. A. van Zorge, J. H. van Wijnen, R. M. C. Theelen, K. Olie and M. van der Berg, *Chemosphere*, 19 (1989) 1881.
239 F. W. Kutz, D. G. Barnes, E. W. Bretthauer, D. P. Bottimore and H. Greim, *Toxicol. Environ. Chem.*, 26 (1990) 99.
240 B. Brunström and L. Andersson, *Arch. Toxicol.*, 62 (1988) 263.
241 B. Brunström, *Arch. Toxicol.*, 64 (1990) 188.
242 T. W. Sawyer and S. H. Safe, *Chemosphere*, 14 (1985) 79.
243 R. Bannister, D. Davis, T. Zacharewski, I. Tizard and S. H. Safe, *Toxicology*, 46 (1987) 29.
244 B. Astroff, T. Zacharewski, S. H. Safe, M. P. Arlotto, A. Parkinson, P. Thomas and W. Levin, *Mol. Pharmacol.*, 33 (1988) 231.
245 D. Davis and S. H. Safe, *Toxicol. Lett.*, 48 (1989) 35.
246 M. E. Hahn, J. A. Goldstein, P. Linko and T. A. Gasiewicz, *Arch. Biochem. Biophys.*, 270 (1989) 344.
247 B. Astroff and S. H. Safe, *Toxicology*, 59 (1989) 285.
248 L. Sargent, Y. P. Dragan, C. Erickson, C. J. Laufer and H. C. Pitot, *Carcinogenesis*, 12 (1991) 793.
249 N. Kannan, S. Tanabe and R. Tatsukawa, *Bull. Environ. Contam. Toxicol.*, 41 (1988) 267.
250 G. Di Bella, A. Daghetta and M. Riva, *Ind. Aliment.*, 28 (1989) 929.
251 *Bundesgesetzblatt*, 1 (1988) 422.
252 B. Kratochvil and J. K. Taylor, *Anal. Chem.*, 53 (1981) 924A.
253 L. H. Keith (Editor), *Principles of Environmental Sampling*, American Chemical Society, Washington, DC, 1988.
254 L. H. Keith, *Environ. Sci. Technol.*, 24 (1990) 610.
255 T. F. Bidleman and C. E. Olney, *Bull. Environ. Contam. Toxicol.*, 11 (1974) 442.
256 D. L. Swackhamer, B. D. McVeety and R. A. Hites, *Environ. Sci. Technol.*, 22 (1988) 664.
257 S. B. Hawthorne, M. S. Krieger and D. J. Miller, *Anal. Chem.*, 61 (1989) 736.
258 P. Larsson, L. Okla, S. O. Ryding and B. Westöö, *Can. J. Fish. Aquat. Sci.*, 47 (1990) 746.
259 T. Nakano, M. Tsuji and T. Okuno, *Atmos. Environ.*, 24A (1990) 1361.
260 C. S. Brownlow and S. S. Que Hee, *Am. Ind. Hyg. Assoc. J.*, 46 (1985) 421.
261 M. Chevreuil, A. Chesterikoff and R. Létolle, *C. R. Acad. Sci. Sér. II*, 306 (1988) 1081.
262 M. Chevreuil, A. Chesterikoff, R. Létolle and L. Granier, *Water Air Soil Pollut.*, 43 (1989) 73.
263 J. C. Duinker and F. Bouchertall, *Environ. Sci. Technol.*, 23 (1989) 57.
264 J. H. Raymer and E. D. Pellizzari, *Int. J. Environ. Anal. Chem.*, 43 (1991) 151.
265 J. P. Thome and Y. Vandaele, *Int. J. Environ. Anal. Chem.*, 29 (1987) 95.
266 T. Cseh, S. Sanschagrin, J. Hawari and R. Samson, *Appl. Environ. Microbiol.*, 55 (1989) 3150.
267 B. G. Oliver and K. D. Nicol, *Chromatographia*, 16 (1982) 336.
268 A. Opperhuizen and P. I. Voors, *Chemosphere*, 16 (1987) 2379.
269 D. J. Gregor and W. D. Gummer, *Environ. Sci. Technol.*, 23 (1989) 561.
270 D. E. Schulz, G. Petrick and J. C. Duinker, *Mar. Pollut. Bull.*, 19 (1988) 526.
271 L. Morselli, S. Zappoli and S. Donati, *Ann. Chim.*, 79 (1989) 677.
272 V. Leoni, G. Puccetti, R. J. Colombo and A. M. D'Ovidio, *J. Chromatogr.*, 125 (1976) 399.
273 M. T. H. J. Hillebrand, J. M. Everaarts, H. Razak, D. Moelyadi Moelyo, L. Stolwijk and J. P. Boon, *Neth. J. Sea Res.*, 23 (1989) 369.
274 M. Chevreuil, L. Granier, A. Chesterikoff and R. Létolle, *Water Res.*, 24 (1990) 1325.
275 R. J. Maguire and R. J. Tkacz, *Chemosphere*, 19 (1989) 1277.
276 A. Södergren, *Ecotoxicol. Environ. Safety*, 19 (1990) 143.
277 J. Teichman, A. Bevenue and J. W. Hylin, *J. Chromatogr.*, 151 (1978) 155.
278 E. Eduljee, K. Badsha and L. Price, *Chemosphere*, 14 (1985) 1371.
279 D. B. Martin and W. A. Hartman, *J. Assoc. Off. Anal. Chem.*, 68 (1985) 712.
280 R. J. Kominar, F. I. Onuska and K. A. Terry, *J. High Resolut. Chromatogr. Chromatogr. Commun.*, 8 (1985) 585.
281 F. M. Dunnivant and A. W. Elzerman, *J. Assoc. Off. Anal. Chem.*, 71 (1988) 551.
282 N. I. Rubinstein, R. J. Pruell, B. K. Taplin, J. A. Livolsi and C. B. Norwood, *Chemosphere*, 20 (1990) 1097.
283 F. A. Maris, E. Noroozian, R. R. Otten, R. C. J. M. van Dijck, G. J. de Jong and U. A. Th. Brinkman, *J. High Resolut. Chromatogr. Chromatogr. Commun.*, 11 (1988) 197.
284 J. N. Huckins, T. R. Schwartz, J. D. Petty and L. M. Smith, *Chemosphere*, 17 (1988) 1995.
285 J. E. Baker and S. J. Eisenreich, *J. Great Lakes Res.*, 15 (1989) 84.
286 F. I. Onuska and K. A. Terry, *J. High Resolut. Chromatogr.*, 12 (1989) 527.
287 K. C. Jones, *Chemosphere*, 18 (1989) 1665.
288 L. G. Hansen, P. W. Washko, L. G. M. Th. Tuinstra, S. B. Dorn and T. D. Hinesly, *J. Agric. Food Chem.*, 29 (1981) 1012.
289 G. R. Shaw and D. W. Connell, *Environ. Sci. Technol.*, 18 (1984) 18.
290 R. L. Holt, S. Cruse and E. S. Greer, *Bull. Environ. Contam. Toxicol.*, 36 (1986) 651.
291 S. Focardi, C. Fossi, C. Leonzio and R. Romei, *Bull. Environ. Contam. Toxicol.*, 36 (1986) 644.
292 R. A. Morse, T. W. Culliney, W. H. Gutenmann, C. B. Littman and D. J. Lisk, *Bull. Environ. Contam. Toxicol.*, 38 (1987) 271.
293 P. G. Olafsson and A. M. Bryan, *Anal. Lett.*, 20 (1987) 1719.
294 J. Pellantová, K. Hudec, F. Kredl. J. Svobodník and R. Svobodová, *Folia Zool.*, 38 (1989) 79.

295 P. V. Winger, C. Sieckman, T. W. May and W. W. Johnson, *J. Assoc. Off. Anal. Chem.*, 67 (1984) 325.
296 L. Maack and W. C. Sonzogni, *Arch. Environ. Contam. Toxicol.*, 17 (1988) 711.
297 D. L. Stalling, R. C. Tindle and J. L. Johnson, *J. Assoc. Off. Anal. Chem.*, 55 (1972) 32.
298 P. Fernández, C. Porte, D. Barceló, J. M. Bayona and J. Albaigés, *J. Chromatogr.*, 456 (1988) 155.
299 A. Schecter, J. Mes and D. Davies, *Chemosphere*, 18 (1989) 811.
300 W. L. Mauck and L. E. Olson, *Bull. Environ. Contam. Toxicol.*, 17 (1977) 387.
301 D. L. Stalling, J. N. Huckins, J. D. Petty, J. L. Johnson and H. O. Sanders, *Ann. N. Y. Acad. Sci.*, 320 (1979) 48.
302 T. A. Haines, *Water, Air Soil Pollut.*, 20 (1983) 47.
303 J. Mes, L. Marchand and K. Karpinski, *J. Environ. Sci. Health*, A24 (1989) 879.
304 J. Mes, L. Marchand and D. J. Davies, *Environ. Technol.*, 11 (1990) 747.
305 G. Petrick, D. E. Schulz and J. C. Duinker, *J. Chromatogr.*, 435 (1988) 241.
306 D. L. Swackhamer and R. A. Hites, *Environ. Sci. Technol.*, 22 (1988) 543.
307 G. L. LeBel and D. T. Williams, *J. Assoc. Off. Anal. Chem.*, 69 (1986) 458.
308 H. Goerke and K. Weber, *Mar. Environ. Res.*, 29 (1990) 205.
309 J. Batty, R. A. Leavitt, N. Biondo and D. Polin, *Arch. Environ. Contam. Toxicol.*, 19 (1990) 283.
310 U. Skarén, *Ann. Zool. Fenn.*, 25 (1988) 271.
311 S. Tanabe, N. Kannan, T. Wakimoto and R. Tatsukawa, *Int. J. Environ. Anal. Chem.*, 29 (1987) 199.
312 J. de Boer, *Chemosphere*, 17 (1988) 1803.
313 E. Bacci, D. Calamari, C. Gaggi, R. Fanelli, S. Focardi and M. Morosini, *Chemosphere*, 15 (1986) 747.
314 L. A. Shane and B. Bush, *Ecotoxicol. Environ. Safety*, 17 (1989) 38.
315 R. J. Hesselberg and D. D. Scherr, *Bull. Environ. Contam. Toxicol.*, 11 (1974) 202.
316 S. S. Que Hee, J. A. Ward, M. W. Tabor and R. R. Suskind, *Anal. Chem.*, 55 (1983) 157.
317 L. L. Needham, V. W. Burse and H. A. Price, *J. Assoc. Off. Anal. Chem.*, 64 (1981) 1131.
318 V. W. Burse, L. L. Needham, M. P. Korver, C.R. Lapeza, Jr., J. A. Liddle and D. D. Bayse, *J. Assoc. Off. Anal. Chem.*, 66 (1983) 32.
319 M. Luotamo, J. Järvisalo and A. Aitio, *Environ. Health Perspect.*, 60 (1985) 327.
320 V. W. Burse, S. L. Head, M. P. Korver, P. C. McClure, J. F. Donahue and L. L. Needham, *J. Anal. Toxicol.*, 14 (1990) 137.
321 W. H. Newsome and J. B. Shields, *Int. J. Environ. Anal. Chem.*, 10 (1981) 295.
322 L. G. M. Th. Tuinstra, W. A. Traag and H. J. Keukens, *J. Assoc. Off. Anal. Chem.*, 63 (1980) 952.
323 B. Bush, J. T. Snow and S. Connor, *J. Assoc. Off. Anal. Chem.*, 66 (1983) 248.
324 J. Mes and L. Marchand, *Bull. Environ. Contam. Toxicol.*, 39 (1987) 736.
325 E. Dewailly, A. Nantel, J. P. Weber and F. Meyer, *Bull. Environ. Contam. Toxicol.*, 43 (1989) 641.
326 M. P. Seymour, T. M. Jefferies, A. J. Floyd and L. J. Notarianni, *Analyst (London)*, 112 (1987) 427.
327 K. Norén and J. Sjövall, *J. Chromatogr.*, 422 (1987) 103.
328 L. R. Snyder, in E. Heftmann (Editor), *Chromatography*, Reinhold, New York, 2nd ed., 1967, Ch. 4, p. 43.
329 J. Lawrence and H. M. Tosine, *Bull. Environ. Contam. Toxicol.*, 17 (1977) 49.
330 D. T. Williams and G. L. LeBel, *Chemosphere*, 20 (1990) 33.
331 F. Krédl and I. Breyl, in *Proceedings of the Seminar on Polychlorinated Biphenyl Residues*, Brno, January 1983, published in the supplementary volume of *Acta Hyg. Epidemiol. Microbiol.*, Institute of Hygiene and Epidemiology, Prague, and Research Institute of Preventive Medicine, Bratislava, No. 10, 1984, p. 59.
332 L. G. Hansen, J. M. Sullivan, C. C. Neff, P. E. Sanders, R. J. Lambert, V. R. Beasley and E. Storr-Hansen, *J. Agric. Food Chem.*, 37 (1989) 135.
333 W. Liao, W. D. Smith, T. C. Chiang and L. R. Williams, *J. Assoc. Off. Anal. Chem.*, 71 (1988) 742.
334 D. Davies and J. Mes, *Bull. Environ. Contam. Toxicol.*, 39 (1987) 743.
335 S. J. V. Young, C. Finsterwalder and J. A. Burke, *J. Assoc. Off. Anal. Chem.*, 56 (1973) 957.
336 O. Roerden, K. Reisinger, W. Leymann and C. B. G. Frischkorn, *Fresenius' Z. Anal. Chem.*, 334 (1989) 413.
337 V. W. Burse, M. P. Korver, L. L. Needham, C. R. Lapeza, Jr., E. L. Boozer, S. L. Head, J. A. Liddle and D. D. Bayse, *J. Assoc. Off. Anal. Chem.*, 72 (1989) 649.
338 T. R. Schwartz and R. G. Lehmann, *Bull. Environ. Contam. Toxicol.*, 28 (1982) 723.
339 M. L. Meredith and R. A. Hites, *Environ. Sci. Technol.*, 21 (1987) 709.
340 J. N. Huckins, D. L. Stalling and J. L. Johnson, *J. Assoc. Off. Anal. Chem.*, 59 (1976) 975.
341 A. Opperhuizen and S. M. Schrap, *Chemosphere*, 17 (1988) 253.
342 M. M. Gagnon, J. J. Dodson, M. E. Comba and K. L. E. Kaiser, *Sci. Total Environ.*, 97/98 (1990) 739.
343 S. Jensen and G. Sundström, *Ambio*, 3 (1974) 70.
344 D. L. Stalling, J. Johnson and J. N. Huckins, in F. Coulston and F. Korte (Editors), *Lectures Held at the IUPAC Third International Congress of Pesticide Chemistry, Helsinki, July 1974*, Georg Thieme, Stuttgart, 1975, p. 12.
345 L. M. Smith, T. R. Schwartz, K. Feltz and T. J. Kubiak, *Chemosphere*, 21 (1990) 1063.
346 C. S. Hong and B. Bush, *Chemosphere*, 21 (1990) 173.
347 B. G. Luke, G. W. Johnstone and E. J. Woehler, *Chemosphere*, 19 (1989) 2007.
348 D. L. Stalling, R. J. Norström, L. M. Smith and M. Simon, Chemosphere, 14 (1985) 627.
349 A. Venant, S. Borrel, J. Mallet and E. van Neste, *Analusis*, 17 (1989) 64.
350 L. G. M. Th. Tuinstra, J. A. van Rhijn, A. H. Roos, W. A. Traag, R. J. van Mazijk and P. J. W. Kolkman, *J. High Resolut. Chromatogr.*, 13 (1990) 797.
351 J. L. Sericano, E. L. Atlas, T. L. Wade and J. M. Brooks, *Mar. Environ. Res.*, 29 (1990) 161.

352 S. Jensen, L. Renberg and L. Reutergårdh, *Anal. Chem.*, 49 (1977) 316.
353 D. Veierov and N. Aharonson, *J. Assoc. Off. Anal. Chem.*, 61 (1978) 253.
354 D. Veierov and N. Aharonson, *J. Assoc. Off. Anal. Chem.*, 63 (1980) 202.
355 C. Strang, S. P. Levine, B. P. Orlan, T. A. Gouda and W. A. Saner, *J. Chromatogr.*, 314 (1984) 482.
356 M. Remberger, P. Å Hynning and A. H. Neilson, *J. Chromatogr.*, 508 (1990) 159.
357 D. Rossel, P. Honsberger and J. Tarradellas, *Int. J. Environ. Anal. Chem.*, 31 (1987) 219.
358 L. Granier, M. Chevreuil, A. M. Carru and R. Létolle, *Chemosphere*, 21 (1990) 1101.
359 J. Mes, D. S. Campbell, R. N. Robinson and D. J. A. Davies, *Bull. Environ. Contam. Toxicol.*, 17 (1977) 196.
360 K. Grob, I. Kaelin and A. Artho, *J. High Resolut. Chromatogr.*, 14 (1991) 373.
361 P. Haglund, L. Asplund, U. Järnberg and B. Jansson, *J. Chromatogr.*, 507 (1990) 389.
362 F. I. Onuska, R. J. Kominar and K. A. Terry, *J. Chromatogr.*, 279 (1983) 111.
363 M. D. Mullin, C. M. Pochini, S. McCrindle, M. Romkes, S. H. Safe and L. M. Safe, *Environ. Sci. Technol.*, 18 (1984) 468.
364 E. D. Pellizzari, M. A. Moseley and S. D. Cooper, *J. Chromatogr.*, 334 (1985) 277.
365 F. I. Onuska and K. A. Terry, *J. High Resolut. Chromatogr. Chromatogr. Commun*, 9 (1986) 671.
366 S. D. Cooper, M. A. Moseley and E. D. Pellizzari, *Anal. Chem.*, 57 (1985) 2469.
367 J. W. Rote and J. W. Morris, *J. Assoc. Offic. Anal. Chem.*, 56 (1973) 188.
368 G. R. B. Webster and D. A. Birkholz, in F. W. Karasek, O. Hutzinger and S. H. Safe (Editors), *Mass Spectrometry in Environmental Sciences*, Plenum Press, New York, 1985, Ch. 11, p. 209.
369 E. D. Pellizzari, K. B. Tomer and M. A. Mosseley, in L. H. Keith (Editor), *Advances in the Identification and Analysis of Organic Pollutants in Water*, Ann Arbor Sci. Publ., Ann Arbor, MI, 1981, p. 197.
370 L. E. Slivon, J. E. Gebhart, T. L. Hayes, A. L. Alford-Stevens and W. L. Budde, *Anal. Chem.*, 57 (1985) 2464.
371 A. L. Alford-Stevens, J. W. Eichelberger and W. L. Budde, *Environ. Sci. Technol.*, 22 (1988) 304.
372 N. Kannan, S. Tanabe, M. Ono and R. Tatsukawa, *Arch. Environ. Contam. Toxicol.*, 18 (1989) 850.
373 G. W. Tindall and P. E. Wininger, *J. Chromatogr.*, 196 (1980) 109.
374 J. E. Gebhart, T. L. Hayes, A. L. Alford-Stevens and W. L. Budde, *Anal. Chem.*, 57 (1985) 2458.
375 S. Erhardt-Zabik, J. T. Watson and M. J. Zabik, *Biomed. Environ. Mass Spectrom.*, 19 (1990) 101.
376 E. L. White and M. M. Bursey, *Biomed. Environ. Mass Spectrom.*, 18 (1989) 413.
377 L. D. Sawyer, *J. Assoc. Off. Anal. Chem.*, 61 (1978) 272.
378 M. Dressler, *Selective Gas Chromatographic Detectors*, Elsevier, Amsterdam, 1986, Ch. 9, p. 181.
379 P. Popp, K. H. Bothe, K. Metzner, D. Obst and H. Schön, in E. Leibnitz and G. H. Struppe (Editors), *Handbuch der Gaschromatographie*, Geest & Portig, Leipzig, 1984, Ch. X, p. 335.
380 P. J. McAteer, T. B. Ryerson, M. D. Argentine, M. L. Ware and G. W. Rice, *Appl. Spectrosc.*, 42 (1988) 586.
381 R. P. Eganhouse, B. R. Gould, D. M. Olaguer, C. S. Phinney and P. M. Sherblom, *Int. J. Environ. Anal. Chem.*, 35 (1989) 175.
382 W. Herres, *HRGC–FTIR: Capillary Gas Chromatography–Fourier Transform Infrared Spectroscopy*, Hüthig, Heidelberg, 1987, Ch. 13, p. 107.
383 J. F. Schneider, G. T. Reedy and D. G. Ettinger, *J. Chromatogr. Sci.*, 23 (1985) 49.
384 R. G. Webb and A. C. McCall, *J. Chromatogr. Sci.*, 11 (1973) 366.
385 J. A. Armour, *J. Assoc. Off. Anal. Chem.*, 56 (1973) 987.
386 J. N. Huckins, J. E. Swanson and D. L. Stalling, *J. Assoc. Off. Anal. Chem.*, 57 (1974) 416.
387 J. M. Lin and S. S. Que Hee, *Anal. Chem.*, 57 (1985) 2130.
388 A. de Kok, R. B. Geerdink, R. W. Frei and U. A. Th. Brinkman, *Int. J. Environ. Anal. Chem.*, 11 (1982) 17.
389 M. Cooke, G. Nickless, A. M. Prescott and D. J. Roberts, *J. Chromatogr.*, 156 (1978) 293.
390 A. de Kok, R. B. Geerdink, R. W. Frei and U. A. Th. Brinkman, *Int. J. Environ. Anal. Chem.*, 9 (1981) 301.
391 U. A. Th. Brinkman, G. De Vries, A. de Kok and A. L. de Jonge, *J. Chromatogr.*, 152 (1978) 97.
392 H. L. Issaq, S. D. Fox and G. M. Muschik, *J. Chromatogr. Sci.*, 27 (1989) 172.
393 J. de Boer and Q. T. Dao, *Int. J. Environ. Anal. Chem.*, 43 (1991) 245.
394 J. de Boer and Q. T. Dao, in P. Sandra (Editor), *Proceedings of the 13th International Symposium on Capillary Chromatography, Riva del Garda, May 1991*, Hüthig, Heidelberg, 1991, p. 1367.
395 J. Mes, D. Turton, D. Davies, W. F. Sun, P. Y. Lau and D. Weber, *Int. J. Environ. Anal. Chem.*, 28 (1987) 197.
396 W. Sonzogni, L. Maack, T. Gibson, D. Degenhardt, H. Anderson and B. Fiore, *Arch. Environ. Contam. Toxicol.*, 20 (1991) 56.
397 M. N. Hasan and P. C. Jurs, *Anal. Chem.*, 60 (1988) 978.
398 M. N. Hasan and P. C. Jurs, *Anal. Chem.*, 62 (1990) 2318.
399 J. Krupčík, P. A. Leclercq, A. Šímová, P. Suchánek, M. Čollák and J. Hrivňák, *J. Chromatogr.*, 119 (1976) 271.
400 J. Krupčík, P. A. Leclercq, J. Garaj and A. Šímová, *J. Chromatogr.*, 191 (1980) 207.
401 J. C. Duinker, D. E. Schulz and G. Petrick, *Mar. Pollut. Bull.*, 19 (1988) 19.
402 A. H. Roos, P. G. Kienhuis, W. A. Traag and L. G. M. Th. Tuinstra, *Int. J. Environ. Anal. Chem.*, 36 (1989) 155.
403 B. Larsen and J. Riego, *Int. J. Environ. Anal. Chem.*, 40 (1990) 59.
404 W. Vetter, B. Luckas and W. Haubold, *Chemosphere*, 23 (1991) 193.
405 J. T. Borlakoglu, J. P. G. Wilkins, C. H. Walker and R. R. Dils, *Comp. Biochem. Physiol. C.*, 97 (1990) 151.
406 D. W. Kuehl, B. C. Butterworth, J. Libal and P. Marquis, *Chemosphere*, 22 (1991) 849.
407 H.-Ö. Knöppler, W. Mücke and W. Gedek, *Chemosphere*, 17 (1988) 1963.

408 K. Norén, A. Lundén, J. Sjövall and Å. Bergman, *Chemosphere*, 20 (1990) 935.
409 E. Franchi and S. Focardi, *Sci. Total Environ.*, 102 (1991) 223.
410 P. de Voogt, D. E. Wells, L. Reutergårdh and U. A. Th. Brinkman, *Int. J. Anal. Chem.*, 40 (1990) 1.
411 R. Fischer and K. Ballschmiter, *Fresenius' Z. Anal. Chem.*, 332 (1988) 441.
412 R. Fischer and K. Ballschmiter, *Fresenius' Z. Anal. Chem.*, 335 (1989) 457.
413 W. L. Zielinski, Jr., M. M. Miller, G. Ulma and S. P. Wasik, *Anal. Chem.*, 58 (1986) 2692.
414 J. de Boer, Q. T. Dao and R. van Dortmond, in P. Sandra (Editor), *Proceedings of the 13th International Symposium on Capillary Chromatography, Riva del Garda, May 1991*, Hüthig, Heidelberg, 1991, p. 225.
415 K. Ballschmiter, R. Bacher, R. Fischer, A. Mennel, U. Riehle and M. Swerev, in P. Sandra (Editor), *Proceedings of the 13th International Symposium on Capillary Chromatography, Riva del Garda, May 1991*, Hüthig, Heidelberg, 1991, p. 501.
416 U. A. Th. Brinkman, J. W. L. Seetz and H. G. M. Reymer, *J. Chromatogr.*, 116 (1976) 353.
417 U. A. Th. Brinkman, A. de Kok, G. de Vries and H. G. M. Reymer, *J. Chromatogr.*, 128 (1976) 101.
418 L. S. Kaminsky and M. J. Fasco, *J. Chromatogr.*, 155 (1978) 363.
419 M. Fránek (Research Institute of Veterinary Medicine, Brno), personal communication.
420 S. H. Safe, G. Mason, T. Sawyer, T. Zacharewski, M. Harris, C. Yao, B. Keys, K. Farrell, M. Holcomb, D. Davis, L. Safe, J. Piskorska-Pliszczynska, B. Leece, M. A. Denomme, O. Hutzinger, H. Thoma, B. Chittim and J. Madge, *Toxicol. Ind. Health*, 5 (1989) 757.
421 D. E. Tillitt, J. P. Giesy and G. T. Ankley, *Environ. Sci. Technol.*, 25 (1991) 87.
422 D. E. Tillitt, G. T. Ankley and J. P. Giesy, *Mar. Environ. Res.*, 28 (1989) 505.
423 D. W. Nebert and H. V. Gilboin, *J. Biol. Chem.*, 243 (1968) 6242.
424 R. J. Pohl and J. R. Fouts, *Anal. Biochem.*, 107 (1980) 150.
425 D. E. Tillitt, G. T. Ankley, D. A. Verbrugge, J. P. Giesy, J. P. Ludwig and T. J. Kubiak, *Arch. Environ. Contam. Toxicol.*, 21 (1991) 91.
426 C. A. Bradfield and A. Poland, *Mol. Pharmacol.*, 34 (1988) 682.
427 C. A. Bradfield, A. S. Kende and A. Poland, *Mol. Pharmacol.*, 34 (1988) 229.
428 L. Zikovsky and M. Badillo, *J. Radioanal. Nucl. Chem.*, 122 (1988) 51.
429 J. Jeník, A. Vojteková, M. Kopanica and V. Stará, *Sci. Pap. Inst. Chem. Technol. Pardubice*, 49 (1986) 195.
430 S. R. Finch, D. A. Lavigne and R. P. W. Scott, *J. Chromatogr. Sci.*, 28 (1990) 351.
431 W. Horwitz, R. K. Laverne and W. K. Boyer, *J. Assoc. Off. Anal. Chem.*, 63 (1980) 1344.
432 P. Hall and B. Selinger, *Anal. Chem.*, 61 (1989) 1465.
433 J. F. Uthe, C. J. Musial and R. K. Misra, *J. Assoc. Off. Anal. Chem.*, 71 (1988) 369.
434 L. G. M. Th. Tuinstra, A. H. Roos, D. E. Wells and B. Griepink, *Mikrochim. Acta, I.*, (1989) 1.
435 J. U. Skaare and A. Polder, *Arch. Environ. Contam. Toxicol.*, 19 (1990) 640.
436 J. U. Skaare, N. Hedlund Markussen, G. Norheim, S. Havgen and G. Holt, *Environ. Pollut.*, 66 (1990) 309.
437 L. M. Hernández, M. A. Fernández and M. J. González, *Bull. Environ. Contam. Toxicol.*, 43 (1989) 725.
438 R. Guitart, J. L. Riu, A. Puigdemont and M. Arboix, *Bull. Environ. Contam. Toxicol.*, 44 (1990) 555.
439 S. Racanelli, B. Pavoni, A. Marcomini and A. A. Orio, *Sci. Total Environ.*, 79 (1989) 111.
440 J. Jan and M. Tratnik, *Bull. Environ. Contam. Toxicol.*, 41 (1988) 809.
441 J. E. Portman, *Dana*, 8 (1989) 95.
442 J. T. Borlakoglu, J. P. G. Wilkins, C. H. Walker and R. R. Dils, *Comp. Biochem. Physiol. C.*, 97 (1990) 161.
443 I. A. Stenhouse and K. S. Badsha, *Chemosphere*, 21 (1990) 563.
444 D. Hrubá, H. Dubský, J. Totušek and H. Koukalová, *J. Hyg. Epidemiol. Microbiol.*, 32 (1988) 273.
445 B. Luckas and M. Oehme, *Chemosphere*, 21 (1990) 79.
446 A. Scheckter, P. Fürst, C. Fürst, W. Groebel, J. D. Constable, S. Kolesnikov, A. Beim, A. Boldonov, E. Trubitsun, B. Vlasov, D. C. Hoang, C. D. Le and T. Q. Hoang, *Chemosphere*, 20 (1990) 799.
447 B. Morton, *Mar. Pollut. Bull.*, 20 (1989) 310.
448 N. Kannan, S. Tanabe, T. Okamoto, R. Tatsukawa and D. J. H. Phillips, *Environ. Pollut.*, 62 (1989) 223.
449 K. Fujiwara, *Environmental and Food Contamination in Japan*, Nakagyo-ward, Kyoto, 1974.
450 A. S. Perry, I. Sidis and A. Zemach, *Bull. Environ. Contam. Toxicol.*, 45 (1990) 523.
451 K. L. E. Kaiser, K. R. Lum, M. E. Comba and V. S. Palabrica, *Sci. Total Environ.*, 97/98 (1990) 23.
452 A. J. Niimi and B. G. Oliver, *Environ. Sci. Technol.*, 23 (1989) 83.
453 J. E. Baker and S. J. Eisenreich, *Environ. Sci. Technol.*, 24 (1990) 342.
454 E. A. Marti and D. E. Armstrong, *J. Great Lakes Res.*, 16 (1990) 369.
455 T. R. Schwartz and D. L. Stalling, *Arch. Environ. Contam. Toxicol.*, 20 (1991) 183.
456 F. I. Onuska and S. Davies, *Int. J. Environ. Anal. Chem.*, 43 (1991) 137.
457 D. T. Williams and G. L. Le Bel, *Chemosphere*, 22 (1991) 1019.
458 J. Japenga, W. J. Wagenaar, W. Salomons, L. D. Lacerda, S. R. Patchineelam and C. M. Leitão Filho, *Sci. Total Environ.*, 75 (1988) 249.
459 B. A. Knoppers, L. D. Lacerda and S. R. Patchineelam, *Mar. Pollut. Bull.*, 21 (1990) 381.
460 S. W. Fowler, *Mar. Environ. Res.*, 29 (1990) 1.
461 P. G. Ryan, A. D. Connell and B. D. Gardner, *Mar. Pollut. Bull.*, 19 (1988) 174.
462 B. N. Ames, R. Magaw and L. Swirsky Gold, *Science*, 236 (1987) 271.
463 R. D. Kimbrough, *J. Toxicol. Environ. Health*, 30 (1990) 261.
464 B. N. Ames, *Sci. Total Environ.*, 104 (1991) 159.
465 S. Tanabe, N. Kannan, A. Subramanian, S. Watanabe and R. Tatsukawa, *Environ. Pollut.*, 47 (1987) 147.

Journal of Chromatography, 595 (1992) 45–52
Elsevier Science Publishers B.V., Amsterdam

CHROM. 23 843

Solvatochromic hydrogen bond donor acidity of cyclodextrins and reversed-phase liquid chromatographic retention of small molecules on a β-cyclodextrin-bonded silica stationary phase

Jung Hag Park*, Myung Duk Jang and Moon Ju Shin

Department of Chemistry, College of Science, Yeungnam University, Kyongsan 712-749 (South Korea)

(First received August 19th, 1991; revised manuscript received October 30th, 1991)

ABSTRACT

Values of the Kamlet–Taft hydrogen bonding (HB) donor acidity (α) and dipolarity/polarizability (π*) parameters for α-, β- and γ-cyclodextrins (CDs) are reported. They possess HB donor acidities in the range 0.21–0.12 and dipolarity/polarizability parameters of about 0.43. Both values are smaller than those for free aliphatic alcohol analogues. The reversed-phase liquid chromatographic retention behaviour of some small molecules on the β-CD bonded silica was compared with that on an octadecylsilylsilica based on the linear solvation energy relationship. It was found that the factors affecting retention on the two stationary phases are very different in that on the ODS column cavity formation and type A HB interactions determine retention whereas on the β-CD column dipolar and type A HB interactions determine retention. Differences in the retention properties of β-CD and ODS phases are rationalized in terms of types of solute–stationary phase interactions involved in the retention process.

INTRODUCTION

Cyclodextrins (CDs) are cyclic oligosaccharides traditionally formed by the action of *Bacillus macerans* amylose on starch. CDs contain six to twelve glucose units which are bonded through α-(1,4) linkages. Among them the three smallest homologues, α-, β- and γ-CD, are commercially available [1]. They have the shape of a hollow truncated cone, the interior of which forms a relatively hydrophobic cavity. The ability of CDs to form inclusion complexes with a variety of compounds has been extensively utilized in many industrial, pharmaceutical, agricultural and other related applications [1,2]. CDs have also been extensively employed in separation science and their applications in liquid chromatography (LC) have recently been reviewed [3–5].

The driving force of complexation is not yet fully understood, but it is widely accepted that the stabilities of CD inclusion complexes are governed by factors such as hydrogen bonding, hydrophobic interactions, solvation effects and the guest molecule's size and shape. To date only a little work has been done to characterize the cavity of the CDs with regard to their polarity [6–8]. CDs have, depending on their size, 18–24 primary and secondary hydroxyl groups on their upper and lower rims, which may undergo hydrogen bonding (HB) interactions with incoming guest molecules. However, HB donor acidity or HB acceptor basicity has not been studied so far. In this paper, we report for the first time the determination of Kamlet–Taft solvatochromic HB donor acidity values (α) [9,10] for α-, β-, and γ-CDs from proton NMR chemical shifts. The α parameter is most conveniently obtained from measurements of the frequency of maximum absorption (ν_{max}) of selected indicators in the solvent of interest [10]. However, electronic absorption spectroscopy could not be employed for the measurement of the α

0021-9673/92/$05.00

values of CDs for the following reason. The most important limitation of application is the lack of a suitable solvent in which CDs show reasonable solubility and an easily measurable shift in ν_{max} occurs on addition of CD. The α value of the solvent must be zero so that HB between the indicator as the HB acceptor and the solvent as the HB donor will not affect the shift in ν_{max}. Dimethyl sulphoxide (DMSO) and N,N-dimethylformamide (DMF) dissolve CDs well and their α values are zero, but in these solvents no appreciable shifts in ν_{max} could be observed when CD was dissolved in the solvent containing an indicator.

In this work, the α values of CDs were conveniently calculated from a correlation of proton NMR chemical shifts of some aliphatic primary and secondary alcohols with their α values. DMSO was chosen as the solvent because the assignments of NMR chemical shifts for CD protons in this solvent were known [11,12]. As DMSO itself is fairly strong HB acceptor base [whose HB acceptor basicity value (β) = 0.76], one has to choose carefully a reference base compound that is a stronger HB acceptor base than the solvent DMSO so that HB interactions between the reference base and alcohol molecules predominate over those between DMSO and alcohol molecules. The size of the reference base should also be small enough to fit entirely into α-CD, whose cavity is the smallest among the three CDs. Hexamethylphosphoramide (HMPA) (β = 1.00), which is the strongest HB acceptor base in the Kamlet–taft scale, meets the above requirements. HB interactions between the acceptor and the donor decreases the electron shielding at the hydrogen of the donor according to the spillover effect [13]. The chemical shift (δ) of a donor proton in the presence of HMPA should then be downfield of that in the solvent alone. The extent of the downfield shift ($\Delta\delta$, ppm) should increase with increasing HB donor acidity of the donor and should be more pronounced for a dilute solution in which the concentration of the reference base is much greater than that of the donor so that isolated donor molecules are surrounded mainly by HMPA molecules. The downfield shifts ($\Delta\delta$) of alcohols thus measured are correlated with their α values, and then the $\Delta\delta$ values of CDs are measured and α values are calculated from this correlation.

Since the introduction of silica-bonded cyclodextrins as high-performance liquid chromatographic stationary phases, they have been widely used in separations of positional, geometric and optical isomers and of simple molecules in both normal- and reversed-phase (RP)modes [4,5]. The major contributor to the separation of these compounds is inclusion complexation and the stabilities of these complexes should affect the elution of the compounds. Factors governing the separation have been discussed [14–16]. It is known that for chiral recognition the analyte must fit into the CD cavity as closely as possible [14]. In addition to the size requirement, HB interactions of the analyte with hydroxyl groups of CD are also essential to chiral recognition [15]. It was suggested that complex formation involves HB interactions with the secondary hydroxyls of CD followed by movement into the cavity [16]. Despite the importance of CD–analyte interactions, few studies on the determination of the types and relative strengths of various CD–analyte intermolecular interactions and their effects on the retention behaviour of analytes has been reported. In this work, we examined the retention behaviour of some small molecules on a β-CD-bonded silica stationary phase in RP-LC based on the linear solvation energy relationships (LSERs) [17,18] to deconvolute the types and relative strengths of CD–analyte interactions affecting retention, and compared the results with those obtained on an ODS stationary phase.

Kamlet, Taft and co-workers applied the LSER approach and their solvatochromic parameters, π^* (polarity/polarizability), β (HB acceptor basicity) and α (HB donor acidity) to *ca.* 600 processes [17,18], including a large number of systems of immediate relevance of chromatography, such as Rohrschneider's gas–liquid partition coefficients [19], retention of McReynold's solutes on polymeric silicone oil gas chromatographic phases [20], and retention in normal- [21] and reversed-phase LC [22–25]. According to the LSER formalism, when applied to phase-transfer processes, a general solute or solvent property (*SP*) can be correlated via the use of three types of terms as follows [17,18]:

$$SP = SP_0 + \text{cavity term} + \text{dipolar term} + \text{hydrogen bonding term(s)} \quad (1)$$

where SP_0 denotes the value of *SP* when all the three terms in the equation are zero. The cavity

term is usually taken as the product of the solute Van der Waals molar volume (V_I) and the square of the Hildebrand solubility parameter (δ) of the solvent. The dipolar term is the product of the solute π^* and the solvent π^*. The π^* parameter measures a combination of the dipolarity and polarizability of a compound. The hydrogen bonding (HB) terms are written as a cross product of the solute α and the solvent β (type B HB) and the product of the solute β and the solvent α (type A HB). In chromatographic retention, SP in the equation below denotes a logarithmic capacity factor, the subscript 2 designates a solute property and the subscripts s and m denote the stationary and mobile phases, respectively:

$$\log k' = \log k'_0 + M(\delta_s^2 - \delta_m^2)V_{I,2}/100 + S(\pi_s^* - \pi_m^*)\pi_2^* + B(\alpha_s - \alpha_m)\beta_2 + A(\beta_s - \beta_m)\alpha_2 \quad (2)$$

where the coefficients M, S, A and B are the fitting parameters.

When a system with a fixed pair of mobile and stationary phases is considered, eqn. 2 is reduced to

$$\log k' = \log k'_0 + mV_{I,2}/100 + s\pi_2^* + b\beta_2 + a\alpha_2 \quad (3)$$

The coefficients m, s, b and a are obtained by multiple linear regression of $\log k'$ *vs.* the solute parameters. The sign and magnitude of the coefficients measure the direction and relative strength of different types of solute–stationary (or mobile) phase interactions affecting retention for a given pair of mobile–stationary phase conditions. When the capacity factors for a series of solutes measured on two different stationary phase columns using a mobile phase of the same composition are examined, the mobile phase parameters in eqn. 2 (δ_m^2, π_m^*, α_m and β_m) are fixed. Any variations in the coefficients m, s, b and a are then determined only by the variations in the stationary phase properties (δ_s^2, π_s^*, α_s and β_s). The values of the coefficients m, s, b and a can be used to compare the corresponding interaction properties of the stationary phases of interest. This approach has been found useful for the characterization of the chromatographic properties of some stationary phases for use in normal [21] and reversed-phase LC [26,27]. We compared the retention properties of β-CD-bonded silica with those of octadecylsilylsilica (ODS) based on the above approach.

EXPERIMENTAL

Chemicals

α-, β- and γ-CD obtained from Aldrich (Milwaukee, WI, USA) were purified by recrystallization from water and dried under vacuum at 80°C. Methanol, ethanol, 1-propanol, 2-propanol, 1-butanol, DMSO and HMPA obtained from Aldrich were dried and fractionally distilled before use as described [28].

Apparatus

NMR spectra were measured at 25°C using a Varian Model EM-360 60-MHz continuous-wave NMR spectrometer with tetramethylsilane (TMS) as the internal reference.

Procedure

The concentration of HMPA was maintained in large excess ([HMPA] > 3 *M*) over of the concentration of hydroxyl groups of alcohols or CDs (0.1 *M*). The chemical shifts of the donor (alcohols and CDs) were measured at concentrations of 0.5, 0.3 and 0.1 *M*. Changes in the chemical shift in this concentration range were negligible. The shifts for the 0.1 *M* donor solution were measured throughout the study, as these values can be safely assumed to be the infinite dilution values. Figs. 1 and 2 show the NMR spectra for ethanol and β-CD in DMSO and in a DMSO solution of HMPA, respectively. The OH proton signals for alcohols and CDs appear within the range accessible with HMPA and DMSO. Very small amounts of water and other impurities in DMSO may be responsible for some of the scatter in the data, but we believe that they do not significantly affect the correlation. Fig. 3 shows the plot of α *vs.* measured $\Delta\delta$ values for dichloromethane and some HB aliphatic alcohols. A reasonably good linear relationship is observed between $\Delta\delta$ and α values (r = 0.984, S.D. = 0.017).

RESULTS AND DISCUSSION

In DMSO solution of HMPA, signals only for O_2H and O_3H hydroxyls of CDs could be observed (see Fig. 2). Table I lists measured $\Delta\delta$ and estimated HB donor acidity values for the O_2H and O_3H hydroxyl groups of α-, β- and γ-CDs. The O_2H hydroxyl has a greater HB donor acidity than the O_3H

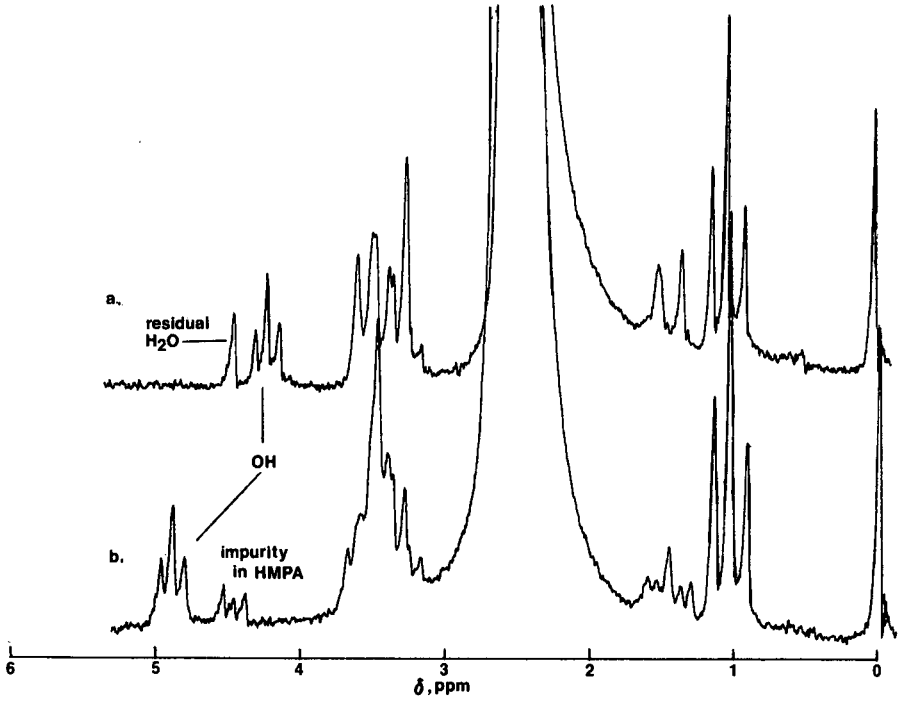

Fig. 1. NMR spectra for ethanol in (a) DMSO and (b) DMSO containing HMPA.

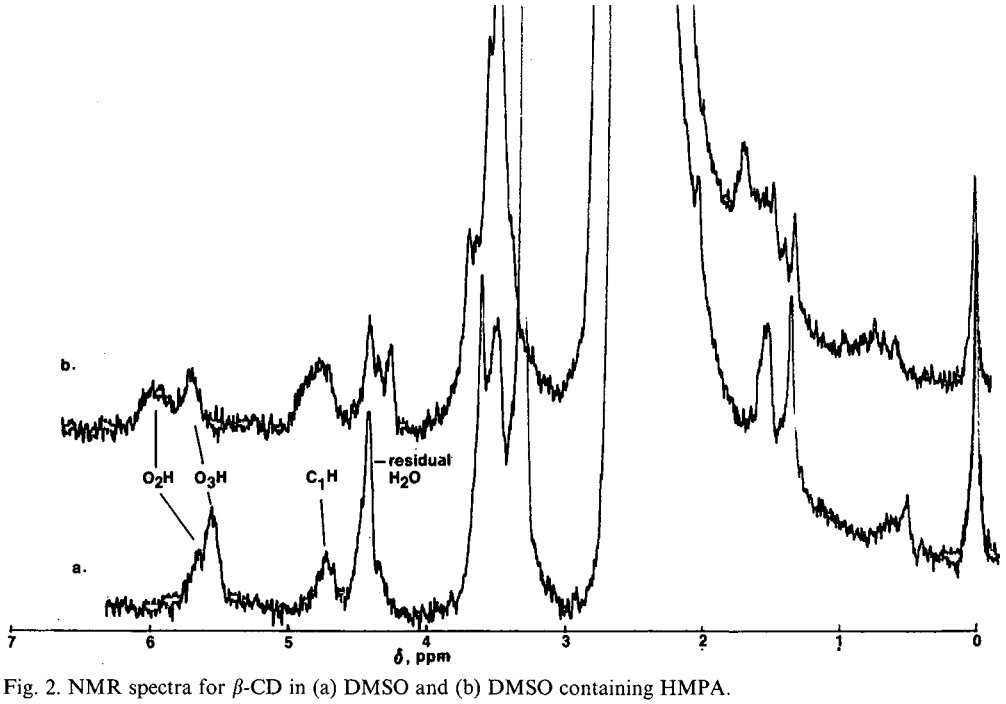

Fig. 2. NMR spectra for β-CD in (a) DMSO and (b) DMSO containing HMPA.

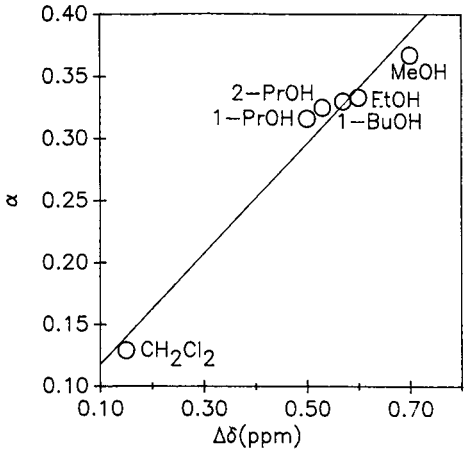

Fig. 3. Plot of HB donor acidity (α) *vs.* $\Delta\delta$. The α values are from Abraham *et al.* [29]. Me = Methyl; Et = ethyl; Pr = propyl; Bu = butyl.

hydroxyl. This is in agreement with the fact that the chemical shift of the O_2H proton is downfield with respect to that for the O_3H proton, indicating that HB interactions with HMPA are stronger for the O_2H hydroxyl. The HB donor acidities of α- and β-CD are the same and greater than that for γ-CD. In view of the fact that the strongest interactions between the guest (HMPA) and CD can occur when the guest is included in the CD cavity with a snug fit [30], a smaller HB donor acidity value for γ-CD is indicative of that the cavity size of γ-CD is too large for HMPA to fit snugly. Overall the HB donor acidities of these secondary hydroxyl groups of CDs are smaller than that for the corresponding hydroxyl group of 2-propanol (α = 0.325 [29]). It is likely that smaller HB donor acidities of CDs than that of the corresponding secondary alcohol are due to the intramolecular hydrogen bond between the O_2H and O_3H hydroxyl groups, which are strong enough to exist even in DMSO [11] and also compete with HMPA in the process of hydrogen bond formation. The HB acceptor basicity of CDs could not be obtained in the solution phase either by electronic absorption spectroscopy or by the present NMR methodology because of the lack of a solvent whose β value is zero.

TABLE I

$\Delta\delta$ (ppm) AND α VALUES FOR CD HYDROXYL PROTONS

Parameter	α-CD		β-CD		γ-CD	
	O_2H	O_3H	O_2H	O_3H	O_2H	O_3H
$\Delta\delta$	0.31	0.15	0.31	0.16	0.22	0.10
α	0.21	0.14	0.21	0.14	0.17	0.12

Determination of the dipolarity/polarizability parameter (π^*) of CDs by the above methodologies in the solution phase is also not feasible for the same reason as for β. The π^* values of CDs may be estimated from the *Py* values [31,32], which are known to represent the polarity of the solvent. The π^* values [33] of some aliphatic alcohols (methanol, ethanol, 1-propanol, 2-propanol, 1-butanol and 2-methoxyethanol) are well correlated with their *Py* values [32], as shown by the following equation:

$$\pi^* = 0.03(\pm 0.03) + 0.43(\pm 0.03)Py \quad (4)$$

$$n = 6,\ r = 0.989,\ \text{S.D.} = 0.01$$

The values of *Py* for CDs have recently been reported [6]. The π^* values calculated from the *Py* values using eqn. 4 are 0.787, 0.428 and 0.431 for α-, β- and γ-CD, respectively. The π^* values for β- and γ-CD are similar but the value for α-CD seems too high. The π^* value of α-CD is believed to be in error as the reported *Py* value of α-CD is known to be erroneous [6]. It has been suggested that pyrene molecules, the probe for use in the determintation of the *Py* value, are too large to fit into the cavity of α-CD [6]. As with the α values for CDs, the π^* values for CDs are lower than those for aliphatic alcohols.

The π^* and α values estimated as above are for free solution CDs. The π^* and α values for bound CDs as in a bonded silica stationary phase would not be the same as the values in solution, as bound CDs are in a different environment owing to microheterogeneity [34,35]. However, it is not expected that the interaction properties of CD will vary much between the free and bound states. Assuming that π^* and α values calculated as above are equally applicable to free or bound CD as in a mobile phase modifier and in bound silica stationary phase, we may compare the solvation ability of CDs. As an example, the solvation ability of β-CD (π^* = 0.43 and α = 0.14–0.21) are more closely approximated by the alkanes (*e.g.*, hexadecane, π^* = 0.08 [36], α = 0.00) than water (π^* = 1.09, α = 1.17 [33]) or

TABLE II

CAPACITY FACTORS[a] AND PROPERTIES OF SOME SOLUTES USED IN MULTIPLE REGRESSION ANALYSES BASED ON THE LSER

Solute	$V_I/100$	π^*	β	α	Log k'	
					β-CD	ODS
Mesitylene	0.769	0.47	0.13	0	−0.678	–
Toluene	0.592	0.55	0.11	0	−0.119	0.785
Benzene	0.491	0.59	0.10	0	0.124	0.497
Anisole	0.630	0.73	0.32	0	−0.237	0.470
Methyl benzoate	0.736	0.76	0.39	0	−0.194	0.410
o-Toluidine	0.660	0.73	0.47	0.13	−0.538	−0.051
m-Toluidine	0.660	0.69	0.51	0.13	−0.538	−0.036
Aniline	0.562	0.73	0.50	0.13	−0.432	−0.229
N-Methylaniline	0.660	0.73	0.47	0.12	−0.409	0.209

[a] Mobile phase: methanol–water (60:40, v/v) [39].

aqueous organic mobile phases ($\pi^* = 1.66$–0.66 [37], $\alpha = 1.17$–0.58 [38]) for solute sizes suitable for the β-CD cavity. This also suggests, according to the LSER (eqn. 2), that the chromatographic properties of β-CD-bonded silica as the stationary phase would be different from those of ODS. Chang *et al.* [39] reported RP–LC capacity factors for a set of solutes on both β-CD-bonded silica and ODS stationary phases in methanol–water mobile phases. We examined these data based on the LSER (eqn. 3) to see how different the two stationary phases are in terms of the type and strengths of interactions with the solutes (see Table II for retention and property data). As cavity formation processes are involved in any transfer processes and β-CD is dipolar and HB donating, we started with regressing capacity factors on the β-CD-bonded silica using the three-parameter equation including the $V_I/100$, π^* and β parameters:

$$\log k' = -0.92(\pm 0.43) - 0.03(\pm 0.39)V_I/100 + 2.77(\pm 0.56)\pi^* - 2.33(\pm 0.31)\beta \quad (5)$$

$n = 9$, $r = 0.964$, S.D. $= 0.088$

Interestingly, the coefficient for the cavity formation term ($V_I/100$) is statistically zero, indicating that the cavity formation process is not affecting the retention of the solutes under study on the β-CD bonded silica. It is not likely that the cavity formation processes truly do not affect the retention process. The model (eqn. 5) may be incomplete because of omission of the solute α parameter. We therefore applied the four-parameter equation including the α parameter:

$$\log k' = 0.53(\pm 1.31) - 0.27(\pm 1.03)V_I/100 + 2.26(\pm 1.68)\pi^* - 1.78(\pm 1.72)\beta - 0.87(\pm 2.68)\alpha \quad (6)$$

$n = 9$, $r = 0.965$, S.D. $= 0.097$

There is no improvement in the goodness of fit and the coefficients for both the $V_I/100$ and α parameter turned out to be statistically zero. This indicates that the two-parameter equation including only π^* and β parameters is appropriate for the representation of retention behaviour on the β-CD bonded phase:

$$\log k' = -0.90(\pm 0.25) + 2.76(\pm 0.48)\pi^* - 2.31(\pm 0.27)\beta \quad (7)$$

$n = 9$, $r = 0.964$, S.D. $= 0.079$

We also checked on the basis of the Ehrenson test [40] whether the resulting three-parameter equation with inclusion of the α term in eqn. 7 improves the fit, and found that the α term is statistically not significant. It should be noted, however, that the data set does not include any HB donor solute stronger than toluidine ($\alpha = 0.13$), so that the dependence on HB donor acidity remains uncertain. The above results indicate that the retention beha-

TABLE III

COMPARISON OF THE COEFFICIENTS IN LSER EQUATIONS FOR RETENTION ON THE β-CD-BONDED SILICA AND ODS STATIONARY PHASES

Column	*m*	*s*	*b*	*a*
β-CD	N.E.[a]	1.45	−1.73	N.E.
ODS	2.52	N.E.	−2.35	N.E.

[a] N.E. = No effect on retention.

viour of the solutes studied on the β-CD bonded phase is well represented by the LSER of eqn. 7. We do not have a firm explanation for the insignificance of the cavity formation term in the retention process on the β-CD-bonded silica. All the analytes studied are of size compatible with the β-CD cavity and it is likely for the transfer process from the mobile phase to the β-CD bonded to silica that cavity formation is not necessary as a cavity for the incoming molecule already exists in β-CD, whereas in other common stationary phases a cavity must be first made for the incoming solute. The CD cavities are known to be hydrophobic [41] and therefore the energetically unfavoured polar–apolar interaction between the included water and the CD cavity is readily substituted without an appreciable expense of energy by the more favoured apolar–apolar interaction between the guest and the CD cavity [42]. However, the above explanation is at best speculative and remains to be confirmed. To this end, retention data for analytes of more varied but still compatible size with the CD cavity should be studied.

Retention data on ODS were examined in a similar fashion to those on the β-CD-bonded silica. The resulting LSER equation is

$$\log k' = -0.46(\pm 0.27) + 2.52(\pm 0.50)V_I/100 - 2.35(\pm 0.22)\beta \quad (8)$$

$$n = 8,\ r = 0.980,\ \text{S.D.} = 0.08$$

As previously observed [22–24], retention on ODS is mainly determined by cavity formation and the solute HB acceptor basicity. The coefficients for the terms in eqns. 7 and 8 are summarized in Table III for comparison. It can be seen that the types of intermolecular interactions affecting retention are different on the two stationary phases and hence there are disparate chromatographic selectivities toward a given set of solutes. On ODS the cavity formation term is the major factor affecting retention whereas on β-CD-bonded silica this term has no effect. On ODS the dipolar interaction term has no effect on retention but on β-CD-bonded silica this term acts to increase the retention. Similar trends in the sign and size of the coefficients in the LSER equations were also observed for retention data in mobile phases with different methanol compositions. As mentioned above, in order for this comparison of the chromatographic properties of the two stationary phases to be validated, a greater number of solutes of widely varying sizes and chemical properties than used in this study must be employed.

ACKNOWLEDGEMENT

This work was supported by the Korea Science and Engineering Foundation under Grant 901-0304-012-1.

REFERENCES

1 J. Szejtli, *Cyclodextrin Technology*, Kluwer, Dordrecht, 1988.
2 W. Saenger, *Angew. Chem., Int. Ed. Engl.*, 19 (1980) 344.
3 W. L. Hinze, *Sep. Purif. Methods*, 10 (1981) 159.
4 D. W. Armstrong and W. Demond, *J. Chromatogr. Sci.*, 22 (1984) 411.
5 D. W. Amrstrong, A. Alak, K. Bui, W. Domond, T. Ward, T. E. Riehl and W. L. Hinze, *J. Inclusion Phenom.*, 2 (1984) 533.
6 K. W. Street, Jr., *J. Liq. Chromatogr.*, 10 (1987) 655.
7 A. Nag and K. Bhattacharyya, *Chem. Phys. Lett.*, 151 (1988) 474.
8 A. Nag. T. Kundu and K. Bhattacharyya, *Chem. Phys. Lett.*, 157 (1989) 83.
9 R. W. Taft and M. J. Kamlet, *J. Am. Chem. Soc.*, 98 (1976) 2886.
10 M. J. Kamlet, J. L. M. Abboud and R. W. Taft, *Prog. Phys. Org. Chem.*, 13 (1981) 485.
11 B. Casu, M. Reggiani, G. G. Galls and A. Vigevanik, *Tetrahedron*, (1966) 3061.
12 M. St.-Jacques, P. R. Sundararaian, K. J. Taylor and R. H. Marchessault, *J. Am. Chem. Soc.*, 98 (1976) 1386.
13 V. Gutmann, *The Donor–Acceptor Approach to Molecular Interactions*, Plenum Press, New York, 1978.
14 D. W. Armstrong, *J. Liq. Chromatogr.*, 7 (1984) 353.
15 D. W. Armstrong, T. J. Ward, R. D. Armstrong and T. E. Beesly, *Science*, 232 (1985) 1132.
16 E. N. Arnold, T. S. Lillie and T. E. Beesley, *J. Liq. Chromatogr.*, 12 (1989) 337.
17 M. J. Kamlet and R. W. Taft, *Acta. Chem. Scand., Ser. B.*, (1985) 611.

18 R. W. Taft, J. L. M. Abboud, M. J. Kamlet and M. H. Abraham, *J. Solution Chem.*, 14 (1985) 153.
19 M. J. Kamlet, R. W. Taft, P. W. Carr and M. H. Abraham, *J. Chem. Soc., Faraday Trans. 1*, 78 (1982) 1689.
20 J. E. Brady, D. Bjorkman, C. D. Herter and P. W. Carr, *Anal. Chem.*, 56 (1984) 278.
21 J. H. Park and P. W. Carr, *J. Chromatogr.*, 465 (1989) 123.
22 P. C. Sadek, P. W. Carr, R. M. Doherty, M. J. Kamlet, R. W. Taft and M. H. Abraham, *Anal. Chem.*, 57 (1985) 2971.
23 P. W. Carr, R. M. Doherty, M. J. Kamlet, R. W. Taft, W. Melander and Cs. Horváth, *Anal. Chem.*, 58 (1986) 2674.
24 J. H. Park, P. W. Carr, M. H. Abraham, R. W. Taft, R. M. Doherty and M. J. Kamlet, *Chromatographia*, 25 (1988) 373.
25 J. H. Park, M. D. Jang and S. T. Kim, *Bull. Korean Chem. Soc.*, 11 (1990) 297.
26 J. H. Park, *Bull. Korean Chem. Soc.*, (1990) 568.
27 J. H. Park, M. D. Jang and S. M. Kwon, *J. Chromatogr.*, submitted for publication.
28 J. A. Riddick, W. B. Bunger, and T. K. Sakano, *Organic Solvents*, Wiley, New York, 4th ed., 1986.
29 M. H. Abraham, P. L. Grellier, D. V. Prior and R. P. Duce, *J. Chem. Soc., Perkin Trans. 2*, (1989) 699.
30 J. F. Wojcik, *Bioorg. Chem.*, 12 (1984) 130.
31 D. C. Dong and A. Winnik, *Photochem. Photobiol.*, 35 (1982) 17.
32 D. C. Dong and M. A. Winnik, *Can. J. Chem.*, 62 (1984) 2560.
33 M. J. Kamlet, J. L. M. Abboud, M. H. Abraham and R. W. Taft, *J. Org. Chem.*, 49 (1983) 2877.
34 C. H. Lochmuller, D. B. Marshall and D. R. Wilder, *Anal. Chim. Acta*, 130 (1981) 31.
35 C. H. Lochmuller, D. B. Marshall and J. M. Harris, Anal. Chim. Acta, 131 (1981) 263.
36 J. E. Brady and P. W. Carr, *J. Phys. Chem.*, 89 (1985) 1813.
37 W. J. Cheong and P. W. Carr, *Anal. Chem.*, 60 (1988) 820.
38 J. H. Park, M. D. Jang, D. S. Kim and P. W. Carr, *J. Chromatogr.*, 513 (1990) 107.
39 C. A. Chang, H. Abdel-Aziz, N. Melchor, Q. Wu, K. E. Pannell and D. W. Armstrong, *J. Chromatogr.*, 347 (1985) 51.
40 S. Ehrenson, *J. Org. Chem.*, 44 (1979) 1793.
41 W. Schlenk and V. M. Sand, *J. Am. Chem. Soc.*, 83 (1961) 2312.
42 M. L. Grayeski and E. Woolf, in L. J. Kricka (Editor), *Analitical Applications of Bioluminescence and Chemiluminescence (Proceedings of 3rd International Symposium)*, Academic Press, London, 1984, p. 565.

Journal of Chromatography, 595 (1992) 53–61
Elsevier Science Publishers B.V., Amsterdam

CHROM. 23 891

Validation of chromatographic retention models in reversed-phase high-performance liquid chromatography by fitting experimental data to the relevant equations

Nina Sadlej-Sosnowska

Drug Institute, 30/34 Chełmska Str., 00-725 Warsaw (Poland)

Irma Śledzińska

Institute of Physics, Warsaw University of Technology, 75 Koszykowa Str., 00-662 Warsaw (Poland)

(First received January 3rd, 1991; revised manuscript received October 8th, 1991)

ABSTRACT

Capacity factors (k') were measured for five steroid hormones in the binary mobile phases methanol–water and acetonitrile–water as a function of methanol and acetonitrile concentration. The results were interpreted in terms of five models of chromatographic retention selected from the many that have been published. The R factor statistic based on the F distribution was used for testing the goodness of fit of the models to the experimental data.

INTRODUCTION

The development of chromatographic methodology and the accumulation of numerous experimental data have been continuously accompanied by interest in the theory of chromatographic retention. This has resulted in various simplified models of the mutual interactions between stationary phase, solutes to be chromatographed and components of the mobile phase. Such chromatographic systems are relatively complicated, so any model can reflect only some aspects of the physico-chemical processes significant to the retention behaviour of a given solute in its environment. These models are most frequently characterized by the functional dependence between capacity factor, k', and the composition of the mobile phase. In reversed-phase high-performance liquid chromatography (RP-HPLC), the mobile phase is a mixture of water and a miscible organic solvent ("modifier"); the composition of the mobile phase is expressed by the volume fraction φ or mole fraction x of the latter. Various models anticipate different relationships connecting k' with φ or x, and the relevant constants have different physical meaning.

Authors of individual approaches or researchers interpreting their experimental results in terms of a given model may state that the goodness of fit of the experimental data to a functional dependence $k'(\varphi)$ or $k'(x)$ supports the theoretical premises on which this dependence is based. Such an implication seems to be well founded. Nevertheless, attempts to interpret any given set of data using more than one theoretical approach and to compare the results are lacking. Among many models and consequently mathematical relationships reported in the literature, we have selected five: (A) Snyder–Soczewiński displacement model [1–3], assuming monolayer adsorption of the solute or solvent on the stationary phase; (B) Scott–Kucera model [4,5] assuming also monolayer adsorption and taking into account dispersion interactions between the solvent and

0021-9673/92/$05.00

solute in the mobile phase; (C) model of Jaroniec and co-workers [6,7], taking into consideration self-association of one component of a binary mobile phase and association of solute molecules with that component; (D) the most universally adopted in RP-LC exponential relationship for $k'(\varphi)$ introduced first for partition chromatography [8,9], assumed to be empirical [10] but it can be justified by consideration of the partition ratio of a substance between the stationary and mobile phases using the Kemula–Buchowski equation [8]; and (E) the Dill lattice statistical thermodynamic theory [11,12] underlying the affinity of the solute for the grafted chains. The same functional (quadratic) dependence was deduced by Schoenmakers and co-workers [13–15]; they introduced solubility parameters for the calculation of intermolecular forces, based on the Hildebrand theory of regular solutions. The same expression was derived by Jandera *et al.* [16]; their model also emphasizes intermolecular interactions between the solute and the mobile phase.

Models A, B and C were elaborated for normal-phase chromatographic systems but we have tried to check them also in RP-LC.

The above-mentioned approaches yield the following functional dependences between k' and φ or x:

$$\text{(A)} \quad \log k' = -(A_s/n_B)\log x + \log k'_B \tag{1}$$

$$\text{(B)} \quad 1/k' = A' + B'\varphi \tag{2}$$

$$\text{(C)} \quad 1/k'x = \alpha + \beta x \tag{3}$$

$$\text{(D)} \quad \log k' = -S\varphi + \log k'_w \tag{4}$$

$$\text{(E)} \quad \log k' = a\varphi^2 + b\varphi + c \tag{5}$$

Some of the parameters have well defined physical meanings, *e.g.*, k'_B in eqn. 1 is the capacity factor in pure organic modifier, k'_w the capacity factor in pure water, A_s the surface area of the adsorbed solute molecule and n_B the surface area of the adsorbed molecule of organic modifier; more complex interpretations of other parameters have been given.

The usefulness of eqns. 1–4 for the interpretation of experimental data was checked by plotting them with the use of coordinates that ought to produce a linear plot. For example, representation of experimental points by functional eqn. 1 ought to give a straight line if the coordinates ($\log k'$, $\log x$) are used.

Eqn. 1, elaborated primarily for adsorption chromatography and applied in such systems [17], has also been used for RP bonded phases in the analysis of proteins [18]. Eqns. 2 and 3 (similarly to eqn. 1) were devised for adsorption, normal-phase chromatography, and to our knowledge have not been applied to RP systems. Eqn. 4 has been successfully applied to the interpretation of chromatographic data in numerous papers [10,19–29]; in most of them the relationship $\log k' = f(\varphi)$ was linear, with few exceptions. The quadratic function in eqn. 5 described the retention of various aromatics [13], including amines and phenols.

Apart from the relationships mentioned above, one can find in the literature many more theoretical approaches and methods of chromatographic data interpretation, *e.g.*, those relating retention to the polarity of the mobile phase [30] and more rigorous models [31] introducing a number of physico-chemical constants that are difficult to determine.

Taking into consideration that the same set of data could be satisfactorily described by different authors by two entirely different approaches [28,32], we decided to try to establish how our own results would fit the several models quoted above. For this purpose we chose a group of five steroid hormones: prednisolone (**1**), hydrocortisone (**2**), methylprednisolone (**3**), testosterone (**4**) and progesterone (**5**).

EXPERIMENTAL

HPLC system

The HPLC system used was a Pye Unicam PU 4100 (pump, oven and UV detector), with a Varian fluorescence detector (for the measurement of void volume, V_0) and Shimadzu R6A integrator. The chromatograms of steroid compounds were monitored at 240 nm. The column used was Partisil 10 ODS (25 cm × 4.6 mm I.D.), maintained at 35 or 22°C with a flow-rate of 1.5 ml/min. V_0 was determined by two techniques: (1) as proposed by Neidhart *et al.* [33], involving the doping of the mobile phase with a fluorophore (quinine sulphate), injection of undoped mobile phase and measuring the decrease in fluorescence; by this method V_0 was determined separately in each mobile phase; and (2) a static method, giving V_0 (static), in which the column was successively filled with two solvents of different density (carbon tetrachloride and isopropanol) and weighed after each filling [34]. This

method gives the maximum value of V_0 (total column porosity). The dead volume was measured after switching the column out of the system and connecting the detector directly with the injection valve. It was equal 0.13 ml both for UV and fluorescence detectors.

Sample preparation

The steroid concentrations were 4 μg/ml ± 10%, always prepared in a given mobile phase (methanol–water or acetonitrile–water) of varying composition.

RESULTS AND DISCUSSION

Determination of the capacity factors, k'

For the five steroid hormones, k' values were investigated with several methanol–water and acetonitrile–water mobile phase compositions. For the calculation of k' (and other dependent parameters) it is necessary to determine V_0, yet there is no universally accepted method for the accurate measurement of this value. The variety of methods for V_0 determination were reviewed by Smith *et al.* [35]; most of them were tried by us. The method proposed by Neidhart *et al.* [33] seemed to be the most reliable. V_0 decreased with increasing fraction of organic modifier, according to the predictions of the statistical mechanical theory of retention [36]. For acetonitrile–water it ranged from 2.86 to 2.64 ml and for methanol–water from 2.85 to 2.80 ml. The static void volume, V_0 (static), the upper limit of V_0, was also determined and used for further calculation because it is well defined and does not depend on the composition of the mobile phase; the results of all other methods for V_0 determination depend not only on the mobile phase composition but also on the substance chosen as a void volume marker. V_0 (static) was equal 3.03 ml. Of the other methods used for V_0 determination, the breakthrough and minor disturbance methods with methanol–water mixtures gave the results which, within experimental error, were identical with the value obtained by static method, but with acetonitrile–water mixtures the breakthrough method, at low acetonitrile concentrations, gave results higher than the upper (static) limit, indicating retention of acetonitrile in the system; at higher acetonitrile concentrations the values obtained by the breakthrough method were,

TABLE I

k' VALUES FOR STEROID HORMONES ON PARTISIL ODS WITH METHANOL–WATER PHASES AT 35°C

φ = Methanol volume fraction; x = methanol mole fraction.

Compound	V_0										
	$\varphi = 0.30$	0.35	0.40	0.45	0.50	0.55	0.60	0.65	0.70	0.75	0.80
	$x = 0.160$	0.193	0.229	0.267	0.308	0.352	0.400	0.453	0.509	0.572	0.640
1	14.5	7.83	4.46	2.62	1.32	1.00	0.72				
2	15.3	8.26	4.71	2.76	1.41	1.06	0.79				
3		14.5	7.79	4.34	2.03	1.50	0.98	0.64			
4				15.1	7.95	4.62	2.93	1.81	1.26	0.89	
5					17.2	8.94	5.19	2.97	1.90	1.25	0.85
	V_0 (static)										
	$\varphi = 0.30$	0.35	0.40	0.45	0.50	0.55	0.60	0.65	0.70	0.75	0.80
	$x = 0.160$	0.193	0.229	0.267	0.308	0.352	0.400	0.453	0.509	0.572	0.640
1	13.6	7.31	4.14	2.40	1.17	0.87	0.60				
2	14.4	7.71	4.37	2.54	1.25	0.93	0.66				
3		13.6	7.27	4.03	1.84	1.34	0.85	0.52			
4				14.2	7.38	4.26	2.66	1.61	1.09	0.75	
5					16.0	8.30	4.76	2.69	1.68	1.08	0.71

within experimental error, identical with those of the method proposed by Neidhart *et al.* [33].

Taking into consideration the above results, we decided to calculate values of k' with double V_0 data, as mentioned under Experimental, and to see if the results of fitting k' to eqns. 1–5 would depend on the choice of V_0. The experimental data are given in Tables I and II.

Statistical analysis of data

The experimental k' values were fitted to eqns. 1–5 using the least-squares method (linear regression). The resulting parameters and correlation coefficients r are given in Tables III–VII. Standard deviations of the parameters are given in parantheses and correspond to the last digit.

A high value of the correlation coefficient r is often considered as validation of an assumed equation. For example, Jaffé [37] arbitrarily classified the goodness of fit into the categories excellent, good (satisfactory) and fair, corresponding to r values of at least 0.99, 0.95 and 0.90, respectively. The tabulated r values are all >0.95 and in most instances >0.99 (Tables III–VII).

However, it was pointed out by Ehrenson *et al.* [38] that the correlation coefficient gives a non-linear acceptability scale, with good and bad correlations often crowded in the range 0.9–1.0, particularly for small samples. Therefore, the conclusions based on this value should be treated with caution.

The R factor statistic, extensively used among crystallographers [39] and employed by Ehrenson [40] for free energy relationship fitting, seems to be a more appropriate measure of the goodness of fit. The generalized R factor [41] is defined as

$$R = \left[\frac{\sum_i (f_i^{obs} - f_i^{calc})^2 \omega_{ii}}{\sum_i (f_i^{obs})^2 \omega_{ii}} \right]^{1/2} \quad (6)$$

where f^{obs} are a set of observed functions and f^{calc} are a set of calculated values for them in some parametrized model representation; ω_{ii} are elements of a diagonal weight matrix and are proportional to the inverse squares of the corresponding uncertainties of the experimental f_i^{obs} values. The statistical character of the chromatographic processes and

TABLE II

k' VALUES FOR STEROID HORMONES ON PARTISIL ODS WITH ACETONITRILE–WATER MOBILE PHASES AT 22°C

φ = Acetonitrile volume fraction; x = acetonitrile mole fraction.

Compound	V_0												
	$\varphi = 0.18$	0.20	0.24	0.28	0.32	0.36	0.40	0.44	0.48	0.52	0.56	0.60	0.64
	$x = 0.070$	0.079	0.098	0.113	0.139	0.162	0.186	0.212	0.241	0.271	0.304	0.340	0.379
1	13.9	9.57	4.94	3.06	2.03	1.42	1.02						
2	14.2	9.99	5.18	3.20	2.12	1.49	1.09						
3		18.1	8.61	5.06	3.13	2.10	1.46	1.07					
4					11.4	7.24	4.77	3.31	2.55	1.95	1.58		
5							12.6	7.91	5.61	3.98	2.98	2.38	1.84
	V_0 (static)												
	$\varphi = 0.18$	0.20	0.24	0.28	0.32	0.36	0.40	0.44	0.48	0.52	0.56	0.60	0.64
	$x = 0.070$	0.079	0.098	0.113	0.139	0.162	0.186	0.212	0.241	0.271	0.304	0.340	0.379
1	13.2	8.84	4.38	2.63	1.68	1.14	0.78						
2	13.5	9.23	4.60	2.76	1.76	1.20	0.84						
3		16.8	7.71	4.43	2.66	1.75	1.17	0.82					
4					10.0	6.30	4.09	2.80	2.11	1.59	1.24		
5							11.0	6.85	4.79	3.36	2.46	1.94	1.47

TABLE III

CONSTANTS OF THE FUNCTIONAL RELATIONSHIP BETWEEN k' AND x, CALCULATED BY SUBSTITUTING DATA FROM TABLES I AND II INTO EQN. 1

r = Linear regression correlation coefficient; meaning of $\mathscr{R}$ is explained in the text.

Compound	V_0							
	Methanol				Acetonitrile			
	Log k'_B	A_s/n_B	r	$\mathscr{R}$	Log k'_B	A_s/n_B	r	$\mathscr{R}$
1	−1.53(7)	3.4(1)	0.997	1.02	−1.96(7)	2.66(7)	0.998	4.16
2	−1.49(7)	3.4(1)	0.997	1.11	−1.92(7)	2.65(7)	0.998	5.26
3	−1.49(7)	3.7(1)	0.997	1.24	−1.91(7)	2.84(8)	0.998	4.05
4	−0.99(5)	3.7(1)	0.998	4.48	−1.15(7)	2.54(9)	0.996	3.69
5	−0.90(4)	4.1(1)	0.998	5.23	−0.89(6)	2.68(9)	0.996	3.69
	V_0 (static)							
	Methanol				Acetonitrile			
	Log k'_B	A_s/n_B	r	$\mathscr{R}$	Log k'_B	A_s/n_B	r	$\mathscr{R}$
1	−1.64(7)	3.5(1)	0.997	1.03	−2.23(6)	2.87(6)	0.999	3.01
2	−1.60(7)	3.5(1)	0.997	1.09	−2.17(6)	2.84(6)	0.999	4.14
3	−1.62(7)	3.8(1)	0.997	1.05	−2.13(7)	3.01(8)	0.998	2.76
4	−1.09(5)	3.8(1)	0.998	3.70	−1.31(6)	2.67(9)	0.997	4.68
5	−1.00(3)	4.3(1)	0.999	4.67	−1.04(5)	2.80(9)	0.997	3.46

TABLE IV

CONSTANTS OF THE FUNCTIONAL RELATIONSHIP BETWEEN k' AND φ, CALCULATED BY SUBSTITUTING DATA FROM TABLES I AND II INTO EQN. 2

r = Linear regression correlation coefficient; meaning of $\mathscr{R}$ is explained in the text.

Compound	V_0							
	Methanol				Acetonitrile			
	A'	B'	r	$\mathscr{R}$	A'	B'	r	$\mathscr{R}$
1	−1.4(2)	4.5(6)	0.965	3.61	−0.7(1)	4.0(4)	0.980	9.56
2	−1.3(2)	4.1(5)	0.968	3.24	−0.7(1)	3.8(3)	0.981	17.3
3	−1.8(3)	4.8(7)	0.954	2.84	−0.8(1)	3.6(4)	0.973	12.8
4	−1.6(2)	3.5(4)	0.965	3.20	−0.7(1)	2.3(1)	0.991	6.85
5	−1.9(3)	3.6(5)	0.956	10.9	−0.7(1)	1.9(1)	0.988	5.62
	V_0 (static)							
	Methanol				Acetonitrile			
	A'	B'	r	$\mathscr{R}$	A'	B'	r	$\mathscr{R}$
1	−1.7(3)	5.3(6)	0.958	4.26	−1.0(2)	5.3(6)	0.971	6.69
2	−1.6(3)	4.8(6)	0.961	3.98	−0.9(2)	4.9(5)	0.974	9.48
3	−2.2(3)	5.8(7)	0.951	3.29	−1.0(2)	4.7(6)	0.964	6.58
4	−1.9(3)	5.0(7)	0.958	7.80	−0.9(1)	2.9(2)	0.987	11.9
5	−2.2(7)	4.3(7)	0.952	5.84	−0.9(1)	2.4(2)	0.984	5.76

TABLE V

CONSTANTS OF THE FUNCTIONAL RELATIONSHIP BETWEEN k' AND x, CALCULATED BY SUBSTITUTING DATA FROM TABLES I AND II INTO EQN. 3

r = Linear regression correlation coefficient; meaning of $\mathscr{R}$ is explained in the text.

Compound	V_0							
	Methanol				Acetonitrile			
	α	β	r	$\mathscr{R}$	α	β	r	$\mathscr{R}$
1	−1.9(3)	13(1)	0.989	1.08	−1.53(3)	36.4(2)	1.0	1.05
2	−1.7(2)	12(1)	0.987	1.03	−1.38(4)	34.0(3)	1.0	1.65
3	−2.1(2)	12(1)	0.990	1.59	−1.56(5)	27.9(3)	1.0	1.66
4	−1.3(1)	5.7(2)	0.996	2.42	−0.57(9)	9.0(4)	0.994	2.94
5	−1.4(1)	4.9(3)	0.993	5.72	−0.51(5)	5.2(2)	0.997	1.99
	V_0 (static)							
	Methanol				Acetonitrile			
	α	β	r	$\mathscr{R}$	α	β	r	$\mathscr{R}$
1	−2.4(3)	16(1)	0.987	1.25	−2.5(1)	49(1)	0.999	1.95
2	−2.2(2)	15(1)	0.988	1.16	−2.3(1)	46(1)	0.999	2.16
3	−2.7(2)	14(1)	0.983	2.06	−2.3(2)	37(1)	0.997	1.93
4	−1.7(2)	6.8(3)	0.993	3.85	−0.90(7)	11.8(3)	0.998	2.03
5	−1.8(2)	6.0(3)	0.989	11.5	−0.75(4)	6.7(3)	0.999	1.35

TABLE VI

CONSTANTS OF THE FUNCTIONAL RELATIONSHIP BETWEEN k' AND φ, CALCULATED BY SUBSTITUTING DATA FROM TABLES I AND II INTO EQN. 4

r = Linear regression correlation coefficient; meaning of $\mathscr{R}$ is explained in the text.

Compound	V_0							
	Methanol				Acetonitrile			
	Log k'_w	S	r	$\mathscr{R}$	Log k'_w	S	r	$\mathscr{R}$
1	2.4(1)	4.4(2)	0.993	1.93	2.0(1)	5.1(3)	0.990	4.26
2	2.4(1)	4.4(2)	0.992	2.01	2.0(1)	5.0(4)	0.990	5.34
3	2.7(1)	4.5(2)	0.992	1.95	2.3(1)	5.0(3)	0.989	4.66
4	2.9(1)	4.1(2)	0.995	5.84	2.1(1)	3.6(2)	0.991	7.55
5	3.3(1)	4.3(2)	0.996	7.11	2.4(1)	3.4(2)	0.993	3.98
	V_0 (static)							
	Methanol				Acetonitrile			
	Log k'_w	S	r	$\mathscr{R}$	Log k'_w	S	r	$\mathscr{R}$
1	2.5(1)	4.6(2)	0.994	1.84	2.0(1)	5.5(3)	0.990	3.82
2	2.5(1)	4.6(2)	0.993	1.79	2.0(1)	5.4(3)	0.991	4.77
3	2.7(1)	4.7(2)	0.994	1.67	2.2(1)	5.3(3)	0.990	3.41
4	3.0(1)	4.2(2)	0.996	3.33	2.1(1)	3.5(2)	0.992	5.74
5	3.4(1)	4.5(2)	0.997	6.69	2.4(1)	3.6(2)	0.994	3.91

TABLE VII

CONSTANTS OF THE FUNCTIONAL RELATIONSHIP BETWEEN k' AND φ, CALCULATED BY SUBSTITUTING DATA FROM TABLES I AND II INTO EQN. 5

r = Linear regression correlation coefficient; meaning of $\mathscr{R}$ is explained in the text.

Compound	V_0									
	Methanol					Acetonitrile				
	a	b	c	r	$\mathscr{R}$	a	b	c	r	$\mathscr{R}$
1	5.31(4)	−9.2(1)	3.47(4)	0.998	1.34	11.7(1)	−11.8(1)	2.88(4)	0.999	2.12
2	5.61(4)	−9.5(1)	3.53(4)	0.998	1.38	11.7(1)	−11.7(1)	2.88(3)	1.0	2.87
3	5.54(4)	−10.1(1)	4.01(4)	0.998	1.01	10.2(1)	−11.6(1)	3.14(4)	0.999	2.25
4	4.81(2)	−9.8(1)	4.63(3)	1.0	1.15	7.0(1)	−9.7(1)	3.45(3)	1.0	1.16
5	4.54(2)	−10.2(1)	5.21(3)	1.0	1.05	5.7(1)	−9.3(1)	3.92(3)	0.999	1.57
	V_0 (static)									
	Methanol					Acetonitrile				
	a	b	c	r	$\mathscr{R}$	a	b	c	r	$\mathscr{R}$
1	4.65(4)	−8.8(1)	3.37(4)	0.998	1.53	11.7(1)	−12.2(1)	2.92(4)	0.999	3.11
2	5.01(4)	−9.1(1)	3.44(4)	0.998	1.36	11.7(1)	−12.2(1)	2.93(3)	1.0	3.31
3	4.69(4)	−9.4(1)	3.85(4)	0.998	1.01	10.3(1)	−11.9(1)	3.17(4)	0.999	2.44
4	4.39(2)	−9.5(1)	4.52(3)	1.0	1.14	6.5(1)	−9.5(1)	3.73(3)	1.0	1.21
5	4.07(2)	−9.8(1)	5.07(3)	1.0	1.13	5.4(1)	−9.2(1)	3.85(3)	1.0	1.52

many sources of random and systematic errors make the evaluations of the weight ω_{ii} very difficult. Therefore, we arbitrarily put $\omega_{ii} = 1$ in all our calculations.

It should be noted that the numerator in eqn. 6 is the root-mean-square deviation of the fitted set, being the explicit variable in the least-squares procedure.

Different mathematical formulations of the retention model are virtually equivalent to different data sets (*i.e.*, $1/k'$, $1/k'x$, $\log k'$, φ, x) taken into account in the calculations.

It is well known that each set of experimental data can be approximated by a polynomial of sufficiently high order.

Eqns. 1–4 assume a linear relationship of the variables (a polynomial of order one) and eqn. 5 a quadratic relationship (polynomial of order two). To verify the goodness of fit of a given equation to the experimental data, the hypothesis that the approximation by the polynomial of order p-1 is as good as the approximation by the polynomial of order p was tested. Therefore, the higher power terms were added, *i.e.*, quadratic to eqns. 1–4 and cubic to eqn. 5.

The ratio

$$\mathscr{R} = R_{p-1}/R_p$$

was compared with

$$\mathscr{R}_{1,n-p-1,\alpha} = \left(\frac{1}{n-p-1} \cdot F_{1,n-p-1,\alpha} + 1\right)^{1/2} \qquad (7)$$

where F is the well known Fisher (Snedecor) distribution [42] and n is the number of experimental points. If $\mathscr{R} > \mathscr{R}_{1,n-p-1,\alpha}$, the hypothesis that the polynomial of order $p-1$ provides as good a fit as the polynomial of order p may be rejected on the $100\alpha\%$ significance level. Consequently, we may conclude that the approximation of the data by the polynomial of order $p-1$ does not give a satisfactory fit. Of course, an increase in a polynomial order

always improves the agreement, and we must weigh the utility of the equation (we prefer a model with a smaller number of parameters) against the increased accuracy given by a proper choice of the significance level α. The rejection at a significance level of 1% may be regarded as "highly significant" (see ref. 41, p. 48).

The above procedure (method) seems to be particularly useful for comparison of models D and E. In these models, the same variables ($\log k'$ and φ) are used and eqn. 5 is obtained by adding a quadratic term to eqn. 4.

For the remaining models, the validation of the linear approximation was tested. The calculated values of $\mathscr{R}$ are shown in Tables III–VII; they should be compared with the values $\mathscr{R}_{1,4,0.01} = 2.51$ and $\mathscr{R}_{1,3,0.01} = 3.52$ for models A–D and E, respectively.

CONCLUSIONS

From Tables III–VII, we can see that for models A, B, D and E the differences between parameters calculated for V_0 and V_0 (static) are in most instances not greater than the sum of the corresponding standard deviations. The correlation coefficients are also very similar and values of $\mathscr{R}$ calculated for the two dead volumes lead to the same conclusions regarding the goodness of fit. This is not true for model C, for which the parameters α and β change significantly. The $\mathscr{R}$ values given in Table V (calculated for V_0) indicate that the hypothesis about the approximation of data by a straight line cannot be rejected at the 99% confidence level for four compounds (exceptions are compound **5** in methanol–water and **4** in acetonitrile–water). For V_0 (static) the $\mathscr{R}$ values are different and the hypothesis must be rejected for two compounds in methanol–water and for three in acetonitrile–water. Further considerations are based on the r and $\mathscr{R}$ values calculated for V_0 as void volume.

Table V shows that higher values of correlation coefficients are not always correlated with smaller values of $\mathscr{R}$. For example, for compound **5** in methanol–water $\mathscr{R} = 5.72$ and $r = 0.993$, but for **2**, $\mathscr{R} = 1.03$ corresponds to $r = 0.987$. Comparison of the approximation of the experimental data for these two compounds by a straight line (see Fig. 1) indicates that the $\mathscr{R}$ value is a more reliable measure of the goodness of fit. In agreement with this R value criterion, models A and D cannot be rejected only for compounds **1–3** in methanol–water (see Tables III and VI). For model D it is equivalent to the

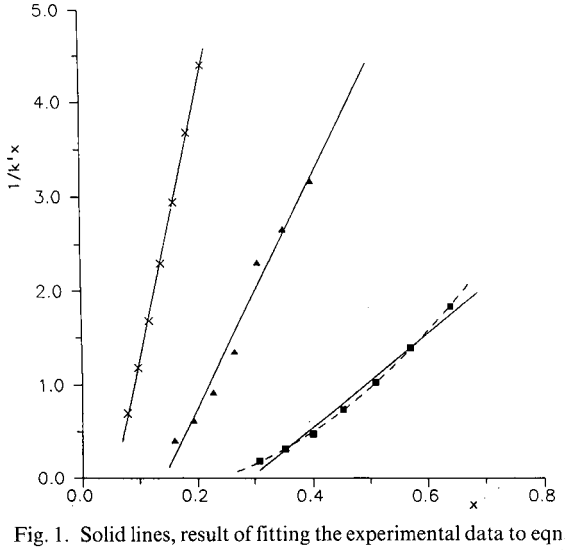

Fig. 1. Solid lines, result of fitting the experimental data to eqn. 3 (model C); dashed line, fitting the experimental data to eqn. 3 with added second-order term. × = Compound **3**, acetonitrile–water; ▲ = compound **2**, methanol–water; ■ = compound **5**, methanol–water.

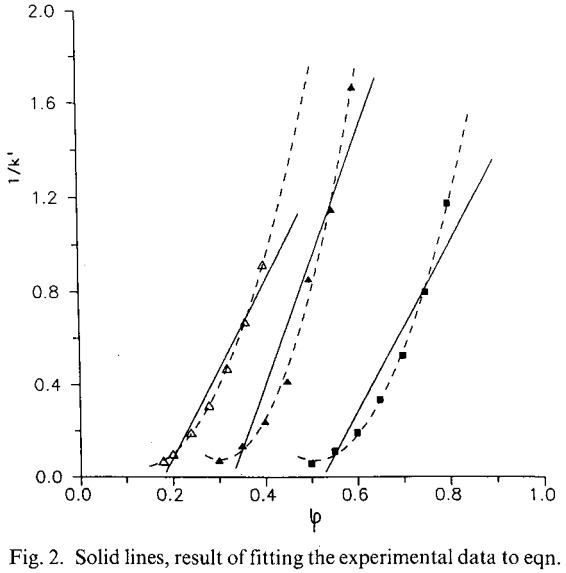

Fig. 2. Solid lines, result of fitting the experimental data to eqn. 2 (model B); dashed line, fitting the experimental data to eqn. 2 with added second-order term. △ = compound **2**, acetonitrile–water; ▲ = compound **1**, methanol–water; ■ = compound **5**, methanol–water.

conclusion that only for those data sets can we not choose between this model and model E. The latter, as can be seen from Table VII, describes satisfactorily the experimental data for all the compounds.

Model B should be rejected for all the compounds (see Table IV). Fig. 2 shows us that eqn. 2 corresponding to this model is inadequate for the approximation of our experimental data.

According to Jaffé's classification [37], the goodness of fit of the experimental data by model B is good and by models A, C, D and E is excellent even in cases when the points evidently do not follow a straight line. Hence we can conclude that the estimation of the goodness of fit based on correlation coefficients cannot be sufficiently discriminating.

It must be pointed out that our method of verification of the models does not give any indication of how to improve the equations in accordance with the physico-chemical premises of these models. Addition of a higher power term serves only for the evaluation of the goodness of fit of an original equation.

ACKNOWLEDGEMENT

This investigation was supported by a grant from the Ministry of Health and Social Welfare under MZ VII-155 to N.S.-S.

REFERENCES

1 L. R. Snyder, *Principles of Adsorption Chromatography*, Marcel Dekker, New York, 1968, Ch. 8.
2 E. Soczewiński, *Anal. Chem.*, 41 (1969) 179.
3 L. R. Snyder, *Anal. Chem.*, 46 (1974) 1384.
4 R. P. W. Scott and P. Kucera, *J. Chromatogr.*, 112 (1975) 425.
5 R. P. W. Scott, *J. Chromatogr.*, 122 (1976) 35.
6 M. Jaroniec and J. Piotrowska, *J. High Resolut. Chromatogr. Chromatogr. Commun.*, 3 (1980) 257.
7 M. Jaroniec, J. A. Jaroniec and W. Gołkiewicz, *J. High Resolut. Chromatogr. Chromatogr. Commun.*, 4 (1981) 89.
8 E. Soczewiński and C. A. Wachtmeister, *J. Chromatogr.*, 7 (1962) 311.
9 E. Soczewiński and G. Matysik, *J. Chromatogr.*, 32 (1968) 458.
10 L. R. Snyder, J. W. Dolan and J. R. Gant, *J. Chromatogr.*, 165 (1979) 31.
11 K. A. Dill, *J. Phys. Chem.*, 91 (1987) 1980.
12 P. Y. Ying, J. G. Dorsey and K. A. Dill, *Anal. Chem.*, 61 (1989) 2540.
13 P. J. Schoenmakers, H. A. H. Billiet and L. de Galan, *J. Chromatogr.*, 149 (1978) 519.
14 P. J. Schoenmakers, H. A. H. Billiet and L. de Galan, *J. Chromatogr.*, 218 (1981) 261.
15 R. Tijssen, H. A. H. Billiet and J. Schoenmakers, *J. Chromatogr.*, 122 (1976) 185.
16 P. Jandera, H. Colin and G. Guiochon, *Anal. Chem.*, 54 (1982) 435.
17 E. Soczewiński, *J. Chromatogr.*, 388 (1987) 91.
18 X. Geng and F. E. Regnier, *J. Chromatogr.*, 296 (1984) 15.
19 J. A. Schmidt, R. A. Henry, R. C. Williams and J. F. Dieckman, *J. Chromatogr. Sci.*, 9 (1971) 645.
20 S. R. Abbott, J. R. Berg, P. Achener and R. L. Stevenson, *J. Chromatogr.*, 126 (1976) 421.
21 B. L. Karger, J. R. Gant, A. Hartkopf and P. H. Weiner, *J. Chromatogr.*, 128 (1976) 65.
22 K. Karch, I. Sebestian, I. Halász and H. Engelhardt, *J. Chromatogr.*, 122 (1976) 171.
23 A. Hulshoff and J. H. Perrin, *J. Chromatogr.*, 129 (1976) 263.
24 N. Tanaka and E. R. Thornton, *J. Am. Chem. Soc.*, 99 (1977) 7300.
25 J. W. Dolan, J. R. Gant and L. R. Snyder, *J. Chromatogr.*, 165 (1979) 31.
26 I. Atamna, E. Grushka, H. Colin and G. Guiochon, *Chromatographia*, 19 (1984) 48.
27 H. Engelhardt and H. Muller, *Chromatographia*, 19 (1984) 77.
28 H. A. Cooper and R. J. Hurtubise, *J. Chromatogr.*, 360 (1986) 313.
29 A. Opperhuizen, T. L. Sinnige, J. M. D. van der Steen and O. Hutzinger, *J. Chromatogr.*, 388 (1987) 51.
30 W. J. Cheong and P. W. Carr, *Anal. Chem.*, 61 (1989) 1524.
31 Cs. Horváth, W. Melander and I. Molnár, *J. Chromatogr.*, 125 (1976) 129.
32 T. Kowalska, *Chromatographia*, 27 (1989) 628.
33 B. Neidhart, K. P. Kringe and W. Brockmann, *J. Liq. Chromatogr.*, 4 (1981) 1875.
34 G. E. Berendsen, P. J. Schoenmakers, L. de Galan, G. Vigh and Z. Varga-Puchony, *J. Liq. Chromatogr.*, 3 (1980) 1669.
35 R. J. Smith, C. S. Nieass and M. S. Wainwright, *J. Liq. Chromatogr.*, 9 (1986) 1387.
36 J. G. Dorsey and K. A. Dill, *Chem. Rev.*, 89 (1989) 331.
37 H. H. Jaffé, *Chem. Rev.*, 53 (1953) 191.
38 S. Ehrenson, R. T. C. Brownlee and R. W. Taft, *Prog. Phys. Org. Chem.*, 10 (1973) 1.
39 W. C. Hamilton, *Acta Crystallogr.*, 18 (1965) 502.
40 S. Ehrenson, *J. Org. Chem.*, 44 (1979) 1793.
41 W. C. Hamilton, *Statistics in Physical Science*, Ronald Press, New York, 1964.
42 G. W. Snedecor and W. Cochran, *Statistical Methods*, Iowa State University Press, Ames, IA, 6th ed., 1967.

Journal of Chromatography, 595 (1992) 63–75
Elsevier Science Publishers B.V., Amsterdam

CHROM. 23 932

Chromatographic resolution on methylbenzoylcellulose beads

Modulation of the chiral recognition by variation of the position of the methyl group on the aromatic ring

Eric Francotte* and Romain M. Wolf

Pharmaceutical Research, K-122.P.25, Ciba-Geigy Ltd., 4002 Basle (Switzerland)

(First received October 16th, 1991; revised manuscript received December 5th, 1991)

ABSTRACT

The preparation of cellulose-based chiral stationary phases (CSPs) in the pure polymer form (*i.e.*, without an achiral support such as silica gel), according to a process already reported for benzoyl cellulose, was extended to substituted benzoylcellulose derivatives. The chiral recognition abilities of benzoylcellulose and *o*-, *m*- and *p*-methylbenzoylcellulose were compared. The four CSPs are shown to exhibit different selectivities and in numerous instances an inversion of the elution order was observed on the different methylbenzoylcellulose CSPs, indicating that the CSPs undergo different interactions with the same racemic solute. The broad variety of racemic structures that can be resolved on the four CSPs indicate the great application potential of the new cellulose-based sorbents. This should be the case especially for preparative separations, as the materials are not deposited on an achiral supporting matrix and thus have a higher loading capacity than coated CSPs.

INTRODUCTION

There is an increasing demand for the isolation of the enantiomerically pure forms of new chiral biologically active compounds owing to the necessity to investigate the relationships between the stereochemistry of these compounds and their biological activity. Therefore, the individual enantiomers should be isolated easily and at low cost with high optical purity, in amounts adequate for performing biological tests, toxicological studies and even, at a later stage, clinical or field tests. Chromatography on chiral stationary phases has been recognized as a useful tool in respect of these requirements and is now established as a simple, efficient and generally applicable method for this purpose.

Among the numerous chiral stationary phases (CSPs) that have been investigated and developed during the last decade, cellulose-based phases have been identified as very versatile and useful chiral sorbents for the separation of enantiomers [1]. Numerous applications have been reported on microcrystalline cellulose triacetate (CTA I) used in the pure polymeric form [1] and a variety of other cellulose derivatives have been introduced for the same purpose by Okamoto *et al.* [1] as a coating of *ca.* 20% polymer weight on silica. Most of these silica-coated materials are now commercially available and they show very different selectivities depending on the derivatizing groups on cellulose.

We recently developed a process for the preparation of benzoylcellulose beads in the pure cellulosic form, avoiding the use of the expensive macroporous silica support, and producing a material that consists of 100% chiral sorbent, resulting in a high loading capacity [2,3]. Owing to the excellent chro-

0021-9673/92/$05.00

matographic properties and its high loading capacity, this new chiral sorbent is useful for both analytical applications and preparative purposes. Using the same procedure we prepared further benzoylcellulose derivatives in the pure polymer form [2] and examined their chiral recognition abilities. In this study, we investigated the influence of the position of the methyl group of methylbenzoylcellulose on the chiral recognition abilities of the CSP. For this purpose a series of racemic compounds were chromatographed on benzoylcellulose and on *o*-, *m*- and *p*-methylbenzoylcellulose.

EXPERIMENTAL

Preparation of the chiral phases

General procedure for the preparation of methylbenzoylcellulose (ortho-, meta- or para). To a suspension of 10 g of microcrystalline cellulose in a mixture of 100 ml of pyridine and 45 ml of triethylamine containing 0.2 g of dimethylaminopyridine are slowly added at room temperature 40 g of toluoyl chloride (*ortho-*, *meta-* or *para*). The temperature rises to 40–50°C. After the addition, the mixture is stirred for 20 h at 120°C under nitrogen. After cooling to room temperature, the solid mass obtained is treated with 4 l of methanol. The insoluble part is filtered and washed twice with methanol. The product is dissolved in dichloromethane and precipitated twice in ethanol. The light brown powder is dried for 2 days at 100°C under vacuum. Yield: 95–98%. Elemental analysis: methylbenzoylcellulose (*ortho-*, *meta-* or *para-*) $(C_{30}H_{28}O_8)_n$, calculated, C 69.8, H 5.5, O 24.8%; *o*-methylbenzoylcellulose (OMBC), found C 69.2, H 5.5, O 25.3%; *m*-methylbenzoylcellulose (MMBC), found C 69.3, H 5.5, O 25.2%; *p*-methylbenzoylcellulose (PMBC), found C 69.5, H 5.6, O 24.9%.

p-Methylbenzoylcellulose beads. A solution of 10 g of *p*-methylbenzoylcellulose dissolved in a mixture of 300 ml of dichloromethane and 50 ml of heptanol is added dropwise to an aqueous solution (240 ml) of sodium lauryl sulphate (0.7%) stirred mechanically at 400 rpm in a 1-l flask. After the addition, stirring is maintained and the emulsion is heated at 40–42°C (bath temperature) to remove the dichloromethane slowly by distillation. After complete removal of dichloromethane, the residual suspension is filtered and the solid is washed first with water and then with ethanol. The powder is dried under vacuum at 80°C for 20 h (yield 9.5 g, 95%). The material consists of more or less spherical particles of cellulose benzoate as determined by electron microscopy [3] (size 5–10 μm) and can be used directly for chromatographic separations. The specific surface are determined by the BET method was 69 m^2/g. Differential scanning calorimetric (DSC) analysis of the material showed a melting point at 267°C.

m-Methylbenzoylcellulose beads. Analogously, 10 g of *m*-methylbenzoylcellulose in 300 ml of dichloromethane and 50 ml of heptanol are added to an aqueous solution (240 ml) of sodium lauryl sulphate (0.7%). After removal of the dichloromethane, the solid is washed and dried (yield, 9.4 g, 94%). The particle size was 10–20 μm, specific surface area 58 m^2/g and melting point by DSC 246°C.

o-Methylbenzoylcellulose beads. A solution of 5 g of *o*-methylbenzoylcellulose dissolved in a mixture of 300 ml of tetrahydrofuran (THF) and 12 ml of heptanol is added dropwise to an aqueous solution (300 ml) of sodium lauryl sulphate (0.7%) stirred mechanically at 400 rpm in a 1-l flask. After the addition, stirring is maintained and the emulsion is heated at 70–75°C (bath temperature) to remove the THF slowly by distillation. After complete removal of THF the residual suspension is filtered and the solid is washed first with water and then with ethanol. The powder is dried under vacuum at 80°C for 20 h (yield 4.9 g, 98%). The material consists of more or less spherical particles of cellulose methylbenzoate (size 5–20 μm) and can be used directly for chromatographic separations. The specific surface area determined by the BET method was 36 m^2/g. DSC analysis of the material showed a melting point at 246°C.

Chromatographic conditions

The methylbenzoylcellulose beads were slurry packed as a suspension in hexane–isopropanol (9:1) or methanol in stainless-steel high-performance liquid chromatographic (HPLC) columns (25 × 0.46 cm I.D.). The columns were washed with the same mobile phase until UV absorption was no longer detected at a wavelength of 254 nm. Chromatography was performed using the same mobile phase composition (hexane–isopropanol or metha-

nol) at a constant flow-rate (usually 1 ml/min). The dead time of the columns was determined by injection of 1,3,5-tri-*tert.*-butylbenzene used as a non-retained compound. Typically, 10 μl of a 1% solution of racemate dissolved in the mobile phase used for chromatography were injected.

General

Solvents were of analytical-reagent grade. All compounds synthesized in this work were characterized spectroscopically (^{1}H NMR, IR) and gave satisfactory elemental analyses. NMR measurements were recorded on a Bruker VM 250-MHz spectrometer. X-ray measurements were performed on a Philips powder diffraction instrument as described previously [3]. Melting points were determined by DSC on a Mettler TA3000 system.

Apparatus

The HPLC experiments were performed with a modular liquid chromatograph composed of an Altex Model 110A pump and a Shimadzu Model UV-120-02 multi-wavelength UV detector in series with a Perkin-Elmer Model 241 LC polarimeter equipped with an 80-μl cell (length 10 cm). Both signals (UV absorption and optical rotation) were recorded and processed by an IBM PC-AT3 microcomputer, via a DYSC WD 24 analogue interface module using MAXIMA 820 chromatographic software (Carlo Erba, Milan, Italy).

RESULTS AND DISCUSSION

Preparation of stationary phases

Analogously to the preparation of benzoylcellulose beads reported recently [3], *p*- and *m*-methylbenzoylcellulose beads were prepared from a suspension of the corresponding cellulose derivative dissolved in dichloromethane, in water containing sodium lauryl sulphate and in the presence of a long aliphatic chain alcohol (Fig. 1). In the case of *o*-methylbenzoylcellulose, when using dichloromethane as a solvent, the specific surface area of the beads produced is very low, resulting in very bad chromatographic properties. In contrast, when *o*-methylbenzoylcellulose (OMBC) is dissolved in THF, a good specific surface area is obtained, yielding an efficient chromatographic support material. X-ray investigations (Fig. 2) and DSC measure-

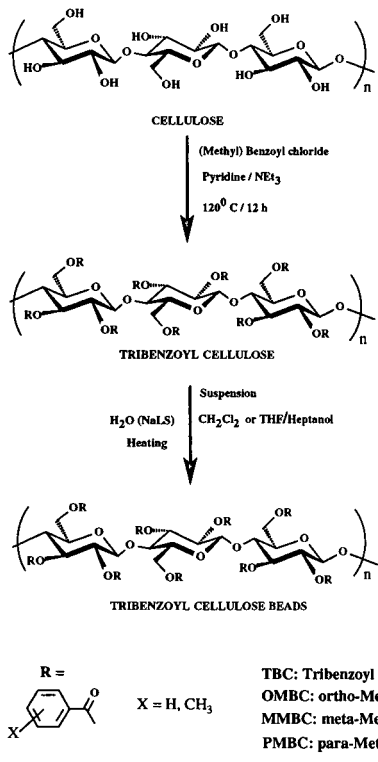

Fig. 1. Preparation of methylbenzoylcellulose beads.

ments (see Experimental) indicate that the different cellulose derivatives are at least partially crystalline, confirming the necessity to have a certain supramolecular structure in the polymer in order to achieve good chiral recognition.

Chromatographic resolutions

In order to investigate the influence of the position of the methyl group attached to the benzoyl moiety on the chiral recognition ability, various classes of racemates were chromatographed on benzoylcellulose and on the different methylbenzoylcellulose derivatives. The cellulose-based chiral stationary phases were found to exhibit very different selectivities, behaving like completely different sorbents.

The acetate derivatives of various racemic aliphatic alcohols or diols were chromatographed on the different benzoylcellulose esters reported in this work and the results are summarized in Table I. The best resolutions of the enantiomers are clearly obtained with unsubstituted tribenzoylcellulose

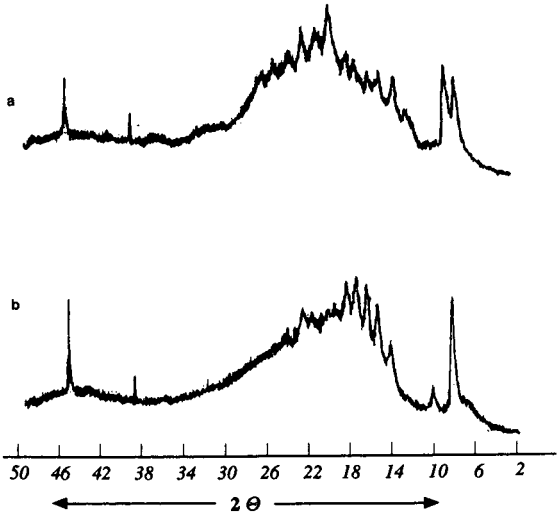

Fig. 2. X-ray powder diffractograms of (a) MMBC and (b) PMBC beads (after annealing of the samples for 45 min at 200°C).

(TBC), whereas the substituted methylbenzoyl derivatives exhibit only poor chiral recognition, independently of the position of the methyl group. *p*-Methylbenzoylcellulose (PMBC) shows virtually no selectivity. These results indicate that TBC is the most appropriate CSP for relatively small molecules, especially for aliphatic compounds (Fig. 3), as we have illustrated more widely in a previous paper [3].

We have reported previously [3] that numerous racemic aryl alkanols can be well resolved on TBC beads. The comparative results presented in Table II confirm that TBC is generally the most appropriate stationary phase for the resolution of this class of compounds, except for **12**, which is not resolved on TBC but very well on MMBC. Only partial resolutions could be achieved for phenylethanol (**7**) and phenylpropanol (**8**) on MMBC and PMBC. Moreover, in the series of phenylalkanol derivatives **7**–

TABLE I

CHROMATOGRAPHIC RESULTS FOR ACETATE DERIVATIVES OF ALIPHATIC ALCOHOLS

k'_2 = Capacity factor of the more strongly retained enantiomer and, in parentheses, its absolute configuration or sign of the optical rotation at 365 nm; α = separation factor; HPLC column, 25 × 0.46 cm I.D.; mobile phase, hexane–2-propanol (90:10). Ac = Acetyl; Et = ethyl.

Compound	Structure	Parameter	Chiral stationary phase			
			TBC	OMBC	MMBC	PMBC
1	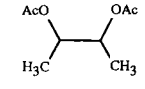	k'_2	6.98 (+)	1.82	10.66 (−)	2.35
		α	3.13	1.00	1.21	1.00
2	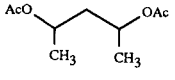	k'_2	1.80 (−)	0.59 (−)	2.28	2.18
		α	1.32	1.00	1.00	1.00
3	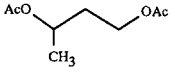	k'_2	10.24 (−)	1.78	4.75	3.54
		α	2.14	1.00	1.11	1.00
4		k'_2	3.62 (−)	0.57	2.28 (+)	2.14
		α	1.48	1.00	1.22	1.00
5	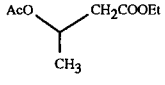	k'_2	5.04 (+)	1.39 (+)	2.60	2.72
		α	1.40	1.0	1.00	1.00
6	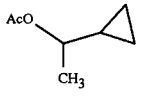	k'_2	2.67 (−)	1.86	0.90 (−)	0.10 (−)
		α	1.19	1.00	1.0	1.0

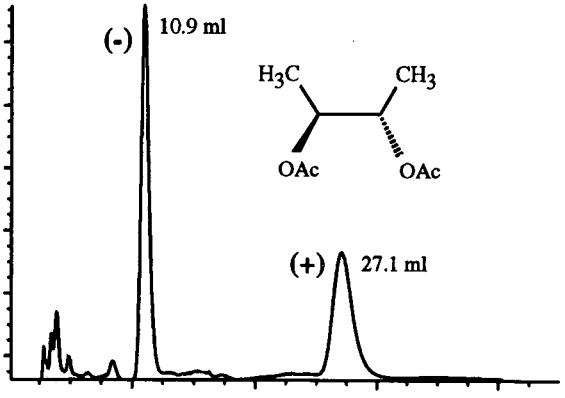

Fig. 3. Chromatographic separation of the enantiomers of racemic 2,3-butanediol diacetate (**1**) on TBC beads. HPLC column, 25 × 0.46 mm I.D.; mobile phase, hexane–2-propanol (9:1); flow-rate, 1 ml/min.

11, the separation factors and the capacity factors decrease on TBC as the chiral centre carrying the alcohol function is further away from the phenyl ring. The inversion of the elution order observed for **12** as the position of the methyl group on the CSP is changed from the *ortho* to the *meta* position and again from the *meta* to the *para* position clearly demonstrates that small alterations of the chemical structure of the cellulose-based CSP (even far away from the chiral carbon centres located on the sugar moieties) can totally modify the chiral recognition ability of the CSPs.

The chromatographic results summarized in Table III for a series of 3-phenylcyclopentanone and cylohexanone derivatives show that the chiral recognition is strongly dependent on the substituent attached to the phenyl ring of the racemic solute. The enantiomers of the 3-phenylcyclopentanone derivatives **17** and **18** are only resolved on MMBC, but the elution order is reversed for both compounds (*S* more retained for **17** and *R* for **18**), indicating that the interaction mechanisms are different. Both compounds have been preparatively re-

TABLE II

CHROMATOGRAPHIC RESULTS FOR ARYLAKANOLS

For definitions and chromatographic conditions, see Table I.

Compound	Structure	Parameter	Chiral stationary phase			
			TBC	OMBC	MMBC	PMBC
7	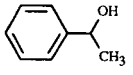	k'_2	5.06 (*R*)	0.63 (*R*)	3.81 (*R*)	3.95 (*R*)
		α	1.76	1.0	1.15	1.13
8	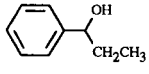	k'_2	2.72 (*R*)	0.54 (*R*)	3.02 (*R*)	3.35 (*R*)
		α	1.43	1.0	1.12	1.05
9	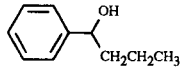	k'_2	2.62 (+)	0.38 (+)	2.38	2.62
		α	1.48	1.0	1.00	1.00
10	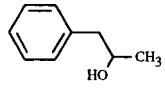	k'_2	2.03 (+)	0.57 (+)	2.41 (−)	3.08
		α	1.10	1.0	1.0	1.00
11	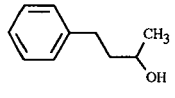	k'_2	1.47 (+)	0.46	2.26	2.62
		α	1.0	1.0	1.00	1.00
12	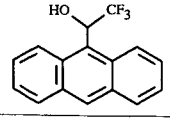	k'_2	5.92	3.97 (*S*)	38.14 (*R*)	22.80 (*S*)
		α	1.00	1.25	1.84	1.18

TABLE III

CHROMATOGRAPHIC RESULTS FOR PHENYLCYCLOALKANONE DERIVATIVES

For definitions and chromatographic conditions, see Table I.

Compound	Structure	Parameter	Chiral stationary phase			
			TBC	OMBC	MMBC	PMBC
13	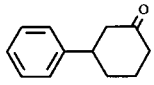	k'_2 α	3.80 1.00	5.90 (+) 1.51	7.36 (+) 1.0	6.32 (−) 1.0
14	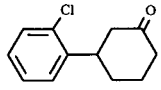	k'_2 α	4.27 (−) 1.0	5.83 (+) 1.40	7.45 (+) 1.0	5.61 (−) 1.0
15	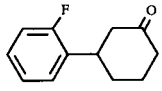	k'_2 α	3.60 (−) 1.0	4.38 (+) 1.36	4.96 (−) 1.0	4.78 (−) 1.0
16	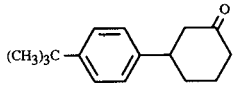	k'_2 α	1.46 (−) 1.0	0.96 (−) 1.0	8.41 (+) 1.96	2.83 (+) 1.0
17	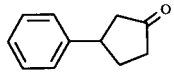	k'_2 α	7.09 (*R*) 1.0	5.49 (*R*) 1.0	12.75 (*S*) 1.12	9.36 (*S*) 1.0
18	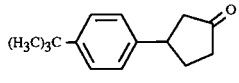	k'_2 α	2.39 (*S*) 1.0	1.48 (*R*) 1.0	6.00 (*R*) 1.32	4.60 (*R*) 1.0

solved as intermediates for the synthesis of new fungicides [4]. The enantiomers of 3-phenylcyclohexanone and of both *o*-halo-3-phenylcyclohexanone derivatives **14** and **15** (Fig. 4) are only separated on OMBC, whereas the *tert.*-butyl derivative **16** (Fig. 4) is only resolved on MMBC, as in the case of the corresponding cyclopentanone derivative **18**. Moreover, for most of the cycloalkanone derivatives we observed variations of the elution order depending on the position of the methyl group on the methylbenzoylcellulose CSP.

Various alkyl and phenyl lactone derivatives were

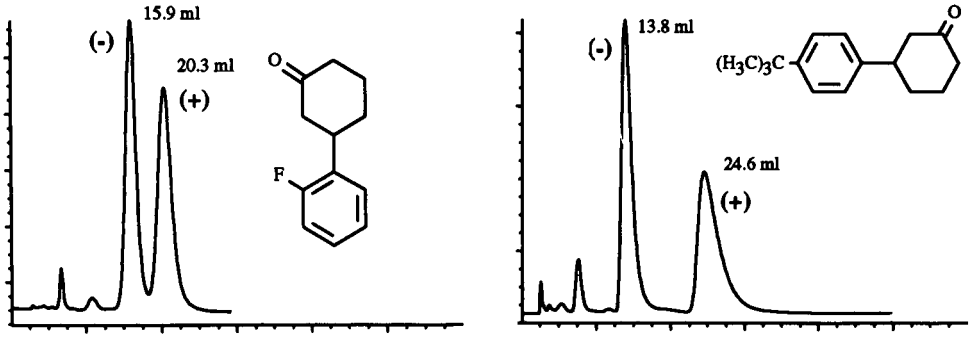

Fig. 4. Chromatographic resolution of the racemic cyclohexanone derivatives **15** on OMBC (left) and **16** on MMBC (right). For chromatographic conditions, see Fig. 3.

TABLE IV

CHROMATOGRAPHIC RESULTS FOR LACTONE DERIVATIVES 19–25

For definitions and chromatographic conditions, see Table I. Et = ethyl; Pr = propyl; Bu = butyl; Hex = hexyl;

Compound	Structure	Parameter	Chiral stationary phase			
			TBC	OMBC	MMBC	PMBC
19a	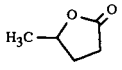	k'_2 α	17.29 (*S*) 1.15	5.80 (*R*) 1.0	10.94 (*S*) 1.05	10.90 1.00
19b	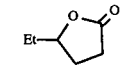	k'_2 α	11.83 (*R*) 1.06	4.49 (*R*) 1.0	7.28 (*S*) 1.0	8.45 1.00
19c	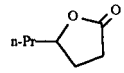	k'_2 α	9.47 (*R*) 1.04	3.69 (*R*) 1.0	6.17 (*S*) 1.04	7.30 1.0
19d	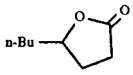	k'_2 α	6.14 1.00	3.06 1.00	5.20 1.00	5.66 1.00
19e	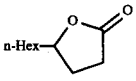	k'_2 α	4.00 1.00	2.23 1.0	3.85 1.00	4.14 1.00
20	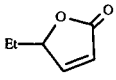	k'_2 α	17.15 (*R*) 1.17	5.39 (*R*) 1.0	10.00 1.00	11.71 1.00
21	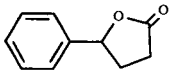	k'_2 α	36.90 (*R*) 1.39	13.18 1.00	27.22 (*R*) 1.24	27.90 1.00
22	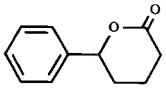	k'_2 α	37.76 (+) 1.17	16.32 1.00	23.70 1.00	33.64 (−) 1.08
23	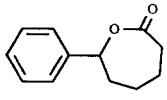	k'_2 α	13.53 1.66	8.98 3.19	7.51 1.00	11.48 1.00
24	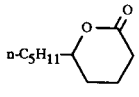	k'_2 α	4.95 (+) 1.13	2.29 (−) 1.0	3.77 1.00	4.53 1.00
25	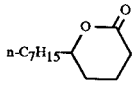	k'_2 α	3.67 (+) 1.08	1.79 1.00	2.45 1.00	3.55 1.00

chromatographed on TBC, OMBC, MMBC and PMBC (Table IV). In the series of five- and six-membered ring lactones, the best enantiomeric resolution is always observed on the TBC beads CSP. For the alkyl-substituted lactones, the separation factors decrease as the length of the alkyl substituent increases, contrasting with the results obtained with cellulose triacetate [5], where a maximum α value was reached for the butyl derivative **19d**. The inversion of the elution order on TBC between the methyl **19a** (*S* more strongly retained) and the ethyl **19b** (*R* more retained) derivative cannot be explained.

The size of the lactone ring also has a strong in-

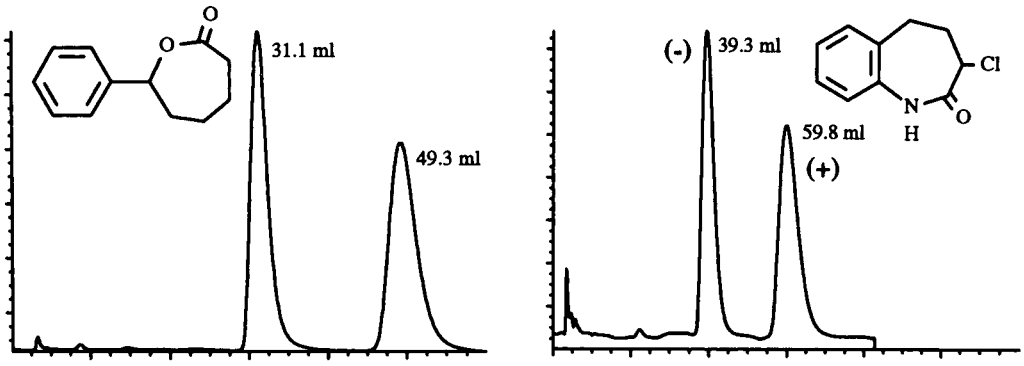

Fig. 5. Chromatographic resolution of both seven-membered-ring compounds **23** (left) and **28** (right) on TBC beads. For chromatographic conditions, see Fig. 3.

fluence on the separation, as indicated by the chromatographic results of the phenyl lactone derivatives **21–23** on the four different CSPs. While the enantiomers of phenylbutyrolactone (**21**) and phenylvalerolactone (**22**) are better separated on TBC beads, the seven-membered ring lactone derivative **23** is better resolved on OMBC (Fig. 5).

Racemic acylated nitrogen compounds or weakly basic nitrogen derivatives can also be resolved on CSPs consisting of cellulose esters. This is illustrated by the chromatographic resolution of **28** (Fig. 5) and **29** on TBC, of **30** on OMBC and of **31** on MMBC (Table V). For the resolution of racemic molecules with a C_2 axis of symmetry, PMBC seems to be the most appropriate CSP, as observed for binaphthol (**26**) and the biphenyl derivative **27** (Table V). For these compounds, which exhibit very high capacity factors using hexane–2-propanol as a mobile phase, pure methanol as the eluent strongly reduces the retention time, without a decrease in selectivity, however. The results obtained with both glycidyl ether derivatives **32** and **33** show that the CSP is very sensitive to the steric hindrance of the solute. For the methyl-substituted compound **32**, OMBC exhibits the best chiral recognition, whereas for the *tert.*-butyl derivative **33**, PMBC gives the best selectivity.

In addition to the racemic compounds presented before, a variety of racemic drugs and biocides were investigated on the four cellulose-based CSPs. Although a prediction of the separation was not possible, we could identify in most instances at least one among the four different investigated CSPs which was able to separate the enantiomers efficiently (Table VI). Even for analogous structures we found that the best selectivity was not necessarily achieved on the same CSP. For example, for the hypnotic drugs mephobarbital (**40**) and hexobarbital (**41**), the former is better resolved on MMBC and the latter on TBC. Racemic thalidomide (**42**), which is not soluble in hexane–2-propanol (9:1), was chromatographed with methanol as the mobile phase and a baseline resolution was achieved on PMBC (Fig. 6). The enantiomers of glutethimide (**39**) are well resolved either on OMBC or on PMBC (Fig. 6), whereas the metabolite **43** of methsuximide, a five-membered ring imide analogue of glutethimide, is better resolved on TBC. The resolution of the methyl ester of the non-steroidal anti-inflammatory drug (NSAID) oxindazac (**34**) was easily achieved on MMBC, similarly to other propionic acid methyl ester derivatives. The four isomers of the fungicide CGA 80000 (**38**) [6] can be baseline separated on MMBC (Fig. 8). This example illustrates the ability of MMBC to recognize simultaneously the chirality at the carbon centre of the lactone ring and the atrope isomerism induced by the hindered rotation of the trisubstituted phenyl ring around the nitrogen atom. Although the selectivity exhibited by TBC for the enantiomeric separation of the anti-cancer agent **35** [7] is higher with hexane–2-propanol (60:40) as the mobile phase (α = 3.55), the resolution can also be performed with methanol. Moreover, the selectivity can be considerably enhanced by addition of water to the methanol mobile phase (Fig. 8).

The various examples reported in Tables I–VI show that the cellulose-based CSPs are very versatile and in many instances also complementary in their selectivities. The dependence of the chiral recognition ability of methylbenzoylcellulose on the position of the methyl substituent on the phenyl group has already been observed for the corresponding silica-coated CSPs [8], but no inversion of the elution order for the same solute has so far been reported. The inversion of the elution order observed for many racemates (compounds **10**, **12–17**, **19a–c**, **26**, **28–32**), as illustrated in Fig. 9 for com-

TABLE V

CHROMATOGRAPHIC RESULTS FOR MISCELLANEOUS RACEMIC COMPOUNDS

For definitions and chromatographic conditions, see Table I.

Compound	Structure	Parameter	Chiral stationary phase			
			TBC	OMBC	MMBC	PMBC
26	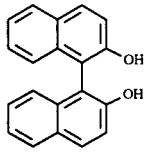	k'_2	1.43	7.89	32.45 (*R*)	63.11 (*S*)
		α	1.00	1.00	1.17	1.45
		k'_2	0.62 (*S*)[a]	–	–	2.45 (*S*)[a]
		α	1.0	–	–	1.42[a]
27	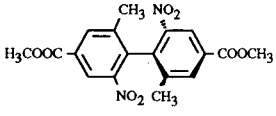	k'_2	72.75	31.10	22.82	129.51
		α	1.00	1.00	1.00	1.25
		k'_2	5.33[a]	–	–	9.09
						(–)[a]
		α	1.00	–	–	1.24[a]
28	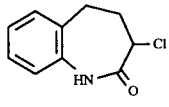	k'_2	16.63 (+)	8.05 (–)	15.86 (+)	13.50 (+)
		α	1.57	1.0	1.22	1.10
29	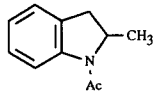	k'_2	19.20 (–)	3.58 (+)	8.70 (–)	9.01 (–)
		α	2.53	1.0	1.22	1.0
30	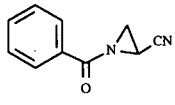	k'_2	37.05 (*R*)	16.21 (*R*)	33.02 (*S*)	24.16 (*S*)
		α	1.16	1.19	1.16	1.10
31	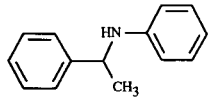	k'_2	11.16 (*R*)	2.56 (*R*)	18.85 (*R*)	13.27 (*S*)
		α	1.13	1.16	1.43	1.10
32	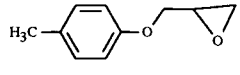	k'_2	7.21 (*R*)	3.69 (*S*)	10.09 (*R*)	11.23 (*R*)
		α	1.15	1.31	1.15	1.12
33	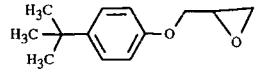	k'_2	2.51	1.28	6.04	6.95
		α	1.00	1.00	1.11	1.19

[a] Mobile phase: methanol.

TABLE VI

CHROMATOGRAPHIC RESULTS FOR VARIOUS DRUGS AND BIOCIDES

For definitions and chromatographic conditions, see Table I.

Compound	Structure	Parameter	Chiral stationary phase			
			TBC	OMBC	MMBC	PMBC
34	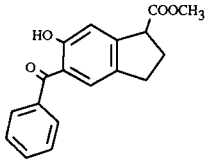	k'_2 α	15.83 1.28	5.95 1.00	25.11 2.29	27.81 1.05
35	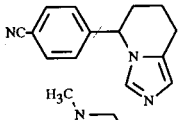	k'_2 α	2.26 (+)[a] 1.62[a]	– –	– –	1.93 (+)[a] 1.10[a]
36	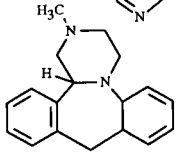	k'_2 α	1.17 (−)[a] 1.0[a]	– –	– –	2.92 (+)[a] 1.31[a]
37	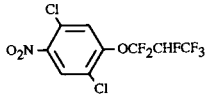	k'_2 α	2.96 (−) 1.24	1.63 1.28	5.33 1.00	4.62 1.00
38	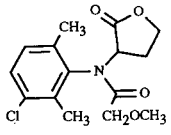	k'_2 α k'_2 α	– – – –	– – – –	14.40 (+)[b] 2.11[b] 23.53 (+)[b] 2.30[b]	14.16 (+)[b] 1.29[b] 14.65 (+)[b] 1.34[b]
39	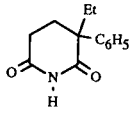	k'_2 α	17.74 (−) 1.23	17.31 (−) 1.76	32.26 1.31	28.14 (−) 1.65
40	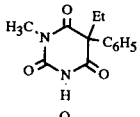	k'_2 α	16.33 1.00	11.92 1.29	38.27 1.30	53.44 1.0
41	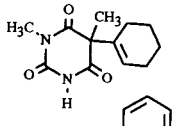	k'_2 α	19.87 1.46	8.21 1.0	21.49 1.0	37.32 1.28
42	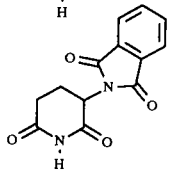	k'_2 α	2.59 (−)[a] 1.26	– –	– –	4.26 (−)[a] 1.39
43	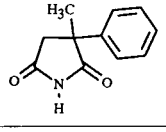	k'_2 α	20.86 1.00	12.96 1.00	19.95 1.20	42.04 1.56

[a] Mobile phase: methanol.

[b] Mobile phase: hexane–2-propanol (60:40).

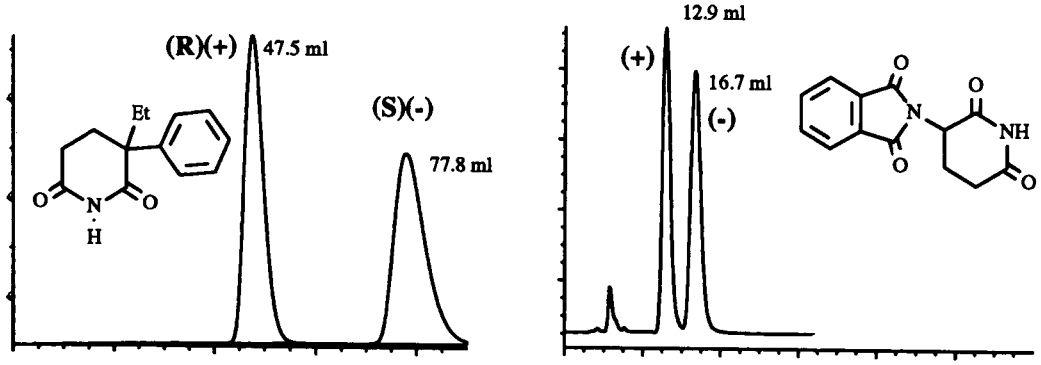

Fig. 6. Chromatographic resolution on PMBC of racemic glutethimide (**39**) (left) (for chromatographic conditions, see Fig. 3) and thalidomide (**42**) (right) (chromatographic conditions as in Fig. 3, but with methanol as the mobile phase).

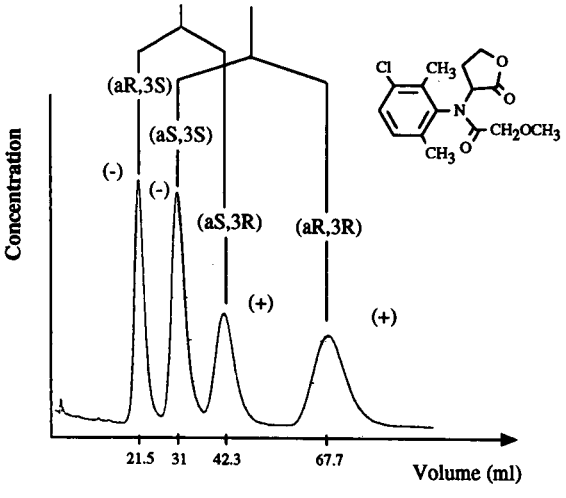

Fig. 7. Chromatographic resolution of the four optical isomers of CGA 80 000 on MMBC. HPLC column 25 × 0.46 cm I.D.; mobile phase, hexane–2-propanol (6:4); flow-rate, 1 ml/min.

pounds **12, 30** and **31**, demonstrates the dramatic influence of the position of the methyl radical attached to the benzoyl group on the chiral recognition, showing that the three methylbenzoylcellulose derivatives behave like totaly different sorbents. The preparative separation of the enantiomers of **30** on MMBC and the absolute configuration have been reported previously [9]. The elution order of the enantiomers of **31** has been determined by injection of the individual enantiomers obtained by condensation of the corresponding enantiomers of phenylethylamine with bromobenzene [10].

The great differences in selectivities exhibited by TBC, OMBC, MMBC and PMBC indicate that very slight modifications of the substituents or its position on the benzoyl group can lead to important alterations of the shape of the chiral receptors. This shape is defined by the arrangement of the polymer

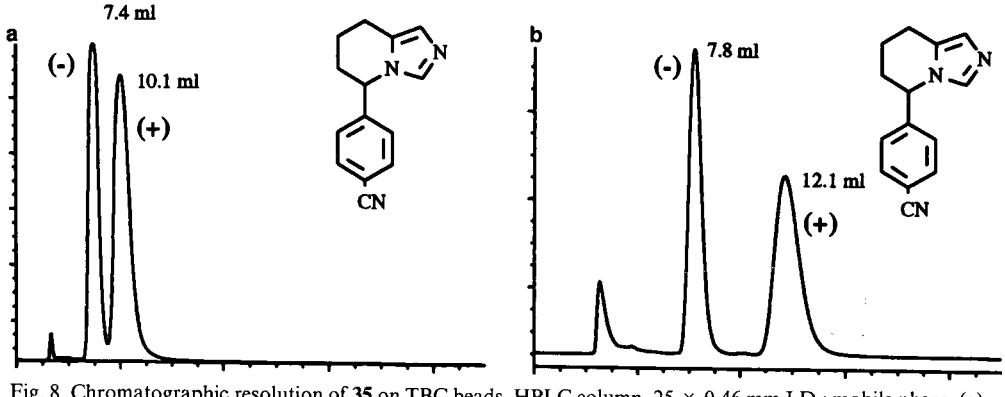

Fig. 8. Chromatographic resolution of **35** on TBC beads. HPLC column, 25 × 0.46 mm I.D.; mobile phase, (a) methanol at a flow-rate of 1 ml/min and (b) methanol–water (95:5) at a flow-rate of 0.5 ml/min.

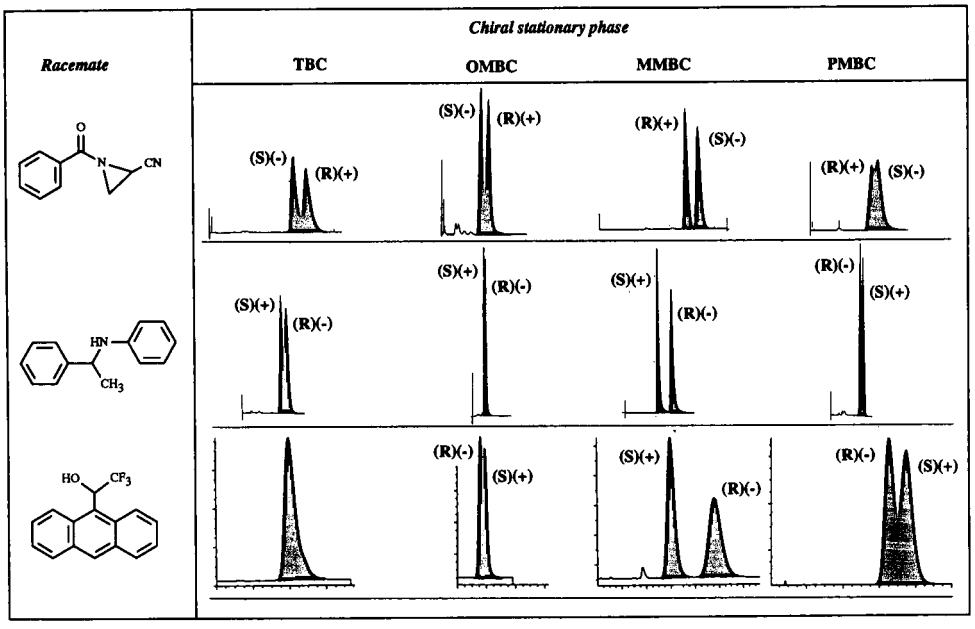

Fig. 9. Analytical resolutions of racemic compounds **30** (top), **31** (middle) and **12** (bottom) on TBC, OMBC, MMBC and PMBC beads. For chromatographic conditions, see Fig. 3.

chains and/or by the actual conformation of the benzoyl groups. Although achiral *per se*, the benzoyl groups can obviously transfer the chiral information of the sugar moiety to which they are attached, further into the space around the polymer chains, thus creating chiral cavities.

Whereas the main-chain conformation of the polymer is presumably not dramatically affected by slight variations on the phenyl groups, the conformation of the phenyl groups themselves is certainly altered. Also, the packing of the polymer chains in ordered (crystalline or at least semi-crystalline) arrays must be affected. The influence of the supramolecular structure of cellulose derivatives on their chiral recognition has been revealed by studies carried out on cellulose triacetate [11]. In this instance, a change in the actual crystalline packing scheme, without any chemical changes, was found to reverse the elution order of some enantiomers. It is therefore not surprising that the presence and position of a methyl group on the phenyl group of methyl benzoylcellulose can induce similar effects. However, these effects are a clear indication that the chiral recognition process on cellulose derivatives is based on a large number of weak, well balanced, interactions and not, or only rarely, on a few, but very well defined, strong interactions between distinct atom groups (*e.g.*, hydrogen bonds or π-π interactions). This may explain the surprisingly broad range of different racemic compounds that can be resolved on derivatized cellulose CSPs.

These results also illustrate the difficulty of making predictions concerning a separation. Although some empirical rules can be applied, it is very difficult to decide by a rational method which CSP has to be used for a given compound.

The new CSPs described in this work are not only suitable for analytical purposes but also, because of their high loading capacity, they are particularly useful for preparative separations as we have already demonstrated for benzoylcellulose beads (TBC) [3]. Such preparative applications will be reported later.

CONCLUSIONS

Various cellulose-based CSPs have been prepared in the pure polymeric form (without supporting material) according to a new process. By simple variation of the position of the methyl substituent on

the phenyl group of the methylbenzoylcellulose CSPs, completely different chiral recognition abilities have been observed. In some instances, even an inversion of the elution order of the enantiomers has been observed, depending only on the position of the methyl group.

In most instances, a good resolution of the racemates could be achieved on at least one of the benzoylcellulose CSPs, indicating that the four different CSPs have complementary selectivities. These results demonstrate that a large number of racemates can probably be resolved with a limited number of cellulose derivatives, starting from the same inexpensive material, cellulose. Although a rationalization of the influence of the derivatizing group of cellulose is still impossible, the versatility of the cellulose derivatives offers a large application potential. Mechanistically, the results suggest that supramolecular effects (crystal packing) play an important role in the chiral recognition, in accordance with our previous investigations on cellulose triacetate [11]. A better understanding of these effects could lead to a controlled modulation of the chiral recognition by variations of the substituent and its position on the phenyl group of the respective benzoylcellulose derivatives.

ACKNOWLEDGEMENTS

Thanks are due to Miss G. Baisch and Mrs. M.-L. Piccolotto for excellent technical assistance. We thank Professor A. Eschenmoser (ETH, Zürich) for providing the racemate **30** and Drs. J. Drabek, W. Eckhardt, W. Fisher, A. Huxley and M. Lang, Ciba-Geigy, Basle, for supplying the racemates **37**, **38**, **31**, **16–18** and **35**, respectively. We are grateful to Dr. A. Burkhard (Ciba-Geigy) for recording X-ray powder diffractograms.

REFERENCES

1 T. Shibata, K. Mori and Y. Okamoto, in A. M. Krstuvolic (Editor), *Chiral Separation by HPLC—Applications to Pharmaceutical Compounds*, Wiley, New York, 1989, pp. 336–398.
2 E. Francotte and G. Baisch, *Eur. Pat.*, EP 0316 270 A2 (1988).
3 E. Francotte and R. M. Wolf, *Chirality*, 3 (1991) 43.
4 A. Huxley-Tencer, E. Francotte and M. Bladocha-Moreau, *Pestic. Sci.*, in press.
5 E. Francotte and D. Lohmann, *Helv. Chim. Acta*, 70 (1987) 1569.
6 W. Eckhardt, E. Francotte, J. Herzog, W. Kunz and P. Margot, *Pestic. Sci.*, submitted for publication.
7 R. E. Steele, L. B. Mellor, W. K. Sawyer, J. M. Wasvary and L. J. Browne, *Steroids*, 50 (1987) 147.
8 Y. Okamoto, R. Aburantani and K. Hatada, *J. Chromatogr.*, 389 (1987) 95.
9 S. Drenkard, J. Ferris and A. Eschenmoser, *Helv. Chim. Acta*, 73 (1990) 1373.
10 W. Fischer, Ciba-Geigy, Basle, unpublished results.
11 E. Francotte, R. M. Wolf, D. Lohmann and R. Müller, *J. Chromatogr.*, 347 (1985) 25.

Journal of Chromatography, 595 (1992) 77–88
Elsevier Science Publishers B.V., Amsterdam

CHROM. 23 913

Preparation of nitrophenylethylsilylated silica gel and its chromatographic properties in the separation of polychlorinated dibenzo-*p*-dioxins

Kazuhiro Kimata, Ken Hosoya, Nobuo Tanaka* and Takeo Araki

Kyoto Institute of Technology, Department of Polymer Science and Engineering, Matsugasaki, Sakyo-ku, Kyoto 606 (Japan)

D. G. Patterson, Jr.

Centers for Disease Control, Toxicology Branch, Atlanta, GA 30333 (USA)

(First received October 18th, 1991; revised manuscript received November 25th, 1991)

ABSTRACT

Nitrophenylethylsilylated (NPE) silica gel was prepared from phenylethylsilylated silica gel by direct nitration, and its chromatographic properties were compared with those of C_{18} and pyrenylethyl (PYE) bonded phase in reversed-phase high-performance liquid chromatography. The NPE phase showed preferential retention for aromatic compounds, especially for those with dipolar character. In contrast, PYE phase showed preferential retention for symmetrically substituted aromatic compounds. The combination of NPE and PYE phases provided the selectivity required for the separation of isomers of polychlorinated aromatic compounds, namely polychlorodibenzo-*p*-dioxins (PCDDs). The two stationary phases, having aromatic functionalities of opposite nature, also provided the possibility of structural assignment of PCDD isomers based on the chromatographic retention on the two phases.

INTRODUCTION

Reversed-phase high-performance liquid chromatography (RP-HPLC) has been used for the separation of extremely wide ranges of compounds owing to its high performance and the applicability of alkylsilylated silica packing materials (C_{18}). In addition, several packing materials capable of charge-transfer interactions have been reported. This adds more selectivity to RP-HPLC, whereas the most popular silica C_{18} packing materials separate solutes mainly based on their total hydrophobic properties. Although steric discrimination by the alkyl groups in the stationary phase has been observed [1–3], the interaction between the bonded alkyl groups and solutes is believed to be weak [4].

Pyrenylethylsilylated (PYE) silica gel offered much greater selectivity towards molecules with a difference in planarity in aromatic and alicyclic structures [5]. Graphite carbon packing materials have been reported to be even more selective for these compounds based on the strong planarity recognition, charge-transfer interactions and the contribution of dispersion forces [6–9]. These two types of packing materials possess common features in that the planar binding sites having electron-donating and hydrophobic properties contribute to the retention process [9].

When applied to the separation of polychlorinated aromatic compounds, PYE phase permitted the separation of polychloropyrenes [10] and most of the 22 isomers of tetrachlorodibenzo-*p*-dioxins (TCDDs) [11]. Another charge-transfer type of stationary phase having an electron-withdrawing group on an aromatic ring, nitrophenylethylsilylated (NPE) silica gel, permitted the separation of TCDD isomers [12], which was not possible with either C_{18} or PYE phases. Although nitrophenyl-

0021-9673/92/$05.00

bonded phases have been used in RPLC [13] and in many chiral stationary phases, no systematic application of such bonded phases has been reported for the separation of chlorinated aromatic compounds in RP-HPLC.

We report here a simple method for the preparation of NPE phase from readily available phenylethylsilylated (PE) silica gel, and some of the properties of the resulting NPE phase. The combination of the two charge-transfer-type stationary phases, PYE and NPE, and also C_{18}, not only increases the separation capabilities but also provides structural information for isomeric aromatic compounds with multiple substituents, because the NPE and PYE phases possess considerable differences in the dipolar character of the aromatic moieties.

EXPERIMENTAL

Equipment

The HPLC system consisted of an LC-6A pump, a SIL-6A automatic sample injector, an SPD-6A variable-wavelength UV detector, a C-R5A data processor (Shimadzu, Kyoto, Japan) and an RI-8 refractive index detector (Tosoh, Tokyo, Japan). Measurements with chlorinated dioxins were carried out at the Centers for Disease Control (Atlanta, GA, USA) by using a Beckman System Gold HPLC system (Model 126 pump and Model 166 UV detector; Beckman Instruments, San Ramon, CA, USA). The column temperature was maintained at 30°C by using a thermostated water-bath.

Preparation of NPE phase

Concentrated nitric acid (2.5 ml) was added dropwise to 4.0 g of phenylethylsilylated silica gel (particle size 5 μm, prepared from Develosil, Nomura Chemicals, Seto, Japan) suspended in 50 ml of acetic anhydride at 0°C, and the mixture was stirred for 1 h in an ice-bath. The reaction mixture was filtered with a PTFE membrane filter, and the particles were washed with 100 ml of acetic acid. The silica particles were further washed successively with 100 ml each of ethyl acetate, methanol, methanol–water (80:20, v/v), methanol and chloroform before drying. Trimethylsilylation was carried out with this material. Toluene and isopropylbenzene were nitrated under similar conditions in order to examine the reactivity of benzene derivatives.

Structure determination of the NPE phase

The NPE silica (5 g) was dissolved in dilute hydrofluoric acid (1:1, v/v) (30 ml), and the resulting organic portion was chromatographically separated [C_{18} column, methanol–water (70:30, v/v) as eluent]. NMR measurements, were carried out on an XL 200 NMR instrument (Varian, Sunnyvale, CA, USA).

Materials

The NPE prepared as above, PYE (particle size 5 μm, Cosmosil 5-PYE, Nacalai Tesque, Kyoto, Japan) and C_{18} (particle size 5 μm, Cosmosil 5-C_{18}) packing materials were packed into stainless-steel tubes (15 or 10 cm × 4.6 mm I.D.). Polychlorodibenzo-*p*-dioxin (PCDD) mixtures were prepared at the Centers for Disease Control as described previously [14], and 0.1–1.0 μl of toluene solutions (*ca.* 1 mg/ml) were injected. Other chemicals and HPLC-grade solvents were obtained commercially.

RESULTS AND DISCUSSION

Preparation of NPE phase

Direct nitration of PE silica was employed to produce NPE phase. This approach avoids the complicated synthesis of nitrophenylsilanes to be used for the preparation of bonded phases. The precursor PE silica is readily available.

Nitration of monosubstituted benzenes usually results in a mixture of isomeric products. Fig. 1 shows the variation of the composition of the reaction mixture for the nitration of toluene and isopropylbenzene. The reactions proceeded to more than 95% completion in 15 min in both instances. The nitration of toluene with concentrated nitric acid in acetic anhydride gave *o*- and *p*-nitrotoluene in a 65:35 ratio. In contrast, isopropylbenzene mainly resulted in nitration at the *para* position (75%) owing to the steric repulsion by the bulky isopropyl group. The results agreed well with those reported [15].

The nitration of PE silica was carried out for 1 h under the same reaction conditions. The surface coverages of NPE and other bonded phases are listed in Table I. Elemental analysis indicates the presence of one nitro group per phenyl ring on NPE. Up to 25% loss of PE bonded phase owing to the decomposition of the stationary phase under the high-

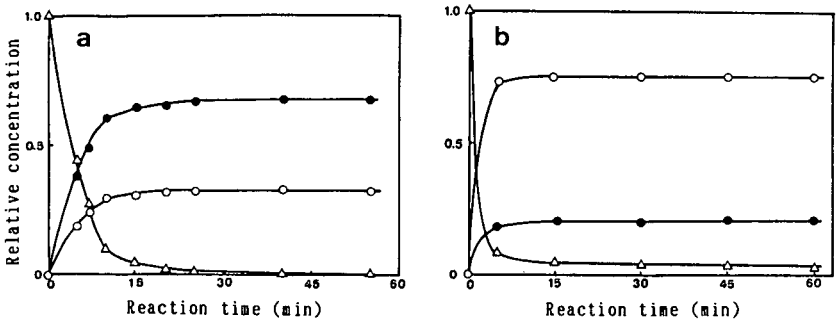

Fig. 1. Nitration of (a) toluene and (b) isopropylbenzene. Vertical axis represents relative concentrations. (△) Starting material; (○) *para*-substituted product; (●) *ortho*-substituted product. Determined by RP-HPLC. Column, C_{18} (15 cm × 4.6. mm I.D.); mobile phase, (a) methanol–water (60:40, v/v); (b) methanol–water (70:30, v/v).

ly acidic reaction condition was noted. Although the nitration afforded good reproducibility (± 1%) in terms of capacity factors (k' values) for hydrocarbons, esters and ketones, for the three preparations of NPE phases from one batch of PE silica gel, poorer reproducibility (± 2.8% in k') was observed for dipolar molecules such as dinitrobenzenes or dinitronaphthalenes. The separation factors between *o*- and *p*-dinitrobenzene were in the range 1.54 ± 0.05 on the seven NPE phases prepared from three different batches of silica gel. The two dinitrobenzenes showed reversal of the elution order between NPE and PE phases, and gave poorer reproducibility than the other compounds.

In order to determine the structure of the bonded nitrophenylethyl group, the NPE silica was subjected to hydrofluoric acid degradation followed by chromatographic separation and subsequent NMR spectroscopy. Fig. 2 shows the chromatogram obtained for the hydrofluoric acid degradation products. The ratio between the areas of peaks A and B was found to be 28:72 based on the response of the refractive index detector.

The NMR spectra obtained for the two fractions indicated that peak B contained a 2-*p*-nitrophenylethyldimethylsilyl group. The steric requirement of the bonded phenylethyl group resulted in selective nitration at the *para* position.

Chromatographic properties of NPE phase

The hydrophobic property of NPE phase, as measured by the separation factor between toluene and benzene, was much smaller than those of C_{18} and PYE and similar to that of PE silica. NPE

TABLE I

SURFACE COVERAGE AND CHROMATOGRAPHIC PROPERTIES OF PACKING MATERIALS

Stationary phase	Elemental Analysis[a]			Surface coverage (μmol/m^2)	Separation factor (k')			
	H (%)	C (%)	N (%)		CH_3[b]	$COOCH_3$[b]	PAH[c]	(C_6H_6)[d]
C_{18}	3.68	19.17	0	3.22	1.96	0.80	6.25	(3.36)
PYE	1.82	18.45	0	2.99	1.83	1.86	24.4	(1.86)
PE	1.72	11.50	0	3.42	1.60	1.20	4.04	(1.47)
NPE	1.44	9.25	1.04[e]	2.56	1.58	1.39	11.5	(0.96)

[a] Prior to trimethylsilylation.
[b] The k' ratios between toluene and benzene, and between methyl benzoate and benzene in methanol–water (60:40, v/v).
[c] The k' ratio between triphenylene and benzene in methanol–water (90:10, v/v).
[d] The k' value of benzene in methanol–water (60:40, v/v).
[e] Corresponds to 1.02 NO_2 group per phenyl group.

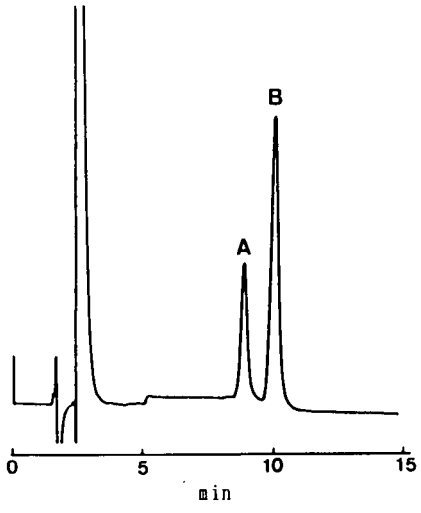

Fig. 2. Separation of hydrofluoric acid degradation products of NPE phase by RP-HPLC. Column, C_{18} (15 cm × 4.6 mm I.D.); mobile phase, methanol–water (70:30, v/v).

phase shows selective retention of polar and polycyclic aromatic compounds compared to PE phase, as shown in Table I. PYE showed the influence of charge-transfer interactions.

Fig. 3 shows the plot of log k' values for benzene derivatives against log P values obtained in a 1-octanol–water liquid–liquid partition system [16]. The C_{18} phase showed good linearity, indicating that the hydrophobic interaction played a major role in the retention process. PYE showed a positive deviation for compounds with either electron-withdrawing or electron-donating substituents. This is similar to the case with carbon packing material [9].

It is interesting to note the similar behaviour of the PYE and NPE phases, both selectively retaining polar compounds compared with non-polar solutes such as alkylbenzenes. There is, however, a slight difference between these two aromatic stationary phases. The NPE phase showed a slightly greater

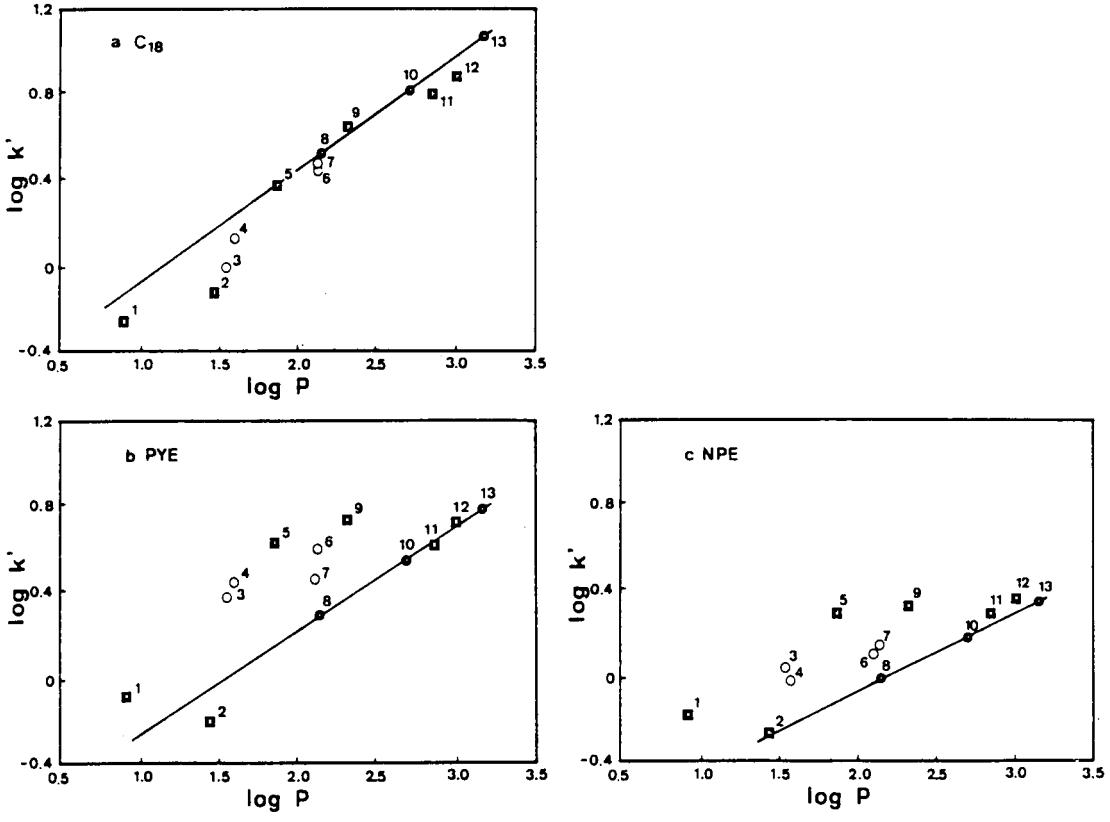

Fig. 3. Plots of log k' values against log P values for monosubstituted benzenes. (1) NH_2; (2) OH; (3) CN; (4) $COCH_3$; (5) NO_2; (6) $COOCH_3$; (7) OCH_3; (8) H; (9) $N(CH_3)_2$; (10) CH_3; (11) Cl; (12) Br; (13) C_2H_5. Mobile phase, methanol–water (60:40, v/v). Column: (a) C_{18}; (b) PYE; (c) NPE. The straight lines were drawn through the plots for (8), (10) and (13).

preference for substituted benzenes with OH, NH_2, $N(CH_3)_2$, Cl, Br and NO_2 groups (squares in Fig. 3) than the PYE phase, which favoured other compounds with electron-withdrawing substituents (open circles in Fig. 3).

The chromatograms in Fig. 4 show a preferential retention of dinitronaphthalenes (peaks 1 and 2) on the charge-transfer-type phases compared with the C_{18} phase. The difference between PYE and NPE is also clearly noticeable. Whereas 1,5-dinitronaphthalene (peak 2) was preferentially retained by the PYE phase, 1,8-dinitronaphthalene (peak 1) was retained longer on the NPE phase. This cannot be explained by consideration of charge-transfer interaction between the aromatic rings.

The results with the NPE phase in Figs. 3 and 4 indicate the presence of strong dipole–dipole interactions. The molecule of 1,8-dinitronaphthalene possesses the two nitro group dipoles aligned for a much greater dipolar interaction with the bonded nitrophenyl group than 1,5-dinitronaphthalene. Similarly, *o*-dinitrobenzene was retained longer

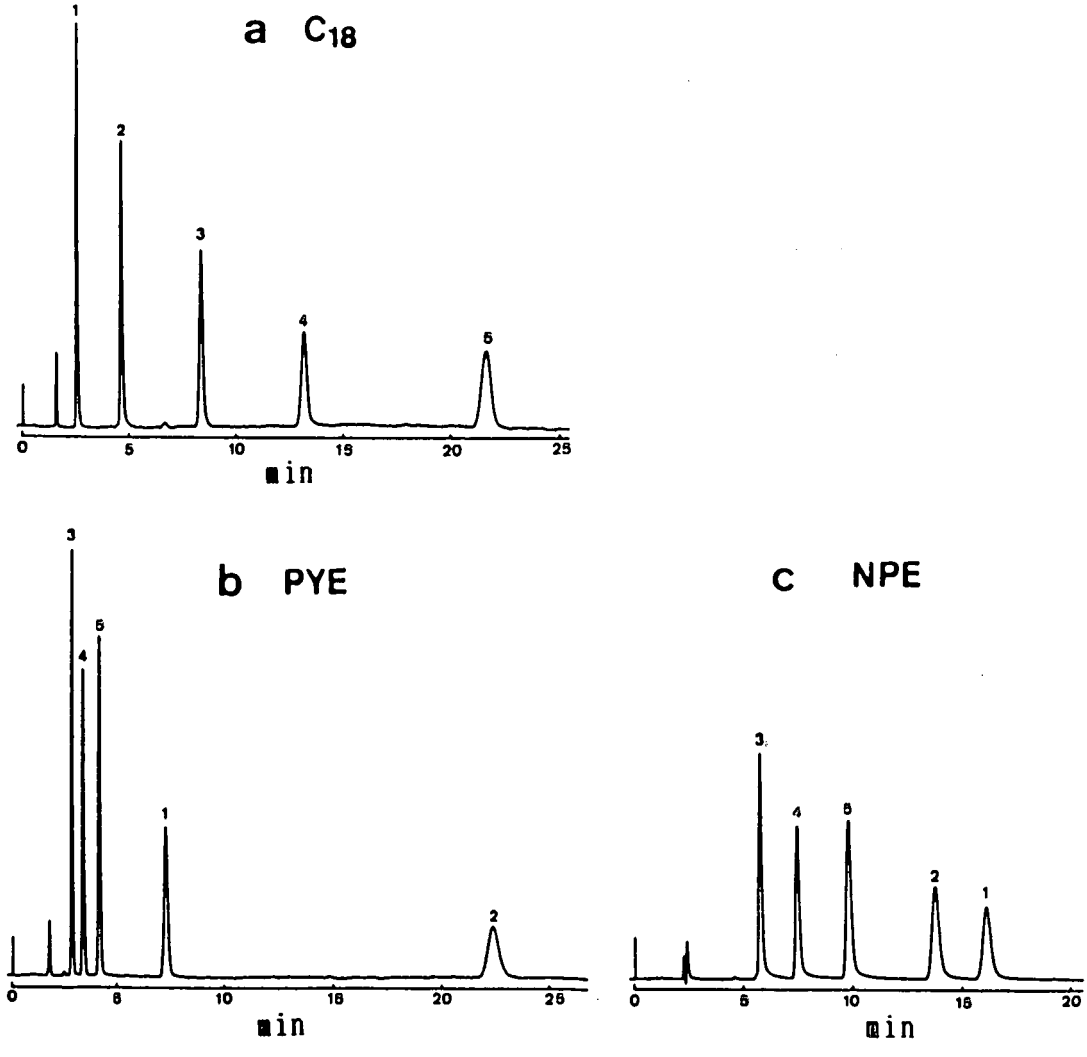

Fig. 4. Separation of naphthalene derivatives. Mobile phase and column: (a) C_{18}, methanol–water (70:30, v/v); (b) PYE, methanol–water (90:10, v/v); (c) NPE, methanol–water (70:30, v/v). Solutes: (1) 1,8-dinitronaphthalene; (2) 1,5-dinitronaphthalene; (3) naphthalene; (4) 1-methylnaphthalene; (5) 1,5-dimethylnapthalene.

than *p*-dinitrobenzene on NPE phase, whereas the elution order was reversed on PYE phase, and on PE phase.

Separation of polychlorinated aromatic compounds

The three stationary phases, NPE, PYE and C_{18}, showed substantial differences in the retention selectivity toward polychlorinated aromatic compounds. As shown in Fig. 5a, the C_{18} phase showed a preferential retention of polychlorobenzenes with chlorine atoms in *meta* positions to each other. PYE phase preferentially retained those with the chlorine atoms located as far apart as possible from each other. In contrast, NPE phase showed the greatest retention for polychlorobenzenes with an *ortho* arrangement of the chlorine groups. This tendency is similar to the example in Fig. 4, where 1,8-dinitronaphthalene with aligned dipoles was preferentially retained by NPE phase. The least hydrophobic 1,2,3,4-tetrachlorobenzene showed the shortest retention among the three tetrachlorobenzenes on C_{18} and PYE and the greatest retention on NPE phase.

The complete reversal of the elution order of tetrachlorobenzenes between NPE and PYE phase suggests the possibility of providing structural information for isomeric polychlorinated aromatic compounds such as PCDDs based on their chromatographic behaviour. In addition, the present combination of the C_{18}, PYE and NPE stationary phases is expected to increase the separation capability for the closely related PCDD isomers.

The separation of all the congeners of PCDDs is extremely difficult, whereas PCDDs having different numbers of chlorine atoms can be separated by high-resolution gas chromatography (HRGC) [17]. Therefore, several groups of TCDDs are currently measured together in environmental analysis [18–20]. The combintaion of RP-HPLC on C_{18} phase and normal-phase HPLC on silica gel distinguished most of the 22 TCDD isomers, but with several pairs remaining unidentified even with the use of

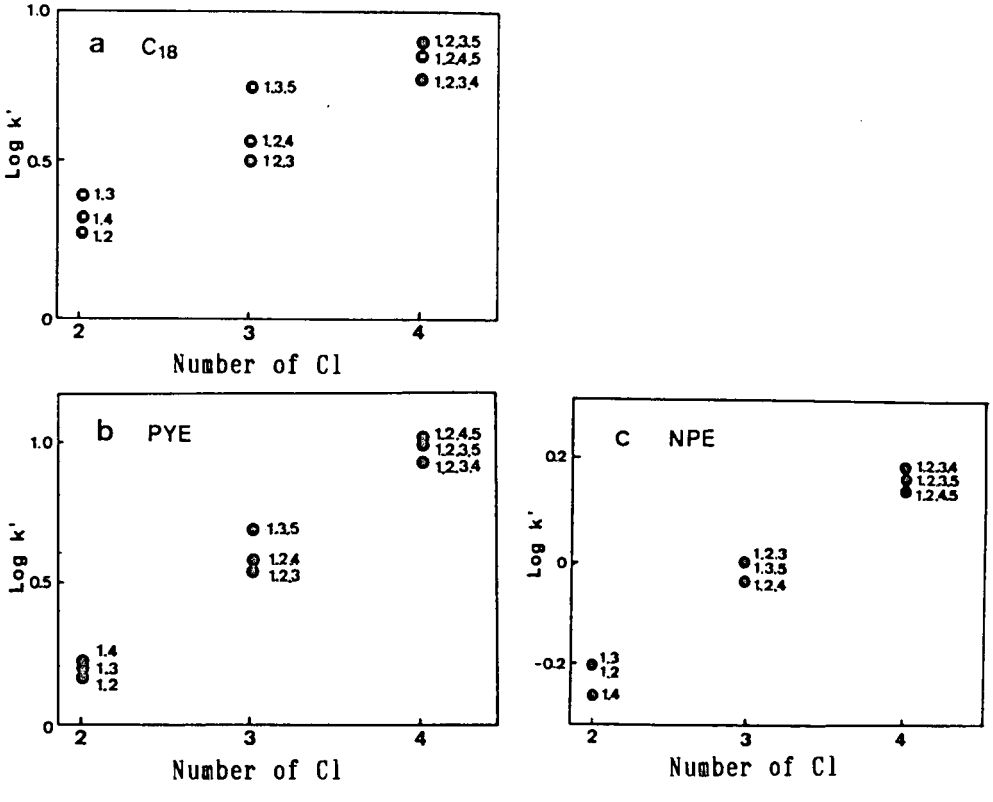

Fig. 5. Retention of polychlorobenzenes. Mobile phase, methanol–water (80:20, v/v). Column: (a) C_{18}; (b) PYE; (c) NPE.

HRGC [21]. In the past, the difficulty with isomer separation led to ambiguous structural assignments, especially when two isomers were present in a mixture at similar concentrations. Some structural assignments have been performed based on Fourier transform IR and NMR spectra by using mixtures [14,22–24]. Many TCDDs in HRGC have been identified by using the photolysis of hexachlorodibenzo-*p*-dioxins (HxCDDs) with known structures [25].

TABLE II

STRUCTURES OF PCDD ISOMERS

Starting materials		PCDD products	
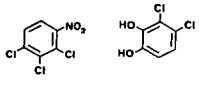		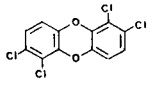	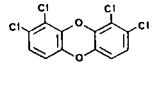
		1,2,6,7-TCDD	1,2,8,9-TCDD
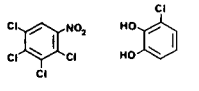		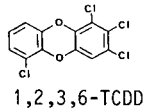	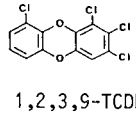
		1,2,3,6-TCDD	1,2,3,9-TCDD
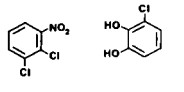		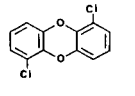	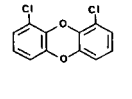
		1,6-DCDD	1,9-DCDD
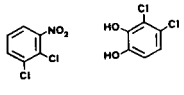		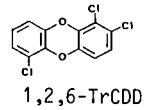	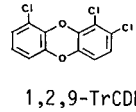
		1,2,6-TrCDD	1,2,9-TrCDD
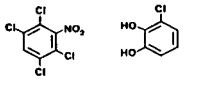		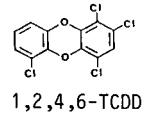	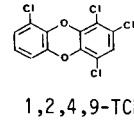
		1,2,4,6-TCDD	1,2,4,9-TCDD
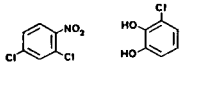		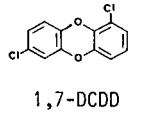	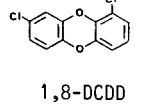
		1,7-DCDD	1,8-DCDD
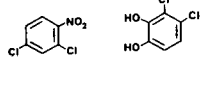		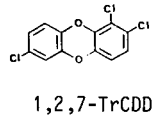	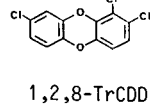
		1,2,7-TrCDD	1,2,8-TrCDD
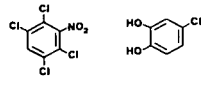		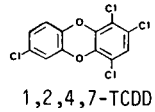	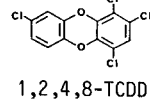
		1,2,4,7-TCDD	1,2,4,8-TCDD

The isolation of each PCDD congener is also required in order to examine individual toxicity and teratogenicity. Many PCDDs, however, are necessarily produced as a mixture owing to the Smiles rearrangement during the preparation reaction [26,27]. Table II shows several pairs of PCDD isomers co-produced during preparation that need to be separated. For example, the reaction of 3,4-dichlorocatechol with 2,3,4-trichloronitrobenzene results in a mixture of 1,2,6,7- and 1,2,8,9-TCDD. The separation and identification of 1,2,6,7- and 1,2,8,9-TCDDs and 1,2,3,6- and 1,2,3,9-TCDDs have been reported [28], and these TCDDs were used here to show how the retentions of PCDDs on PYE and NPE phases can be related to their structures.

Figs. 6 and 7 show the separation of synthetic mixtures of 1,2,6,7- and 1,2,8,9-TCDDs and 1,2,3,6- and 1,2,3,9-TCDDs on C_{18}, PYE and NPE phases. The identities of the peaks were provided by comparison of the retention on C_{18} phase [28] and the peak size ratios with the reported values [14]. On C_{18} and PYE phases, the isomers existing in a greater amount with less steric congestion among the chlorine atoms, 1,2,6,7- and 1,2,3,6-TCCD, were retained longer than 1,2,8,9- and 1,2,3,9-TCDD, respectively. In contrast, 1,2,8,9- and 1,2,3,9-TCCD were retained longer than 1,2,6,7- and 1,2,3,6-TCDD, respectively, on the NPE phase. The opposite retention order of these TCDDs on PYE and NPE phases is in agreement with the results for polychlorobenzenes (Fig. 5) and dinitronaphthalenes (Fig. 4).

The retention on C_{18} phase is primarily determined by the hydrophobic property of the solute [4]. As chlorine atoms on an aromatic ring increase the hydrophobic property [16], compounds with isolated chlorine substituents are retained longer than those with sterically congested chlorine atoms owing to the greater hydrophobic surface areas. Hence the proximity between the 1- and 9-chlorine atoms resulted in a smaller retention of 1,2,8,9-TCDD and 1,2,3,9-TCDD than 1,2,6,7-TCDD and 1,2,3,6-TCDD, respectively, on C_{18} phase.

As the greatest retention was observed on PYE phase for the polychlorobenzenes with minimum steric congestion due to the most favourable

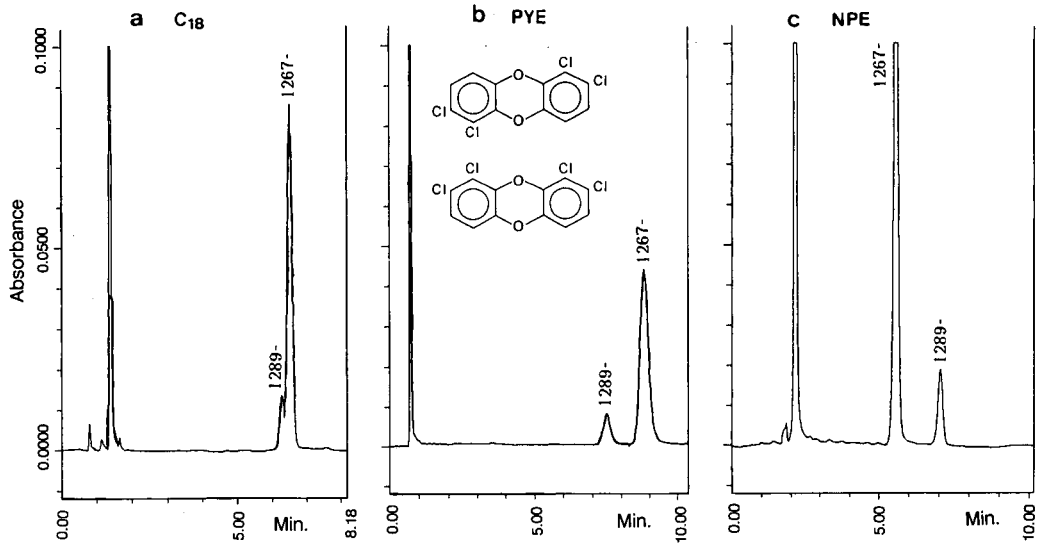

Fig. 6. Separation of 1,2,6,7- and 1,2,8,9-TCDDs. Mobile phase and column: (a) C_{18}, 15 cm, methanol–water (90:10, v/v) at 2 ml/min; (b) PYE, 10 cm, methanol at 2 ml/min; (c) NPE, 15 cm, methanol–water (90:10, v/v) at 1 ml/min.

charge-transfer interactions, the longer retention times for 1,2,6,7-TCDD and 1,2,3,6-TCDD than 1,2,8,9-TCDD and 1,2,3,9-TCDD, respectively, are readily understandable. In contrast, the TCDDs with the greater steric congestion among the chlorine atoms, existing as minor components in reaction mixtures, are retained longer than the more symmetrically substituted TCDDs by NPE phase. This is presumably due the more aligned dipoles in 1,2,8,9- or 1,2,3,9-TCDD than in 1,2,6,7- or 1,2,3,6-TCDD, respectively, as with dinitronaphthalenes and polychlorobenzenes.

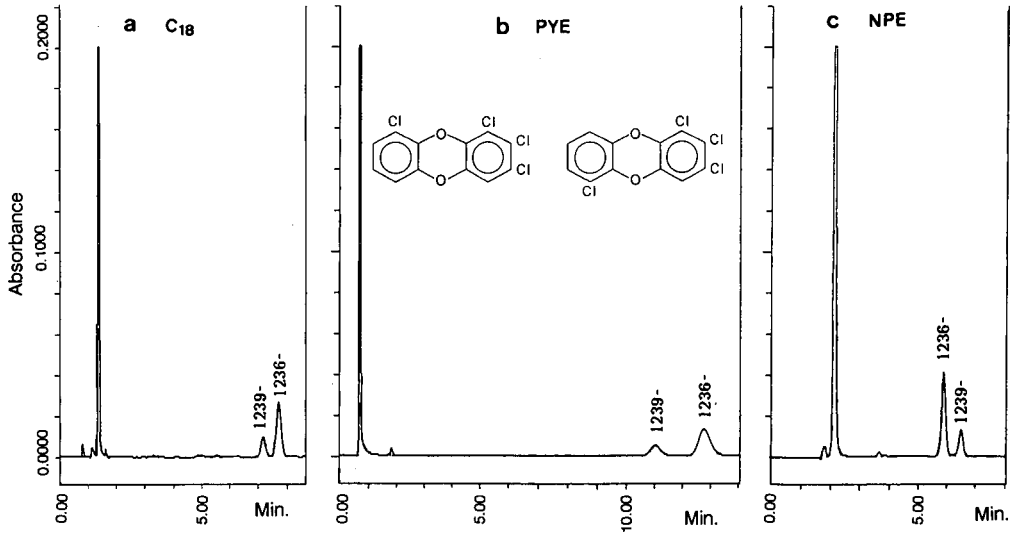

Fig. 7. Separation of 1,2,3,6- and 1,2,3,9-TCDDs. Conditions as in Fig. 6.

Possibility of structural assignment for PCDDs based on retention on NPE and PYE phases

Difficulties in separation are usually encountered for PCDDs with product ratios close to unity, which also made the spectroscopic structural assignment more difficult when dealing with a mixture. The results showing the clear reversal of the elution order on PYE and NPE phases indicate the possibility of structural assignment for such PCDD isomers that have been providing difficulties. The following reports the first attempts at the application of the chromatographic system with a combination of NPE and PYE phases to the structural assignment of PCDDs.

The separation and identification of two pairs of TCDD isomers, 1,2,4,6- and 1,2,4,9-TCDDs and 1,2,4,7- and 1,2,4,8-TCDDs, are particularly interesting, because these TCDDs have not been separated by either HRGC or RP-HPLC on C_{18} phase. Normal-phase chromatography on silica gel separated these TCDD isomers, but identification was not achieved [21,28]. We previously reported the separation of 1,2,4,6- and 1,2,4,9-TCDDs using NPE [12] and 1,2,4,7- and 1,2,4,8-TCDDs using PYE [11], but could not provide definite structure assignments. In this study, we included 1,6- and 1,9-dichlorodibenzo-*p*-dioxins (DCDDs) and 1,2,6- and 1,2,9-trichlorodibenzo-*p*-dioxins (TrCDDs) with 1,2,4,6- and 1,2,4,9-TCDDs, and 1,7- and 1,8-DCDDs and 1,2,7- and 1,2,8-TrCDDs with 1,2,4,7- and 1,2,4,8-TCDDs for the following reasons. First, these DCDD and TrCDD isomers are assumed to be easier to separate than the TCDDs, because of the greater difference in dipolar character. Second, the chromatographic behaviour of the DCDDs and the TrCDDs would give structural information for the TCDDs by taking into account the effect of additional chlorine atoms. Third, the structural assignment of DCDDs and TrCDDs is also important.

Fig. 8 shows the chromatograms of 1,6- and 1,9-DCDDs, 1,2,6- and 1,2,9-TrCDDs and 1,2,4,6- and 1,2,4,9-TCDDs on C_{18}, PYE and NPE phase. The C_{18} phase showed the greater retentions for the DCDD and TrCDD isomers present in greater amounts, which are assumed to be the isomers possessing sterically less congested structures. PYE phase showed a preference for PCDDs with more symmetrical chlorine substitution, generally giving a similar retention order to C_{18} phase. NPE phase also gave easy separations of 1,6- and 1,9-DCDDs and 1,2,6- and 1,2,9-TrCDDs. The elution orders,

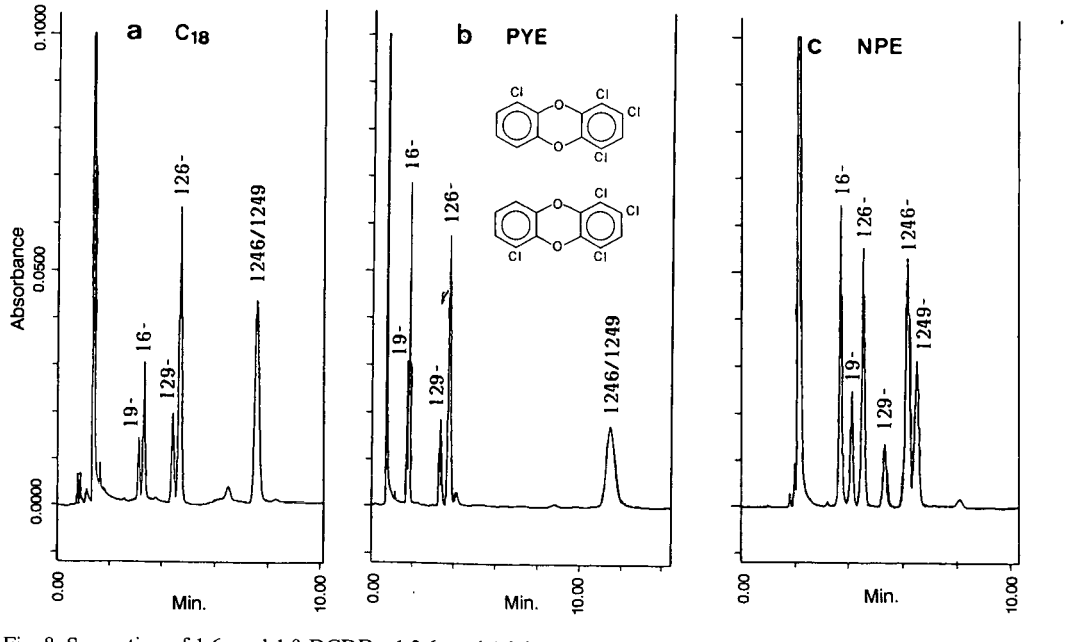

Fig. 8. Separation of 1,6- and 1,9-DCDDs, 1,2,6- and 1,2,9-TrCDDs and 1,2,4,6- and 1,2,4,9-TCDDs. Conditions as in Fig. 6.

however, are reversed from those on C_{18} or PYE phase. The results are understandable on the basis of the interaction of the more aligned dipoles of 1,9-DCDD and 1,2,9-TrCDD with NPE phase compared with 1,6-DCDD and 1,2,6-TrCDD, respectively.

Based on these considerations, the late-eluting peaks on C_{18} and PYE with the greater size are tentatively assigned to 1,6-DCDD and 1,2,6-TrCDD, as shown in Fig. 8. The present assignment is consistent with the results with 1,2,6,7- and 1,2,8,9 - TCDDs and 1,2,3,6- and 1,2,3,9-TCDDs.

Although 1,2,4,6- and 1,2,4,9-TCDDs have not been separated by using either C_{18} or PYE phase, NPE phase permitted the easy separation of these TCDDs. The chromatographic behaviour of the three pairs of isomers are expected to follow a similar tendency with the successive addition of chlorine atoms first at the 2-position and then at the 4-position to the original 1,6- and 1,9-DCDD skeleton. Thus the second peak on NPE existing in a smaller amount is tentatively assigned to 1,2,4,9-TCDD, which agrees with its more dipolar character than 1,2,4,6-TCDD (Table III) [29]. This assignment,

TABLE III

RETENTION OF PCDDs IN RP-HPLC AND STRUCTURE ASSIGNMENTS

PCDD mixture	*k'* value (proportion, %)			Dipole moment[e] (D)	Heat of formation[e] (kcal/mol)
	C_{18}[b]	PYE[c]	NPE[d]		
1,2,8,9-/	6.39 (11)	10.4 (12)	2.64 (12)	4.220	−40.488
1,2,6,7-	6.66 (89)	12.4 (88)	1.91 (88)	0.023	−40.913
	[α = 1.04][a]	[α = 1.19]	[α = 0.72]		
1,2,3,9-/	8.08 (25)	16.1 (32)	2.53 (25)	4.121	−40.012
1,2,3,6-	8.72 (75)	18.8 (68)	2.20 (75)	3.095	−40.324
	[α = 1.08]	[α = 1.17]	[α = 0.87]		
1,9-/	2.74 (29)	1.67 (28)	1.17 (29)		
1,6-	2.96 (71)	1.86 (72)	0.96 (71)		
	[α = 1.08]	[α = 1.11]	[α = 0.82]		
1,2,9-/	4.21 (22)	4.18 (22)	1.78 (22)		
1,2,6-	4.53 (78)	4.81 (78)	1.38 (78)		
	[α = 1.08]	[α = 1.15]	[α = 0.78]		
1,2,4,9-/	7.95[f]	16.6[f]	2.37 (38)	2.922	−40.436
1,2,4,6-			2.19 (62)	2.178	−40.458
			[α = 0.92]		
1,8-/	3.53[f]	1.78[f]	3.33 (37)		
1,7-			2.90 (63)		
			[α = 0.87]		
1,2,8-/	5.20[f]	4.28[f]	5.43 (27)		
1,2,7-			4.60 (73)		
			[α = 0.85]		
1,2,4,8-/	9.21[f]	14.6 (43)	7.94 (41)	1.607	−42.533
1,2,4,7-		15.3 (57)	7.67 (59)	0.623	−42.552
		[α = 1.05]	[α = 0.96]		

[a] α = *k'* ratio between the peak of larger size and the peak of smaller size.
[b] Mobile phase: methanol–water (90:10, v/v), flow-rate 2.0 ml/min.
[c] Mobile phase: methanol, flow-rate 2.0 ml/min.
[d] Mobile phase: methanol–water (90:10, v/v), except for 1,7- and 1,8-DCDDs, 1,2,7- and 1,2,8-TrCDDs and 1,2,4,7- and 1,2,4,8-TCDDs, which were chromatographed using methanol–water (80:20, v/v), flow-rate 1.0 ml/min.
[e] Ref. 29.
[f] Insufficient separation was observed.

however, contradicts the previous one [14] based on NMR and Fourier transform IR spectra of the mixture.

So far we have been using the different peaks sizes in each PCDD pair only for tracing the elution order. However, the relationship between retention order and relative peak size is clearly noticeable in Figs. 6–8. In each pair of PCDDs co-produced during preparation, the isomer present in excess was generally retained longer on C_{18} and PYE phases.

The results are explainable as follows, assuming that thermodynamic equilibrium is reached during the preparation reaction which involves the rapid Smiles rearrangement [26,27]. Sterically less hindered species should be preferentially produced owing to the greater thermodynamic stability via a common spirocyclic intermediate. Strong 1,9-nonbonded (repulsive) interaction via ether oxygen is suggested for dioxins having chlorine atoms at 1- and 9-positions that deform ether linkages [30]. The heats of formation of such TCDDs were accordingly smaller than those of TCDDs with less steric congestion [29], as shown in Table III.

Thus 1,2,6,7-TCDD and 1,2,3,6-TCDD were produced more than 1,2,8,9-TCDD and 1,2,3,9-TCDD, respectively. Similarly, 1,6-DCDD is expected to be produced more than 1,9-DCDD, and 1,2,6-TrCDD more than 1,2,9-TrCDD. It would be of interest to examine the difference between the present results and those with HxCDDs [26] with respect to the reaction conditions and the work-up procedure. Spectroscopic and X-ray crystal analysis will be required to confirm the assignments, although the structural assignment with proton NMR may be increasingly difficult for DCDDs and TrCDDs because of coupling.

Fig. 9 gives another example showing the possibility of the combined use of NPE and PYE phases in establishing the structures of TCDDs. The structure assignments of 1,2,4,7- and 1,2,4,8-TCDDs based on NMR and IR spectrometry were contradictory, even after the separation of the isomers on PYE phase [14,22,23].

Mixtures of 1,7- and 1,8-DCDDs and 1,2,7- and 1,2,8-TrCDDs were readily separated with NPE phase, in spite of the difficulties in separation on C_{18} and PYE phases. Again, the compounds present in smaller amounts were retained longer on NPE phase, and tentatively assigned to 1,8-DCDD and 1,2,8-TrCDD as in Fig. 9c, because they presumably possess the more aligned dipoles and the greater steric congestion in each pair.

Although the separation between 1,2,4,7- and 1,2,4,8-TCDDs on NPE phase is only partial, the elution order on NPE was clearly reversed from that on PYE phase. Taking into account the retention order and the peak size ratios of 1,7- and 1,8-DCDDs and 1,2,7- and 1,2,8-TrCDDs, the TCDD isomer present in the greater amount, or the first peak on NPE phase, can be tentatively assigned to 1,2,4,7-TCDD, which supports the previous structural assignment based on NMR [23]. In Fig. 9, it is noticeable that the steric discriminations with 1,7- and 1,8-DCDD skeletons in terms of the product

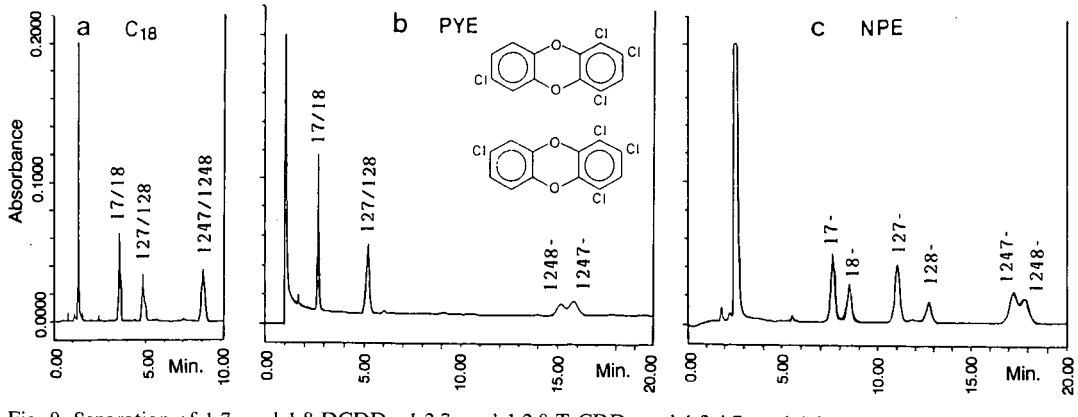

Fig. 9. Separation of 1,7- and 1,8-DCDDs, 1,2,7- and 1,2,8-TrCDDs and 1,2,4,7- and 1,2,4,8-TCDDs. Mobile phase and column: (a) C_{18}, 15 cm, methanol–water (90:10, v/v) at 2 ml/min; (b) PYE, 15 cm, methanol at 2 ml/min; (c) NPE, 15 cm, methanol–water (80:20, v/v) at 1 ml/min.

ratios and chromatographic separation were enhanced by the addition of a chlorine atom at the 2-position and reduced by a chlorine atom at the 4-position, as occurred with those with 1,6- and 1,9-DCDD skeletons in Fig. 8.

The interpretation of Figs. 8 and 9 is consistent with the results with 1,2,6,7- and 1,2,8,9-TCDDs and 1,2,3,6- and 1,2,3,9-TCDDs in terms of retention on NPE and PYE phases, which is related to the dipolar character, and the peak size ratios, related to the thermodynamic stability or the steric congestion. The present interpretation of the retention tendency on NPE phase based on the effect of the more aligned dipoles on one isomer seems to agree with the relative magnitude of dipole moments calculated for these TCDDs (Table III) [29].

The present results clearly indicate the utility of PYE and NPE phases, and the need for further studies. The identification of each congener, based on isolation and structure determination, is essential for assessing environmental safety with respect to the chlorinated aromatic compounds. The chromatographic method, not frequently used for structure determinations, is very straightforward in the present instance, and will be effective for isomers having differences in dipolar character, including PCDDs, chloronaphthalenes and chlorobiphenylenes, especially when spectroscopic methods are associated with difficulties.

ACKNOWLEDGEMENTS

This work was supported in part by the Monbusho International Joint Research Program (No. 03044089), funded by the Ministry of Education. We are grateful to Drs. E. R. Barnhart and L. R. Alexander of the Centers for Disease Control, US Public Health Service, Professor K. Fukunishi of Kyoto Institute of Technology, Professor S. Terabe of Himeji Institute of Technology and Professor H. Miyata of Setsunan University for helpful suggestions.

REFERENCES

1 N. Tanaka, K. Sakagami and M. Araki, *J. Chromatogr.*, 199 (1980) 327.
2 L. C. Sander and S. A. Wise, *Anal. Chem.*, 56 (1984) 504.
3 K. Jinno, T. Nagoshi, N. Tanaka, M. Okamoto, J. C. Fetzer and W. R. Biggs, *J. Chromatogr.*, 392 (1987) 75.
4 N. Tanaka and E. R. Thornton, *J. Am. Chem. Soc.*, 99 (1977) 7300.
5 N. Tanaka, K. Hosoya, Y. Tachibana, M. Araki, K. Tanaka and A. Kaji, *J. Chromatogr. Sci*, 27 (1989) 735.
6 J. H. Knox, B. Kaur and G. R. Millward, *J. Chromatogr.*, 352 (1986) 3.
7 B. J. Bassler and R. A. Hartwick, *J. Chromatogr. Sci*, 27 (1989) 162.
8 E. Skutchanova, L. Feltl, E. Smolkova-Keulemansova and J. Skutchan, *J. Chromatogr.*, 292 (1984) 233.
9 N. Tanaka, T. Tanigawa, K. Kimata, K. Hosoya and T. Araki, *J. Chromatogr.*, 549 (1991) 29.
10 E. R. Barnhart, D. L. Ashley, V. V. Reddy and D. G. Patterson, *J. High Resolut. Chromatogr. Chromatogr. Commun.*, 9 (1986) 528.
11 E. R. Barnhart, D. G. Patterson, N. Tanaka and M. Araki, *J. Chromatogr.*, 445 (1988) 145.
12 K. Kimata, K. Hosoya, N. Tanaka, T. Araki, E. R. Barnhart, D. G. Patterson and S. Terabe, *J. High Resolut. Chromatogr.*, 13 (1990) 137.
13 L. Nondek, *J. Chromatogr.*, 373 (1986) 61.
14 L. T. Gelbaum, D. G. Patterson, D. L. Ashley and D. F. Groce, *Chemosphere*, 17 (1988) 551.
15 R. O. C. Norman and R. Taylor, *Electrophilic Substitution in Benzenoid Compounds*, Elsevier, Amsterdam, 1965, Ch. 3.
16 R. F. Rekker, *Hydrophobic Fragmental Constant*, Elsevier, Amsterdam, 1977, Ch. 3.
17 H. R. Buser and C. Rappe, *Anal. Chem.*, 56 (1984) 442.
18 H. R. Buser and C. Rappe, *Anal. Chem.*, 52 (1980) 2257.
19 C. Rappe, S. Marklund, L.-O. Kjeller, P.-A. Bergqvist and M. Hansson, in L. H. Keith, C. Rappe and G. Choudhary (Editors), *Chlorinated Dioxins and Dibenzofurans in the Total Environment, II*, Butterworth, Boston, MA, 1985. Ch. 29.
20 H. Miyata, K. Takayama, J. Ogaki, M. Mimura and T. Kashimoto, *Toxicol. Environ. Chem.*, 17 (1988) 91.
21 T. J. Nestrick, L. L. Lamparski and R. H. Stehl, *Anal. Chem.*, 51 (1979) 2273.
22 J. Grainger, E. R. Barnhart, D. G. Patterson and D. Presser, *Appl. Spectrosc.*, 42 (1988) 321.
23 D. L. Ashley, V. V. Reddy and D. G. Patterson, *Magn. Res. Chem.*, 27 (1989) 117.
24 D. G. Patterson, V. V. Reddy, E. R. Barnhart, D. L. Ashley, C. R. Lapeza, L. R. Alexander and L. T. Gelbaum, *Chemosphere*, 19 (1989) 233.
25 H. R. Buser, *Chemosphere*, 8 (1979) 251.
26 A. S. Kende and M. R. DeCamp, *Tetrahedron Lett.*, (1975) 2877.
27 A. P. Gray, S. P. Cepa and J. S. Cantrell, *Tetrahedron Lett.*, (1975) 2873.
28 M. L. Taylor, T. O. Tiernan, B. Ramalingam, D. J. Wagel, J. H. Garrett, J. G. Solch and G. L. Ferguson, in L. H. Keith, C. Rappe and G. Choudhary (Editors), *Chlorinated Dioxins and Dibenzofurans in the Total Environment, II*, Butterworth, Boston, MA, 1985, Ch. 2.
29 C. J. Koester and R. A. Hites, *Chemosphere*, 17 (1988) 2355.
30 J. Grainger, V. V. Reddy and D. G. Patterson, Jr., *J. Appl. Spectrosc.*, 42 (1988) 643.

Journal of Chromatography, 595 (1992) 89–101
Elsevier Science Publishers B.V., Amsterdam

CHROM. 23 924

Evaluation of reversed-phase liquid chromatographic columns for recovery and selectivity of selected carotenoids

Katherine S. Epler and Lane C. Sander

Organic Analytical Research Division, Chemical Science and Technology Laboratory, National Institute of Standards and Technology, Gaithersburg, MD 20899 (USA)

Regina G. Ziegler

Environmental Epidemiology Branch, Epidemiology and Biostatistics Program, Division of Cancer Etiology, National Cancer Institute, Bethesda, MD 20892 (USA)

Stephen A. Wise and Neal E. Craft*

Organic Analytical Research Division, Chemical Science and Technology Laboratory, National Institute of Standards and Technology, Gaithersburg, MD 20899 (USA)

(First received September 17th, 1991; revised manuscript received November 28th, 1991)

ABSTRACT

Sixty commercially available and five experimental liquid chromatography columns were evaluated for the separation and recovery of seven carotenoid compounds. Methanol- and acetonitrile-based solvents (either straight or modified with ethyl acetate or tetrahydrofuran) were compared to determine which solvent systems and which columns provided better selectivity and recovery. Methanol-based solvents typically provided higher recoveries than did acetonitrile-based solvents. Polymeric C_{18} phases generally provided better selectivity for the difficult separation of lutein and zeaxanthin than did monomeric C_{18} phases.

INTRODUCTION

Epidemiologists have observed a lower incidence of lung cancer in people who have an above-average intake of fruits and vegetables [1,2]. Studies also suggest that the intake of fruits and vegetables may reduce the risk of cancers of the mouth, pharynx, larynx, esophagus, stomach, colon, rectum, bladder, and cervix [2]. Because low serum levels of β-carotene are associated with the subsequent development of lung cancer, β-carotene may be the protective factor present in the fruits and vegetables [2]. However, the lowered incidence of cancer may be due to other carotenoids that are co-ingested with the β-carotene, and serum levels of these other carotenoids have not been adequately studied. Liquid chromatography (LC) has been used to separate and measure β-carotene in serum [3] with concurrent measurement of α-carotene [4–10] and sometimes lycopene [11–18]. In addtion to numerous *cis/trans* geometric isomers, human blood serum contains at least six structurally distinct carotenoids. To determine which carotenoid compound(s) may provide anti-cancer effects, it is important to separate and measure the major carotenoids in serum and in food. Consequently, a number of workers have reported the measurement of carotenoids other than lycopene, α-, and β-carotene in serum

0021-9673/92/$05.00

[19–31], in skin [32], in human milk [33] and in foods [34–48].

The majority of carotenoid separations reported in the literature involve the use of reversed-phase LC, generally on a C_{18} stationary phase, although a few normal-phase LC separations have been reported [21,24,35]. Most workers using reversed-phase LC have used one of the following solvent systems: an acetonitrile-based eluent, an acetonitrile-based eluent to which ammonium acetate has been added, or a methanol-based eluent.

Acetonitrile-based eluents are used most frequently. In 1979, Zakaria *et al.* [49] separated lycopene, α-carotene, and β-carotene in tomatoes on a C_{18} column using a mixture of chloroform and acetonitrile. In 1983, Nelis and De Leenheer [19] reported LC separations on C_{18} columns using acetonitrile or acetontrile and 8% methanol with various organic modifiers added [tetrahydrofuran (THF), diisopropyl ether, chloroform, dichloromethane, ethyl acetate]. Most workers have adapted one of these mixtures so that it provides acceptable results on their particular LC column [4,5,8,9,11–13,16–18,20,22,25,26,30,31,35,38,40,46,48]. Khachik and co-worker [37,41,42,47] typically add hexane to a mixture of methanol, acetonitrile, and methylene chloride. Other workers have used acetonitrile modified with THF and water [36], with water and 2-propanol [44,45], or in a 1:1 mixture with ethanol [27].

The second basic method was described by Peng [6], and employs a mixture of acetonitrile, THF, methanol, and ammonium acetate. This method has been adapted by Nierenberg *et al.* [3,14,29], Kalman *et al.* [10], and Culling-Berglund *et al.* [32].

Methanol-based separations cited include the use of straight methanol [15] or methanol that has been modified with THF or chloroform [35], with water and THF [7], with water and butanol [23], and with hexane [28].

Carotenoid separations reported in the literature employ a wide variety of C_{18} and other reversed-phase columns from different manufacturers. Several workers have compared separations on a small number of commercially available columns: Nelis and De Leenheer [19] have described the effects of five organic modifiers on retention and selectivity of carotenoids on two different C_{18} columns. Bushway [35] has compared the selectivity of eight columns (two normal-phase and six reversed-phase) using several different solvent systems. Lauren and McNaughton [50] have compared ten reversed-phase columns with respect to alfalfa carotenoids' elution order, retention time, peak height and shape, etc. using acetonitrile and ethyl acetate with or without 0.1% *n*-decanol.

Recovery of carotenoids from the LC column is an important factor in carotenoid analysis. Frequently, serum carotenoid concentrations are near the detection limit so maximum sensitivity is necessary for accurate carotenoid measurements. This can only be achieved if carotenoid recovery is essentially 100%. Similarly, since epidemiological studies continue for extended periods, reproducibility is extremely important to the outcome of studies. Therefore only LC columns offering consistent and maximum recovery can yield the most meaningful results. Finally, there is a need to correlate carotenoid analysis by LC to older spectrophotometric measurements. If LC columns do not provide complete and consistent recovery of carotenoids, then LC measurements cannot be correlated with spectrophotometric measurements of carotenoids. Only one limited study has been reported that compared serum carotenoids measured by LC to total carotenoid concentration determined statically in a spectrophotometer [20]. We have compared sixty-five reversed-phase LC columns (primarily C_{18}-modified silica) for selectivity and recovery of a mixture of seven carotenoids, six of which are present in the serum of most American populations. This is the first study to report absolute recovery of carotenoids from LC columns.

EXPERIMENTAL[a]

Test mixture

An ethanol solution containing approximately 2 to 10 mg/l each of lutein (Kemin Industries, Des Moines, IA, USA); zeaxanthin, β-cryptoxanthin (Atomergic Chemetals, Farmingdale, NY, USA); echinenone (Hoffmann-La Roche, Nutley, NJ,

[a] Certain commercial equipment, instruments, or materials are identified in this report to specify adequately the experimental procedure. Such identification does not imply recommendation or endorsement by the National Institute of Standards and Technology, nor does it imply that the materials or equipment identified are necessarily the best available for the purpose.

USA); lycopene (extracted from tomato paste); and α- and β-carotene (Sigma, St. Louis, MO, USA) was prepared, and 2-ml aliquots of this solution were stored in amber glass vials at −20 °C. The respective concentrations of the compounds in the mixture were sufficiently different to provide some indication of identity based on chromatographic peak area. Prior to injection, 100 μl THF were added to a vial of the carotenoid mixture, and the mixture was placed in an ultrasonic bath for 10 min to ensure dissolution. This solution was then transferred to a vial and placed in an autosampler where it was held at a constant temperature of 15°C; the autosampler injected a 20-μl aliquot of the solution onto the column being tested.

Chromatographic conditions

A liquid chromatograph pumped the mobile phase at a rate of 1.5 ml/min. Solvents were premixed so as not to depend on reproducible mixing by the pump; the solvents were sparged with helium. The column being tested was held at 27°C by the LC column oven.

Columns

A list of the columns tested, serial number, manufacturer, and classification of the bonded C_{18} stationary phase (polymeric, monomeric, or intermediate [51]) is provided in Table I. Reversed-phase columns that were potentially useful for the separation of carotenoids were donated by LC column manufacturers. Columns prepared from different production lots from the same manufacturer were also requested in order to assess reproducibility. Several columns that were currently in use in our laboratory were tested as well. Most of the columns tested were C_{18}, 250 × 4.6 mm I.D., with 5-μm particles. All columns were made of stainless steel. All columns were alkyl-silane modified silica, except for the Biotage Unisphere Polybutadiene, which was modified alumina. The polymeric/monomeric/intermediate classification given in Table I refers to the type of stationary phase modification procedure, and is described in detail in the Results and Discussion section, as is the separation factor ($\alpha_{TBN-BaP}$ value) to which it is related.

Eluents based in methanol and acetonitrile were used in this study. Butylated hydroxytoluene-stabilized THF and ethyl acetate modifiers were added to the mobile phase for those columns that failed to elute all seven compounds with a capacity factor ($k' \leq 11$. Both THF [3,6,7,10,11,14,22,29,32,35,36,43] and ethyl acetate [19,50] have been used for carotenoid separations and represent two different solvent selectivity groups, III and VI, respectively. (Chlorinated solvents such as methylene chloride and chloroform were not tested because of a previous report of carotenoid losses caused by the hydrochloric acid that may be a trace contaminant in these solvents [52].) Prior to performing a separation, each column was flushed with THF at 1.5 ml/min for 4 min to remove any compounds remaining on the column from a previous run. The column was then equilibrated at 1.5 ml/min for 15 min with a given eluent. In cases where 100% methanol or acetonitrile eluted the compounds from the column with a $k' < 7$, no attempt was made to increase retention by the addition of water because of the minimal solubility of carotenoids in water and the opportunity for on-column precipitation [19,23].

Recovery determination

The photodiode array detector (Model 990, Waters, Milford, MA, USA) used to monitor the LC effluent acquired absorbance spectra from 350 to 500 nm with 20 scans/s at 2-s intervals. Data were acquired for 25 min at 0.5 a.u.f.s. Spectral data were used for peak identification when necessary. Visible absorbance at 450 nm was recorded by the data system for the quantitative comparison discussed below.

For the recovery study, the column was replaced with a 195-cm length of PTFE tubing (0.8-mm I.D.) to provide "peak" dispersion similar to the LC column. Using ethanol as the mobile phase, a 20-μl injection of the test mixture was considered to have a peak area that represented 100% recovery. Five such replicate measurements were made at the beginning and at the end of each day's work. With a column in place, the individual areas of the integrated peaks were totalled, and the total area was normalized to the average area of the 10 replicate injections when no column was used. Because the test mixture contained small quantities (1 to 7%) of impurities that certain columns may have been capable of resolving, all peaks eluting from a column were measured, not just the seven main peaks.

The linearity of the detector response was verified

TABLE I

LIST OF COLUMNS USED

Columns are C_{18} except where noted.

	Supplier	Column name	Serial No.	$\alpha_{TBN/BaP}$[a]	Classification[b]
1	Beckman	Ultrasphere ODS	9UE1898	1.92	Monomeric
2	Beckman	Ultrasphere ODS	8UE2757	2.01	Monomeric
3	Beckman	Ultrasphere ODS DABS	7UE2306	2.00	Monomeric
4	Analytichem	Sepralyte C18	072851-18	1.82	Monomeric
5	Separations Group	Vydac 218TP	890130-16	0.83	Polymeric
6	Separations Group	Vydac 201TP	890130-23	0.78	Polymeric
7	Separations Group	Vydac 201TP	890131-26	0.80	Polymeric
8	Biotage	Unisphere-PBD[c]	2167	3.06	Monomeric
9	ES Industries	Gamma Bond C18	19589-57-17992	1.86	Monomeric
10	ES Industries	Chromegabond C22 (C_{22})	19589-4-58-17994	1.83	Monomeric
11	ES Industries	Chromegabond MC18	19589-4-57-17991	1.73	Monomeric
12	Supelco	LC-18	18744F	2.03	Monomeric
13	Supelco	LC-18	18745F	2.02	Monomeric
14	Supelco	LC318	110224	2.05	Monomeric
15	Supelco	LC318	110232	2.04	Monomeric
16	Supelco	LC-PAH	81695	0.70	Polymeric
17	Analytichem	Sepralyte C18	071912-14	1.92	Monomeric
18	Alltech	Adsorbosphere C18	08039GA	2.01	Monomeric
19	EM Science	LiChrospher 100 RP-18	86554563	1.45	Intermediate
20	Serva	Octadecyl	03118	1.84	Monomeric
21	Serva	Triacontyl (C_{30})	–[d]		
22	J&W	Accusphere ODS	9050825	2.07	Monomeric
23	J&W	Accusphere ODS	9072526	1.96	Monomeric
24	MacMod	Zorbax RX C8 (C_8)	AU2642	2.33	Monomeric
25	Perkin Elmer	Pecosphere C18	1119	2.00	Monomeric
26	YMC	A303	42511	1.97	Monomeric
27	YMC	AMP303	4259	2.01	Monomeric
28	YMC	AP303	4250	2.06	Monomeric
29	J.T. Baker	exper WP C18[e]	1294-43	0.57	Polymeric
30	J.T. Baker	exper WP C18[e]	1294-26	0.93	Polymeric
31	J.T. Baker	exper WP C18[e]	1294-29	0.73	Polymeric
32	J.T. Baker	exper WP C18[e]	1239-64C	1.42	Intermediate
33	J.T. Baker	exper WP C18[e]	1239-64D	0.22	Polymeric
34	ES industries	Chromegabond PFP[f]	19589-4-58-17993	0.88	Polymeric
35	ES Industries	Chromegabond BF-C18	21389-4-60-18079	1.04	Intermediate
36	J.T. Baker[g]	Bakerbond C18	A29113-01	1.25	Intermediate
37	J.T. Baker[g]	Bakerbond WP C18	B36097.25	0.51	Polymeric
38	J.T. Baker[g]	Bakerbond WP C18	none	0.54	Polymeric
39	J.T. Baker[g]	Bakerbond WP C18	B33125.16	1.09	Intermediate
40	Keystone Sci.	ODS Hypersil	03708	1.95	Monomeric
41	Shiseido	Capsell Pak C18	SG120	1.99	Monomeric
42	Nacalai Tesque	Cosmosil 5C18-P Waters	391-03	2.04	Monomeric
43	Nacalai Tesque	Cosmosil 5C18 Waters	390-47	1.85	Monomeric
44	Waters	Nova-Pak C18	T93242	1.97	Monomeric
45	YMC	ASP303-5	42541	2.05	Monomeric
46	Hewlett-Packard	ODS Hypersil	79926OD-584	1.98	Monomeric
47	Hewlett-Packard	LiChrospher 100 RP-18	79925OD-584	1.50	Intermediate
48	Brownlee	Spheri-5 ODS	102454	1.26	Intermediate
49	Bio-Rad	Hi-Pore RP318	890215-11 No. 82	0.59	Polymeric
50	Macherey-Nagel	Nucleosil 5 PAH	90702B	0.36	Polymeric
51	Rainin[g]	Microsorb C18	10681	1.78	Monomeric
52	Phase Separations	Spherisorb S5 PAH	23/123 00-1046	0.82	Polymeric
53	Phase Separations	Spherisorb S5 ODS	29/69 19-1372	1.68	Intermediate

TABLE I (*continued*)

Supplier	Column name	Serial No.	$\alpha_{TBN/BaP}$[a]	Classification[b]
54 Phase Separations	Spherisorb S5 ODS	30/35 06-10-F1	1.50	Intermediate
55 Carlo Erba	Erbasil 5 C18/L	517250502	1.76	Monomeric
56 Carlo Erba	Erbasil 5 C18/M	517250503	1.28	Intermediate
57 Carlo Erba[h]	Erbasil 5 C18/H	517250504	0.91	Polymeric
58 Brownlee	Spheri-5 RP-18	109083	1.92	Monomeric
59 MacMod	Zorbax RX C18	880967.902	1.50	Intermediate
60 Phenomenex	Ultracarb 5 ODS20	PP/4953C	1.95	Monomeric
61 Phenomenex	Ultracarb 5 ODS30	PP/4954C	2.01	Monomeric
62 J.T. Baker	Bakerbond WP C18	1314-13	0.89	Polymeric
63 J.T. Baker	Bakerbond WP C18	DS097	0.67	Polymeric
64 Brownlee	Spheri-5 ODS	102402	1.42	Intermediate
65 MacMod[g]	Zorbax ODS	F36560	1.80	Monomeric

[a] Relative retention of 1,2:3,4:5,6:7,8-tetrabenzonaphthalene (TBN) to benzo[a]pyrene (BaP); see Results and Discussion section or ref. 51.
[b] As determined by evaluation of SRM 869 (see refs. 51 and 53).
[c] PBD = polybutadiene.
[d] Returned to supplier before value could be determined.
[e] Experimental columns with varying surface coverage.
[f] PFP = pentafluorophenol.
[g] Used in laboratory prior to evaluation in this study.
[h] Not tested due to excessive backpressure (>200 bar).

by injecting varying amounts of the mixture of seven carotenoids. The detector response was linear from 50 to 300% of the amount injected for evaluation of the columns.

RESULTS AND DISCUSSION

Sixty-five reversed-phase LC columns (Table I) were evaluated to determine selectivity and recovery of selected carotenoids. Lutein, zeaxanthin, β-cryptoxanthin, echinenone, lycopene, and α- and β-carotene were selected for use in the test mixture, and are shown in Fig. 2. Excluding echinenone, which is present in the human populations that consume echinoderms (sea urchins, starfish), these compounds account for more than 90% of the carotenoids present in American serum [20]. Echinenone was included because it has intermediate polarity and has been used as an internal standard for carotenoid measurements [20].

Column classification

A system has been developed for the classification of C_{18} stationary phases based on their separation of a mixture of polycyclic aromatic hydrocarbons (PAHs) [51]. The application of this classification scheme has proven useful for selecting columns for separating PAH isomers and steroids, two classes of compounds with rigid molecular

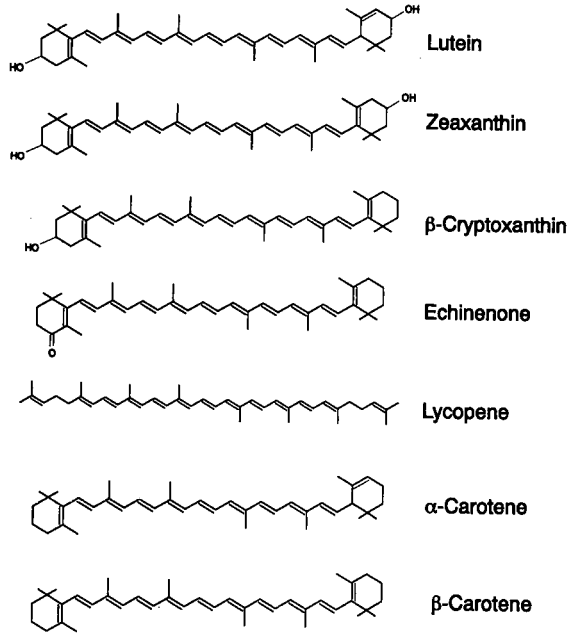

Fig. 1. Structures of carotenoids used in test mixture.

structures [51]. Because carotenoid isomers also have a rigid structure, it was thought that the classification scheme might provide insight into retention mechanisms for carotenoids, as well as provide assistance in column selection.

The C_{18} columns in this study were classified into three stationary phase types using Standard Reference Material (SRM) 869, Column Selectivity Test Mixture for Liquid Chromatography [51,53]. The SRM is a mixture of three PAHs: benzo[*a*]pyrene (BaP), 1,2:3,4:5,6:7,8-tetrabenzonaphthalene (TBN), and phenanthro [3,4-*c*]phenanthrene. Columns were classified by calculating the relative retention of TBN to BaP. The resulting $\alpha_{TBN-BaP}$ values were grouped as follows: those columns with an $\alpha_{TBN-BaP}$ less than 1 are classified as polymeric, those with an $\alpha_{TBN-BaP}$ between 1 and 1.7 are classified as intermediate, and those with an $\alpha_{TBN-BaP}$ greater than 1.7 are classified as monomeric. The $\alpha_{TBN-BaP}$ values for each column are provided in Table I. These values may not be directly comparable for the five columns whose stationary phases were not C_{18}. Nonetheless, 35 of the columns tested were classified as monomeric, 17 were polymeric and 12 were intermediate at 27°C.

This classification scheme is strongly related to the procedures used in the bonded-phase synthesis, *i.e.*, monomeric phases prepared by the reaction of silica with monofunctional silanes (usually in the absence of water) have properties that differ from polymeric phases prepared by reaction of silica with trifunctional silanes in the presence of water. (The third group is an arbitrary classification for which phase chemistry is less certain; this group has properties that are intermediate to the monomeric and polymeric classes.)

Selectivity

Optimum carotenoid selectivity of each column was difficult to assess, since a mobile phase was not tailored for each. Our design was limited to an isocratic, nonaqueous binary mobile phase separation, with the capacity factor, k', manipulated through the addition of THF or ethyl acetate such that $7 \leqslant k' \leqslant 11$. Under the defined conditions, lutein and zeaxanthin were the most difficult carotenoids to resolve due to their structural similarity and early elution.

No monomeric C_{18} column evaluated in this study was able to resolve lutein and zeaxanthin using methanol or methanol-based solvents. Using acetonitrile-based solvents, monomeric C_{18} columns were sometimes able to separate this pair partially. The polymeric C_{18} columns were usually able to separate lutein and zeaxanthin. Typical chromatograms for columns classified as monomeric, polymeric, and intermediate are shown in Figs. 2, 3 and 4, respectively; chromatographic conditions are described in those figures. In Table II, resolution (R) and α values for zeaxanthin/lutein and β-carotene/lycopene are shown for a representative one-third of the columns. The actual frequency and inability of a class of columns to separate lutein and zeaxanthin is represented, *i.e.*, if one in every three monomeric columns failed to separate lutein and zeaxanthin, then one of every three numbers shown for the monomeric columns in Table II is for a column that failed to separate this pair. Using monomeric and most intermediate columns, the elution of lycopene was followed by that of α- and β-caro-

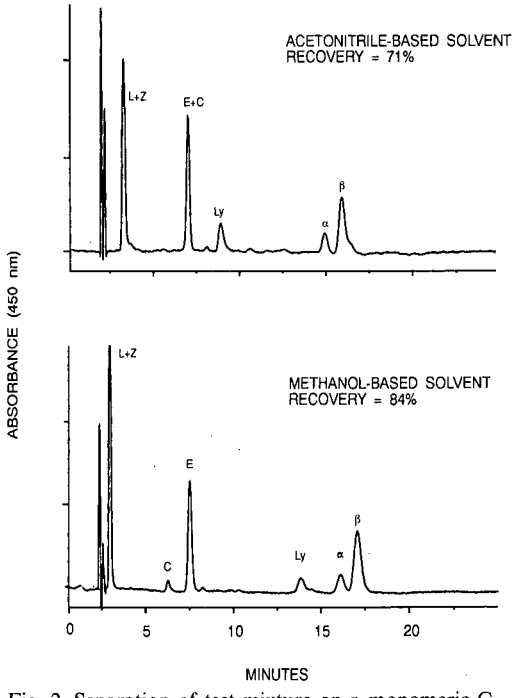

Fig. 2. Separation of test mixture on a monomeric C_{18} phase. Eluent is THF–methanol (10:90) or THF–acetonitrile (15:85) at a flow-rate of 1.5 ml/min. Legend: L = lutein, Z = zeaxanthin, C = β-cryptoxanthin, E = echinenone, Ly = lycopene, α = α-carotene, β = β-carotene.

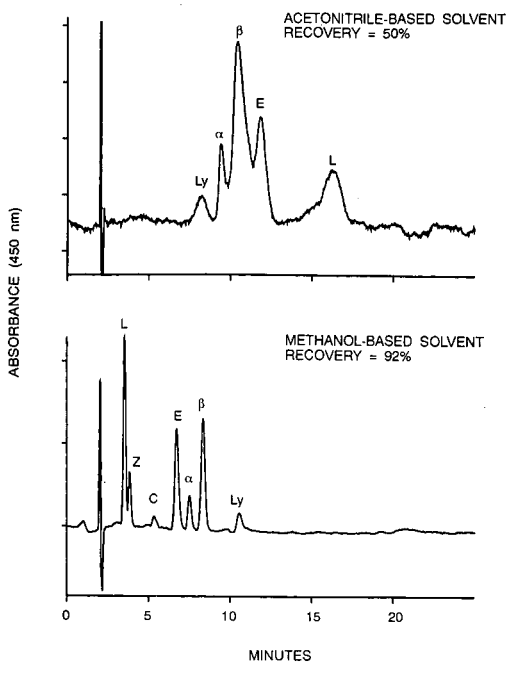

Fig. 3. Separation of test mixture on a polymeric C_{18} phase. Eluent is 100% methanol or 100% acetonitrile at a flow-rate of 1.5 ml/min. For legend, see Fig. 2.

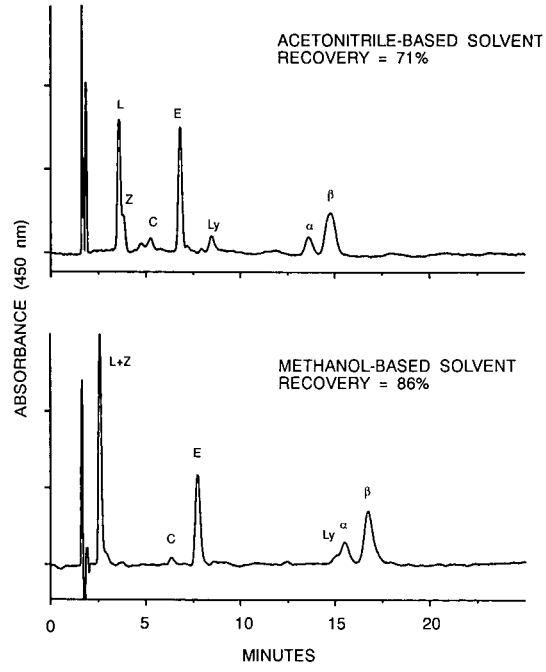

Fig. 4. Separation of test mixture on an intermediate C_{18} phase. Eluent is THF–methanol (7.5:92.5) or THF–acetonitrile (12.5:87.5) at a flow-rate of 1.5 ml/min. For legend, see Fig. 2.

TABLE II

RESOLUTION (R) AND SELECTIVITY (α) FOR ZEAXANTHIN/LUTEIN (Z/L) AND β-CAROTENE/LYCOPENE (B/Ly) ON SELECTED C_{18} COLUMNS USING METHANOL AND THF–METHANOL COMPARED TO THE TBN/BaP α VALUE ON THOSE COLUMNS

Column[a]	Character	$\alpha_{Z/L}$	$R_{Z/L}$	$\alpha_{B/Ly}$	$R_{B/Ly}$	$\alpha_{TBN/BaP}$
22	Monomeric	1	0	1.28	13	2.07
14	Monomeric	1	0	1.20	6.2	2.05
18	Monomeric	1	0	1.28	14	2.01
25	Monomeric	1	0	1.18	7.8	2.00
41	Monomeric	1	0	1.24	7.8	1.99
44	Monomeric	1	0	1.29	13	1.97
26	Monomeric	1	0	1.27	12	1.97
40	Monomeric	1	0	1.29	12	1.95
1	Monomeric	1	0	1.28	13	1.92
20	Monomeric	1	0	1.19	7.4	1.84
11	Monomeric	1	0	1.36	7.9	1.73
53	Intermediate	1	0	1.15	10	1.68
59	Intermediate	1	0	1.24	13	1.50
19	Intermediate	1	0	2.16	19	1.45
35	Intermediate	1.20	2.9	0.91	6.0	1.04
30	Polymeric	1.18	2.9	0.78	8.0	0.93
5	Polymeric	1.21	2.9	0.83	5.8	0.83
6	Polymeric	1.23	4.0	0.74	12	0.78
16	Polymeric	1.22	4.4	0.74	12	0.70
49	Polymeric	1.26	3.9	0.70	16	0.59
37	Polymeric	1.32	4.6	0.56	35	0.51

[a] See Table I for column descriptions.

tene. Using polymeric columns, the elution order often changed to α-carotene, β-carotene, lycopene, thus the α- values for the polymeric columns (and one intermediate column) in Table II are less than one. In general, if the column could resolve lutein and zeaxanthin, then lycopene eluted after α- and β-carotene. Quackenbush and Smallidge [54] and Bushway [35] have also observed that Vydac 201TP and 218TP columns, which are polymeric, reverse the order of elution of lycopene and β-carotene compared to other (monomeric) columns that they tested, although they did not recognize the monomeric or polymeric phase synthesis of the columns as the cause. Polymeric phases have also been reported to provide better separation of certain carotenoids and their *cis* isomers [35,54,55].

To investigate whether the selectivity for selected carotenoids correlates with the selectivities for the PAHs, $\alpha_{TBN/BaP}$ values for the columns are also shown in Table II. On the polymeric columns, $\alpha_{TBN/BaP}$ and $\alpha_{zeaxanthin/lutein}$ are correlated (correlation coefficient, $r = -0.94$), as are $\alpha_{TBN/BaP}$ and $\alpha_{\beta\text{-carotene/lycopene}}$ ($r = 0.86$). Despite the small sample size ($n = 6$ polymeric columns), there is more than 95% confidence that a correlation does exist, according to Pearson Product Moment correlation coefficient tables [56]. There is no correlation between the $\alpha_{TBN/BaP}$ and the $\alpha_{zeaxanthin/lutein}$ on the monomeric columns because all the $\alpha_{zeaxanthin/lutein}$ values are 1, as is the case for most of the intermediate columns' $\alpha_{zeaxanthin/lutein}$ values. There is also no correlation between the $\alpha_{TBN/BaP}$ and the $\alpha_{\beta\text{-carotene/lycopene}}$ on both the monomeric and intermediate columns. Thus, the $\alpha_{TBN/BaP}$ values are useful for predicting whether a column will be able to separate lutein and zeaxanthin inasmuch as it indicates whether the column is monomeric, polymeric, or intermediate, since mainly polymeric columns are capable of resolving this pair. However, it is not useful for predicting whether an intermediate column will be able to resolve lutein and zeaxanthin, nor can it predict how much separation of lycopene and β-carotene a monomeric or intermediate column is likely to provide.

For most columns it was necessary to add a mobile phase modifier to elute compounds with a $k' \leqslant 11$. The choice of modifier (THF or ethyl acetate) did not significantly affect selectivity for either lutein/zeaxanthin or lycopene/β-carotene, the two pairs that were examined. Columns that failed to resolve lutein and zeaxanthin using methanol-based solvents failed using each modifier. On a few columns, the use of one modifier in acetonitrile did provide higher α values than the other, but the difference was not great enough to significantly improve resolution. THF did not consistently provide higher α values than ethyl acetate or vice versa. For the separation of lycopene and β-carotene, selectivity differed slightly using acetonitrile-based mobile phases on some columns. On one or two columns using methanol-based solvents, the α values for lycopene and β-carotene may have been more significantly affected by the choice of modifier. Again, THF was not consistently better or worse than ethyl acetate at providing greater resolution.

Pore size of the column can affect the selectivity for carotenoids of sufficiently different size (*e.g.*, lycopene and β-carotene, zeaxanthin and β-carotene) but does not affect selectivities for carotenoids of very similar sizes (*e.g.*, α-carotene and β-carotene). In a comparison of four monomeric columns from the same manufacturer (column 45, 26, 27 and 28), the only difference being pore size of the silica substrate (*i.e.*, 60, 120, 200 and 300 Å, respectively), both $\alpha_{\beta\text{-carotene/lycopene}}$ and $\alpha_{\beta\text{-carotene/zeaxanthin}}$ decrease with increasing pore size. This also holds true for a comparison of two other sets of wide-pore columns and their narrow-pore counterparts (columns 12 and 13, 100 Å *vs.* columns 14 and 15, 300 Å; column 36, 120 Å *vs.* column 37, 300 Å). In addition, as pore size decreases, more modifier must be added in all three cases to elute all seven compounds with a $k' \leqslant 11$. This is as expected since the greater surface area of the base silica of the narrow-pore columns results in a higer carbon load. Although absolute retention of carotenoids increases with decreasing pore size (and increasing carbon loading), α values for similarly sized carotenoids do not change with column pore size. An example of this trend is the α values for β-carotene/α-carotene, which are the same for the sets of columns described above.

Recovery

Sample losses on the column are critical to the sensitivity and precision of an LC method and to quantitative analysis. Carotenoid recoveries ranging from 0 to almost 100% were observed. Recovery was dependent on the mobile phase, stationary phase type classification, and possibly the column bed support frit material.

Mobile phase. On almost all the columns tested, the use of methanol or methanol-based solvents provided a higher recovery of the carotenoids than did the use of acetonitrile of acetonitrile-based solvents, as shown by the mean recoveries given in Table III. When using acetonitrile-based mobile phases, the THF modifier resulted in a higher percent recovery on most columns than did the ethyl acetate. This difference in recovery was less noticeable when the methanol-based eluents were used. Addition of a modifier was not necessary for about half the columns when methanol was used and about one-third of the columns when acetonitrile was used. Typically, it took less THF than ethyl acetate to elute the compounds with $k' \leqslant 11$, and methanol required less modifier than acetonitrile, which is contrary to expectations based on solvent strength parameters, where acetonitrile is classified as a stronger solvent than methanol [57]. However, this observation is consistent with the findings of Nelis and De Leenheer, who reported that methanol acts as a stronger solvent than acetonitrile for the separation of carotenoids on C_{18} columns [19]. Since recoveries were lower and no improvements in selectivity were observed, ethyl acetate-modified solvents are not discussed further to simplify data analysis. Henceforth each column has just two sets of results: 100% methanol and 100% acetonitrile, or THF–methanol and THF–acetonitrile if it was necessary to use a modifier.

TABLE III

AVERAGE RECOVERY OF CAROTENOIDS ON ALL COLUMNS TESTED USING DIFFERENT MOBILE PHASES

THF or ethyl acetate are added to methanol and acetonitrile as modifiers such that $7 \leqslant k'_{max} \leqslant 11$.

Mobile phase	Recovery ± S.D. (%)
100% methanol	84 ± 8 (n = 29)[a]
Methanol–THF	86 ± 11 (n = 35)
Methanol–ethyl acetate	82 ± 12 (n = 35)
100% Acetonitrile	56 ± 19 (n = 21)
Acetonitrile–THF	68 ± 17 (n = 43)
Acetonitrile–ethyl acetate	47 ± 17 (n = 43)

[a] n = Number of columns.

Acetonitrile-based solvents are typically used for the carotenoid separations reported in the literature [3–12,14,17–20,22,25,26,29–38,40–48]. However, our studies show that recoveries using acetonitrile and acetonitrile-based eluents are generally lower than those obtained using methanol and methanol-based eluents. Nelis and De Leenheer [19] reported that the incorporation of methanol in acetonitrile-based solvents dramatically enhanced selectivity, which they speculated was due to hydrogen bonding. Most of the acetonitrile-based methods reported in the literature do involve the use of some methanol [3,6,7,9–11,14,17,19,20,22,26,29–35,37,38,40–44,46–48]. To determine whether the addition of methanol improved recovery as well as selectivity, a column that had provided 0% recovery when run with 100% acetonitrile and 77% recovery with 100% methanol was tested with a methanol–acetonitrile (10:90) mixture. Recovery with respect to the 100% acetonitrile run improved only slightly (up from 0 to 2%). A run using methanol–acetonitrile (20:80) as the eluent resulted in 4% recovery. Thus the addition of methanol did improve recovery marginally. The column tested performed poorly using 100% acetonitrile; it would be unfair to say that recovery on all columns using acetonitrile-based solvents would also show only a 2% increase in recovery with the addition of methanol.

The poor performance of certain columns appears to be real and not an artifact. When poorly performing columns were rechecked at a later date, performance had not changed. In addition, recovery was not affected when various sample sizes were injected (from 5 μl to 100 μl). Lauren and McNaughton [50] recommend the addition of 0.1% n-decanol to the mobile phase to improve performance by minimizing adsorption. We did not find n-decanol to be effective in improving the performance of columns with poor recoveries using acetonitrile-based solvents. However, we have observed that flushing the column with an ammonium acetate buffer improves recovery on these columns when an acetonitrile-based mobile phase is used. We have also found that the addition of ammonium acetate to the mobile phase improves recoveries.

To determine the reproducibility of recovery results, one column from each of the three classification groups was retested about four months after the initial test. Columns that had required 100%

methanol were selected to eliminate any effect caused by slight variations in the mobile phase composition. Columns were also selected that had provided recoveries greater than 80% in the first test. Relative standard deviations ranged from 2.5 to 5.6%. An insufficient number of runs were made on individual columns to allow statistical comparisons of methanol or methanol-based and acetonitrile or acetonitrile-based recoveries for each column; however, based on the reproducibility studies, 6% represents a liberal estimate of the relative standard deviation. Using this estimate of variability, columns with a 12% difference in recovery between methanol- and acetonitrile-based eluents would be significantly different. Columns are grouped according to their recoveries using methanol or THF–methanol and acetonitrile or THF–acetonitrile in Table IV.

Selective recovery. Experiments were performed to determine whether certain carotenoids contributed a greater share to recovery losses than did the other carotenoids. Individual carotenoids were injected into the system, both with and without a column, as described. Two monomeric-phase and three polymeric-phase columns were tested. All columns had previously required 100% methanol for elution of the carotenoids in less than 25 min. Four of the columns had required 100% acetonitrile; one required THF–acetonitrile (5:95). Two trends in recovery were observed. Losses of zeaxanthin and β-carotene, which each contain two β-rings (Fig. 1), were greater than losses of lutein and α-carotene, which each contain one β- and one ε-ring. Within the group of β,β-carotenoids used in the mixture (zeaxanthin, β-cryptoxanthin, echinenone, and β-carotene), recovery increased as polarity decreased: less zeaxanthin, a dihydroxy carotenoid, was recovered than β-cryptoxanthin, a monohydroxy carotenoid. Less β-cryptoxanthin was recovered than echinenone, a mono-keto carotenoid. And less echinenone was recovered than β-carotene, a hydrocarbon carotenoid. This trend also holds true for the two β,ε-carotenoids used in the mixture. The recovery of the dihydroxy carotenoid, lutein, was less than that of the hydrocarbon carotenoid, α-carotene.

Stationary phase. In these carotenoid studies, as a rule, polymeric phases required the least modifier (a mean value of 2% THF in methanol, 3% THF in acetonitrile) and monomeric phases required the most (a mean value of 6% THF in methanol, 9% THF in acetonitrile) to elute all seven compounds from the column within the k' range allowed ($7 \leqslant k' \leqslant 11$). Intermediate phases required an intermediate amount of modifier (4% THF in methanol, 6% THF in acetonitrile). Percent recovery across the three groups did not vary consistently. Recovery results for columns divided into the three classification groups are shown in Table V. Thirty percent of the columns gave >90% recovery using

TABLE IV

COLUMNS USED IN THIS STUDY GROUPED ACCORDING TO PERCENT RECOVERIES

Recovery (%)	Columns
Using methanol or THF–methanol:	
90–100	3 5 7 11 15 21 23 24 26 27 28 29 30 32 41 42 43 44 45 52 65
80–89	1 2 4 6 8 10 12 13 14 16 17 18 19 22 25 31 35 37 38 39 40 46 47 48 49 50 51 53 54 58 59 60 61
70–79	20 33 36 55 63 64
60–69	42 62
50–59	9
40–49	–
30–39	56
Using acetonitrile or THF–acetonitrile:	
90–100	43 50 51
80–89	2 3 23 27 37 49 60 61
70–79	1 4 8 12 13 18 21 22 26 30 32 41 42 45 47 52 58 59
60–69	5 10 25 28 29 33 36 44 48 65
50–59	9 11 14 15 17 20 24 31 38 40 46
40–49	6 7 16 19 35 39 62 64
30–39	63
20–29	–
10–19	–
0–9	53 54 55 56

TABLE V

AVERAGE PERCENT RECOVERY FOR POLYMERIC, INTERMEDIATE, AND MONOMERIC COLUMNS TESTED

Eluent	Polymeric	Intermediate	Monomeric
MeOH[a]	83%	79%	88%
ACN[b]	62%	46%	67%

[a] MeOH = methanol and methanol-based eluents.
[b] ACN = acetonitrile and acetonitrile-based eluents.

methanol or THF–methanol as the solvent; of these, 70% were classified as monomeric and the remaining 30% were classified as polymeric.

In several cases, columns were available that contained the "same" packing material from different lots. Recovery results and k' values for selected compounds using THF–methanol for columns from different production lots are presented in Table VI. Mean recoveries for many of the columns appear to be different, but performance of Tukey's Multiple Comparison test [58] on these data shows that there is no difference between the mean recoveries at a 95% confidence level for almost all the column pairs.

Retention times of carotenoids using columns from different stationary phase lots varied substantially. (On one pair of columns, there was a 15% difference in β-carotene's retention time.) This variability can arise from two sources: the base silica from which the stationary phase is prepared and reproducibility of the bonding procedure. Most LC column manufacturers obtain silica from outside suppliers, and differences between column lots is strongly related to differences in the silica—particle size, pore size, surface area, silanol activity, and trace metal contamination. Thus, column lot differences can exist for both monomeric and polymeric phases. The only way to ensure reproducible columns is to purchase columns packed with the same production lot of stationary phase.

Column bed support frits. It has been suggested that losses occurring on column frit materials may be partially responsible for low recoveries of carotenoids [3,23]. Data from two sets of columns that were identical except for the presence of different frits are presented in Table VII. Although recoveries were slightly lower for stainless steel frits, no significant differences in recoveries between these sets of columns were detected. Later studies in which frits were placed in series (without a column in the system) showed no significant difference in recovery using stainless steel, titanium, or "biocompatible" frits.

In 1986, Nierenberg and Lester [3] observed dif-

TABLE VI

COMPARISON OF k' AND RECOVERY FOR COLUMNS FROM DIFFERENT LOTS

Column[a]	k'			Recovery (%)	n^b
	Lutein	Echinenone	β-carotene		
4	0.30	2.91	8.38	87	3
17	0.20	2.75	8.08	82	3
12	0.26	2.60	7.07	92	3
13	0.20	2.66	7.25	89	3
14	0.27	2.21	5.86	88	3
15	0.30	2.31	6.07	90	5
16	0.73	1.83	2.80	86	5
66[c]	0.66	2.00	2.95	92	5
40	0.43	3.18	8.22	86	3
46	0.49	3.06	7.76	92	3
48	0.35	3.24	8.16	86	3
64	0.38	3.57	9.18	78	3
37	1.03	3.00	4.81	82	3
62	0.74	2.58	3.89	87[d]	4
63	0.59	2.60	3.82	73[d]	2

[a] See Table I for column descriptions.
[b] n = Number of runs.
[c] Supelco LC-PAH column tested after the completion of the other analyses.
[d] Statistical difference in recovery as determined by Tukey's Multiple Comparisons.

TABLE VII

COMPARISON OF k' AND RECOVERIES ON COLUMNS WITH DIFFERENT FRIT MATERIALS

Column[a]	Frit	k'			Recovery (%)	n
		Lutein	Echinenone	β-carotene		
6	SS[b]	0.75	2.46	3.30	86	5
7	Ti	0.75	2.53	3.42	88	5
1	SS	0.28	2.85	8.27	87	5
3	Ti	0.29	3.02	8.93	92	5
2	Hast	0.33	2.98	8.54	93	5

[a] See Table I for column description.
[b] SS = Stainless steel; Ti = titanium; Hast = Hastelloy.

ferences in recovery when they switched to a new column of the same brand from the same manufacturer, but with a different kind of frit, and they attributed these differences to the use of different frits (stainless steel *vs.* Hastelloy). They also observed this phenomenon when two columns were packed with the same lot of packing material, topped with either stainless steel or Hastelloy frits. During our studies, it was observed that a certain previously unused column did not provide the same recovery or retention times as its older, used, counterpart, but that the "new" column gradually attained the retention and recovery characteristics of the "old" column with repeated use. Columns that had been used in our laboratory prior to this study have been marked in Table I, in the event that results for these columns have been affected by previous use in the laboratory.

CONCLUSIONS

Several conclusions concerning the selectivity and recovery of carotenoids in reversed-phase LC can be drawn from this study: (1) In general, separations using acetonitrile or the frequently employed acetonitrile-based solvents resulted in lower recoveries than separations using methanol or methanol-based solvents. (2) Monomeric C_{18} columns generally provided high recoveries, but they were unable to resolve lutein and zeaxanthin using methanol or methanol-based eluents, which were the solvents yielding the highest recoveries. (3) Polymeric C_{18} columns were usually able to resolve lutein and zeaxanthin in methanol-based solvents, but on average had lower recoveries than monomeric C_{18} columns. (4) Using methanol-based solvents, the retention time of lycopene is greater than that of β-carotene on most polymeric columns. (5) Columns with the "same" stationary phases from different lots do not necessarily elute compounds with the same retention times. (6) When using a new column, it may be necessary to make several preliminary runs before the separation (*i.e.*, retention times, recovery, selectivity) becomes reproducible and comparable to that expected based on the performance of the corresponding "old" column. (7) The most appropriate system for the separation of carotenoids would probably include the use of a polymeric C_{18} column (to allow separation of lutein and zeaxanthin) and a methanol-based mobile phase (to obtain a high percent recovery).

ACKNOWLEDGEMENTS

This work was supported in part by the National Cancer Institute, Division of Cancer Etiology, Agreement No. Y01-CP9-0513. We extend our thanks to the many companies who supplied us with their columns for this study.

REFERENCES

1 R. Peto, R. Doll, J. D. Buckley, and M. B. Sporn, *Nature, (London)*, 290 (1981) 201.
2 R. G. Ziegler, *Am. J. Clin. Nutr.*, 53 (1991) 251S.
3 D. W. Nierenberg and D. C. Lester, *J. Nutr. Growth Cancer*, 3 (1986) 215.
4 W. J. Driskell, J. W. Neese, C. C. Bryant and M. M. Bashor, *J. Chromatogr.*, 231 (1982) 439.

5 W. J. Driskell, M. M. Bashor and J. W. Neese, *Clin. Chem.*, 29 (1983) 1042.
6 Y. M. Peng, J. Beaudry, D. S. Alberts and T. P. Davis, *J. Chromatogr.*, 273 (1983) 410.
7 C. C. Tangney, *J. Liq. Chromatogr.*, 7 (1984) 2611.
8 W. J. Driskell, A. D. Lackey, J. S. Hewett and M. M. Bashor, *Clin. Chem.*, 31 (1985) 871.
9 K. W. Miller and C. S. Yang, *Anal. Biochem.*, 145 (1985) 21.
10 D. A. Kalman, G. E. Goodman, G. S. Omenn, G. Bellamy and B. Rollins, *J. Natl. Cancer Inst.*, 79 (1987) 975.
11 C. R. Broich, L. E. Gerber and J. W. Erdman, Jr., *Lipids*, 18 (1983) 253.
12 N. Katrangi, L. A. Kaplan and E. A. Stein, *J. Lipid Res.*, 25 (1984) 400.
13 K. W. Miller, N. A. Lorr and C. S. Yang, *Anal. Biochem.*, 138 (1984) 340.
14 D. W. Nierenberg, *J. Chromatogr.*, 339 (1985) 273.
15 D. B. Milne and J. Botnen, *Clin. Chem.*, 32 (1986) 874.
16 V. J. Gatautis and K. H. Pearson, *Clin. Chim. Acta*, 166 (1987) 195.
17 Y. Ito, R. Sasaki, M. Minohara, M. Otani and K. Aoki, *Clin. Chim. Acta*, 169 (1987) 197.
18 G. Wang, M. M. Root, X. Ye, J. Chen and T. C. Campbell, *J. Micronutr. Anal.*, 5 (1989) 3.
19 H. J. C. F. Nelis and A. P. De Leenheer, *Anal. Chem.*, 55 (1983) 270.
20 J. G. Bieri, E. D. Brown and J. C. Smith, Jr., *J. Liq Chromatogr.*, 8 (1985) 473.
21 R. Ohmacht, Gy. Tóth and G. Voigt, *Chromatographia*, 22 (1986) 189.
22 M. Stacewicz-Sapuntzakis, P. E. Bowen, J. W. Kikendall and M. Burgess, *J. Micronutr. Anal.*, 3 (1987) 27.
23 W. A. MacCrehan and E. Schönberger, *Clin. Chem.*, 33 (1987) 1585.
24 R. Ohmacht, Gy. Tóth and G. Voigt, *J. Chromatogr.*, 395 (1987) 609.
25 L. A. Kaplan, J. A. Miller and E. A. Stein, *J. Clin. Lab. Anal.*, 1 (1987) 147.
26 C. S. Yang and M. J. Lee, *J. Nutr. Growth Cancer*, 4 (1987) 19.
27 A. L. Sowell, D. L. Huff, E. W. Gunter and W. J. Driskell, *J. Chromatogr.*, 431 (1988) 424.
28 G. Cavina, B. Gallinella, R. Porra, P. Pecora and C. Suraci, *J. Pharm. Biomed. Anal.*, 6 (1988) 259.
29 L. R. Cantilena and D. W. Nierenberg, *J. Micronutr. Anal.*, 6 (1989) 127.
30 A. B. Burua, R. O. Batres, H. C. Furr and J. A. Olson, *J. Micronutr. Anal.*, 5 (1989) 291.
31 B. Olmedilla, F. Granado, E. Rojas-Hidalgo and I. Blanco, *J. Liq. Chromatogr.*, 13 (1990) 1455.
32 A. J. Culling-Berglund, S. A. Newcomb, M. Gagne, W. S. Morfitt and T. P. Davis, *J. Micronutr. Anal.*, 5 (1989) 139.
33 Y. Kim, C. English, P. Reich, L. E. Gerber and K. L. Simpson, *J. Agric. Food Chem.*, 30 (1990) 1930.
34 J. C. Bauernfeind, *J. Agric. Food Chem.*, 20 (1972) 456.
35 R. J. Bushway, *J. Liq. Chromatogr.*, 8 (1985) 1527.
36 J. L. Bureau and R. J. Bushway, *J. Food Sci.*, 51 (1986) 128.
37 F. Khachik, G. R. Beecher, and N. F. Whittaker, *J. Agric. Food Chem.*, 34 (1986) 603.
38 J. F. Fisher and R. L. Rouseff, *J. Agric. Food Chem.*, 34 (1986) 985.
39 C. Fisher and J. A. Kocis, *J. Agric. Food Chem.*, 35 (1987) 55.
40 P. W. Simon and Z. Y. Wolff, *J. Agric. Food Chem.*, 35 (1987) 1017.
41 F. Khachik and G. R. Beecher, *J. Chromatogr.*, 449 (1988) 119.
42 F. Khachik and G. R. Beecher, *J. Agric. Food Chem.*, 36 (1988) 929.
43 S. Scalia and G. W. Francis, *Chromatographia*, 28 (1989) 129.
44 B. Czinkotai, H. G. Daood, P. A. Biacs and F. Hajdu, *J. Liq. Chromatogr.*, 12 (1989) 2707.
45 P. A. Biacs, H. G. Daood, A. Pavisa and F. Hajdu, *J. Agric. Food Chem.*, 37 (1989) 350.
46 M. I. Heinonen, V. Ollilainen, E. K. Linkola, P. T. Varo and P. E. Koivistoinen, *J. Agric. Food Chem.*, 37 (1989) 655.
47 F. Khachik, G. R. Beecher and W. R. Lusby, *J. Agric. Food Chem.*, 37 (1989) 1465.
48 M. I. Heinonen, *J. Agric. Food Chem.*, 38 (1990) 609.
49 M. Zakaria, K. Simpson, P. R. Brown and A. Krstulovic, *J. Chromatogr.*, 176 (1979) 109.
50 D. R. Lauren and D. E. McNaughton, *J. Liq. Chromatogr.*, 9 (1986) 2013.
51 L. C. Sander and S. A. Wise, *LC · GC*, 5 (1990) 378.
52 G. Britton, *Methods Enzymol.*, 111 (1985) 113.
53 *Certificate of Analysis, SRM 869, Column Selectivity Test Mixture for Liquid Chromatography*, National Institute of Standards and Technology, Gaithersburg, MD, 1990.
54 F. W. Quackenbush and R. L. Smallidge, *J. Assoc. Off. Anal. Chem.*, 69 (1986) 767.
55 N. E. Craft, L. C. Sander and H. F. Pierson, *J. Micronutr. Anal.*, 8 (1991) 209.
56 N. R. Ullman, *Elementary Statistics*, Wiley, New York, 1978.
57 L. R. Snyder, *Introduction to Modern Liquid Chromatography*, Wiley, New York 1979.
58 H. Schessé, *The Analysis of Variance*, Wiley, Chichester, 1959.

Journal of Chromatography, 595 (1992) 103–111
Elsevier Science Publishers B.V., Amsterdam

CHROM. 23 884

Physical and biochemical characterization of five commercial resins for immunoaffinity purification of factor IX

John Tharakan*

Howard University, Department of Chemical Engineering, Washington, DC 20059 (USA)

Frank Highsmith

University of Maryland, Department of Chemical Engineering, College Park, MD 20742 (USA)

David Clark and William Drohan

American Red Cross, Plasma Derivatives Laboratory, Rockville, MD 20855 (USA)

(First received June 26th, 1991; revised manuscript received November 19th, 1991)

ABSTRACT

The American Red Cross has developed an immunoaffinity chromatography method to purify human coagulation factor IX (FIX) to homogeneity using monoclonal antibodies (MAb) that bind FIX in the presence of divalent cations. The MAb is immobilized on Sepharose CL2B, a soft gel with a low pressure tolerance as well as poor large-scale performance characteristics, including low reusability, and resin crumbling and deterioration. In this study, we examined several commercially available resin supports. Aside from Sepharose CL2B, we studied two other cross-linked agaroses, as well as two synthetic polymer supports. Immobilization chemistries included cyanogen bromide activation of agarose, 2-fluoro-2 methylpyridinium toluene-4-sulfonate activation of one of the synthetic polymer as well as aldehyde group reduction by $NaCNBH_3$ to form secondary amine linkages on one of the cross-linked agaroses. To determine the feasibility of using the resins in large-scale immunoaffinity chromatographic purification of FIX, we studied physical and biochemical properties of the resins. The physical characteristics studied included the crushability of the resins under pressure as well as ability to support increasing flow-rates at increasing pressures. The biochemical examination of the various resins focused on efficiency of antigen capture by the immobilized antibody ligand and the effect of flow-rate on MAb efficiency, where we found that very low flow-rates slightly increased the capacity of the MAb.

The results demonstrate a straightforward method of assessing the feasibility of using particular resins in large-scale affinity purification.

INTRODUCTION

The separation of proteins from complex mixtures using immunoaffinity chromatography is being increasingly applied to large-scale processes [1]. In the development of these large-scale processes, it is important to select a resin that effectively separates the desired protein while being capable of supporting high flow-rates and resisting extensive crushing.

The American Red Cross has developed a large-scale immunoaffinity process [2] based on the use of a divalent cation-dependent monoclonal antibody (MAb) [3] coupled to Sepharose CL2B (Pharmacia, Uppsala, Sweden) to produce highly pure human coagulation factor IX (FIX), an essential protein involved in the blood clotting cascade. This resin support is also being utilized in the development of various other immunoaffinity-purified plasma protein products. In the course of the process devel-

0021-9673/92/$05.00

opment, we discovered that the CL2B resin was not capable of supporting a high flow-rate without developing a significant back pressure. We also observed that the maximum pressure that the CL2B resin could withstand without being crushed was less than 0.3 bar. To operate the process at this low pressure involved an unacceptable lengthening of the process time and attendant decreases in process efficiency. The CL2B resin performed well as far as the ability to bind high levels of FIX and the purity of the product obtained. In earlier studies, for example, comparing hydrazide and CNBr-activated immunosorbents [4], the CNBr-CL2B resin performed as well or better than the other resins tested.

However, in order to decrease process time while maintaining the purity of the FIX produced, we explored the use of several other MAb support resins, two other agarose-based resins as well as two synthetic polymer supports. In this paper, we report the data from our investigations.

MATERIALS AND METHODS

Resins

The resins used in the flow and compression studies as well as the immunoaffinity chromatography studies are listed in Table I. They have been identified by letter to facilitate labeling and their major characteristics are listed, including pore exclusion limit, pressure limit and the maximum supportable linear flow-rate. Manufacturer's of the resins are also identified.

Pressure/flow experiments

Fig. 1 illustrates the experimental apparatus used to measure resin compression and the relationship between pressure and flow for each of the resins tested. In each experiment, the resin was packed into the column (C10/20, 200 mm × 10 mm I.D., adjustable bed depth, Pharmacia) and allowed to settle under gravity. The upper flow adapter was then inserted to the upper level of the resin bed and then the pressure source connected. Pressure was increased in the feed source tank and flow-rate and resin bed height were measured. After reaching the pressure limit of the column (2 bar), the pressure was decreased and the flow-rate and column height were measured again. The volumetric flow-rate was divided by the column cross sectional area (0.7854 cm^2) and expressed as a linear flow-rate (cm/min).

TABLE I

RESINS COMPARED IN FLOW AND GEL COMPRESSION STUDIES AND FACTOR IX AFFINITY CHROMATOGRAPHY

Resin label	Resin type	Exclusion[a] limit (dalton)	Pressure[a] limit (bar)	Maximum[a] linear flow-rate (cm/min)	Coupling chemistry	MAb density immobilized (mg MAb/ml resin)	Manufacturer
A	2% Cross-linked agarose	$20 \cdot 10^6$	<0.1	0.25	CNBr activation	1.0	Pharmacia (Piscataway NJ, USA)
B[b]	6% Cross-linked agarose	$4 \cdot 10^6$	1.0	>35	NC	–	Pharmacia
C	6% Cross-linked agarose	$6 \cdot 10^6$	2	50	Aldehyde reduction	1.0, 0.5[a]	Sterogene (Arcadia, CA, USA)
D	Azlactone copolymer		>3.5	>32	Amino group reduction	0.96[a]	3M (St. Paul, MN, USA)
E[c]	Poly-acrylate	$10 \cdot 10^6$	6.9	2.5	FMP activation	1.55[a]	Bioprobe (Tustin, CA, USA)

[a] Data reported by manufacturer.
[b] Resin B not tested in affinity studies.
[c] Resin E not tested in flow studies.

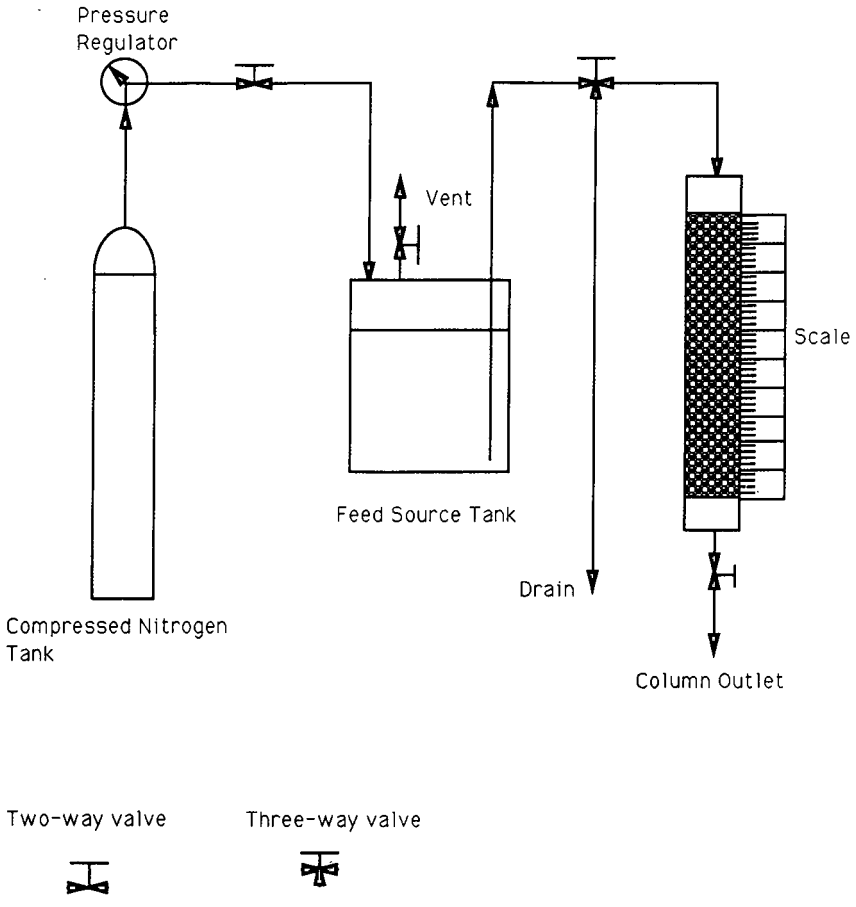

Fig. 1. Experimental apparatus for flow-rate and resin compression studies.

The change in bed height was expressed in terms of the percent change in resin bed volume.

Factor IX binding and immunoaffinity chromatography

The experimental apparatus used for the FIX binding and chromatography studies is illustrated in Fig. 2. The various resins were obtained from the respective manufacturers with MAb coupled at the densities indicated in Table I. The experimental conditions employed are listed in Table II. The resins were packed into a column (G10 × 150, 150 mm × 10 mm I.D., adjustable bed depth, Amicon, Danvers, MA, USA) and allowed to settle under gravity. The upper flow adapter was inserted to the upper level of the resin bed and the resin was then equilibrated with 10 m*M* $MgCl_2$, 100 m*M* NaCl, 20 m*M* imidazole, pH 7.2. The load material was immunoaffinity-purified FIX [5]. $MgCl_2$ was added to this to a final concentration of 40 m*M* and then it was filtered through a 0.2 μm filter (Sterivex, Millipore, Bedford, MA, USA) and loaded onto the column. The column was then washed with 1.0 *M* NaCl, 20 m*M* imidazole, 10 m*M* $MgCl_2$, pH 7.2 until the absorbance at 280 nm was <0.01. The bound proteins were then eluted with 20 m*M* sodium citrate, 110 m*M* NaCl, pH 6.8. Elution was considered complete after the absorbance reached the baseline. The column was regenerated with 2.0 *M* NaCl, 100 m*M* sodium citrate, pH 7.2. The flow-through material from the load, wash, elution and regeneration steps was collected in pools and as-

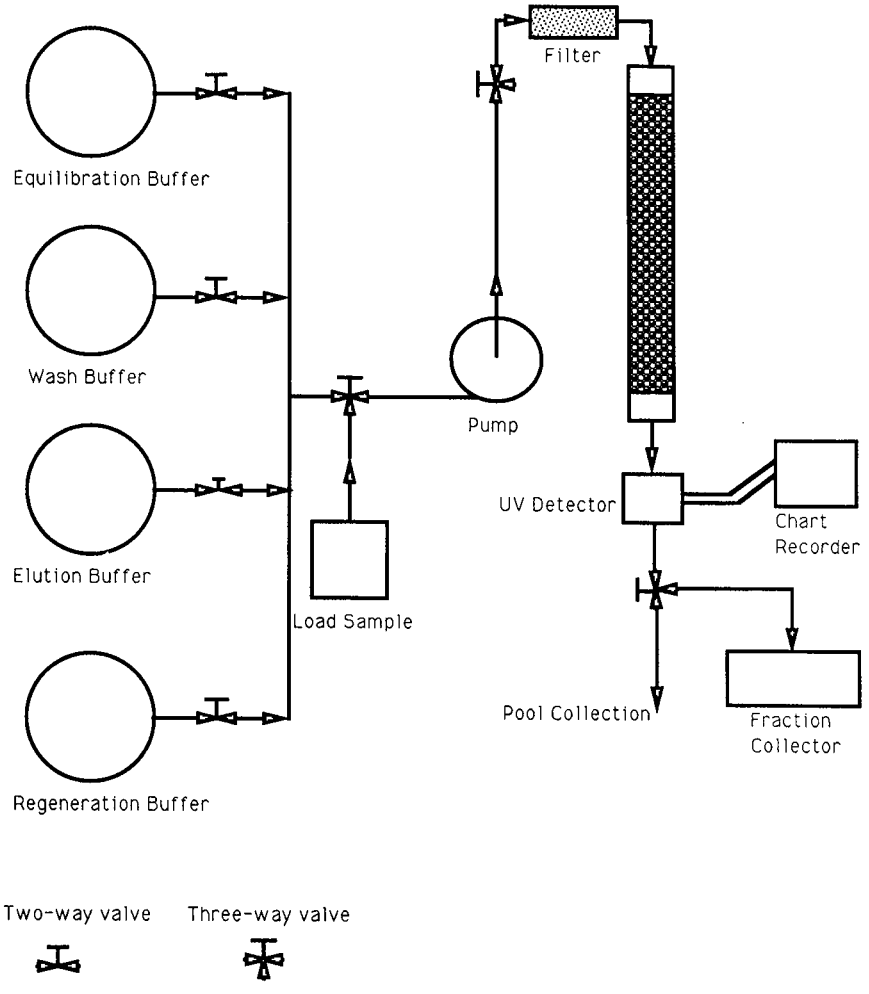

Fig. 2. Experimental apparatus for immunoaffinity purification studies.

sayed for FIX activity and protein content. All chemical were reagent grade from Sigma (St. Louis, MO, USA).

To study the effect of flow-rate on MAb capacity and efficiency, resin C was chosen at a MAb density of 1.0 mg MAb/ml. In these experiments, the volumetric flow-rates were varied from 0.35 to 5.0 ml/min. Using similar methods as described above, the capacity of the MAb was calculated as well as the recovery of FIX.

Factor IX Activity assay

FIX activity was measured using a one-stage coagulation assay [6] of the sample against a pooled plasma standard. Details of the assay procedure are available from Menache *et al.* [7].

Protein assay

Total protein was calculated from the absorbance at 280 nm, after subtracting scatter at 320 nm, assuming an extinction coefficient of 13.3 [8]. It was possible to calculate the protein mass balance as the starting material was essentially a single protein of highly pure FIX.

RESULTS AND DISCUSSION

In Fig. 3A, the effect of pressure on flow-rate is

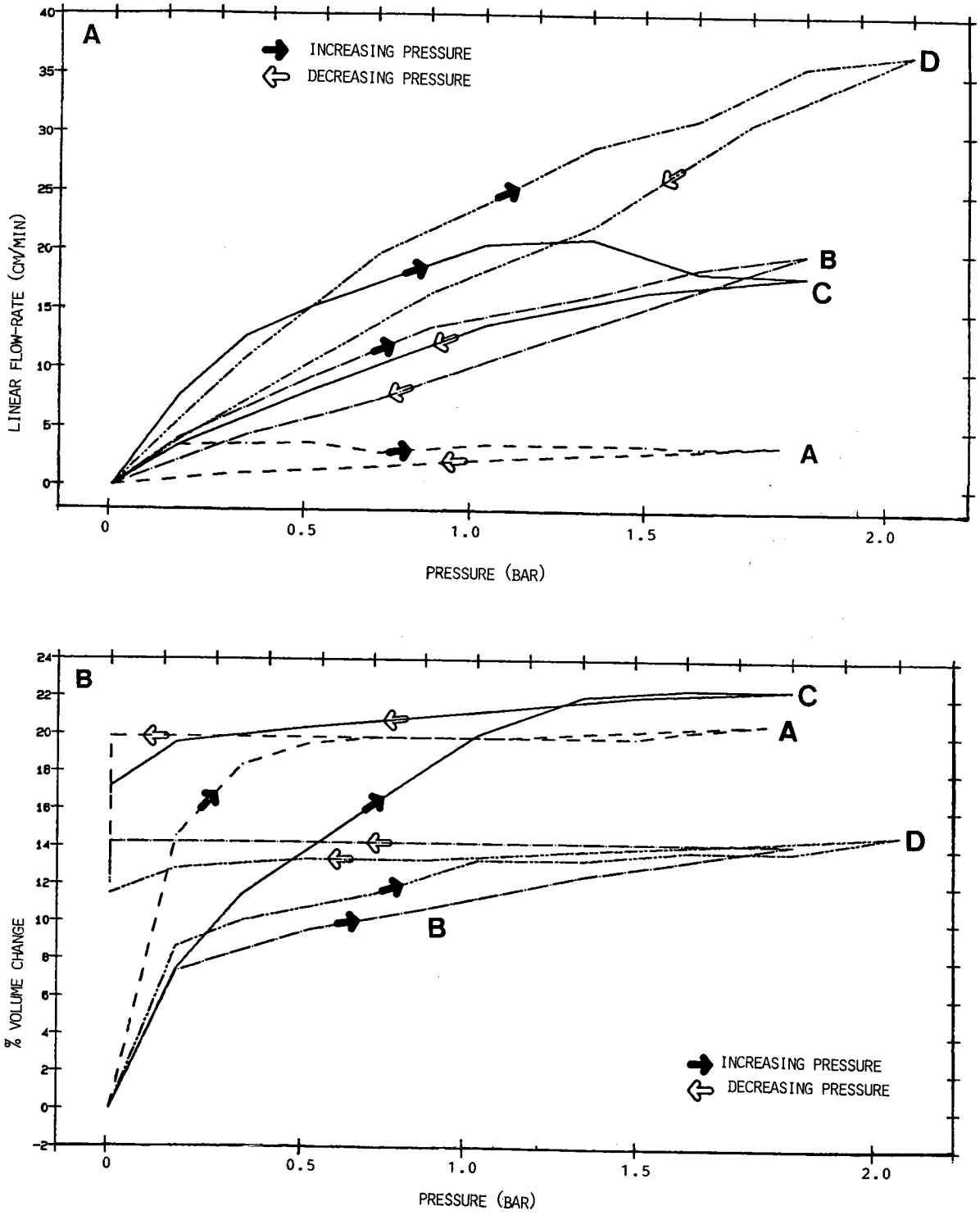

Fig. 3. Comparison of (A) linear flow-rate and (B) volume change in resins A, B, C and D.

shown. As the pressure on the resins is increased the flow-rate increases upto a certain point. This trend is common to all the resins studied. In the case of resin A (a 2% cross-linked agarose), the increase in flow-rate levels off after 0.136 bar. The pressure was then decreased within an hour of reaching this maximum point. As the pressure decreases, the flow-rate demonstrates hysteresis-type behaviour, suggesting that the structure of the resin may have been altered under pressures greater than the specified pressure limit (see Table I). This structural alteration may include irreversible deformation of the resin that results in a configuration that offers greater resistance to flow, hence the lower flow-rate at similar pressures for the decreasing pressure regime. Resins B and C (both 6% cross-linked agaroses) and resin D (a synthetic polymer) demonstrate a greater ability to support higher flow-rates at greater pressure, a consequence of their ability to support higher pressure drops (Table I). However, each resin demonstrated hysteresis behaviour for the flow-rate when the pressure was decreased, even though the maximum pressure limit was not reached. This would suggest that (1) all the soft resins undergo some irreversible compression upon the application of pressure, and (2) the synthetic polymers undergo some degree of compaction. For all the resins tested in this manner, the resins were allowed to "relax" under atmospheric conditions after the entire experiment, and then pressure was applied again. Although quantitative data was not recorded, we observed that the resins supported lower flow-rates for a given pressure drop, suggesting again that some irreversible deformation may have occurred during the first application of pressure. A more thorough evaluation of this phenomenon would require studies that explicitly compare the time-based behaviour of the elasticity of the resins. Resin D shows the least resistance to flow, probably due to its synthetic polymeric structure. However, it is interesting to note that even in this case hysteresis in flow-rate is observable. Resin E was not tested in flow studies.

Fig. 3B shows the volume change that the resins undergo upon application of pressure. The change in volume is a measure of the compression of the resins under pressure. Comparison of Fig. 3A and B suggests that there is no direct correlation between the effect of pressure on flow-rate and resin volume. For example, one of the 6% cross-linked agaroses (C) and the 2% cross-linked agarose (A) undergo

TABLE II

IMMUNOAFFINITY PURIFICATION EXPERIMENTAL CONDITIONS

Experimental condition	Resin					
	A	C	C'[a]	D	D'[b]	E[c]
Column volume[d] (ml)	5.0	5.5	5.1	2.0	2.5	4.3
MAb density (mg MAb/ml resin)	1.0	1.0	0.5	0.97	0.97	1.55
FLow-rate[e] (ml/min)	1 ± 0.1	0.99 ± 0.1	0.97 ± 0.1	0.31 ± 0	0.96 ± 0.05	0.95
Feed concentration of FIX[e] (units/ml)	108 ± 9	111 ± 3	111 ± 3	110 ± 3	104 ± 5	115
FIX/MAb load ratio[e] (units FIX loaded/ mg MAb immobilized)	101 ± 9	104 ± 2	108 ± 6	112 ± 3	100 ± 0.5	108

[a] Resin C' was the same as resin C except the density of MAb on C' was halved.
[b] Resin D' is the same as resin D, but the flow-rate in experiments with D' were increased by a factor of three.
[c] Mean and standard deviation were not calculated for resin E.
[d] The cross-sectional area of the column was 0.7854 cm^2.
[e] Mean ± standard deviation (n = 4).

similar changes in volume, although demonstrating very different flow-rate capacities. This suggests that the compression of the resin, the reduction in supportable flow-rate and the irreversible deformation of the resin are interconnected but not in a straightforward manner. Studies specifically targetted at the relationship between volume change and supportable flow-rate for each resin are indicated.

Table III shows the results of the binding and elution studies. Since all the resins were challenged with the same ratio of FIX to immobilized MAb, the percent of FIX protein not bound is an indication of the ability of the immobilized MAb to bind FIX. Resin A demonstrates the highest capacity for FIX. Resin C and C′ perform similarly, the main difference being in the percent of MAb that is active. As resin C′ contains half the amount of MAb as C, these results suggest that at lower immobilization densities less MAb is available for FIX to bind to. Interestingly, previous work in this laboratory demonstrated that at resin densities ranging from 1.0 to 9.7 mg MAb/ml, the higher MAb densities bound less FIX. Working with other antibodies and ligands, Eveleigh and Levy [9] demonstrated that higher ligand densities lead to lower capacity, and suggested that steric hinderances at high ligand densities decreased the accessibility of the ligand. The results obtained here suggest that there may be a threshold density at which the benefits of more immobilized MAb are offset by increasing steric or diffusional hinderances that result in lower MAb utility and activity. At the very low immobilization densities of 0.5 to 1.0 mg MAb/ml, however, the more MAb immobilized the more FIX bound.

Resin D and E did not perform well in comparison to A and C (with the highest amount of active MAb), suggesting that the MAb immobilized on these resins may have lost activity during the immobilization step. The synthetic polymers tested demonstrated the poorest activity of MAb. It should be pointed out that the coupling chemistries utilized for MAb immobilization (listed in Table I) were different for each resin studied. The chemistries employed were those recommended as the optimum choice by the respective manufacturer. Coupling chemistry has a definite impact on the efficiency of affinity purification using immobilized MAbs. Different coupling chemistries have given rise to variation in the ability of ligand to bind ligate [9] and in the stability of immobilized ligands [11]. There is an

TABLE III

MAb UTILITY AND CAPACITY AND FACTOR IX BINDING AND ELUTION TO RESINS

	Resin					
	A	C	C′	D	D′	E[b]
% of load FIX protein unbound[a]	13 ± 3	21 ± 5	24 ± 10	52 ± 4	25 ± 6	95
% of load FIX protein eluted[a]	65 ± 3	52 ± 14	65 ± 3	39 ± 3	53 ± 9	13[c]
Utility of FIX binding to MAb[a,d] (units FIX bound/ mg MAb immobilized)	93 ± 8	95 ± 4	79 ± 5	12 ± 0.1	51 ± 2	1.5
% of MAb active[e]	69 ± 6	71 ± 3	59 ± 4	9 ± 0.08	38 ± 1.5	1.1

[a] Means ± standard deviation (n = 4).

[b] Mean and standard deviation were not calculated for resin E. Although only one experiment is reported, resin E repeatedly did not bind FIX. The data reported is the best of all experiments performed.

[c] The summed recovery of protein in the case of resin E was > 100%, possibly because of UV absorbing material leaching from this resin.

[d] MAb binding efficiency is calculated by subtracting the total unitage of FIX that does not bind to the affinity resin from the total FIX unitage loaded.

[e] The percent of active MAb is calculated assuming that a theoretical maximum (100%) of two moles of FIX binds per mole of MAb.

TABLE IV

PURITY OF FACTOR IX PRODUCED BY DIFFERENT RESINS

The specific activity of the product was calculated by dividing the measured activity by the calculated protein concentration. A 100% pure solution of Factor IX has a theoretical specific activity that can range between 200 and 250 units/mg [9].

Resin	Specific activity (units FIX/mg protein) (mean ± S.D., $n=4$)
A	182 ± 15
B	252 ± 24
C	148 ± 3
D	69 ± 2
D′	243 ± 25
E	28[a]

[a] Mean and standard deviation were not calculated for resin E. Although only one experiment is reported, the data reported are the best of all experiments performed with resin E.

optimum coupling chemistry for each resin used, one that is usually recommended by the resin manufacturer after extensive testing. However, the specificity of coupling protocol to resin most likely extends to a specificity for different ligands as well. Thus, what works best for one ligand–resin couple may not be optimum for another ligand on the same resin. It is likely that these factors affected our results and lead to the wide variation in MAb utility and activity.

Table IV shows FIX specific activity, which is a measure of the purity and activity of the FIX recovered from each immunoaffinity resin. Resins A, C and D′ demonstrate that they are capable of producing very pure FIX products. Due to difficulties inherent in assaying very pure FIX preparations [12], specific activities around 200 units FIX/mg are considered to be around or at the maximum possible [10]. Resin E consistently did not perform well according to any of the criteria.

Fig. 4 shows the effect of flow-rate on MAb ca-

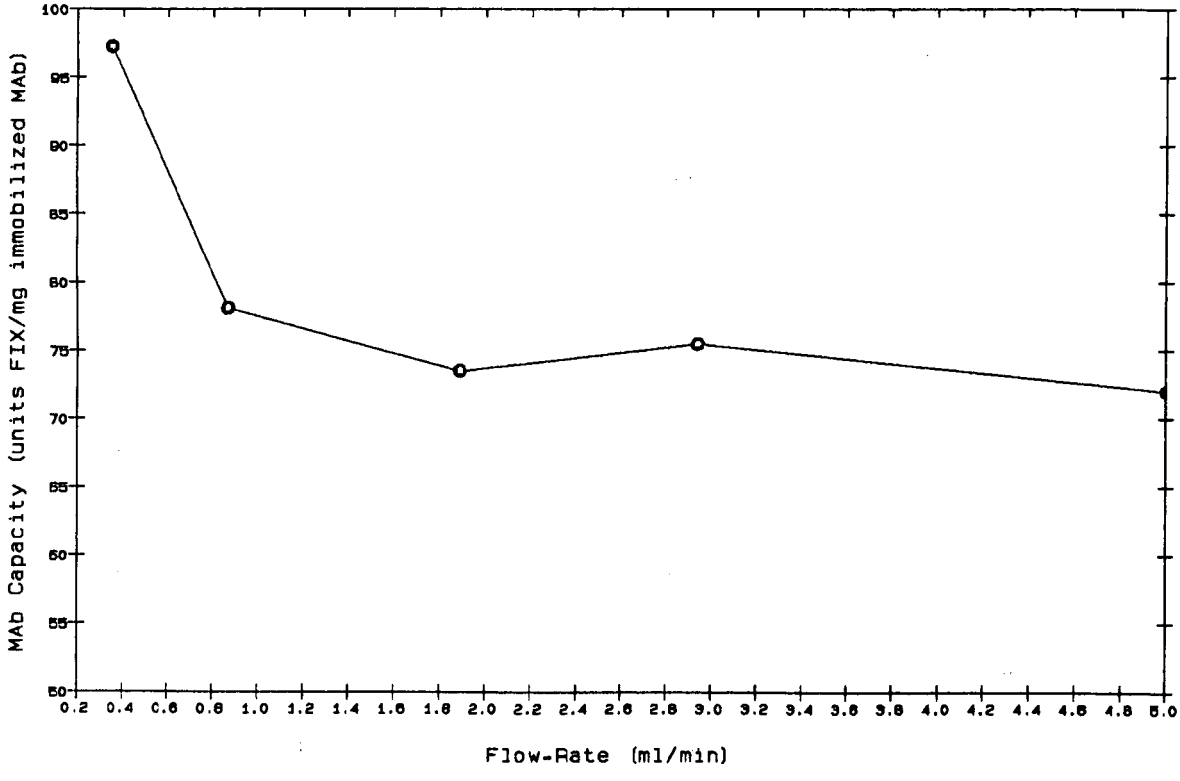

Fig. 4. Effect of flow-rate on the capacity of MAb immobilized on resin C at 1.0 mg/ml resin.

pacity (defined as the units of FIX bound per mg of immobilized MAb) for resin C. There is a slight decrease in the capacity of the MAb as the flow-rate is increased from 0.35 to 1.0 ml/min. After this point, further increases in flow-rate do not demonstrate a significant decrease in the amount of FIX bound by the MAb. The small decrease in capacity suggests that slight kinetic or diffusive effects may influence the binding of FIX. As the flow-rate increases, residence time for the FIX in the immunoaffinity resin bed decreases and thus the time available for the FIX to migrate (diffusion) to MAb immobilized inside the bead and bind (kinetics) to it decreases. Earlier work [2] suggested that FIX purification on Sepharose CL2B was not affected by increases in flow-rate. The lower limit of the flow-rate in those experiments [2] (in an identical column) was 1.0 ml/min. When the flow-rate is decreased below 1.0 ml/min, it is likely that the process approaches a batch load, thus increasing time for FIX binding and concomittantly increasing MAb capacity. Another factor may have been the resin used. In the earlier studies [2], the resin used was 2% cross-linked agarose, instead of the 6% cross-linked agarose (resin C) used here. Increased cross-linking may magnify diffusive resistance and thus increase the effect of flow-rate as shown by the slight increase demonstrated here. Further research will focus on investigating the effect of the degree of cross-linking of the resin substrate on immobilized MAb capacity.

For resin D, the results obtained at a reduced flow-rate was the reverse of those obtained with resin C, as shown in Table III. A three-fold decrease in flow-rate (D') resulted in a four-fold decrease in MAb utility and % MAb active. This difference in response may be caused by the different coupling chemistries employed (Table I). The exact reason is not clear and a thorough study of flow-rate effects on resin D will yield more comprehensive results.

From these experimental comparisons, it appears that of all the resin tested, the 6% cross-linked agarose would be the most amenable to larger scale purification of FIX using this MAb. It can support a high pressure and flow-rate while not undergoing extensive compression. At the same time, it yields an extremely pure FIX preparation as demonstrated by the specific activity of the recovered FIX. It should be stressed that these results obtain for the ligand–ligate pair of this MAb and FIX. As has been emphasized by numerous investigators, these results cannot be extended to other ligand–ligate–resin systems.

CONCLUSIONS

All the resins tested consistently bound FIX, except for E which was as consistent in its inability to bind FIX. Although resin A performs well according to FIX binding, elution and purity criteria, its ability to support high flow-rates is severely restricted at higher pressures. Resins C and D, a 6% cross-linked agarose and a synthetic polymer, respectively, both performed well according to the physical criteria. Resin C is, however, better in the efficiency with which it binds FIX. Resin E did not perform satisfactorily. Studies on the effect of flow-rate demonstrated a slight increase in the capacity of MAb on resin C at very slow flow-rates.

The conclusions reached in this study cannot be directly extended to other resin–ligand systems. However, they do illustrate a systematic evaluation of the suitability of various resins for large-scale immunoaffinity purification processes.

REFERENCES

1 D. C. Yanis, *Bio/Technology*, 5 (1987) 1290.
2 J. Tharakan, F. Highsmith, D. Clark and W. Drohan, W., *J. Chromatogr.*, 522 (1990) 153–162.
3 H.-L. Wang, J. Steiner, F. Battey and D. Strickland, *Fed. Proc.*, 46B (1987) 2119.
4 R. D. Madurawe, C. L. Orthner, J. Tharakan, F. A. Highsmith, W. N. Drohan and W. H. Velander, *J. Chromatogr.*, 558 (1991) 55.
5 J. P. Tharakan, S. I. Miekka, H. E. Behre, B. D. Kolen, D. M. Gee, W. N. Drohan and D. B. Clark, *Throm. Haem.*, 62 (1989) 56.
6 R. Biggs (Editor), *Human Blood Coagulation Haemostasis and Thrombosis*, Blackwell Scientific, Oxford, 1st Ed., 1972, p. 64.
7 D. Menache, H. E. Behre, C. L. Orthner, H. Nunez, H. D. Andersen, D. C. Triantaphyllopoulos and D. P. Kosow, *Blood*, 64 (1984) 1220.
8 H. A. Liebman, S. A. Limentani, B. C. Furie and B. Furie, *Proc. Natl. Acad. Sci. U.S.A.*, 82 (1985) 3879.
9 J. W. Eveleigh and D. E. Levy, *J. Solid-Phase Biochem.*, 2(1) (1977) 45.
10 J. Tharakan, D. Strickland, W. Burgess, W. N. Drohan and D. B. Clark, *Vox Sang.*, 58 (1990) 21.
11 H. Sato, T. Kidaka and M. Hori, *Appl. Biochem. Biotech.*, 15 (1987) 145.
12 S. I. Miekka, *Thromb. Haem.*, 58 (1987) 349.

Journal of Chromatography, 595 (1992) 113–119
Elsevier Science Publishers B.V., Amsterdam

CHROM. 23 917

Immobilization of monoclonal antibodies for affinity chromatography using a chelating peptide

Pius Loetscher, Lone Mottlau and Erich Hochuli*

F. Hoffmann-La Roche Ltd., Pharma Research, New Technologies, 4002 Basle (Switzerland)

(First received October 1st, 1991; revised manuscript received November 26th, 1991)

ABSTRACT

A procedure was developed for oriented immobilization of monoclonal antibodies on a solid support. The technique involves the specific oligosaccharide-directed covalent modification of the monoclonal antibody (mAb) with the chelating peptide, Lys–Gly–$(His)_6$, in conjunction with immobilized metal ion affinity chromatography. Chelating peptide–mAb conjugates with a molar ratio of 2.2 retained full antigen binding activity. On immobilization of the modified antibodies on a nickel affinity resin, the molar antigen binding ratio was 1.4. The high antigen binding capacity is indicative of oriented immobilization providing maximum access for the antigen. The described method can be used for the preparation of high-capacity immunosorbents for affinity chromatography and it is applicable for all immunoglobulin classes.

INTRODUCTION

Immobilized antibodies are widely used for the efficient purification of a broad spectrum of proteins in biochemistry and biotechnology [1]. For instance, large-scale purification of recombinant interferon α-2a involves affinity chromatography using immobilized monoclonal antibodies directed against human leukocyte interferon [2].

Numerous different procedure have been developed to couple antibodies to solid supports [3,4]. In general, antibodies are cross-linked to the matrix through stable covalent bonds. Most of the methods are based on either random amino acid- or selective oligosaccharide-directed immobilization of antibodies. Random coupling through the amino acid side-chains is often accompanied with a partial or complete loss of antigen binding capacity owing to reduced efficiency of antibody–antigen interactions [5]. However, the decrease in bonding activity can be minimized by oligosaccharide-directed coupling of antibodies to solid supports. Oligosaccharide chains are primarily located on the Fc portion of the immunoglobulin molecules. Thus, antibodies immobilized by their oligosaccharide moieties are oriented in such way that most of the antigen binding activity is retained. Antigen/antibody molar ratios as high as 1.6 have been obtained, corresponding to an increase in binding activity of up to 400% compared with the random coupling [6–8].

Immobilized metal ion affinity chromatography was introduced in 1975 by Porat *et al.* [9]. It takes advantage of the selective interaction between biomolecules containing groups for metal complexation and immobilized metal ions. The nitrilotriacetic acid (NTA) adsorbent, when charged with Ni^{2+} ions, has a high affinity for proteins and peptides containing adjacent histidines [10]. A large number of engineered fusion proteins and protein fragments having a polyhistidine affinity peptide at the C- and/or N-terminus were successfully purified using this Ni^{2+} chelate affinity hromatography [11,12].

In this paper we describe a novel procedure for oriented immobilization of monoclonal antibodies (mAbs). It combines the site-specific covalent modification of the oligosaccharide moiety of immunoglobulins with Ni^{2+} chelate affinity chromatography. A hexahistidine peptide (chelating peptide) is

0021-9673/92/$05.00

chemically conjugated to the aldehyde groups generated on the carbohydrate side-chains of the monoclonal anti-human leukocyte interferon antibody LI-8. The selective interaction of the histidine-containing peptide with the Ni^{2+} ions bound to the NTA resin results in an oriented immobilization of the antibodies which retain most of the antigen binding activity.

EXPERIMENTAL

Materials

Dansylcadaverine, sodium metaperiodate and sodium cyanoborohydride were purchased from Fluka (Buchs, Switzerland). Polyacrylamide supplies, Tween-20, Econo-Pac 10DG desalting columns and coupling buffer were obtained from Bio-Rad Labs. (Richmond, CA, USA). Sephadex G-25 and Sepharose CL-6B were supplied by Pharmacia (Uppsala, Sweden). Coomassie Blue R-250 protein assay reagent was purchased from Pierce (Rockford, IL, USA). C-grade guanidine hydrochloride was obtained from SKW Trostberg (Trostberg, Germany). All other chemicals were of the highest purity available. The chelating peptide Lys–Gly–$(His)_6$ was synthesized by A. Trzeciak, Hoffmann-La Roch (Basle, Switzerland). The following materials were kindly provided by members of Hoffmann-La Roche: NTA resin having a capacity of 9.1 μequiv./ml and monoclonal antibody (LI-8) directed against human leukocyte interferon by A. Schacher, and highly purified recombinant interferon α-2a by U. Ettlin.

Oligosaccharide-directed modification of mAb (LI-8)

The monoclonal anti-human leukocyte interferon antibody [13] was site-specifically modified on the oligosaccharide moiety with either dansylcadaverine or the chelating peptide, Lys–Gly–$(His)_6$. Prior to the oxidation of the oligosaccharides on the Fc region, the storage buffer of the antibody [0.1 *M* potassium phosphate (pH 7.2)–0.1 *M* NaCl] was exchanged with coupling buffer (pH 5.5) using Econo-Pack 10DG columns. Sodium metaperiodate stock solution (21 mg/ml)m was added to the mAb solution (4 mg/ml) at one tenth the final volume. After shaking for 1 h in the dark at room temperature, the mixture was passed through an Econo-Pack 10DG column equilibrated with coupling buffer (pH 5.5) in order to remove the excess of sodium metaperiodate. The oxidized antibody was incubated with dansylcadaverine at various molar ratios or with a 270-fold molar excess of chelating peptide for 1 h at room temperature. After addition of sodium cyanoborohydride to a final concentration of 10 m*M*, the incubation was continued for up to 20 h. The modified mAb was recovered by passing the reaction mixture through a Sephadex G-25 column (20 × 2.6 cm I.D.) equilibrated with 0.1 *M* Tris–HCl (pH 7.0)–1 *M* NaCl.

Chromatography

The NTA ligand and Ni^{2+} ion content of the metal chelate affinity resin [10] used in this study was 9.1 μequiv./ml of packed resin. The mAb modified with the chelating peptide and dissolved in 0.1 *M* Tris–HCl (pH 7.0)–1 *M* NaCl buffer was loaded on to a 1–2-ml Ni^{2+}–NTA affinity column equilibrated with the same buffer at a flow-rate of 0.5 ml/min. After extensive washing with loading buffer in order to remove unmodified antibody molecules, the column was equilibrated with 0.1 *M* sodium phosphate (pH 8.0)–0.2 *M* NaCl buffer and the antigen, interferon α-2a, was applied at a flow-rate of 0.1 ml/min. The bound interferon α-2a was eluted with 0.1 *M* sodium phosphate (pH 7.0)–0.2 *M* NaCl buffer containing 2 *M* guanidine hydrochloride and 0.1% Tween-20. The immobilized antibody could be eluted by washing the column with 0.1 *M* acetic acid (pH 4.0)–0.15 *M* NaCl.

Sodium dodecylsulphate–polyacrylamide gel electrophoresis (SDS–PAGE)

Modified mAb and samples from the metal affinity chromatography were analysed by SDS-PAGE. Proteins were electrophoresed on 12.5% SDS polyacrylamide gels by the method of Laemmli [14]. The gels stained with Coomassie Blue R-250 were scanned using a Hirschmann Elscript 400 densitometer.

Protein determination

The protein content was determined according to Bradford [15] with bovine serum albumin as a standard or by measuring the UV absorption at 280 nm using a molar absorptivity of 1.4 for mAb (LI-8) and 1.0 for interferon α-2a.

Fluorescence measurement

Coupling of dansylcadaverine to the oxidized mAb was monitored by fluorescence spectrometry using a Kontron (Zurich, Switzerland) spectrofluorimeter. Samples containing dansylcadaverine in phosphate-buffered saline were excited at 350 nm and the emission was measured at 550 nm.

Amino acid analysis

For the determination of the amount of chelating peptide coupled to the antibody, the conjugates were assessed by amino acid analyses. Amino acid analysis was performed according to a modified method of Spackman *et al.* [16]. The instrumentation consisted of a Kontron Liquimat II amino acid analyser.

Assay of antigen binding activity

Antigen binding activity was measured by an enzyme immunoassay as described [17].

RESULTS AND DISCUSSION

Labeling of mAb with fluorescent dansylcadaverine

Dansylcadaverine [N-(5-aminophenyl)-5-dimethylamino-1-naphthalensulphonamide] was used as a model agent for the development of a suitable coupling procedure. Dansylcadaverine is a fluorescent amine [18]. Incorporation of the primary amine of dansylcadaverine into the monoclonal anti-human leukocyte interferon antibody (LI-8) can be quantified easily and rapidly by measuring the fluorescence. Therefore, coupling conditions for the chelating peptide were optimized with this fluorescent compound. The procedure involved oxidation of the oligosaccharides of the mAb and subsequent condensation of the generated aldehydes with the primary amines. The resulting Schiff base was reduced by cyanoborohydride to stabilize the linkage. After separation of residual free fluorescent label by gel filtration, the incorporation of dansylcadaverine was assayed spectrofluorimetrically. The extent of antibody cross-linking which can occur by reaction of the aldehyde groups with primary amines of the antibody was assessed by SDS-PAGE. The results of these studies are summarized in Table I.

A high concentration of dansylcadaverine was needed to quench antibody cross-linking. A molecular excess of less than 150-fold resulted in almost complete antibody cross-linking (data not shown). Using a 270-fold molar excess of the reporter molecule, we found a molar coupling ratio of 1.9, whereas Rodwell *et al.* [19] attached an average number of five chelating agent molecules to the mouse monoclonal anti-phosphocholine immunoglobulin M under slightly different conditions. The attachment of dansylcadaverine was dependent on prior oxidation of the antibody with sodium periodate and it was drastically affected by reducing the reaction time. Surprisingly, increasing the molar ratio of dansylcadaverine to mAb did not result in a higher degree of modification. The fraction of cross-linked antibody molecules, however, was reduced. The issue of antibody cross-linking is addressed in the following section.

Taken together, these observations indicate that conjugates with the required chelating peptide/mAb molar ratio of 1–2 can potentially be obtained by

TABLE I

EFFECT OF VARYING EXPERIMENTAL CONDITIONS ON THE MODIFICATION OF mAb WITH DANSYLCADAVERINE

The amount of coupled dansylcadaverine was determined by measuring the fluorescence. The increase in fluorescence intensity (excitation at 350 nm and emission at 550 nm) was linear in the range 1.5–60 nmol/ml dansylcadaverine. The percentage of mAb cross-linked during the modification reaction was determined by SDS-PAGE followed by densitometry.

Oxidation with periodate	Dansylcadaverine (molar excess)	Reduction with cyanoborohydride (time)	mol dansylcadaverine / mol mAb	Cross-linked mAb (%)
+	270	Overnight	1.9	41
−	270	Overnight	0	0
+	1000	Overnight	1.8	28
+	270	4 h	0.1	28

TABLE II

CHARACTERIZATION OF CHELATING PEPTIDE–mAb CONJUGATES

Chelating peptide–mAb conjugates were prepared as described under Experimental. The extent of coupled chelating peptide was determined by amino acid analysis, the percentage of the cross-linked mAb fraction by densitometry of SDS polyacrylamide gels stained with Coomassie Blue R-250 and the antigen binding activity by enzyme immunoassay. Each result is the mean ± standard deviation of three independent experiments. IBU, interferon binding units.

Species	mol peptide / mol mAb	Cross-linked mAb (%)	Antigen binding activity (IBU/μg)
Conjugates	2.20 ± 0.08	43.1 ± 3.1	11019 ± 975
mAb	–	–	9892

incubating the periodate-oxidized mAb overnight with about a 300-fold molar excess.

Chelating peptide coupling

The results in Table II show that under the experimental conditions identified for the dansylcadaverine coupling, a similar number of the chelating peptide Lys–Gly–$(His)_6$ could be coupled to mAb LI-8. Further, SDS-PAGE of the modified mAb also revealed a similar fraction of cross-linked antibodies (Fig. 1). The main species of the high-molecular-mass fraction migrated on the SDS polyacrylamide gel with an apparent molecular mass of about 200 000. This band probably represents cross-linked heavy chains resulting from inter- and/or intramolecular Schiff base formation, as the relative amount of the heavy chain in the conjugate fraction is reduced compared with the control antibody. A solid-phase immunoassay based on the "sandwich" principle [17] was used to determine whether cross-linking and incorporation of the chelating peptide were paralleled by a decrease in the antigen binding activity of the antibody. The conjugated mAb exhibited the same ability to bind interferon α-2a as the parental molecule (Table II), thereby demonstrating that neither the attachment of the peptide to the carbohydrate residues nor antibody cross-linking during the coupling reaction affected the accessibility of the antigen binding site. Therefore, it is very likely that the linkage sites for the formation of cross-linked antibody molecules are not located in the regions near or at the antigen binding site.

The data in Table II are also in good agreement with several reports showing that oligosaccharide-directed covalent modification of antibodies with reporter molecules has no measurable effect on the antigen binding activity [19–21]. In these studies, a wide range of different reporter molecules, including liposomes [20], vitamins [21], chelating agents [19], chlorin e_6 coupled to dextran molecules [22] containing either amines [19,22] or hydrazides [20,21] as functional groups, were used. The potential applications of such carbohydrate-labelled antibodies in basic research, diagnostics or immunotherapy were reviewed by O'Shannessy and Quarles [23].

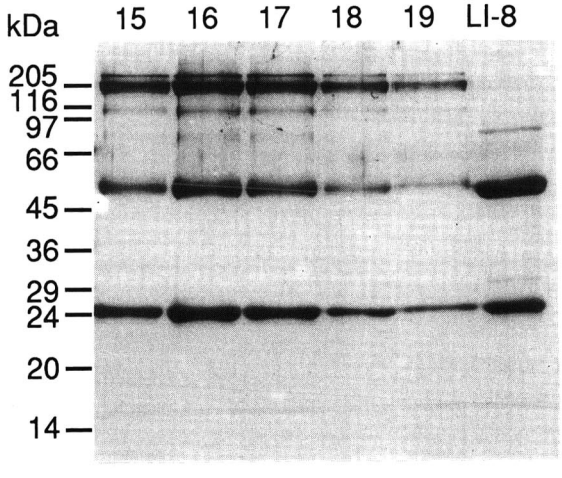

Fig. 1. Electrophoretic analysis of His–mAb conjugates. mAb was modified with the chelating peptide as described under Experimental. The conjugates present in the fractions (Nos. 15–19) eluting from the Sephadex G-25 gel filtraton column were separated on a 12.5% SDS polyacrylamide gel and stained with Coomassie Blue R-250. Positions of Sigma molecular mass markers are indicated on the left-hand side. LI-8, unmodified monoclonal antibody. kDa = kilodalton.

Immunoaffinity chromatography

To prepare an immunoaffinity absorbent for interferon α-2a, we made use of the high-affinity binding of neighbouring histidine residues to immobilized Ni^{2+} ions. The mAb modified on the oligosaccharides with Lys–Gly–$(His)_6$ peptide (His–mAb) was applied to the Ni^{2+}–NTA resin. Using 0.1 *M* Tris–HCl (pH 7.0)–1 *M* NaCl as buffer system, over 92% of the His–mAb conjugates bound to the Ni^{2+} chelate matrix, whereas mAbs lacking the histidine peptide were completely recovered in the flow-through fraction (Fig. 2). These results indicate that at least one chelating peptide is attached to more than 90% of the monoclonal antibody molecules and that the immobilized Ni^{2+} ions selectively interact with the hexahistidine label. In addition, even if the mAb contained surface-accessible metal ion binding sites, no stable complexes were formed under these conditions. The interaction of the hexahistidine peptide with immobilized Ni^{2+} ions has been found to be extremely stable; even harsh conditions such as the presence of chaotropic agents (6 *M* guanidine hydrochloride or 8 *M* urea

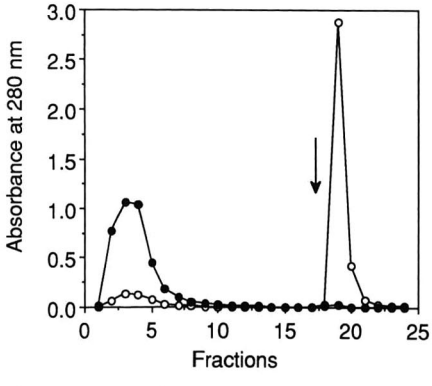

Fig. 2. Characteristics of the binding to and elution from the Ni^{2+}–NTA matrix of His–mAb conjugates and mAb. Modified mAb (10.7 mg) and control mAb (8.7 mg) in 0.1 *M* Tris–HCl (pH 7.0)–1 *M* NaCl buffer were applied to identical 2-ml Ni^{2+} chelate affinity columns. The columns were washed with the same buffer followed by elution of the bound protein with 0.1 *M* acetic acid (pH 4.0)–0.15 *M* NaCl. Absorbance measured at 280 nm of the collected fractions (3.5 ml) from (○) His–mAb conjugate and (●) mAb runs. Arrow indicates the position of the buffer change. The differences in peak height and width for the modified mAb and the control mAb might be due to non-specific interactions of the control mAb with the absorbent at pH 7. These interactions seem not to be manifest for the modified mAb at pH 4.

[11,12] did not release the histidine peptide from the metal complex. Further, equilibrium binding analyses showed that the complex of the dihydrofolate reductase fusion protein bearing a C-terminal hexahistidine peptide extension with Ni^{2+} ions immobilized on the NTA resin had an apparent dissociation constant (K_d) of $0.7 \cdot 10^{-6}$ *M* under identical experimental conditions (not shown).

To demonstrate that the immobilized antibodies were oriented in a way that allowed maximum interaction with the antigen, an excess of highly purified interferon α-2a was loaded on to the immunometal chelate affinity column. As shown by the data in Table III, an interferon α-2a/mAb molar ratio of 1.43 was obtained in the first binding–elution cycle. Importantly, these results showed that immobilization of the modified mAb on the solid support had a minimal effect on the antigen binding activity. Most of the activity was retained, indicating that the antigen binding F_{ab} regions were oriented away from the matrix, allowing efficient recognition and capture of the antigen. As the Ni^{2+}–histidine complexes are acid sensitive (Fig. 2), the most commonly employed acid-elution strategy in immunoaffinity chromatograpy cannot be applied to elute specifically the antigen from the antibody column. The empirically determined solvent for the recovery of bound interferon α-2a consisted of a phosphate buffer (pH 7.0) containing 2 *M* guanidine hydrochloride and 0.1% Tween-20. While 75% of the interferon α-2a were released under these conditions, the remaining 25% were retained on the immunosorbent in the first cycle (Table III). As verified by SDS-PAGE, there was no detectable leakage of His–mAbs or His–mAb–interferon complexes during the elution with the chaotropic agent (Fig. 3). Subsequent binding–elution cycles showed that whereas the binding capacity decreased to an antigen/mAb molar ratio of 1 and stabilized at this level, the amount of recovered interferon α-2a increased to 90%. These results indicate that the observed reduction in antigen binding activity is not due to denaturation of the immobilized mAb, but rather to the blocking of potential binding sites by non-eluted interferon α-2a. Increasing the guanidine hydrochloride concentration to 4 *M* for a higher recovery of the antigen destroyed about 70% of the mAb activity. Preliminary experiments showed that the developed immuno-metal chelate affinity

TABLE III

ANTIGEN BINDING AND ELUTION PROPERTIES OF HIS–mAb CONJUGATES IMMOBILIZED ON THE Ni^{2+}–NTA RESIN

The mAb modified with the chelating peptide was immobilized on a 1-ml Ni^{2+}–NTA column. A four-fold molar excess of highly purified interferon α-2a in 0.1 *M* sodium phosphate (pH 8.0)–0.2 *M* NaCl was applied to the column. After extensive washing, the bound protein was eluted with 0.1 *M* sodium phosphate (pH 7.0)–0.2 *M* NaCl–2 *M* guanidine hydrochloride–0.1% Tween-20. This cycle was repeated three times. The amount of immobilized His–mAb conjugates was 9.7 mg.

Cycle	Interferon bound (mg)	mol interferon / mol mAb	Interferon eluted	
			mg	%
1	1.81	1.43	1.34	74
2	1.30	1.03	1.13	87
3	1.15	0.91	1.06	92

sorbent can also be applied for the purification of recombinant interferon α-2a from a crude bacterial extract (data not shown).

The concept of oriented immobilization of antibodies on solid supports through a "binding protein" has been described for the avidin–biotin system, which exploits the strong binding forces exhibited between the protein and the vitamin [24–26]. In this procedure, biotin hydrazide is selectively coupled to the oxidized carbohydrate residues of mAbs [21], and the biotinylated antibodies are then immobilized on glass beads coated with streptavidin. Unfortunately, no quantitative binding and elution data were reported.

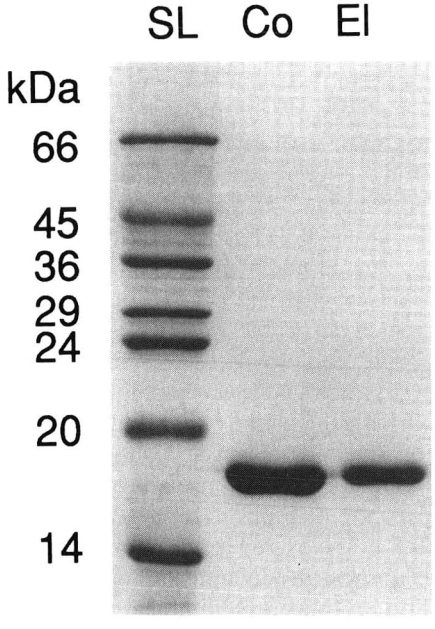

Fig. 3. SDS-PAGE of interferon α-2a recovered from the immuno-metal chelate affinity column. Interferon α-2a was bound to and eluted from the immunosorbent as described in Table III. The eluted protein was separated on a 12% SDS polyacrylamide gel and stained with Coomassie Blue R-250. The lanes represent samples of control interferon α-2a (Co), of interferon α-2a eluted from the immunoaffinity column (EI) and of the low-molecular-mass marker from Sigma (S_L).

In summary, although the inability to recover the bound antigen by acid elution might limit the potential of the described method to some extent, the possibility of differential elution of the antigen, antigen–antibody complex and antibody may be of general use in the wide variety of immuno-chromatographic separation techniques.

ACKNOWLEDGEMENTS

We thank M. Manneberg for performing the amino acid analysis and U. Hennes for measuring the antigen binding activity. We are grateful to U. Ettlin for providing the highly purified interferon α-2a and to A. Schacher for providing the NTA resin and the monoclonal LI-8. We also thank Dr. H. Loetscher for critical reading of the manuscript and for help in preparing the figures.

REFERENCES

1 P. Mohr and K. Pommerening, *Affinity Chromatography: Practical and Theoretical Aspects*, Marcel Dekker, New York, 1985.

2 E. Hochuli, *Chimia*, 40 (1986) 408.
3 D. J. O'Shannessy, *J. Chromatogr.*, 510 (1990) 13.
4 K. Ernst-Cabrera and M. Wilchek, *Trends Anal. Chem.*, 7 (1988) 58.
5 C. Schneider, R. A. Newman, D. R. Sutherland, U. Asser and M. F. Graves, *J. Biol. Chem.*, 257 (1982) 10766.
6 M. C. Little, C. J. Siebert and R. S. Matson, *Bio-Chromatography*, 3 (1988) 156.
7 V. S. Prisyazhnoy, M. Fusek and Y. B. Alakhov, *J. Chromatogr.*, 424 (1988) 243.
8 W. L. Hoffmann and D. J. O'Shannessy, *J. Immunol. Methods*, 112 (1988) 113.
9 J. Porath, J. Carlsson, I. Olsson and G. Belfrage, *Nature (London)*, 258 (1975) 598.
10 E. Hochuli, H. Dobeli and A. Schacher, *J. Chromatogr.*, 411 (1987) 177.
11 D. Stuber, H. Matile and G. Garotta, *Immunol. Methods*, 4 (1990) 121.
12 E. Hochuli, W. Bannwarth, H. Dobeli, R. Gentz and D. Stuber, *Bio/Technology*, 6 (1988) 1321.
13 T. Staehelin, D. S. Hobbs, H.-F. Kung, C.-Y. Lai and S. Pestka, *J. Biol. Chem.*, 256 (1981) 9750.
14 U. K. Laemmli, *Nature (London)*, 227 (1970) 680.
15 M. M. Bradford, *Anal. Biochem.*, 72 (1976) 248.
16 D. H. Spackman, W. H. Stein and S. Moore, *Anal. Biochem.*, 30 (1958) 1190.
17 U. Hennes, W. Jucker, E. A. Fischer, Th. Krummenacher, A. V. Palleroni, P. W. Trown, S. Linder-Ciccolunghi and M. Rainisio, *J. Biol. Standard.*, 15 (1987) 231.
18 L. Lorand and L. K. Campbell, *Anal. Biochem.*, 44 (1971) 221.
19 J. D. Rodwell, V. L. Alvarez, C. Lee, A. D. Lopes, J. W. F. Goers, H. D. King, H. J. Powsner and T. J. McKearn, *Proc. Natl. Acad. Sci. U.S.A.*, 83 (1986) 2632.
20 M.-M. Chua, S.-T. Fan and F. Karush, *Biochim. Biophys. Acta*, 800 (1984) 291.
21 D. J. O'Shannessy, M. J. Dobersen and R. H. Quarles, *Immunol. Lett.*, 8 (1984) 273.
22 A. R. Oseroff, D. Ohuoha, T. Hasan, J. C. Bommer and M. L. Yarmush, *Proc. Natl. Acad. Sci. U.S.A.*, 83 (1986) 8744.
23 D. J. O'Shannessy and R. H. Quarles, *J. Immunol. Methods*, 99 (1987) 153.
24 T. M. Phillips and S. C. Frantz, *J. Chromatogr.*, 444 (1988) 13.
25 J. V. Babashak and T. M. Phillips, *J. Chromatogr.*, 444 (1988) 21.
26 T. M. Phillips, *Clin. Chem.*, 34 (1988) 1689.

Journal of Chromatography, 595 (1992) 121–124
Elsevier Science Publishers B.V., Amsterdam

CHROM. 23 892

Stationary phase effect on enantioselectivity of dansyl phenylalanine in microcolumn liquid chromatography with γ-cyclodextrin as mobile phase additive

Toyohide Takeuchi*

Research Center for Resource and Energy Conservation, Nagoya University, Chikusa-ku, Nagoya 464 (Japan)

Norikazu Nagae

Nomura Chemical Co., 1-6 Sumiredai, Seto 489 (Japan)

(First received October 24th, 1991; revised manuscript received November 21st, 1991)

ABSTRACT

The effects of the stationary phase on enantioselectivity were examined in microcolumn liquid chromatography using γ-cyclodextrin as a mobile phase additive. The stationary phases examined were octadecyldimethylsilica, octyldimethylsilica and trimethylsilica. Dansyl phenylalanine enantiomers were employed as test analytes. For the octadecyldimethylsilica stationary phases the effect of surface coverage on enantioselectivity was not significant. The retention behaviours observed for the octadecyldimethylsilica and octyldimethylsilica were similar, but different from those observed for the trimethylsilica stationary phase.

INTRODUCTION

Cyclodextrin-bonded stationary phases were investigated to determine the resolution of optical isomers in liquid chromatography (LC) [1–4]. The use of cyclodextrins as mobile phase additives in LC is another approach to determining chiral resolution. Three kinds of cyclodextrins are commercially available, which differ in the number of the glucose unit, *viz.* α-, β- and γ-cyclodextrin. γ-Cyclodextrin has so far been applied to the enantiomeric resolution of norgestrel [5], 1,1′-binaphthyl-2,2′-diyl hydrogenphosphate [6] and dansyl amino acids [7]. In a previous study [7], it was found that enantioselectivity was affected by the concentrations of γ-cyclodextrin and acetonitrile in the mobile phase. In this paper, the effect of the stationary phase on enantioselectivity has been examined in microcolumn LC using γ-cyclodextrin as the mobile phase additive.

EXPERIMENTAL

Apparatus

The microcolumn LC system was assembled in the laboratory and comprised an MF-2 microfeeder (Azumadenki Kogyo, Tokyo, Japan) equipped with an MS GAN-050 gas-tight syringe (0.5 ml; Ito, Fuji, Japan), an ML-522 microvalve injector with an injection volume of 20 nl (Jasco, Tokyo, Japan), a separation column, a UVIDEC 100V UV detector (Jasco) with a laboratory-made microflow cell, and a Chromatopac C-R4AX data processor (Shimadzu, Kyoto, Japan). The separation column was prepared from fused-silica tubing of 15 cm × 0.35 mm I.D. The flow-rate of the mobile phase was 2.8 μl/min. The separation was carried out at room temperature, *i.e.* 25°C.

The stationary phases employed were Develosil octadecyldimethylsilica (ODS), octyldimethylsilica (C_8) and trimethylsilica (TMS) (Nomura Chemical,

0021-9673/92/$05.00

TABLE I

PHYSICAL DATA OF THE PACKING MATERIALS EMPLOYED IN THIS WORK

Packing materials	Functional group	C[a] (%)	Surface coverage[b] (μmol/m^2)
Develosil TMS-5	Trimethyl	5	5.3
Develosil C_8-5	Octyldimethyl	13	3.6
Develosil ODS-P-5	Octadecyldimethyl	11	1.4
Develosil ODS-N-5	Octadecyldimethyl	16	2.1
Develosil ODS-5	Octadecyldimethyl	20	3.1

[a] The values represent the carbon contents and contain the amount of trimethylsilane used for end capping.
[b] The values show the surface coverage before end capping.

Seto, Japan), and the surface properties of these packing materials are compared in Table I. In the text, surface coverage refers to the coverage of the silica by the bonded phase. The various ODS packings are seen to vary widely in their coverage by bonded phase. All of the packing materials are end capped with trimethylsilane. The original silica gel used for the preparation of these packing materials has the following dimensions and surface properties: specific surface area 340 m^2/g; average particle diameter 5 μm; average pore diameter 120 Å; specific pore volume 1.0 ml/g.

Reagents

High-performance liquid chromatography (HPLC) grade distilled water and reagent-grade γ-cyclodextrin were obtained from Wako (Osaka, Japan). Dansyl derivatives of phenylalanine (Phe) were supplied by Sigma (St. Louis, MO, USA). Other reagents were obtained from Wako, unless otherwise stated. The reagents were used without further purification.

RESULTS AND DISCUSSION

The dependence of the retention behaviours of the analytes on the acetonitrile concentration was examined. The logarithm of the capacity factor (k') was plotted as a function of the acetonitrile concentration, as shown in Figs. 1 and 2, in which linear relationships between the two parameters are observed. In this work, the concentration of γ-cyclodextrin was kept constant (30 mM). The capacity factors were calculated by assuming that nitrate was

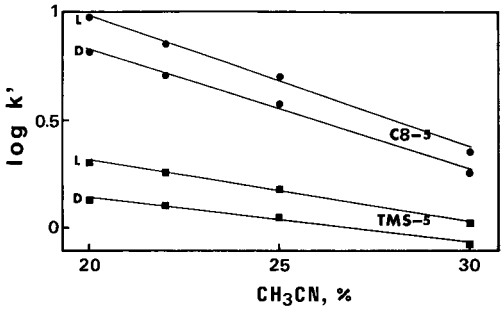

Fig. 1. Relationships between the logarithm of the capacity factor (k') and the acetonitrile concentration for the TMS and C_8 stationary phases. Columns: TMS-5 and C_8-5. Mobile phase: acetonitrile–water mixture containing 30 mM γ-cyclodextrin and 50 mM ammonium acetate. Flow-rate: 2.8 μl/min. Analytes: D = dansyl-D-Phe; L = dansyl-L-Phe.

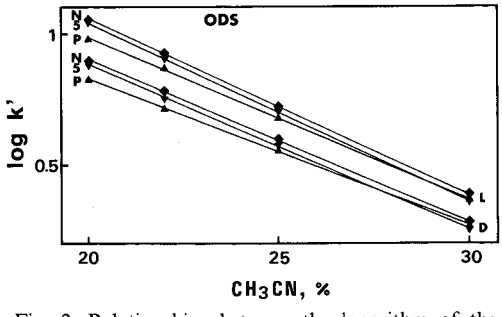

Fig. 2. Relationships between the logarithm of the capacity factor and the acetonitrile concentration for the ODS stationary phases. Columns: P = ODS-P-5; N = ODS-N-5; 5 = ODS-5. Other operating conditions as in Fig. 1.

not retained on the stationary phase. In all cases dansyl D-Phe was eluted before dansyl L-Phe. Among the ODS stationary phases examined, ODS-N-5 gave the largest capacity factor. The C_8 stationary phase gave nearly the same capacity factor as those observed with the ODS stationary phases.

Fig. 3 shows the separation factor (α) as a function of the acetonitrile concentration. The separation factor increases with decreasing acetonitrile concentration in the mobile phase, which suggests that the enantioselectivity can be improved by decreasing the acetonitrile concentration but with an increase in the analysis time. It was found that the TMS stationary phase provided the largest separation factor when the acetonitrile concentration was kept constant. The varying surface coverage has no effect on the separation factor for the ODS stationary phases.

The separation factor is plotted as a function of the capacity factor of the L-isomer in Fig. 4. Much larger values of the separation factor were achieved for the TMS stationary phase in comparison with the other stationary phases. It is seen again that varying the surface coverage of the ODS stationary phases has no effect on the relationship between the two parameters.

The resolution (R_s) is commonly expressed as follows:

$$R_s = \frac{\alpha - 1}{4} \cdot \frac{k'}{1 + k'} \cdot N^{1/2} \quad (1)$$

where N is the theoretical plate number. Here, we define the resolution coefficient (R_s^*) as follows:

$$R_s^* = \frac{\alpha - 1}{4} \cdot \frac{k'}{1 + k'} \quad (2)$$

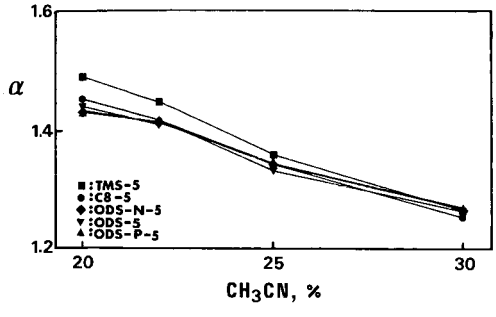

Fig. 3. Separation factor (α) as a function of the acetonitrile concentration. Operating conditions as in Figs. 1 and 2.

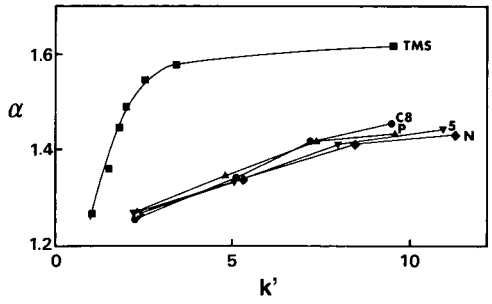

Fig. 4. Separation factor as a function of the capacity factor of the L-isomer. Operating conditions as in Figs. 1 and 2.

If the same theoretical plate numbers are achieved, better resolution can be achieved under the conditions which generate a larger R_s^* value.

Fig. 5 shows the relationships between R_s^* and acetonitrile concentration. At the same acetonitrile concentration, the TMS stationary phase gave smaller R_s^* values than the other stationary phases, because the capacity factor produced by the TMS stationary phase is much smaller than that of the other stationary phases, as demonstrated in Figs. 1 and 2. However, by using a mobile phase containing a lower concentration of acetonitrile, the capacity factor for the TMS stationary phase can be increased, which in turn improves the R_s^* value. This is because, if the same capacity factor is achieved for the TMS stationary phase as the other stationary phases, the separation factor of the former stationary phase is larger than that of the latter, as demonstrated in Fig. 4. On the other hand, the ODS and C_8 stationary phases showed almost the same

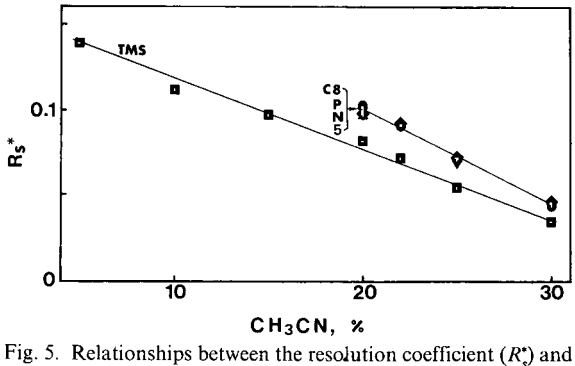

Fig. 5. Relationships between the resolution coefficient (R_s^*) and the acetonitrile concentration. Operating conditions as in Figs. 1 and 2.

relationships between the two parameters. Unfortunately, since the TMS column prepared in this work exhibited a somewhat poorer column efficiency than the other columns, the resolution (R_s) obtained with the TMS column was less than that with the other columns.

In conclusion, enantioselectivity in the present separation mode can be improved by the careful selection of the stationary phase as well as the mobile phase additives.

REFERENCES

1 D. W. Armstrong and W. Demond, *J. Chromatogr. Sci.*, 22 (1984) 411.
2 K. G. Feitsma, B. F. H. Drenth and R. A. de Zeeuw, *J. High Resolut. Chromatogr. Chromatogr. Commun.*, 7 (1984) 147.
3 D. W. Armstrong, X. Yang, S. M. Han and R. A. Menges, *Anal. Chem.*, 59 (1987) 2594.
4 A. M. Stalcup, H. L. Jin and D. W. Armstrong, *J. Liq. Chromatogr.*, 13 (1990) 473.
5 M. Gazdag, G. Szepesi and L. Huszar, *J. Chromatogr.*, 351 (1986) 128.
6 T. Takeuchi, *J. High Resolut. Chromatogr.*, 14 (1991) 560.
7 T. Takeuchi, *J. Microcol. Sep.*, submitted for publication.

Journal of Chromatography, 595 (1992) 125–135
Elsevier Science Publishers B.V., Amsterdam

CHROM. 23 936

Reversed-phase chromatographic behaviour of β-endorphin: evidence of conformational change

Lynda S. Monger* and Cedric J. Olliff

Pharmaceutical Sciences Research Group, Brighton Polytechnic, Moulsecoomb, Brighton, E. Sussex, BN2 4GJ (UK)

(First received April 2nd, 1991; revised manuscript received October 29th, 1991)

ABSTRACT

The effect of alteration in isocratic mobile phase constituents, composition of sample solution, flow-rate and column temperature on the reversed-phase chromatographic behaviour of β-endorphin was investigated. β-Endorphin was shown to be particularly sensitive to the concentration of organic modifier within the mobile phase. The relative contact area of β-endorphin was demonstrated to be less than that of the much smaller molecule, γ-endorphin, indicating that β-endorphin is in a folded form under the mobile phase conditions utilised. Buffer molarity and pH were implicated in the conformational transition of β-endorphin. In addition, the micro-environment of β-endorphin prior to its injection onto the high-performance liquid chromatographic (HPLC) column is crucial to its chromatographic behaviour. Manipulation of the sample solvent environment produced reversible conformational modifications ultimately resulting in asymmetric and even split peaks. This phenomenon was more clearly seen when altering HPLC flow-rate. Elevation of HPLC column temperature provided additional evidence of structural change in β-endorphin, with further conformational forms of this molecule being observed at higher temperatures. This work suggests that the chromatography of β-endorphin involves a complex mechanism of separation which cannot be adequately explained by the two-state model of kinetic processes.

INTRODUCTION

High-performance liquid chromatography (HPLC) has rapidly attained prominence as a powerful separation mode for proteins and peptides. It is perhaps not surprising therefore that such an effective method of separation has been utilised for β-endorphin prior to analysis by radioimmunoassay. Numerous reversed-phase HPLC systems now exist for β-endorphin and employ a variety of solvent conditions [1–6]. Unfortunately, however, little is known of the chromatographic interactions of β-endorphin and the corresponding behaviour of this molecule during elution.

It has been shown that chromatographic conditions, particularly the stationary phase, can affect hydrophobic interactions that normally stabilise native protein conformations [7]. This can lead to proteins undergoing slow dynamic interconversion resulting in broad asymmetrical peaks and even multiple peaks, which correspond to the native and denatured forms, if the kinetic processes of conformational change are slow or irreversible during elution [8]. This phenomenon has been observed with a variety of proteins such as papain [9], ribonuclease A [10,11], lysozymes [12] and myoglobin [12]. Anomalous band broadening of β-endorphin has been observed during size-exclusion chromatography in the presence of dodecyl sulphate [13] and with reversed-phase HPLC [14,15], demonstrating the propensity of β-endorphin to change structure during separation.

It is now well documented that the conformational stability of β-endorphin is affected by changes in solvent environment. In water β-endorphin is almost devoid of secondary structure [16–21], however, methanol [18,21,22] and trifluoroethanol [16,17,23,24] have been shown to induce conformational transition. Helicity is augmented by increasing the percentage of organic solvent, yielding 50 and 60% α-helix at 90% methanol and 100% trifluoroethanol, respectively. Similar promotion of helix

0021-9673/92/$05.00

formation has been reported in the presence of sodium dodecyl sulphate [21,22] and various lipids [25]. In general, much higher concentrations of organic solvents are required to achieve the same effect as a surfactant in inducing an ordered structure. The occurence of helixing has, however, been noted at concentrations as low as 10% methanol and trifluoroethanol [22]. Thus it might be postulated that both a mobile phase containing organic solvent plus the influence exerted by a hydrophobic HPLC stationary phase may contribute to conformational change of β-endorphin.

Although it might be hypothesises that β-endorphin undergoes conformational change during HPLC, the only data available is from gradient elution studies [14,15]. This paper therefore investigates the chromatographic behaviour of β-endorphin utilising an isocratic system and the consequence of varying mobile phase constituents such as the percent of organic modifier, pH and buffer molarity and in addition, the effect of altering the solvent composition of the sample solution.

Investigations to characterise conformational change in proteins caused by reversed-phase HPLC have been undertaken using elevated column temperature and increased flow-rates [10,26,27]. Temperature enhances denaturation, while changes in flow-rate will allow alternative conformations to be eluted, provided that the rate of change is of the same order as the retention time. These methodologies were thus employed here in an attempt to further characterise the chromatographic behaviour of β-endorphin.

EXPERIMENTAL

Materials

Purified β-endorphin (human sequence) was purchased from Sigma (Dorset, UK) as was α-endorphin, γ-endorphin, Met-enkephalin and Leu-enkephalin. Acetonitrile (HPLC-S grade) was obtained from Rathburn (Scotland, UK), ammonium acetate (HPLC grade) from Fisons (Loughborough, UK) and orthophosphoric acid (Aristar) and potassium dihydrogenphosphate (Aristar) from BDH (Dorset, UK). High-purity water was produced by double destilling, de-ionising and filtering through 0.45-μm nylon membrane filter (Gelman Sciences, Northampton, UK).

Equipment and operating conditions

All chromatographic experiments were performed using a SP8750 organiser and SP8770 pump (Spectra-Physics, Herts., UK) with a Rheodyne injection valve, coupled with a single-pen chart recorder. Detection was obtained by a UV–VIS detector (LC871 Pye, Cambridge, UK) at 210 and 275 nm or electrochemical detection (ED) by either a LCA 15 EDT electrochemical detector (EDT Research, London, UK) or a 5100A Coulochem electrochemical detector, guard cell 5020 and analytical cell 5011 (loaned by Severn Analytical, Beds., UK). A reversed-phase C_{18} Nucleosil 300 Å, 7-μm analytical (250 mm × 4.9 mm I.D.) and guard (50 mm × 4.9 mm I.D.) columns (Hichrom, Berks., UK) were employed.

The standard mobile phase constituents comprised acetonitrile–0.1 *M* potassium dihydrogenphosphate adjusted to pH 2.3 with Aristar phosphoric acid (32:68), at a flow-rate of 1 ml/min. These conditions were varied systematically and are reported in the appropriate sections that follow. Samples were injected manually via a 50μl loop. Sample concentration varied between 5 and 10 μg/ml but was sufficiently small to avoid column overloading. Chromatograms were recorded and analysed with respect to peak height, peak area, retention time, capacity factor (k'), peak asymmetry factor (A_s) and the effective theoretical plate height equivalent (H_{eff}) was calculated for those peaks that could be adequately described as Gaussian [28].

RESULTS AND DISCUSSION

Effects of HPLC mobile phase constituents on the chromatographic behaviour of β-endorphin

Percent of acetonitrile. It was demonstrated that β-endorphin is extremely sensitive to solvent polarity. A narrow range of elution was exhibited for β-endorphin of between 30 and 34% acetonitrile, 29% retaining the molecule indefinitely on the column and 36% eluting it in the solvent front (Table I). Similar steep elution profiles for other polypeptides have been observed [5,29,30].

The effect of acetonitrile concentration on the elution of α- and γ-endorphin as well as for Met and Leu enkephalin were studied under similar conditions. Results are given in Table I.

The displacement model theory developed by

TABLE I

THE EFFECT OF VARYING THE PERCENTAGE ACETONITRILE ON k' VALUES FOR MET-ENKEPHALIN, LEU-ENKEPHALIN, α-ENDORPHIN, β-ENDORPHIN AND γ-ENDORPHIN

Acetonitrile (%)	k'				
	γ-Endorphin	α-Endorphin	β-Endorphin	Leu-enkephalin	Met-enkephalin
26	2.9	0.6	–	1.4	0.9
27	2.4	0.5	–	1.3	0.8
28	1.7	0.5	–	1.1	0.6
30	0.9	0.4	2.8	0.8	0.6
31	–	–	1.0	–	–
32	0.5	0.3	0.8	0.6	0.4
33	–	–	0.7	–	–
34	–	–	0.5	–	–
35	–	–	0.3	–	–

Geng and Regnier[31] can be used to estimate the relative contact areas between these solute molecules and the stationary phase due to the adsorption process. According to this theory (k') can be expressed as

$$\log k' = \log I - Z \log D$$

where D is the molar concentration of the organic modifier, Z is a measure of the contact area of the absorbed peptides and I represents a measure of the relative binding strength of individual polypeptides under a fixed mobile phase composition.

Linear relationships were obtained for plots of $\log k'$ as a function of $\log D$ for α-endorphin, γ-endorphin, Met-enkephalin and Leu-enkephalin (as shown by their correlation coefficients in Table II), the plot for β-endorphin was, however, curvilinear (Fig. 1). The values of Z for the above peptides are given in Table II, and that for β-endorphin was taken from the slope at 32% acetonitrile. Even though β-endorphin is nearly twice the molecular weight of γ-endorphin it has a slightly smaller contact area which would suggest that it is in a folded form under these conditions. Similarly, it can be argued that α-endorphin is folded having a contact area slightly smaller than the five amino-acid peptides, Leu- and Met-enkelphalin.

pH. The effect of changes in aqueous phase pH on the elution of β-endorphin was determined by HPLC–ED. A pH range of between 2.3–4.0 was attained with H_3PO_4, all other mobile phase constituents remained constant. Table III details alterations observed in the chromatographic performance of β-endorphin.

Peak area was shown to increase from pH 2.3–3.2 ($p < 0.05$), however, a dramatic and significant decrease ($p < 0.01$) occurred at pH 4.0 (Table 3). This observation supports the findings of others that a low pH of between 2.0–3.0 is required if maximum chromatographic efficiency of pro-opiomelanocortin-related peptides is to be obtained [4,32]. Identical k' values were gained between pH 2.3–3.2, however at pH 4.0 k' was significantly increased ($p < 0.01$). This suggests variation in the interaction of β-endorphin with the stationary phase, and is shown by the change in H_{eff}. While the β-endorphin molecule, having a pI at pH 9.9 [33], will be positively charged between pH 2.3–4.0, localised change

TABLE II

VALUES OF Z AND CORRELATION COEFFICIENTS (r) FOR A RANGE OF ENDOGENOUS OPIOIDS

	γ-Endorphin	α-Endorphin	Leu-enkephalin	Met-enkephalin	β-Endorphin
Z	8.8	3.2	4.5	4.1	7.2
r ($n=5$)	0.997	0.999	0.992	0.976	

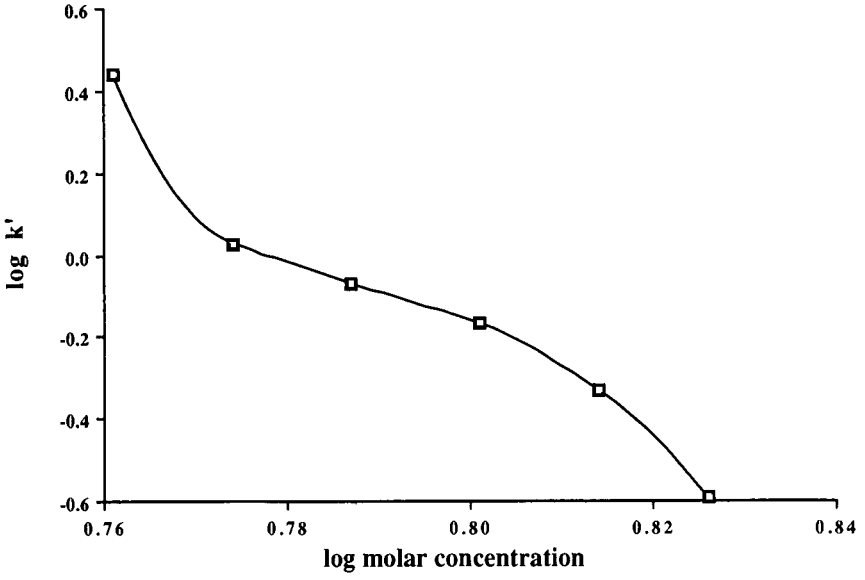

Fig. 1. Effect of mobile phase polarity on the chromatographic retention of β-endorphin: log k' for β-endorphin *versus* log molar concentration of acetonitrile.

in the ionisation of the acidic/carboxylic side chains of glutamic acid and the C-terminal may be possible at the higher end of this pH range. It is postulated, therefore, that the dramatic reduction in peak area, the change in k' and H_{eff} is the result of negatively charged regions of the molecule causing slight conformational change, possibly reducing the tyrosine accessibility and thus the signal generated and changing the interaction of the molecule with the stationary phase.

TABLE III

EFFECTS OF VARYING AQUEOUS PHASE pH ON THE CHROMATOGRAPHIC PERFORMANCE OF β-ENDORPHIN [MOBILE PHASE CH_3CN–0.1 *M* KH_2PO_4 (32:68), ACIDIFICATION GAINED WITH ARISTAR H_3PO_4]

	pH			
	2.3	2.8	3.2	4.0
Peak area (mm^2)	69	76	97[a]	49[b]
k'	1.4	1.4	1.4	2.1[b]
H_{eff} (μm)	472	472	472	200[b]

[a] Mann Witney "U" Test; $p<0.05$ [39].
[b] Mann Witney "U" Test; $p<0.01$.

Molarity. Effects of changes in molarity of KH_2PO_4 on the peak area of β-endorphin were investigated using EDT-ED. A constant pH of 2.3 was maintained throughout by adjustment with Aristar H_3PO_4. Results detailing peak areas as a function of molarity are illustrated in Table IV. A sharp peak area–molarity profile was demonstrated with the greatest peak area being recorded at 0.1 *M* KH_2PO_4, while peak resolution deteriorated above and below 0.1 *M* KH_2PO_4 (Table IV). The reduction in peak asymmetry noted from 0.01 to 0.1 *M* KH_2PO_4, pH 2.3 can perhaps be explained by a

TABLE IV

EFFECTS OF VARYING AQUEOUS PHASE MOLARITY (0.010–0.150 *M* KH_2PO_4) ON THE CHROMATOGRAPHIC PERFORMANCE OF β-ENDORPHIN [MOBILE PHASE CH_3CN–KH_2PO_4, pH 2.3 (32:68)]

Molarity	k'	A_s	Peak area (mm^2)
0.010	2.2	9.0	95
0.050	1.9	28.0	145
0.075	1.6	20.0	178
0.100	1.1	1.0	262
0.150	1.0	0.4	184

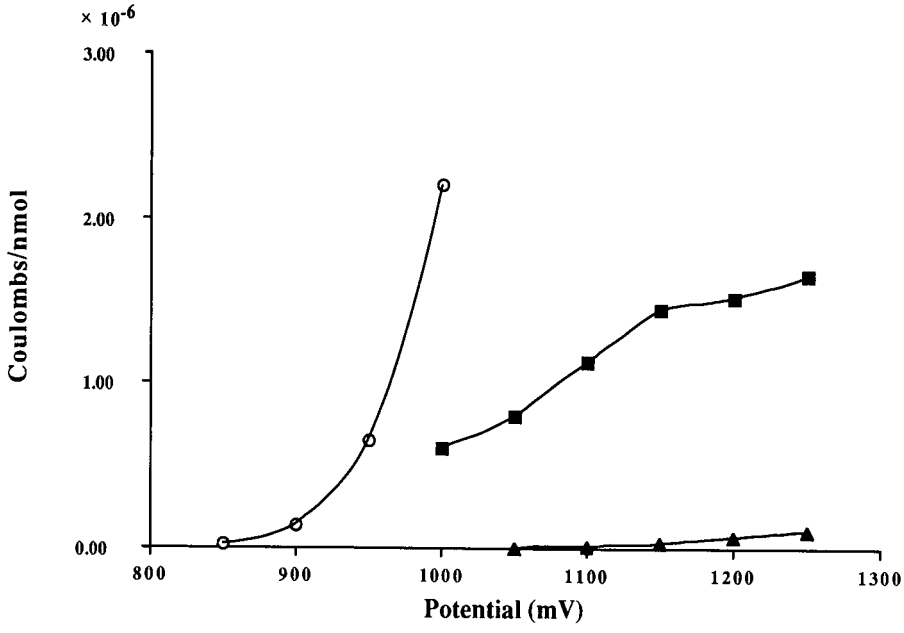

Fig. 2. Hydrodynamic voltammograms of β-endorphin (■), tyrosine (○) and methionine (▲) gained utilising a LCA 15 EDT electrochemical detector.

conformational change of β-endorphin from a more unstructured to a relatively more structured form. The higher buffer molarities (>0.1 *M*) required for β-endorphin chromatography, have been reported to be mandatory for reproducible high-efficiency chromatography of other polypeptides [33].

Comparison of the sensitivity to detection of tyrosine, methionine and β-endorphin. Hydrodynamic voltammograms constructed for β-endorphin and its two major electrochemically active amino acids, tyrosine and methionine are shown in Fig. 2. Tyrosine displays superior electrochemical activity to β-endorphin, suggesting that the activity of β-endorphin is not an additive function of electrochemical activity of the constituent amino acids. Methionine, conversely, would only be expected to contribute fractionally to the activity of β-endorphin. Although β-endorphin contains one methionine and two tyrosine residues within its structure it exhibits a dramatically lower sensitivity to oxidation per mole than tyrosine. Whilst some of this difference can be attributed to the lower mobility of β-endorphin, calculations (shown in Table V) indicate that another phenomenon is occurring.

The notion that β-endorphin exhibits α-helix conformation might be postulated as an appropriate explanation. This premise is supported by Lichtarge *et al.* [18] finding that in organic modifier β-endorphin undergoes conformation changes, inducing an α-helix structure between residues Tyr 1–Thu 12,

TABLE V

THE OBSERVED AND CALCULATED RATIO DIFFERENCE BETWEEN THE SIGNAL GENERATED FOR TYROSINE TO THAT OF β-ENDORPHIN AT VARYING POTENTIALS

The ratio difference between tyrosine and β-endorphin due to differences in diffusion coefficients (D_C) was calculated based on the assumption of spherical molecules where $D_C \propto 1/MW^{0.333}$. The two tyrosine residues present in β-endorphin have been considered in the calculation. MW = molecular weight.

Potential (mV)	Ratio difference	
	Observed	Calculated
1000	3.60	1.34
1050	5.25	1.34
1100	4.97	1.34
1150	4.27	1.34
1200	4.41	1.34
1250	4.36	1.34

Leu 14–Lys 28 and a β-turn between Lys 28–Glu 31. The tyrosine residues at positions 1 and 27 are thus an integral part of the changes in conformation which may result in the shielding of active amino acids and thus a loss of activity.

Environmentally induced conformational changes in β-endorphin

The effect of reconstituting β-endorphin in varying percentages of CH_3CN and KH_2PO_4 on HPLC chromatograms. Lyophilised samples of β-endorphin were reconstituted with varying percentages of CH_3CN and 0.1 *M* KH_2PO_4 adjusted to pH 2.3 with H_3PO_4 (v/v) to achieve a range of 0 to 50% acetonitrile. The final concentration of β-endorphin was 5 μg/ml (samples A) or 10 μg/ml (samples B) irrespective of the solvent composition. HPLC–UV analysis of β-endorphin at both 210 nm (samples A) and 275 nm (samples B) was then undertaken. This allowed the effect of sample solvent environment on the subsequent chromatography of β-endorphin to be established (Table VI).

A similar relationship is apparent for peak area at both wavelengths, an increase being observed from 0 to 30% CH_3CN but a decrease noted thereafter (Table VI). This can perhaps be attributed to the internalisation of the tyrosine and phenylalanine residues in β-endorphin, as at 275 nm the aromatic absorption of these amino acids has been dramatically reduced. At 38 and 40% CH_3CN concentrations, asymmetrical peaks appeared which had progressed to be either large shoulders or split peaks at 50% CH_3CN (*i.e.* Fig. 3). While the interaction of β-endorphin with the mobile and stationary phase did not change, denoted by a markedly constant k' value, the chromatographic efficiency was demonstrated to be increasingly jeopardised as the percentage of acetonitrile rose in the reconstitution fluid. It might be assumed therefore that when β-endorphin is injected onto the HPLC column in a solution containing higher concentrations of acetonitrile than that present in the mobile phase, that the conformational modifications which would be expected to result, as the molecule restructures to orientate itself in the mobile phase (*i.e.* 32% CH_3CN–0.1 *M* KH_2PO_4, pH 2.3), are significantly slower than its life time on the column.

To further verify the above observations and to establish whether conformational changes are reversible, additional analysis was undertaken. A sample of β-endorphin (10 μg/ml) was reconstituted and divided equally into two aliquots and diluted to make final concentrations of 5 μg/ml of β-endorphin in either CH_3CN–KH_2PO_4, pH 2.3 (30:70) (A) or CH_3CN–KH_2PO_4, pH 2.3 (50:50) (B). Each sample was assessed for its β-endorphin content using HPLC–UV (210 nm), peak areas and k' values were recorded. To check reversibility, sample B was further processed by altering the proportions of solvent present to that of (A); CH_3CN–KH_2PO_4, pH 2.3 (30:70) (C), and then re-analysed (Table VII).

It was demonstrated that the conformational change of β-endorphin, induced by variation in the proportions of CH_3CN and KH_2PO_4, is completely

TABLE VI

EFFECTS OF SAMPLE SOLVENT ENVIRONMENT ON THE SUBSEQUENT CHROMATOGRAPHIC PERFORMANCE OF β-ENDORPHIN

Lyophilised β-endorphin samples were reconstituted with varying percentage of CH_3CN to 0.1 *M* KH_2PO_4 pH 2.3 and chromatographically analysed utilising a mobile phase of CH_3CN–KH_2PO_4, pH 2.3 (32:68).

nm	Parameter	CH_3CN in the reconstitution solution (%)									
		0	10	20	25	30	32	34	36	38	40
210	Peak area (mm^2)	154.0	221.0	274.0	325.0	332.0	325.0	301.0	256.0	234.0	179.0
	±S.D. (mm^2)	11.0	26.0	16.0	5.0	9.5	24.0	28.5	25.5	8.5	1.5
	k'	0.9	0.9	0.9	0.9	0.9	0.9	1.0	1.0	0.9	0.9
275	Peak area (mm^2)	–	–	–	64.5	69.0	67.0	51.0	36.0	25.0	18.2
	±S.D. (mm^2)	–	–	–	1.0	2.5	3.0	2.0	2.5	2.0	1.5
	k'	–	–	–	0.8	0.9	0.8	0.9	0.9	0.8	0.8

[a] S.D. ± Standard deviation ($n = 5$).

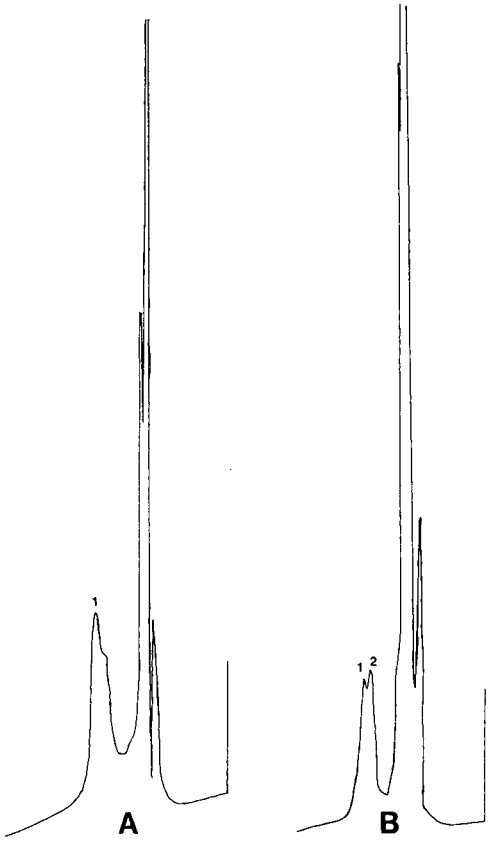

Fig. 3. Reversed-phase chromatographic behaviour of β-endorphin as a result of changes in sample solvent composition prior to injection onto the HPLC column. Chromatograms are those which were gained when a sample of β-endorphin was reconstituted with either (A) CH_3CN–KH_2PO_4, pH 2.3 (40:60) or (B) CH_3CN–KH_2PO_4, pH 2.3 (50:50). The first and second eluting peaks are denoted by 1 and 2, respectively. Isocratic mobile phase constituents were CH_3CN–KH_2PO_4 (adjusted to pH 2.3 with Aristar H_3PO_4) (32:68).

reversible. The HPLC–UV response obtained for β-endorphin in solvent B, as measured by peak area and k', returns to the original values gained for solvent A. It is evident therefore that a slight alteration in the sample solvent environment and the subsequent chromatography of β-endorphin may be manifested as a major change in chromatographic performance.

The effect of HPLC flow-rate on β-endorphin chromatograms. Assessment of the chromatographic performance of certain proteins has been studied by varying the HPLC flow-rate [10,11,27]. This provides a method of altering the retention time of a molecule, thereby enabling a reversibly denatured protein to be eluted at varying stages during its transition back to its native form. An examination of the equilibration rate of β-endorphin was thus undertaken by manipulating the flow-rate and assessing the corresponding chromatograms. HPLC–UV conditions utilised were those routinely used, CH_3CN–0.1 *M* KH_2PO_4 adjusted to pH 2.3 with H_3PO_4 (32:68). β-Endorphin samples reconstituted in this mobile phase and in addition, varying percentages of CH_3CN and 0.1 *M* KH_2PO_4 adjusted to pH 2.3 with H_3PO_4 were subjected to changes in flow-rate. Each sample of β-endorphin was 5 μg/ml, with the same sample being injected at all investigatory flow-rates. The relationship between flow-rate, peak area, k', retention time and solvent composition is demonstrated in Table VIII. As might be expected, retention time increases with decreasing flow-rate, the relationship of the increase proving to be similar, reflected by the k' values, irrespective of the sample solvent concentration. Thus the nature of interaction between molecule, stationary and mobile phase is therefore, perhaps alike.

In support of findings documented earlier, the sample solvent environment prior to HPLC analysis was again shown to directly affect the chromatographic behaviour of β-endorphin by dramatically altering the size and shape of the peak. Furthermore, the samples' solvent environment was also demonstrated to influence changes in peak area with altered flow-rates.

A decrease in flow-rate resulted in an increase in peak area, this increase when expressed as a ratio of the peak area at 1 ml/min was shown to be the same

TABLE VII

REVERSIBLE CHANGES IN THE CHROMATOGRAPHIC PEAK AREA OF β-ENDORPHIN AS A CONSEQUENCE OF ALTERATIONS IN THE SAMPLE SOLVENT ENVIRONMENT PRIOR TO CHROMATOGRAPHY

Sample	Proportion of CH_3CN: KH_2PO_4	Peak area (mm^2)	k'	
A	30 : 70	328		0.8
B	50 : 50	108	0.7[a]	0.8
C	30 : 70	333		0.8

[a] Developing peak.

TABLE VIII

THE EFFECT OF FLOW-RATE ON THE CHROMATOGRAPHY OF β-ENDORPHIN RECONSTITUTED WITH VARYING PERCENTAGE OF CH_3CN TO 0.1 *M* KH_2PO_4, pH 2.3 AND ANALYSED UTILISING A MOBILE PHASE OF CH_3CN–0.1 *M* KH_2PO_4, pH 2.3 (32:68)

Flow-rate (ml/min)	Ratio difference	Reconstitution of β-endorphin (% acetonitrile)									
		32%					36%				
		Peak area	Ratio difference	Peak area · flow-rate	R.T.[a]	*k'*	Peak area	Ratio difference	Peak area · flow-rate	R.T.	*k'*
1.0	1.25	337	1.3	337	6.3	0.75	225	1.2	255	6.2	0.88
0.8	1.66	439	1.5	351	7.7	0.75	300	1.9	240	7.5	0.79
0.6	2.50	517	2.4	310	10.1	0.90	485	2.8	291	10.0	0.72
0.4		821		328	15.2	0.73	720		288	14.9	0.77
Flow-rate (ml/min)	Ratio difference	Reconstitution of β-endorphin (% acetonitrile)									
		40%					50%				
		Peak area	Ratio difference	Peak area · flow-rate	R.T.	*k'*	Peak area	Ratio difference	Peak area · flow-rate	R.T.	*k'*
1.0	1.25	204	1.2	204	6.5	0.80	110	1.1	110	6.6[b]	0.83
0.8	1.66	252	1.3	202	7.6	0.81	120	1.3	96	7.8[b]	0.86
0.6	2.50	275	1.6	165	10.1	0.80	147	1.4	88	10.2[b]	0.76
0.4		336		134	14.6	0.73	150		60	15.4[b]	0.75

[a] R.T. = Retention time.
[b] Developing peak.

as the ratio change in flow-rate for samples of β-endorphin in both the CH_3CN–KH_2PO_4 (32:68) and CH_3CN–KH_2PO_4 (36:64). In higher acetonitrile concentrations, however, ratio differences in peak area are much smaller (Table VIII) than might be anticipated. In addition, when the peak areas are multiplied by their respective flow-rate a constant value should be gained [28], and while the CH_3CN–KH_2PO_4 (32:68) and CH_3CN–KH_2PO_4 (36:64) peak areas do yield such a value, CH_3CN–KH_2PO_4 (40:60) and CH_3CN–KH_2PO_4 (50:50) do not (Table VIII). These inconsistencies at higher acetonitrile concentrations might be explained by the conformational state of β-endorphin.

The reduction in β-endorphin peak area noted at all flow-rates for both CH_3CN–KH_2PO_4 (40:60) and CH_3CN–KH_2PO_4 (50:50) is perhaps due to the molecule being in a more structured form. Thus, if this is true then the conformation of β-endorphin prior to analysis is crucial to its chromatographic performance.

Chromatographically induced changes in other proteins have been ascertained and are described by a two-state model [9,11] where the native and denatured peaks are inversely related. If β-endorphin is helical or partially helical in the mobile phase and is reversibly denatured by the stationary phase, then the molecule would be expected to fold to reform the native peak on its elution from the column, as has been shown for other proteins [9,10]. Such a phenomenon is, however, not apparent. Findings do suggest though that β-endorphin does have the propensity to alter structure when reconstituted and introduced onto the column in higher percentages of acetonitrile. In addition the occurrence of asymmetrical and split peaks provide evidence that a further confirmation of β-endorphin can exist and may be induced under certain conditions, although an adequate explanation of such phenomena cannot yet be given. Information obtained therefore, only highlights that the chromatography of β-endorphin involves a complex mechanism of separation, which is particularly sensitive to the micro-environment of the molecule and suggests that a more complex model as described for other proteins [8] is required to explain the dynamic effects of β-endorphin.

The effect of HPLC column temperature on β-endorphin chromatograms. To study further the chromatographically induced conformational change of β-endorphin, thermal denaturation was utilised. This technique has been used by other investigators in an attempt to characterise the denaturated and native forms of proteins [10,26,27]. The column temperature was thermostatically controlled by a

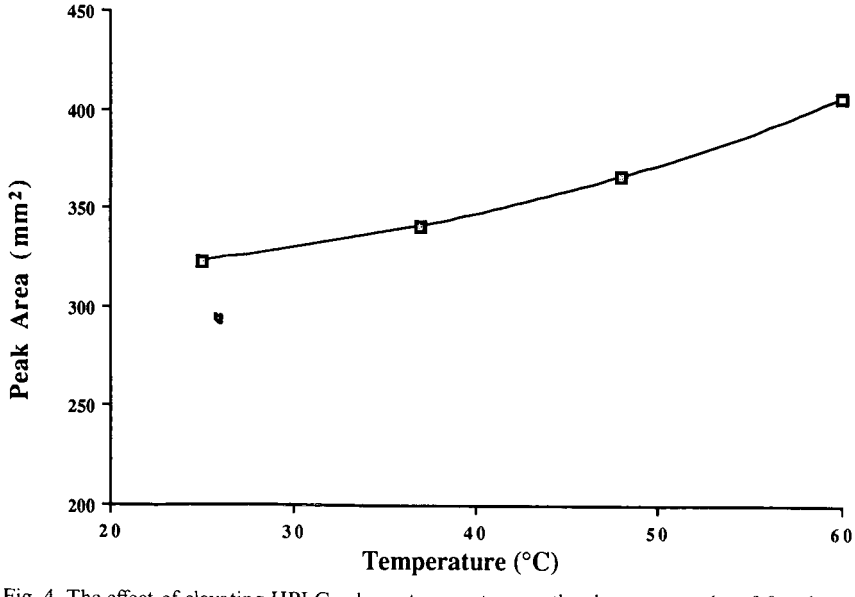

Fig. 4. The effect of elevating HPLC column temperature on the chromatography of β-endorphin, measured as changes in peak area (mm^2).

condenser. A thermocouple 4939 (Comark Electronics), was placed between the column and the jacket so that temperature could be accurately measured. The same sample of β-endorphin (5 μg/ml) was used at all temperatures; 25, 37, 48 and 60°C, so as to ensure that any difference observed in peak area could be ascribed to temperature alone, rather than changes in sample concentration. Results are demonstrated in Fig. 4, and show an increase in peak area with an increase in temperature. As temperature is known to destructure proteins, then it can be assumed that β-endorphin is transformed from a helical structure to a denatured random coil, thus altering the micro-environment of the absorbing amino acids resulting in an increase in response. These data support previous findings [13,14] that β-endorphin is helical during detection after undergoing HPLC at room temperature (25°C).

In addition to the increase in peak area caused by a rise in temperature, the introduction of a small peak was observed at 37°C which persisted up to 64°C where this peak began to split. Interestingly, these peaks eluted prior to the main peak. As it is thought that a denatured protein exposes additional internal hydrophobic residues, which increase its interaction with the stationary phase and thereby lengthen the retention time [27], then it might be supposed that these early eluting peaks represent a more folded form of the molecule than the main peak. The appearance of the split peak can perhaps only be explained by the emergence of another conformational form of β-endorphin.

Substantiating the hypothesis that the main peak of β-endorphin is unfolding, data gained demonstrates an increase in k' with elevated temperature (Table IX), which would normally be expected to decrease [34]. Elevated temperature will facilitate the denaturation of a peptide resulting in more sites being available to associate with the stationary phase, thereby lengthening the retention time. It might therefore be suggested that the main eluted peak, in this instance, represents an increasingly unfolded form of β-endorphin. These findings further demonstrate that the dynamic processes involved do not fit a simple two-state kinetic model.

TABLE IX

EFFECT OF COLUMN TEMPERATURE ON k' VALUES OF THE MAIN ELUTED PEAK OF β-ENDORPHIN [MOBILE PHASE UTILISED WAS CH_3CN–0.1 M KH_2PO_4, pH 2.3 (32:68)]

Temperature (°C)	k'		
	Peak 1	Peak 2	Peak 3
25			0.9
37		0.8	0.95
48		0.8	1.0
60		0.8	1.05
64	0.7	0.8	1.1

CONCLUSIONS

The observation that β-endorphin has the propensity to alter conformation during HPLC analysis [14,15] has been confirmed within this study. Mobile phase constituents, such as organic modifier, pH and buffer molarity dramatically alter the chromatographic behaviour of β-endorphin. The exact mechanisms involved cannot be predicted from the present work, although it would seem that the interaction of the molecule is not just reliant upon the sorbent and mobile phase but also the structure of β-endorphin prior to injection onto the column.

Conformational change of proteins normally occurs over a time span of 0.1 to 100 S [35]. Thus depending on the rate of equilibration between the native and denatured protein, whether it is possible to study the HPLC-induced conformational transition by manipulating the flow-rate. If this conformational process is rapid one peak will appear on the chromatogram, however, two or more peaks will be evident if the rate is slow [36]. Results gained can only partially be explained by the above, as while an extra peak did appear at slower flow-rates it was evident only as a consequence of variation in the micro-environment of the sample prior to chromatography. It is apparent therefore that the conformational change of β-endorphin, in this instant, cannot be adequately explained by the two-state model of kinetic processes.

The way in which β-endorphin folds is unknown, although some of the general assumptions forwarded for proteins [35] may apply here. In addition, as β-endorphin contains a proline at residue 13 it is possible that *cis–trans* isomerisation occurs, promoting conformational change of this peptide. This

phenomenon has altered the chromatographic performance of other peptides causing band spreading and peak distortion [36–38].

From this work it can be concluded that β-endorphin can undergo conformational changes during HPLC and that the sample solvent prior to injection can dramatically alter the chromatogram.

REFERENCES

1 F. Bach, R. Ekman and F. Jensen, *Regul. Peptides.*, 16 (1986) 189.
2 M. Dennis, C. Lazure, N. Seidah and M. Chretien, *J. Chromatogr.*, 266 (1983) 163.
3 K. Hermann, R. Lang, T. Unger, C. Bayer and D. Ganten, *J. Chromatogr.*, 312 (1984) 273.
4 S. Mousa and D. Couri, *J. Chromatogr.*, 267 (1983) 191.
5 E. Nice and M. O'Hare, *J. Chromatogr.*, 162 (1979) 401.
6 R. Venn, *J. Chromatogr.*, 423 (1987) 93.
7 S. Lau, A. Taneja and R. Hodges, *J. Chromatogr.*, 317 (1984) 129.
8 M. Hearn, A. Hodder and M. Aguilar, *J. Chromatogr.*, 327 (1985) 47.
9 K. Benedek, S. Dong and B. Karger, *J. Chromatogr.*, 317 (1984) 227.
10 S. Cohen, K. Benedek, Y. Tapuhi and B. Karger, *Anal. Biochem.*, 144 (1985) 275.
11 X. Lu, K. Benedek and B. Karger, *J. Chromatogr.*, 359 (1986) 19.
12 A. Sadler, R. Micanovic, G. Katzenstein, R. Lewis and R. Middaugh, *J. Chromatogr.*, 317 (1984) 93.
13 M. Hearn, *Life Sci.*, 41 (1987) 897.
14 M. Hearn and M. Aguilar, *J. Chromatogr.*, 352 (1986) 35.
15 M. Hearn and M. Aguilar, *J. Chromatogr.*, 397 (1987) 47.
16 P. Bayley, C. Snell and D. Smyth, *Biochem. Soc. Trans.*, 5 (1977) 683.
17 M. Hollosi, M. Kajtar and L. Graf, *FEBS Lett.*, 74 (1977) 185.
18 O. Lichtarge, O. Jardetzky and C-H. Li, *Biochemistry*, 26 (1987) 5916.
19 W. Mattice and R. Robinson, *Biochem. Biophys. Res. Commun.*, 101 (1981) 1311.
20 W. Mattice and R. Robinson, *Biopolymers*, 20 (1981) 1421.
21 J. Yang, T. Brewley, G. Chi Chen and C-H. Li, *Proc. Natl. Acad. Sci. U.S.A.*, 74 (1977) 3235.
22 M. Jibson and C-H. Li, *Int. J. Pept. Proteins Res.*, 18 (1981) 297.
23 L. Graf, M. Hollosi, I. Barna, K. Hermann, J. Borvendeg and N. Ling, *Biochem. Biophys. Res. Commun.*, 95 (1980) 1623.
24 R. Hammonds, A. Hammonds, N. Ling and D. Puett, *J. Biol. Chem.*, 257 (1982) 2990.
25 C. Wu, N. Lee, H. Loh, J. Yang and C-H. Li, *Proc. Natl. Acad. Sci. U.S.A.*, 76 (1979) 3656.
26 R. Ingraham, S. Lau, A. Taneja and R. Hodges, *J. Chromatogr.*, 327 (1985) 77.
27 E. Parente and D. Wetlaufer, *J. Chromatogr.*, 314 (1984) 337.
28 C. Simpson, *Practical High Performance Liquid Chromatography*, Heyden & Son, London, 1976.
29 J. Di Bussolo, *Liquid Chromatogr.*, June (1984) 20.
30 J. Smith and M. O'Hare, in E. Reid, B. Scales and I. Wilson (Editors), *Bioactive analytes including CNS drugs, peptides and enantiomers*, Plenum, New York, 1986, pp. 17–36.
31 X. Geng and F. Regnier, *J. Chromatogr.*, 296 (1984) 15.
32 M. O'Hare and E. Nice, *J. Chromatogr.*, 171 (1979) 209.
33 A. Santagestino, G. Giagnoni, P. Fumagalli, D. Pavesi and E. Torretta, *Biochem. Biophys. Res. Commun.*, 104 (1982) 576.
34 K. Cohen, K. Schellenberg, K. Benedek, B. Karger, B. Grego and M. Hearn, *Anal. Biochem.*, 140 (1984) 223.
35 J. Andrade and V. Haldy, *Advances in Polymer Science 79*, Springer, Berlin, 1986.
36 W. Melander, H. Lin, J. Jacobson and Cs. Horváth, *J. Phys. Chem.*, 88 (1984) 4527.
37 J. Creighton, *8th International Biophysics Congress U.K.*, International Union of Pure and Applied Biophysics and The Royal Society of London, London, 1984, p. 165.
38 D. Henderson and J. Mello, *J. Chromatogr.*, 499 (1990) 79.
39 S. Siegel, *Non-Parametric Statistics for the Behavioural Sciences*, McGraw-Hill, London, 1956.

Journal of Chromatography, 595 (1992) 137–142
Elsevier Science Publishers B.V., Amsterdam

CHROM. 23 873

Comparison of colorimetric and chromatographic determination of *tert.*-butylpyrocatechol

E. Hlavačková and R. Reya

Cables and Insulating Materials Research Institute, Továrenská 14, 815 71 Bratislava (Czechoslovakia)

(First received July 5th, 1991; revised manuscript received November 12th, 1991)

ABSTRACT

A high-performance liquid chromatographic method for the determination of 4-*tert.*-butylpyrocatechol (TBC) in styrene after its preconcentration by a solid-phase extraction technique is compared with a colorimetric method based on absorbance measurement of TBC products formed with alkaline hydroxide. The differences between the results obtained with both methods when applied to technical samples and samples enriched with prepared TBC oxidation products are discussed. It is assumed that in the high-performance liquid chromatographic method only unchanged TBC is determined, while in the colorimetric method its transformation products are also included. Apparently, oxidation products contribute to a measurement which represents neither the concentration of remaining TBC nor the total concentration of TBC and its oxidation products in the sample.

INTRODUCTION

Technical styrene undergoes undesirable polymerization during shipping, storage and technological processes and it is therefore stabilized with 4-*tert*-butylpyrocatechol (TBC) in the concentration range 10–50 ppm. For industrial applications, the content of TBC in the monomer is an important criterion. Colorimetric methods have been frequently used for its determination. The total amount of TBC is currently determined by an alkaline method [1] utilizing the formation of coloured oxidation products with sodium hydroxide. A similar principle is applied in the test method of the American Society for Testing and Materials (ASTM) [2] for determination of total TBC content in light hydrocarbons. In another method the intensity of the yellow-coloured complex of TBC with ferric chloride is measured by a suitable photoelectric photometer.

The above-mentioned methods are not capable of distinguishing between original TBC and its transformation products formed during inhibition processes. Another colorimetric method is based on the reduction of Fe^{3+} with inhibitor to Fe^{2+} and on the measurement of the absorbance of its complex with 1,10-phenanthroline. The above method is limited to the non-oxidized form of phenolic and the total amount of aminic inhibitors and has been applied to the quantitative analysis of the following inhibitors: TBC, hydroquinone, 2,6-*tert.*-butyl-4-methylphenol and *n*-phenyl-*n'*-izopropyl-*n*-phenylendiamine [3]. Later the same authors [4] published a paper dealing with the comparison of photocolorimetric methods for determination of the total content and unchanged portion of inhibitors.

High-performance liquid chromatography (HPLC) has also been shown to be a useful method for determination of phenolic inhibitors, antioxidants and light stabilizers [5–9]. An HPLC method was developed for the determination of 4-*tert*-butylphenol and TBC by Gaguardi *et al.* [10]. For the determination of only the active form of TBC in butadiene an HPLC method was published by Oomens *et al.* [11].

In a recent paper we have reported an HPLC method [12] for determination of TBC in styrene. The separation conditions were similar to those in

0021-9673/92/$05.00

the above-mentioned method [11], but a solid-phase extraction (SPE) technique for preconcentration and preseparation of TBC from styrene was used. In the present study the results of a comparison of HPLC and an alkali colorimetric method for the determination of TBC in styrene are presented and discussed.

EXPERIMENTAL

Reagents and chemicals

TBC of analytical grade was obtained from Fluka (Switzerland) and styrene of technical grade stabilized with TBC was obtained from Kautshuk (Czechoslovakia) as well as from Prochema (Austria).

The oxidized form of TBC was prepared from TBC by reaction with sodium hydroxide [11] in various modifications. For TBC_{OX}, each solution of TBC in 1 *M* sodium hydroxide was mixed for 30 min; moreover TBC_{OXI} was mixed and saturated with oxygen for 30 min; TBC_{OXII} was saturated with oxygen for only 15 min; TBC_{OXIII} was saturated with oxygen for only 10 min; TBC_{OXIV} was saturated with oxygen for 5 min, and TBC_{OXV} was prepared without saturation. In Table I the concentrations of TBC in such prepared samples are shown.

Solvents and reagents for both HPLC and colorimetric determination, all analytical grade, were from Lachema (Czechoslovakia); acetic acid was used as received without purification; methanol, chloroform and *n*-heptane were glass-distilled; water was doubly distilled.

Calibration standards and standard samples were prepared by addition of 2–32 ml of TBC stock solution (0.113 g of TBC in 1000 ml of inhibitor-free styrene) to inhibitor-free styrene.

TABLE I

HPLC ANALYSIS OF TBC_{OX} IN THE MOBILE PHASE

Sample	TBC found (mean ± R.S.D.) (%)
TBC_{OXI}	0
TBC_{OXII}	6.74 ± 4.66
TBC_{OXIII}	16.72 ± 5.03
TBC_{OXIV}	66.36 ± 4.85
TBC_{OXV}	105.06 ± 5.93

Inhibitor-free styrene was prepared by washing the monomer three times with an equal volume of a 1 *M* solution of sodium hydroxide in water followed by washing with water until neutral to litmus.

Methods

For chromatographic determination of TBC in styrene, an HPLC [12] method was used.

For colorimetric determinations of TBC in styrene the ASTM test method [1] was applied using a Model 559 UV–VIS spectrophotometer from Perkin Elmer (USA), wavelength 700–800 nm, with PTFE-covered glass rectangular cells: *d* (optical path length of cell) = 10 mm, scan speed = 480 nm/min, slit = 2 nm.

RESULTS AND DISCUSSION

The calibration graph in Fig. 1, in which curve A shows the dependence of absorbance on TBC concentration, was constructed on the basis of spectrophotometric measurements at a wavelength of 485 nm. It can be seen that this dependence is not linear but cubic, with the following parameters: $y = -4.11 \cdot 10^{-3} + 3.79 \cdot 10^{-3} x + 5.87 \cdot 10^{-5} x^2 - 3.53 \cdot 10^{-3} x^3$. However, at TBC concentrations above 18 ppm a linear relationship is obtained with a correlation coefficient $r = 0.9994$.

It was assumed that this non-linearity at low concentrations is due to the procedure of extracting TBC from styrene with 1 *M* sodium hydroxide.

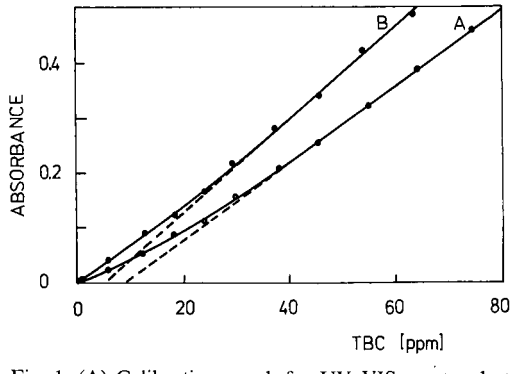

Fig. 1. (A) Calibration graph for UV–VIS spectrophotometric measurements. (B) Dependence of absorbance on TBC concentration after reaction with 1 *M* sodium hydroxide.

However, this assumption was not confirmed by the following experiments. Various amounts of TBC were weighed directly into 1 *M* sodium hydroxide, then shaken for the same time as in the above method in an arbitrary atmosphere. Finally the absorbance of the solution was measured at a wavelength of 485 nm at 1-min intervals for 18–20 min. These experimental values were expressed as the dependence of absorbance on TBC concentrations. It was found that the curve thus obtained, curve B in Fig. 1, also conforms to a cubic relationship at lower concentrations. This is most likely because of the oxidation processes of TBC followed by decomposition of products formed in alkaline medium; moreover, the relative portion of air present is higher at lower concentrations. The influence of the time on the reaction of TBC with sodium hydroxide is shown in Fig. 2. A continuous decrease of absorvance with time, which is linear after 12–15 min, can be seen.

This phenomenon can be explained with the help of Fig. 3, in which the absorbance of the TBC mixture with sodium hydroxide was continuously recorded at intervals of 4–60 min. Such UV–VIS spectra are characteristic of a system in which the compounds undergo mutual chemical changes.

From the results obtained it can be concluded that the reaction time of 15 min prescribed by the ASTM method [1] must be rigidly adhered to.

The calibration graph of the HPLC method for the determination of TBC [12], unlike that of the colorimetric analysis, shows a linear relationship with a correlation coefficient of 0.9998. The direct measurement of unchanged TBC by the former method is the reason for this behaviour.

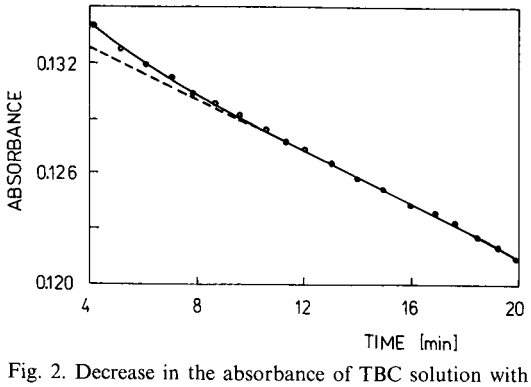

Fig. 2. Decrease in the absorbance of TBC solution with time (18.33 ppm TBC in 1 *M* sodium hydroxide).

For the comparison of both methods, standards, technical samples of styrene and samples containing oxidation products were analysed.

Standard samples

Table II summarizes the results of the analysis of various TBC concentrations performed in nine parallel determinations with HPLC and three parallel determinations with the UV–VIS spectrophotometric method. The accuracy of these results was confirmed by the Student and Lord test; evaluation of the comparison was confirmed by the Moor test at a significance level of 0.5. The results represented by confidence intervals agree well with the amounts added in both methods, when applied to standard (model) samples.

Technical samples

The results of the analysis of three technical styrenes are shown in Table III. Various differences between the HPLC and UV–VIS spectrophotometric measurements can be seen. HPLC separation of the above samples is illustrated in Fig. 4. Serious differences can be seen in these three chromatograms of technical styrenes. They can be explained by the presence of various amounts and types of TBC transformation products. The type and amount of these products are strongly dependent

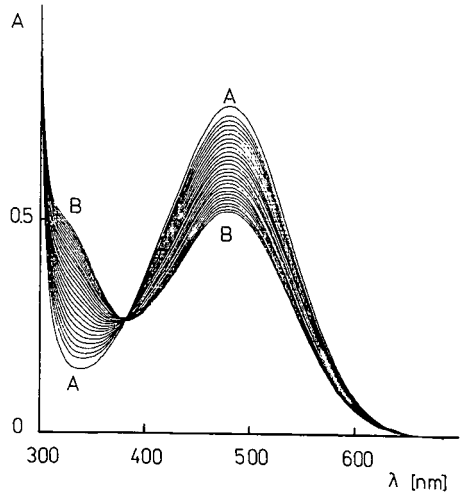

Fig. 3. UV–VIS spectra of 9.06 ppm TBC in 1 *M* sodium hydroxide scanned at 2-min time intervals: (A) reaction time 4 min; (B) reaction time 60 min.

TABLE II

RESULTS OF HPLC AND UV–VIS SPECTROPHOTOMETRY OF STANDARD SAMPLES

TBC added (ppm)	TBC found (ppm)	
	HPLC (mean ± S.D.)	UV–VIS (mean ± S.D.)
4.52	4.42 ± 0.53	4.33 ± 0.44
13.56	–	13.41 ± 0.59
22.60	22.47 ± 0.63	23.45 ± 1.57
40.68	39.95 ± 0.95	41.73 ± 0.93
58.76	58.08 ± 0.90	59.28 ± 1.86

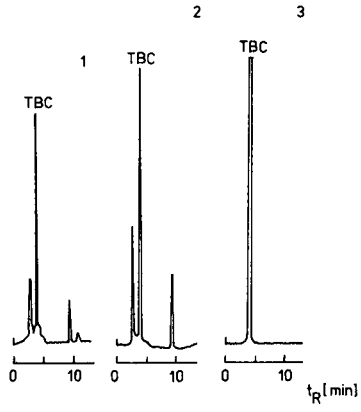

Fig. 4. Chromatograms of TBC in three technical styrenes (see Table III). Chromatographic conditions: reversed-phase glass column Separon SGX C_{18}, 5 μm particle size, 150 × 3.3 mm I.D., mobile phase, methanol–water–acetic acid (67:32:1, v/v/v); flow-rate, 0.5 ml/min; UV detector wavelength, 280 nm; injection, 20-μl sample with fixed loop.

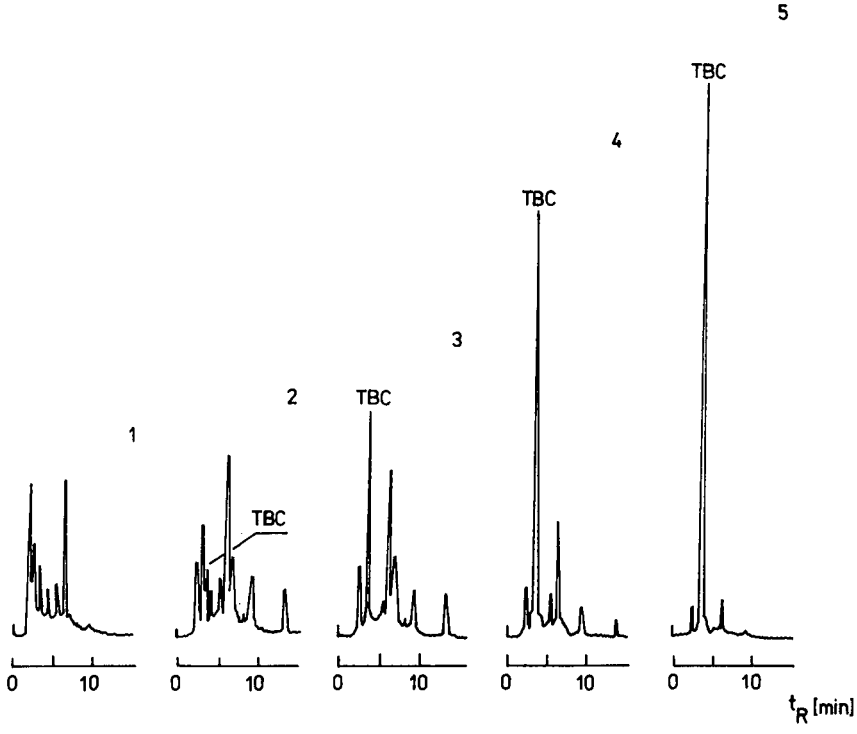

Fig. 5. Chromatograms of TBC oxidation products in styrenes (see Table IV). Chromatographic conditions as above. 1 = TBC_{OXI}; 2 = TBC_{OXII}; 3 = TBC_{OXIII}; 4 = TBC_{OXIV}; 5 = TBC_{OXV}.

TABLE III

THE RESULTS OF HPLC AND UV–VIS SPECTROPHOTOMETRY OF TECHNICAL SAMPLES

Sample No.	TBC found (ppm)	
	HPLC (mean ± S.D.)	UV–VIS (mean ± S.D.)
1	15.76 ± 1.90	17.52 ± 0.37
2	18.38 ± 1.84	26.70 ± 1.85
3	42.38 ± 0.27	44.96 ± 2.01

on storage time and temperature. It is evident that these conditions were different in individual styrene samples.

Styrene with TBC_{ox}

From the results of the HPLC method it can be seen that an increasing amount of original (unchanged) TBC remained as the saturation time with oxygen decreased. It is evident that the composition of the mixture strongly depends on the reaction conditions. HPLC separation of TBC-free styrene enriched with all prepared oxidation products as described in the Experimental section is shown in Fig. 5.

Finally, the results of styrene enriched with TBC_{ox} by both mentioned methods are shown in Table IV. Significant differences in the TBC content as determined by both methods can be observed. However, the TBC concentrations obtained by spectrophotometry are remarkably higher than the results obtained by HPLC, which may be because in the former method both the oxidation products of TBC and the products of interaction of TBC with styrene radicals are included.

CONCLUSIONS

From the results obtained it is evident that the main differences between the HPLC and UV–VIS spectrophotometric methods are as follows. With HPLC, TBC is separated from its oxidation products and thus is determined in unchanged form. With UV–VIS spectrophotometry the absorbance of the reaction products with alkaline hydroxide as a whole is measured. Therefore the results of both methods, in the absence of TBC oxidation products, as in the standard samples and in the technical styrenes, include only traces of TBC transformation products. But significant differences were observed in samples of technical styrenes which had been stored for a long time under poor conditions and in model styrenes enriched with TBC oxidation products.

TABLE IV

HPLC AND UV–VIS SPECTROPHOTOMETRIC RESULTS OF STYRENE ENRICHED WITH TBC_{ox}

Sample	TBC_{ox} added (ppm)	TBC found (ppm)	
		HPLC (mean ± S.D.)	UV–VIS (mean ± S.D.)
1. TBC_{oxI}	40.80	0	20.33 ± 0.18
2. TBC_{oxII}	41.36	2.77 ± 0.23	29.94 ± 0.65
3. TBC_{oxIII}	41.96	10.64 ± 0.39	31.55 ± 1.27
4. TBC_{oxIV}	40.16	20.58 ± 0.36	29.73 ± 0.49
5. TBC_{oxV}	40.48	35.59 ± 0.61	36.83 ± 0.76

It can be concluded that the UV–VIS spectrophotometry alone, although a simple and effective method, is not applicable for severely aged styrene samples. For this purpose, as well as for investigation of transformation processes of TBC during styrene storage and synthesis of polymeric materials on styrene basis, the HPLC method should be preferred.

ACKNOWLEDGEMENT

The authors thank Dr. O. Mlejnek for his invaluable advice and assistance in preparing this paper.

REFERENCES

1 ANSI/ASTM D2120-82, *Inhibitor p-tert.-Butylpyrocatechol in Styrene Monomer*, ASTM, Philadelphia, PA.
2 ANSI/ASTM D1157-59 (reapproved 1978), *Total Inhibitor content (TBC) of Light Hydrocarbons*, ASTM, Philadelphia, PA.
3 G. A. Kotova, N. K. Loginova and R. A. Kuznecova, *Promyschlenost*, 8 (1981) 6.
4 G. A. Kotova, N. K. Loginova and R. A. Kuznecova, *Sb. Nauch. Tr. NII Monomerov Dlya Sintetich. Kauchuka*, 4 (1981) 34.
5 D. N. Armentrout, J. D. Melean and M. W. Long, *Anal. Chem.*, 51 (1979) 1039.
6 J. Firth and I. Rix, *Analyst*, 111 (1986) 129.
7 R. B. Walter and J. F. Johnson, *J. Polym. Sci.*, 15 (1980) 29.
8 Y. Kitada, Y. Veda, M. Yamamoto, K. Shinomiya and H. Makazawa, *J. Liq. Chromator.*, 8 (1985) 47.

9 D. Monteanu, A. Isfan, C. Isfan and I. Timcul, *Chromatographia*, 23 (1987) 7.
10 L. Gaguardi, A. Cimorelli, G. Cavazzutti and L. Montanarella, *J. Chromatogr.*, 486 (1989) 433.
11 A. C. Oomens, F. G. Schuurhuis and M. E. Skelly, *J. Liq. Chromatogr.*, 7 (1984) 2143.
12 E. Hlavačková, O. Mlejnek and D. Berek, *J. Liq. Chromatogr.*, 13 (1990) 3053.

Journal of Chromatography, 595 (1992) 143–148
Elsevier Science Publishers B.V., Amsterdam

CHROM. 23 926

Fluorescence detection of trichothecene mycotoxins as coumarin-3-carbonyl chloride derivatives by high-performance liquid chromatography

Huguette Cohen* and Bernadette Boutin-Muma

Laboratory Services Division, Food Production and Inspection Branch, Agriculture Canada, Building No. 22, C.E.F., Ottawa, Ontario K1A 0C6 (Canada)

(First received September 9th, 1991; revised manuscript received November 28th, 1991)

ABSTRACT

A new and simple procedure was developed for the determination of trichothecenes mycotoxins by high-performance liquid chromatography using fluorescence detection. The procedure involves the synthesis of the derivatizing reagent, coumarin-3-carbonyl chloride, and its use in the esterification of T-2, HT-2, T-3 and T-4. A clean-up procedure was used using silica cartridge to remove the excess reagent peaks. The esterified toxins were simultaneously separated on a reversed-phase column using acetonitrile–water containing acetic acid as the mobile phase and detected by fluorescence. The minimum detectable amounts of T-2 and its metabolites were 2.0 ng and 0.83 ng, respectively, at a signal-to-noise ratio of 2 and injection volume of 10 μl.

INTRODUCTION

Trichothecene mycotoxins are mold metabolites produced by various strains of Fusarium, Trichoderma, Myrothecium, and other species of imperfect fungi. The group is characterized by the 12,13-epoxy-trichothec-9-ene ring system. In blood T-2 and HT-2 are easily interconverted and hydrolyzed to T-3 and T-4 toxins (Fig. 1, compound 3). T-2 and its derivatives belong to the group that does not contain a carbonyl function at C-8 conjugated with a double bond in 9–10 [1]. The absence of this δ-β-enone feature prevents these compounds from being detected by UV absorption.

Numerous analytical methods have been published. The most frequently employed methods are thin-layer chromatography (TLC) [2,3], enzyme-linked immunoassay (ELISA) [4–7], gas chromatography [8–10] combined with mass spectrometry [11], or with tandem mass spectrometry [12], or thermospray liquid chromatography–mass spectrometry [13,14]. The use of the coumarin-3-carbonyl chloride as derivatization reagent permits the fluorescence detection of the hydroxyl function of the trichothecenes. Acylation is commonly used for labelling hydroxy compounds and permits rapid and quantitative derivatization. A pre-column derivatization has been reported to form a chromophore with *p*-nitrobenzoyl chloride with an absorption maximum at 254 nm, the method has the disadvantages that the reagent gives an interfering peak and also a large number of organic compounds absorb at this low wavelength [15]. A more recent post-column derivatization technique involves an alkaline decomposition to form formaldehyde and a modified Hantzch reaction with methylacetoacetate and ammonium acetate [16]. This procedure was suitable for deoxynivalenol (DON), nivalenol, fusarenone trichothecenes that contain a carbonyl function at C-8, but not for T-2 and its derivatives. Polycyclic aromatics such as anthracene-3-carboxylic chloride have been employed for the determination T-2 toxin and DON.

Coumarins as fluorophore possess a high molecular extinction coefficient and quantum yields. For trace analyses, derivatization of the target com-

0021-9673/92/$05.00

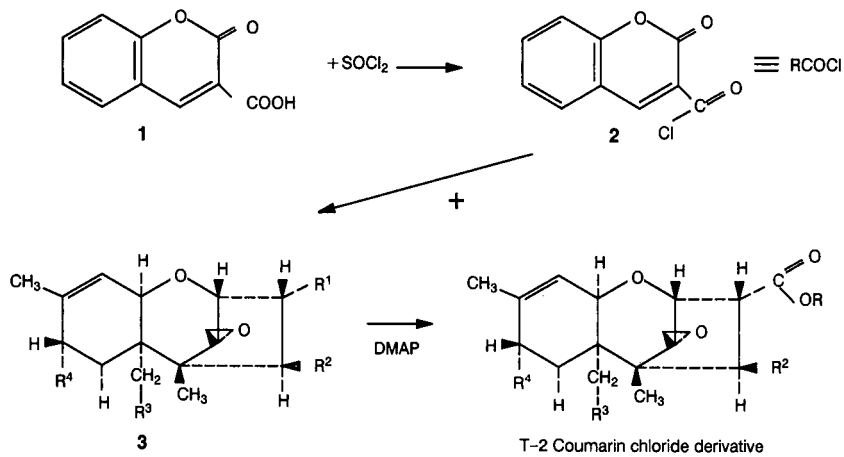

Trichothecene	R^1	R^2	R^3	R^4
HT-2 toxin	OH	OH	OAC	$OCOCH_2CH(CH_3)_2$
T-2 toxin	OH	OAC	OAC	$OCOCH_2CH(CH_3)_2$
T-3 toxin	OH	OH	OH	$OCOCH_2CH(CH_3)_2$
T-4 toxin	OH	OH	OH	OH

Fig. 1. Structures of trichothecenes.

pounds offers significant advantages such as improving selectivity. A coumarin-3-carbonyl chloride derivative has been successfully applied to hydroxy compounds such as hydroxy-steroids and prostaglandins [17]. In the present work, we have sucessfully empolyed coumarin-3-carboxylic acid chloride to derivativze T-2 and its "major metabolites" for analyses by high-performance liquid chromatography (HPLC). The reaction is represented in Fig. 1 below.

EXPERIMENTAL

Chemicals and materials

Coumarin-3-carboxylic acid, 4-dimethylamino pyridine (DMAP), thionyl chloride (99%) were obtained from Aldrich (Milwaukee, WI, USA). Trichothecenes were obtained from Sigma St. Louis, MO, USA). Silica gel cartridges were purchased from BDH (Toronto, Canada). LDX filters were purchased from Chromatographic Sciences (Montreal, Canada). Water was purified using a Millipore Milli-Q system. All other solvents were glass distilled or HPLC grade from BDH (Toronto, Canada).

Apparatus

A Perkin-Elmer LS-4 liquid chromatograph equipped with microprocessor control delivery system and an auto-injector ISS-sampling system was employed. An RP-18, 5-μm column (250 × 4.6 mm I.D.) protected with a RP-18, 7-μm guard column (15 × 3.2 mm I.D.) was used. Mobile phase was acetonitrile-water (65:35, v/v) containing 0.75% acetic acid and flow-rate of 1 ml/min. Fluorescence detection conditions were excitation at 292 nm and emission at 425 nm, both with 10 nm slit widths.

Electron impact mass spectra were obtained with Kratos MS 25 or VG 15-250 spectrometers set at 70 eV.

Methods

Synthesis of coumarin-3-carbonyl chloride. Coumarin-3-carboxylic acid (5 g) was suspended in dry dichloromethane (30 ml) and refluxed while adding thionyl chloride (10 ml) dropwise. A drying tube packed with calcium chloride was placed in the outlet of the condenser. The mixture was refluxed for 40 min. Some dichloromethane was added to prevent dryness. On completion of the reaction the solvent was evaporated under vacuum at 50°C. The residues were dissolved in anhydrous chloroform and the solution was heated with careful addition of hexane until the solution turned cloudy. Yellow pale crystals (3.83 g) were obtained on cooling,

yield 70%; m.p.: 143°C (uncorrected). The mass spectrum had peaks at m/z 208 (M^+, 8%, agrees for $C_{10}H_5C10_3$), 173 ($M^+ - Cl$), 145 ($M^+ - COCl$).

Preparation of standard solution. (i) Trichothecene standards T-2: 25 mg, dissolved in 100 ml toluene to obtain a concentration of 0.25 μg/μl; HT-2: 5 mg; T-3: 5 mg; T-4: 5 mg, three standard solutions at concentration of 50 ng/μl in 100 ml toluene solution were prepared. These standard solutions were stored at 4°C and brought to room temperature before use. (ii) Coumarin-3-carbonyl chloride 65 mg was dissolved in 20-ml volumetric flask, to obtain a concentration of 3.25 μg/μl. (iii) 4-Dimethylaminopyridine (DMAP) 130 mg was dissolved in volumetric flask (20 ml) to obtain a concentration of 6.5 μg/μl.

Derivatization conditions. All glassware were rinsed with toluene before use. In 15-ml screw cap conical tube, 10 μl of each trichothecene standard solution was evaporated to near dryness under slow stream of nitrogen. To each tube, 10 μl of DMAP 6.5 μg/μl solution was added, followed by the addition of 10 μl of the coumarin reagent. The tube was closed and the mixture incubated at 80°C for 20 min. The mixture was then cooled in ice water and then purification procedure followed as detailed below.

Preparation of the standard curves. To obtain the calibration curve, a series of standard solution containing each of the four toxins was used at concentration between 0.01 and 0.5 μM. DMAP was added at concentrations between 0.13 and 3.98 μM and the carbonyl chloride between 0.037 and 1.125 μM. Derivatization was carried out as mentioned in the derivatization procedure.

Purification of the reaction mixture. The silica gel cartridge was pre-conditioned first with 5 ml of chloroform–methanol (70:30) and then 5 ml of benzene. The cooled reaction mixture was then quantitively transferred to the silica gel column with benzene (5 × 1 ml). The benzene fractions were discarded, then a mixture ethyl acetate–hexane (80:20, 5 × 2 ml) was added to the column and discarded. The derivatized trichothecenes were eluted with ethyl acetate–hexane (90:10, 2 × 7 ml). The eluate was collected and evaporated to dryness under a gentle flow of nitrogen. To the residues 1 ml of the HPLC mobile phase: acetonitrile–water (65:35) containing 0.75% acetic acid was added, the solution filtered through LXD filter (4.5 μm) and 10 μl injected into an HPLC system.

RESULTS AND DISCUSSIONS

Reaction conditions were optimised by investigating variables such as solvent, reagent ratio, temperature and reaction times. The effect of benzene and methylene chloride as solvent was investigated. This later solvent gave an additional peak in the chromatogram. The optimum molar ratio of the derivatizing reagent–base–sample was 1:3:0.5. No improvement in peak height was obtained when the relative porportion of the derivatizing reagent was greater than 1. The unreacted reagents eluted near the solvent front and their peaks show little tailing, also the peaks of interest eluted far from the solvent front.

Each toxin was tested for temperature effect, the derivatization of T-2 and HT-2 was least affected by temperature. The derivatization was optimal at room temperature and remained unchanged at higher temperatures. However, the best peak response for T-3 and T-4 was obtained when a reaction temperature of 80°C and a reaction time of 20 min was used. A longer time didn't change the peak height.

The limit of detection which was defined as the lowest instrumental signal was obtained at 0.83 ng/10 μl injection for HT-2, T-3, T-4 and at 2.0 ng/10 μl injection for T-2, when the signal to noise ratio (S/N) was 2. It appears that the detection limit for HT-2, T-3 and T-4 was lower than for T-2 because T-2 has only one hydroxyl, HT-2 two hydroxyl, T-3 three and T-4 four for derivatization. The fluorescence properties of the toxins increase as the number of the chromophores undergoing esterification increases.

The HPLC separation was performed with acetonitrile–water (65:35), and 0.75% of acetic acid was added to the HPLC mobile phase, in order to separate all four derivatives. No reaction was observed between the mobile phase and the derivatizing agent. The purification using preconditioned silicagel cartridge gave very good recoveries. Table I summarizes the recoveries obtained for various trichothecenes. The recoveries ranged from 80–100%. In the HPLC mobile phase, the derivatives were stable at room temperature up to 10 days.

TABLE I

PERCENT RECOVERY OF MIXTURE OF T-2, HT-2, T-3, T-4 AFTER SILICA GEL PURIFICATION

Trichothecenes	Concentration (ng/μl)	Recovery ± R.S.D. (%)[a]
T-2	125	100 ± 8.09
HT-2	25	102 ± 3.78
T-3	25	91 ± 9.22
T-4	25	80 ± 4.77

[a] Relative standard deviation ($n = 3$).

Fig. 2 displays the chromatogram of a single injection of T-2, HT-2, T-3, T-4; (a) before and (b) after clean up on silica Sep-pak column; (c) a blank of the reaction mixture containing only reagents. As shown, most of the excess reagent peaks are eliminated in 2b. Fig. 3 displays the standard curve for the four trichothecenes. Excellent linearities with correlation co-efficient over 0.996 were obtained for all toxins (Table II). The highest relative standard deviation (R.S.D.) obtained for all trichothecene standards is $\leqslant 5\%$ (Table III), except for T-4 which

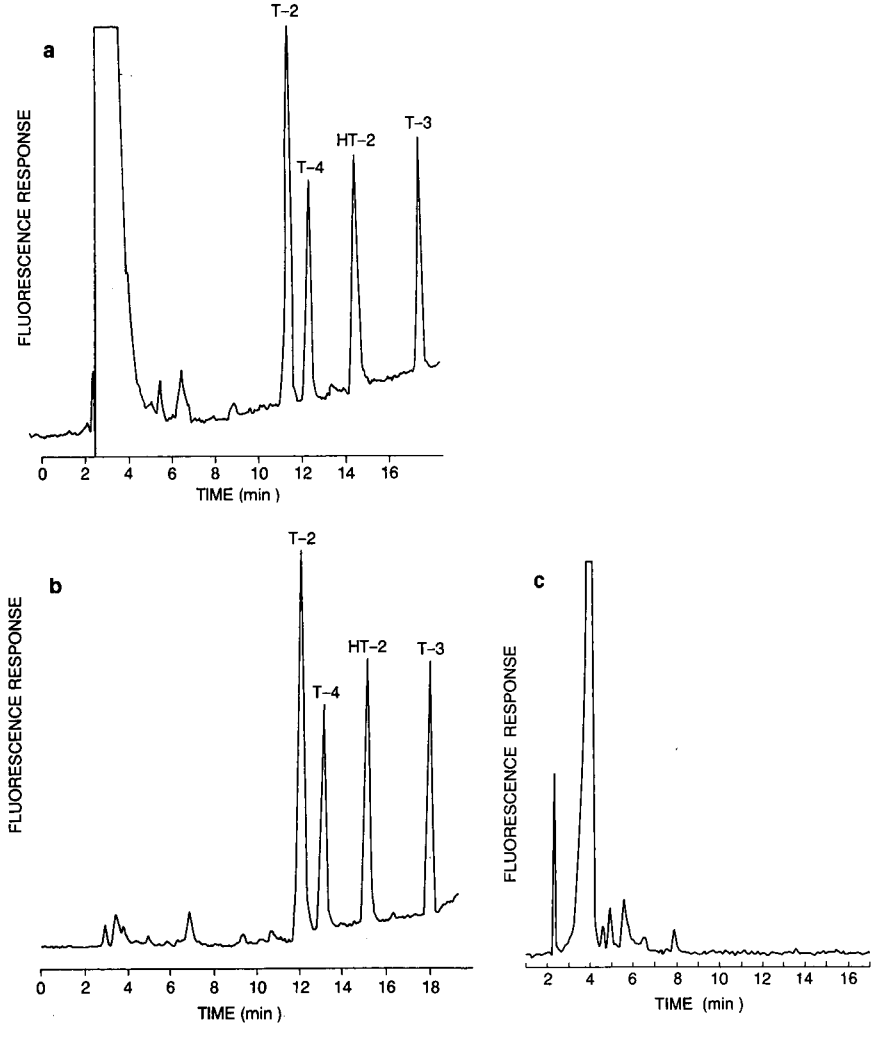

Fig. 2. Chromatogram of derivatization reaction mixtures of T-2, T-4, HT-2, T-3: (a) Before clean-up on a silica gel cartridge; (b) after clean-up on a silica cartridge; (c) a blank of the reaction mixture containing only reagents. HPLC conditions: reversed-phase chromatography on RP-18, 5 μm, 250 × 4.9 mm I.D. Mobile phase, acetonitrile–water (65:35 v/v) containing 0.75% acetic acid at 1 ml/min. Detection, excitation and emission at 292 nm and 425 nm respectively, same conditions for a, b and c.

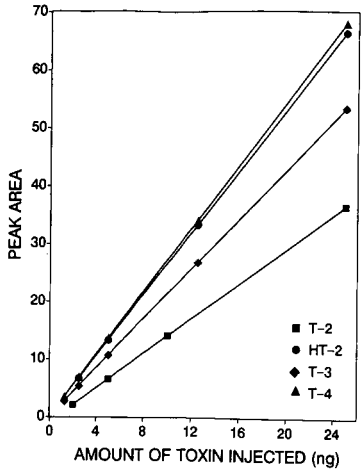

Fig. 3. A plot of concentration *vs.* peak area of derivatives of various mycotoxins.

TABLE II

LINEAR REGRESSION DATA AND CORRELATION COEFFICIENTS (r) FOR DERIVATIZED TRICHOTHECENES

$y = mx + b$

Mycotoxins	Slope m (ng^{-1})	Intercept b	Correlation coefficient of calibration graphs r
T-2	$1.5 \cdot 10^3$	$-8.48 \cdot 10^2$	0.9961
HT-2	$2.2 \cdot 10^3$	$-4.1 \cdot 10^3$	0.9960
T-3	$2.14 \cdot 10^3$	$-4.88 \cdot 10^2$	0.9963
T-4	$2.88 \cdot 10^3$	$-5.70 \cdot 10^3$	0.9902

TABLE III

CHROMATOGRAPHIC DATA FOR TRICHOTHECENE MYCOTOXINS

Mycotoxins	Retention time mean ± S.D.[a] (min)	Detection limit (ng/10 μl)	R.S.D.[c] (% Peak Area)
T-2	12.5 ± 0.46	2.0	3.65 (12.5)[b]
HT-2	15.1 ± 0.79	0.83	5.78 (12.5)
T-3	17.9 ± 0.70	0.83	5.31 (12.5)
T-4	13.6 ± 0.63	0.83	10.05 (12.5)

[a] $n = 4$.
[b] The numbers in parentheses are the relevant concentrations in ng/10 μl.
[c] $n = 4$.

was 10%. The reason for the large deviation has not been determined.

CONCLUSION

The synthesis of the coumarin-3-carboxyl chloride is simple and straight forward and its use as a derivatization reagent has proven quite efficient because of its high reactivity with hydroxyl group(s). The derivatization must be carried out in aprotic solvent to prevent hydrolysis to the parent acid. The proposed method for the determination of tricothecenes is very sensitive and rapid, it allows the simultaneous separation, detection and quantification of more than one mycotoxin in a short time. Therefore determination of at least 20 samples in 8 hours was possible. The detection limits are quite low for all trichothecenes. Although the applicability of the method has not yet been assessed, it offers a good scheme for separating solvent as well as the interfering peaks from the peaks of desired compounds. The toxins are very well separated from each other for easy detection and quantification. Futhermore this method can be used for the selective determination of other tricothecenes with similar functional groups.

REFERENCES

1 R. Cole and R. Cox (Editors), *Handbook of Toxic Fungal Metabolites*, 1981, Academic Press, New York, 1981, p. 152.
2 A. Sano, Y. Asabe, S. Takitani and Y. Ueno, *J. Chromatogr.*, 235 (1982) 257–265.
3 L. S. Lee and B. Skau, *J. Liq. Chromatogr.*, 4 (1981) 43–62.
4 M. R. A. Morgan, *Tetrahedron.*, 45 (1989) 2237–2249.
5 S. L. Fan-Titan, X. Y. Chun and F. S. Chu, *J. Assoc. Offic. Chem.*, 70 (1987) 657–661.
6 R. C. Lee, R. D. Wei and F. S. Chu., *J. Assoc. Offic. Anal. Chem.*, 72 (1989) 345–348.
7 J. Douglas, A. Kariman and R. W. Giese, *J. Immunol. Methods*, 131 (1990) 77–82.
8 P. M. Scott, P.-Y. Lay and S. R. Kanhere, *J. Assoc. Offic. Anal. Chem.*, 64 (1981) 1364–1371.
9 P. Begley, B. E. Foulger, P. D. Jeffrey, R. M. Black and R. W. Read, *J. Chromatogr.*, 367 (1986) 87–101.
10 H. Cohen, M. Lapointe, *J. Assoc. Offic. Anal. Chem.*, 67 (1984) 1105–1107.
11 C. J. Mirocha, R. A. Pawlosky, K. Chatterjee, S. Watson and W. Hayes, *J. Assoc. Off. Anal. Chem.* 66 (1983) 1485–1499.
12 R. D. Plattner, M. N. Beremand and R. Powell, *Tetrahedron*, 45 (1989) 2251–2262.
13 E. Rajakyla, K. Laasasenaho and P. J. D. Sakkers, *J. Chromatogr.*, 384 (1987) 391–402.

14 R. D. Smith , H. R. Udseth and B. W. Wright, *J. Chromatogr. Sci*, 23 (1985) 192–199.
15 R. Maycok and D. Utley, *J. Chromatogr.*, 347 (1985) 429–433.
16 A. Sano, S. Matsutani, M. Suzuki and S. Takitani, *J. Chromatogr.*, 410 (1987) 427–436.
17 K. E. Karlson, D. Wiesler, M. Alasandro and M. Novotny, *Anal. Chem.*, 57 (1985) 229–234.

Journal of Chromatography, 595 (1992) 149–154
Elsevier Science Publishers B.V., Amsterdam

CHROM. 23 927

Ion-exclusion chromatography using mobile phases containing β-cyclodextrin

Bronislaw K. Głod☆, Paul R. Haddad* and Peter W. Alexander

Department of Analytical Chemistry, University of New South Wales, P.O. Box 1, Kensington, N.S.W. 2033 (Australia)

(First received August 14th, 1991; revised manuscript received November 20th, 1991)

ABSTRACT

Ion-exclusion chromatography of some aromatic carboxylic acids is performed using an Aminex HPX-87H organic acids column with a mobile phase comprising ethanol–water (20:80, v/v) containing camphorsulphonic acid and β-cyclodextrin. Retention volumes of the solutes increased with increasing mobile phase concentration of camphorsulfonic acid. On the other hand, some solutes (gallic, *o*-nitrobenzoic, acetylsalicylic and *m*-nitrobenzoic acids) showed a decrease in retention volume when the mobile phase concentration of β-cyclodextrin was increased. This behaviour was attributed to the formation of inclusion complexes in the mobile phase, leading to an equilibrium shift which decreases the amount of solute in the stationary phase and hence its retention. This provides an additional parameter for control of the solute retention. A theoretical equilibrium model is presented which considers the equilibrium reactions occurring in the chromatographic system. Retention data are then used to evaluate the equilibrium constants for these reactions. In this way, the inclusion constant for each solute may be determined.

INTRODUCTION

Ion-exclusion chromatography, first introduced by Wheaton and Baumann [1] in 1953, involves the use of strong anion- or cation-exchange resin for the separation of ionic solutes from weakly ionized or neutral solutes. In this mode of chromatography ionic solutes tend to be repelled (or excluded) from the resin, whilst neutral solutes are able to penetrate the resin and are hence retained. In addition to the charge on the solute, several other factors are known to play a part in the retention process; these include the size and especially the hydrophobicity of the solute [2].

The mechanism by which acidic solutes may be separated by ion-exclusion chromatography using a cation-exchange resin has been described previously [3–6]. We now introduce a further parameter which exerts an influence on retention in this form of chromatography, namely the concentration of an inclusion compound in the eluent. β-Cyclodextrin (CD) was selected as a model inclusion compound. The most characteristic property of cyclodextrins is their remarkable ability to form molecular inclusion compounds with some organic and inorganic compounds and also with ions. The stereoselective nature of CD inclusion has been exploited in high-performance liquid chromatography (HPLC) through the use of chemically bonded CD–silica stationary phases and by the application of CD as a mobile phase component. CD was first utilized as a mobile phase modifier by Uekama et al. [7] for ion-exchange chromatography and later applied [8–11] to reversed-phase HPLC. The main purpose of the present paper is to demonstrate that CD may also be utilized as an eluent component in ion-exclusion chromatography. A simple scheme describing the separation process occurring in this system is proposed and equations relating the distribution coefficient of a solute to the concentration of CD are derived. These equations are used to calculate in-

☆ Present address: Institute of Physical Chemistry of the Polish Academy of Sciences, Kasprzaka 44/52, 01-224 Warszaw, Poland.

0021-9673/92/$05.00

clusion constants for some aromatic carboxylic acids.

THEORY

The ion-exclusion system under study consists of an eluent comprising an acid buffer (designated as HB) and CD, used in conjunction with a sulfonated cation-exchange resin. Aromatic carboxylic acids (designated as HR) are used as solutes. This system can be described after making some simplifying assumptions (some of which are similar to those used previously [3–6]: (i) An equilibrated column is used, so that the concentrations of the buffer and CD in the eluent remain constant during the experiment. (ii) The functional (sulphonic acid) groups on the resin are completely dissociated and their concentration is much higher than that of the solute. (iii) Only neutral molecules (that is undissociated solute, HR, and the inclusion complex, CD–HR) exist in the stationary phase. (iv) Both neutral and ionic species exist in the mobile phase. (v) The eluent buffer acid is completely dissociated and its concentration is much higher than that of the solute. (vi) CD exists only in the mobile phase [9,10] and its concentration is much higher than that of the solute. (vii) Eluent components (especially the buffer) do not form inclusion compounds with CD.

From assumption (v) we can write:

$$c_B = [B^-]_m \tag{1}$$

where c_B is the analytical buffer concentration and the subscript m refers to the mobile phase. Since the hydrogen ions originate only from the buffer dissociation, then:

$$c_B = [H^+]_m \tag{2}$$

From assumptions (vi) and (vii) we can write:

$$c_D = [CD]_m \tag{3}$$

where c_D is the analytical concentration of CD and $[CD]_m$ is the concentration of this species in the eluent. The chromatographic system can be described by the set of equilibria illustrated in Fig. 1. These equilibria incorporate the acid dissociation constant of the sample (K_a), the partition coefficients of the solute (K_1) and the inclusion complex (K_2), the formation constants for inclusion complexes of HR and R^- (K_3–K_7), and the acid dissociation constant of the inclusion complex (K_8). Expressions for these equilibrium constants are given below:

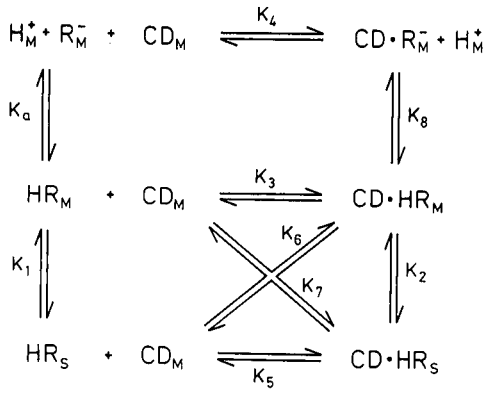

Fig. 1. Schematic representation of the equilibrium reactions existing in the chromatographic system under study.

$$K_a = \frac{[H^+]_m [R^-]_m}{[HR]_m} \tag{4}$$

$$K_1 = \frac{[HR]_s}{[HR]_m} \tag{5}$$

$$K_2 = \frac{[CD\text{–}HR]_s}{[CD\text{–}HR]_m} \tag{6}$$

$$K_3 = \frac{[CD\text{–}HR]_m}{[CD]_m [HR]_m} \tag{7}$$

$$K_4 = \frac{[CD\text{–}R^-]_m}{[CD]_m [R^-]_m} \tag{8}$$

$$K_5 = \frac{[CD\text{–}HR]_s}{[CD]_m [HR]_s} \tag{9}$$

$$K_6 = \frac{[CD\text{–}HR]_m}{[CD]_m [HR]_s} \tag{10}$$

$$K_7 = \frac{[CD\text{–}HR]_s}{[CD]_m [HR]_m} \tag{11}$$

$$K_8 = \frac{[CD\text{–}R^-]_m [H^+]_m}{[CD\text{–}HR]_m} \tag{12}$$

where the subscript s refers to the stationary phase. The overall distribution coefficient for the solute HR in the presence of CD is given by the concentration ratio of all forms of HR in the stationary phase to that in the mobile phase. That is:

$$K_9 = \frac{[HR]_s + [CD\text{–}HR]_s}{[HR]_m + [R^-]_m + [CD\text{–}HR]_m + [CD\text{–}R^-]_m} \quad (13)$$

K_9 can be calculated from the chromatographic retention data, as follows:

$$K_9 = \frac{V_R - V_m}{V_s} \quad (14)$$

where V_R, V_m and V_s are the retention, void and inner volumes, respectively. Under conditions where CD is absent from the mobile phase, the overall distribution coefficient becomes:

$$K_{10} = \frac{[HR]_s}{[HR]_m + [R^-]_m} \quad (15)$$

$$K_1 = \frac{K_{10}(c_B + K_a)}{c_B} \quad (16)$$

and from eqns 7–9, 13 and 16 it is possible to derive

$$K_9 = \frac{K_1 c_B + K_1 K_5 c_D c_B}{c_B + K_a + K_3 c_D c_B + K_4 K_a c_D} \quad (17)$$

Values of K_3, K_4 and K_5 can be estimated from values of K_9 obtained at different values of c_D and c_B. Thus, K_5 can be calculated by using two concentrations of CD, designated by the superscripts (1) and (2), using the equation:

$$K_5 = [K_1 c_B K_9^{(1)} K_9^{(2)} c_D^{(1)} c_D^{(2)} + K_9^{(1)} K_9^{(2)} c_D^{(1)} c_D^{(2)} (K_a + c_B)]/[K_1 c_B c_D^{(1)} c_D^{(2)} (K_9^{(2)} - K_9^{(1)})] \quad (18)$$

Similarly, K_3 and K_4 can be calculated using two concentrations of the eluent buffer [again designated by the superscripts (1) and (2)], using the equations:

$$K_3 = [K_1 K_9^{(1)} K_9^{(2)} c_B^{(1)} c_B^{(2)} (K_5 c_D + 1) + K_9^{(1)} K_9^{(2)} c_B^{(1)} c_B^{(2)}]/K_9^{(1)} K_9^{(2)} c_B^{(1)} c_B^{(2)} c_D \quad (19)$$

and

$$K_4 = (K_1 c_B^{(1)} + K_1 K_5 c_B^{(1)} c_D - K_9^{(1)} c_B^{(1)} - K_9^{(1)} K_a - K_3 K_9^{(1)} c_B^{(1)} c_D)/K_a K_9^{(1)} c_B^{(1)} \quad (20)$$

The remaining constants can then be calculated from the following equations:

$$K_7 = K_1 K_5 \quad (21)$$

$$K_6 = \frac{K_3}{K_1} \quad (22)$$

$$K_2 = \frac{K_7}{K_3} = \frac{K_5}{K_6} \quad (23)$$

$$K_8 = \frac{K_a K_4}{K_3} \quad (24)$$

EXPERIMENTAL

Instrumentation

Chromatographic studies were performed using a Millipore-Waters (Milford, MA, USA) Model 510 HPLC pump, a U6K universal injector and a Model 484 Tunable Absorbance Detector. Chromatograms were recorded using an ABB (Vienna, Austria) SE 120 recorder. The column used was a Bio-Rad (Richmond, CA, USA) Aminex HPX-87H organic acid analysis column (300 × 7.8 mm I.D.). The void and inner volumes of this column were determined by the method described in ref. 3 and were found to be 3.4 ml and 9.2 ml, respectively.

Reagents

CD was obtained from Chinoin (Budapest, Hungary) and (1*R*)-(−)-10-camphorsulphonic acid (98%) from Aldrich (Milwaukee, WI, USA). Other reagents were of analytical-reagent grade and were used without further purification. Water was triply distilled and was passed through a Millipore (Bedford, MA, USA) Milli-Q water purification apparatus. Eluents were filtered through a 0.45-μm membrane filter and were degassed in an ultrasonic bath prior to use.

RESULTS AND DISCUSSION

Chromatograms of solute acids (2-naphthol-6-sulphonic, sulphanilic, barbituric, gallic, *o*-nitrobenzoic, acetylsalicylic, salicylic and *m*-nitrobenzoic) with the mobile phases containing different concentrations of CD and camphorsulphonic acid (used here as a buffer) are presented in Figs. 2 and 3, respectively. The dependence of retention volume of the analysed acids on CD concentration is given in Fig. 4. These figures show that the addition of CD to the mobile phase reduces the retention volume of solutes forming inclusion complexes. The same effect has been observed in reversed-pase HPLC [8,10]. In contrast, an increase in the concen-

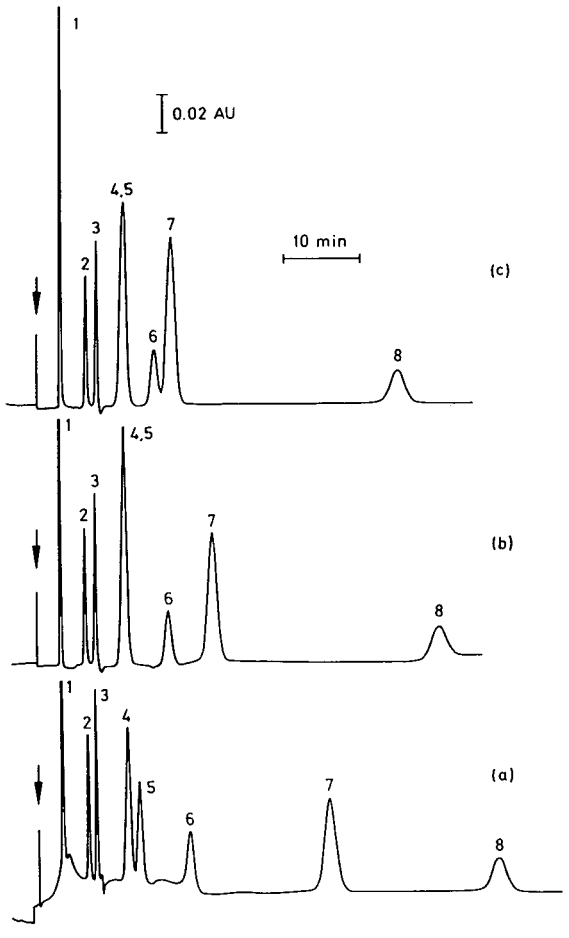

Fig. 2. Chromatograms of 2-naphthol-6-sulphonic (1), sulphanilic (2), barbituric (3), gallic (4), *o*-nitrobenzoic (5), acetylsalicylic (6), salicylic (7) and *m*-nitrobenzoic (8) acids at different CD concentrations in the mobile phase: (a) 0; (b) $5 \cdot 10^{-3}$ and (c) $1 \cdot 10^{-2}$ *M*. Conditions: Aminex HPX-87H organic acids column. Mobile phase: ethanol–water (20:80, v/v) containing 10^{-3} *M* camphorsulphonic acid and the indicated concentrations of CD, operated at a flow-rate of 0.5 ml/min.

tration of camphorsulphonic acid causes an increase in the retention volume. This results from the decreased dissociation of the solute acids and is in accordance with previous observations on retention in ion-exclusion chromatography [3,4]. Calculated values (from eqns. 16–24) of the thermodynamic constants are presented in Table I, with the exception of those for 2-naphthol-6-sulphonic acid, sulphanilic acid and barbituric acid since addition of CD to the mobile phase produced virtually no changes in retention for these species.

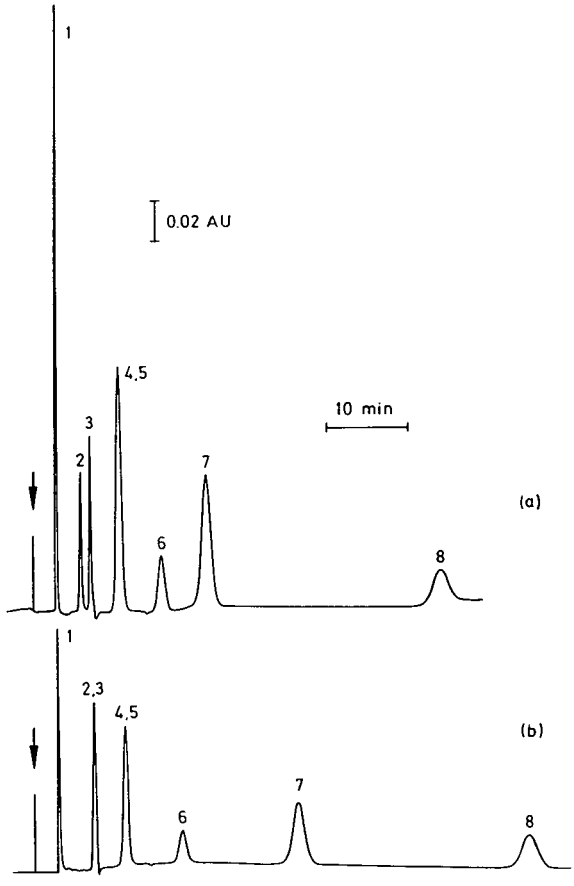

Fig. 3. Chromatograms of aromatic acids at different camphorsulphonic acid concentrations: (a) 10^{-3} *M*, (b) 10^{-2} *M*. Other conditions as for Fig. 2.

When a purely ion-exclusion mechanism operates, a dependence between the retention volume of a solute and its acid dissociation constant is observed. Retention volumes fall in the range between the column void volume and the sum of column void and inner volumes. The distribution coefficient falls in the range between zero (for strong acids, which are anionic and therefore are completely excluded) and one (for neutral solutes, which have unrestricted access to the occluded liquid in the stationary phase). In our experiments the mechanism for solute retention is rather more complex, as evidenced by the fact that the distribution coefficients (K_{10}) of aromatic carboxylic acids in the absence of CD are greater than 1. This is caused by hydrophobic interactions (K_1) between the solute and the resin and this effect is especially high on the polystyrene–divi-

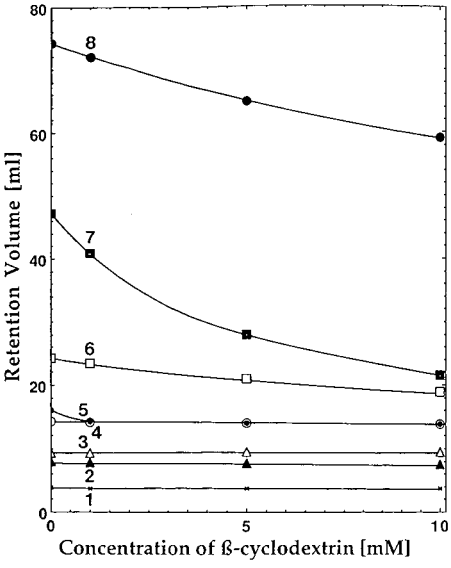

Fig. 4. Dependence of the retention volume of aromatic acid solutes on the concentration of CD in the mobile phase. Chromatographic conditions as for Fig. 2.

nylbenzene resin used as a result of π–π interactions. Of course, the distribution coefficient K_{10} is controlled not only by K_1 but also by the solute dissociation constant K_a.

The situation becomes even more complicated after the addition of CD to the mobile phase. For example the adsorption of the inclusion complex CD–HR (described by the constant K_2) is influenced by two dissociation constants (K_a and K_8). From a mathematical standpoint all unknowns can be obtained by solving eqns. 1–8, 13 and 15. Only the constants K_1–K_4 are necessary to describe the system, with the remaining constants being dependent. The constants K_3–K_7 each describe different mechanisms which might contribute to the retention of the solute. The values shown in Table I suggest that no single mechanism is predominant. However, some general trends may be elucidated.

It is known [8,9] that CD shows greatest interactions with aromatic compounds of the type investigated in this study. Some structural effect can also be observed by comparing the thermodynamic constants describing the formation of inclusion complexes (K_3–K_7 in Table I) for *o*- and *m*-nitrobenzoic acids. For each constant, the value obtained for *o*-nitrobenzoic acid is the higher, showing that the *ortho* isomer forms the stronger inclusion complexes. This behaviour probably results from steric effects and from the fact bonding with CD is more prevalent for the *ortho* isomer.

As can be seen from Fig. 1, solute complexation resulting in the formation of inclusion complexes existing in the mobile phase (K_3, K_4 and K_6) will result in decreased solute retention. Additionally, the inclusion complexes of the acids studied are characterised by smaller hydrophobic adsorption on the stationary phase, as evidenced by the relative magnitudes of K_1 and K_2 in Table I. These factors combine to suggest that decreased solute retention should be expected when inclusion complexes are formed, especially when the retention of the solute is high in the absence of CD. This behaviour is evident in Fig. 4. Comparison of K_3 and K_6 in Table I also suggests that the complexation of the adsorbed solute by CD is smaller than that for the solute in the mobile phase.

In conclusion we can state that it is possible to apply CD as a mobile phase modifier in ion-exclusion chromatography and that this modifier permits the attainment of selectivity effects which differ from those achieved by the conventional method of varying the pH of the mobile phase. Moreover, it is

TABLE I

VALUES OF THE THERMODYNAMIC CONSTANTS DEFINED BY EQNS. 5–15

Solute acid	K_a	K_1	K_2	K_3	K_4	K_5	K_6	K_7	K_8	K_{10}
Sulphanilic	$4.68 \cdot 10^{-4}$	0.73	3.0	177	250	200	241	730	$6.6 \cdot 10^{-4}$	0.5
Barbituric	$9.23 \cdot 10^{-5}$	0.7	0.8	159	54	159	229	187	$3.1 \cdot 10^{-5}$	0.6
Gallic	$3.89 \cdot 10^{-5}$	1.23	0.8	470	860	481	384	375	$1.1 \cdot 10^{-4}$	1.2
o-Nitrobenzoic	$6.76 \cdot 10^{-3}$	10.6	1.3	298	178	332	281	378	$4.0 \cdot 10^{-5}$	1.4
Acetylsalicylic	$2.69 \cdot 10^{-5}$	2.33	2.4	16	138	13	7.0	38	$2.3 \cdot 10^{-3}$	2.3
Salicylic	$1.00 \cdot 10^{-3}$	9.52	0.8	265	126	22	28	210	$4.8 \cdot 10^{-4}$	4.8
m-Nitrobenzoic	$3.2 \cdot 10^{-4}$	10.2	3.3	69	8.7	21	6.8	227	$4.1 \cdot 10^{-5}$	7.7

interesting to note that a few simple experiments enable us to calculate many thermodynamic constants. These constants are of fundamental importance in other chromatographic and electrochemical techniques which use CD. Whilst the precision of chromatographic methods for the calculation of such constants is not high, these methods are very rapid.

ACKNOWLEDGEMENTS

We thank Professor Danuta Sybilska from the Institute of Physical Chemistry of the Polish Academy of Sciences for kindly providing β-cyclodextrin.

REFERENCES

1 R. M. Wheaton and W. C. Bauman, *Ind. Eng. Chem.*, 45 (1953) 228.
2 P. R. Haddad and P. E. Jackson, *Ion Chromatography: Principles and Applications* (*Journal of Chromatography Library*, Vol. 46), Elsevier, Amsterdam 1990, pp. 202–212.
3 B. K. Głod and W. Kemula, *J. Chromatogr.*, 366 (1986) 39.
4 B. K. Głod, A. K. Piasecki and J. Stafiej, *J. Chromatogr.*, 457 (1988) 43.
5 B. K. Głod and R. Nowakowski, in preparation.
6 B. K. Głod, P. W. Alexander and P. R. Haddad, in preparation.
7 K. Uekama, F. Hirayama, S. Nasu, N. Matuso and T. Irie, *Chem. Pharm. Bull.*, 261 (1978) 3477.
8 D. Sybilska, J. Lipkowski and J. Wojcikowski, *J. Chromatogr.*, 253 (1988) 95.
9 D. Sybilska in W. L. Hinze and D. W. Armstrong (Editors), *Ordered Media in Chemical Separations* (*A.C.S. Symposium Series*, No. 342), American Chemical Society, Washington, DC, 1987, p. 218.
10 D. Sybilska and J. Zukowski, in A. M. Krstulovic (Editor), *Chiral Separations by HPLC —Application to Pharmaceutical Compounds*, Ellis Horwood, Chichester, 1988.
11 K. Shimada, T. Oe, Y. Hirose and Y. Komine, *J. Chromatogr.*, 478 (1989) 339.

Journal of Chromatography, 595 (1992) 155–162
Elsevier Science Publishers B.V., Amsterdam

CHROM. 23 958

Quantitative analysis of total resin acids by high-performance liquid chromatography of their coumarin ester derivatives

Desmond E. Richardson*

Research Laboratory, Australian Newsprint Mills Ltd., Boyer, Tasmania 7140 (Australia)

John B. Bremner and Barry V. O'Grady

Chemistry Department, University of Tasmania, G.P.O. Box 252C, Hobart, Tasmania 7001 (Australia)

(First received August 19th, 1991; revised manuscript received December 3rd, 1991)

ABSTRACT

A method for the quantitative analysis of resin acids in effluent and water samples using high-performance liquid chromatography is described. Resin acids in aqueous samples are extracted by passage through C_{18} solid-phase cartridges at pH 9. The (7-methoxycoumarin-4-yl) methyl (MMC) and (7-acetoxycoumarin-4-yl) methyl (MAC) esters are quantitatively formed at room temperature by the reaction of resin acids with 4-bromomethyl-7-methoxycoumarin and 4-bromomethyl-7-acetoxycoumarin respectively, in the presence of potassium carbonate. The effect of potassium carbonate particle size, exposure to light, presence of residual water, and derivatisation reagent: resin acid ratio on their formation are described. The MMC esters of resin acids may be detected by UV absorption at 318 nm at concentrations >20 $\mu g\ l^{-1}$, while the (7-hydroxycoumarin-4-yl) methyl esters, obtained by post-column alkaline hydrolysis of the resin acid MAC (RAMAC) esters, enable the detection of resin acids by fluorescence spectrophotometry to levels below 1 $\mu g\ l^{-1}$. The method has been compared to gas chromatographic analysis of the carboxylic acid methyl esters and shows no evidence of any interferences by other carboxylic acids. The method is routinely used by two newsprint mills for environmental monitoring of resin acids in effluent.

INTRODUCTION

Resin acids are released from softwoods in both mechanical and chemical pulping processes [1]. They are toxic to marine life at low concentrations, having 96-h LC_{50} values ranging from 0.5 to 1.1 mg l^{-1} [2–4], and also accumulate in fish tissue [5,6]. Attempts have been made to estimate effluent toxicity on the basis of chemical composition and LC_{50} values for pure components [2,7–8]. Resin and fatty acids have also been implicated with occurrences of pitch deposits on paper machines and in pulping equipment [9].

The routine monitoring of resin acids in a variety of matrices is therefore necessary and has required the development of analytical techniques for their extraction and analysis. Extraction techniques have been predominantly based on solvent extraction using diethyl ether [10,11], dichloromethane [10,12–13], light petroleum–acetone–methanol [11], and methyl *tert.*-butyl ether [14]. Solid-phase extraction techniques have also been used to isolate resin acids from rosin, paper mill deposits, and process streams [15,16]. The most common instrumental technique used in recent years is that of capillary gas chromatography (GC) of the methyl esters of resin acids [17–19]. More recently, the inherent sensitivity of the electron capture detector has been utilised to measure pentafluorobenzyl esters of resin acids [20].

While high-performance liquid chromatography (HPLC) has been used for qualitative analysis of mixtures containing resin acids [21–26], and for

0021-9673/92/$05.00

quantitative measurement of one resin acid (dehydroabietic acid) [22,27], it has not been used for quantitative analysis of total resin acids in a mixture. The two major barriers to their quantitation by HPLC are the difficulty in separating the various resin acid isomers, and the lack of a suitable chromophore for their detection, particularly for the non-conjugated resin acids [1].

Bromomethyl coumarin compounds containing substituents on the aromatic ring and other bromoalkyl-aromatic compounds have been used to form esters with carboxylic acids [28–35]. The derivatisation procedures have used 4-bromomethyl-7-methoxycoumarin (4BrMMC) [28–31], 4-bromomethyl-6,7-dimethoxycoumarin [32], 3-bromomethyl-6,7-dimethoxy-1-methyl-2(1H)-quinoxalinone [33], and 4-bromomethyl-7-acetoxycoumarin (4BrMAC) [34,35] to form fluorescent derivatives of carboxylic acids from a variety of matrices. More recently micellar phase transfer catalysis procedures have been developed around 4BrMMC [36] and 9-bromomethylacridine [37] and applied to the analysis of fatty acids in plasma.

This paper describes the application of these derivatisation techniques to the analysis of resin acids in effluents as an alternative to existing methods of analysis with a view to developing a simple method with low detection limits and using small sample volumes. Both UV and fluorescence properties of the coumarin-4-yl methyl esters of resin acids were investigated based on the reactions shown in Fig. 1. A procedure based on the formation of coumarin-4-yl methyl esters of resin acids from 4BrMMC and 4BrMAC has been developed and used successfully for environmental monitoring of two newsprint mills' effluent for over two years. Factors affecting the quantitative formation, spectrophotometric properties, and HPLC separation of coumarin-4-yl methyl esters of resin acids from 4BrMMC and 4BrMAC are discussed in this paper.

EXPERIMENTAL

Materials and reagents

The resin acids (dehydroabietic, isopimaric, neoabietic, palustric, abietic, levopimaric and sandaracopimaric) were obtained from Helix Biotech (Vancouver, Canada) and used without further pu-

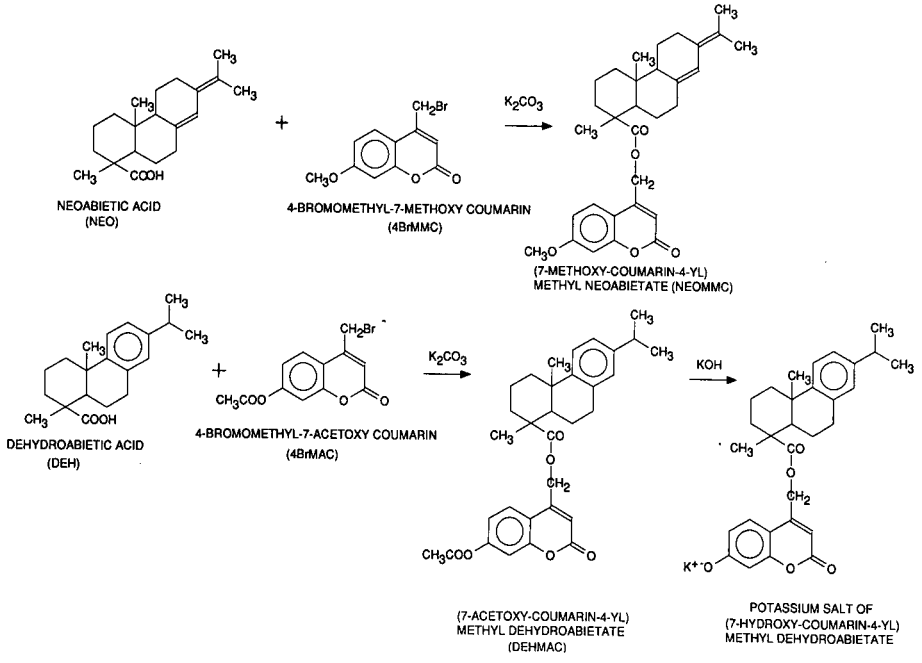

Fig. 1. Reaction schemes for formation of (7-methoxycoumarin-4-yl) methyl neoabietate and (7-hydroxycoumarin-4-yl) methyl dehydroabietate.

rification. Dehydroabietic (DEH), isopimaric (ISO), and neoabietic (NEO) acid were found by GC assay to be >98% pure, while the remainder contained 5%–15% of other resin acids. 4BrMMC was obtained from Sigma (St. Louis, MO, USA), while 4BrMAC was synthesised from 4-methylumbelliferone according to the method of Tsuchiya *et al.* [34]. HPLC-grade acetonitrile, dichloromethane and methanol, and spectroscopic grade acetone were used throughout. Water was obtained from a Millipore Milli-Q water purification system. All other reagents were analytical-reagent grade. Analytichem C_{18} 3-ml Bond Elut solid-phase extraction columns (part. No. 607303) were used to extract effluent samples. Samples were placed in a Branson B-220 ultrasonic bath for the derivatisation process.

Spectrophotometric analyses

Quantum yields of the resin acid derivatives of 4BrMMC and 4BrMAC were measured according to an established method [38] using a Perkin-Elmer LS-5 fluorescence spectrophotometer connected to a Perkin-Elmer 3600 data station with quinine sulfate (Sigma) and 9,10-diphenylanthracene (Aldrich) as reference standards. A Varian DMS 90 UV–VIS spectrophotometer was used to record UV spectra.

Extraction and derivatisation

The volume of sample to be extracted, normally within the range of 2–100 ml, was chosen so that it contained no more than 50 μg of resin acids. This was to ensure that the ratio of derivatisation reagent to resin acid was sufficient to obtain quantitative conversion to the RAMMC or RAMAC ester. The pH of samples containing more than 10 mg l^{-1} of suspended solids was adjusted to 11 with solid potassium hydroxide. The samples were then filtered through Whatman No. 4 filter paper. The pH was then reduced to 9 with dilute H_2SO_4 and the conductivity increased to >2 mS cm^{-1} with solid NaCl. The Bond Elut cartridges were conditioned by rinsing successively with 2 ml acetone, 3 ml methanol and 3 ml water. The effluent sample was then passed through the solid phase extraction cartridge at 20 cmHg vacuum. Excess water was removed from the extraction cartridge by applying vacuum for at least 15 min after all sample had passed through. The adsorbed resin acids and other organic material were eluted into a light-protected 2-ml vial by adding sequentially 0.5 ml acetone, 2 × 0.5 ml dichloromethane and 0.5 ml methanol. The solvent was then removed under a gentle stream of nitrogen. The derivatisation was performed *in situ* in the vial in the presence of 4–5 mg of finely ground potassium carbonate (>100 μm) by adding 0.50 ml of 0.0074 *M* 4BrMMC or 0.01 *M* 4BrMAC (in acetone), and 1.00 ml of acetone, and placing it in an ultrasonic bath for 10 min at 25°C. The potassium carbonate was prepared by grinding with a mortar and pestle for 10 min and measuring the particle size by optical microscopy. The vial was kept tightly sealed with a PTFE-lined septum to ensure no loss of solvent between derivatisation and analysis. The potassium carbonate was allowed to settle before presenting the sample for HPLC analysis.

Standards were prepared by placing a known quantity of dehydroabietic acid and isopimaric acid in a vial before addition of the derivatising reagent. The method of external standards was used for calibration.

HPLC analysis

Both the (methoxycoumarin-4-yl) methyl (MMC) esters and the (acetoxycoumarin-4-yl) methyl (MAC) esters were separated using a Rainin Dynamax C_8 5-μm 25 cm × 4 mm reversed-phase column (80-325-C5) fitted with a Rainin Dynamax guard column (80-300-G5) and a 2-μm in-line filter to remove any traces of particulate potassium carbonate. A Varian 5060 ternary gradient HPLC system (fitted with a Rheodyne 7126 injection valve (20-μl loop) and a Varian Model 9090 autosampler) was used to deliver an acetonitrile–water (70:30, v/v), solvent mix at 1.5 ml min^{-1}. A linear gradient to acetonitrile–water (90:10, v/v) was generated at 2.5% min^{-1} where it was held for 5 min before returning to the initial solvent conditions.

The MMC esters were detected using a Varian UV100 variable-wavelength detector set at 318 nm. The MAC esters did not fluoresce but were hydrolysed post-column to the fluorescent (7-hydroxymethylcoumarin-4-yl) methyl ester of the resin acid by the addition of 0.2 *M* potassium hydroxide in methanol–water (80:20, v/v) at a flow-rate of 0.5 ml min^{-1}. The fluorescence signal was measured with a Perkin-Elmer Model LS4 fluorescence spectrophotometer with the excitation monochromator set

at 375 nm (slit width 15 nm), and the emission monochromator set at 475 nm (slit width 20 nm). The detector signal was processed by a Varian DS654 data system.

The composition of hydrolysis products from the addition of alkali to resin acid MAC (RAMAC) esters was determined using a Varian 9060 Polychrom photodiode array detector.

Gas chromatography analysis

The evaporated extracts from the Bond Elut cartridges were made to react with diazomethane (in diethyl ether) to form resin acid methyl esters. Heptadecanoic acid was added to the sample, prior to methylation, as an internal standard. The methylated extracts were reconstituted in acetone for injection onto a Varian 3600 gas chromatograph fitted with a 30 m × 0.32 mm HP-1 column (Hewlett-Packard) film thickness 1.05 μm and a Varian 1075 split/splitless injector (used in the splitless mode). Data were processed on a Varian Vista 402 data system.

RESULTS AND DISCUSSION

Spectophotometric properties

Resin acid MMC (RAMMC) esters were prepared and isolated as pure compounds [1] so that their spectral properties could be examined. While they were all found to have a molar absorptivity of 13600 ± 260 l mol^{-1} cm^{-1} at 318 nm, their fluorescence quantum yield was found to be dependent on resin acid structure, with the RAMMC esters of conjugated diene acids (abietic, neoabietic, palustric, and levopimaric) having a quantum yield about half that of the RAMMC esters of non-conjugated resin acids (dehydroabietic, isopimaric, and sandaracopimaric). Furthermore the quantum yield was affected by the water content of the HPLC solvent mixtures, in a similar fashion to that reported for fatty acid MMC esters [31]. It was concluded therefore that RAMMC esters could only be measured by UV detection.

RAMAC esters had a molar absorptivity of 8200 ± 150 l mol^{-1} cm^{-1}at 310 nm, and therefore could also be detected quantitatively by UV detection. However, because the molar absorptivity was lower than that for the RAMMC esters, UV detection was not used for RAMAC derivatives. RAMAC esters did not fluoresce until they were hydrolysed to the (7-hydroxycoumarin-4-yl) methyl esters. The fluorescence quantum yields of hydrolysed DEHMAC, ISOMAC, and NEOMAC (representing aromatic, non-conjugated diene, and conjugated diene resin acid structures, respectively) were 0.28 ± 0.01, 0.30 ± 0.02, and 0.26 ± 0.02 respectively. In contrast to the RAMMC esters, their quantum yields were the same regardless of resin acid structure, and did not vary significantly over the range of water–solvent proportions encountered in their HPLC separation. The fact that the fluorescence response was independent of resin acid structure enabled the use of a single resin acid to represent the response of all resin acids, and therefore measure quantitatively the total resin acid concentration, even though they co-eluted when analysed by HPLC. Investigation of the products of hydrolysis using a photodiode array detector revealed that at room temperature the predominant hydrolysis product was the (7-hydroxycoumarin-4-yl) methyl ester. Comparison of sample spectra with authentic compounds revealed that no significant free resin acid was formed. This finding is in contrast to the alkaline hydrolysis of fatty acid MAC esters in which it has been claimed that both the acetoxy and carboxylate ester linkages are hydrolysed [34].

HPLC separation

Measurements of the capacity factors (k') of both the MMC and MAC esters on C_{18} and C_8 columns showed that, while DEHMMC (and DEHMAC) eluted with a lower k' than the non-aromatic RAMMC (and RAMAC) esters, the latter had almost identical k' regardless of resin acid structure, and eluted with a narrower distribution of k' on a C_8 column than on a C_{18} column. The resin acid, pimaric acid, was not available as a pure standard, and hence the k' of its MMC and MAC esters could not be measured. However, GC analysis of effluent from a mechanical pulping process containing pimaric acid (10–15% of total resin acid content) showed good agreement between results for the two types of measurement. The k' values of chlorinated resin acids were not measured as only effluent from mechanical pulp mills was evaluated by this technique.

Fig. 2 is a chromatogram of the MMC esters of several fatty acids ($C_{16:0}$, $C_{16:1}$, $C_{18:0}$, $C_{18:1}$, and

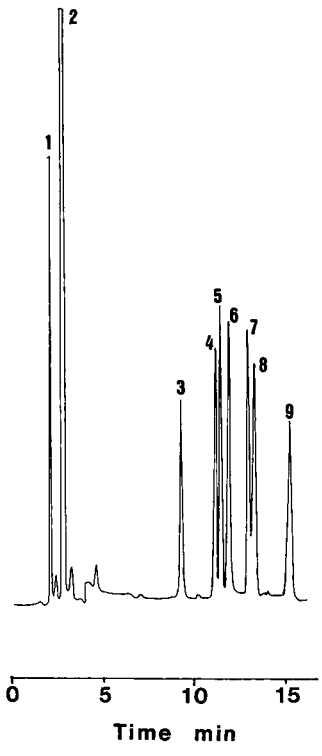

Fig. 2. Chromatogram showing response of 200 ng (each) of MMC esters of resin and fatty acids. HPLC conditions: Column, Rainin Dynamax C_8 5-μm 25 cm × 4 mm (80-325-C5) + Rainin Dynamax guard column (80-300-G5); initial solvent acetonitrile–water (70:30, v/v), to acetonitrile–water (90:10, v/v) at 2.5% min^{-1}, UV detection at 318 nm. Peaks: 1 = acetone; 2 = 4BrMMC; 3 = DEHMMC; 4 = non-aromatic resin acid MMC esters; 5 = $C_{16:1}$ MMC; 6 = $C_{18:2}$ MMC; 7 = $C_{16:0}$ MMC; 8 = $C_{18:1}$ MMC; 9 = $C_{18:0}$ MMC.

$C_{18:2}$), dehydroabietic acid and isopimaric acid. Resolution of these components in particular is important as this range of fatty acids is commonly found in extracts and pulping effluents from softwoods such as *Pinus radiata*. Baseline resolution of $C_{16:1}$ MMC from ISOMMC was almost achieved with the solvent program and column shown. A similar separation was achieved for RAMAC esters.

Reaction conditions

The main purpose of this technique was to develop a method that was robust enough to be used in a paper mill by technical staff for routine environmental monitoring. It was also for this reason that the procedure had to be as simple as possible and not involve exposure to hazardous chemicals. Several published methods for formation of fatty acid MMC and MAC esters require the use of the highly toxic crown ether 18-crown-6 [29,34,35]. A key factor in eliminating the crown ether catalyst was to reduce the particle size of the potassium carbonate used to form the resin acid salt which reacted with the bromomethyl coumarin. The effect of reducing the potassium carbonate to a small particle size (< 100 μm) was to bring about quantitative formation of the RAMMC ester in less than 10 min compared to > 1 h for potassium carbonate used directly as received.

Some procedures highlight the need to protect the reaction mixture from visible light due to the photodecomposition of both 4BrMMC and 4BrMAC [29,35]. Exposure of either of these reagents to light causes rapid decomposition to products that either cannot form derivatives with carboxylic acids, or form adducts that interfere in the analysis of the target compounds [1]. The effect of exposing resin acids to light whilst performing the derivatisation was quite dramatic for the conjugated diene resin acids (neoabietic, abietic, levopimaric and palustric), and was manifested by degradation of the resin acid coumarin ester after about 20 min exposure time. This phenomenon was not observed for the non-conjugated diene resin acids such as isopimaric acid, nor for dehydroabietic acid.

The extraction of aqueous samples using solid-phase extraction cartridges can result in traces of water being eluted along with the resin acids unless great care is taken to dry the cartridges by drawing air through them for some time after all sample has been adsorbed. The tolerance of the procedure to the presence of traces of water was determined by addition of known amounts of water to the reaction mixture. The maximum amount of water that could be tolerated in the reaction was 4% (v/v) or 60 μl in a total of 1.50 ml. An amount of water greater than 4% resulted in a significant decrease in yield, approaching 0 at 20% water.

An important consideration in a derivatisation reaction is to have a sufficient excess of reagents to ensure that quantitative conversion to the desired product occurs at all sample concentrations. The excess required to achieve this for both 4BrMMC and 4BrMAC was investigated by allowing isopi-

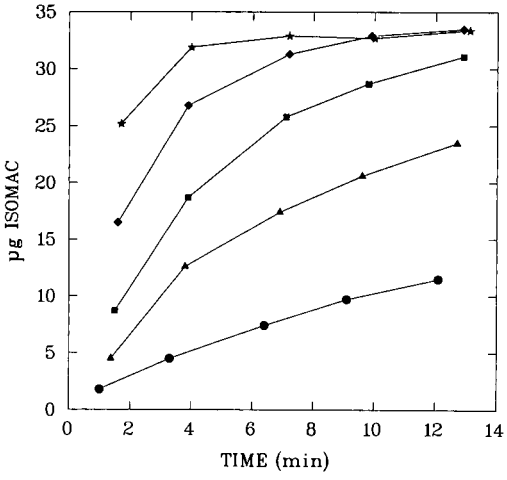

Fig. 3. Effect of BrMAC:ISO molar ratio on yield of ISOMAC. BrMAC:ISO ratio: ● = 1:1; ▲ = 2.5:1; ■ = 5:1; ◆ = 10:1; ★ = 20:1. Theoretical yield, 34.4 μg.

maric acid to react with 4BrMAC and 4BrMMC over a range of molar excesses of bromomethylcoumarin to isopimaric acid. Fig. 3 shows that a 10-fold excess was sufficient to ensure that quantitative conversion occurred after 10 min.

Acetonitrile was investigated as an alternative solvent to acetone in which to perform the derivatisation but it was found to be inferior due to the faster reaction in acetone compared to acetonitrile. The enhanced rate in acetone has been ascribed to the greater dispersion of charge in the transition state complex in a solvent with medium dielectric constant (such as acetone, ε (25°C) = 20.7) than in a solvent with a larger dielectric constant, (acetonitrile ε (25°C) = 36.2) [39].

Application to effluent and water samples

Some important factors in developing a reliable extraction and chromatographic technique for routine trace organic analysis are quantitative recovery of spiked samples, freedom from interference, reproducible chromatographic separation over the range of sample conditions likely to be encountered, correlation with other established methods, and ease of use. Recoveries of DEH and non-aromatic resin acids (added to effluent samples at the 1 mg l^{-1} level) using the solid-phase adsorption method and analysis of their MMC esters, averaged 95±8%, and 91±11%, respectively, over a six-month period. It was found that a slightly alkaline extraction (pH 9) was necessary to obtain good recoveries, due to adsorption of resin acids on glassware and plasticware when these are used to manipulate samples at pH < 7.

Use of the solid phase extraction technique for resin acid extraction has several advantages over solvent extraction methods, including elimination of emulsions, lower solvent consumption, and the ability to handle large sample volumes. The loss of analyte by breakthrough, or preferential adsorption of other extractives, are two potential disadvantages of the procedure. Elimination of interfering compounds in solid-phase extraction of pulp and paper effluents has been achieved by the addition of 15% (v/v) methanol to the sample [16]. Presumably competition for adsorption sites between resin acids and other components was reduced by minimising the adsorption of lignin material [16]. The high recoveries of resin acids from effluent containing very little lignin was achieved in this work without methanol addition.

GC mass spectrometric analysis of samples of effluent containing extractives from both *Pinus radiata* and various *Eucalyptus* species showed that the only carboxylic acids present which were likely to interfere with either RAMMC or RAMAC esters were fatty acids of chain length 16 carbons or greater. The HPLC conditions chosen were able to resolve satisfactorily both the RAMMC and RAMAC esters from the nearest fatty acid ($C_{16:1}$) MMC or MAC ester. The amount of $C_{16:1}$ fatty acid to resin acid can, in effluent, vary significantly depending upon whether the effluent has been biologically treated. Excellent separation of the resin acid (RAMMC or RAMAC) from the $C_{16:1}$ fatty acid ester can be obtained over a wide range of resin acid: $C_{16:1}$ fatty acid ratios. Fig. 4 shows the separation obtained in the case of an untreated effluent when the ratio is high, whereas Fig. 5 shows the separation when the amounts of resin and fatty acids are approximately equal.

The choice of which derivatisation reagent to use is dependent on the concentration of resin acid present in the sample and the type of detector available to the analyst. Formation of RAMMC esters combined with UV detection enabled a concentration of resin acid >20 μg l^{-1} to be measured using effluent volumes of 50 ml. RAMAC esters, however, could

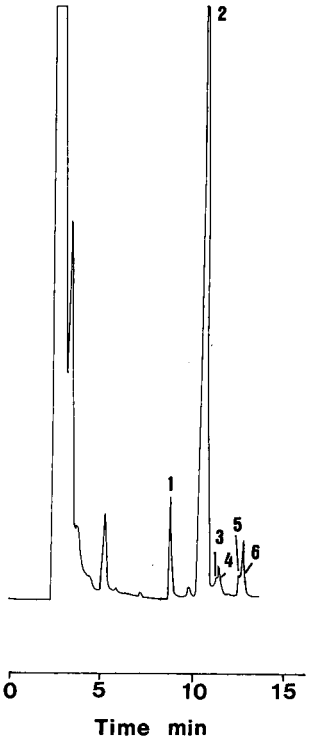

Fig. 4. Chromatogram of total resin acids in softwood pulping effluent, containing 3 mg l^{-1} of resin acids. Peaks: 1 = DEHMMC; 2 = non-aromatic resin acid MMC esters; 3 = $C_{16:1}$ MMC; 4 = $C_{18:2}$ MMC; 5 = $C_{16:0}$ MMC; 6 = $C_{18:1}$ MMC. HPLC conditions as in Fig. 2.

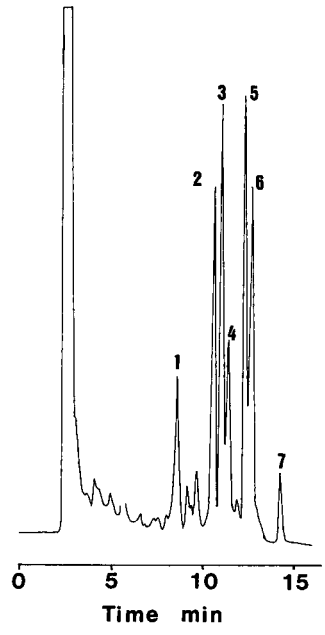

Fig. 5. Chromatogram of total resin and fatty acids in biologically treated effluent containing 20 μg l^{-1} resin acids. Peaks: 1 = DEHMAC; 2 = non-aromatic resin acid MAC Esters; 3 = $C_{16:1}$ MAC; 4 = $C_{18:2}$ MAC; 5 = $C_{16:0}$ MAC; 6 = $C_{18:1}$ MAC; 7 = $C_{18:0}$ MAC. HPLC conditions as in Fig. 2, except that fluorescence detection at excitation wavelength 375 nm and emission wavelength 475 nm was used instead of UV detection.

be formed and their hydroxycoumarin esters detected by fluorescence detection where resin acid concentrations down to 1 μg l^{-1} were to be measured.

Correlation of the total resin acid results obtained by HPLC with those obtained by analysis of the methyl esters by capillary GC was undertaken to ensure that good agreement was obtained. The correlation coefficients, slopes and intercepts obtained by linear least-squares analysis of the data (Table I) showed that, within experimental error,

TABLE I

CORRELATION COEFFICIENTS FOR TOTAL RESIN ACID MEASUREMENTS BY HPLC *vs.* GC

HPLC values determined using resin acid esters, GC values determined using resin acid methyl esters (RAME).

HPLC assay (x-axis), using	GC assay (y-axis), using	R^2	Slope	95% C.L.[c]	Intercept	95% C.L.
RAMMC	RAME	0.9936	0.9518	0.054	0.0220	0.0478
RAMAC[a]	RAME	0.9890	1.011	0.075	0.0438	0.0641
RAMAC[b]	RAME	0.8110	0.9855	0.287	0.0068	0.0089

[a] High concentration samples (0.20–1.60 mg l^{-1})
[b] Low concentration samples (0.005–0.080 mg l^{-1})
[c] C.L. = Confidence level.

the correlation between the HPLC method (using both derivatives) and the GC method, was excellent.

CONCLUSIONS

Resin acids reacted readily with both 4BrMMC and 4BrMAC at 25°C, without the need for a crown ether catalyst, to form RAMMC and RAMAC derivatives, respectively. They were separated from the esters of other carboxylic acids such as fatty acids present in pulp and paper effluents (derived from mechanical pulping processes), by reversed-phase HPLC using a C_8 stationary phase and an acetonitrile–water gradient. The high quantum yield of the (7-hydroxycoumarin-4-yl) methyl esters (obtained by post-column alkaline hydrolysis) enabled total resin acids to be measured at levels down to 1 $\mu g\ l^{-1}$ in water using solid-phase extraction at a slightly alkaline pH.

ACKNOWLEDGEMENTS

The assistance of Australian Newsprint Mills in financing this work is gratefully acknowledged. We also thank Dr. G. Ettershank for access to fluorescence spectrophotometry equipment at Monash University. The assistance of Ian Jewell, Pat Deprez and Tony Parsons in developing the solid-phase extraction method is acknowledged.

REFERENCES

1 D. E. Richardson, *Ph. D. Thesis*, University of Tasmania, Hobart, 1987.
2 J. M. Leach and L. T. K. Chung, *US EPA Report EPA-600/2-80-206*, US Department of Commerce, National Technical Information Service, December 1980.
3 J. M. Leach and A. N. Thakore, *J. Fish Res. Board Can.*, 32 (1975) 1249.
4 J. M. Leach and A. N. Thakore, *Tappi*, 59 (2) (1976) 129.
5 A. Oikari, B. Holmbom, E. Anas and H. Bister, *Pap. Puu*, 64 (1982) 251.
6 A. Oikari, B.-E. Lonn, M. Castren, T. Nakari, B. Snickars-Nikinmaa, H. Bister and E. Virtanen, *Water Res.*, 17 (1983) 81.
7 L. T. K. Chung, H. P. Meier and J. M. Leach, *Tappi*, 62 (12) (1979) 71.
8 B. Holmbom and K.-J. Lehtinen, *Pap. Puu*, 62 (1980) 673.
9 L. H. Allen, *Pulp Pap. Can.*, 76 (5) (1975) T139.
10 D. E. Richardson and H. Bloom, *Appita*, 35 (1982) 477.
11 D. H. McMahon, *Tappi*, 63 (9) (1980) 101.
12 V. E. Turoski, M. E. Kuehnl and B. F. Vincent, *Tappi*, 64 (1981) 117.
13 S. A. Turner and B. K. Wallin, *Tappi*, 68 (8) (1985) 108.
14 R. H. Voss and A. Rapsomatiotis, *J. Chromatogr.*, 346 (1985) 205.
15 K. M. Sweeney, *Tappi*, 71 (1988) 137.
16 S. Backa, A. Brolin and N. O. Nilvebrant, *Tappi*, 72 (8) (1989) 139.
17 D. F. Zinkel and C. C. Engler, *J. Chromatogr.*, 136 (1977) 245.
18 B. Holmbom, *J. Amer. Oil Chem. Soc.*, 54 (1977) 289.
19 D. O. Foster and D. F. Zinkel, *J. Chromatogr.*, 248 (1982) 89.
20 H. B. Lee, T. E. Peart and J. M. Carron, *J. Chromatogr.*, 498 (1990) 367.
21 W. Kamutzki and Th. Krause, *Das Papier (Darmstadt)*, 34, nr. 10A (1980) 29.
22 R. K. Symons, *J. Liq. Chromatogr.*, 4 (1981) 1807.
23 R. C. Cambie, B. A. Grigor and T. Mee-Ing, *Aust. J. Chem.*, 34 (1981) 1073.
24 J. P. Kutney, M. Singh, G. Hewitt, P. J. Salisbury, B. R. Worth, J. A. Servizi, D. W. Martens and R. W. Gordon, *Can. J. Chem.*, 59 (1981) 2334.
25 J. P. Kutney, M. Singh, E. Dimitriadis, G. M. Hewitt, P. J. Salisbury, B. R. Worth, J. A. Servizi, D. W. Martens and R. W. Gordon, *Can. J. Chem.*, 59 (1981) 3350.
26 J. P. Kutney, E. Dimitriadis, G. M. Hewitt, M. Singh and B. R. Worth, *Helv. Chim. Acta*, 65 (1982) 661.
27 D. E. Richardson, B. V. O'Grady and J. B. Bremner, *J. Chromatogr.*, 268 (1983) 341.
28 W. Dunges, *Anal. Chem.*, 49 (1977) 442.
29 S. Lam and E. Grushka, *J. Chromatogr.*, 158 (1978) 207.
30 W. Dunges and N. Seiler, *J. Chromatogr.*, 145 (1978) 483.
31 J. B. F. Lloyd, *J. Chromatogr.*, 178 (1979) 249.
32 R. Farinotti, Ph. Siard, J. Bourson, S. Kirkiacharian, B. Valeur and G. Mahuzier, *J. Chromatogr.*, 269 (1983) 81.
33 M. Yamaguchi, S. Hara, R. Matsunaga, M. Nakamura and Y. Ohkura, *J. Chromatogr.*, 346 (1985) 227.
34 H. Tsuchiya, T. Hayashi, H. Naruse and N. Takagi, *J. Chromatogr.*, 234 (1982) 121.
35 H. Tsuchiya, T. Hayashi, M. Sato, M. Tatsumi and N. Takagi, *J. Chromatogr.*, 309 (1984) 43.
36 F. A. L. van der Horst, M. H. Post and J. J. M. Holthuis, *J. Chromatogr.*, 456 (1989) 201.
37 F. A. L. van der Horst, M. H. Post, J. J. M. Holthuis and U. A. Th. Brinkman, *J. Chromatogr.*, 500 (1990) 443.
38 A. T. Rhys-Williams, S. A. Winfield, and J. N. Miller, *Analyst (London)*, 108 (1983) 1067.
39 R. W. Alder, R. Baker and J. M. Brown, *Mechanism in Organic Chemistry*, Wiley-Interscience, London, 1971.

Journal of Chromatography, 595 (1992) 163–168
Elsevier Science Publishers B.V., Amsterdam

CHROM. 23 877

High-performance liquid chromatography of histamine and 1-methylhistamine with on-column fluorescence derivatization

Koichi Saito*, Masakazu Horie and Norihide Nose

Saitama Institute of Public Health, 639-1, Kamiokubo, Urawa-shi, Saitama 338 (Japan)

Kazuya Nakagomi

Fermentation Research Institute, 1-1-3 Higashi, Tukuba, Ibaragi 305 (Japan)

Hiroyuki Nakazawa

Department of Pharmaceutical Science, National Institute of Public Health, 4-6-1, Shirokanedai, Minato-ku, Tokyo 108 (Japan)

(First received August 27th, 1991; revised manuscript received November 11th, 1991)

ABSTRACT

An on-column fluorometric derivatization method was developed for the determination of histamine and 1-methylhistamine (HMs) by high-performance liquid chromatography. The system for the derivatization consisted only of a commercially available single-plunger pump and a reversed-phase C_{18} column supported on synthetic polymer with a mobile phase of acetonitrile and alkaline borate buffer solution containing *o*-phthalaldehyde as a derivatization reagent. It required no additional reaction system as for a post-column derivatization method. Injected HMs might be derivatized to a fluorophore on the inlet site of the high-performance liquid chromatographic column, followed by chromatography on the same column. Optimization of the on-column reaction conditions resulted in a simple and sensitive analytical method for the determination of HMs with excellent reproducibility and linearity of 0.05–5 μg/ml of both HMs. Application of this method to the determination of HMs in food samples resulted in a limit of quantification of 0.05 mg/100 g and in a greater than 95% overall mean recovery at a fortification of 0.1 mg/g of both HMs. This method was furthermore applicable to the determination of histamine released from rat peritoneal mast cells.

INTRODUCTION

Histamine, an inflammatory substance released from mast cells, is regarded as one of the chemical mediators which are generally known as autacoids. Each mediator plays an important role in living systems, and there is a need in clinical medicine to monitor procedures involving them and their metabolites, such as 1-methylhistamine.

However, it is known that allergic intoxication sometimes occurs with the intake of histamine-contaminated food, such as spoiled fish or fish products. The amount of histamine formed depends on the species of fish, the composition of the bacterial population, temperature, and the handling and storage of the fish. Shimidu [1] suggested that the critical concentration for toxic reactions is 60 mg/100 g. Therefore, there has also been a need to develop a simple routine analysis method to determine histamine in order to control the quality and evaluate the safety of various kinds of foods.

A number of analytical methods such as bioassay [2], fluorocolorimetry [3], enzyme isotope assay [4], gas chromatography (GC) [5] and high-performance liquid chromatography (HPLC) [6–11] have so far been used for the determination of histamine in

0021-9673/92/$05.00

a variety of substances. Most reports on the HPLC method which has been widely used in many fields have employed the pre-column [6–8] or post-column [9–11] derivatization technique using *o*-phthalaldehyde (OPA) [7–11] or dansyl chloride [6] as a fluorescence labelling reagent. However the pre-column procedure suffers from certain disadvantages, such as the requirement for carefully controlled reaction conditions and the time involved. Furthermore, the reaction product is inferior in terms of reproducibility because of its very limited stability.

On the other hand, a post-column procedure is claimed to be less troublesome than a pre-column procedure and can eleminate its drawbacks, but it requires expensive additional equipment for the chromatographic system. Further, peak broadening and dilution of samples are caused by the addition of post-column reagent.

The present paper proposes an on-line and on-column derivatization method employing a polymer C_{18} column with the mobile phase containing OPA reagents. This method was designed to overcome some of the drawbacks of the current derivatization method. The on-column method discussed in this paper is applicable to the quantitative analysis of histamine in various foods and in rat peritoneal mast cells.

EXPERIMENTAL

Chemicals and reagents

Standard solutions of histamine and 1-methylhistamine (HMs) were prepared by dissolving histamine dihydrochloride (Tokyo Kasei Kogyo, Tokyo, Japan) and 1-methylhistamine dihydrochloride (Sigma, St. Loius, MO, USA) in 0.05 *M* hydrochloric acid. Acetonitrile used was of HPLC grade (Wako Pure Chemical Industries, Osaka, Japan), water was glass-distilled and deionized. N-Acetyl-L-cysteine (NAC) was of biochemical grade (Merck, Darmstadt, Germany) and OPA (Tokyo Kasei Kogyo) and all other chemicals were of analytical-reagent grade and used without further purification.

Amberlite CG-50 (type I, 100–200 mesh; Rohm and Haas, Philadelphia, PA, USA) for the clean-up column was conditioned with 0.2 *M* sodium acetate buffer (pH 4.6) according to a conventional method, and the wet resin was then packed in a glass column (135 mm × 9 mm I.D.) at a height of 1 cm.

Apparatus

The HPLC system consisted of an LC-6A pump (Shimadzu, Kyoto, Japan), a Model 7125 injector (Rheodyne, Berkeley, CA, USA) with a 20-μl volume loop and a Model RF-535 fluorescence detector (Shimadzu) set at excitation and emission wavelengths of 340 and 450 nm, respectively. The recording and integrating device was a Chromatopac C-R6A (Shimadzu). The analytical column was an Asahipak ODP-50 (150 mm × 4.6 mm I.D.; Asahi Chemical Industry, Kanagawa, Japan).

The HPLC mobile phase used was acetonitrile–50 m*M* sodium tetraborate (borax) aqueous solution (18:82, v/v) containing 1 m*M* OPA and 1 m*M* NAC. The prepared mobile phase was transferred to an amber glass bottle and shielded from exposure to sunlight. The mobile phase was prepared daily and run isocratically at ambient temperature at a flow-rate of 0.5 ml/min.

Food sample preparation

A sample of 1 g of food was homogenized in a 10-ml volumetric test tube with 4 ml of 5% trichloroacetic acid for 1 min, then brought to a total volume of 10 ml with water. After centrifugation at 1800 *g* for 5 min, the supernatant was filtered with Toyo Roshi No. 5B filter paper. A 1-ml aliquot of the filtrate was neutralized to pH 6–7 with 1 *M* sodium hydroxide, followed by addition of 1 ml of 1 *M* acetate buffer (pH 4.6) and dilution with water to a total volume of 5 ml. The solution was then placed on an Amberlite CG-50 column and eluted at a flow-rate of less than 1 ml/min. After washing the column with 15 ml of 0.2 *M* acetate buffer (pH 4.6) and subsequently with 5 ml of water, HMs were eluted with 3 ml of 0.05 *M* hydrochloric acid. The first 1 ml was discarded, and the subsequent 2-ml eluates were taken as the HMs fraction. The fraction was evaporated to dryness *in vacuo*, and the residue was dissolved with 1 ml of 0.05 *M* hydrochloric acid. A portion of the 10-μl volume of this final solution was injected for HPLC analysis.

Stability of OPA-labelled HMs

The stability of the OPA-labelled histamine obtained by the proposed method and by a batchwise operation, *i.e.* the pre-column method, was examined as follows. For the on-column method, the delivery of mobile phase was stopped exactly 2 min

after injection of histamine (10 ng), and after certain periods had elapsed (10, 20, 30 and 60 min) the mobile phase was made to flow again. The HPLC column was thermostated at 25 ± 0.5°C throughout the experiment. For the pre-column method, 1 μg of histamine was incubated in 1 ml of the solution of the HPLC mobile phase used for the on-column method at 25 ± 0.5°C. After an elapsed period (10, 20, 30 and 60 min), 10-μl aliquots were injected into the HPLC system. The mobile phase used was a mixture of acetonitrile–50 m*M* borax (18:82, v/v) without OPA–NAC, and other conditions were similar to those for the on-column method.

Measurement of histamine release from rat peritoneal mast cells

Mast cells were separated from the peritoneal cavity fluid of Wistar rats using the method described by Nakagomi *et al.* [12]. Each test material (compound 48/80, mastoparan and somatostatin) was added to the mast cell suspension (20 μl) and the mixture was incubated at 37°C for 10 min. The reaction was terminated by cooling the mixture in an ice bath. After centrifugation at 1500 *g* for 5 min, 30 μl of the supernatant were taken, and the same volume of 0.1 *M* hydrochloric acid was added. A portion of the 10-μl volume of this final solution was injected for HPLC analysis without further purification. In this case, HPLC conditions were slightly modified: the HPLC column size used was 250 mm × 4.6 mm I.D., and the column was thermostated at 40 ± 0.5°C throughout the experiment. Other conditions were similar to those already described.

RESULTS AND DISCUSSION

The histamine introduced from an injector was presumed to be derivatized spontaneously to its OPA derivative at the inlet site of the HPLC column in the presence of the OPA reagent in the mobile phase, and the derivative was subsequently chromatographed on the same column. Therefore, the parameters examined, which were varied in order to effect the required reactivity and separation, were the concentration of the OPA, NAC, borax and acetonitrile in the mobile phase, its pH and the column temperature. The column employed for the on-column derivatization method was an Asahipak ODP-50, which is a polymer-supported C_{18} column advertised as being tolerant towards alkaline eluent. For the active thiol compound which is indispensable for the OPA-labelling reaction, NAC was used, because it has only a faint odour, whereas β-mercaptoethanol and ethanethiol, which have been used until now, are stinking liquids and difficult to handle.

The optimum concentrations of OPA–NAC in the mobile phase were examined with a mixture of acetonitrile–50 m*M* borax (18:82, v/v) containing 0.1–5 m*M* OPA–NAC. The molar ratio of OPA and NAC concentration was always set at equivalence. Fig. 1A shows that each peak area increased with increasing concentration (0.1–1 m*M*) of OPA–NAC and reached a plateau in the range 1–2 m*M*. As for the peak shape, symmetrical peaks were observed above 0.5 m*M* OPA–NAC, while slightly leading and tailing shapes were observed below 0.2 m*M*. On the other hand, the constant capacity factor (k') values in Fig. 1A suggested that the separation of OPA-labelled HMs was not influenced by the OPA or NAC concentration. Since the lower concentration of OPA–NAC was desirable for the HPLC background chromatogram, 1 m*M* OPA–NAC was chosen for subsequent work.

The derivatization of histamine with OPA is generally best carried out at alkaline pH, approximately pH 10. As might be expected, there was a significant drop in the peak area as the pH was lowered below 9, while a plateau was observed above pH 9.5 (see Fig. 1B). Symmetrical peaks were observed above pH 9, while leading or tailing peaks were observed below pH 8.5. The k' values of the HMs showed immutability regardless of the pH variation. Since the pH of the mixed solution of acetonitrile and 50 m*M* borax aqueous solution (18:82, v/v) containing 1 m*M* OPA–NAC was in the range 9.5–10, no additional pH adjustment was employed for subsequent work.

Fig. 1C shows the effect of the borax concentration. The peak area of both HMs increased with increasing borax concentration in the range 5–40 m*M* and reached a plateau over the range 40–70 m*M*. The variation in k' values showed a pattern similar to that of the peak area.

The variation in the acetonitrile concentration hardly influenced the peak area of the HMs, while

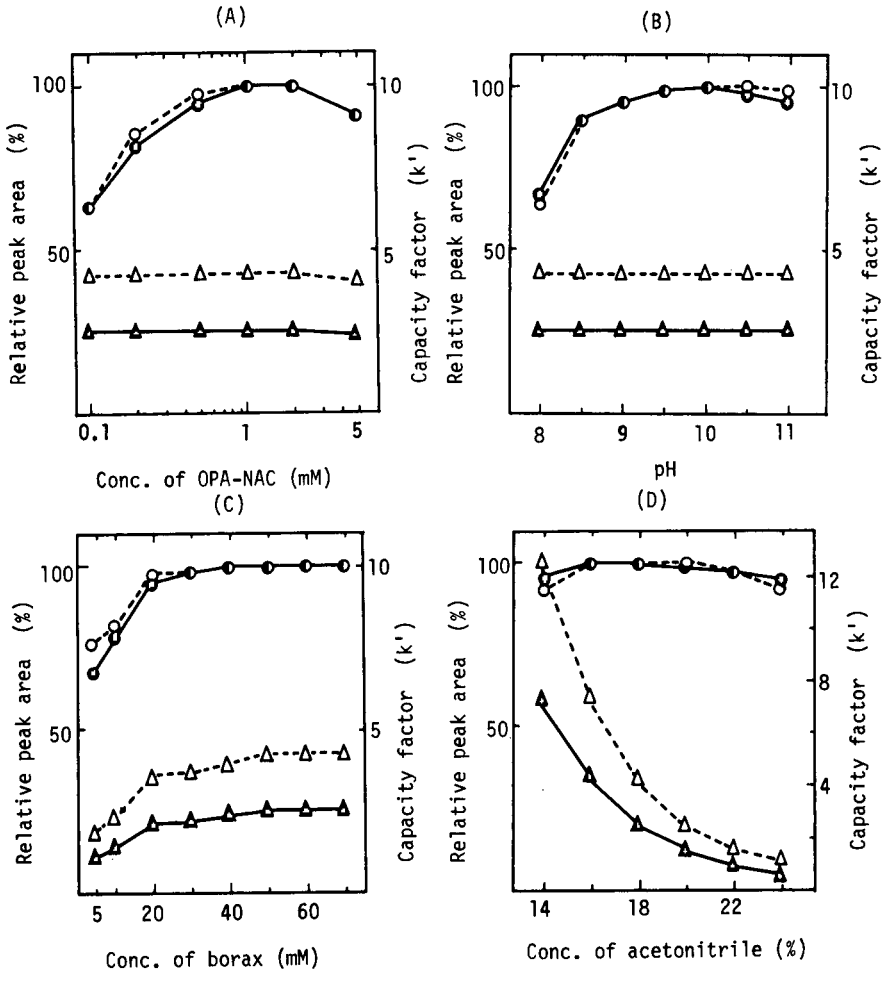

Fig. 1. Effect of (A) OPA–NAC concentration, (B) pH, (C) borax concentration and (D) acetonitrile concentration of the mobile phase on relative peak area (● = histamine; ○ = 1-methylhistamine) and capacity factor (▲ = histamine; △ = 1-methylhistamine). The mobile phase conditions were as follows: (A) 18% acetonitrile in 50 m*M* borax containing various concentrations of OPA–NAC; (B) 18% acetonitrile in 50 m*M* borax (adjusted to various pH values) containing 1 m*M* OPA–NAC; (C) 18% acetonitrile in various concentrations of borax containing 1 m*M* OPA–NAC; (D) various concentrations of acetonitrile in 50 m*M* borax containing 1 m*M* OPA–NAC. Flow-rate: 0.5 ml/min. Injection: 10 ng for both histamine and 1-methylhistamine. HPLC column: Asahipak ODP-50 (150 mm × 4.6 mm I.D.); column temperature: 25°C.

the k' values decreased with increasing acetonitrile concentration, as shown in Fig. 1D. When the acetonitrile concentration was *ca.* 18%, the k' values of both HMs were in the range 2–5, and the HMs showed good baseline separation. On the basis of these results, the mobile phase of acetonitrile–50 m*M* borax (18:82, v/v) containing 1 m*M* OPA–NAC was determined to be optimum for the proposed methodology.

As for the column temperature, relatively constant values for the HMs peak areas were obtained in the range 25–50°C, and a slightly declining tendency was observed above 50°C. The k' values of both HMs decreased with increasing temperature. Therefore, we usually performed experiments at ambient temperature.

Reproducibility and linearity

The precision and linearity of the on-column derivatization method were examined. The repetitive analyses ($n = 5$) of the HMs standard solution (0.05, 0.5 and 5 μg/ml) gave a corresponding relative stan-

dard deviation (R.S.D.) of the peak area for each concentration: 1.2, 0.5 and 0.8% for histamine; 1.3, 1.2 and 0.9% for 1-methylhistamine. The R.S.D. (n = 15) of the retention times was 0.5% for histamine and 0.3% for 1-methylhistamine.

The calibration graphs of peak area *versus* HMs concentration showed excellent linearity over the range 0.05–5 μg/ml for both HMs. The detection limit was 0.5 ng (signal-to-noise ratio = 3) for both HMs.

Stability of the OPA-labelled histamine

According to the report by Simmons and Johnson [13], an isoindole form of an OPA-labelled primary amino compound exhibites fluorescence but gradually convertes to a non-fluorescent substance because of its instability. Therefore, the stability of the OPA-labelled histamine in the HPLC column was compared with that in a batchwise solution. As a result, the decreasing fluorescence of the fluorophore, *i.e.* the decomposition reaction, was revealed to be a pseudo-first-order reaction for both methods. The rate constant obtained was $1.8 \cdot 10^{-3}$ min^{-1} for the on-column method and $3.6 \cdot 10^{-3}$ min^{-1} for the batchwise operation. Based on these results, the OPA-labelled histamine was more stable in the HPLC column than in a batchwise solution. Owing to a mutual interaction with the octadecyl group and/or the polymer support, the fluorophore was supposed to be more rigid in the HPLC column than in the batchwise solution. Further, though a steric effect of the octadecyl group was supposed to play an important role in the derivatization and decomposition reaction, the exact role is unclear at this point in time. However, there is no problem with pratical application of the on-column method because of the reproducibility of retention time and peak area and the linearity of wide-range calibration.

Extraction and clean-up

Sample extraction methods currently used for HMs detection in various foods require a clean-up step before quantitative analysis. A procedure described by Kawabata *et al.* [14] was slightly modified: the resin volume of the clean-up column was reduced on a scale of *ca.* one fifth. This shortened the total analytical time considerably and made this part of the procedure more convenient. The HMs adsorbed on the Amberlite CG-50 column were found in the 3 ml of 0.05 *M* hydrochloric acid eluate after washing with 15 ml of 0.2 *M* acetate buffer followed by 5 ml of water. No HMs were found in the 1.5 ml of the first eluate, where other impurities, such as amino acids when present in foods, were found. Therefore, the 1-ml of the first eluate was discarded with the subsequent 2-ml eluates taken as the HMs fraction. Fig. 2 shows typical chromatogram of HMs standard (A) and soy sauce (B) after removal of impurities.

Recovery study and analysis of commercial samples

Table I summarizes the recoveries of the HMs from commercial samples of dried sardine, soy sauce and soybeen paste fortified with 10 mg/100 g of each HM. Overall mean recoveries greater than 95% and standard deviations of 3% were obtained with every sample.

The histamine content found in fish and some kinds of commercial bean products varied from 0.07 to 20.0 μg/g, as shown in Table II. On the other hand, 1-methylhistamine was found not to be present in these samples.

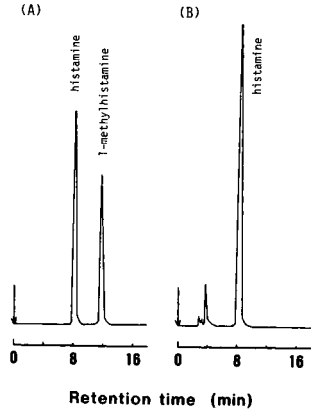

Fig. 2. Typical chromatograms of histamine and 1-methylhistamine from (A) a standard (10 ng for both histamine and 1-methylhistamine) and (B) soy sauce (14 ng of histamine) after clean-up. The ordinate shows relative fluorescence intensity. HPLC column: Asahipak ODP-50 (150 mm × 4.6 mm I.D.); mobile phase: acetonitrile–50 m*M* borax (18:82, v/v) containing 1 m*M* OPA–NAC; flow-rate: 0.5 ml/min; column temperature: 25°C.

TABLE I

RECOVERIES OF HISTAMINE AND 1-METHYLHISTAMINE ADDED TO FISH AND SOY PRODUCTS

Sample[a]	Recovery (mean ± S.D., n = 5)	
	Histamine	1-Methylhistamine
Sardine	96.5 ± 2.0	97.0 ± 2.7
Soy sauce	99.3 ± 1.5	98.1 ± 0.6
Bean paste	99.1 ± 1.2	99.7 ± 0.8

[a] Histamine and 1-methylhistamine were added to each sample at the level of 10 mg/100 g.

Analysis of histamine released from rat peritoneal mast cells

The applicability of this proposed method to the measurement of histamine-releasing activities of drugs, such as compound 48/80, mastoparan and somatostatin, which are well known to induce histamine release from mast cells, was examined. In this application, the purification procedure of the test solution was omitted, since the coexistent substance in the matrix was less than in the food samples. As shown in Fig. 3, the chromatograms were found not to contain any peaks that interfered with the measurement of the histamine peak. Histamine added at a level of 1 μg/ml to each test solution was quantitatively recovered (98.3–100.3%). Therefore, the assay developed here for the measurement of histamine released from rat peritoneal mast cells was sufficiently practical for routine analysis.

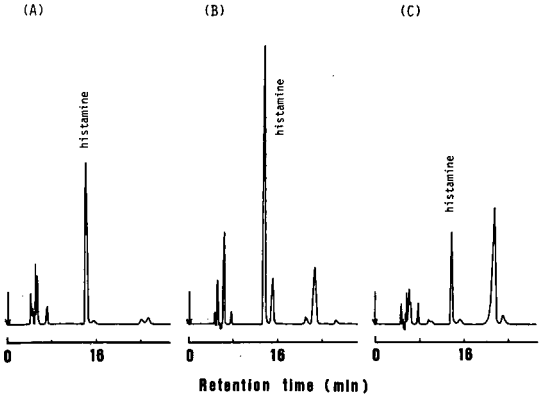

Fig. 3. Typical chromatograms of histamine released from rat peritoneal mast cells induced by (A) 1 μg/ml compound 48/80, (B) 10 μ*M* mastoparan and (C) 10 μ*M* somatostatin. The ordinate shows relative fluorescence intensity. HPLC column: Asahipak ODP-50 (250 mm × 4.6 mm I.D.); mobile phase: acetonitrile–50 m*M* borax (18:82, v/v) containing 1 m*M* OPA–NAC; flow-rate: 0.5 ml/min; column temperature: 40°C.

TABLE II

CONTENTS OF HISTAMINE AND 1-METHYLHISTAMINE IN VARIOUS FOODS

Determination limit: 0.05 mg/100 g; N.D. = not detected.

Sample	Histamine (mg/100 g)	1-Methylhistamine (mg/100 g)
Sardine	0.09	N.D.
Pacific saury	0.2	N.D.
Dry tuna	1.44	N.D.
Shelfish (n = 10)	0.29–2.73	N.D.
Soy sauce (n = 7)	0.08–20.0	N.D.
Bean paste (n = 10)	0.07–7.71	N.D.
Fermented soybeans	N.D.	N.D.

In conclusion, the on-column derivatization method described here is simple, highly sensitive, specific and routinely useful for the quantitative analysis of HMs in various foods and in rat peritoneal mast cells. This method resolves the problem associated with the stability of the fluorophore produced in the reaction of OPA with HMs and, moreover, it is convenient and can be readily incorporated into existing laboratory HPLC system as a new derivatization method.

REFERENCES

1 W. Shimidu, *Bull. Jpn. Soc. Sci. Fish*, 21 (1955) 365.
2 J. R. Vane, *Br. J. Pharmacol.*, 20 (1964) 360.
3 P. A. Shore, A. Burkhalter and V. H. Cohn, Jr., *J. Pharmacol. Exp. Ther.*, 127 (1959) 182.
4 R. E. Shaff and M. A. Beaven, *Anal. Biochem.*, 94 (1979) 425.
5 H. Mita, H. Yasueda and T. Shida, *J. Chromatogr.*, 221 (1980) 1.
6 A. Yamatodani, T. Seki, M. Taneda and H. Wada, *J. Chromatogr.*, 144 (1977) 141.
7 Y. Tsuruta, K. Kohashi and Y. Ohkura, *J. Chromatogr.*, 224 (1981) 105.
8 E. Kasziba, L. Flancbaum and J. C. Fitzpatrick, *J. Chromatogr.*, 432 (1988) 407.
9 F. Perini, J. B. Sadow and C. V. Hixon, *Anal. Biochem.*, 94 (1979) 431.
10 A. Yoshida and A. Nakamura, *J. Food Hyg. Soc. Japan*, 23 (1982) 339.
11 Y. Arakawa and S. Yachibana, *Anal. Biochem.*, 158 (1986) 20.
12 K. Nakagomi, M. Takeuchi, H. Tanaka, N. Tomizuka and T. Nakajima, *J. Antibiotics*, 43 (1990) 462.
13 S. S. Simmons, Jr. and D. Johnson, *J. Org. Chem.*, 43 (1978) 2886.
14 T. Kawabata, Y. Uchida and T. Akano, *Bull. Jpn. Soc. Sci. Fish.*, 26 (1960) 1183.

Journal of Chromatography, 595 (1992) 169–177
Elsevier Science Publishers B.V., Amsterdam

CHROM. 23 919

Purity assay of sodium mercaptododecaborate by high-performance liquid chromatography

Bohumír Grüner* and Zbyněk Plzák

Institute of Inorganic Chemistry, Czechoslovak Academy of Sciences, 250 68 Řež near Prague (Czechoslovakia)

Ivan Vinš

Tessek Ltd., Křižovnická 3, 110 00 Prague 1 (Czechoslovakia)

(First received October 18th, 1991; revised manuscript received November 25th, 1991)

ABSTRACT

A simple high-performance liquid chromatographic (HPLC) method for purity monitoring and determination of $[B_{12}H_{11}SH]^{2-}$ (**I**) and its oxidation impurities $[B_{12}H_{11}SSB_{12}H_{11}]^{4-}$ (**II**) and $[B_{12}H_{11}S(O)SB_{12}H_{11}]^{4-}$ (**III**) is presented. The method is based on the use of the hydroxyethylmethacrylate sorbent Separon HEMA-BIO 300 and 100 m*M* sodium perchlorate in 0.01 *M* phosphate buffer as mobile phase. Common HPLC equipment with direct spectrophotometric detection in the range 200–210 nm was used throughout. The minimal detectable amounts of the sodium salts of anions **I**, **II** and **III** at 204 nm were $8.6 \cdot 10^{-8}$, $8.8 \cdot 10^{-9}$ and $6.4 \cdot 10^{-8}$ g, respectively. The application of the method to the study of the stability of the sodium salt of **I** in solution revealed a strong positive effect of trace amounts of Cu^{+} in enhancing the $Na_2B_{12}H_{11}SH$ oxidation rate.

INTRODUCTION

The disodium salt of the *closo*-undecahydro-1-mercaptododecaborate anion, $[B_{12}H_{11}SH]^{2-}$ (**I**) (Fig. 1), is the most widely used agent in boron neutron capture therapy (BNCT) of brain tumours [1].

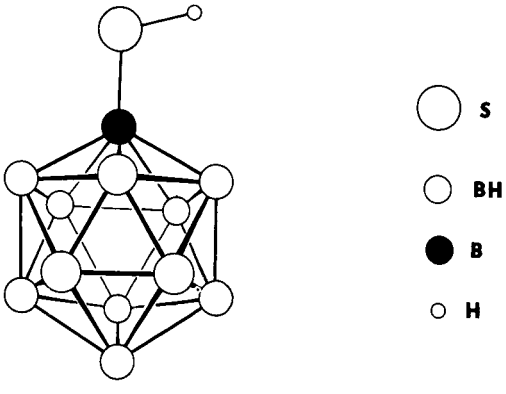

Fig. 1. Framework of the *closo*-$[B_{12}H_{11}SH]^{2-}$ anion.

BNCT is based on the selective accumulation of a boron compound in the malignant tissue, followed by subsequent destruction of the tumour cells by α-particles produced from the nuclear reaction of the ^{10}B nuclei contained in the isotopically enriched $[^{10}B_{12}H_{11}SH]^{2-}$ anion with thermal neutrons.

The known syntheses of the sodium salt of anion **I** proceed via several steps [2,3] and the final product can contain a wide range of impurities, as do the most important precursors $[(C_2H_5)_3NH]_2B_{12}H_{12}$ and $[(CH_3)_4N]_2B_{12}H_{11}SH$ [2]. The crystallinity of the final and intermediate products does not seem to be a valid indications of purity, as seemingly pure crystals have often been found to be mixtures [4]. When the intermediate product, *closo*-$[(C_2H_5)_3NH]_2B_{12}H_{12}$, is not sufficiently pure, some smaller cage *closo*-borate impurities and $[B_{12}H_{12}]^{2-}$ anion derivatives may be transferred to the final product.

The mercapto group of the sodium salt of **I** is sensitive to oxidation, yielding compounds of higher toxicity, sodium salts of anions **II** and **III** being

0021-9673/92/$05.00

the main oxidation products [4–8]. Efficient quantitative monitoring of the oxidation products during both the transformation of mercaptododecaborate to the drug form and its storage is therefore necessary.

The physical and chemical properties of the anion **I** and other *closo*-hydroborate impurities are very similar. The sodium salts are hygroscopic and highly soluble in water. The main factors governing the solution behaviour of this class of compounds are derived from the properties of relatively highly charged symmetrical boron cages. Consequently, these salts behave as very strong inorganic electrolytes, simultaneously exhibiting hydrophobic properties comparable to those of organic aromatic molecules, which causes the mixtures of such compounds to be difficult to separate.

Thin-layer chromatography [4] and capillary isotachophoretic methods [6,7] have been developed to determine the purity of the sodium salt of anion **I**, but the resolution of both methods is insufficient for all contaminants.

Recently, a paper dealing with the preparation of some oxidation products of the caesium salt of **I** was published [8] that included a short description of an HPLC method based on ion-pair chromatography on octadecyl silica using UV detection at 254 nm for determining both the oxidation impurities and the parent compound. We have recently reported the influence of separation conditions on the separation of some *closo*-$[B_{12}H_{12}]^{2-}$ derivatives on differently surface-modified Separon HEMA hydroxyethylmethacrylate sorbents [9], and in this study we have tried to extend the scope of the method to the separation of the anion **I** and its oxidation impurities, anions **II** and **III**.

EXPERIMENTAL

Columns

A broad range of cartridge glass columns (150 × 3.3 mm I.D.) packed with Separon HEMA hydroxyethylmethacrylate supports were provided by Tessek (Prague, Czechoslovakia). The columns were packed with low-capacity (0.03–0.1 mequiv./g) sorbents for ion-exchange chromatography or ion-exclusion chromatography [Separon HEMA-S 1000 Q-L (quarternary ammonium groups, 10 and 12 μm), Separon HEMA-S 1000 DEAE (diethylaminoethyl groups, 12 μm) and Separon HEMA-BIO 1000 CM (carboxy groups, 7 μm)], and with supports for hydrophobic interaction chromatography or the separation of biomolecules (Separon HEMA-S 1000, 10 and 12 μm; Separon HEMA-BIO 300, lot 3401, 12 and 15 μM, lot 1311, 10 μm; and Separon HEMA-BIO 1000, 10 μm).

Eluents

Deionized water produced with a Milli-Q apparatus (Millipore) was used throughout. All chemicals were of analytical-reagent grade [Lachema (Brno, Czechoslovakia) and Laborchemie (Apolda, Germany)]. The eluents were prepared by dissolving the calculated amount of electrolyte either in water or in 0.01 *M* phosphate buffer with the pH adjusted with sodium hydroxide solution. The eluents were filtered before use through a 0.45-μm filter and degassed under vacuum.

Apparatus

A simple isocratic HPLC system was used, consisting of a pulseless dual-piston high-pressure VCR 40 pump and a six-port sampling valve K 1 with 20- or 50μl loops (Development Workshops of the Czechoslovak Academy of Sciences, Prague, Czechoslovakia), an LCD 2040 variable-wavelength (190–360 nm) UV spectrophotometric detector (Laboratory Instruments, Prague, Czechoslovakia), a PKS-1 column holder (Tessek) equipped with a heating glass jacket with circulating water from a thermostated bath, a Servogor 2s line recorder (Brown Boveri, Germany) and a CI 100 integrator (Laboratory Instruments).

A Pye Unicam system consisting of a PU 4010 pulseless dual-piston pump, PU 4031 oven, PU 4700 autoinjector with a 20-μl sample loop, a PU 4021 diode-array UV detector and a PU 4850 computer with PU Chromascan software routines was used for optimization of the spectrophotometric detection mode.

Sample preparation

The free acid and sodium and tetramethylammonium salts of anion **I** were prepared in the Institute of Inorganic Chemistry, Czechoslovak Academy of Sciences, by a modified published procedure [2,3].

The tetramethylammonium salts of anion **II** was prepared by the oxidation of an aqueous solution of

the free acid of **I** by oxygen. The oxidation course was monitored by the HPLC method under discussion and stopped at the moment when the peak of **I** had disappeared and the solution contained the maximum amount of anion **II** together with a smaller amount of anion **III**. The pure tetramethylammonium salt was obtained by adding 10% tetramethylammonium hydroxide at pH 8.5–9 and a five recrystallization from a weakly basic aqueous solution. The tetramethylammonium salt of **III** was prepared by oxidation of the free acid of **I** by hydrogen peroxide and threefold recrystallization of product resulting from the precipitation with 10% aqueous tetramethylammonium hydroxide from a weakly basic aqueous solution. The purity of the products was monitored by HPLC. Individual products were identified *via* ^{1}H and ^{11}B NMR spectroscopy by comparing their NMR chemical shifts with published data [2].

Solid substances used in the preparation of standard solutions were dried *in vacuo* over P_2O_5 at 50°C.

Free acids or sufficiently water-soluble salts of the *closo*-$[B_{12}H_{12}]^{2-}$ derivatives, *e.g.*, salts with Li^+, Na^+, K^+, Rb^+, Cs^+, NH^+_4, $N(CH_3)^+_4$ counter cations, were directly injected as aqueous 0.05–10 μmol/ml solutions. Sparingly soluble compounds, *e.g.*, salts with bulky cations, were converted into sufficiently soluble forms before injection using standard ion-exchange techniques or suitable metathetical methods [10]. Before injection all samples were filtered through a 0.45-μm nylon microfilter (Tessek).

Data evaluation

ADSTAT statistical software (TriloByte, Prague, Czechoslovakia) was used for data evaluation and regression analysis.

RESULTS

As in the previous study [9], we employed a wide range of both types of hydroxyethylmethacrylate sorbents modified for ion-exchange chromatography and unmodified for hydrophobic interaction chromatography to try to effect a reasonable separation of anion **I** and its oxidation impurities. On all types of materials, the dependence of the capacity factor (k') on the mobile phase (aqueous $NaClO_4$) ionic strength, pH and acetonitrile content and on the separation temperature in the range 20–60°C was studied. As a result, the behaviour of anion **I** was established as being analogous to that of other monosubstituted *closo*-$[B_{12}H_{12}]^{2-}$ derivatives. On all materials used, the k' values for anion **I** follow well the order of monosubstituted derivatives (see Fig. 2, for example), lying between those of *closo*-$[B_{12}H_{12}]^{2-}$ and *closo*-$[B_{12}H_{12}Cl]^{2-}$. The retention on unmodified materials increases with increasing concentration of $NaClO_4$ in the mobile phase up to 0.1 *M* following a slight decrease at higher concentrations. Therefore, such chromatographic behaviour can be attributed to the hydrophobic interaction of *closo*-hydroborate anions with hydrophobic sites of the hydroxyethylmethacrylate polymer [9]. With materials for ion-exchange chromatography, ion-exchange interaction

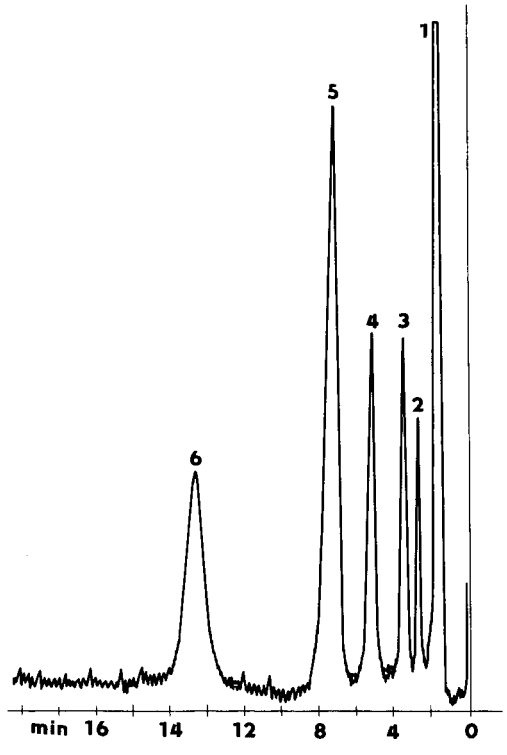

Fig. 2. Example of the separation of the unsubstituted *closo*-$[B_{12}H_{12}]^{2-}$ anion and some of its monosubstituted derivatives, including the *closo*-$[B_{12}H_{11}SH]^{2-}$ anion. Column, Separon HEMA-BIO 300 (12 μm); eluent, 0.1 *M* $NaClO_4$ in 0.01 *M* phosphate buffer (pH 8.5); flow-rate, 0.5 ml/min; detection, UV at 205 nm; temperature of separation, 40°C. Peaks: 1 = $[B_{12}H_{11}OH]^{2-}$; 2 = $[B_{12}H_{12}]^{2-}$; 3 = $[B_{12}H_{11}SH]^{2-}$; 4 = $[B_{12}H_{11}Cl]^{2-}$; 5 = $[B_{12}H_{11}Br]^{2-}$; 6 = $[B_{12}H_{11}I]^{2-}$.

makes the separation mechnism more complex, causing some trailing of the peaks of anion **I**.

Unfortunately, the oxidation products **II** and **III** with molecular structures based on two *closo*-$[B_{12}H_{12}]^{2-}$ moieties linked by sulphur bridges [3,5] did not follow the typical chromatographic behaviour of the uncoupled *closo*-hydroborate anion derivatives mentioned above. As a result, substantial changes in the selectivity of anions **II** and **III** on individual materials were observed, the most significant being those in the elution order of both oxidation impurities and anion **I**. On most of the materials used, the k' values of the anions **II** and **III** were smaller than that of the anion **I**, causing a poor resolution. Such chromatographic behaviour of impurities cannot be explained on the basis of a simple hydrophobic interaction model as for the corresponding parent compounds. Owing to these difficulties we considered only the practical aspects of the separation study. Of all the materials used, only Separon HEMA-BIO 300, lot 3401, 12 and 15 μm sorbents allowed a reasonable separation of anion **I** and the two well known oxidation impurities **II** and **III** along with at least three other unknown contaminants which were undoubtedly formed by subsequent oxidation reactions of anions **II** and **III**. One of two such additional peaks (compounds **IV** and **V**) in Fig. 3, can be probably ascribed to the recently reported [8] sulphinylsulphone $[B_{12}H_{11}SO\text{-}SO_2B_{12}H_{11}]^{4-}$.

The best separation conditions for a routine purity assay of anion **I** arising from optimization proce-

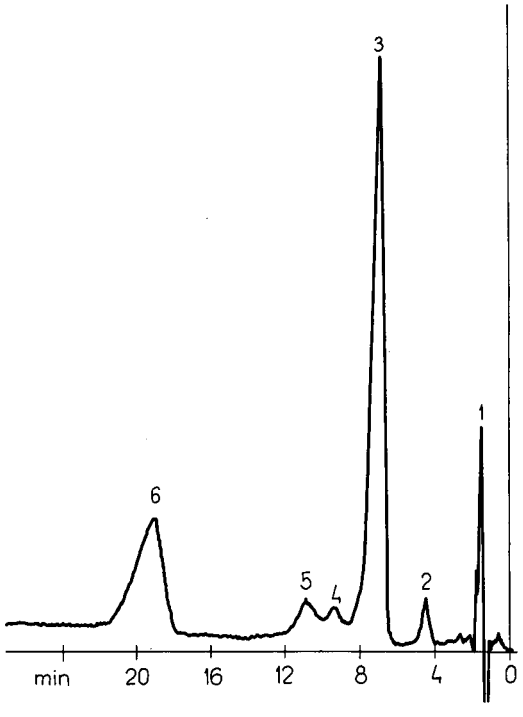

Fig. 3. Separation of highly oxidized sample of $Na_2B_{12}H_{11}SH$ in distilled water after an 8-day air exposure. Initial concentration, 5.7 μmol/ml. Column, Separon HEMA-BIO 300 (12 μm); eluent, 0.1 *M* $NaClO_4$ in 0.01 *M* phosphate buffer (pH 8.5); flow-rate, 0.5 ml/min; detection, UV at 204 nm; temperature of separation, 25°C; injection volume, 50 μl. Peaks: 1 = unknown; 2 = $[B_{12}H_{11}SH]^{2-}$ (**I**); 3 = $[B_{12}H_{11}SSB_{12}H_{11}]^{4-}$ (**II**); 4,5 = unknown hydroborate impurities (**IV** and **V**); 6 = $[B_{12}H_{11}S(O)\text{-}SB_{12}H_{11}]^{4-}$ (**III**).

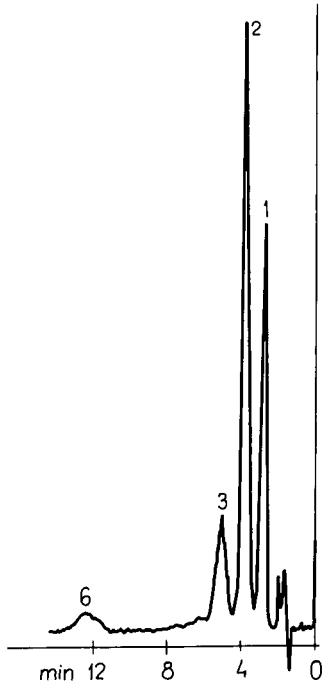

Fig. 4. Separation of a sample of an aqueous solution of the drug form (containing 8% of sodium salt of anion **II**) of $Na_2B_{12}H_{11}SH$ (concentration 1.14 μmol/ml, diluted for analysis) in Milli-Q-purified water after 8 days of air exposure. Temperature, 40 °C; other separation conditions as in Fig. 3. Peaks: 1 = $[B_{12}H_{12}]^{2-}$ (internal standard); 2 = $[B_{12}H_{11}SH]^{2-}$ (**I**); 3 = $[B_{12}H_{11}SSB_{12}H_{11}]^{4-}$ (**II**); 6 = $[B_{12}H_{11}S(O)SB_{12}H_{11}]^{4-}$ (**III**).

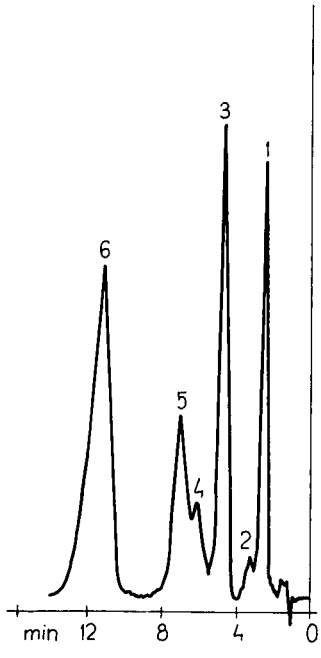

Fig. 5. Separation of a sample of an aqueous solution of the drug form (containing 8% of the sodium salt of anion II) of $Na_2B_{12}H_{11}SH$ (concentration 1.14 μmol/ml) in Milli-Q-purified water after 5 days of air exposure in the presence of a trace amount of Cu^+ (130 μg/l). Chromatographic conditions as in Fig. 4. Peaks: 1 = $[B_{12}H_{12}]^{2-}$ (internal standard); 2 = unknown impurity; 3 = $[B_{12}H_{11}SSB_{12}H_{11}]^{4-}$ (**II**); 4,5 = unknown hydroborate impurities (**IV** and **V**); 6 = $[B_{12}H_{11}S(O)SB_{12}H_{11}]^{4-}$ (**III**).

dures are shown in Figs. 3–5. Separation at ambient temperature 25°C (Fig. 3) can be recommended for samples with a high degree of oxidation of anion **I**, giving a better resolution of anions **II**, **IV** and **V** (compare with the separation of another highly oxidized sample in Fig. 5 at 40°C). The procedure at 25°C can also be employed for the purity assay of $[(C_2H_5)_3NH]_2B_{12}H_{12}$, which is a significant intermediate product in the synthesis (Fig. 6). It is strongly recommended that the analysis of this compound, prepared as described [11], is performed before the sulphydrylation step of *closo*-$[B_{12}H_{12}]^{2-}$ [2,3] in order to avoid either transfer of *closo*-hydroborate impurities to the final product or a decrease in the yield of **I**.

Additional desirable analyses can be performed by applying the above-mentioned type of sorbent using different eluent compositions and a separation temperature of 40°C (Fig. 7). Thus the $[B_{12}H_{11}SCSC_6H_4NCH_3]^-$ anion, an intermediate adduct of N-methylbenzothiazole-2-thione with the *closo*-$[B_{12}H_{12}]^{2-}$ anion formed in the sulphydrylation step [2] of the synthesis of **I** can be determined. However, this compound has never been found as an impurity in the usual samples of *closo*-$[B_{12}H_{11}SH]^{2-}$ used for biomedical applications.

The calculated k' values of all the compounds under discussion are summarized in Table I.

Detection and detection limits

The UV spectra of compounds **I**, **II** and **III** recorded during the chromatographic experiment at the peak maxima using a PU 4021 diode-array spectrometric detector are shown in Fig. 8. The spectra indicate that *closo*-$[B_{12}H_{11}SH]^{2-}$ exhibits a maximum at 204 nm and its oxidation impurities, **II** and **III**, at 204 and 207 nm, respectively. In the shorter (down 200 nm) and longer (up to 210) wavelength regions, a relatively large decrease in the absorbance can be observed, and the use of wavelengths outside the 200–210 nm range thus leads to a marked decrease in the direct UV detection sensitivity.

With the use of the LCD 2040 UV spectrophotometric detector at 204 nm the minimum detectable amounts (defined as the amount of solute that caus-

TABLE I

CAPACITY FACTORS k' OF THE *closo*-HYDROBORATE ANION UNDER DISCUSSION

Chromatographic conditions: column, cartridge glass column, Separon HEMA-BIO 300 (12 μm); eluent, 0.1 *M* $NaClO_4$ in 0.01 *M* phosphate buffer (pH 8.5); detection, UV at 204 nm; flow-rate, 0.5 ml/min; temperature, 25 or 40°C.

Anion	k'	
	25°C	40°C
$[B_{10}H_{10}]^{2-}$	0.33	
$[B_{12}H_{12}]^{2-}$	1.66	1.25
$[B_{12}H_{11}SH]^{2-}$	2.75	2.08
$[B_{12}H_{11}SSB_{12}H_{11}]^{4-}$	4.6	3.2
IV	6.7	3.9
V	8.2	4.6
$[B_{12}H_{11}S(O)SB_{12}H_{11}]^{4-}$	15.2	8.7
$[B_{12}H_{11}SCSC_6H_4NCH_3]^-$		8.9[a]

[a] Eluent: 0.1 *M* $NaClO_4$ in acetonitrile–water (25:75).

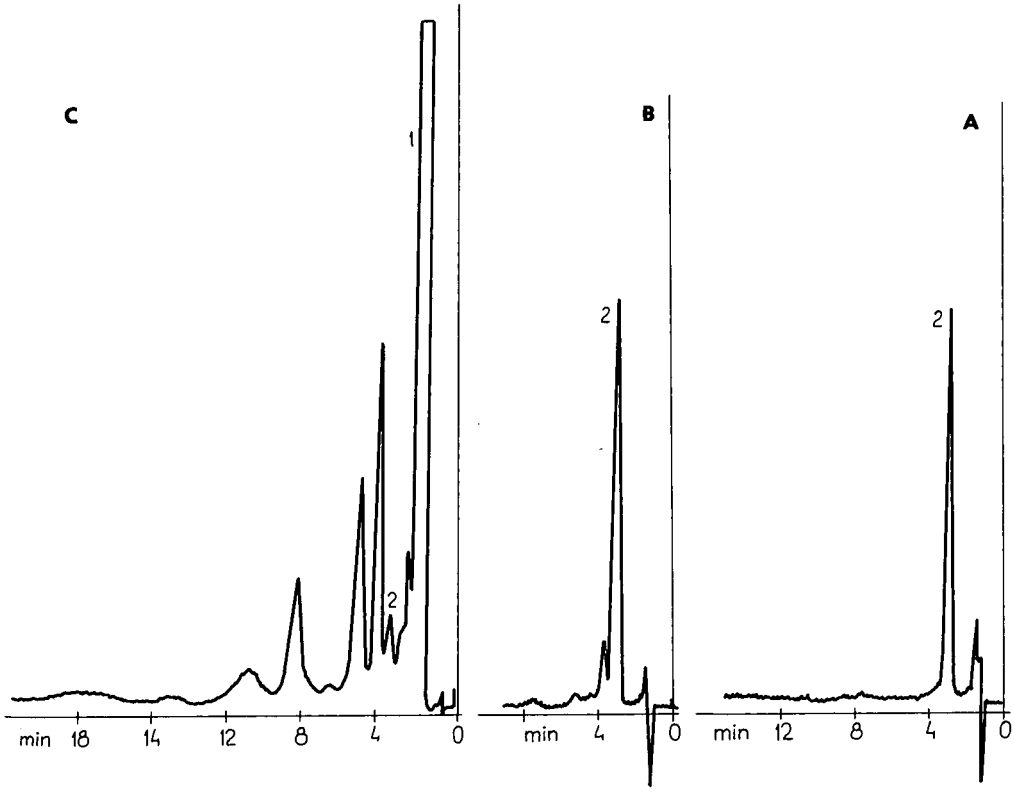

Fig. 6. Determination of impurities in samples of $[B_{12}H_{12}]^{2-}$ anion prepared as described [10]. (A) Pure anion $[B_{12}H_{12}]^{2-}$ after purification process; (B) crude product before purification) (C) mixture of hydroborate impurities isolated from the crude product. Chromatographic conditions as in Fig. 3. Peaks: 1 = $[B_{10}H_{10}]^{2-}$; 2 = $[B_{12}H_{12}]^{2-}$; other peaks, unknown hydroborate impurities.

es a detector signal of twice the noise intensity) were $8.6 \cdot 10^{-8}$, $8.8 \cdot 10^{-9}$ and $6.4 \cdot 10^{-8}$ g for the sodium salt of anion **I** and anions **II** and **III**, respectively.

Calibration

The calibration graphs for the anions **I–III** were measured using standard solutions of non-hygroscopic tetramethylammonium salts instead of highly hygroscopic sodium salts with variable water contents. The calibration graphs are shown in Fig. 9. The relationships between peak area and amount of the tetramethylammonium salts of anions **I, II** and **III** was linear up to concentrations of 50, 26 and 50 mg/ml, respectively. As no other peaks or baseline drift were observed, it was concluded that no oxidation of the compounds actually occurred.

*Stability of anion **I** in aqueous solutions*

Recent papers dealing with the isotachophoretic determination of anion **I** [7] and the preparation of its oxidation products [8] initiated studies of the oxidation processes involving $Cs_2B_{12}H_{11}SH$ in aqueous solutions exposed to air. Nevertheless, comparison of the experimentally determined estimates of the oxidation rates thus obtained indicates some discrepancies.

As we have found, dissolution of real analytical samples of the sodium salt of the anion **I** in different lots of distilled water in the course of analyses and the use of chemicals of different quality in the syntheses cause considerable fluctuations in the oxidation rates during the storage of aqueous samples (*e.g.*, compare Figs. 3 and 4). Therefore, a study of the influence of several factors, including metal impurities, on the stability of aqueous solutions of **I** was performed.

Additions of Fe^{2+}, Co^{2+}, Ni^{2+} and Cr^{3+} salts to the Milli-Q-purified water solutions of the sodium

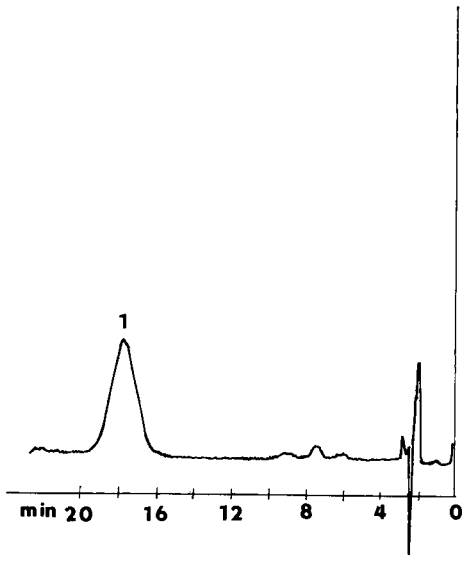

Fig. 7. determination of the $[B_{12}H_{11}SCSC_6H_4NCH_3]^-$ anion (peak 1), an intermediate adduct of N-methylbenzothiazole-2-thione with the *closo*-$[B_{12}H_{12}]^{2-}$ anion formed in the sulphydrylation step [2] of the synthesis of **I**. Temperature, 45°C; eluent, 0.1 *M* solution of $NaClO_4$ in acetonitrile–water (25:75).

salt of anion **I** (drug form containing 8% of sodium salt of **II**; Léčiva Měcholupy, Czechoslovakia) in amounts corresponding to ten times smaller molar concentrations than that of **I** caused a decrease in the concentration of anion **I** only at the beginning of a 10-day study, owing to the formation of a weakly dissociated salt. On the other hand, addition of Cu^+ ions at a comparatively low concentration affected the oxidation rate very strongly. This effect is exemplified in Figs. 5 and 10, showing that the presence of a trace amount of Cu^+ caused complete oxidation of anion **I** within a few days. Moreover, the replacement of Cu^+ with Cu^{2+} increased the oxidation rate within the initial 3 h of oxidation, which resulted in an increased content of anion **II** in the sample. However, the composition of the products after an 8-day period was identical with that in the presence of Cu^+, which seems to be consistent with the involvement of a Cu^+–Cu^{2+} equilibrium in the oxidation mechanism. Another experiment indicated that the addition of Fe^{3+} causes an equivalent part of anion **I** to be oxidized to generate a mixture of compound **III** with an unknown oxidation product **IV**. In agreement with earlier findings [4], the oxidation of $Na_2B_{12}H_{11}SH$ with hydrogen peroxide gave anion **III** directly, but we also identified two other peaks of unknown oxidation impurities (**IV** and **V**), in small amounts, in the corresponding reaction mixture.

The above-mentioned observations indicate that the oxidation rate can be affected by the presence of trace amounts of some transition metal ions and probably also by other substances present in the water used. Indeed, in samples of compounds of anion **I** dissolved in the commonly used distilled water (single distillation step), the disappearance of anion **I** was observed after 8–20 days (an example is shown in Fig. 3), depending on the initial concen-

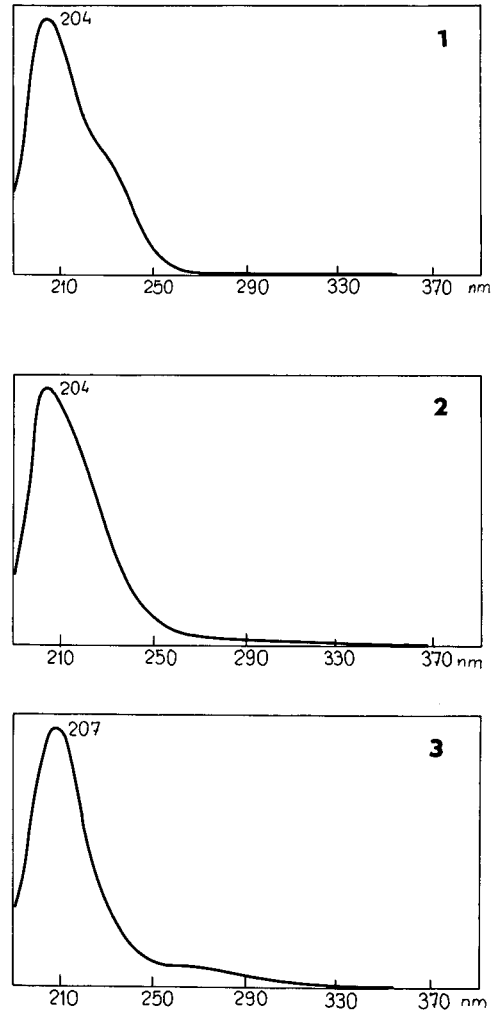

Fig. 8. Plots of UV spectra of anions **I**–**III**. 1 = $[B_{12}H_{11}SH]^{2-}$ **I**; 2 = $[B_{12}H_{11}SSB_{12}H_{11}]^{4-}$ **II**; 3 = $[B_{12}H_{11}S(O)SB_{12}H_{11}]^{4-}$ **III**.

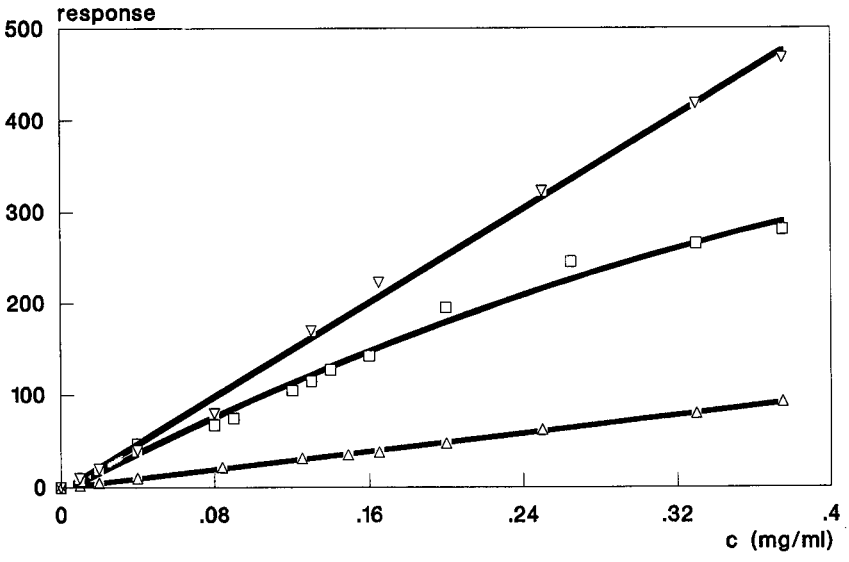

Fig. 9. Calibration graphs for tetramethylammonium salts of anions **I–III**. Chromatographic conditions as in Fig. 4; detection, UV at 204 nm; sensitivity, 0.16 a.u.f.s. Curves: △, $[B_{12}H_{11}SH]^{2-}$ **I**; □, $[B_{12}H_{11}SSB_{12}H_{11}]^{4-}$ **II**; ▽, $[B_{12}H_{11}S(O)SB_{12}H_{11}]^{4-}$ **III**.

tration of **I** (0.1–5.46 μmol/ml). It was also found that the free acid of anion **I** exhibited lower and the tetramethylammonium salt higher stability than the sodium salt under comparable conditions.

In contrast, the stability of solutions of the sodium salt of **I** in Milli-Q-purified water was appreciably higher. Three standard solutions (0.65, 1.14 and 2.20 μmol/ml) of the drug form of $Na_2B_{12}H_{11}SH$ (containing 8% of the sodium salt of **II**) were used in this study. The samples were analysed at 24 h intervals over a period of 10 days. The first and third sample were also analysed after a 123-day exposure to air. At the end of the 10-day period, the concentration of anion **I** was found to be almost unchanged (Fig. 4), with only 2% (w/w) of the sodium salt of **III** being generated from the oxidation of the anion **II** present. After 123 days, a 28% and 31% decrease in the content of anion **I** and corresponding increases of 14 and 17% of **II** and 11 and 12% of the sodium salt ion **III** in the samples of initial concentrations 2.2 and 0.65 μmol/ml, respectively were found. At least three additional but unidentified oxidation impurities with k' values lower than that of anion **I**, which were not found in the most concentrated sample, could be detected in the most diluted sample.

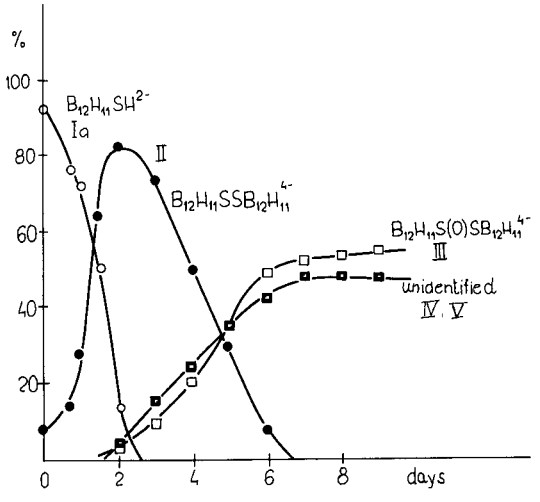

Fig. 10. Time course of the oxidation of the drug form of the sodium salt of anion **I** (1.14 μmol/ml) in aqueous solution (Milli-Q-purified water) in the presence of a trace amount of Cu^+ (130 μg/l). The curve represents the percentage of sodium salts of anions **I–III** and unknown hydroborate impurities **IV** and **V**.

CONCLUSIONS

A simple, rapid and quantitative method, based on HPLC on the hydroxyethylmethacrylate Separon HEMA-BIO 300 (12 μm) sorbent, was devel-

oped for purity assay and determination of $Na_2B_{12}H_{11}SH$. Optimum separation was obtained using 0.1 *M* aqueous $NaClO_4$ in 0.01 *M* phosphate buffer (pH 8.5) as the mobile phase and direct UV detection at 204 nm. The method can also be used for sensitive detection and determination of both of the most significant oxidation impurities, $Na_4B_{12}H_{11}SSB_{12}H_{11}$ and $Na_4B_{12}H_{11}S(O)SB_{12}H_{11}$.

The oxidation study also revealed an unexpectedly high resistance of aqueous $Na_2B_{12}H_{11}SH$ solutions oxidation when sufficiently pure water is used for sample preparation. An appreciable effect of trace amounts of Cu^+ on the increase in the oxidation rate was demonstrated.

ACKNOWLEDGEMENTS

We are grateful to Mr. V. Opočenský (Analytical Department, Léčiva Měcholupy, Czechoslovakia) for the method verification and permission to publish the UV spectra. They thank Drs. J. Plešek, B. Štíbr and T. Jelínek from the Institute of Inorganic Chemistry, Czechoslovak Academy of Sciences, for the samples of $(H_3O)_2B_{12}H_{11}SH$, $[(CH_3)_4]_2B_{12}H_{11}SH$ and $Na_2B_{12}H_{11}$ and Dr. S. Heřmánek for the identification of individual compounds by ^1H and ^{11}B NMR spectroscopy. Dr. B. Štíbr is thanked for helpful discussions.

REFERENCES

1 H. Hatanaka, *Boron Neutron Capture Therapy for Tumors*, Nishimura, Nigata City, 1986, p. 349.
2 E. I. Tolpin, G. R. Wellum and S. A. Berley, *Inorg. Chem.*, 17 (1978) 2867.
3 J. Plešek, B. Štíbr, T. Jellínek and S. Heřmánek, unpublished results.
4 G. R. Wellum, E. I. Tolpin, L. P. Andersen and R. Sneath, *J. Chromatogr.*, 103 (1975) 153.
5 G. R. Wellum, E. I. Tolpin, A. H. Soloway and A. Kacmarczyk, *Inorg. Chem.*, 16 (1977) 2120.
6 I. Ikeuchi and T. Amano, *Chem. Pharm. Bull.*, 26 (1978) 2619.
7 I. Ikeuchi and T. Amano, *J. Chromatogr.*, 396 (1987) 273.
8 K. Nagasawa, Y. Ikenishi and Y. Nakagawa, *J. Organomet. Chem.*, 391 (1990) 139.
9 B. Grüner, Z. Plzák and I. Vinš, *J. Chromatogr.*, 588 (1991) 201.
10 H. C. Miller and E. L. Muetterties, *Inorg. Synth.* 10, (1967) 90.
11 J. Plešek, E. Drdáková and B. Štíbr, *Czech. Pat.*, 238 254 (1986).

Journal of Chromatography, 595 (1992) 179–184
Elsevier Science Publishers B.V., Amsterdam

CHROM. 23 961

High-performance liquid chromatography of sulphonamides extracted from bovine and porcine muscle by solid-phase dispersion

L. V. Walker*, J. R. Walsh and J. J. Webber

Regional Veterinary Laboratory, Department of Agriculture, P.O. Box 406, Hamilton, Victoria 3300 (Australia)

(First received July 16th, 1991; revised manuscript received December 16th, 1991)

ABSTRACT

A method has been developed for the analysis of sulphonamides in bovine and porcine muscle, based on solid-phase dispersion. Muscle tissue was blended with pre-washed C_{18} coated silica (55–105 μm), and the resulting homogeneous solid packed into a polypropylene syringe barrel. Fatty material was washed from the sample using hexane, and the sulphonamide analytes eluted with dichloromethane. The collected fraction was dried under nitrogen and reconstituted in 20% methanol in 0.01 *M* sodium acetate/acetic acid (pH 5) buffer. After sonication and filtration, the sample was analysed by high-performance liquid chromatography on a C_{18} column using UV diode array detection. Individual sulphonamides could be detected down to 0.01 ppm, whilst analyte identity could be confirmed by diode array spectrum down to 0.02 ppm.

INTRODUCTION

The maximum residue limit (MRL) in Australia for sulphamethazine and sulphadiazine in bovine and porcine muscle tissue is 0.1 ppm. A method for sulphonamide extraction from muscle was therefore required which would allow assays in the 0.02–0.05 ppm range, with very low signal-to-noise ratios at the MRL.

Extraction of sulphonamides from tissues traditionally has been performed by any of a large number of variations on liquid–liquid partitioning [1–5], or more recently by liquid extraction followed by solid-phase extraction [6,7]. A new extractive technique has been described, solid-phase dispersion (SPD) [8], and applied to the extraction of sulphonamides from milk [9], pig muscle [10], fish [11] and infant formula [12]. In this method, the sample was dispersed over a large area of C_{18} derivatised silica —typically 0.5 g of tissue over 1000 m^2 of surface area, allowing practically total exposure of the sample to an extracting solvent. The dispersed material is packed into a column (a syringe barrel) and eluted according to a normal-phase chromatographic sequence with a relatively low volume (< 10 ml) of dichloromethane, from which a sample is easily prepared for chromatography.

In the method presented below, the SPD technique has been modified to allow greater sensitivity and higher sample throughput than the original published method [8], applied to the analysis of spiked and incurred sulphonamide residues in bovine and porcine muscle, and then applied in surveillance and monitoring testing programs in Australia.

MATERIALS AND METHODS

Chemicals

Hexane, ethyl acetate (Nanograde; Mallinckrodt, Paris, KY, USA), acetonitrile, methanol, dichloromethane (HPLC grade; Waters, Milford, MA, USA), sulphisomidine, sulphadiazine, sulphathiazole, sulphamerazine, sulphamethazine (Sigma, St.

0021-9673/92/$05.00

Louis, MO, USA), anhydrous sodium acetate (AnalaR grade; BDH, Kilsyth, Australia), acetic acid (analytical-reagent grade; Mallinckrodt).

Disposables

Plastic weighing trays (80 mm × 80 mm × 20 mm); No. 22 scalpel blades (Swann-Morton, Sheffield, UK); C_{18} silica (Waters Preparative C_{18}; 55–105 μm, 125 Å pore size, end-capped, 12% carbon load); 10-ml and 1- or 2-ml polypropylene disposable syringes (Terumo, Melbourne, Australia); filter paper Whatman 541 (Whatman, Maidstone, UK); silanised glass wool; 0.45-μm disposable disc filters with slip Luer fitting (FlowPore D26; Flow Laboratories Australasia, North Ryde, Australia); Luer-Lock needles; 1.25 × 38 mm (Becton Dickinson, Singapore); autosampler vials.

Equipment

Sample preparation. 20- or 50-ml glass syringe barrel, for washing C_{18} solid phase; Sample evaporator (Turbovap; Zymark, Hopkinton, MA, USA); ultrasonic bath (FX-8; Unisonics, Sydney, Australia).

Liquid chromatograph. Varian Star System (Varian, Walnut Creek, CA, USA), comprising a 9010 ternary pump, 9065 diode array UV spectrophotometer (190–367 nm range), 9095 autosampler (6-port Valco, 1-ml loop), data handling and system control PC (Varian Star software).

LC columns. C_{18} Novapak 100 mm × 8 mm Radial-Pak cartridge (end-capped, 4-μm particle, 60 Å pore, 7% carbon load) and μBondapak C_{18} guard column (end-capped, 6–12 μm, 125 Å, 11% carbon load) (Waters).

Chromatographic conditions

LC solvents. (A) 0.01 *M* sodium acetate, buffered to pH 5 with acetic acid; (B) 100% acetonitrile.

LC conditions. Flow-rate, 2.4 ml/min. Start, 100% A; 8 min, A–B (60:40); 12 min, A–B (60:40); 15 min, 100% A; 20 min, 100% A.

Preparation of solid phase

Bulk C_{18}-coated silica (C_{18}) was washed in twice its own volume of hexane, dichloromethane, ethyl acetate and methanol (in succession) by drawing the solvent through a glass syringe packed with C_{18}. The C_{18} was air-dried after the methanol wash, and has an indefinite shelf life once sealed away.

Sample preparation

For successful assay of a muscle sample for sulphonamides, the tissue must be of high quality. The assay required meat trimmed free of fat and connective tissue.

Slivers of trimmed frozen muscle were then shaved off using a scalpel, and transferred directly to a plastic weighing tray for a final sample mass of 1 g. At this stage, the sample was either spiked with sulphonamides for a recovery assay, or spiked with 100 μl of 1 μg/ml sulphisomidine in methanol as an internal standard. To this was added 2.5 g of the washed and dried C_{18}. Each sample was then ground into a homogeneous solid, using a test tube as the pestle. The blending was performed using a pressing and light grinding action, rather than an outright grinding action, to minimise crushing of the silica. The blended material was shredded using the pestle and a spatula and then packed into 10-ml polypropylene syringe barrels which had the outlets plugged with silanised glass wool. The sample was topped off with a disc of filter paper and then compressed down to approximately 4 ml, using the syringe plunger from which the rubber end and plastic support had been cut off to give a flat-ended plunger.

The column was then filled to the top with hexane, which was either allowed to drain through, or aspirated through under a mild vacuum. Air was then blown through or a mild vacuum applied to the column to remove excess hexane and give a dry-appearing sample. The column was then filled to the top with dichloromethane, and again either aspirated or allowed to drain directly into a 50 ml Turbovap tube, until the column appeared dry. The collected fraction was reduced to dryness in the Turbovap under dry nitrogen. The dried extract was then reconstituted in 200 μl of methanol, vortex mixed, and a further 800 μl of the first chromatographic mobile phase added. The sample was again vortex mixed, and then placed in an icewater-filled ultrasonic bath for 15–20 min. The resulting opaque suspension was drawn up in a 1- or 2-ml disposable syringe, and filtered, through a 25-mm diameter 0.45-μm filter, into HPLC autosampler vials.

Sample analysis

A 300-μl volume sample was injected for each run, although up to 1 ml could be used if desired.

UV absorbance was monitored at 263 nm, with a usable diode array range of 220–367 nm available for confirmation of compounds by their spectral characteristics.

RESULTS AND DISCUSSION

The determination of sulphonamide residues in muscle tissue on a regular basis requires an assay that is fast and relatively cheap and has a high degree of repeatability. To allow other laboratories to adopt the method without great capital outlay, the equipment required for the assay must also be readily available and reuseable, or if not, of low enough cost to be disposable.

To this end the solid-phase dispersion method was examined for use in this assay. Initial work was performed at the 1 ppm level using readily available Waters C_{18} (in the ratios of the initial work [8]). This indicated far higher recoveries than had been found with the more traditional wet extractive methods of analysis: around 90–100% recovery for sulphadiazine, sulphamerazine and sulphamethazine. Further examination revealed only slightly lower recoveries at 0.1 ppm. The process was re-examined in an effort to increase the sample size to 1 g or more, in a final volume of 1 ml. It was found that a sample of 1 g of tissue to 2.5–3 g of C_{18} was readily prepared without loss of recovery. The method as developed allowed the detection and quantitation to 0.01 ppm and diode array confirmation down to 0.02 ppm for sulphadiazine, sulphathiazole, sulphamerazine and sulphamethazine.

Chromatograms of a 0.1-ppm standard, an unspiked muscle and a muscle sample spiked at 0.1 ppm are given in Fig. 1A–C. The spiked muscle gave recoveries (intra-assay) of 85% for sulphadiazine, 37% for sulphathiazole, 80% for sulphamerazine and 76% for sulphamethazine. Results for these muscle samples spiked at 0.1 ppm are given in Table I, along with inter-assay data taken from 12 successive spikes associated with actual assays made with this method. Muscle samples spiked at 0.05 ppm gave recoveries equivalent to those obtained at 0.1 ppm, although the relative standard deviation (R.S.D.) of sulphadiazine and sulphathiazole increased markedly at the lower level. Results for these muscle samples spiked at 0.05 ppm are also presented in Table I. Four replicates are used at

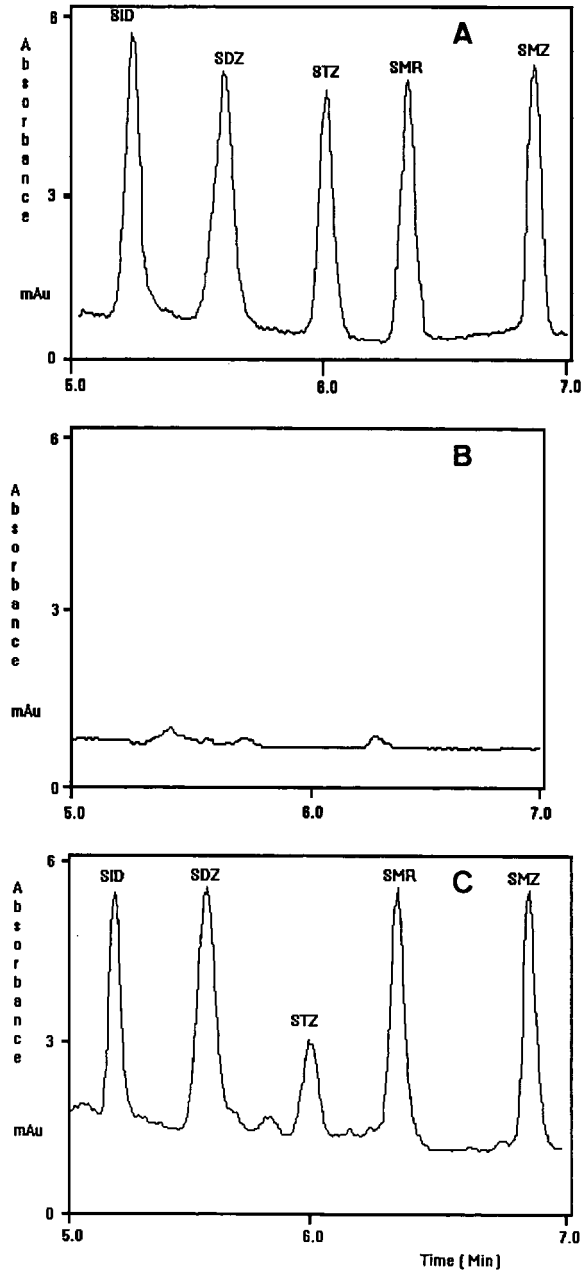

Fig. 1. (A) Chromatogram of 0.1 ppm standard; (B) chromatogram of unspiked bovine muscle; (C) chromatogram of 0.1 ppm spiked bovine muscle. SID = sulphisomidine; SDZ = sulphadiazine; STZ = sulphathiazole; SMR = sulphamerazine; SMZ = sulphamethazine. Chromatographic conditions: Absorbance monitored at 263 nm; gradient 0–40% acetonitrile over 8 min, hold 4 min, 40–0% acetonitrile over 3 min, hold at 100% acetate buffer for 5 min; flow-rate 2.4 ml/min.

TABLE I

INTRA- AND INTER-ASSAY RECOVERY OF SULPHONAMIDE ANALYTES FROM BLANK CALF MUSCLE SPIKED AT 0.1 PPM AND 0.05 PPM

Chromatographic conditions as in Fig. 1.

Analyte	Spike value (ng/g)	Intra-assay (n = 4)			Inter-assay (n = 12)	
		Mean (ng/g)	Recovery (%)	R.S.D. (%)	Recovery (%)	R.S.D. (%)
Spiked at 0.1 ppm						
Sulphadiazine	130	110	85	5	71	10
Sulphathiazole	103	38	37	8	38	31
Sulphamerazine	99	80	80	4	82	16
Sulphamethazine	104	79	76	6	80	10
Spiked at 0.05 ppm						
Sulphadiazine	65	50	77	22		
Sulphathiazole	52	22	42	27		
Sulphamerazine	50	41	82	2		
Sulphamethazine	52	38	73	8		

each spike level, to allow calculation of standard deviation and recovery percentages.

Fig. 2 shows the resulting chromatogram from an animal which was injected with a therapeutic dose of sulphamethazine approximately one week prior to slaughter. The level of sulphamethazine found was 0.10 ppm (corrected for recovery data of Table I). The diode array spectrum for sulphamethazine in the incurred residue sample *vs.* the sulphamethazine spectrum of the standard is given in Fig. 3.

Fig. 4 shows the spectrum of sulphisomidine added to the incurred residue sample *vs.* the sulphisomidine spectrum from the standard. Sulphisomidine, as an internal standard, may be used for calculation of analyte quantities but is also useful as a reference marker in chromatographic runs. The sulphisomi-

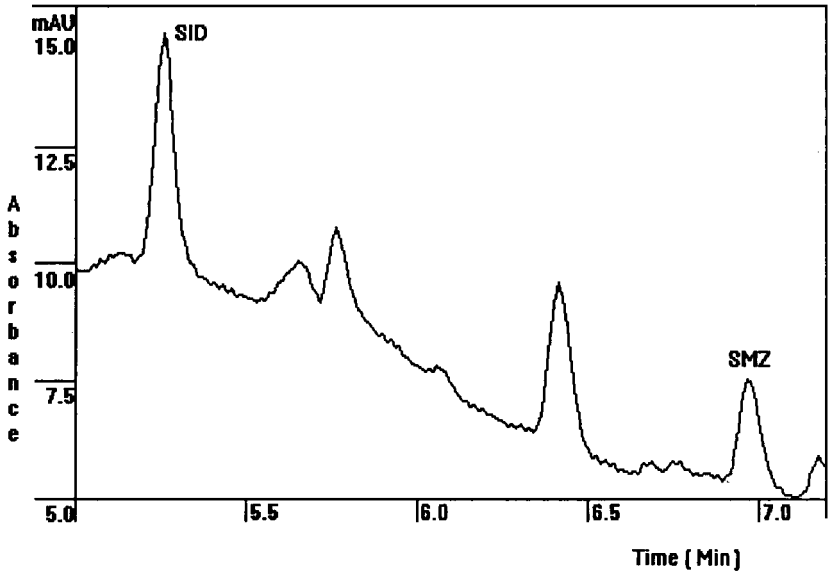

Fig. 2. Chromatogram of incurred sulphamethazine sample. SID = Sulphisomidine; SMZ = sulphamethazine. Chromatographic conditions as in Fig. 1.

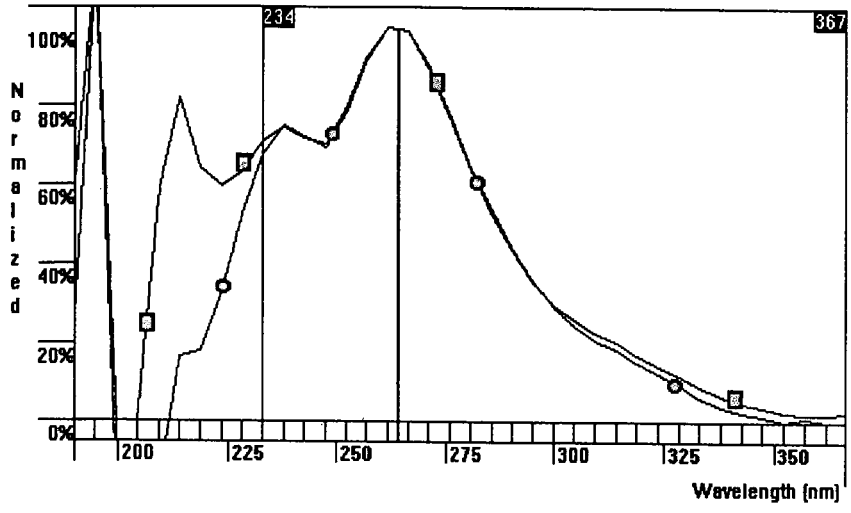

Fig. 3. Diode array spectrum of sulphamethazine from the incurred sample *vs.* sulphamethazine from the standard in Fig. 1A. ◘ = Incurred sample; O = standard.

dine peak may be recognised by its characteristic spectra (see Fig. 4), and used as an indicator for the relative position of the other analyte peaks if the retention times have moved during an extended period of operation (*e.g.*, overnight).

Other C_{18} packings were tried in the course of the method development. Two different 40-μm packings were obtained: Analytichem (originally specified [8]) and Davisil (Alltech, Deerfield, IL, USA). These had the theoretical advantage of larger surface area, giving higher sample loads. In practice it was found that a larger quantity of solid phase was required to form a dry homogenate with the tissue, and the material was generally more difficult to handle and blend than the coarser Waters material. The finer packings tended to "clump" together, and the homogenate was formed when enough C_{18} was added to coat and blend through the tissue matrix. The coarser Waters material tended to cut through and fragment the tissue matrix with significantly

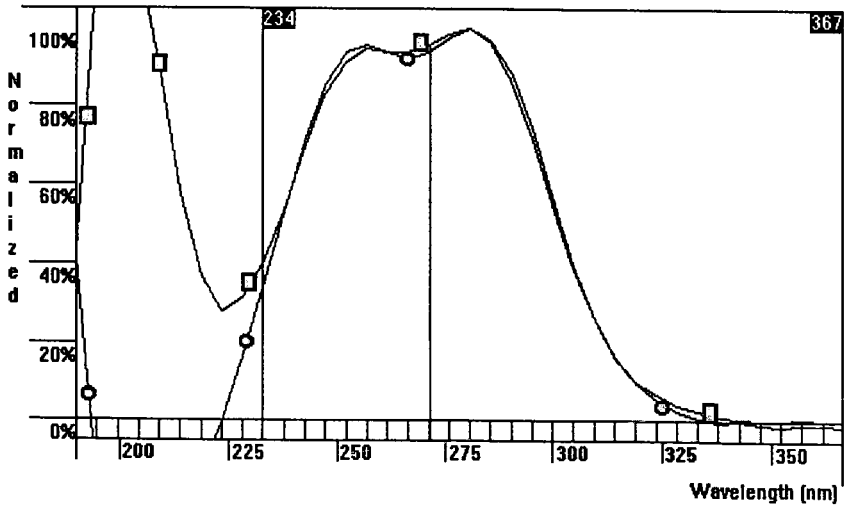

Fig. 4. Diode array spectrum of internal standard sulphisomidine in incurred SMZ sample *vs.* sulphisomidine in the standard of Fig. 1A. ◘ = Incurred SMZ sample; O = standard.

less effort, whilst tending to "clump" less even on very moist tissue. The 40-μm packings proved to be inferior overall, with recoveries well below that obtained with the Waters material. This was found to be caused partly by vacuum cavitation in the packed bed during washing and eluting. Elution under gravity improved the yield, although not to the level obtained with the Waters material. Whilst the SPD method may be used with gravity or vacuum elution, the sample throughput is significantly increased by vacuum elution. The restrictions inherent in using the fine grade C_{18} packings, both from the sample preparation and elution aspects, were felt to be unacceptable.

The SPD method allows for fast sample extraction and clean-up whilst using a minimum of extraction solvent. This technique, unlike traditional solvent extraction procedures, is quite easily expanded to allow a single operator to process multiple samples in one day (up to 20).

A limitation inherent in the method is that of sample size. If a sample much greater than 1 g is used, the sample preparation becomes more time consuming in both blending and eluting. If scaling-up was required, it would actually be easier to prepare the sample in multiple batches of 1 g, and elute all of the columns into the one Turbovap tube for drying. The speed of the method would be seriously jeopardised if more than 5 g of sample were required. Loss of sample homogeneity through directly taking 1 g of a tissue sample has not to date appeared as a problem. The method has performed well in Australian quality assurance programmes, competing successfully against a variety of liquid-extraction and solid-phase extraction methods, all using homogenized muscle samples.

The use of UV diode array detection in the assay allowed for the positive identification of sulphonamide analytes without actually having to re-run the samples in question. The acetate buffer used had significant advantages over similar pH phosphate, citrate or oxalate buffers with respect to the operation and use of a diode array instrument. The detector used had an operational wavelength range from 190 to 367 nm, but absorption from the acetonitrile and the acetate buffer reduced this range to 220–367 nm. The phosphate, citrate and oxalate buffers tended to raise the lower operational wavelength to around 250 nm. As the absorbance maxima for three of the five sulphonamides was 263 nm, spectral information useful or vital for analyte confirmation was lost. Confirmation of an analyte from its 220–367 nm spectrum was readily made against library spectra from samples spiked at 0.1 ppm (such as Fig. 1C). Library referencing could be made either manually (post-run) or as an extension of the automated post-run computing sequence. The library spectra were found to be of more use if taken from chromatograms of spiked samples, as this provided the background which was otherwise missing from pure standards. This also allowed the analyte species to be confirmed down to 0.02 ppm.

The SPD method opens up possible sample sources which would not be considered feasible by the more traditional wet extraction methods. As only 1 g of quality tissue is required, muscle biopsies are possible, and may be of great value in trace-back operations, similar to those followed for organochlorine residues monitoring in Australia. Similarly, the small sample required could allow for random monitoring of carcasses at an abattoir with minimal or no damage to the carcass.

REFERENCES

1 H. J. Lindsay, P. J. Smith and P. J. Love, presented at the *10th Australian Symposium on Analytical Chemistry, Brisbane, August 28–September 1, 1989.*
2 R. F. Bevill, R. M. Sharma, S. H. Meachum, S. C. Wozniak, D. W. A. Bourne and L. W. Dittert, *Am. J. Vet. Res.*, 38 (7) (1977) 973–977.
3 B. L. Cox and L. F. Krzeminski, *J. Assoc. Off. Anal. Chem.*, 65 (6) (1982) 1311–1315.
4 H. Holmsberg, J. R. Andersen, E. Larsen, C. T. Petersen, K. Knudsen and C. Friis, *Proceedings of the 35th International Congress of Meat Science and Technology, Denmark, 1989,* pp. 646–649.
5 S. C. Mutha, T. L. Brown, B. Chamberlain and C. E. Lee, *J. Agric. Food Chem.*, 25 (3) (1977) 556–558.
6 M. Horie, K. Saito, Y. Hoshino, N. Nose, N. Hamada and H. Nakazawa, *J. Chromatogr.*, 502 (1990) 371–378.
7 N. Haagsma and C. van de Water, *J. Chromatogr.*, 333 (1985) 256–261.
8 S. A. Barker, A. R. Long and C. R. Short, *J. Chromatogr.*, 475 (1989) 353–361.
9 A. R. Long, C. S. Short and S. A. Barker, *J. Chromatogr.*, 502 (1990) 87–94.
10 A. R. Long, L. C. Hsieh, M. S. Malbrough, C. R. Short and S. A. Barker, *J. Agric. Food Chem.*, 38 (1990) 423–426.
11 A. R. Long, L. C. Hsieh, M. S. Malbrough, C. R. Short and S. A. Barker, *J. Assoc. Off. Anal. Chem.*, 73 (6) (1990) 868–871.
12 A. R. Long, L. C. Hsieh, M. S. Malbrough, C. R. Short and S. A. Barker, *J. Liq. Chromatogr.*, 12 (1989) 1601–1612.

Journal of Chromatography, 595 (1992) 185–192
Elsevier Science Publishers B.V., Amsterdam

CHROM. 23 851

Aqueous high-performance size-exclusion chromatographic assay for high-molecular-weight impurities in ceftiofur sodium

Michael J. Dunn and David A. Hahn*

The Upjohn Company, Control Development, 4823-259-12, Kalamazoo, MI 49001 (USA)

(First received July 9th, 1991; revised manuscript received November 4th, 1991)

ABSTRACT

An aqueous high-performance size-exclusion chromatographic assay for high-molecular-weight (HMW) impurities in ceftiofur sodium bulk drug is described. The assay uses a sodium dodecyl sulfate micellar mobile phase to provide complete recovery of the analyte from a glycerylpropyl-bonded silica column. Using 254-nm absorbance detection corrected for relative detector response, the assay provides a linear response and complete recovery of HMW impurities. The relative standard deviation for repeated assay of a single bulk drug lot is 2.5%, with systematic variation of column, mobile phase batch, analyst, laboratory, instrument and day. The detection limit is 0.03%.

INTRODUCTION

The β-lactam antibiotics, which include both the cephalosporins and the penicillins, have long been known to contain autologous high-molecular weight (HMW) impurities [1,2]. These HMW impurities are considered potential antigens, but have been reported to be weakly antigenic, at most, when administered parenterally [3]. In contrast, HMW conjugates between β-lactams and proteins have been reported to induce allergic reactions.

Formation of HMW impurities in aqueous solutions of penicillins or cephalosporins is well documented [4,5] and these materials have been characterized chemically and immunologically. HMW impurities from penicillins have been reported to be amide-linked polymers of β-lactam ring-opened degradation products of the parent antibiotic [4–7]. We have found no published data on the structure of cephalosporin-related HMW impurities, although efforts to identify such materials are occasionally mentioned parenthetically. High-performance aqueous size-exclusion methods have been developed to determine HMW impurities in both penicillins and cephalosporins [8–10].

Ceftiofur sodium (Sterile Powder Naxcel) is a cephalosporin antibiotic marketed by Upjohn for the treatment of bovine respiratory disease. During analytical development, thin-layer chromatography (TLC) indicated the presence of HMW impurities in ceftiofur sodium bulk drug which were not detected using a reversed-phase gradient high-performance liquid chromatographic (HPLC) assay. A high-performance size-exclusion chromatographic (HP-SEC) method was developed to determine the HMW impurities, using an aqueous mobile phase to provide adequate analyte solubility. Competing separation mechanisms typical of aqueous SEC assays were encountered, including ion exclusion, adsorption and salting-out effects [11]. Addition of micellar sodium dodecyl sulfate (SDS) to the mobile phase was required in order to obtain complete recovery of HMW impurities from the analytical column. Previously published methods [8–10] were investigated; none provided complete recovery of ceftiofur HMW impurities from the column.

This paper describes the development of a quantitative aqueous HPSEC assay for these HMW impurities in ceftiofur sodium bulk drug, with particular attention to optimizing resolution and achieving complete recovery. Validation of the method for use in pharmaceutical quality control is also described.

EXPERIMENTAL

Reagents

Ceftiofur sodium and ceftiofur hydrochloride bulk drug lots were provided by Upjohn (Kalamazoo, MI, USA). Deionized water was prepared using a Milli-Q purification system (Millipore, Bedford, MA, USA). HPLC-grade solvents were obtained from Baxter, Burdick and Jackson (Muskegon, MI, USA). Other reagents were of analytical-reagent grade obtained from Mallinckrodt (St. Louis, MO, USA) or Aldrich (Milwaukee, WI, USA). All reagents and solvents were used as received.

Chromatography

The assay uses a 250 mm × 4 mm I.D. LiChrospher 100 DIOL (5-μm particle size) glyceryl-propyl (diol) silica column with 100 Å pore size (EM Science, Cherry Hill, NJ, USA). Other chromatographic experiments utilized 250 mm × 4 mm I.D., 5μm particle size silica columns: LiChrospher Si 100 silica (EM Science), Zorbax TMS C_1 bonded phase (MAC-MOD, Chadds Ford, PA, USA), Vydac Protein C_4 bonded phase (Separations Group, Hysperia, CA, USA), Zorbax C_8 bonded phase (MAC-MOD), Zorbax ODS C_{18} bonded phase (MAC-MOD), Zorbax CN cyano bonded phase (MAC-MOD), Brownlee aminopropyl-bonded phase (Brownlee Labs., Santa Clara, CA, USA) and a TSK 2000 SW aqueous size-exclusion column with proprietary inactivation chemistry (Phenomenex, Torrance, CA, USA).

The HPLC system consisted of a Beckman (Fullerton, CA, USA) Model 110A isocratic pump, a Rheodyne (Cotati, CA, USA) Model 7135 loop injection valve with pressure bypass and either an LDC UV-Monitor III 254 nm line source detector (LDC/Milton Roy, Riviera Beach, FL, USA) or a Waters Model 410 differential refractive index detector (Millipore–Waters, Milford, MA, USA). Chromatographic data were collected and analyzed using an in-house VAX-based (Digital Equipment, Maynard, MA, USA) chromatographic data system. Data analysis was performed using SAS Version 5.16 (SAS Institute, Cary, NC, USA).

The mobile phase for the optimized HPSEC assay procedure was made by preparing a 0.005 *M* potassium orthophosphate solution, adjusting the pH to 7.5 with the addition of concentrated potassium hydroxide solution, adding 1% (w/v) SDS, stirring until completely dissolved and vacuum filtering/degassing through a 0.45-μm nylon-66 filter (Rainin, Woburn, MA, USA). Other mobile phases were prepared similarly, as indicated under Discussion. The pH was measured using a Sargent-Welch (Skokie, IL, USA) pH 6000 with an S-30072-15 combination electrode.

Samples for assay were dissolved at *ca.* 0.1 mg/ml in mobile phase and 20 μl were injected, avoiding contact with plastic vial caps or tubing (*ca.* 2 μg on-column). The flow-rate of the system was maintained at 1.0 ml/min. Elution volumes of totally included and totally excluded analytes were approximated using sodium nitrate and blue dextran, respectively. The peak-area percentage of the HMW impurities was determined, and this was divided by a relative response factor (*RRF*) of 0.81 to account for the relative detector response. Correction for co-eluting low-molecular-weight impurities, if any, is accomplished using data from a separate low-molecular-weight impurities assay. The weight percentage of HMW impurities can be calculated, if desired, from the peak-area percentage result (corrected for *RRF*) using as-is major component potency and low-molecular-weight impurities data from separate HPLC assays.

Preparation of isolated HMW impurities

Isolated HMW impurities were prepared by dissolving 10 g of a ceftiofur sodium lot containing HMW impurities in 200 ml of 0.1 *M* sodium phosphate buffer (pH 7). The solution was filtered through a 45-mm Diaflo Model YM2 1000-dalton (nominal) ultrafiltration membrane (Amicon, Danvers, MA, USA) fitted to an Amicon Model 8050 stirred ultrafiltration cell. The material retained on the membrane was rinsed with two 50-ml portions of water, dissolved from the top of the membrane in *ca.* 5 ml of water, frozen in liquid nitrogen and

freeze-dried using a Labconco (Kansas City, MO, USA) Model 75035 vacuum freeze-drying apparatus. The purity and HPSEC elution profile of the isolated material were determined using the HPSEC impurities assay.

Absolute recovery from column

Recovery of HMW impurities from the column was investigated by directly comparing the amount eluted from the column with the amount injected. Filled loop injection was used to control the injection volume precisely. First, 20 μl of a solution of isolated HMW material (8.5 μg) were injected onto the column and the total effluent was collected. Then the same volume was injected without a column in-line and the effluent was collected. The amount of each collected solution was determined gravimetrically, the absorbance at 254 nm was measured for each solution and the percentage recovery was calculated.

Relative response factor

The *RRF* is the ratio of the chromatographic detection response of the analyte per unit weight to that of ceftiofur. The *RRF* for HMW impurities relative to ceftiofur was determined using two approaches. In the first, the absorbance at 254 nm was determined using a line source detector for separate mobile phase solutions containing a known concentration of either the HMW impurities or ceftiofur. The resulting mass absorptivities were then ratioed to determine the relative response. In the second approach, the slope of the recovery study uncorrected amount found *vs.* amount added data is taken as the *RRF*. Absorption spectra of ceftiofur and isolated HMW impurities were measured using a Hewlett-Packard (Palo Alto, CA, USA) Model 8450A diode-array spectrophotometer or a Hewlett-Packard Model 1090A chromatograph with a diode-array detector.

Recovery study

A bulk drug lot of ceftiofur hydrochloride containing 1.86% of HMW impurities was spiked with isolated HMW impurities up to 7.86%. The peak-area percentage of HMW impurities was determined using the optimized assay with an *RRF* of 0.81 and the percentage of recovery was calculated for each point.

RESULTS AND DISCUSSION

During early analytical development for ceftiofur sodium, a non-migrating impurity was detected in a silica TLC impurities screen. Visible amounts of a non-eluting impurity were also noted at the inlet of a reversed-phase HPLC column used for ceftiofur impurities assays. These materials were hypothesized to be HMW impurities, and this was confirmed by their retention on an ultrafiltration membrane with a 1000-dalton nominal molecular weight cut-off, about twice the 522.56-dalton molecular weight of ceftiofur free acid. However, ultrafiltration does not provide definitive molecular weight information because retentivity depends on molecular size, shape and hydration, and at low molecular weights the correlation between retentivity and molecular weight is not as great as at higher molecular weight. Because the HMW impurities could not be assayed using existing methods, a separate chromatographic assay was developed.

Several types of stationary phase were screened to determine the most suitable chromatographic mode for the separation, inlcuding C_1, C_4, C_8 and C_{18} bonded-phase columns, a silica column, cyano and aminopropyl bonded-phase columns, and two different aqueous size-exclusion columns. For each column, mobile phase pH, organic content and buffer concentration were varied in attempts to obtain an acceptable separation. Both ceftiofur sodium and the HMW impurities show high aqueous solubility and generally low non-aqueous solubility, and ceftiofur solution stability is reduced at basic or acidic pH, focusing consideration on aqueous-based near-neutral mobile phases. Aqueous size-exclusion chromatography was the only investigated chromatographic mode in which the HMW impurities were eluted from the column at mobile phase pH below 8. The LiChrospher DIOL size-exclusion column (100-Å pore size) was selected for further assay development. This silica-based column is inactivated by a glycerylpropyl-bonded phase, and has a reported fractionation range of about 10^3–10^5 dalton [11].

The assay development goals were optimization of the mobile phase to achieve complete recovery of both the HMW impurities and ceftiofur from the column and acceptable resolution between the HMW impurities and ceftiofur, determination of an

appropriate UV absorbance *RRF* for the HMW impurities and validation of the assay for use in pharmaceutical quality control.

Mobile phase optimization: selectivity and absolute recovery

In aqueous SEC, non-size-exclusion mechanisms can contribute to retention, potentially affecting both recovery and resolution. Non-elution of the HMW impurities from both reversed- and normal-phase HPLC systems suggested that adsorption might make recovery difficult. Additionally, ceftiofur's negative charge at neutral pH makes ionic contributions to the separation mechanism likely.

The ionic strength of the mobile phase is critical to selectivity. Without salt, the HMW impurities and ceftiofur eluted together in the totally excluded volume. Under these conditions, negatively charged compounds such as ceftiofur tend to be retained less than neutral species on silica-based SEC columns because of coulombic repulsion from residual silanols near the stationary phase pores. This effect is mitigated by increasing the mobile phase ionic strength [11], which provides a shielding effect. With increasing salt concentration, ceftiofur was more strongly retained and separation from the HMW impurities was achieved. At salt concentrations above 10 m*M*, the retention volume of ceftiofur peak became greater than totally included volume of the column, suggesting an increasing contribution from adsorption.

The recovery of both the HMW impurities and ceftiofur decreased with increasing salt concentration. Although acceptable resolution between the HMW impurities and the ceftiofur peak and complete recovery of ceftiofur were achieved with a pH 7.5 mobile phase containing 5 m*M* potassium phosphate, HMW impurities recovery from the column was less than about 75%.

Complete recovery and acceptable resolution were achieved by increasing the mobile phase solvent strength by adding micellar SDS. The 1% (w/v) SDS in the final assay procedure is about 35 m*M*, exceeding the SDS critical micelle concentration (*ca.* 5 m*M* in the 13 m*M* ionic strength buffer). Using this micellar mobile phase, an absolute recovery of HMW impurities of 100.9 ± 5.7% [95% confidence limit (CL)] was determined at *ca.* 8.5 μg of HMW material injected, as described under Experimental. The addition of organic modifiers such as acetonitrile, methanol or tetrahydrofuran to the aqueous mobile phase was alternatively attemped, but did not improve the recovery, and degraded the resolution between ceftiofur and the HMW impurities at higher concentrations (*e.g.*, > 25% acetonitrile).

The separation obtained using the final HPSEC assay procedure is shown in Fig. 1. The HMW impurity peaks elute before the major component peak at retention times of *ca.* 1–2.2 min. Ceftiofur and most other low-molecular-weight impurities elute at about 2.7 min. The resolution between ceftiofur and the closest eluting HMW impurity peak is *ca.* 3.6, and is sufficient for accurate determination of the HMW impurities.

Several impurities with molecular weights similar to that of ceftiofur, which are determined using a separate HPLC assay, co-elute with the HMW impurities. This was determined by assaying isolated HMW peaks from the HPSEC separation using the separate assay for low-molecular-weight impurities. The co-elution is speculated to result from interaction of the co-eluting low-molecular-weight impurities with the SDS micelles, which have a hydrodynamic radius of about 30 Å (aggregation number near 60), and would therefore elute between the excluded peak and the included peak on the LiChrospher DIOL 100 Å column. The peak areas of the co-eluting low-molecular-weight impurities can be subtracted from the total peak area found in the HPSEC procedure, but significant amounts of these are rarely observed.

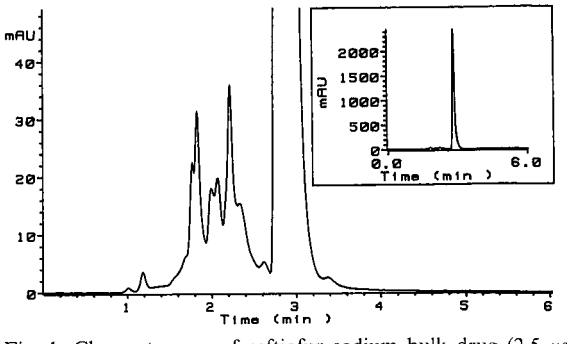

Fig. 1. Chromatogram of ceftiofur sodium bulk drug (2.5 μg on-column). Column, EM Science LiChrospher 100 DIOL, 5 μm (250 mm × 4.6 mm I.D.); mobile phase, 0.005 *M* KH_2PO_4 (pH 7.5) containing 1% SDS; flow-rate, 1.0 ml/min; detection, 254 nm.

Linearity, recovery and response factor determination

The detector peak-area response is linear over the range 0.005–9.25 μg of isolated HMW impurities injected (r^2 = 0.999999; residuals apparently random), which corresponds to about 0.25–460% of the amount of bulk drug injected in the assay procedure. This range encompasses the amount injected in the absolute recovery experiment (8.5 μg) and thus allows complete absolute recovery to be inferred over the entire linear range. An insignificant *y*-intercept (−1110 μV s: estimated standard deviation (ESD) = 5716) shows the absence of additive bias and is consistent with complete recovery. The same mobile phase without SDS provided a lower recovery throughout the investigated range of 0.1–14.46 μg HMW impurities injected (75.3% at 13.25 μg of HMW material injected), and progressively lower recoveries with lower levels of HMW impurities injected on to the column.

HMW impurities present in ceftiofur sodium are determined on a peak-area percentage basis relative to the major component peak using UV absorbance detection at 254 nm. The difference in chromatographic detector response between the analyte and the major component is accounted for by dividing the area percentage result by an *RRF*, the ratio of the mass response of the analyte to that of the major component.

The *RRF* used in this work is 0.81 ± 0.01 (95% CL), the least-squares regression slope from the recovery study discussed below. The value agrees with an *RRF* of 0.80 measured directly by rationing the 254-nm absorbance of isolated HMW impurities in mobile phase solution to that of ceftiofur. These experimental values are near 1.0, consistent with a possible structural relationship between the HMW impurities and ceftiofur suggested by the qualitative similarity between their absorbance spectra.

These approaches require a knowledge of the purity of both the isolated HMW impurities and the ceftiofur lot used for comparison. Because insufficient isolated HMW material was available for complete material balance assays, it was assumed that these purity values were identical. Additionally, it was assumed (throughout this work) that the isolated HMW impurities are structurally representative of those present in bulk drug lots. The HPSEC elution profile of the isolated HMW impurities is shifted to earlier elution times than that of the impurities normally found in bulk drug lots. However, the diode-array detector absorbance spectra of the HMW impurity peaks in bulk drug lots are similar to those of the isolated materials, suggesting that the structure of the isolated HMW impurities is similar to that of the impurities normally observed.

These assumptions were tested by using two different approaches to determine the *RRF* directly for materials naturally present in bulk drug, with no assumptions regarding analyte purity. A set of measurements using TLC with similar-response detection based on spray-reagent derivatization gave an *RRF* of 0.87 ± 0.17 (95% CL) [12]. Data from a separate experiment using the HPSEC assay with refractive index detection proved more difficult to interpret because both positive and negative peaks occurred in the HMW impurities region. An *RRF* of 0.85 was calculated by integrating both positive and negative peaks with respect to the same baseline. These results are consistent with the *RRF* value assigned using isolated HMW impurities, and thus support the assumptions.

The spiked recovery is acceptable over a range of 0.3–6.0 wt.% HMW impurities added. In this study, the peak-area percentage of HMW impurities was determined for a bulk drug lot of ceftiofur hydrochloride that had been spiked with isolated HMW impurities. This bulk drug lot contained the lowest level of HMW impurities that had been observed at that time. If the relative detector response difference is not taken into account, the least-squares regression slope for these data is 0.81 ± 0.01 (95% CL). This slope was assigned as the assay *RRF* value, as discussed above. Recovery data are given in Table I, the "HMW impurities found" values being calculated using an *RRF* of 0.81. At each spiking level, the percentage of HMW impurities recovered is within 1 assay standard deviation (see below) of the amount added. The recovery is linear, as shown by a least-squares r^2 value of 0.9997 and apparently random residuals. The slope (found *vs.* added) is 1.002 ± 0.005 (ESD), and the *y*-intercept is not significantly different from zero (0.08 ± 0.04 ESD) when the data are corrected for the 1.86% ± 0.10% (95% CL) HMW impurities found in the ceftiofur hydrochloride bulk drug lot used in the spiking study.

TABLE I

RECOVERY OF SPIKED HMW IMPURITIES

Percentage found data are corrected for mobile phase blank and a detection *RRF* of 0.81 (see text). The adjusted percentage found is the difference between the actual percentage found and the percentage of HMW impurities assayed in the ceftiofur hydrochloride lot used in the spiking study (1.86%).

HMW impurities added (%)	HMW impurities found (%)		Regression residuals (% HMW impurities)
	Actual	Adjusted	
0.27	2.18	0.32	−0.031
0.26	2.21	0.35	0.007
0.56	2.49	0.63	−0.007
0.56	2.47	0.61	−0.029
0.55	2.56	0.70	0.069
1.16	3.14	1.28	0.030
1.11	3.09	1.23	0.041
1.13	2.99	1.13	−0.080
3.02	4.94	3.08	−0.026
3.01	4.97	3.11	0.016
3.01	4.97	3.11	0.009
5.97	7.88	6.02	−0.040
5.90	7.84	5.98	−0.009
5.86	7.86	6.00	0.051

Limit of detection

The limit of detection (L_D) can be defined by the expression $L_D = Y_{bl} + 6S_{bl}$ [13,14], where Y_{bl} is the average signal of the baseline and S_{bl} is the standard deviation of the baseline. Using this definition, L_D is the smallest peak-height value that can be distinguished from the highest probable excursion of the baseline with 99.86% certainty, assuming a normal noise distribution. A standard deviation of $15.3 \cdot 10^{-6}$ absorbance units was measured for the chromatogram baseline from an entire run, excluding only the mobile phase disturbance discussed below. This corresponds to an L_D of 0.03% for HMW impurities, based on peak height.

Precision and ruggedness

The recovery of HMW impurities and the resolution of ceftiofur from the closest eluting HMW peak were studied as a function of mobile phase composition by assaying a ceftiofur sodium bulk drug lot using the same column with systematically varying mobile phase compositions, as detailed in Table II. The selected mobile phase is on relatively flat area of both the resolution and recovery response surfaces, predicting acceptable ruggedness with respect to small variations in mobile phase composition. The relative 95% confidence limit on individual recovery results is *ca.* ±5.6% at the HMW impurities level present (5.4%), based on relative assay variability (see below). Recovery values significantly greater than 100% are due to decreasing resolution, which results in the assignment of an increasing portion of the ceftiofur peak area to the HMW impurities.

Precision and ruggedness were further investigat-

TABLE II

MOBILE PHASE RUGGEDNESS

Conditions are given under Experimental. Mobile phase S is used in the assay.

Mobile phase	SDS (%)	Phosphate (%)	Resolution	Recovery (%)
1	0.1	1.0	3.05	81
2	0.1	5.0	4.01	84
3	0.1	10.0	4.93	69
4	1.0	1.0	2.68	106
5	1.0	5.0	3.60	101
6	3.0	1.0	1.65	112
7	3.0	5.0	1.63	110
8	3.0	10.0	1.43	110

ed by assaying a single ceftiofur sodium bulk drug lot using five different columns on six different days and in three separate laboratories. The individual assay value standard deviation is 0.16% for the 60 assays, corresponding to a relative standard deviation of 2.5% and a relative 95% confidence limit of $\pm 5.6\%$ [using $t(\alpha = 0.975; n = 59)$ and assuming a single assay value]. Analysis of variance (ANOVA) showed no significant effect on assay results at the 95% confidence level due to different columns, days, laboratories or analysts.

Mobile phase blank

A series of small peaks reproducibly elutes at the totally excluded volume when a blank injection is made, as shown in the top chromatogram in Fig. 2. Although a blank correction can be performed, the presence of a significant blank would compromise the ruggedness of the method, and extensive efforts were made to eliminate this blank.

The artifact peaks were observed only with mobile phases containing micellar SDS, and only when using Rheodyne Model 7125 or 7126 injection valves, which do not include a pressure by-pass. The blank peaks are reduced by an order of magnitude (to *ca.* 0.05% of the total peak area) by replacing the stator and stator face assembly in a Model 7126 with an assembly incorporating a pressure bypass, as shown in the bottom chromatogram in Fig. 2.

The modified valves contain the same solvent

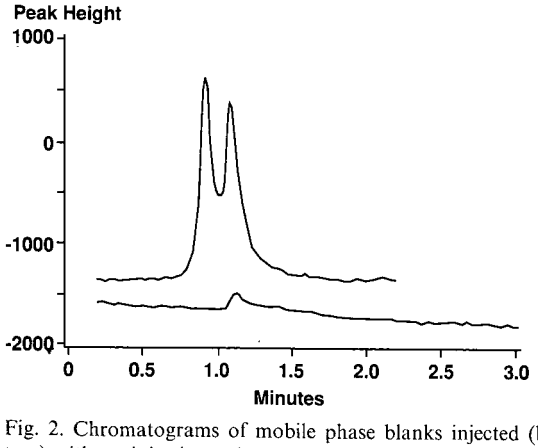

Fig. 2. Chromatograms of mobile phase blanks injected (bottom) with an injection valve equipped with a pressure by-pass and (top) with an injection valve not equipped with a pressure by-pass. The ordinate (peak height) is in μV; 1 V = 1 absorbance unit.

contact materials as the unmodified valves. Exhaustive cleaning of the dismantled injection valve with organic solvents and (separately) nitric acid failed to reduce the magnitude of the blank, and the size of the artifact peaks remains constant even after many repeated injections. Identical blanks are observed for manual injections and autosampler injections for a given valve, ruling out other autosampler components as a primary blank source. These results suggest that the blank somehow results from the high-pressure transient during valve switching. However, high-pressure extraction of components of the injection valve materials does not appear to explain fully the observed blank peaks. Micellar solubilization has been reported to be a relatively weak function of pressure [15,16]. Either increased or decreased solubility of less than about 10% has been reported, depending on the solute, surfactant structure and applied pressure. This contrasts with the order of magnitude decrease in the blank obtained by incorporating the pressure bypass.

No explanation for the blank peaks has been proposed to date which is consistent with all of the available information. Use of Rheodyne Model 7135 and 7125-075, which have the by-pass equipped stator and stator face assembly, or Rheodyne Model 7125 and 7126 valves rebuilt with stator and stator face assemblies with pressure by-pass is recommended to limit the magnitude of the blank. Extractable material from plastic to which the sample may be exposed before injection can also contribute to the blank peak, and plastic autosampler sample path tubing and plastic vial caps are therefore avoided.

CONCLUSIONS

The described size-exclusion chromatographic assay of HMW impurities in ceftiofur sodium bulk drug is suitable for use in pharmaceutical quality control. The method exhibits linear response and complete recovery of HMW impurities, with a relative standard deviation of 2.5%.

ACKNOWLEDGEMENTS

The authors acknowledge helpful discussions with John Stodola and a number of other co-work-

ers in Control Development at Upjohn, and thank Upjohn for supporting this work.

REFERENCES

1 F. R. Batchelor, J. M. Dewdney, J. G. Feinberg and R. D. Weston, *Lancet*, i (1967) 1175.
2 G. T. Stewart, *Lancet*, i (1967) 1177.
3 A. C. Munroe, J. M. Dewdney, H. Smith and A. W. Wheeler, *Int. Arch. Allergy Appl. Immunol.*, 50 (1976) 192.
4 H. Smith and A. C. Marshall, *Nature (London)*, 232 (1971) 45.
5 G. T. Stewart, B. T. Butcher, S. S. Wagle and M. K. Stanfield, in J. F. Johnson and R. S. Porter (Editors), *Liquid Crystals and Ordered Fluids*, Plenum Press, New York, 1970, p. 33.
6 M. K. Stanfield, B. L. Warren and F. H. Wilson, *Liq. Cryst. Ordered Fluids*, 3 (1978) 89.
7 H. Aki, N. Sawai, K. Yamamoto and M. Yamamoto, *Pharm. Res.*, 8 (1991) 119.
8 H. Ueno, M. Nishikawa, M. Muranaka and Y. Horiuchi, *J. Chromatogr.*, 207 (1981) 425.
9 M. Iwata, H. Tokiwa and T. Matuhasi, *Int. Arch. Allergy Appl. Immunol.*, 70 (1983) 132.
10 *Fed. Regist.*, 50 (1985) 48396.
11 H. G. Barth, *J. Chromatogr. Sci.*, 18 (1980) 409.
12 M. J. Dunn and D. A. Hahn, in preparation.
13 D. L. Massart, A. Dijkstra and L. Kaufman, *Evaluation and Optimization of Laboratory Methods and Analytical Procedures*, Elsevier, Amsterdam, 1987, p. 150.
14 Analytical Methods Committee, *Analyst (London)*, 1 (1987) 112.
15 N. Nishikido, M. Kishi and M. Tanaka, *J. Colloid Interface Sci.*, 94 (1983) 348.
16 N. Nishikido, K. Abiru and N. Yoshimura, *J. Colloid Interface Sci.*, 113 (1986) 356.

Journal of Chromatography, 595 (1992) 193–202
Elsevier Science Publishers B.V., Amsterdam

CHROM. 23 861

Screening of organophosphorus pesticides using liquid chromatography–atmospheric pressure chemical ionization mass spectrometry

Seiji Kawasaki and Hiroshi Ueda

Department of Laboratory Medicine, Saga Medical School Hospital, Nabeshima, Saga 849 (Japan)

Hideo Itoh

Department of Internal Medicine, Taisei Hospital, Fussa, Tokyo 197 (Japan)

Jutaro Tadano*

Department of Laboratory Medicine, Saga Medical School Hospital, Nabeshima, Saga 849 (Japan)

(First received May 7th, 1991; revised manuscript received October 28th, 1991)

ABSTRACT

Screening and identification of organophosphorus pesticides in blood from patients suffering from acute agricultural chemical toxicity were established by a liquid chromatography–atmospheric pressure chemical ionization mass spectrometric method. To determine 21 pesticides, it was necessary to monitor both positive and negative ions. This method could easily screen for 21 organophosphorus pesticides in less than 30 min. By comparison with a gas chromatographic–mass spectrometric method, the chemicals indicated a similar extent of specificity and within equivalent detection limits, thus satisfying clinical requirements completely.

INTRODUCTION

In modern society, many drugs and related compounds are readily accessible. Among these, agricultural chemicals have been comparatively easy to obtain, and these agents continue to be seported in patients with acute drug toxicity as a result of accidental or suicide-intended consumption. It is vital that methods for rapid detection and determination are available to assist in diagnosis and the application of therapeutic countermeasures.

Current analyses of agricultural chemicals involve methods such as gas chromatography (GC) [1–3], high-performance liquid chromatography (HPLC) [4,5] and gas chromatography–mass spectrometry (GC–MS) [6–9]. Among these, GC and HPLC using retention times as criteria are acceptable quantitative methods and are the methods of choice for a number of agricultural chemicals. These methods are reliable, but the identification of an unknown in a matrix that has not been validated may be problematic. GC–MS shows high reliability for both quantitative and qualitative analysis because of the characteristic peaks of compounds in the mass spectra. However, GC–MS has the disadvantage of the decomposition of some thermally unstable substances in the column or derivatization of the specimen during the GC separation.

In recent years, liquid chromatography–mass spectrometry (LC–MS) has been developed to overcome the above problems without losing the specificity of the qualitative analysis of GC–MS [10–20]. In this study, we attempted to detect and screen 21 organophosphorus pesticides (OPs) of compara-

0021-9673/92/$05.00

tively high toxicity by subjecting blood from patients suffering from acute agricultural chemical toxicity to liquid chromatography–atmospheric pressure chemical ionization mass spectrometry (LC–APCI-MS).

EXPERIMENTAL

Pesticides

Twenty-one OPs with consumptions exceeding 10^5 l or 100 tons per year in Saga Prefecture, Kyushu, Japan, were studied: chlorpyrifos (O,O-diethyl O-3,5,6-trichloro-2-pyridyl phosphorothioate), chlorpyrifos-methyl (O,O-dimethyl O-3,5,6-trichloro-2-pyridyl phosphorothioate), diazinon (O,O-diethyl O-2-isopropyl-6-methylpyrimidin-4-yl phosphorotioate), dichlorvos (2,2-dichlorovinyl dimethyl phosphate), dimethoate (O,O-dimethyl S-methylcarbomoylmethyl phosphorodithioate), dimethylvinphos [2-chloro-1-(2′,4′-dichlorophenyl) vinyl dimethyl phosphate], disulfoton (O,O-diethyl S-2-ethylthioethyl phosphorodithioate), ediphenphos (O-ethyl S,S-diphenyl phosphorodithioate), EPN (O-ethyl O-4-nitrophenyl phenyl phosphorothioate), ethion [O,O,O′,O′-tetraethyl S,S′-methylene bis(phosphorodithioate)], fenitrothion (O,O-dimethyl O-4-nitro-*m*-tolyl phosphorothioate), fenthion (O,O-dimethyl O-4-methylthio-*m*-tolyl phosphorothioate), IBP (O,O-diisopropyl S-benzyl phosphorothioate), isoxathion (O,O-diethyl O-5-phenylisoxazol-3-yl phosphorothioate), malathion [S-1,2-bis(ethoxycarbonyl)ethyl O,O-dimethyl phosphorodithioate], methidathion (S-2,3-dihydro-5-methoxy-2-oxo-1,3,4-thioadiazol-3-ylmethyl O,O-dimethyl phosphorodithioate), parathion (O,O-diethyl O-4-nitrophenyl phosphorothioate), parathion-methyl (O,O-dimethyl O-4-nitrophenyl phosphorothioate), phenthoate (S-α-ethoxycarbonylbenzyl O,O-dimethyl phosphorodithioate), propaphos (4-methylthiophenyl dipropyl phosphate) and pyridaphenthion [O,O-diethyl O-(2,3-dihydro-3-oxo-2-phenylpyridazine-6-yl)phosphorothioate].

Dimethylvinphos was supplied by Sankyo Agricultural Chemical Manufacturing and the other twenty pesticides were purchased from Wako. All chemicals were dissolved in methanol–in water (70:30, v/v) to prepare standard solutions.

Instruments and chromatographic conditions

The HPLC system consisted of an intelligent pump (Model L-6200; Hitachi), an ultraviolet (UV) spectrophotometer (Model L-4000; Hitachi) and a sample injector (Model 7125, with a 200-μl sample loop; Rheodyne). The column was packed with μBondapak C_{18} (30 cm × 3.9 mm I.D., 10-μm average particle size; Waters Assoc.). The mobile phase was methanol–water and elution was performed with a 20-min linear gradient from 70% to 90% (v/v) methanol at a flow-rate of 1.0 ml/min and at room temperature. Methanol was of HPLC grade (Wako) and distilled deionized water purified using a Milli-Q II system (Millipore) was used.

The HPLC system was connected with a mass spectrometer (Model M-2000; Hitachi) via an atmosphere pressure chemical ionization (APCI) interface of the non-equilibrium type [19]. The interface was set with a vaporizer temperature of 250°C, a nebulizer temperature of 400°C, an ionization needle electrode current of 5 μA and a drift voltage of 230 V. The mass spectrometer was adjusted to a vacuum pressure of $1 \cdot 10^{-4}$ Pa, an ion-source slit width of 500 μm, a collector slit width of 400 μm, an accelerated electrical potential of 4 kV, and a secondary electronic step-up tube electrical potential supply of 1.3 kV, and a mass range (m/z) of 0–500 was scanned at 8-s intervals.

Total ion current (TIC) chromatography was applied in the range m/z 200–500 with both UV spectrophotometric and MS detection.

Serum extract

Standard solutions of OPs were added to Lyphocheck drug-free serum (Bio-Rad Labs.) to give a final concentration of 2.0 μg/ml. A 1.5-ml volume of this sample together with 2.0 ml of 0.2 *M* phosphate buffer (pH 7.0) was applied to an Extrelut No. 3 column (E. Merk) and allowed to stand for 10 min. A volume of 15 ml of *n*-hexane–diethyl ether (8:2, v/v) was used for elution. The eluate obtained was evaporated to dryness under a steam of nitrogen at 40°C, the residue was dissolved in 150 μl of methanol–water (70:30, v/v) and 100 μl of this solution were injected into the LC–APCI-MS apparatus.

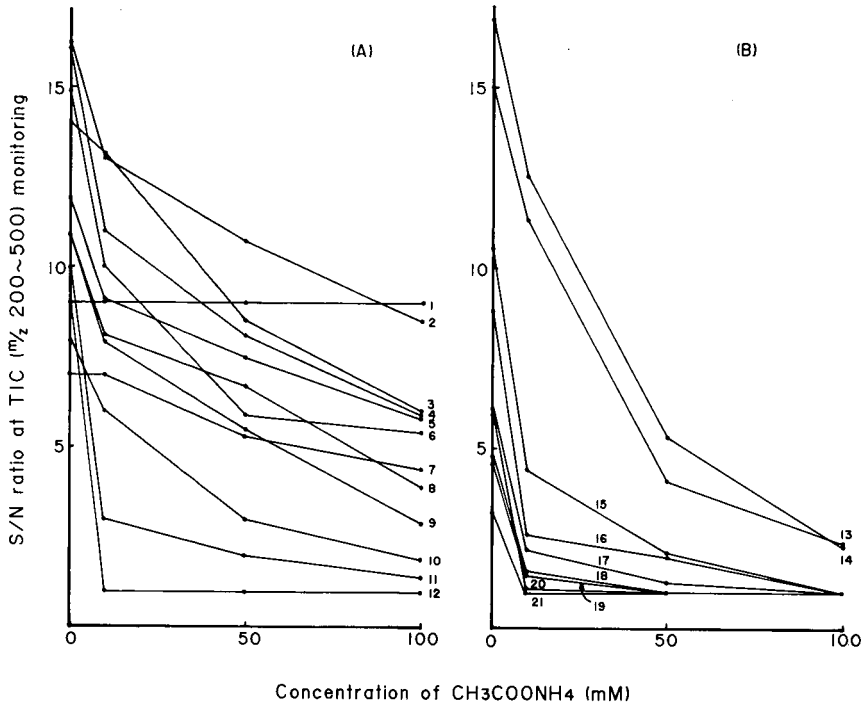

Fig. 1. Effects of ammonium acetate concentration in the mobile phase on the determination sensitivity with TIC monitoring. Mobile phases of 0, 10, 50 and 100 m*M* ammonium acetate–methanol (3:7, v/v) were used. (A) Positive-ion measurement mode; (B) negative-ion measurement mode. 1 = diazinon; 2 = dimethoate; 3 = propaphos; 4 = pyridaphenthion; 5 = ediphenphos; 6 = dimethylvinphos; 7 = IBP; 8 = malathion; 9 = isoxathion; 10 = phenthoate; 11 = dichlorvos; 12 = fenthion; 13 = parathion-methyl; 14 = fenitrothion; 15 = parathion; 16 = methidathion; 17 = EPN; 18 = disulfoton; 19 = ethion; 20 = chlorpyrifos-methyl; 21 = chlorpyrifos.

RESULTS

Selection of ionization mode (positive or negative ions) for measurement

After analyses of standards of the 21 OPs by LC–APCI-MS, the chemicals were classified into three groups: diazinon, dichlorvos, dimethoate, IBP, isoxathion, malathion and propaphos were detectable only with the positive-ion measurement mode, chlorpyrifos, chlorpyrifos-methyl, disulfoton, ethion, EPN, fenitrothion, parathion and parathion-methyl were detectable only with the negative-ion measurement mode and dimethylvinphos, edifenphos, fenthion, methidathion, penthoate and pyridaphenthion were detectable with both the positive- and negative-ion measurement modes. In the last group, methidathion was determined in the negative-ion mode whereas the other five were detected with high sensitivity in the positive-ion mode.

Selection of mobile phase

In LC, a salt is often added to the mobile phase to enhance the separation efficiency. However, as the possible use of the type of salt is limited, acetic acid and ammonium acetate are generally used. To study the effects on the sensitivity of determination of adding ammonium acetate to the mobile phase, the signal-to-noise ratio (S/N) in TIC was measured when 1.0 μg of standards was determined using 10, 50 or 100 m*M* ammonium acetate buffer (pH 7.0)–methanol (3:7, v/v) as the mobile phase.

Ammonium acetate did not affect the detection sensitivity for diazinon, but for the other 20 chemicals marked decreases in sensitivity occured as the ammonum acetate concentration increased (Fig. 1).

Further, except for diazinon and fenthion, the $[M + NH_4]^+$ ion was produced on addition of ammonium acetate to the mobile phase for the other ten chemicals in the determination of positive ions.

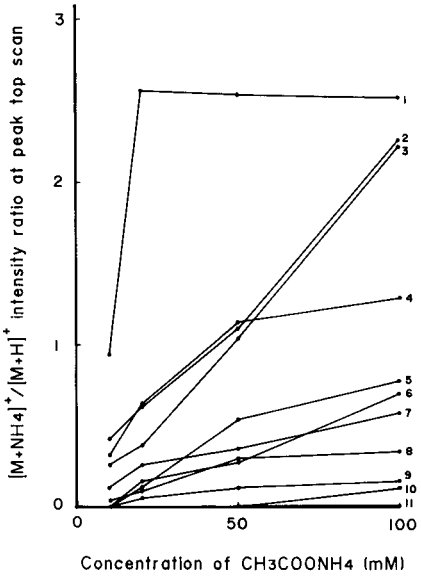

Fig. 2. Effect of ammonium acetate concentration in the mobile phase on $[M + NH_4]^+$ pseudo-molecular ion production. Mobile phases of 0, 10, 50 and 100 m*M* ammonium acetate–methanol (3:7, v/v) were used. 1 = malathion; 2 = dichlorvos; 3 = phenthoate; 4 = dimethylvinphos; 5 = IBP; 6 = ediphenphos; 7 = propaphos; 8 = dimethoate; 9 = isoxathion; 10 = pyridaphenthion; 11 = diazinon.

The ratio of the $[M + NH_4]^+$ intensity to that of the $[M + H]^+$ intensity showed a proportional increase with respect to increase in ammonium acetate concentration (Fig. 2). On the other hand, the $[M + NH_4]^+$ ion was not produced for diazinon. For fenthion, the use of a mobile phase containing 10 m*M* ammonium acetate did not allow the detection of this compound.

Conditions of APCI interface

In LC–APCI-MS, the vaporizer temperature is the limiting factor for the sensitivity of determination. Using methanol–water (70:30, v/v) as the mobile phase, 1.0 μg of the respective OP standard solution was injected and applying TIC chromatography, the *S/N* was derived (Fig. 3). The range of the vaporizer temperature for suitable detection was comparatively narrow; for the determination of positive ions for twelve compounds and negative ions for nine compounds the ranges were 230–250 and 250–270°C, respectively.

Mass spectra

Based on the determination conditions above, mass spectra of 21 OP standard solutions were de-

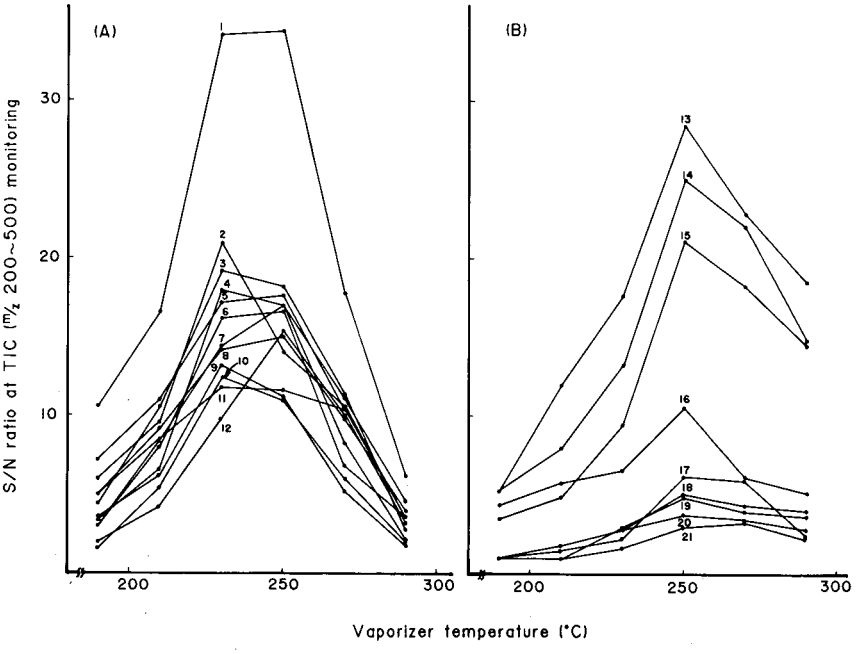

Fig. 3. Influence of the vaporizer temperature on determination sensitivity with TIC monitoring. Mobile phase, methanol–water (70:30, v/v). (A) Positive-ion measurement mode; (B) negative-ion measurement mode. 1 = Dimethoate; 2 = pyridaphenthion; 3 = dimethylvinphos; 4 = dichlorvos; 5 = propaphos; 6 = ediphenphos; 7 = isoxathion; 8 = diazinon; 9 = malathion; 10 = phenthoate; 11 = IBP; 12 = fenthion; 13 = fenitrothion; 14 = parathion-methyl; 15 = parathion; 16 = methidathion; 17 = disulfoton; 18 = EPN; 19 = chlorpyrifos-methyl; 20 = ethion; 21 = chlorpyrifos.

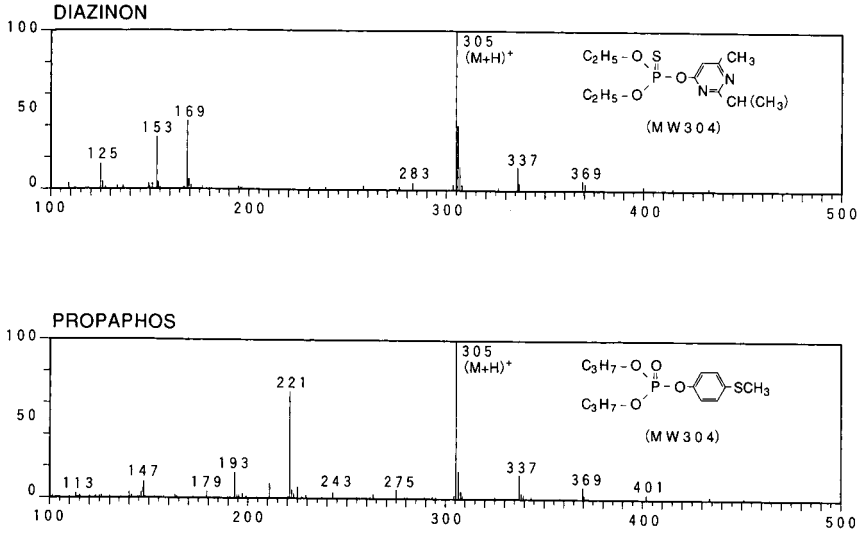

Fig. 4. Mass spectrum (positive-ion measurement mode), showing the positive-ion LC-APCI mass spectra of diazinon and propaphos as examples. These two compounds have a molecular weight of 304 and the $[M + H]^+$ pseudo-molecular ion appeared at m/z 305 as a base peak. However, a fragment ion appeared at m/z 221 with high intensity only with propaphos. Hence the two compounds showed different mass spectral patterns. LC conditions: column, μBondapak C_{18} (30 cm × 3.9 mm I.D., 10-μm average particle size); elution with methanol–water with a 20-min linear gradient from 70% to 90% (v/v) methanol; flow-rate, 1.0 ml/min at room temperature. APCI interface conditions: vaporizer temperature, 250°C, nebulizer temperature, 400°C; ionization needle electrode current, 5 μA; drift voltage, 230 V. MS conditions: ion-source slit width, 500 μm; collector slit width, 400 μm; acceleration electrical potential, 4 kV; secondary electronic step-up tube electrical potential supply, 1.3 kV; m/z range scanned, 0–500; scan rate, 8-s intervals. MW = Molecular weight.

termined. In the determination of positive ions of twelve compounds, $[M + H]^+$ pseudo-molecular ions of high intensity were registered. The $[M + CH_3OH + H]^+$ ion with methanol attached was also observed, although with a low intensity. Moreover, two or three fragment ions, which indicated a simple mass spectrum overall, were indicated (Fig. 4).

For the nine compounds whose negative ions were determined, none produced any $[M - H]^-$ pseudo-molecular ions. The seven compounds disulfoton, ethion, EPN, fenitrothion, methidathion, parathion and parathion-methyl showed fragment ions with monodealkylation replaced by an ether bond. Two or three other fragment ions indicated a simple overall mass spectral pattern. For chlorpyrifos and chlorpyrifos-methyl, $[M - Cl + O; M - 19]^-$ ions showed a standard peak without yielding $[M - H]^-$ pseudo-molecular ions, indicating a mass spectral pattern different from that of the other seven compounds (Fig. 5).

Chromatograms

Chromatograms obtained by injecting 1.0 μg each of the OP standard solutions are presented in Fig. 6A and B. Determination of positive ions was achieved by monitoring the $[M + H]^+$ pseudo-molecular ions. For the negative ions, determination of chlorpyrifos and chlorpyrifos-methyl was based on $[M - Cl + O]^-$ ions, whereas $[M - alkyl]^-$ ions were monitored for the other seven compounds. The total time needed was less than 20 min. However, complete separation for determining the 21 compounds was not attained.

Detection limits

Using standard solutions of the 21 OPs, the detection limits with TIC Monitoring and mass fragmentography were derived for S/N = 3 (Table I). Comparison of the detection limits given by GC, HPLC and GC–MS method showed that the values were slightly inferior with TIC monitoring. Mass fragmentography gave the best results.

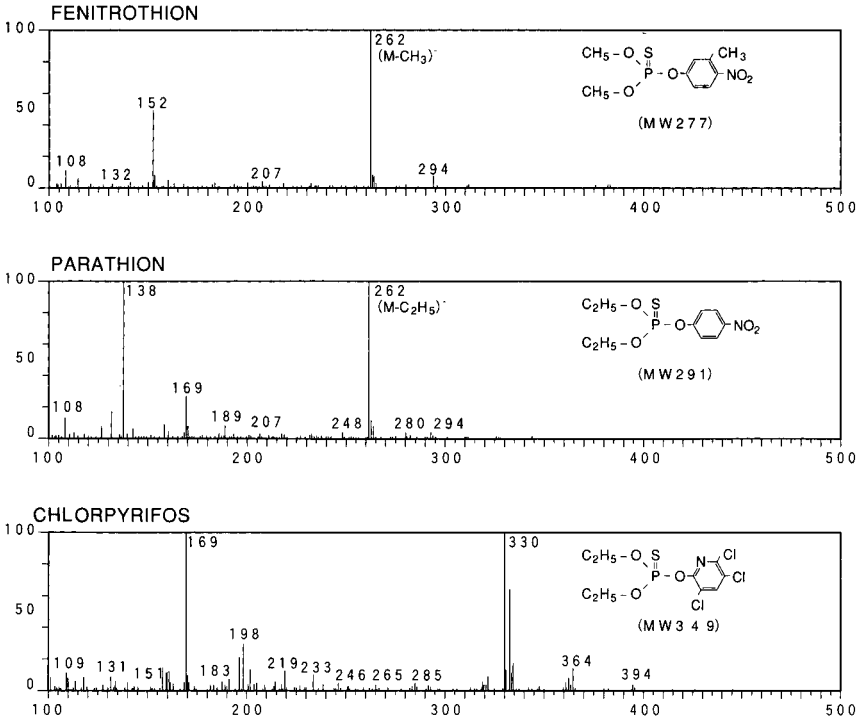

Fig. 5. Mass spectrum (negative-ion measurement mode), showing the negative-ion LC-APCI mass spectra of fenitrothion, parathion and chlorpyrifos as examples. For fenitrothion and parathion, the $[M - alkyl]^-$ fragment ion appeared at m/z 262 as a base peak. However, other fragment ions also appeared at m/z 152 for fenitrothion and at m/z 138 for parathion, so these two compounds showed different mass spectral patterns. In chlorpyrifos, the $[M - Cl + O]^-$ fragment ion appeared as the base peak. LC, APCI interface and MS conditions as in Fig. 4.

Recovery test

OP standard solutions were added to drug-free serum at 2.0 μg/ml. Using this as the sample, measurements were made with UV detection. The mean recovery for each compound ($n = 5$) ranged from 80.3 to 101% (Table II).

DISCUSSION

It is important to perform rapid detection and quantitative analysis and of samples from patients acutely affected with agricultural chemical toxicity in order to be able to take appropriate countermeasures. Many methods for OPs are available, among which GC–MS shows extremely high specificity. However, the use of GC as a separation procedure is impracticable with thermally instable substances and complicated determination procedures involving derivatives are necessary, in addition to other difficulties arising in *in vivo* sample analysis. In recent years, LC—MS has been developed as a practical method that overcomes the disadvantages of GC–MS without losing specificity [10–20].

The 21 OPs studied were classified into three groups that were detectable by only positive-ion measurement, by only negative-ion measurement by both positive- and negative-ion measurement. In LC–MS determinations, the production of positive or negative ions depends considerably on the acidity of the substance in question, and the determination of negative ions for compounds of high acidity has been reported to be appropriate [21]. In the present experiments, we monitored the negative ions for nine compounds and examined the sensitivity. Of these, EPN, fenitrothion, parathion and parathion-methyl contain a nitro group within the molecule. The effects observed are believed to be due to pseudo-acids formed by electron attachment. The

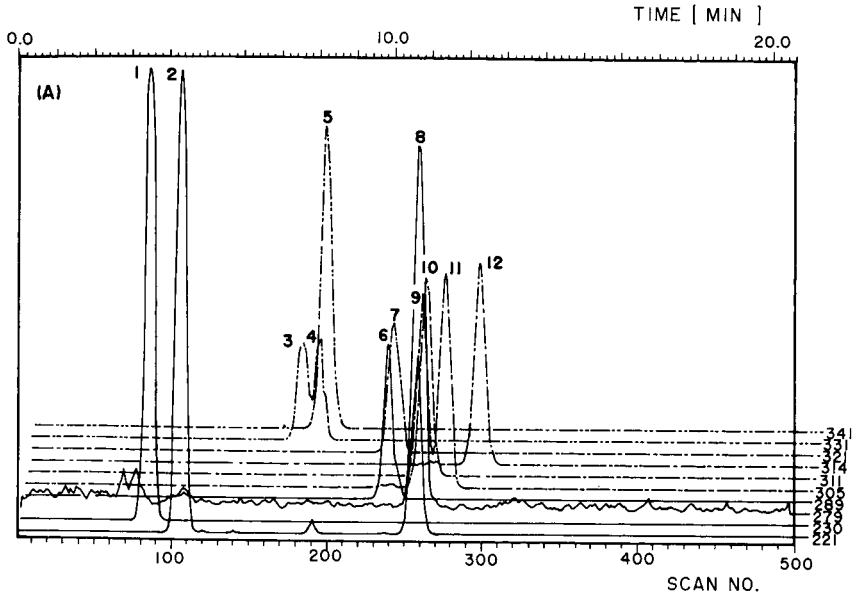

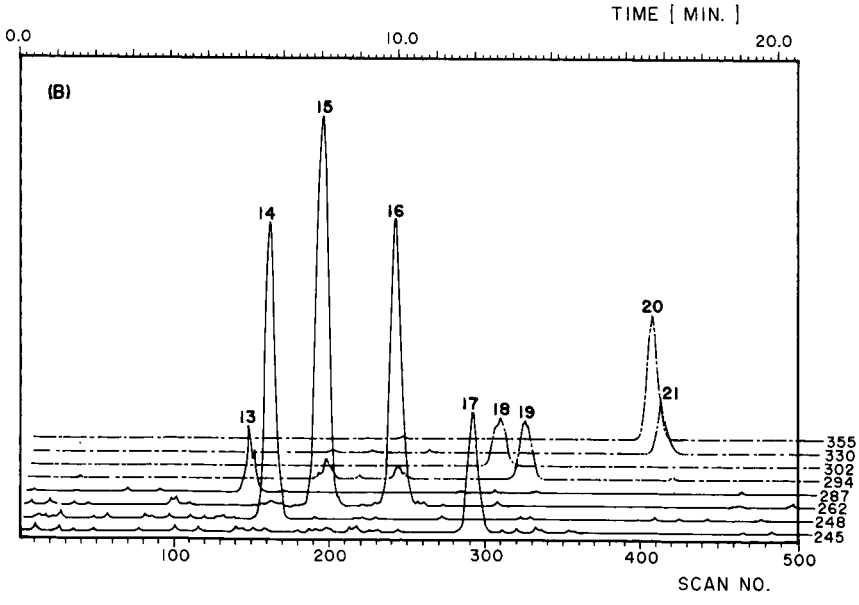

Fig. 6. Mass chromatograms: (A) positive-ion measurement mode; (B) negative-ion measurement mode. LC, APCI interface and MS conditions as in Fig. 4. Peaks: 1 = dimethoate (*m/z* 230); 2 = dichlorvos (*m/z* 221); 3 = malation (*m/z* 331); 4 = dimethylvinphos (*m/z* 331); 5 = pyridaphenthion (*m/z* 341); 6 = IBP (*m/z* 289); 7 = phenthoate (*m/z* 321); 8 = fenthion (*m/z* 279) 9 = propaphos (*m/z* 305, 221); 10 = ediphenphos (*m/z* 311); 11 = diazinon (*m/z* 305); 12 = isoxathion (*m/z* 314); 13 = methidathion (*m/z* 287); 14 = parathion-methyl (*m/z* 248); 15 = fenitrothion (*m/z* 262); 16 = parathion (*m/z* 262); 17 = disulfoton (*m/z* 245); 18 = chlorpyrifos-methyl (*m/z* 302) 19 = EPN (*m/z* 294); 20 = ethion (*m/z* 355); 21 = chlorpyrifos (*m/z* 330).

TABLE I

DETECTION LIMITS

The detection limits during TIC monitoring or mass fragmentography were derived with S/N ratio = 3. LC, APCI interface and MS conditions as in Fig. 4.

Measurement mode	Pesticide	Detection limit (ng)	
		TIC monitoring	Selected ion monitoring
Positive-ion	Diazinon	200	5.0
	Dichlorvos	100	2.0
	Dimethoate	100	2.0
	Dimethylvinphos	200	5.0
	Ediphenphos	200	5.0
	Fenthion	200	20.0
	IBP	200	5.0
	Isoxathion	200	5.0
	Malathion	200	5.0
	Phenthoate	200	5.0
	Propaphos	200	5.0
	Pyridaphenthion	200	5.0
Negative-ion	Chlorpyrifos	1000	50.0
	Chlorpyrifos-methyl	1000	50.0
	Disulfoton	500	20.0
	EPN	1000	50.0
	Ethion	500	10.2
	Fenitrothion	200	2.0
	Methidathion	500	10.0
	Parathion	200	2.0
	Parathion-Methyl	200	2.0

results suggest that the choice between positive- and negative-ion detection also depends on the LC mobile phase conditions, but the detection of both types of ions should be performed when attempting to screen OPs using LC–APCI-MS.

pH adjustment and addition of salt to the mobile phase have sometimes been applied with the aim of enhanceing the separation efficiency in reversed-phase LC. However, as the LC eluate is transferred to the vaporizer via a capillary tube at high temperature, non-volatile salts cannot be used in this method. Although some volatile buffers can be used as the mobile phase in LC–MS, acetic acid and ammonium acetate have generally been adopted and their usefulness is well recognized [22]. From experiments in which the effects of acetic acid and ammonium acetate on the determination sensitivity of OPs were examined, except for diazinon, as the ammonium acetate concentration in the mobile phase increased, a drastic decrease in sensitivity was observed for the other 20 compounds. As ammonium acetate has a higher proton affinity than OPs, the decrease in sensitivity when ammonium acetate buffer is added may be due to the formation of NH_4^+ ions rather than OP^+ ions. It follows, therefore, that it is not appropriate to add ammonium acetate to the mobile phase solvent in the LC–APCI-MS determination of OPs. Although we did not perform the appropriate measurements in this study, other volatile buffers may possibly not have this adverse effect.

The difference in proton affinity between the reagent ion and the analyte has been reported to be a limiting factor the production of pseudo-molecular ions in APCI-MS in general [23]. In this work, even increases in ammonium acetate concentration did not induce the production of $[M + NH_4]^+$ ion for diazinon (for which the determination of positive ions is applied). However, for ten compounds, increases in salt concentration were accompanied by increases in the ratio of $[M + NH_4]^+$ intensity to $[M + H]^+$ intensity (Fig. 2). These findings indicate

TABLE II

EXTRACTION RECOVERIES OF ORGANOPHOSPHORUS PESTICIDES

OP standard solutions were added to drug-free sera to give a final concentration of 2.0 μg/ml as test samples. Measurement was performed using UV spectrophotometric detection, and concentrations of test samples were calculated from peak areas. LC conditions as in Fig. 4.

Pesticide	Mean recovery (%) ($n=5$)
Positive-ion measurement	
Diazinon	97.2
Dichlorvos	80.3
Dimethoate	81.4
Dimethylvinphos	92.2
Ediphenphos	86.0
Fenthion	85.0
IBP	92.1
Isoxathion	81.0
Malathion	87.1
Penthoate	89.3
Propaphos	91.2
Pyridaphenthion	101.7
Negative-ion measurement	
Chlorpyrifos	85.5
Chlorpyrifos-methyl	88.5
Disulfoton	89.0
EPN	82.4
Ethion	98.6
Fenitrothion	92.0
Methidathion	95.3
Parathion	88.1
Parathion-methyl	93.6

that the production of pseudo-molecular ions in APCI-MS is dependent not only on the difference in the proton affinity of the molecules, but also on the molecular concentration of the reagent gas.

The results of determinations using methanol–water (70:30, v/v) as the mobile phase indicated that the determination sensitivity of LC–APCI-MS is markedly influenced by the size of the droplets of the LC eluate, *i.e.* by the vaporizer temperature. Appropriate temperature ranges for positive- and negative-ions measurements were 230–250 and 250–270°C, respectively. The vaporizer temperature was confirmed to have a great influence on the efficacy of ionization (Fig. 3). From such findings, deciding on the appropriate vaporizer temperature of the LC–APCI-MS method, consideration should be given to the volatility of the mobile phase used (*i.e.*, the organic solvent content in the mobile phase), and not merely to the properties of the analyte. It would be inappropriate to employ an organic solvent concentration that is very different from that in the mobile phase in the gradient elution method. In our experiments, we employed linear gradient elution from 70% to 90% methanol in 20 min. From the results obtained with 1.0 μg of OP standard solution, although elution of the respective compound was completely monitored within 20 min where the determinations were based on positive and negative ions, separation of the mixture was incomplete. However, as these pesticides are rarely multiply present in patients acutely intoxicated with agricultural chemicals, and it is possible to observe the spectral pattern, detection of a particular compound can be achieved. However, given sufficient time for elution to proceed, separation can be enhanced. In some instances, as the peaks which were eluted later from the column showed a broad shape, a decrease is S/N ensued, resulting in a decrease in the detection sensitivity.

The detection limits under the determination conditions employed were 2–50 and 200–1000 ng using selected ion monitoring (SIM) and TIC monitoring procedures, respectively. TIC monitoring is a procedure that cannot be excluded in the establishment of the causative factors in cases of acute agricultural chemical toxicity, and the detection limit of 200–1000 ng is slightly inferior to that of GC–MS [23–25]. However, in our experience, emergency cases admitted with OP intoxication usually register blood concentrations from 0.5 to a few tens of μg/ml, and TIC monitoring is therefore applicable.

Numerous mass spectra of OPs have been reported [17–19, 26–33]. In the APCI-MS determination of positive ions, high-intensity $[M + H]^+$ ions have been observed. Whereas in negative-ion determinations the thermospray method has been used to generate M^- and $[M - H]^-$ ions for OPs, only fragment ions have been noted without the production of $[M - H]^-$ pseudo-molecular ions in the APCI method. In addition, as originally reported, come groups of specific fragment ions of OPs are observed with regard to the detection of unknown peaks, but the specificity is not inferior to that of GC–MS. Further, numerous cluster ions derived from meth-

anol and water in the mobile phase occur at $m/z < 200$. Therefore, TIC chromatograms in the low-mass range show an unstable baseline, resulting in a decrease in S/N. This is the reason why we monitored the TIC chromatogram in the m/z range 200–500. By avoiding the production of cluster ions in such a manner, it is possible to monitor TIC chromatograms at even lower mass range. In other words, it is a possible means to enhance the detection limit.

CONCLUSIONS

We have attempted to screen OPs in blood by an LC–APCI-MS method. Its detection ability was comparable to that of GC–MS. Using TIC monitoring, our method, which is inferior to GC–MS analysis, was found to be a useful approach for determinating substances in patients with acute agricultural chemical toxicity. SIM was equal to other methods. With efforts to decrease cluster ions derived from the mobile phase components and by using columns of smaller inner diameters, we could decrease sample dilution by the mobile phase within the column and therefore procure sharp peaks for more efficient detection. Enhanced detection sensitivity can be further expected with the present method.

REFERENCES

1 M. Riva and A. Carisano, *J. Chromatogr.*, 42 (1969) 464.
2 B. J. McDermott, J. A. Double and M. C. Bibby, *J. Chromatogr.*, 338 (1985) 335.
3 R. Benecke, B. Vetter and R. A. de Zeeuw, *J. Chromatogr.*, 417 (1987) 287.
4 M. DeBerardinis, Jr. and W. A. Wargin, *J. Chromatogr.*, 246 (1982) 89.
5 C. M. Sparacino and J. W. Hines, *J. Chromatogr. Sci.*, 14 (1976) 549.
6 G. van der Velde and J. F. Ryan, *J. Chromatogr. Sci.*, 13 (1975) 322.
7 H. J. Stan, *Chromatographia*, 10 (1977) 233.
8 A. K. Singh, D. W. Hewetson and K. C. Jordan, *J. Chromatogr.*, 369 (1986) 83.
9 J. P. G. Wilkins, A. R. C. Hill and D. F. Lee, *Analyst (London)*, 110 (1985) 1045.
10 C. Blakely, J. Carmody and M. Vestal, *J. Am. Chem. Soc.*, 102 (1980) 5931.
11 C. Blakely, J. Carmody and M. Vestal, *Anal. Chem.*, 52 (1980) 1636.
12 E. Harin and M. Vestal, *Anal. Chem.*, 53 (1982) 1492.
13 C. Blakely and M. Vestal, *Anal. Chem.*, 55 (1983) 750.
14 D. Liberato, C. Fenselau and A. Yergey, *Anal. Chem.*, 55 (1983) 1741.
15 R. Voyksner, J. Bursey and E. Pellizzari, *Anal. Chem.*, 56 (1984) 1507.
16 R. Voyksner, J. Hines and E. Pellizzari, *Biomed. Mass Spectrom.*, 11 (1984) 616.
17 D. Barceló, F. A. Maris, R. B. Geerdink, R. W. Frei, G. J. de Jong and U. A. Th. Brinkman, *J. Chromatogr.*, 394 (1987) 65.
18 A. Farran, J. De Pablo and D. Barcelo, *J. Chromatogr.*, 455 (1988) 163.
19 D. Barcelo, *Biomed. Environ. Mass Spectrom.*, 17 (1988) 363.
20 Y. Kato and Y. Numajiri, *J. Chromatogr.*, 562 (1991) 81.
21 K. Hiraoka, *Shitsuryo Bunseki*, 28 (1980) 185.
22 C. K. Lim and T. J. Peters, *J. Chromatogr.*, 316 (1984) 397.
23 K. Hiraoka, *Shitsuryo Bunseki*, 26 (1978) 1.
24 K. Adachi, N. Ohokuni and T. Mitsuhashi, *J. Assoc. Off. Anal. Chem.*, 67 (1984) 798.
25 K. Sasaki, T. Suzuki and Y. Saito, *J. Assoc. Off. Anal. Chem.*, 70 (1987) 460.
26 H. J. Stan, *Fresenius' Z. Anal. Chem.*, 287 (1977) 104.
27 K. L. Busch, M. M. Bursey and G. W. Sovocool, *Appl. Spectrosc.*, 32 (1978) 388.
28 H. J. Stan and G. Kellner, *Biomed. Mass Spectrom.*, 9 (1982) 483.
29 C. E. Parker, C. A. Haney and J. R. Hass, *J. Chromatogr.*, 237 (1982) 233.
30 C. E. Parker, C. E. Haney and J. R. Hass, *J. Chromatogr.*, 242 (1982) 77.
31 C. E. Parker, K. Yamaguchi and J. R. Hass, *J. Chromatogr.*, 319 (1985) 273.
32 T. Cairns and E. G. Siegmund, *J. Assoc. Off. Anal. Chem.*, 70 (1987) 858.
33 A. G. John and D. Andrzejewski, *Applications of New Mass Spectrometry Techniques in Pesticide Chemistry*, Wiley-Interscience, New York, 1987, p. 187.

Journal of Chromatography, 595 (1992) 203–208
Elsevier Science Publishers B.V., Amsterdam

CHROM. 23 920

Stereochemical analysis of betamethasone and dexamethasone by derivatization and high-performance liquid chromatography

Su-Hwei Chen, Shou-Mei Wu and Hsin-Lung Wu*

Graduate Institute of Pharmaceutical Sciences, Kaohsiung Medical College, Kaohsiung 807 (Taiwan)

(First received July 23rd, 1991; revised manuscript received November 12th, 1991)

ABSTRACT

A simple and economical high-performance liquid chromatographic method has been developed for the simultaneous determination of betamethasone and dexamethasone. The method is based on the derivatization of the structural epimers of betamethasone and dexamethasone with a homochiral reagent, N-carbobenzoxy-L-phenylalanine. The derivatives obtained were easily recognized by a non-chiral silica column with *n*-hexane–dichloromethane–isopropanol (100:100:4, v/v/v) as a mobile phase and a good separation was obtained for quantitation. The method was satisfactorily applied to the determination of betamethasone and dexamethasone in tablets.

INTRODUCTION

Betamethasone (BTM) and dexamethasone (DXM), illustrated in Fig. 1, are highly potent fluorinated glucocorticoids and are widely used for the treatment of inflammation, allergies and adrenal cortex insufficiency. BTM has been reported to have a slightly stronger glucocorticoid effect [1] and is more expensive than DXM.

The official methods of the United States Pharmacopeia (USP) [2] for the determination of BTM and DXM are based on reversed-phase high-performance liquid chromatography (HPLC) with C_{18} and C_8 columns, respectively. Although a number of liquid chromatographic methods [3–13] have been described for the determination of BTM, DXM, or their analogues in various samples, to the authors' knowledge, no HPLC methods have been reported for the simultaneous determination of BTM and DXM. This is mainly due to the close structural similarity of the epimers of BTM and DXM which unfavourably affects their separation.

An attempt was made to increase the stereochemical differences between the epimers by derivatization with a commercially available homochiral reagent, N-carbobenzoxy-L-phenylalanine (N-CBZ-Phe). A good separation of the derivatives of BTM and DXM was given on an achiral silica column.

In this paper, an HPLC–UV derivatization method for the simultaneous determination of BTM and DXM is described. Its application to the determination of BTM and DXM in commercial tablets was satisfactory. Further development of the method for the simultaneous determination of BTM, DXM and their analogues in drugs used illegally, such as for promoting zootechnical performance and enhancing the effect of herbal medicine, will be useful.

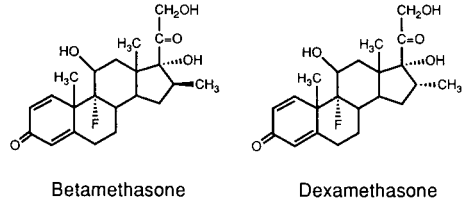

Betamethasone Dexamethasone

Fig. 1. Structures of betamethasone and dexamethasone.

0021-9673/92/$05.00

EXPERIMENTAL

Materials

BTM, DXM and phenacetin (internal standard, I.S.) (Sigma, St. Louis, MO, USA), N-CBZ-Phe, N,N'-dicyclohexylcarbodiimide (DCC) and 4-dimethylaminopyridine (DMAP) (TCI, Tokyo, Japan), dichloromethane and *n*-hexane (Fisher, Fair Lawn, USA), and isopropanol and silica gel 60 (70–230 mesh) (E. Merck, Darmstadt, Germany) were used without further treatment and all reagents used were of analytical-reagent grade.

HPLC conditions

A Water-Millipore LC system with a U6K injector and a Model 484 UV–VIS detector was used. A Nova-Pak silica column (75 × 3.9 mm I.D., 4 μm) with a disposable Resolve silica precolumn (10 μm; bed volume < 100 μl) (Waters-Millipore) and a mixed solvent of *n*-hexane–dichloromethane–isopropanol (100:100:4, v/v/v) at a flow-rate of 1.0 ml/min were used. The column eluate was monitored at 240 nm. The solvents were degassed with a vacuum filter before use.

Mass and NMR spectrometry

Mass spectra were obtained on a JEOL JMS-HX 110 mass spectrometer with fast atom bombardment (FAB) of xenon as the ionization mode and an acceleration energy of 10 kV. ^{13}C NMR spectra were recorded in C^2HCl_3 on a Varian VXR 300 spectrometer. The nature of the ^{13}C resonance was deduced from distortionless enhancement by polarization transfer experiments performed by using polarization transfer pulses of 90 and 135°, respectively.

Derivatization procedures

Solutions of BTM, DXM, phenacetin, N-CBZ-Phe and DCC were prepared by dissolving the appropriate amount of the respective compounds in dichloromethane.

Procedure for individual determination. A 0.5-ml volume of BTM or DXM solution was added to a 10-ml glass-stoppered test-tube containing 0.2 ml of phenacetin (I.S.) solution (1.2 m*M*) and 0.1 ml of DMAP solution (0.5 m*M*). A 0.1-ml volume of solution of N-CBZ-Phe (90 m*M* for BTM or 20 m*M* for DXM) and DCC (90 m*M* for BTM or 20 m*M* for DXM) was then added. The reaction mixture was shaken mechanically at 30°C for 30 min. A 10-μl aliquot of the solution was determined by HPLC with UV detection.

Procedure for simultaneous determination. A 0.5-ml volume of a solution of BTM and DXM was added to a 10-ml glass-stoppered test-tube containing 0.2 ml of phenacetin (I.S.) solution (1.2 m*M*) and 0.1 ml of DMAP solution (0.5 m*M*). A 0.1-ml volume of each N-CBZ-Phe (100 m*M*) and DCC (100 m*M*) was then added. The reaction mixture was shaken mechanically at 30°C for 1.0 h. A 10-μl aliquot of the solution was then separated by HPLC.

RESULTS AND DISCUSSION

Direct chromatographic separation of BTM and DXM with reversed- and normal-phase HPLC using an achiral column was briefly studied. Reversed-phase HPLC for the separation of BTM and DXM with a C_{18} column (150 × 3.9 mm I.D.; 4 μm) using common mobile phases (at a flow-rate of 1 ml/min), including acetonitrile–water (40:60, v/v) and methanol–water (40:60, v/v) was performed, but BTM and DXM were eluted as a single peak. The separation of BTM and DXM by normal-phase HPLC using a silica column (75 × 3.9 mm I.D.; 4 μm) with a variety of mixed solvents at a flow-rate of 0.8 ml/min was also studied, including dichloromethane–isopropanol (100:4, v/v) and *n*-hexane–dichloromethane–isopropanol (100:100:8, v/v/v). These all resulted in tailing and incomplete resolution of BTM and DXM. Decreasing the polarity of the mobile phase *n*-hexane–dichloromethane–isopropanol (100:100:6, v/v/v) led to tailing peaks not suitable for chromatographic analysis, as shown in Fig. 2.

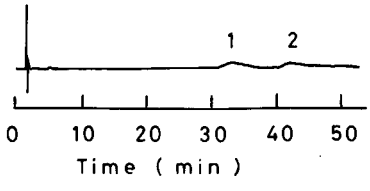

Fig. 2. HPLC chromatogram of an underivatized mixture of BTM and DXM. Peaks: 1 = DXM; 2 = BTM. Conditions: Nova-Pak silica column (75 × 3.9 mm I.D.; 4 μm); mobile phase, *n*-hexane–dichloromethane–isopropanol (100:100:6, v/v/v); flow-rate, 0.8 ml/min; UV detection, 240 nm.

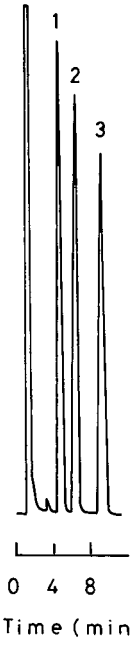

Fig. 3. HPLC chromatogram of the simultaneous determination of a BTM and DXM mixture. Peaks: 1 = Derivative of DXM; 2 = derivative of BTM; 3 = phenacetin (I.S.). Conditions: Nova-Pak silica column (75 × 3.9 mm I.D.; 4 μm); mobile phase, *n*-hexane–dichloromethane–isopropanol (100:100:4, v/v/v); flow-rate, 1.0 ml/min; UV detection, 240 nm.

An analytical strategy for better molecular recognition of BTM and DXM focused on the derivatization of BTM and DXM with a commercially available homochiral reagent, N-CBZ-Phe. As shown in Fig. 3, the resulting derivatives were well resolved by adsorption HPLC with good chromatographic properties of resolution (R_s = 1.59) and selectivity (α = 1.50), indicating that the derivatives of BTM and DXM interact differently with the silica column and the mobile phase. For the optimization of the derivatization conditions for BTM and DXM, some parameters affecting the derivatization reaction were investigated and evaluated by the peak-area ratios of the respective derivative to the I.S. instead of evaluation by the true yield of the derivatives.

Effect of amount of N-CBZ-Phe and DCC

The effects of variable amounts of N-CBZ-Phe and DCC with 0.05 μmol of DMAP on the derivatization of BTM (0.05 μmol) and DXM (0.05 μmol) at 30°C were studied. The results indicated that the amounts of N-CBZ-Phe required for the equilibrium derivatization of BTM and DXM were 9.0 and 2.0 μmol, respectively. The amounts of DCC required for the derivatization of BTM and DXM were also 9.0 and 2.0 μmol, respectively. BTM needs more N-CBZ-Phe to reach equilibrium derivatization in 0.5 h; the derivatization of BTM with smaller amounts of N-CBZ-Phe (2.0 μmol) and DCC (2.0 μmol) resulted in a longer time (about 4.0 h) to attain plateau formation of the derivative with a peak to area ratio equivalent to that obtained with the larger amount. The lower reactivity of BTM is probably because the β-orientation of the two methyl groups at C_{16} and C_{13} sterically affect the esterification of the hydroxyl group at C_{21} with N-CBZ-Phe.

Effect of reaction time

The effects of reaction time were examined for the derivatization of BTM and DXM under the optimum conditions. The results were presented in Fig. 4. The derivatization reaction proceeded under mild conditions and reached equilibrium in a favourably short time of about 0.5 h.

Structural identification of the derivatives

The structural analysis of the isolated derivatives of BTM and DXM was performed by FAB mass spectrometry with 3-nitrobenzyl alcohol as a matrix. The mass spectra obtained are shown in Fig. 5. Quasi-molecular ions of the derivatives of BTM and DXM were found at m/z = 674 $(MH)^+$. This

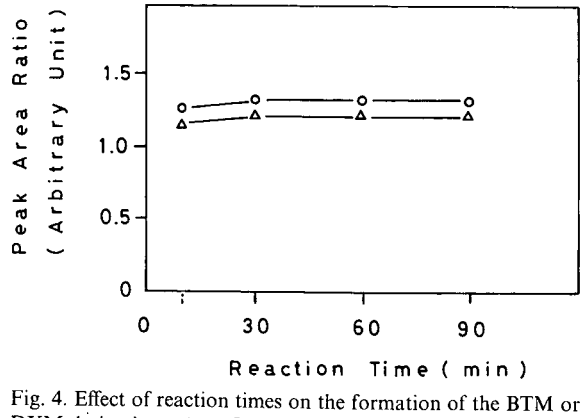

Fig. 4. Effect of reaction times on the formation of the BTM or DXM derivatives. △ = BTM; ○ = DXM.

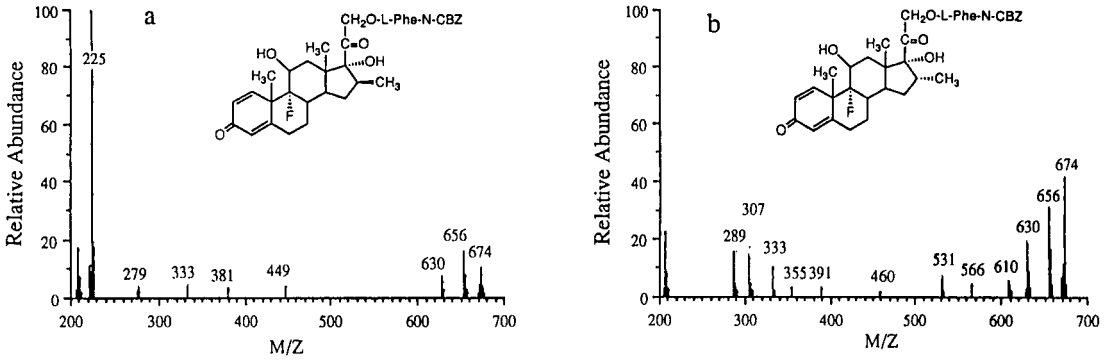

Fig. 5. Mass spectra of (a) BTM and (b) DXM derivatives with FAB ionization. See text for conditions.

indicates that one of the alcohol groups of the epimer was acylated as no higher mass fragments of BTM or DXM were found. In addition, the ion fragments at *m/z* 656 and 333, which correspond to $(MH)^+$ minus water and $(MH)^+$ minus a carbonyl side-chaine at C_{17} on BTM or DXM; the *m/z* fragments at 674 and 333 suggest that the formation of a single ester is from the primary hydroxyl group at C_{21} on BTM or DXM. Furthermore, by comparing the ^{13}C NMR spectra of the derivatives of BTM and DXM with those of underivatized BTM and DXM, an upfield shift of about 7.8 ppm from 212.9 ppm (chemical shift) of C_{20} on BTM to 205.1 ppm of C_{20} on the derivative of BTM and also a parallel upfield shift of 7.4 ppm from 211.7 ppm of C_{20} on DXM to 204.3 ppm of C_{20} on the derivative of DXM were observed. These findings suggest that the hydroxyl group at C_{21} is acylated. The possible hydrogen bonding between the carbonyl group of C_{20} and the hydroxyl group at C_{21} disappears owing to the esterfication of the OH group at C_{21} on BTM or DXM and this leads to the upfield shift of the carbonyl carbon of C_{20} as proposed by Duddeck *et al.* [14]. From the mass and ^{13}C-NMR analyses of the derivatives of BTM and DXM, the position of the ester formation is assigned as at the primary alcohol group of the epimers.

Analytical calibration

Based on the optimum derivatization conditions, the derivatization procedures for the individual and simultaneous determination of BTM and DXM were formulated as described under Experimental. To evaluate the quantitative applicability of this method, five different concentrations of BTM or DXM over the range 1.85–50 nmol (each in 0.5 ml of dichloromethane) were determined to construct a calibration graph. The results indicate good linearity for the determination of BTM and DXM over the range used; for individual determination, the linear regression equations obtained were $y = 0.02539x - 0.002517$ with $r = 0.999$ for BTM and $y = 0.02933x + 0.002376$ with $r = 0.999$ for DXM, where y is the peak area ratio of the glucocorticoid derivative to the I.S., x is the amount in nmol of BTM or DXM and r is the correlation coefficient. Possible linearity to higher concentrations of BTM and DXM was not studied because such concentrations are of no practical use. The detection limits (signal-to-noise ratio 5) of BTM and DXM with a 20-μl aliquot injected were 4.2 and 2.1 pmol, respectively.

Satisfactory results were also obtained for the simultaneous determination of BTM and DXM at five different concentrations in the range 1.85–50 nmol. The linear regression equations obtained were $y = 0.02473x + 0.002410$ with $r = 0.999$ for BTM and $y = 0.02798x + 0.002146$ with $r = 0.999$ for DXM. The reproducibility (relative standard deviation) of the proposed method from ten replicate measurements of 50 nmol of the epimer was 1.43% for BTM and 1.21% for DXM.

Application

One tablet of commercial BTM or DXM was placed in a 10-ml test-tube containing 5.0 ml of distilled water for maceration. It was then triturated with a glass rod and sonicated for 20 min to fully

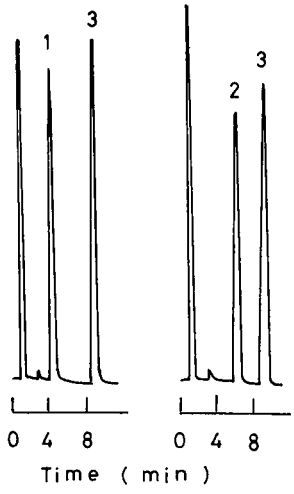

Fig. 6. HPLC chromatograms for the determination of BTM and DXM in tablets. Peaks: 1 Derivative of DXM; 2 = derivative of BTM; 3 = phenacetin (I.S.). Conditions: Nova-Pak silica column (75 × 3.9 mm I.D.; 4 μm); mobile phase, *n*-hexane–dichloromethane–isopropanol (100:100:4, v/v/v); flow-rate, 1.0 ml/min; UV detection, 240 nm.

disintegrate the matrix. The contents of the test-tube were transferred into a 50-ml separator with the aid of 9 ml of dichloromethane and were extracted with an additional three 5-ml portions of dichloromethane. The dichloromethane extracts were filtered through a dichloromethane-treated filter paper into a 25-ml calibrated flask. Dichloromethane was added to the solution and well mixed. A 0.5-ml aliquot of this solution was pipetted into a 10-ml glass-stoppered test-tube and derivatized as described earlier. The HPLC chromatograms obtained are shown in Fig. 6 and the analytical results were presented in Table I. The concentrations of BTM and DXM in the tablets tested were all within 90–110% of the labelled amount of BTM and DXM specified by the current USP. A synthetic test mixture was formulated by mixing an amount of powdered tablets from BTM and DXM equivalent to 0.25 mg of BTM plus 0.25 mg of DXM and this was analysed as described. The results are also shown in Table I. This simultaneous determination of BTM and DXM in a test mixture provides a method to check the illegal use of DXM for BTM or the use of a mixture of DXM and BTM for BTM to reduce costs. The proposed method could therefore be used for the quality control of BTM and DXM in pharmaceutical products.

TABLE I

ASSAY RESULTS FOR BTM AND DXM TABLETS AND THEIR TEST MIXTURE OBTAINED FOR TWO COMMERCIAL SOURCES

Results given as mean ± S.D.

Sample	Amount found (mg per tablet)	Percentage of manufacturer's claim (%)
BTM (0.5 mg per tablet)[a]		
B_1	0.457 ± 0.003	91.4
B_2	0.462 ± 0.004	92.6
B_3	0.468 ± 0.003	93.6
B_4	0.455 ± 0.002	91.0
B_5	0.475 ± 0.005	95.0
B_6	0.471 ± 0.004	94.2
	Mean recovery (%)	93.0
	S.D. (%)	1.58
DXM (0.5 mg per tablet)[a]		
D_1	0.486 ± 0.005	97.2
D_2	0.492 ± 0.004	98.4
D_3	0.487 ± 0.005	97.4
D_4	0.488 ± 0.004	97.6
D_5	0.507 ± 0.006	101.4
D_6	0.510 ± 0.005	102.0
	Mean recovery (%)	99.0
	S.D. (%)	2.14
Test mixture (0.25 mg BTM + 0.25 mg DXM)[b]		
BTM	0.237 ± 0.001	94.5
	S.D. (%)	1.30
DXM	0.257 ± 0.001	102.8
	S.D. (%)	1.13

[a] $n = 3$.
[b] $n = 6$.

Further modification of the method by labelling the epimers with other chromophores or fluorophores is being investigated for the highly sensitive determination of the epimers in various samples of pharmaceutical, clinical or forensic interest.

ACKNOWLEDGEMENT

The authors are grateful to the National Science Council, Taiwan for financial support of part of this work (NSC 81-0412-B-037-06).

REFERENCES

1 H. Kalant and W. H. E. Roschlau, *Principles of Medical Pharmacology*, Decker, Toronto/Philadelphia, 1989, p. 479.
2 *The United States Pharmacopeia*, 22nd ed., The United States Pharmacopeial Convention, Rockville, MD, 1990, pp. 158 and 393.

3 L. G. McLaughlin and J. D. Henion, *J. Chromatogr.*, 529 (1990) 1.
4 Ph. Gaignage, G. Lognary, M. Marlier, M. Severin and Ph. Dreze, *Chromatographia*, 28 (1989) 623.
5 D. Lamiable, R. Vistelle and M. N. H. Millart, *J. Chromatogr.*, 434 (1988) 315.
6 L. L. Ng, *J. Assoc. Off. Anal. Chem.*, 71 (1988) 534.
7 N. Maron, E. A. Cristi and A. A. Ramos, *J. Pharm. Sci.*, 77 (1988) 638.
8 E. A. Bunch, *J. Assoc. Off. Anal. Chem.*, 70 (1987) 967.
9 L. L. Ng, *J. Assoc. Off. Anal. Chem.*, 70 (1987) 829.
10 D. Lamiable, R. Vistelle, H. Millart, V. Sulmont, R. Fay, J. Caron and H. Choisy, *J. Chromatogr.*, 378 (1986) 486.
11 E. W. Smith, J. M. Haigh and I. Kanfer, *Int. J. Pharm.*, 27 (1985) 185.
12 P. M. Plezia and P. L. Berens, *Clin. Chem.*, 31 (1985) 1870.
13 M. C. Petersen, R. L. Nation and J. J. Ashley, *J. Chromatogr.*, 183 (1980) 131.
14 H. Duddeck and D. Rosenbaum, M. Hani, A. Elgamal and M. B. E. Fayez, *Magn. Reson. Chem.*, 24 (1986) 999.

Journal of Chromatography, 595 (1992) 209–219
Elsevier Science Publishers B.V., Amsterdam

CHROM. 23 875

Critical capillary column examination of the relationship between separation number and height equivalent to a theoretical plate and their dependence on temperature

Louis A. Jones*, John J. Glennon and William H. Reiss☆

Department of Chemistry, Box 8204, North Carolina State University, Raleigh, NC 27695-8204 (USA)

(Received August 20th, 1991)

ABSTRACT

Separation numbers (*TZ* values) for the homologous pair C_{11}–C_{12} were determined using a capillary column at 40, 60 and 80°C, as was the height equivalent to a theoretical plate, *h*, for each hydrocarbon at various linear velocities. Increasing temperatures produced both decreasing *TZ* and *h* values, indicating decreased column resolution but suggesting an increase in the number of theoretical plates and hence a contradictory improved column efficiency. The optimum linear velocity required for producing maximum *TZ* was shown to be the expected average of that required to produce h_{min} for C_{11} and C_{12}. Van Deemter-type plots further suggested an inverse relationship between *h* and *TZ*. The following equation was derived: $TZ = (L/5.54)^{\frac{1}{2}} \cdot [(t_r^a - t_r^b)/(t_r^b h_b^{\frac{1}{2}} + t_r^a h_a^{\frac{1}{2}})] - 1$, where t_r is the retention time of consecutive homologues a and b and *L* is the column length. Results using this equation were compared with those obtained with $TZ = [(t_r^b - t_r^a)/(w_{0.5}^a + w_{0.5}^b)] - 1$, where $w_{0.5}$ is the peak width at half-height. The excellent agreement using the data from this study and previous reports clearly shows the concept of *TZ* to be based on sound chromatographic principles.

INTRODUCTION

The concept of the separation number, *TZ*, was first proposed in 1962 [1] and incorporated the retention times and the peak widths at half-height ($w_{0.5}$) of two homologues, a and b, which differed by one CH_2 group:

$$TZ = \frac{t_r^b - t_r^a}{w_{0.5}^a + w_{0.5}^b} - 1 \quad (1)$$

Ettre [2] in a definitive paper on *TZ* and its relationship to other gas chromatographic parameters, viewed the relationship as an indication of column efficiency. He related *TZ* to the resolution *R* of the homologues a and b as defined by the equation

$$R_{b/a} = \frac{2(t_r^b - t_r^a)}{w_b^a + w_b^b} \quad (2)$$

where w_b is the base width. Substitution of the equality $w_{0.5} = w_b/1.699$ in eqn. 1 redefined *TZ* in terms of base widths:

$$TZ = \frac{1.699(t_r^b - t_r^a)}{w_b^a + w_b^b} - 1 \quad (3)$$

Substution of eqn. 2 in eqn. 3 gave

$$TZ = 1.699\left(\frac{R_{b/a}}{2}\right) - 1 = \frac{R_{b/a}}{1.177} - 1 \quad (4)$$

thus relating *TZ* and *R*. Assuming that homologues a and b eluted very close to one another, then the approximation can be made that $w_b^b \approx w_b^a$, which would reduce eqn. 2 to

$$R_{b/a} = \frac{t_r^b - t_r^a}{w_b^b} \quad (5)$$

By assuming that $TZ = 0$ for these homologues, it can be seen from eqn. 4 that $R_{b/a} = 1.177$ and therefore eqn. 5 becomes

☆ Present address: First Brands Corp., 55 Federal Road, Danbury, CT 06810, USA.

0021-9673/92/$05.00

$$1.177 = \frac{\Delta t_r}{w_b} \tag{6}$$

As $w_b = 4\sigma$, $\Delta t = 4.7\sigma$, which gives rise to Ettre's statement [2] that TZ expresses the number of component peaks which are separated by a 4.7σ resolution that can be placed between the peaks of two consecutive alkanes with z and $z + 1$ carbon atoms. Interestingly, there is no inclusion of h (the height equivalent to a theoretical plate) in the relationship.

Subsequently, Jennings and Yabumoto [3] noted that as the column temperature is lowered, relative retentions and TZ increase, leading to the conclusion that the two are related. Rooney and Hartigan [4] showed that "the value of the separation number can be manipulated to give high results if desired". They proposed the approximation $w^b_{0.5}/w^a_{0.5} \approx \alpha$, which, when used in eqn. 1, gave rise to the equation

$$w^b_{0.5} = \frac{t^b_r - t^a_r}{(1 + 1/\alpha)(TZ + 1)} \tag{7}$$

By substitution of eqn. 7 in the equation defining N_{eff}:

$$N_{eff} = 5.54\left(\frac{t^b_r}{w^b_{0.5}}\right)^2 \tag{8}$$

and utilization of the relationship $t^b_r/(t^b_r - t^a_r) = \alpha/(\alpha - 1)$, the following equation was obtained after several rearrangements:

$$TZ = 0.425\left(\frac{\alpha - 1}{\alpha + 1}\right)(N_{eff})^2 - 1 \tag{9}$$

Important to this derivation is the fact that only the peak with the larger t_r or capacity factor is utilized, and again the assumption was made that the peak widths are "approximately" the same.

Krupcik *et al.* [5], using similar substitutions, derived the following equation for the resolution between homologues with $z + 1$ and z carbon atoms:

$$R_{(z+1)/z} = \frac{\alpha - 1}{2} \cdot \frac{(N_z N_{z+1})^{\frac{1}{2}}}{\alpha(N_z)^{\frac{1}{2}} + (N_{z+1})^{\frac{1}{2}}} \tag{10}$$

Then, approximating the number of effective plates by the equation

$$N = \left(N_\infty + \frac{b}{k'}\right)\left(\frac{k'}{1 + k'}\right)^2 \tag{11}$$

where k' is for the later eluting peak of the two homologues, and substituting in eqn. 10, the equation

$$R_{b/a} = \frac{N^{\frac{1}{2}}_\infty}{2} \cdot \frac{\alpha - 1}{\alpha + 1} \tag{12}$$

was obtained. Substituting this equation in eqn. 4 gave the TZ relationship

$$TZ = \frac{N^{\frac{1}{2}}_\infty}{2.35} \cdot \frac{\alpha - 1}{\alpha + 1} - 1 \tag{13}$$

It should be noted that none of the above derivations includes the column length, an important chromatographic parameter.

Both of these groups warned that the temperature dependence makes TZ a value that should be utilized with caution. Indeed, it was described as a "rubber ruler" [5] which should be used carefully or avoided.

We have studied the relationship between TZ and the average carbon number of the two homologues used, $\overline{CH}$ [where $\overline{CH} = (C_b + C_a)/2$] using various temperature-programmed gas chromatographic (TPGC) conditions with various starting temperatures and column flow-rates. Under isobaric conditions (constant head pressure) and using an SP 2100-coated fused-silica capillary column, it was found that TZ was related to $\overline{CH}$ by the equation

$$TZ = a(\overline{CH}) + b \tag{14}$$

for a homologous series of *n*-alkanes, carboxylic acids, methyl esters and alcohols with correlation coefficients >0.95 [6]. The same relationship holds for the TPGC of C_{12}–C_{16} *n*-alkanes at starting temperatures of 40, 50 and 60°C under constant flow conditions (maintained by pressure programming) and isobaric flow. The differences in the two flow conditions resulted in a less negative slope value a under isobaric flow than under constant flow [7]. A plot of the experimentally determined maximum TZ values obtained at a starting temperature of 40°C and the lowest temperature programming rate (TPR) for all $\overline{CH}$s (12.5, 13.5, 14.5, 15.5 and 16.5) *vs.* the starting flow-rates (both constant and isobaric flows) produced an inverse Van Deemter plot. The visualized optimum starting flow-rate of *ca.* 0.9 ml/min at a TPR between 0.86 and 1.35°C/min with a starting temperature of 40°C produced the maximum TZ values for all $\overline{CH}$s, although there was

some evidence that lower flow-rates would be required for the higher molecular weight homologues.

As this suggested the possibility that an inverse relationship between *TZ* and the height equivalent to a theoretical plate (HETP), *h*, might exist, an investigation was initiated to study the changes in *TZ* and *h* as a function of different isothermal temperatures and at various constant flow-rates, and the results are presented in this paper.

EXPERIMENTAL

A Hewlett-Packard Model 5880A gas chromatograph equipped with a Model 7671 autosampler, a flame ionization detector, an electronic flow controller and a split–splitless injector set for a splitting ratio of 200:1 was used. A Level IV microprocessor with an alphanumeric keyboard controlled the temperature programming rates and the column head pressure of the helium carrier gas. Electronically measured retention times (± 0.10 min) and peak width at half-height ($w_{0.5}$), repeatable to $\pm 1\%$, were recorded in the "report annotation" mode [6]. On completion of the gas chromatogram, a specifically designed BASIC program listed the GC parameters for that analysis, giving the oven temperature, the column head pressure and the calculated *TZ* value for the two alkanes. The alkanes used in this study were 99+% pure undecane (C_{11}) and dodecane (C_{12}), obtained from Alltech (Applied Science Labs., Deerfield, IL, USA). These alkanes (*ca.* 300 mg of each) were made up to 10 ml with high-performance liquid chromatographic grade chloroform and 1 ml of this solution was diluted to 50 ml to give a solution that produced on-scale peaks (attenuation 0) for 5–10-μl injections, depending on the column temperature and flow-rate.

A cross-linked DB-5 fused-silica column (25 μm film thickness) (15 m × 0.248 mm I.D.) was used (J&W Scientific, Rancho Cordova, CA, USA) and conditioned for 2 days by microprocessor-controlled repetitive TPGC runs from 100 to 200°C at 10°C/min at an initial helium flow-rate of 1.10 ml/min. The maximum column temperature was never allowed to exceed 250°C, although the manufacturer's recommended T_{max} is 325°C for isothermal operation. When not in use, the column temperature was maintained at 250°C with a continuous helium purge of *ca.* 0.5 ml/min. All runs were performed with injection port and detector temperatures of 275°C. Flow-rates were calculated in triplicate from the electronically determined retention time (t_r) of injected butane using the equation $F = \pi r^2 L/t_r$, where r (cm) is the radius of the column and L (cm) the column length.

RESULTS AND DISCUSSION

The effects of a change in carrier gas flow-rate at three different column temperatures (40, 60 and 80°C) on the *h* values of undecane and dodecane were determined in triplicate and, from the same GC runs, the *TZ* values were determined for the C_{11}–C_{12} homologous pair. The value of *h* (in mm) was calculated for each *n*-alkane from the equation

$$h = \frac{L}{5.54}\left(\frac{w_{0.5}}{t_r}\right)^2 \tag{15}$$

where L (mm) is the column length, $w_{0.5}$ the peak width at half-height and t_r (min) the retention time, *i.e.*, the time required for the alkane to elute from the column after injection.

Table I gives the *TZ* and *h* values calculated from the data generated. Several important facts are apparent. First, as the column temperature increases, the overall *TZ* values decrease, and the maximum *TZ* for each temperature group decreases with increasing temperature. Second, as the column temperature increases, the overall *h* values for each temperature group decrease (reflecting a decrease in t_r and a concomitant decrease in peak broadening), as do the minimum values of *h* for each temperature studied. Although this decrease in *h* would suggest improved column efficiency, the decreasing values of *TZ* indicate that the column resolving power is diminishing.

The Golay equation for a capillary column [8,9] is given by the equation

$$h = \frac{B}{\mu} + C\mu \tag{16}$$

where *h* is the height equivalent to a theoretical plate and μ the linear flow velocity. Using this equation, the data from Table I were used to model the relationships between both *h* and *TZ* and the velocity and/or flow.

$$h = \frac{B}{\mu} + C\mu + D \tag{17}$$

TABLE I

AVERAGE OF TRIPLICATE DETERMINATIONS AT 40, 60 AND 80°C OF h, t_r, FLOW-RATE, μ, AND TZ FOR C_{11} AND C_{12} ALKANES ON A DB-5 FUSED-SILICA CAPILLARY COLUMN (15 m × 0.25 mm I.D.) WITH d_f = 0.25 μm

Column temperature (°C)	Flow-rate (ml/min)	μ[a]	C_{12}			C_{11}			TZ[e]
			t_r[b]	$w_{0.5}$[c]	h[d]	t_r[b]	$w_{0.5}$[c]	h[d]	
40	0.516	17.52	179.31	2.218	0.414	72.88	0.867	0.383	33.51
	0.687	23.33	139.34	1.653	0.381	56.69	0.647	0.352	34.94
	1.10	37.35	85.29	1.087	0.440	34.67	0.431	0.419	32.34
	1.50	50.93	62.86	0.999	0.684	25.56	0.384	0.611	25.98
60	0.409	13.89	63.44	0.758	0.387	29.16	0.345	0.378	30.08
	0.503	17.08	55.22	0.602	0.322	25.34	0.295	0.368	32.30
	0.670	22.75	42.78	0.493	0.360	19.60	0.218	0.334	31.62
	1.08	36.67	26.49	0.303	0.355	12.15	0.145	0.386	31.00
	1.46	49.57	19.44	0.262	0.491	8.91	0.118	0.475	26.73
80	0.489	16.60	20.46	0.232	0.349	10.68	0.121	0.350	16.83
	0.651	22.10	15.69	0.160	0.349	8.18	0.083	0.279	29.96
	1.05	35.65	9.84	0.108	0.326	5.11	0.053	0.295	28.30
	1.42	49.57	7.19	0.086	0.391	3.73	0.045	0.394	25.32

[a] Linear velocity (cm/s).
[b] Retention time (min) S.D. < 6 parts in 1000.
[c] Peak width at half-height (min) S.D. < 3 parts in 100.
[d] Height equivalent to a theoretical plate (mm), S.D. < 2 parts in 1000.
[e] TZ values calculated from eqn. 1, S.D. < 20 parts in 1000.

$$TZ = A - \frac{B}{\mu} - C\mu \tag{17a}$$

It has been shown [10] that the optimum flow-rate, F_{opt}, or velocity, μ_{opt}, can be determined by differentiating eqn. 17 (or 17a) and setting $dh/d\mu$ (or $dTZ/d\mu$, eqn. 17a) equal to zero, giving rise to the equation

$$\mu_{opt} = (B/C)^{\frac{1}{2}} \tag{18}$$

The minimum value of h and the maximum value of TZ can be calculated from the equations

$$h_{min} = D + 2(BC)^{\frac{1}{2}} \tag{19}$$

and

$$TZ_{max} = A - 2(BC)^{\frac{1}{2}} \tag{20}$$

respectively, which are obtained by substituting eqn. 18 into 17 and 17a. These equations were used to calculate the optimum flow-rate or linear velocity necessary to produce the maximum TZ or minimum h at the specified column temperatures used in this study.

Table II gives the coefficients and precision for the relationship between h_{min} and μ_{opt} or F_{opt} (eqns. 18 and 19).

The h values for undecane (C_{11}) and dodecane (C_{12}), obtained at column temperatures of 40, 60 and 80°C, were plotted *versus* the measured linear velocities and are shown in Figs. 1 and 2, respectively. The plots are in accord with those obtained by Desty and Goldup [11] in the definitive 1960 report on their study of coated capillary columns. As they observed, an increase in temperature produces a decrease in h and a small increase in μ_{opt} and/or F_{opt} (Table II). They noted that these temperature changes produced a slight reduction in the resistance to mass transfer or C term (eqn. 13), and also noted the flattening of the curve at low linear velocities in the longitudinal diffusion area with a corresponding decrease in the B term.

Table III gives the coefficients and precision of the relationship between TZ_{max} and μ_{opt} or F_{opt} (eqns. 18 and 20).

The plots for the combined data for TZ and h (C_{11}

TABLE II

COEFFICIENTS FOR THE EQUATION $h = B/\mu + C\mu + D$ FOR THE C_{11} AND C_{12} ALKANES FOR COLUMN TEMPERATURES OF 40, 60 AND 80°C

Alkane	Temperature	B	C	D	R^2	μ_{opt}[a]	F_{opt}[b]	h_{min}[c]
C_{11}	40	10.962	0.019	−0.568	0.994	24.118	0.699	0.341
	60	4.446	0.009	−0.058	0.973	22.342	0.648	0.340
	80	9.178	0.013	−0.411	0.999	27.068	0.785	0.267
C_{12}	40	13.958	0.023	−0.780	0.982	24.530	0.711	0.358
	60	5.320	0.010	−0.146	0.846	22.554	0.654	0.326
	80	6.742	0.010	−0.227	0.927	26.199	0.759	0.288

[a] Optimum linear velocity (cm/s) calculated from eqn. 18.
[b] Optimum flow-rate (ml/min) calculated from $\mu = 34.502\ F$.
[c] Minimum h as calculated from eqn. 19.

and C_{12}) at 40, 60 and 80°C *versus* μ are shown in Figs. 3, 4 and 5, respectively. A comparison of the B and C terms in eqns. 17 and 17a (Tables II and III) show the trend that, with increasing column temperature, both terms decrease. The TZ_{max} values also decrease with increasing column temperature, indicating that the column resolving power or separation capability is being reduced. This reduction in TZ values has been reported previously [3,4,7] and is consistent with the fact that increased temperatures result in decreased t_r and $w_{0.5}$ values owing to an increase in the solute molecular diffusion coefficients in the mobile and stationary liquid phases (D_G and D_L, respectively), particularly for low-molecular weight C_4–C_9 solutes [11].

An examination of plots of TZ and h *versus* measured column linear velocities or flows-rates at 40°C (Fig. 3), 60°C (Fig. 4) and 80°C (Fig. 5) shows that the TZ curve is very nearly the mirror image of the h curve. The optimum flow-rates or velocities for

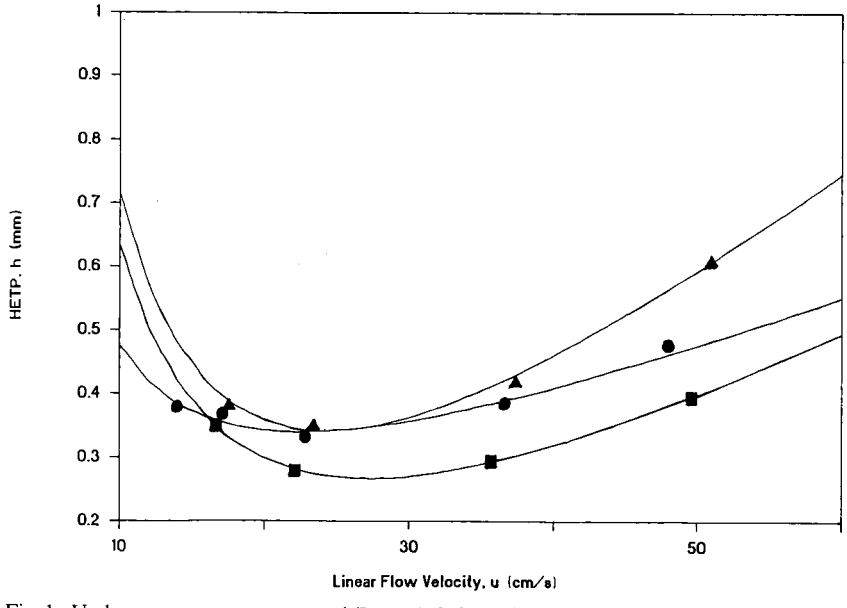

Fig. 1. Undecane: computer-generated (Lotus 1-2-3, version 2.2) plot of the height equivalent to a theoretical plate, h, *versus* linear flow velocity, μ, using a DB-5 fused-silica column, 25 μm film thickness (15 m × 0.248 mm I.D.) with helium as carrier gas. Column temperature: ▲ = 40; ● = 60; ■ = 80°C. Data from Table I.

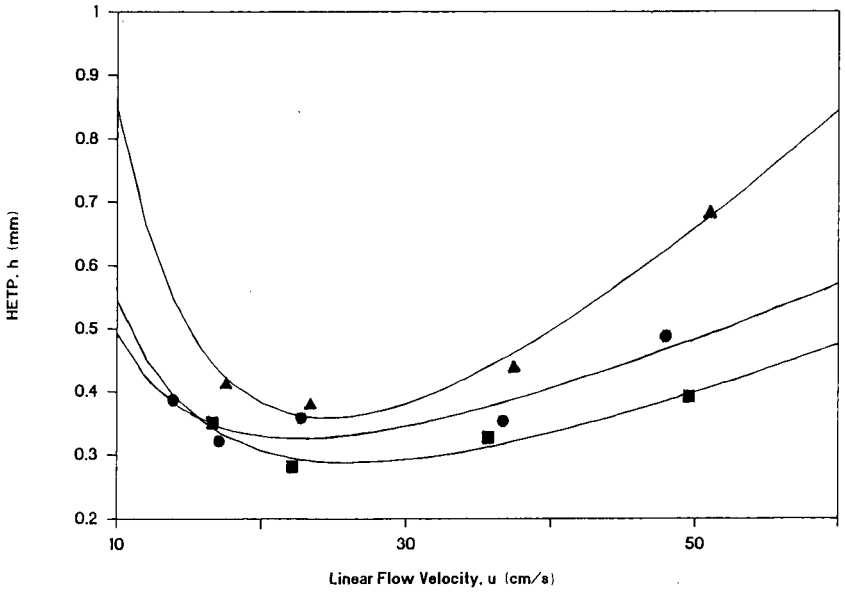

Fig. 2. Dodecane: computer-generated (Lotus 1-2-3, version 2.2) plot of the height equivalent to a theoretical plate, *h versus* linear flow velocity, μ, using a DB-5 fused-silica column, 25 μm film thickness (15 m × 0.248 mm I.D.) with helium as carrier gas. Column temperature: ▲ = 40; ● = 60; ■ = 80°C. Data from Table I.

maximizing TZ values can be seen to be very nearly the average of the μ_{opt} or F_{opt} of the h_{min} for C_{11} and C_{12}, respectively. Therefore, TZ would have a theoretical t_r equal to the average of the t_r values of C_{11} and C_{12} $[(t_r^{11} + t_r^{12})/2]$ and μ_{opt} can be calculated for these two alkanes. The average F_{opt} of these two homologues should approximate the calculated F_{opt} producing TZ_{max}. From Table III, the F_{opt} producing TZ_{max} at 40°C is 0.704 ml/min and the average of F_{opt} for C_{11} and C_{12} (Table II) is 0.705 ml/min. At 60°C, the F_{opt} for TZ_{max} is 0.661 ml/min and the C_{11}–C_{12} average F_{opt} is 0.651 ml/min. Performing the same comparison for 80°C, the TZ_{max} F_{opt} is 0.774 ml/min and the C_{11}–C_{12} average F_{opt} is 0.772 ml/min. The excellent agreement between the average F_{opt} values determined for h and the flow-rate determined for TZ_{max} suggests that there is a relationship between TZ and h. Further, Figs. 3–5 and the equations generated (eqns. 17 and 17a, Tables II and III) indicate that they are inversely related.

The is an equivalence relative to eqn. 1 that can be

TABLE III

COEFFICIENTS FOR THE EQUATION $TZ = A - B/\mu - C\mu$ FOR THE C_{11}–C_{12} ALKANE HOMOLOGUE PAIR FOR COLUMN TEMPERATURES OF 40, 60 AND 80°C

Temperature (°C)	B	C	A	R^2	μ_{opt} [a]	F_{opt} [b]	TZ_{max} [c]
40	385.842	0.653	66.902	0.998	24.301	0.704	35.146
60	196.518	0.378	49.648	0.926	22.804	0.661	32.412
80	317.385	0.446	53.605	0.942	26.689	0.774	29.821

[a] Optimum linear velocity (cm/s) calculated from eqn. 18.
[b] Optimum flow-rate (ml/min) calculated from $\mu = 34.502F$.
[c] Maximum TZ calculated from eqn. 20.

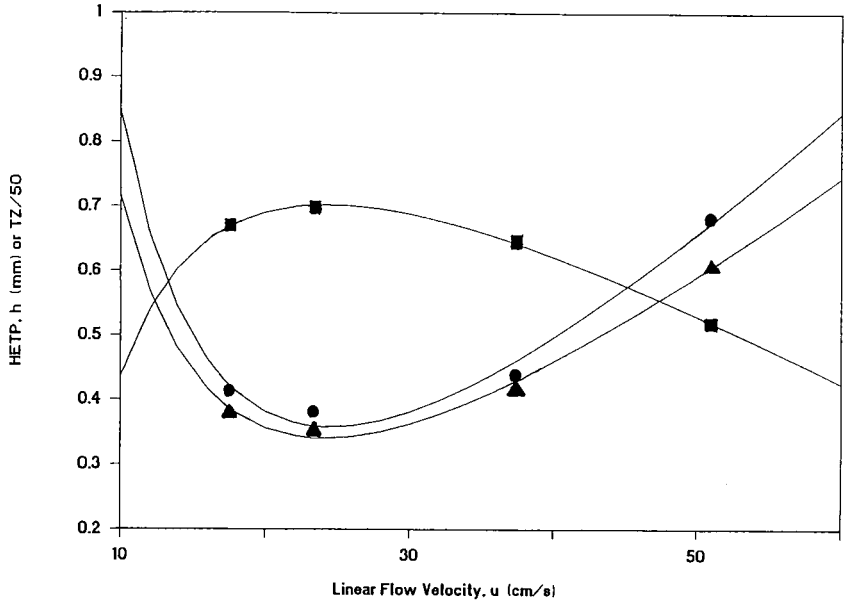

Fig. 3. Computer-generated (Lotus 1–2–3, version 2.2) plot of the height equivalent to a theoretical plate, h, for (▲) C_{11} and (●) C_{12} and ■ *TZ* (C_{11}–C_{12}) *versus* linear flow velocity, μ, using a DB-5 fused-silica column, 25 μm film thickness (15 m × 0.248 mm I.D.) with helium as carrier gas. Column temperature, 40°C.

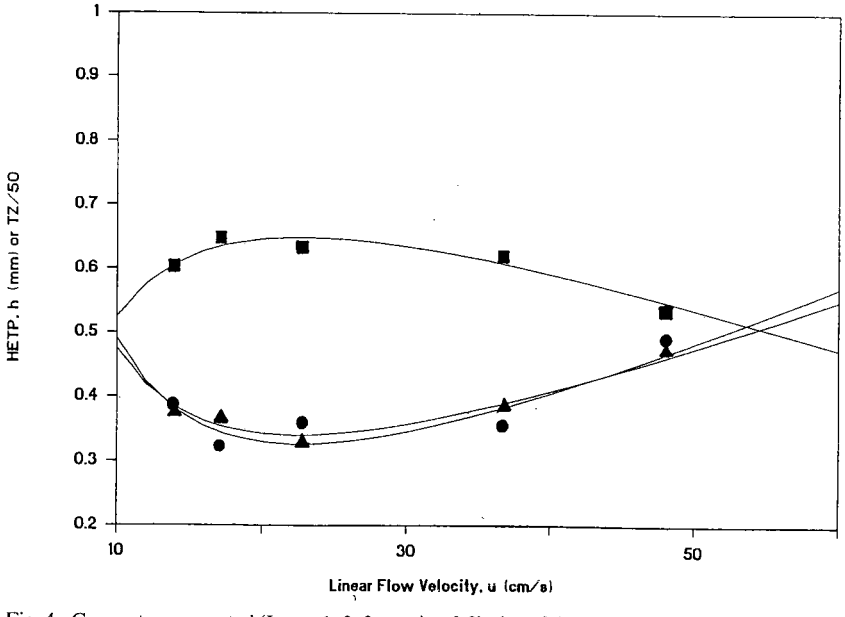

Fig. 4. Computer-generated (Lotus 1–2–3, version 2.2) plot of the height equivalent to a theoretical plate, h for (▲) C_{11} and (●) C_{12} and (■) *TZ* (C_{11}–C_{12}) *versus* linear flow velocity, μ, using a DB-5 fused-silica column, 25 μm film thickness (15 m × 0.248 mm I.D.) with helium as carrier gas. Column temperature, 60°C.

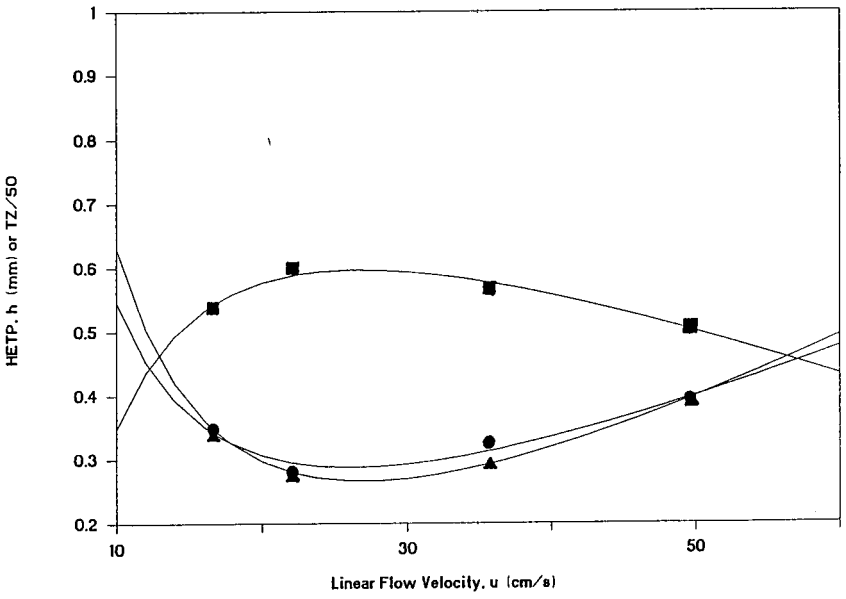

Fig. 5. Computer-generated (Lotus 1–2–3, version 2.2) plot of the height equivalent to a theoretical plate, h, for (▲) C_{11} and (●) C_{12} and (■) TZ (C_{11}–C_{12}) *versus* linear flow velocity, μ, using a DB-5 fused-silica column, 25 μm film thickness (15 m × 0.248 mm I.D.) with helium as carrier gas. Column temperature, 80°C.

shown by rearranging eqn. 15 to give $w_{0.5}$ as a function of h and the column length L as in the equation

$$w_{0.5} = \left(\frac{5.54}{L}\right)^{\frac{1}{2}} h^{\frac{1}{2}} t_r = 1.92 \cdot 10^{-2} h^{\frac{1}{2}} t_r \qquad (21)$$

Substituting this $w_{0.5}$ expression for each homologue in eqn. 1 and solving gives the equation

$$TZ = C \cdot \frac{t_r^b - t_r^a}{t_r^b h_b^{\frac{1}{2}} + t_r^a h_a^{\frac{1}{2}}} - 1 \qquad (22)$$

where $C = (L/5.54)^{\frac{1}{2}}$ or 52.035 for the 15 000-mm column length used in this study.

This is the first time that an equation has been derived for TZ in which the h value for both homologues and the column length are incorporated. Using this relationship and the experimentally determined t_r and h values for C_{11} and C_{12}, as shown in Table I, new TZ values were calculated from eqn. 22 and are compared with those calculated from eqn. 1 in Table IV. The TZ values from eqns. 1 and 22 agree extremely well with each other, as they should since eqn. 21 is simply an alternative definition of $w_{0.5}$.

To test further the derived relationship (eqn. 22), the data reported by Ettre [2] were used for calculation. With a reported column length of 20 m, the constant C becomes 60.080, and utilizing the re-

TABLE IV

TZ VALUES CALCULATED FROM EQN. 1 COMPARED WITH TZ VALUES CALCULATED FROM EQN. 22 FOR COLUMN TEMPERATURES OF 40, 60 AND 80°C FROM THE DATA IN TABLE I

Column temperature (°C)	Flow-rate (ml/min)	TZ (eqn. 1)	TZ (eqn. 22)
40	0.516	33.51	33.51
	0.687	34.94	34.95
	1.10	32.34	32.33
	1.50	25.98	25.97
60	0.409	30.08	30.08
	0.503	32.30	32.29
	0.670	31.62	31.60
	1.08	31.00	30.98
	1.46	26.73	26.73
80	0.489	26.83	26.65
	0.651	29.96	29.95
	1.05	28.30	28.34
	1.42	25.32	25.33

TABLE V

TZ VALUES CALCULATED FROM EQN. 1 COMPARED WITH *TZ* VALUES CALCULATED FROM EQN. 22 USING ETTRE'S [2] DATA FOR A COLUMN 20 m × 0.24 mm I.D. COATED WITH CARBOWAX 20M AT 80°C

Argon flow-rate (ml/min)	Compounds	Carbon No.	t_r (min)	h (mm)	*TZ* (eqn. 22)[a]	*TZ* (eqn. 1)[b]
0.291	*n*-Alkanes	C_{12}	7.07	0.243		
					22.47	22.50
		C_{13}	10.45	0.245		
					26.39	26.40
		C_{14}	16.64	0.256		
	n-Alkanols	C_5	9.24	0.232		
					26.45	26.50
		C_6	14.51	0.239		
					29.85	29.80
		C_7	24.32	0.244		

[a] *TZ* value calculated from eqn. 22, *C* term = 60.080.
[b] *TZ* value calculated [2] from eqn. 1.

ported t_r and $w_{0.5}$ values, the data in Table V were used to calculate the *TZ* values from eqn. 22, and demonstrated again that using the expression for *TZ* that includes h and column length L, the values obtained are essentially the same as those from eqn. 1.

Table VI compares the previously reported *TZ* values of Krupcik *et al.* as calculated with eqn. 1 [5], the values calculated by the combination of eqns. 4 and 10 [5] and those calculated by eqn. 22. In general, the agreement between the eqn. 22 *TZ* values and those determined from eqns. 4 and 10 [5] was better than 99%. However, for those values calculated for the C_8–C_9 homologues with the 19.5-m SE-30 column, large differences existed between the calculated *TZ* value of 13.1 (eqn. 22), the *TZ* value of 16.4 determined from eqns. 4 and 10 [5], and the eqn. 1 *TZ* value of 15.9 [5]. On examining the published data, it was determined that the α-value was 1.82, and not the reported value of 2.10 [5]. Recalculating *TZ* according to their method (eqns. 4 and 10) using this α-value yielded a *TZ* value of 13.07 or 13.1, rather than the reported value of 16.4.

As our method of calculation (eqn. 22) also produced a *TZ* value of 13.1, attention was directed to the validity of the reported *TZ* value of 15.9 for C_8–C_9 [5] obtained from eqn. 1. Given in their Table III [5] were the α-values, the k' values and n (the number of plates) calculated for the hydrocarbons C_8, C_9, C_{10}, C_{11} and C_{12} for selected column lengths and the carrier gas velocity for each of these columns was contained in Table II in the same paper [5]. The velocity given for the column used for the above *TZ* determination (19.5 m × 0.25 mm I.D. SE-30 coated capillary) was 37.1 cm/s, which when substituted in the equation [12]

$$t_0\,(\text{min}) = 1.67 \cdot \frac{L\,(\text{m})}{\mu\,(\text{cm/s})} \qquad (23)$$

gave t_0 = 0.878 min. With this value and the relationship $t_r = k't_0 + t_0$, the t_r values for C_8 and C_9 were found to be 1.66 and 2.31 min, respectively.

For C_8 the number of plates reported (Table III, in ref. 5) was 36 800 and for C_9 46 600, which for a column length of 19.5 m gave h values of 0.530 and 0.418 mm, respectively. Rearranging eqn. 15, these values were used to calculate the $w_{0.5}$ values to three significant figures; C_8 was found to have a $w_{0.5}$ value of 0.020 min and C_9 0.025 min. Rounding these off to 0.02 and 0.03 min gave a *TZ* of 12.0 whereas using the original values gave a *TZ* of 13.1, identical with that calculated above by eqn. 20 and eqns. 4 and 10. It is apparent that $w_{0.5}$ values accurate to three significant figures are necessary for meaningful separation numbers.

TABLE VI

TZ VALUES CALCULATED FROM EQN. 1 COMPARED WITH *TZ* VALUES CALCULATED FROM EQN. 22 USING DATA OF KRUPCIK *et al.* [5]

Flow-rate (ml/min)	Column[a]	Alkane	t_r (min)	h (mm)	*TZ* (eqns. 4 and 10)[b,c]	*TZ* (eqn. 22)	*TZ* (eqn. 1)[c]
1.25	A[d]	C_8	1.80	0.547			
					19.0 (18.8)	19.0	19.0 (19.0)
		C_9	2.62	0.344			
					30.1 (30.2)	30.2	30.2 (30.3)
		C_{10}	4.31	0.270			
					38.4 (38.0)	37.9	37.2 (37.7)
		C_{11}	7.64	0.230			
					43.6 (44.4)	44.4	42.8 (44.3)
		C_{11}	14.59	0.229			
1.09	B[e]	C_8	1.16	0.530			
					16.4 (13.1)	13.1	15.9 (13.2)
		C_9	2.30	0.418			
					24.6 (24.7)	24.8	24.7 (24.9)
		C_{10}	3.83	0.280			
					32.4 (32.4)	32.4	32.5 (32.4)
		C_{11}	6.90	0.272			
					34.8 (34.9)	35.0	35.0 (35.0)
		C_{12}	13.11	0.270			
1.17	C[f]	C_8	3.44	0.322			
					31.7 (30.9)	31.1	31.2 (31.6)
		C_9	5.07	0.283			
					41.2 (41.3)	41.2	41.3 (41.3)
		C_{10}	8.37	0.284			
					48.1 (48.1)	48.3	48.3 (48.2)
		C_{11}	15.06	0.281			
					51.2 (51.3)	51.3	51.3 (51.4)
		C_{12}	28.64	0.304			

[a] Column A: 27 m × 0.25 mm I.D. SE-30-coated capillary; temperature 83°C. Column B: 19.5 m × 0.25 mm I.D. SE-30-coated capillary; temperature 83°C. Column C, 46.5 × 0.25 mm I.D. SE-30-coated capillary; temperature 83°C.
[b] Calculated from eqns. 4 and 10 [5].
[c] Values in parentheses are recalculated; see text.
[d] In eqn. 22, C term = 69.81.
[e] In eqn. 22, C term = 59.33.
[f] In eqn. 22, C term = 91.62.

Having found such large discrepancies, the data in Table III in ref. 5 were recalculated in the manner described and the recalculated values are given in parentheses in the appropriate columns in Table VI. Some of the errors in utilizing eqns. 4 and 10 [5] were found to be related to incorrect calculations of α, whereas errors in the use of eqn. 1 arose from the rounding out off $w_{0.5}$ values.

As was previously noted in the reported derivations of eqns. 4 [2], 9 [4] and 10 [5], all were based on approximations such as equating the $w_{0.5}$ for the two homologues [2], the $w_{0.5}$ fraction of the two homologues being equal to α [4] or the utilization of only the larger k' of the homologous pair in the derivation of eqn. 11. It is apparent from Table I that the $w_{0.5}$ values of a homologous pair are not "approximately" equal. The same can be said for the h values and/or the h values and/or the number of plates. As has been shown, the casual approximating or rounding off of $w_{0.5}$ values can cause a 9% error

in reported values. The excellent agreement between *TZ* values determined using eqn. 1 with $w_{0.5}$ values accurate to three significant figures and eqn. 20, which utilizes *h*, is obvious.

The procedure for determining the optimum flow-rate for h_{min} is the same that provides the optimum flow-rate for TZ_{max} and the inverse relationship between *h* and *TZ* only emphasizes the fact that the concept of *TZ* incorporates proven chromatographic principles. As in any chromatographic study, control of column length and diameter, coating, phase thickness, flow-rate and temperature will control retention time, peak width at half-height (the foundation of plate theory) and, as has been shown, the separation number.

REFERENCES

1 R. Kaiser, *Fresenius' Z. Anal. Chem.*, 189 (1962) 1.
2 L. S. Ettre, *Chromatographia*, 8 (1975) 291.
3 W. Jennings and K. Yabumoto, *J. High Resolut. Chromatogr. Chromatogr. Commun.*, 3 (1980) 177.
4 S. A. Rooney and M. J. Hartigan, *J. High Resolut. Chromatogr. Chromatogr. Commun.*, 3 (1980) 416.
5 I. Krupcik, J. Gorag, G. Guiochon and J. M. Schmitter, *Chromatographia*, 14 (1981) 501.
6 L. A. Jones, S. A. Kirby, C. L. Garganta, T. M. Gerig and J. D. Mulik, *Anal. Chem.*, 55 (1987) 1354.
7 L. A. Jones, C. D. Burton, T. A. Dean, T. M. Gerig and J. R. Cook, *Anal. Chem.*, 59 (1987) 1179.
8 M. G. Golay, in V. J. Coats, N. J. Noebels and I. S. Fagerson (Editors), *Gas Chromatography 1957*, Academic Press, New York, 1958, p. 1.
9 D. H. Desty (Editor), *Gas Chromatography 1958*, Butterworths, London, 1958, p. 139.
10 R. L. Grob, in R. L. Grob (Editor), *Modern Practice of Gas Chromatography*, Wiley, New York, 1977, Ch. 1, p. 72.
11 D. H. Desty and A. Goldup, in R. P. W. Scott (Editor), *Gas Chromatography 1960*, Butterworths, London, 1960, p. 162.
12 J. A. Perry, *Introduction to Analytical Gas Chromatography*, Marcel Dekker, New York, 1981, p. 89.

Journal of Chromatography, 595 (1992) 221–236
Elsevier Science Publishers B.V., Amsterdam

CHROM. 23 876

Van Deemter-type relationship for determining the optimum initial flow-rate and optimum pressure programming rate in temperature/pressure-programmed capillary column gas chromatography utilizing separation numbers

Louis A. Jones*, William H. Reiss☆ and John J. Glennon

Department of Chemistry, Box 8204, North Carolina State University, Raleigh, NC 27695-8204 (USA)

Thomas M. Gerig

Department of Statistics, Box 8203, North Carolina State University, Raleigh, NC 27695-8203 (USA)

(Received August 20th, 1991)

ABSTRACT

Accurate prediction of the optimum conditions for a double-programmed gas chromatographic separation (simultaneous temperature and pressure programming) has been accomplished for the first time using a new relationship analogous to that established by the Van Deemter equation. Separation numbers (*TZ* values) for $\overline{CH}$, the homologous pair average [*e.g.*, $(C_{12} + C_{13})/2 = C_{12.5}$], were determined for a C_{12}–C_{17} series of *n*-alkanes and related to the average of the elution flow-rate, F_e, of the two homologues used to calculate *TZ*. F_e is defined as the flow-rate at the time of solute elution. Conditions for analysis involved the selection of a low temperature programming rate (*TPR*) and four different initial flow-rates (0.677, 1.10, 1.49 and 1.89 ml/min) upon which was superimposed a series of positive and negative pressure programming rates, *PPr*. Graphs of *TZ versus* F_e were parabolic curves which could be described in terms of longitudinal diffusion and resistance to mass transfer. Higher F_es of 1.49 and 1.89 ml/min resulted in straight lines with negative slopes as only resistance to mass transfer was operating. This effect is discussed in terms of laminar and turbulent flow (as predicted by Reynold's number, *Re*). All plots could be modeled by the quadratic expression $TZ = x(F_e)^2 + y(F_e) + z$. By differentiation, the optimum F_e and maximum *TZ* for each $\overline{CH}$ was determined, and, from this, the optimum initial flow-rate and *PPR* could be derived. The example cited is for the data obtained using an initial flow-rate of 0.677 ml/min, a *TPR* of 0.90°C/min starting at 40°C and nine different *PPR*s. The optimum initial flow-rate determined under these conditions was found to be 0.80 ml/min with an optimum *PPR* of 0.12 kPa/min.

INTRODUCTION

To optimize gas chromatographic (GC) analysis, parameters to be controlled include the column, column length, the coating thickness, the column head pressure (carrier gas velocity) and the oven temperature. The efficiency of a column is related to the amount of band broadening that occurs as the solute traverses the column at a particular column (oven) temperature and carrier gas velocity or flow-rate. In practice, column efficiency is expressed in terms of the height equivalent to a theoretical plate (HETP or *h*) under isothermal conditions as determined by the equation

$$h = \frac{L}{5.54}\left(\frac{w_{0.5}}{t_r}\right)^2 \quad (1)$$

☆ Present address: First Brands Corp., 55 Federal Road, Danbury, CT 06810, USA.

0021-9673/92/$05.00

where L is the length of the column, $w_{0.5}$ is the peak width at half-height, and t_r is the retention time of a solute [1].

The Van Deemter equation [2], originally developed for packed columns, reduces to the well known Golay equation when applied to capillary or open-tubular columns [3]:

$$h = \frac{B}{\mu} + C\mu \tag{2}$$

where μ is the linear flow velocity, B relates to molecular diffusion and C reflects the resistance to mass transfer. The optimum flow-rate or velocity (F_{opt} or μ_{opt}), being that producing the minimum h value (h_{min}) for a selected solute under isothermal conditions, can be determined by plotting flow-rate *versus* h. The minimum h and the corresponding flow-rate or velocity can be visually estimated or, alternatively, eqn. 2 can be differentiated, the term $dh/d\mu$ equated to zero and the optimum flow-rate or velocity determined [4] from the equation

$$\mu_{opt} = (B/C)^{\frac{1}{2}} \tag{3}$$

and the minimum value of h from the following equation (obtained from the substitution of eqn. 3 into eqn. 2):

$$h_{min} = 2(BC)^{\frac{1}{2}} \tag{4}$$

In isothermal GC, the boiling points of homologous solutes and their retention times (t_r), are logarithmically related and higher boiling solutes produce large t_rs and peak widths. In a sample of relatively narrow boiling point range, the chromatogram is characterized by poor separation of early-eluting peaks (narrow peak widths) and broad late-eluting peaks. As a solution to this problem, temperature-programmed gas chromatography (TPGC) has become the most widely used separation technique in GC [5].

Under TPGC conditions, peak widths and retention times can be manipulated by the rate of oven temperature increase, or temperature programming rate (*TPR*), and the Van Deemter relationship no longer applies. An equation which describes the TPGC effect on the resolution between two homologues (a and b) differing by one CH_2 group is the separation number or *TZ* value [6,7], as described by the equation

$$TZ = \frac{t_r^b - t_r^a}{w_{0.5}^a + w_{0.5}^b} - 1 \tag{5}$$

where $w_{0.5}$ is the peak width at half-height and t_r the retention time for homologues a and b. The quantity *TZ* is considered to be a measure of the number of peaks separated by 4.7σ resolution that can be placed between two consecutive homologue peaks [8].

Some controversy has been associated with the use of separation number. Rooney and Hartigan [9], in their study of the dependence of *TZ* on isothermal column temperature, related *TZ*, N_{eff} (effective plates) and α by

$$TZ = 0.425\left(\frac{\alpha - 1}{\alpha + 1}\right) N_{eff}^{\frac{1}{2}} - 1 \tag{6}$$

and concluded that the increase in *TZ* with a decrease in column temperature is the result of the increase in α with decreasing temperature. In a study of the dependence of *TZ* on the rate of column heating in TPGC, Jennings and Adam [10] found that increasing the *TPR* resulted in lower *TZ* values of the C_{13}–C_{14} homologue pair at both high (33 cm/s) and low (20 cm/s) velocities, the latter providing the higher *TZ* values. Krupcik *et al.* [11] view the separation number of a column as a "rubber ruler whose length is a function of temperature and is a function not only of the effective plate number which varies with retention as measured by the capacity factor k', but also the relative retention of the *n*-alkanes used ...". However, because of the applicability of *TZ* values to TPGC, Grob *et al.* [12,13] included the *TZ* determination as part of their standardized tests recommended for capillary columns.

We have recently completed an in-depth study of h and the *TZ* values of the homologue pair C_{11}–C_{12} under isothermal column temperature conditions of 40, 60 and 80°C [14]. Coefficients for eqn. 2 were determined, as were the coefficients for an analogous relationship between *TZ* and linear velocity which had been derived:

$$TZ = A - \frac{B}{\mu} - C\mu \tag{7}$$

Eqns. 2 and 7 were differentiated and determination of the optimum linear velocity (μ_{opt}) needed to provide the minimum value of h (h_{min}) for C_{11} and

C_{12} was carried out. The μ_{opt} required for TZ_{max} was found to be the average of the C_{11} and C_{12} optimum linear velocities, consistant with previous work [15] which had shown that the t_r of TZ was the average t_r of the two homologues.

Plots of h and TZ *versus* flow-rate or linear velocity for each temperature suggested an inverse relationship between these two chromatographic measures of column efficiency, and by substituting the equivalence of $w_{0.5}$ derived from eqn. 1 in eqn. 5, the following equation was obtained:

$$TZ = \left(\frac{L}{5.54}\right)^{\frac{1}{2}}\left[\frac{t_r^b - t_r^a}{(h_a)^{\frac{1}{2}}t_r^a + (h_b)^{\frac{1}{2}}t_r^b}\right] - 1 \qquad (8)$$

where L (mm) is the capillary column length and h_a and h_b are the heights equivalent to a theoretical plate for the homologues a and b. TZ values resulting from triplicate determinations using eqns. 5 and 8 were identical or nearly identical and, when the data of Ettre [8] and Krupcik *et al.* [11] were analyzed, similar excellent agreement was obtained, reaffirming the inverse relationship between TZ and h.

The changes in TZ values of a series of homologues as a function of carbon number with varying TPRs and flow-rates has been investigated [15]. Using three different constant head pressure flows (isobaric) and four different TPRs, it was shown that TZ was related to the average carbon number for a homologous pair by the equation

$$TZ = a(\overline{CH}) + b \qquad (9)$$

In eqn. 9, TZ is the determined value for a particular homologous pair average $\overline{CH}$ [*e.g.*, $(C_{12} + C_{13})/2 = C_{12.5}$]. Eqn. 9 was shown to be valid for a homologous series of straight-chain alkanes, carboxylic acids, methyl esters and alcohols with correlation coefficients of >0.95 [15]. A point of concurrence of these equations for each compound class was obtained at a TZ value of *ca.* -1. Eqns. 5 and 6 predict that when the retention times of a and b are equal ($t_r^b = t_r^a$), then $\alpha = 1$, no separation occurs and TZ would equal -1. It was found that the largest TZ values and absolute slopes were obtained with low TPRs and initial flow-rates of *ca.* 0.85 ml/min for a 12 m × 0.25 mm I.D. fused silica SP-2100-coated column.

A subsequent TPR study of the effect on the TZ values of six homologous *n*-alkanes (C_{12}–C_{17}) at starting temperatures of 40, 50 and 60°C under constant head pressure (isobaric flow) or constant flow-rate (maintained by pressure programming) [16] showed that (1) the slope values of eqn. 9 were more negative for isobaric flow than they were for constant flow; (2) CH_C values for isobaric flow were unique to the starting temperature/starting flow-rate/TPR, increasing with increasing flow-rate and starting temperature; (3) under constant flow conditions only one CH_C per starting temperature was observed for all flow-rates/TPRs; and (4) TZ values were optimized at a starting temperature of 40°C and a TPR of 1°C/min with flow-rates of 0.95 ml/min for isobaric flow and 0.89 ml/min for constant flow.

In 1962, Purnell [17] stated that flow programming could lead to chromatographic separations comparable to those obtained by TPGC. Zlatkis *et al.* [18], using a combination of temperature programming and flow programming (*i.e.*, double programming), reduced the time of a capillary column separation of an alkylbenzene mixture to 26 min from the 45 min required when using TPGC alone. Nygren [19] investigated the efficacy of double programming and stated that "flow and temperature programming can be used together in order to maximize the separating power of a capillary column". Ettre *et al.* [20] noted that as the temperature increases from temperature programming, k' will decrease for the same solute resulting in a larger μ_{opt} at higher temperatures. (This temperature dependence of μ_{opt} was observed in our recent study of h and TZ values at 40, 60 and 80°C [14].) Then, for double programming, chromatographic conditions would be conceivably less removed from the optimum than if pressure programming were performed isothermally. These statements, in conjunction with our previous work [14–16] suggested that a study of the changes in TZ as a function of several different pressure programming rates (PPR) superimposed on selected temperature programming rates (TPR) with low starting temperatures might provide further insight into the utility of TZ in capillary column optimization.

The previous approach of relating the initial flow to the TZ of each $\overline{CH}$ [15,16] was deemed inappropriate because, with double programming, the flow-rate was changing with a concomitant change in

temperature. Under TPGC and isobaric or constant flow conditions, each solute elutes at a particular temperature which can be determined by multiplying the *TPR* by the t_r of that solute and adding the result to the starting temperature. Perry [21] defined this temperature as the retention temperature. A similar approach was proposed by Ettre *et al.* [20] in defining elution flow. In isothermal linear carrier gas flow programming, the flow existing at the time the solute elutes (the elution flow-rate, F_e) is defined as being equal to the sum of the initial flow-rate, F_i, plus the product of the solute's t_r and the flow programming rate, r, in ml/min:

$$F_e = F_i + t_r(r) \tag{10}$$

As pressure can be related to flow, an analogous equation for determining the existing head pressure at the time the solute elutes (P_e) can be calculated from the sum of the initial pressure (P_i) and the *PPR* (t_r) product and the pressure related to flow:

$$P_e = P_i + t_r(PPR) \tag{11}$$

As shown previously, the optimum flow for TZ_{max} is determined by the average of the optimum flow of the two homologues [14], and therefore by similar averaging of F_e for these homologues, the calculated F_e for *TZ* and $\overline{CH}$ can be determined.

This paper reports that the *TZ* value for each $\overline{CH}$ can be related to its F_e in a Van Deemter-type equation similar to that derived previously [14]. From this relationship, the optimum starting flow-rate and the optimum *PPR* for the selected starting temperature of 40°C and selected *TPR* can be determined.

EXPERIMENTAL

A Hewlett-Packard Model 5880A gas chromatograph equipped with a Model 7671 autosampler, a flame ionization detector, an electronic flow control, a split–splitless injector set for a splitting ratio of 1:200 and a Level IV microprocessor with an alphanumeric keyboard was used. Helium was utilized as the carrier gas. The "report annotation" mode presented electronically measured values of retention times (±0.10 min) and peak widths at half-height ($w_{0.5}$) repeatable to ±1% [15]. Through "run time" commands at 5-min intervals, a print-out on the chromatogram of the actual column head pressure and its set-point, followed by the actual column/oven temperature and its set-point, provided a constant indication of the linearity of the temperature and pressure programming. On completion of the run, a specifically designed BASIC program listed the GC parameter settings for the particular run (*i.e.*, for oven temperature, initial value, 1-min hold, temperature programming rate, final oven temperature; for column head pressure, initial value, 1-min hold, pressure programming rate, final value; split flow value) and the calculated *TZ* values between the C_{12}–C_{17} *n*-alkane homologues (peaks 1 and 2; 2 and 3; 3 and 4; 4 and 5; 5 and 6).

The six *n*-alkanes used were 99+% pure *n*-dodecane, *n*-tridecane, *n*-tetradecane, *n*-pentadecane, *n*-hexadecane and *n*-heptadecane from Alltech (Applied Science Labs., Deerfield, IL, USA). Approximately 0.3 g of each alkane was weighed and the combined weights made up to 10 ml with high-performance liquid chromatographic grade chloroform. A 1-ml aliquot diluted to 50 ml produced a concentration which resulted in on-scale peaks at an attenuation of 0 for 5-μl injections at the splitting ratio of 1:200.

A cross-linked DB-5 fused-silica capillary column of film thickness 0.25 μm (15 m × 0.248 mm I.D.) (J&W Scientific, Rancho Cordova, CA, USA) was used and was conditioned by microprocessor-controlled repeated TPGC runs from 100 to 200°C at 10°C/min with a helium head pressure of 75 kPa for 2 days. When not in operation, the column was continuously purged at 250°C with helium at *ca.* 0.5 ml/min. The maximum temperature was never allowed ot exceed 250°C, although the manufacturer's recommended maximum temperature was 325°C for isothermal operation. All runs were performed with injection port and detector temperatures set at 275°C with the starting temperature for all runs set at 40°C. Head pressures of 50, 75, 100 and 125 kPa provided initial helium flow-rates (F_i) of 0.677, 1.10, 1.49 and 1.88 ml/min. These, and all other helium flow-rates required for this study, were determined by substituting the t_r of injected butane and into the equation $F = \pi r^2 L/t_r$, where r (cm) is the radius of a column of length L (cm). The *PPR* required to maintain a constant flow-rate during a particular *TPR* was experimentally determined. All other *PPR*s used with an individual *TPR* were chosen to be geometric multiples of the *PPR* re-

quired to maintain a constant flow-rate. In no instance did the pressure required within the run time exceed the previously determined limits of the flow control unit.

Flow-rates for each *PPR* applied to a specific *TPR* were determined by a linear regression of temperature *versus* flow-rate, as described below. The flow-rate was experimentally determined at four temperature points for each *PPR*; the initial conditions of temperature and pressure, two points representing one third and two thirds of the temperature increase of the run time and a final point at a temperature and pressure beyond those required to elute the final alkane, thus ensuring a known range of flow-rates greater than those achieved during the run. At each of these four points, duplicate butane injections were made, flow-rates were calculated as described above and substituted into the equation $F = a(T - 40) + F_i$, where F is the calculated flow-rate, T is the set column temperature and F_i is the measured flow-rate at 40°C and the initial head pressure. Fig. 1 shows the linear regressions of the

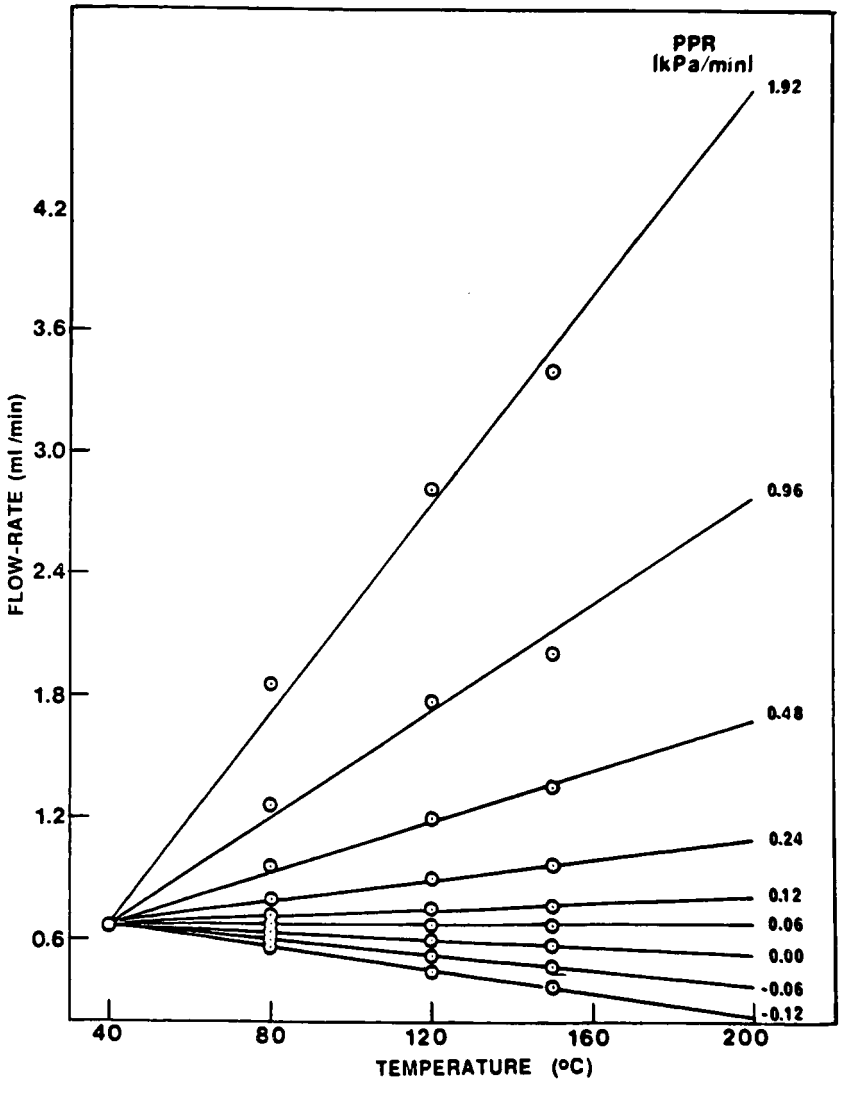

Fig. 1. Flow-rates generated by the indicated *PPR*s imposed on a *TPR* of 0.90°C/min, starting temperature 40°C and starting flow-rate 0.677 ml/min. Equations given in Table I.

TABLE I

COEFFICIENTS FOR THE EQUATION F = SLOPE (T-40) + F_i FOR STARTING TEMPERATURE = 40°C, *TPR* = 0.90°C/min, INITIAL PRESSURE, 50 kPa (0.677 ml/min) FOR VARIOUS *PPRs*[a]

TPR (°C/min)	*PPR* (kPa/min)	Initial flow-rate (ml/min)	Concurrent regression slope (S.D.)	Point of concurrence y-intercept point T	Flow-rate at 225°C (ml/min)[b]
0.90	1.92	0.677	$2.57 \cdot 10^{-2}$ ($7.91 \cdot 10^{-4}$)	40.0	5.43
	0.96		$1.31 \cdot 10^{-2}$ ($3.41 \cdot 10^{-4}$)	40.0	3.10
	0.48		$6.28 \cdot 10^{-3}$ ($1.45 \cdot 10^{-4}$)	40.0	1.84
	0.24		$2.74 \cdot 10^{-3}$ ($7.07 \cdot 10^{-5}$)	40.0	1.18
	0.12		$9.35 \cdot 10^{-4}$ ($4.26 \cdot 10^{-5}$)	40.0	0.846
C.F.[c]	0.06		$-2.99 \cdot 10^{-5}$ ($2.80 \cdot 10^{-6}$)	40.0	0.679
	0.00		$-8.99 \cdot 10^{-4}$ ($5.69 \cdot 10^{-6}$)	40.0	0.507
	−0.06		$-1.85 \cdot 10^{-3}$ ($1.35 \cdot 10^{-5}$)	40.0	0.331
	−0.12		$-2.76 \cdot 10^{-3}$ ($2.70 \cdot 10^{-5}$)	40.0	0.162

[a] T = Selected column temperature; F_i = initial flow-rate. All $R^2 \geqslant 0.992$.
[b] Flow-rate predicted at 225°C from regression equation.
[c] C.F., *PPR* required for constant flow-rate.

relationship between flow-rate and temperature at the indicated *PPRs* for a starting pressure of 50 kPa (0.677 ml/min) and a starting temperature of 40°C at a *TPR* of 0.90°C/min, selected for discussion here. Deviations from linearity became apparent at the higher *PPRs* of 0.96 and 1.92. Table I lists the regression coefficients obtained for these data. The experimentally determined flow-rates for 225°C are included to insure the linearity of the relationship. All R^2 values were at least 0.992. Similar equations were generated for all starting flows and all *TPR*–*PPR* combinations used.

In order to develop the Van Deemter-type relationship, it was necessary to calculate the elution flow-rate, F_e, or the flow-rate existing at the time of elution of $\overline{CH}$ for which *TZ* was calculated. As each hydrocarbon eluted at a characteristic retention time and elution temperature, T_e, dependent on the *TPR*–*PPR* combination used, the determination of T_e for each *TZ* required the averaging of the t_rs of the homologous pair used in calculating the *TZ* value (eqn. 5). As an example, averaging of the t_rs for C_{12} and C_{13} provides the "retention time" for $\overline{CH}$, the average hydrocarbon $C_{12.5}$. Thus, knowing the *TPR* (in this instance 0.90°C/min) and the initial column temperature, one need only know the superimposed *PPR* and, from the appropriate *PPR* line in Fig. 1 or the corresponding equation in Table I, one can calculate the elution flow-rate, F_e, the column flow-rate at the t_r for $\overline{CH}$.

RESULTS AND DISCUSSION

In the previous work relating h and *TZ* [14], a range of constant flow-rates were utilized at isothermal temperatures of 40, 60 and 80°C, the appropriate Van Deemter-type equations were determined and from these equations the optimum flow-rates required to produce minimum h or maximum *TZ* values were calculated. In this work, the objective was to determine not only the *PPR* necessary to provide the maximum *TZ* values for each $\overline{CH}$, but also the optimum starting flow-rates at selected *TPRs*. Hence the starting flow-rates were set by initial head pressures of 50, 75, 100 and 125 kPa, the same as used previously [16], and also the same *TPRs* except that, for the 50-kPa study, two additional rates of 0.90 and 1.80°C/min were added. The starting temperature of 40°C was employed as maximum *TZ* values were obtained with low *TRPs* and starting flow-rates of *ca.* 0.80 ml/min [16].

After concluding this study utilizing all the *TPRs* at the different head pressures (five *TPRs* for 50 kPa and four *TPRs* for 75, 100 and 125 kPa), it was

determined that within each head pressure or flow set, the lowest *TPR* provided the largest *TZ* values using all the superimposed *PPR*s and only these results are shown here. Table II summarizes the *TZ* values and the elution flow-rates, F_e, calculated for each $\overline{CH}$ determined for all *PPR*s superimposed on the lowest *TPR* for each starting head pressure/flow-rate.

Relationship between TZ and PPR

Initially, the *TZ* values for each $\overline{CH}$ obtained were plotted *versus* those *PPR*s used with a starting flow-rate of 50 kPa, 0.677 ml/min, at a *TPR* of 0.90°C/min (as shown in Table II). The plots thus obtained were parabolic curves which fit the model $TZ = a(PPR)^2 + b(PPR) + c$. The coefficients were determined for each $\overline{CH}$, the equations differ-

TABLE II

TZ VALUES AND ELUTION FLOW-RATES, F_e, FOR ALL $\overline{CH}$s AS A FUNCTION OF THE *PPR*s IMPOSED ON THE LOWEST *TPR*s OF INDICATED STARTING PRESSURES AND FLOW-RATES

PPR	Conditions[a]	$\overline{CH}$									
		12.5		13.5		14.5		15.5		16.5	
		TZ	F_e	*TZ*	F_e	*TZ*	F_e	*TZ*	F_e	*TZ*	F_e
1.92	A	34.47	1.487	30.00	1.725	26.07	1.965	22.63	2.202	19.73	2.434
0.96		37.83	1.138	34.25	1.271	30.89	1.403	27.74	1.532	25.04	1.657
0.48		38.82	0.917	35.93	0.986	33.10	1.053	30.50	1.119	28.21	1.182
0.24		38.66	0.787	36.07	0.819	33.49	0.850	31.18	0.880	29.10	0.909
0.12		38.31	0.716	35.72	0.727	33.21	0.738	30.87	0.749	28.85	0.759
0.06 C.F.[b]		37.84	0.678	35.16	0.679	32.56	0.679	31.39	0.679	28.30	0.680
0.00		37.76	0.638	35.31	0.627	32.67	0.616	30.28	0.605	28.10	0.595
−0.06		37.52	0.596	34.83	0.572	32.39	0.548	29.85	0.525	27.48	0.503
−0.12		37.18	0.554	33.95	0.516	31.06	0.479	28.34	0.443	25.67	0.409
2.79	B	30.05	1.898	26.00	2.135	22.61	2.370	19.66	2.601	17.27	2.825
1.40		33.09	1.527	29.65	1.635	26.60	1.777	23.87	1.898	21.61	2.014
0.70		34.95	1.304	31.95	1.364	29.35	1.423	26.85	1.480	24.64	1.535
0.35		35.85	1.180	33.22	1.203	30.67	1.227	28.43	1.249	26.50	1.271
0.17 C.F.[b]		36.37	1.142	33.79	1.154	31.50	1.167	29.30	1.178	27.34	1.190
0.00		36.49	1.038	34.11	1.020	31.81	1.001	29.68	0.983	27.77	0.967
−0.17		36.70	0.966	34.31	0.925	32.04	0.884	29.88	0.845	27.93	0.808
−0.35		37.10	0.833	34.38	0.814	32.03	0.747	29.64	0.681	27.36	0.617
2.24	C	27.72	2.280	23.81	2.576	20.47	2.880	17.79	3.180	15.59	3.473
1.12		30.13	1.973	27.11	2.157	24.28	2.342	21.64	2.523	19.33	2.699
0.56		32.09	1.715	29.33	1.801	26.84	1.889	24.53	1.974	22.47	2.055
0.28		32.87	1.573	30.40	1.605	28.12	1.638	26.60	1.670	24.13	1.700
0.14 C.F.[b]		33.21	1.499	30.86	1.503	28.81	1.507	26.87	1.510	25.06	1.514
0.00		33.71	1.420	31.61	1.392	29.67	1.364	27.75	1.336	26.14	1.310
−0.14		34.01	1.337	32.19	1.276	30.43	1.214	28.77	1.154	27.30	1.095
−0.28		34.89	1.250	32.85	1.153	31.27	1.054	29.16	0.956	28.13	0.862
1.02	D	27.59	2.253	24.68	2.427	22.02	2.610	19.62	2.792	17.40	2.970
0.51		29.12	2.054	26.67	2.137	24.40	2.224	22.48	2.311	20.54	2.394
0.26		29.80	1.944	27.74	1.975	25.69	2.008	23.77	2.040	22.08	2.072
0.13 C.F.[b]		29.90	1.887	28.05	1.891	26.20	1.894	24.39	1.898	22.78	1.902
0.00		30.36	1.825	28.55	1.798	26.91	1.769	25.20	1.741	23.83	1.714
−0.13		30.45	1.762	28.94	1.703	27.52	1.641	26.04	1.579	24.80	1.519
−0.26		30.88	1.692	29.54	1.598	28.30	1.498	27.24	1.398	26.22	1.300

[a] (A) 50 kPa, F_i = 0.677 ml/min, *TPR* 0.90°C/min; (B) 75 kPa, F_i = 1.10 ml/min, *TPR* 1.35°C/min; (C) 100 kPa, F_i = 1.49 ml/min, *TPR* 0.86°C/min; (D) 125 kPa, F_i = 1.88 ml/min, *TPR* 0.60°C/min.

[b] C.F. = The *PPR* required for constant flow-rate.

entiated as described previously [14], and optimum *PPR*s were determined. From these optimum *PPR*s, the maximum *TZ* values were calculated by substitution in the appropriate original equation. The coefficients obtained for each $\overline{CH}$, the PPR_{opt} and TZ_{max} and correlation coefficients are summarized in Table III.

As shown in Table III, TZ_{max} values decrease and PPR_{opt} become smaller as $\overline{CH}$ increases. However, it is apparent that no single *PPR* would provide TZ_{max} for all the $\overline{CH}$s used in this study and no information was available to calculate an optimum starting flow-rate. As a consequence, this approach was abandoned.

Relationship between TZ and F_e

The relationship between *TZ* and F_e was investigated next. When *TZ* was plotted *vs.* the elution flow-rate (F_e) at a particular *TPR* for each $\overline{CH}$, a parabolic curve resulted when the initial flow-rate and *TPR* were low. As the initial flow-rates increased, the parabolicity diminished and increasingly straight lines with negative slopes were observed. Using the data from Table II, the relationship between *TZ* and F_e for all *PPR*s at the lowest *TPR* for each of the following initial pressure/starting flows are shown: Fig. 2 for 50 kPa, 0.677 ml/min, *TPR* 0.90°C/min; Fig. 3 for 75 kPa, 1.10 ml/min, 1.35°C/min; Fig. 4 for 100 kPa, 1.49 ml/min, 0.86°C/min; and Fig. 5 for 125 kPa, 1.88 ml/min, 0.60°C/min. In these plots, the *TZ* values for each $\overline{CH}$ obtained at a particular *PPR* are connected by straight lines, giving rise to the "fan-like" appearance.

Low initial flow-rates, *i.e.*, 0.677 ml/min (50 kPa, Fig. 2) and 1.10 ml/min (75 kPa, Fig. 3), resulted in a

TABLE III

COEFFICIENTS FOR THE EQUATION $TZ = a(PPR)^2 + b(PPR) + c$ USING THE DATA FROM TABLE II FOR 50 kPa, F_i = 0.677 ml/min, *TPR* 0.90°C/min

$\overline{CH}$	a	b	c	R^2	PPR_{opt}	TZ_{max}
12.5	−2.38	2.79	37.79	0.962	0.586	40.03
13.5	−2.76	2.58	35.05	0.932	0.467	36.86
14.5	−2.89	2.12	32.45	0.929	0.367	33.50
15.5	−3.00	1.78	30.02	0.910	0.297	30.72
16.5	−3.22	1.29	27.76	0.884	0.283	28.45

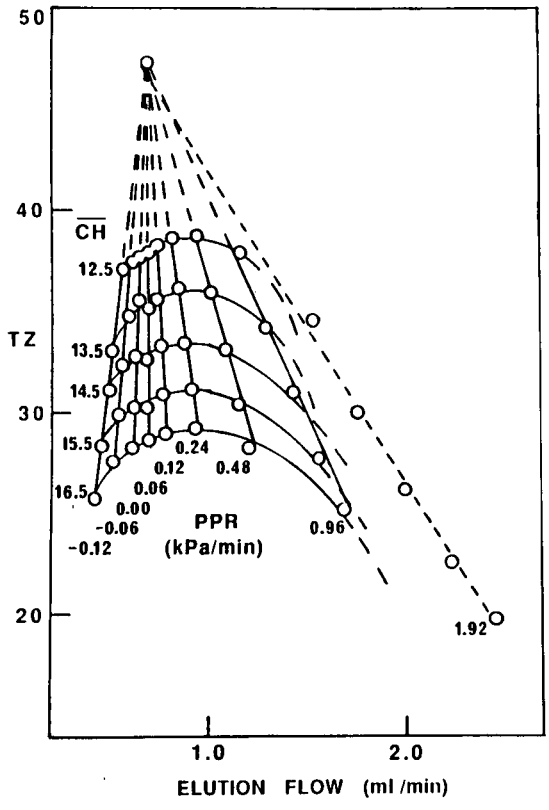

Fig. 2. Elution flow-rate for the *TZ* value of each $\overline{CH}$ for the homologous series C_{12}–C_{17} under the conditions of starting flow-rate 0.677 ml/min (50 kPa), *TPR* of 0.90°C/min and *PPR*s as indicated. Data from Table II.

parabolic relationship between *TZ* and F_e for each $\overline{CH}$ (similar to the *TZ vs.* flow-rate plot obtained in the isothermal study of the effect of flow-rate on *h* and *TZ* [14]). It is apparent that an optimum flow-rate produces maximum *TZ* values. Above the optimum flow-rate, the *TZ* values decrease owing to band broadening resulting from increased resistance to mass transfer. At flow-rates less tham the optimum, the *TZ* values decrease owing to longitudinal diffusion band broadening. For *TPR*s using the higher initial flow-rates of 1.49 ml/min (100 kPa, Fig. 4) and 1.88 ml/min (125 kPa, Fig. 5), the parabolic curvature flattens. A negative *PPR* producing decreasing flow-rates from high starting flow-rates improved the *TZ* values, although they were still significantly lower than those obtained at starting flow-rates of 0.677 ml/min (Fig. 2) or

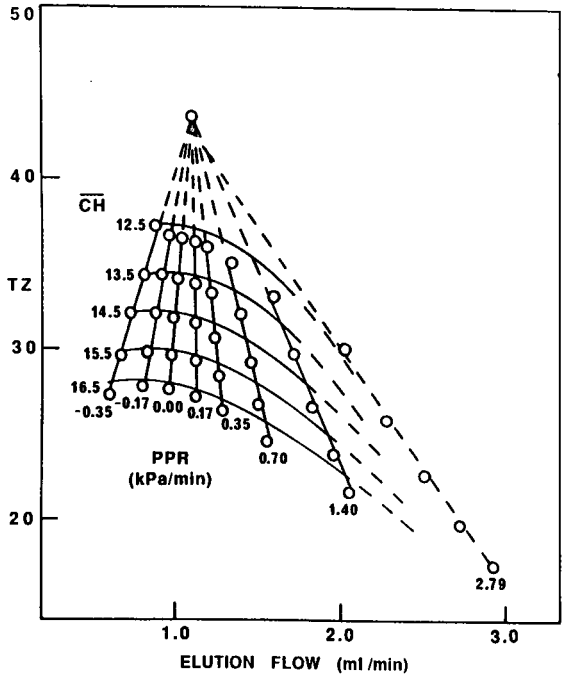

Fig. 3. Elution flow-rate for the TZ value of each $\overline{CH}$ for the homologous series C_{12}–C_{17} under the conditions of starting flow-rate 1.10 ml/min (75 kPa), TPR of 1.35°C/min and PPRs as indicated. Data from Table II.

1.10 ml/min (Fig. 3). As only resistance to mass transfer was operating at these high initial flow-rates, an increasing flow-rate produced larger $w_{0.5}$ values and decreasing TZ values, resulting in a negative slope for each $\overline{CH}$'s relationship between TZ and F_e. A model which adequately describes both the parabolic relationship at low initial flow-rates and the linear relationship at high initial flow-rates is the quadratic equation

$$TZ = x(F_e)^2 + y(F_e) + z \qquad (12)$$

Table IV lists the coefficients, their standard deviations for each $\overline{CH}$ for all the TPR–PPR combinations studied in the 50- and the 125-kPa groups. The 75- and 100-kPa data have been omitted from Table IV as it is clear from Figs. 4 and 5 that higher flow-rates result in the parabolic curve being flattened with the result that the squared term, F_e^2, becomes insignificantly different from zero [as indicated by the large standard deviation for the coefficient x for the 125-kPa data (Table IV)].

Laminar and turbulent flow and their effects on TZ

The flow profile in a column can be either laminar or turbulent [22,23]. Most chromatographic separa-

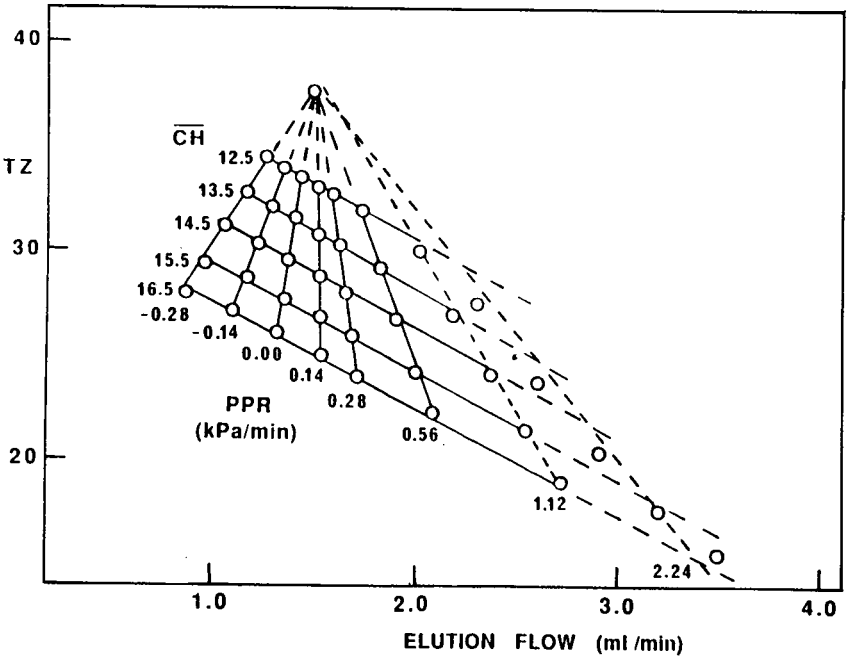

Fig. 4. Elution flow-rate for the TZ value of each $\overline{CH}$ for the homologous series C_{12}–C_{17} under the conditions of starting flow-rate 1.49 ml/min (100 kPa), TPR of 0.86°C/min and PPRs as indicated. Data from Table II.

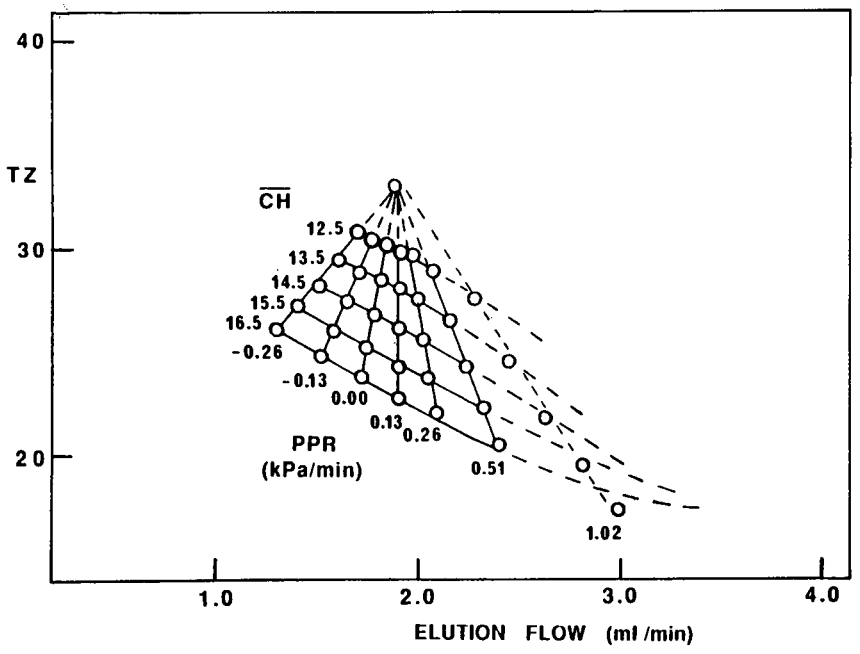

Fig. 5. Elution flow-rate for the *TZ* value of each $\overline{CH}$ for the homologous series C_{12}–C_{17} under the conditions of starting flow-rate 1.88 ml/min (125 kPa), *TPR* of 0.60°C/min and *PPR*s as indicated. Data from Table II.

tions are performed using low flow-rates, which provide a laminar flow profile characterized by a parabolic or "bullet-shaped" flow front. Minimum radial mixing occurs with a laminar flow profile and a solute molecule will, ideally, not deviate from the straight-line path it follows throughout the column. Carrier gas velocity varies with radial position, that is, the velocity at the center of the tube (μ_c) which is slightly faster than the velocity at the tube's inner wall (μ_w). For a straight cylindrical column, the velocity $\mu(r)$ varies with the distance from the center of the column as

$$\mu(r) = 2\mu[1 - (r/R)^2] \tag{13}$$

where r is the radial coordinate (distance from the center of the column), R is the column radius and μ is the mean velocity. The different velocities of each flow path result in peak broadening as the sample molecules at various distances from the column's center reach the detector over a period of time. As flow-rates increase, the onset of turbulent flow occurs when radial mixing flattens the leading edge of the profile and breaks down the parabolic shape [22]. The change in a flow profile from purely laminar to purely turbulent flow is not well defined. The Reynolds number (*Re*) reflects the onset of turbulence. When $Re \lesssim 2100$, flow is purely laminar, and when $Re \gtrsim 4000$, flow is purely turbulent [23]. The Reynolds number is defined by

$$Re = \frac{2\rho\mu R}{n} \tag{14}$$

where ρ (g/cm^3) is the density of the fluid (*i.e.*, the carrier gas), μ (cm/s) is the carrier gas linear velocity, n (μP) is the viscosity of the fluid and R (cm) is the column radius. The continuous radial mixing of the solute molecules associated with turbulent flow has an adverse effect on the ability of the solute to partition between the mobile and stationary phases and results in an increasing deviation in the relationship between *TZ* and F_e as a function of *PPR*.

The high flow-rates that arise from fast positive *PPR*s, especially those resulting in a non-laminar flow profile, result in decreased k' values, larger peak widths and decreased *TZ* values. Martin and Guiochon [24] noted in their study of band broadening in

TABLE IV

COEFFICIENTS AND STANDARD DEVIATIONS FOR THE QUADRATIC REGRESSIONS FOR *TZ VS.* ELUTION FLOW-RATE, F_e, FOR EACH *TPR* OF EACH $\overline{CH}$ FOR THE EQUATION $TZ = x(F_e)^2 + y(F_e) + z$

P_i (kPa)[a]	F_i (ml/min)[b]	*TPR* (°C/min)	$\overline{CH}$	Coefficient			R^2
				x (S.D.)	*y* (S.D.)	*z* (S.D.)	
50	0.677	0.90	12.5	−14.5 (1.48)	25.8 (2.51)	27.2 (1.01)	0.961
			13.5	−13.4 (1.33)	24.2 (2.39)	25.2 (0.995)	0.954
			14.5	−10.9 (1.31)	20.0 (2.49)	24.3 (1.07)	0.935
			15.5	−9.77 (1.00)	18.3 (2.01)	22.6 (0.882)	0.954
			16.5	−8.93 (1.01)	17.4 (2.12)	20.6 (0.952)	0.945
50	0.677	1.80	12.5	−20.5 (1.31)	37.3 (2.31)	19.7 (0.954)	0.982
			13.5	−17.5 (2.08)	32.8 (3.90)	18.9 (1.65)	0.934
			14.5	−14.6 (1.91)	28.7 (3.77)	18.1 (1.64)	0.922
			15.5	−11.7 (1.42)	23.9 (1.31)	17.5 (2.94)	0.932
			16.5	−10.1 (1.35)	21.0 (2.94)	16.6 (1.34)	0.918
50	0.677	3.60	12.5	−16.7 (1.11)	34.0 (2.07)	16.2 (0.864)	0.980
			13.5	−14.3 (1.35)	30.3 (1.13)	15.2 (2.65)	0.960
			14.5	−12.7 (1.21)	27.8 (2.49)	14.0 (1.09)	0.950
			15.5	−11.1 (1.03)	25.0 (2.22)	13.1 (0.989)	0.949
			16.5	−9.75 (1.12)	22.8 (2.51)	12.2 (1.13)	0.922
50	0.677	7.20	12.5	−15.1 (1.19)	33.8 (2.35)	11.3 (1.02)	0.977
			13.5	−13.6 (1.02)	31.3 (2.12)	10.1 (0.943)	0.972
			14.5	−11.4 (1.05)	27.2 (2.30)	9.97 (1.04)	0.953
			15.5	−9.76 (1.06)	13.9 (2.42)	9.73 (1.12)	0.929
			16.5	−8.66 (0.912)	21.9 (2.18)	9.09 (1.02)	0.928
50	0.677	14.40	12.5	−19.6 (1.04)	44.2 (1.73)	1.20 (0.672)	0.998
			13.5	−18.1 (0.829)	41.1 (1.42)	0.859 (0.556)	0.998
			14.5	−17.7 (0.861)	39.8 (1.51)	0.135 (0.594)	0.997
			15.5	−16.2 (0.538)	36.7 (0.962)	0.235 (0.382)	0.998
			16.5	−13.9 (0.337)	32.3 (0.615)	0.965 (0.245)	0.999
125	1.88	0.60	12.5	−1.99 (3.24)	2.76 (1.22)	31.9 (11.4)	0.981
			13.5	−1.48 (1.16)	3.62 (4.33)	32.7 (4.02)	0.996
			14.5	−0.511 (0.399)	−3.41 (1.49)	34.5 (1.37)	0.999
			15.5	0.618 (0.459)	−7.61 (1.71)	36.6 (1.53)	0.998
			16.5	0.899 (0.263)	−8.45 (0.975)	35.6 (0.878)	0.999
125	1.88	1.20	12.5	−2.19 (4.73)	1.30 (1.69)	34.0 (15.1)	0.972
			13.5	−0.212 (2.64)	−5.54 (9.25)	37.9 (8.08)	0.982
			14.5	−0.192 (1.64)	−5.44 (5.65)	35.9 (4.81)	0.988
			15.5	−1.17 (0.823)	−1.62 (2.78)	30.5 (2.31)	0.995
			16.5	−0.0931 (0.644)	−2.47 (2.13)	29.6 (1.73)	0.995
125	1.88	2.40	12.5	−2.71 (1.45)	4.44 (5.12)	29.0 (4.50)	0.988
			13.5	−2.34 (1.07)	2.96 (3.68)	28.5 (3.17)	0.989
			14.5	−1.46 (0.609)	0.0519 (2.06)	29.3 (1.73)	0.995
			15.5	−0.782 (0.308)	−2.56 (1.02)	29.8 (0.837)	0.998
			16.5	−0.664 (0.221)	−2.87 (0.717)	28.5 (0.575)	0.999
125	1.88	3.60	12.5	1.01 (1.54)	−9.68 (5.38)	41.1 (4.67)	0.987
			13.5	0.782 (1.15)	−8.63 (3.91)	37.9 (3.32)	0.988
			14.5	0.619 (0.578)	−7.68 (1.93)	35.0 (1.59)	0.977
			15.5	0.233 (0.417)	−5.21 (1.35)	30.8 (1.08)	0.995
			16.5	−0.595 (0.429)	−3.02 (1.37)	27.5 (1.08)	0.993

[a] Initial pressure.
[b] Initial flow-rate.

TABLE V

PEAK WIDTHS AT HALF-HEIGHT FOR C_{12} AND C_{17} AND REYNOLDS NUMBERS AT EACH *PPR* OF THE *TPR* 0.90°C/min INITIAL FLOW-RATE 0.677 ml/min

	PPR (kPa/min)	C_{12}		C_{17}	
		$w_{0.5}$	*Re*	$w_{0.5}$	*Re*
	1.92[a]	0.131	967	0.252	2236
	0.96	0.137	543	0.205	981
	0.48	0.147	347	0.189	489
	0.24	0.159	254	0.193	289
	0.12	0.168	210	0.200	202
C.F.[b]	0.06	0.173	189	0.208	163
	0.00	0.177	168	0.214	126
	−0.06	0.186	147	0.224	92
	−0.12	0.189	127	0.259	63

[a] Turbulent flow-rates for some CH values.
[b] *PPR* for constant flow-rate.

turbulent flow GC that the plate height increases with increasing gas velocity, indicating an increase in $w_{0.5}$ as shown in Table V. This effect was most evident for the high-molecular-weight solutes and Table V compares the peak widths at half-height of the C_{12} and C_{17} alkanes at all of the *PPR*s of the *TPR* 0.90°C/min, initial flow-rate 0.677 ml/min group. Also attributed to turbulent flow is the deviation from linearity in the relationship between flow-rate and temperature (Fig. 1) at fast *PPR*s when the onset of turbulent flow increases the resistance to flow. This is reflected by the increasing standard deviation in the slope (Table I) as the *PPR* was increased in all *TPR–PPR* combinations considered.

Relationship between TZ and F_e for each $\overline{CH}$ produced by a single PPR

As shown in Table II, the most negative *PPR*, −0.12 kPa/min, resulted in the lowest elution flow-rates for this *TPR* of 0.90°C/min, and produced the largest peak width for C_{17} ($w_{0.5} = 0.259$), because of longitudinal diffusion (Table V). As the *PPR* was increased, the peak width values decreased (longitudinal diffusion minimized), and at the *PPR* of 0.48 kPa/min, a minimum value ($w_{0.5} = 0.189$) was attained for C_{17}. On doubling the *PPR* to 0.96 kPa/min, the resistance to mass transfer increased and the peak width increased by 8.5% to 0.205. When the *PPR* was doubled again, however, to 1.92 kPa/min, non-laminar or turbulent flow-rates were produced (*Re* = 2236) and the peak width increased by 23% to value of 0.252, approximating that of the *PPR* −0.12 kPa/min. Conversely, as the effects of flow-rate changes are most evident for high-molecular-weight solutes, the peak widths for C_{12} did not exhibit the same pattern as those for C_{17}. At the *PPR* of −0.12 kPa/min, the $w_{0.5}$ value for C_{12} was 0.189, which decreased as the *PPR* increased to its maximum of 1.92 kPa/min.

In the Figs. 2–5, each point representing a *TZ* value and its associated F_e is connected horizontally to produce the parabolic curves shown and described by eqn. 12. The standard deviations of the coefficients of the quadratic regressions increased when *PPR*s producing turbulent or near-turbulent flows were included in these calculations. Therefore, values of the coefficients for the quadratic regressions for each $\overline{CH}$ were determined for all *TPR*s omitting those *PPR*s which produce non-laminar flow-rates.

To determine the *TZ* and flow-rate values at the convergence of the vertical line in Figs. 2–5, it was necessary to determine the slopes of each *PPR* line.

As previously mentioned, only two initial flow-rates produced parabolic plots of the *TZ versus* F_e relationship for each $\overline{CH}$ (Fig. 2, $F_i = 0.677$ ml/min, and Fig. 3, $F_i = 1.10$ ml/min). Connecting the *TZ* values obtained for each $\overline{CH}$ of a selected single *PPR* resulted in a straight, near-vertical line or "rib". The lines thus obtained converge at a common *TZ* value which is a function of the original starting flow-rate and all such lines could be described by the equation

$$TZ = a(F_e) + b \qquad (15)$$

Considering only the data in Table II for the F_i of 0.677 ml/min with a *TPR* of 0.90°C/min and excluding the *PPR*s that gave rise to the non-laminar flow and that for constant flow (as under constant flow conditions *TZ* is not a function of flow), the remaining eight *PPR*s gave eight regression lines. The coefficients for eqn. 15 determined for the different starting flow-rates studied are summarized in Table VI.

Recognizing that these lines have a common *TZ* value at the point of concurrence, simultaneous solution of any pair of *PPR* lines for a selected *TPR*

TABLE VI

RELATIONSHIP $TZ = a(F_e) + b$ BETWEEN TZ AND LAMINAR ELUTION FLOW-RATES, F_e, FOR ALL $\overline{CH}$s IN THE VERTICAL LINES OF FIGS. 2–5 AS A FUNCTION OF ALL *PPR*s AT INITIAL FLOW-RATES AND *TPR*s

Conditions[a]	*PPR*	*a*	*b*	R^2
A	0.96	−24.72	65.76	0.998
	0.48	−40.22	75.59	0.999
	0.24	−78.76	100.57	0.999
	0.12	−220.20	195.80	0.999
	C.F.[b] 0.06	−4770.00	3271.88	0.959
	0.00	225.51	−106.14	0.999
	−0.06	107.55	−26.61	0.999
	−0.12	78.90	−6.65	0.999
B	2.79	−13.76	55.68	0.992
	1.40	−23.31	68.04	0.993
	0.70	−44.53	92.83	0.998
	0.35	−103.10	157.83	0.998
	C.F.[b] 0.17	−187.92	250.82	0.998
	0.00	122.21	−90.46	0.999
	−0.17	55.50	−16.98	0.999
	−0.35	41.54	1.43	0.963
C	1.12	−14.90	59.34	0.998
	0.56	−28.20	80.25	0.998
	0.28	−66.69	137.60	0.994
	C.F.[b] 0.14	−547.86	854.36	0.998
	0.00	68.87	−64.19	0.999
	−0.14	27.80	−3.24	0.999
	−0.28	17.70	12.59	0.991
D	1.02	−14.14	59.17	0.997
	0.51	−25.00	80.23	0.997
	0.26	−60.46	147.21	0.998
	C.F.[b] 0.13	−482.35	940.02	0.996
	0.00	58.82	−77.10	0.998
	−0.13	23.28	−10.64	0.999
	−0.26	11.80	10.77	0.995

[a] (A) 50 kPa, F_i = 0.677 ml/min, *TPR* 0.90°C/min; (B) 75 kPa, F_i = 1.10 ml/min, *TPR* 1.35°C/min; (C) 100 kPa, F_i = 1.49 ml/min, *TPR* 0.86°C/min; (D) 125 kPa, F_i = 1.88 ml/min, *TPR* 0.60°C/min.

[b] *PPR* required for constant flow-rate.

will yield the initial flow-rate which, when used in the original equation, will give the concurrent TZ value, TZ_c (method A). Alternatively, use of the known initial flow-rate will permit the calculation of TZ_c (method B). Thus, calculation by method A gives an average F_i of 0.669 ml/min (S.D. = 0.021) and using this F_i in the original equations gave a TZ_c value of 47.22 (S.D. = 1.84). Using method B with a constant flow-rate of 0.677 ml/min gives an average TZ of 47.27 (S.D. = 1.04). The values of F_i and TZ_c thus calculated for all *TPR–PPR* combinations reported here are given in Table VII. The agreement of the TZ_c values determined by both methods is acceptable, as is the agreement between the calculated F_i and that set experimentally.

Determination of TZ_{max}, $F_{e(opt)}$, new F_i and PPR

Previous studies [14,15] have shown that a quadratic relationship such as eqn. 12 can be differentiated to determine the maximum TZ and optimum flow-rate. For each $\overline{CH}$, a different quadratic model (excluding any *PPR*s resulting in non-laminar flow) was derived as shown in Table IV. Then, as described in the derivation of eqns. 3 and 4, differentiating eqn. 12 and setting the slope equal to zero gives

$$\frac{dTZ}{dF_e} = 2x\,(F_e) + y = 0 \qquad (16)$$

and the equation

$$F_{e(opt)} = -y/2x \qquad (17)$$

permits the calculation of the optimum F_e for that $\overline{CH}$. Substituting F_e into eqn. 12 and solving for TZ yields the TZ_{max} value for each $\overline{CH}$ [23]:

TABLE VII

COMPARISON OF TZ_c AND F_i CALCULATED BY METHODS A AND B

Conditions[a]		Method A		Method B
		F_i	TZ_c	TZ_c
A	Average[b]	0.668	47.22	47.27
	S.D.[c]	0.021	1.853	1.038
B	Average[b]	1.148	44.63	44.24
	S.D.[c]	0.087	4.511	1.526
C	Average[b]	1.515	38.26	38.20
	S.D.[c]	0.042	4.106	0.592
D	Average[b]	1.887	33.15	33.15
	S.D.[c]	0.027	0.456	0.353

[a] (A) 50 kPa, F_i = 0.677 ml/min, *TPR* 0.90°C/min; (B) 75 kPa, F_i = 1.10 ml/min, *TPR* 1.35°C/min; (C) 100 kPa, F_i = 1.49 ml/min, *TPR* 0.86°C/min; (D) 125 kPa, F_i = 1.88 ml/min, *TPR* 0.60°C/min.

[b] Average of eight determinations.

[c] Standard deviation of the averages.

TABLE VIII

THEORETICAL MAXIMUM *TZ* AND ITS ASSOCIATED $F_{e(opt)}$ UNDER THE CONDITIONS 50 kPa (F_i = 0.677 ml/min) AND A *TPR* OF 0.90°C/min, FROM THE DIFFERENTIATION OF $TZ = x(F_e)^2 + y(F_e) + z$ (EQN. 12)

$\overline{CH}$	TZ_{max}	$F_{e(opt)}$
12.5	38.68	0.892
13.5	36.13	0.899
14.5	33.47	0.914
15.5	31.17	0.935
16.5	29.09	0.973

$$TZ_{max} = (4xz - y^2)/4x \quad (18)$$

The resulting pairs of TZ_{max} and F_e values for the sample *TPR* 0.90°C/min, 50 kPa (F_i = 0.677 ml/min) are shown in Table VIII and are included in Fig. 6 as solid circles in an expanded plot of Fig. 2. Least-squares regression analysis [25] of the data in Table VIII gave the equation

$$TZ_{max} = -110.6\ (F_e) + 135.8 \quad (19)$$

with $R^2 \geqslant 0.900$.

Knowing that the TZ_C for a *TPR* of 0.90°C/min was 47.27 (Table VII), substitution of this value in eqn. 19 gave an F_i of 0.801 ml/min as the new initial flow-rate. This left only a comparison of the slope values of the regression equations describing the vertical lines or the "ribs" of the fans in Figs. 2 and 6 to determine the *PPR* necessary for the maximum *TZ* values for all the $\overline{CH}$s. The slope values *a* (eqn. 15) for *TZ* and F_e for all the *PPR* lines in Fig. 6 are shown in Table VI and, considering the extreme steepness of the slopes, the above value of −110.6 does not differ greatly from that of −220.4 obtained for the *PPR* of 0.12 kPa at 0.90°C/min (see below).

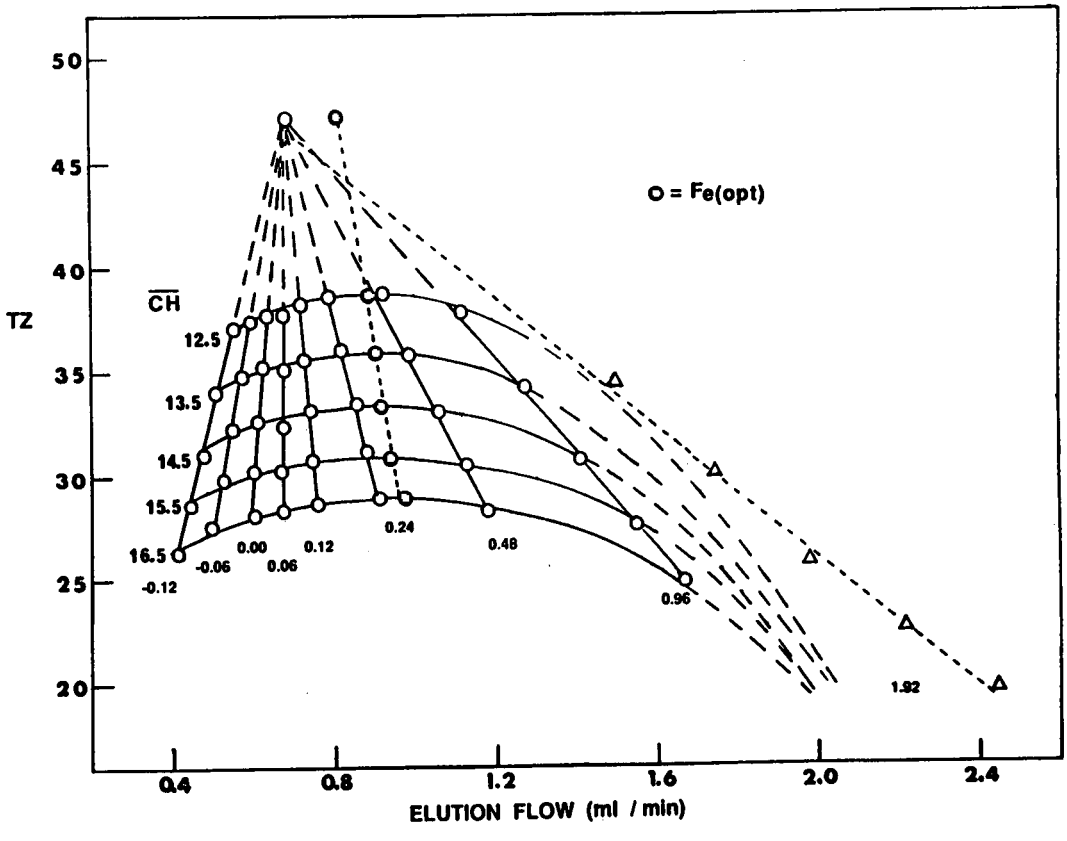

Fig. 6. Expanded version of Fig. 2. Solid circles connected by dashed line are *TZ* and F_e values calculated from eqns. 17 and 18 and are contained in Table VIII.

TABLE IX

COMPARISON OF PREDICTED *TZ* VALUES WITH THOSE EXPERIMENTALLY DETERMINED FOR STARTING FLOW-RATE OF 0.80 ml/min, *TPR* OF 0.90°C/min AND *PPR* OF 0.12 kPa/min

$\overline{CH}$	TZ_{max} (predicted)[a]	*TZ* (found)	$\frac{(TZ_{max} - TZ_{found})}{TZ_{max}} \cdot 100\,(\%)$
12.5	38.68	38.91	−0.595
13.5	36.13	36.35	−0.609
14.5	33.47	33.65	−0.538
15.5	31.17	31.27	−0.321
16.5	29.08	29.04	0.138

[a] See Table VIII.

Further, visual examination of Fig. 6 supports the conclusion that the slope of the new line parallels most closely that of the 0.12 kPa/min *PPR*.

To determine the efficacy and accuracy of the above determination, the C_{12}–C_{17} hydrocarbon mixture was again analyzed utilizing the new calculated starting flow-rate of 0.80 ml/min, a *TPR* of 0.90°C/min and a *PPR* of 0.12 kPa/min. Table IX compares the *TZ* values obtained with those predicted by the calculations as described above. The agreement between the predicted and experimentally determined *TZ* values is acceptable and appears to confirm the applicability of the approach.

The data shown in Table II which gave rise to the shallow parabolic curves (Fig. 6) illustrate that slight changes in the near-optimum *PPR*, as described above, produce small changes in the near-maximum *TZ*, as evidenced by the steep slopes shown in Table VI. To select the optimum velocity for the TPGC separation of a mixture of high- and low-molecular-weight solutes, Jennings [26] proposed a "velocity window" concept in which the optimum velocity is found to be intermediate to that required for the high partition ratio *k* solute (high *h*) and the low-*k* solute (low *h*). These values are proportional to low optimum velocity and high optimum velocity, respectively. The results shown here suggest that a similar "*PPR* window" exists for low *TPR*s and that for acceptable optimization, a *PPR* somewhere between isobaric flow (*PPR* = 0.0) and slightly positive *PPR* (+0.28 kPa/min) will provide a similar *TZ* maximization as shown in the above determination. The new calculated optimum starting flow-rate determined by using the *TPR–PPR* method described herein was *ca.* 0.80 ml/min, whereas by considering only [16] *TPR*, a starting constant flow-rate of 0.89 ml/min was previously calculated. Thus, for a 15 m × 0.25 mm I.D. column, a "*PPR* window" of 0–0.28 kPa/min with a starting flow-rate between 0.80 and 0.89 ml/min for either constant or isobaric flow will provide maximum or near-maximum *TZ* values for a *TPR* of 0.90°C/min.

ACKNOWLEDGEMENT

The authors are indebted to Mr. Terry Schmoeger of Hewlett-Packard for devising the software used to calculate *TZ* in the Level IV microprocessor.

REFERENCES

1 R. L. Grob, in R. L. Grob (Editor), *Modern Practice of Chromatography*, Wiley-Interscience, New York, 1977, Ch. 2, p. 64.
2 J. J. van Deemter, F. J. Zuiderweg and A. Klinkenberg, *Chem. Eng. Sci.*, 5 (1956) 271.
3 M. J. E. Golay, in V. J. Coates, H. J. Noebels and I. S. Fagerson (Editors), *Gas Chromatography 1957*, Academic Press, New York, 1958, pp. 1–13.
4 R. L. Grob, in R. L. Grob (Editor), *Modern Practice of Gas Chromatography*, Wiley-Interscience, New York, 1977, Ch. 2, p. 72.
5 W. E. Harris and W. H. Hapgood, *Programmed Temperature Gas Chromatography*, Wiley, New York, 1966, p. v.
6 N. B. Turkeltaub and A. A. Zuchowitsky, *Fortschriftsberichte Gas Chromatographie, 1959*, Akademie Verlag, Berlin, 1961.
7 R. S. Kaiser, *Fresenius' Z. Anal. Chem.*, 189 (1961) 1.
8 L. S. Ettre, *Chromatographia*, 8 (1975) 291.
9 T. A. Rooney and H. J. Hartigan, *J. High Resolut. Chromatogr. Chromatogr. Commun.*, 3 (1980) 416.
10 W. G. Jennings and S. Adam, *Anal. Biochem.*, 69 (1975) 61.
11 J. Krupcik, J. Garaj, G. Guiochon and J. M. Schmitter, *Chromatographia*, 14 (1981) 501.
12 K. Grob, Jr., G. Grob and K. Grob, *J. Chromatogr.*, 156 (1978) 1.
13 K. Grob, Jr. and K. Grob, *J. Chromatogr.*, 207 (1981) 291.
14 L. A. Jones, J. J. Glennon and W. H. Reiss, *J. Chromatogr.*, 595 (1992) 209.
15 L. A. Jones, S. L. Kirby, C. L. Garganta, T. M. Gerig and J. D. Mulik, *Anal. Chem.*, 55 (1983) 1354.
16 L. A. Jones, C. D. Burton, T. A. Dean, T. M. Gerig and J. R. Cook, *Anal. Chem.*, 59 (1987) 1179.
17 H. Purnell, *Gas Chromatography*, Wiley, New York, 1962, pp. 387–388.
18 A. Zlatkis, D. C. Fenimore, L. S. Ettre and J. E. Purcell, *J. Chromatogr.*, 3 (1965) 75.
19 J. Nygren, *J. Chromatogr.*, 142 (1977) 109.
20 L. S. Ettre, I. Mazor and J. Takacs, *Adv. Chromatogr.*, 123 (1969) 271.

21 J. A. Perry, *Introduction to Analytical Gas Chromatography*, Marcel Dekker, New York, 1981, p. 240.
22 J. A. Jönsson, in J. A. Jönsson (Editor), *Chromatographic Theory and Principles*, Marcel Dekker, New York, 1987, p. 59.
23 J. C. Giddings, *Dynamics of Chromatography*, Marcel Dekker, New York, 1965, p. 218.
24 M. Martin and G. Guiochon, *Anal. Chem.*, 54 (1982) 1533.
25 R. Ellis and D. Gulick, *Calculus with Analytical Geometry*, Harcourt Brace Jovanovich, New York, 2nd ed., 1982, p. 203.
26 W. Jennings, *Analytical Gas Chromatography*, Academic Press, New York, 1987, p. 84.

Journal of Chromatography, 595 (1992) 237–246
Elsevier Science Publishers B.V., Amsterdam

CHROM. 23 915

Activity coefficients in binary liquid mixtures measured by reversed-flow gas chromatography

A. Koliadima, G. Karaiskakis* and N. A. Katsanos

Physical Chemistry Laboratory, University of Patras, 26110 Patras (Greece)

M. Roth

Institute of Analytical Chemistry, Czechoslovak Academy of Sciences, 61142 Brno (Czechoslovakia)

(First received July 8th, 1991; revised manuscript received November 20th, 1991)

ABSTRACT

Three methods of reversed-flow gas chromatography are presented for the determination of activity coefficients in binary liquid mixtures. The systems used were *n*-hexane–*n*-hexadecane and benzene–*n*-octane. The average activity coefficients obtained for *n*-hexane in the first system were close to those given in the literature, when the *n*-hexane mole fraction was close to unity, whereas the values found for benzene in the second system were close to those calculated theoretically, using the Margules equation, when the benzene mole fraction approached zero or unity. On the other hand, the activity coefficients of *n*-octane in the same system were close to the theoretical values only when the *n*-octane mole fraction was close to unity. All these deviations are discussed and possible causes, such as liquid diffusion, fugacity correction and thermal non-equilibrium considered.

INTRODUCTION

The reversed-flow gas chromatography method (RF-GC) has been reviewed several times [1–4], and some more recent papers have been cited [5]. Some of them refer to the determination of activity coefficients in solution [6–8], and are based on a theoretical analysis published in 1984 [9].

It is well known that flow reversals of the carrier gas at various times t_0, by means of a four- or six-port valve (*cf.*, Fig. 1), execute repeated sampling at the junction $x = l'$ of concentration $c(l', t_0)$ of the substances present at this point at t_0. This sampling results in extra chromatographic peaks (sample peaks), such as those shown in Fig. 2. The magnitude of $c(l', t_0)$ in each sampling act is related to the height h of the respective sample peak by the equation [4]

$$h = [2c(l', t_0)]^m \quad (1)$$

where m is the response factor of the detector. For a flame ionization detector, $m = 1$.

The function $c = c(l', t_0)$ has been derived in the past for many special cases pertaining to various physico-chemical parameters and different experimental conditions. One particular case is closely related to the present problem and is given by eqns. 14 and 18 in ref. 9. These equations are a short and a long time approximation, respectively, and apply when a vessel of height L_2 (*cf.*, Fig. 1) contains a pure liquid. The same analysis was employed [6–8] when two- or more component mixtures were placed in a vessel of height y. It is the purpose of this paper to elaborate and extend the theoretical analysis, so that a single equation embraces short and long time in the same experiment.

It is shown in the Appendix that the general solution, based on eqn. 1, takes the form:

$$h = h_\infty - A_1 \exp[-(\alpha + \omega)t_0] + A_2 \exp(-9\alpha t_0) \quad (2)$$

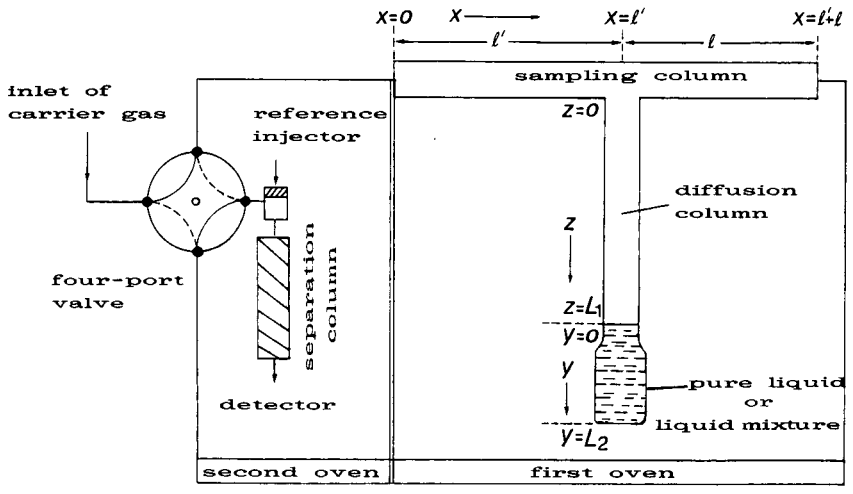

Fig. 1. Experimental set-up for measuring activity coefficients in binary liquid mixtures by RF-GC.

where

$$h_\infty = \frac{2k\alpha}{\alpha+\omega} = \frac{2k_c c_0 a_L}{a_G u}\cdot\frac{\alpha}{\alpha+\omega} \tag{3}$$

$$A_1 = 2k\left(\frac{4}{\pi} - 1 + \frac{\alpha}{\alpha+\omega} + \frac{4}{3\pi}\cdot\frac{\omega}{8\alpha-\omega}\right) \tag{4}$$

$$A_2 = 2k\cdot\frac{4}{3\pi}\cdot\frac{8\alpha}{8\alpha-\omega} \tag{5}$$

$$k = k_c c_0 a_L / a_G u \tag{6}$$

$$\alpha = \pi^2 D/4L_1^2 \tag{7}$$

$$\omega = 2k_c a_L / a_G L_1 \tag{8}$$

where k_c is the mass transfer coefficient for the liquid evaporation, c_0 is the concentration of the vapour which would be in equilibrium with the bulk liquid phase, a_L is the free surface area of the liquid, a_G is the cross-sectional area of the column with height z (*cf.*, Fig. 1), u is the linear velocity of the carrier gas in the sampling column and D is the diffusion coefficient of the vapour into the gases contained in column z, *viz.*, the carrier gas and other vapours.

EXPERIMENTAL

The solutes used were *n*-hexane (pure) and *n*-hexadecane (GC grade, purity >99%) from Merck, *n*-octane (purum) from Fluka and benzene (pure) from Carlo Erba. The nitrogen carrier gas (Linde) had a purity of ⩾99.99%. The chromatographic material for the separation of the components of the mixtures, which was filled into a 64.5-cm separation column, was 11% Apiezon M on Chromosorb P AW DMCS (60–80 mesh).

The apparatus used and the experimental procedure followed have been described in detail elsewhere [8,9]. A conventional gas chromatograph (Pye Unicam Series 104) contained in its oven the sampling column, consisting of two sections of lengths $l' + l = 100 + 100$ cm and the diffusion column with length $L_1 = 114.8$ cm. At the lower end of diffusion column a glass tube ($L_2 = 2.5$ cm) containing the pure liquid or the liquid mixture was connected. One end of the sampling column was connected to the carrier gas supply and the other end to the separation column, which was placed in a second gas chromatographic oven. The end of this column was connected to a flame ionization detector as shown schematically in Fig. 1.

At a given time after placing the pure liquid or the liquid mixture in position, an asymmetric concentration–time curve for the detected vapours was recorded, rising continuously and approaching a limiting plateau. This concentration *vs.* time curve consists of one substance (in the *n*-hexane–*n*-hexadecane system where the vapour pressure of *n*-hexadecane is negligible at the working temperature)

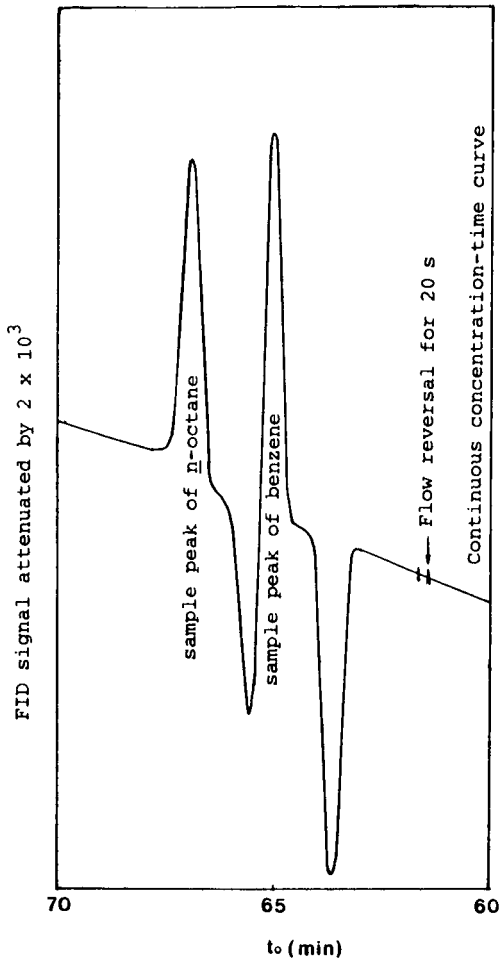

Fig. 2. A reversed-flow chromatogram, showing two sample peaks for the diffusion of benzene and *n*-octane vapours into nitrogen carrier gas at 348.2 K and 1 atm.

or of two substances (in the benzene–*n*-octane system). During the rise period, and also when the plateau was reached, flow reversals for 20 s were effected by means of the four-port valve. When the gas flow was restored to its original direction, one or two sample peaks were recorded (*cf.*, Fig. 2) corresponding to various times t_0 from the beginning.

The carrier gas flow-rate was kept constant in all runs at 0.4 $cm^3\ s^{-1}$ (at ambient temperature). The working temperature was 348.2 K for the evaporation of the mixtures (first oven) and 393.2 K for the separation column (second oven). The pressure drop along the whole system of columns was negligible.

RESULTS AND DISCUSSION

There are three obvious procedures for analysing the experimental data by means of eqn. 2, as follows.

First procedure

The experimental value of h_∞, established after a sufficiently long time, is used and a plot of $\ln(h_\infty - h)$ *vs.* t_0 is constructed according to the following form of eqn. 2:

$$h_\infty - h = A_1 \exp[-(\alpha + \omega)t_0] - A_2 \exp(-9\alpha t_0) \quad (9)$$

An example is given in Fig. 3. As predicted by the equation, this plot becomes linear after a certain time, because the second exponential has decayed to a negligible value, giving

$$\ln(h_\infty - h) = \ln A_1 - (\alpha + \omega)t_0 \quad (10)$$

Having found $\alpha + \omega$ from the slope and A_1 from the intercept of this linear part of the plot, one replots the initial data as

$$\ln\{A_1 \exp[-(\alpha + \omega)t_0] - (h_\infty - h)\} = \ln A_2 - 9\alpha t_0 \quad (11)$$

and finds α from the slope and A_2 from the intercept of the new plot.

Second procedure

Pairs of values h_2 and h_1 are used, measured at equidistant times t_2 and t_1, respectively, *i.e.*, with $\Delta t = t_2 - t_1 =$ constant. Then eqn. 2 gives, on writing it twice, subtracting and rearranging,

$$h_2 - h_1 = A'_1 \exp[-(\alpha + \omega)t_1] - A'_2 \exp(-9\alpha t_1) \quad (12)$$

where

$$A'_1 = A_1\{1 - \exp[-(\alpha + \omega)\Delta t]\} \quad (13)$$

and

$$A'_2 = A_2[1 - \exp(-9\alpha\Delta t)] \quad (14)$$

A plot of $\ln(h_2 - h_1)$ *vs.* t_1 is constructed (*cf.*, Fig. 4), which after some time is approximated by

$$\ln(h_2 - h_1) = \ln A'_1 - (\alpha + \omega)t_1 \quad (15)$$

Having found $\alpha + \omega$ from the slope and A'_1 from the intercept of this linear part, we replot the initial data as

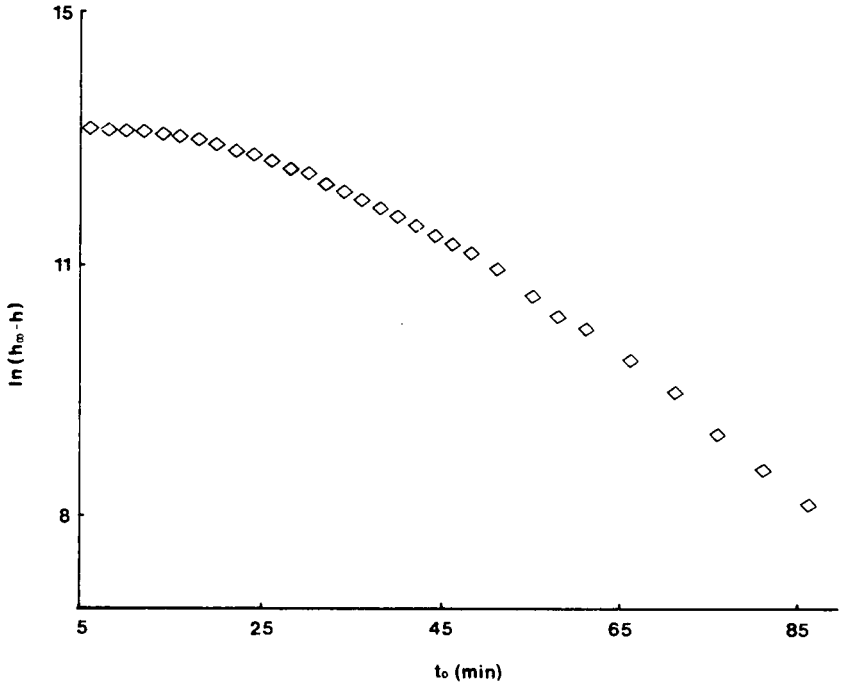

Fig. 3. Example of plotting eqn. 9 for the diffusion of *n*-hexane vapour into nitrogen carrier gas ($\dot{V} = 0.4\ cm^3\ s^{-1}$) at 348.2 K and 1 atm.

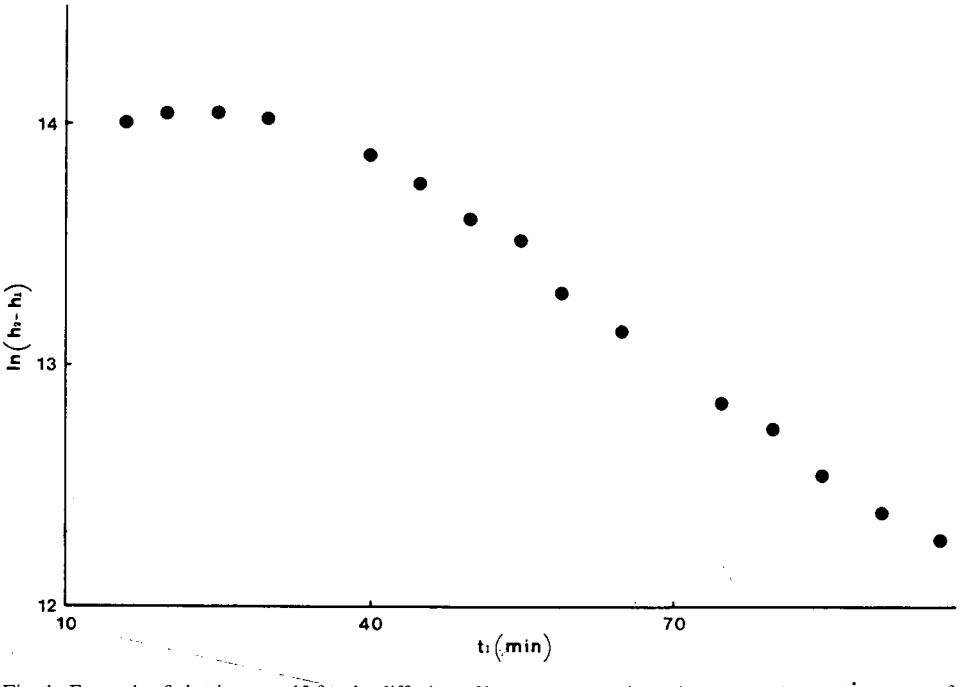

Fig. 4. Example of plotting eqn. 12 for the diffusion of benzene vapour into nitrogen carrier gas ($\dot{V} = 0.4\ cm^3\ s^{-1}$) at 348.2 K and 1 atm.

$$\ln\{A'_1 \exp[-(\alpha + \omega)t_1] - (h_2 - h_1)\} = \ln A'_2 - 9\alpha t_1 \quad (16)$$

and we find α and A'_2 from the slope and the intercept, respectively, of the new plot.

The value of h_∞ can now be calculated from eqn. 2 by substituting in it any pair of h, t_0 values, as A_1, $\alpha + \omega$, A_2 and 9α are all known from the above plots, using also eqns. 13 and 14 and the known value of Δt.

Third procedure

Differentiating eqn. 2 with respect to time, we obtain

$$\frac{dh}{dt_0} = A_1(\alpha + \omega)\exp[-(\alpha + \omega)t_0] - 9\alpha A_2 \exp(-9\alpha t_0) \quad (17)$$

The plot of the experimental data this time should be of ln (dh/dt_0) *vs.* t_0 (*cf.*, Fig. 5), dh/dt_0 being calculated approximately from $\Delta h/\Delta t_0 = (h_2 - h_1)/(t_2 - t_1)$, with t_2 and t_1 as close to each other as possible, and $t_0 = (t_1 + t_2)/2$. Again, this plot, according to eqn. 17, should become after some time

$$\ln(dh/dt_0) = \ln[A_1(\alpha + \omega)] - (\alpha + \omega)t_0 \quad (18)$$

and before this

$$\ln\{A_1(\alpha + \omega)\exp[-(\alpha + \omega)t_0] - dh/dt_0\} = \ln(9\alpha A_2) - 9\alpha t_0 \quad (19)$$

Therefore, as in the previous two procedures, $\alpha + \omega$, A_1, α and A_2 can easily be calculated from the slopes and the intercepts of the two plots described above by eqns. 18 and 19.

It should be noted that when Δt in the second procedure is small, eqn. 12 leads to eqn. 17 with $dh/dt_0 = (h_2 - h_1)/\Delta t$. This is done by expanding the exponentials of eqns. 13 and 14 in MacLaurin series and retaining only the first two terms.

The activities and activity coefficients can be calculated from (a) the experimental h_∞ given by eqn. 3; (b) the A_1 or A_2 values found in the first procedure and given by eqns. 4 and 5, respectively; (c) the A'_1 or A'_2 values found in the second

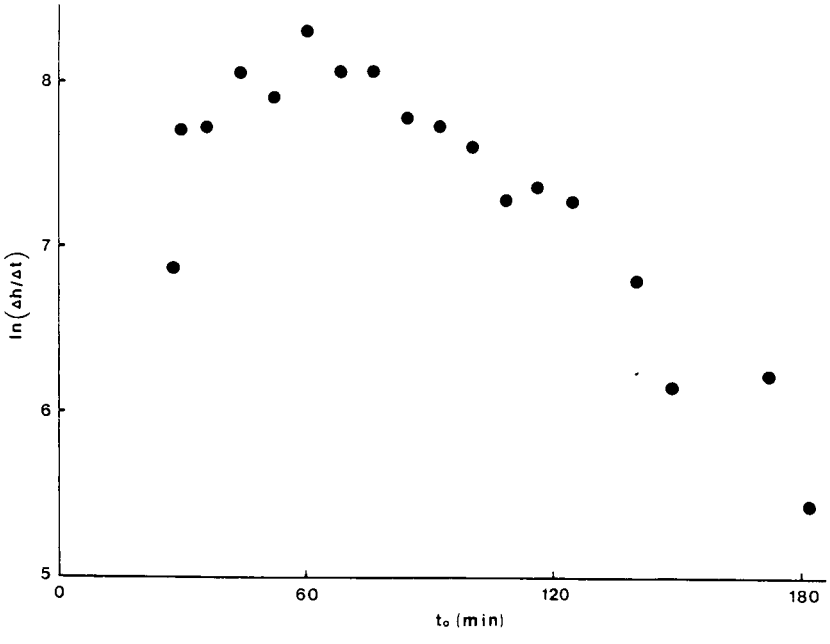

Fig. 5. Example of plotting eqn. 17 for the diffusion of benzene vapour from the benzene–*n*-octane system ($x_1 = 0.5$) into nitrogen carrier gas ($\dot{V} = 0.4$ cm^3 s^{-1}) at 348.2 K and 1 atm.

procedure and given by eqns. 13 and 14, respectively; (d) the A_1 ($\alpha + \omega$) or $9\alpha A_2$ of eqn. 17 in the third procedure. All these parameters contain $k = k_c c_0 a_L / a_G u$ as given by eqn. 6, with k_c being determined from the value of ω (*cf.*, eqn. 8).

Fig. 6 shows the variation of the average activities, as determined by methods (a), (b), (c) and (d) above, of *n*-hexane in the *n*-hexane (1)–*n*-hexadecane (2) system, and of the corresponding literature activities [10] with the *n*-hexane mole fraction. It is seen that the experimental activities, a_1, approach the corresponding literature values only when the *n*-hexane mole fraction approaches unity ($x_1 = 0.93$). This may be due to the fact that either the binary liquid mixtures are not completely homogeneous at the low range of composition or their low composition does not remain constant during the evaporation process. Another possible explanation of this finding may be the diffusion of *n*-hexane into liquid *n*-hexadecane, which was considered negligible in the theoretical treatment.

Let us now examine whether the stirring of the liquid mixture, and hence the liquid diffusion, influences the activities or activity coefficients determined. The experimental activity coefficients, based on the first procedure, for *n*-hexane ($\gamma_1 = 0.842$ with stirring and $\gamma_1 = 0.852$ without stirring) support the hypothesis in the Appendix that the liquid diffusion is negligible. The significance or not of the liquid diffusion with respect to the activity or activity coefficient determination was also examined by changing the volume of the liquid mixture, V. The results, obtained again in the first way ($\gamma_1 = 0.842$ with $V = 1.96$ cm^3 and $\gamma_1 = 0.784$ with $V = 2.72$ cm^3) are not very different, showing that liquid diffusion does not significantly influence the evaporation process of *n*-hexane from the *n*-hexane–*n*-hexadecane system. Comparison of all the *n*-hexane activities, determined by the above four methods at the composition $x_1 = 0.93$, in which the average experimental activity approaches the literature value, with that actually found in the literature [10] shows that method (c) of activity determination is more accurate. On the other hand, comparison of the average diffusion coefficients of the *n*-hexane vapour into the carrier gas nitrogen, calculated from eqn. 7 for the three methods used ($D = 0.386$ cm^2 s^{-1} with the first, $D = 0.488$ cm^2 s^{-1} with the second and $D = 0.834$ cm^2 s^{-1} with the third procedure), with that ($D = 0.388$ cm^2 s^{-1}) obtained by the Füller–Schettler–Giddings (FSG) method [11], shows that the more accurate method, at least

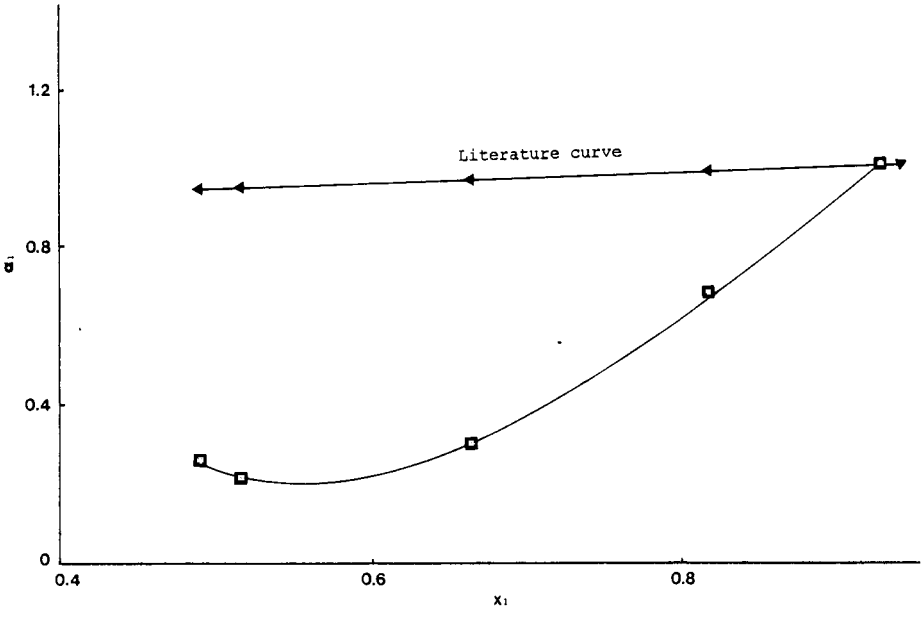

Fig. 6. Variation of the average experimental activities, a_1, of *n*-hexane in the *n*-hexane (1)–hexadecane (2) system, and of the literature activities, with the *n*-hexane mole fraction ($T = 348.2$ K, $P = 1$ atm, $\dot{V} = 0.4$ cm^3 s^{-1}).

for the diffusion coefficient determination, is that based on the first procedure above. This conclusion is supported by the fact that the values of the mass transfer coefficients, $k_{c'}$, determined by the first procedure are closer to those obtained in a previous study [9].

Fig. 7 shows the variation of the benzene average values for activity a_1 in the benzene (1)–*n*-octane(2) system, determined by the four methods mentioned, with the benzene mole fraction, and also the variation of the corresponding theoretical activities with the composition of the mixture. The latter were calculated by the three-suffix Margules equation, resulting from the experimental vapour–liquid equilibrium data [12] for the benzene–*n*-octane system at the working temperature (T = 348.2 K). This equation has the form

$$\ln \gamma_1 = [A_{12} + 2(A_{21} - A_{12})x_1]x_2^2 \quad (20)$$

$$\ln \gamma_2 = [A_{12} + 2(A_{12} - A_{21})x_2']x_1^2 \quad (21)$$

The constants of eqns. 20 and 21, which at T = 348.2 K have the values A_{12} = 0.3516 and A_{21} = 0.4132, were taken from ref. 13.

It can be seen from Fig. 7 that the average experimental activities of benzene approach the theoretical values, calculated from eqn. 20, as the benzene mole fraction approaches unity or zero. The case when $x_1 \rightarrow 1$ is similar to that found for *n*-hexane in the *n*-hexane–*n*-hexadecane system, and is probably due to the same reasons. The second case ($x_1 \rightarrow 0$), which means that the solute component is at infinite dilution, is the ideal condition for studying interactions in solutions by gas chromatography.

Comparison of the activities of benzene in the benzene–*n*-octane system obtained by the three ways

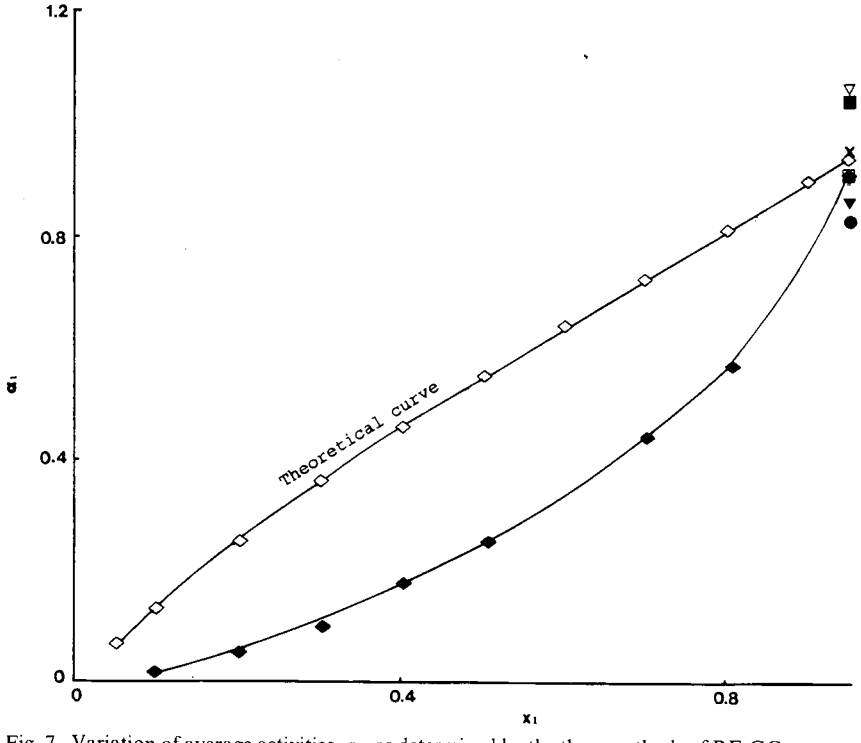

Fig. 7. Variation of average activities, a_1, as determined by the three methods of RF-GC presented, of benzene in the benzene–*n*-octane system, and of the theoretical activities, a_1, as determined from the Margules equation, with the benzene mole fraction (T = 348.2 K, P = 1 atm, $\dot{V}$ = 0.4 cm^3 s^{-1}). First method, × from h_∞, □ from A_1, # from A_2; second method, ■ from A_1, ▽ from A_2'; third method, ▼ from $A_1(\alpha + \omega)$, ● from $9\alpha A_2$; ◆, average values.

mentioned at the higher benzene mole fraction ($x_1 = 0.95$) with that calculated by eqn. 20, and of the average diffusion coefficients for benzene vapour into the carrier gas nitrogen ($D = 0.424$ cm^2 s^{-1} with the first, $D = 1.017$ cm^2 s^{-1} with the second and $D = 0.878$ cm^2 s^{-1} with the third procedure) with that obtained by the FSG method ($D = 0.464$ cm^2 s^{-1}) shows that the accuracy is again better for the method based on the first procedure.

The average experimental activities of *n*-octane, a_2, in the benzene–*n*-octane system, with the corresponding theoretical activities calculated from eqn. 21 at various compositions of the mixture are presented in Fig. 8. It can be seen that the experimental activities approach the theoretical values only when the *n*-octane mole fraction approaches unity. When $x_2 \rightarrow 0$ the experimental activities deviate strongly from the theoretical values, as at the working temperature ($T = 348.2$ K) and in this range of mixture composition the heights of the *n*-octane peaks are too low because of its low vapour pressure.

An effort to draw any conclusion from Fig. 8 regarding the accuracy of the three procedures used was unsuccessful, as the experimental data appear with a large random error.

The deviations pointed out earlier for the activities of *n*-hexane in the *n*-hexane–*n*-hexadecane system and of benzene or *n*-octane in the benzene–*n*-octane system can also be attributed to the effect of the thermal non-equilibrium, as the vessel with height L_2 (*cf.*, Fig. 1) is filled with the liquid mixture at the ambient temperature and needs some time to attain thermal equilibrium.

Finally, one can take into account the fugacity correction for the activities or activity coefficients determined. The fugacity correction for the activity coefficient of *n*-hexane in *n*-hexadecane was calculated using the second virial coefficients of *n*-hexane and the *n*-hexane–nitrogen second cross-virial coefficients obtained by fitting the respective literature data [14] with the Tsonopoulos correlation [15]. For the mixture *n*-hexane–*n*-hexadecane at 333.5 K and an *n*-hexane mole fraction of 0.818, the fugacity-corrected activity of *n*-hexane is 0.713, whereas the fugacity-uncorrected activity is 0.696. Hence the corrected value exceeds the uncorrected one by *ca.* 2.5%, which certainly cannot explain the difference between our results and the literature values, although the fugacity correction should increase as the mole fraction of *n*-hexane decreases. Obviously, more experimental work is necessary in order to investigate these anomalous deviations.

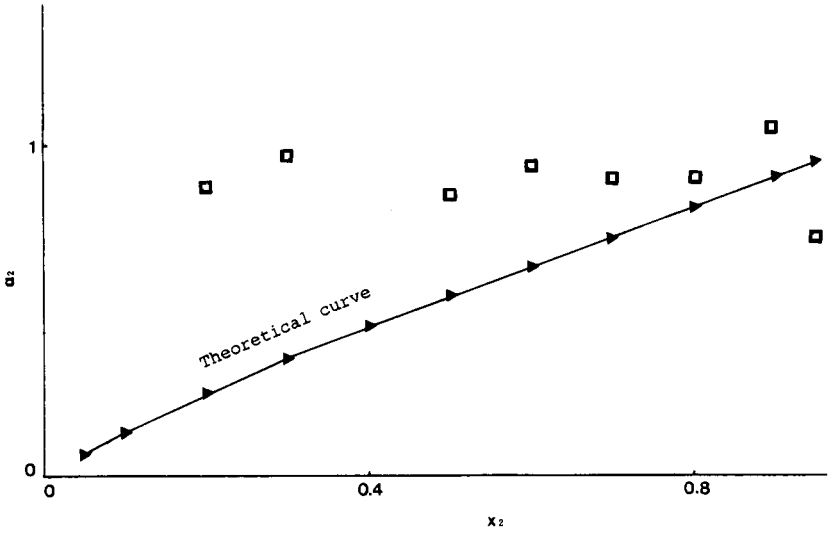

Fig. 8. Plot of the average experimental, a_2, and theoretical activities of *n*-octane in the benzene–*n*-octane system *vs.* the *n*-octane mole fraction ($T = 348.2$ K, $P = 1$ atm, $\dot{V} = 0.4$ cm^3 s^{-1}).

As a general conclusion, it may be said that the three methods of RF-GC presented here should give, under experimental conditions (the evaporation temperature of the solute to be close to its boiling point and the solute mole fraction to be close to zero or unity), activities or activity coefficients for binary liquid mixtures close to those obtained by other techniques or calculated theoretically. The first method appears to be the most accurate, yielding activities, diffusion coefficients and mass transfer coefficients closest to the theoretical values. However, this study shows that there can be differences in the reliability of the results depending on the approach used.

ACKNOWLEDGEMENT

The authors thank Mrs. Margaret Barkoula for assistance.

APPENDIX

The general solution in the form of eqn. 2 will be derived with the help of the coordinates of Fig. 1. The diffusion of a vapour leaving the liquid in vessel L_2 is described by the equation

$$\partial c_z/\partial t_0 = D\partial^2 c_z/\partial z^2 \tag{A1}$$

The initial condition is $c_z(z, 0) = 0$, and the boundary conditions at $z = 0$ are

$$c_z(0, t_0) = c(l', t_0) \quad \text{and} \quad D(\partial c_z/\partial z)_{z=0} = uc(l, t_0) \tag{A2}$$

The boundary condition at the other end, $z = L_1$, of the diffusion column is

$$Da_G(\partial c_z/\partial z)_{z=L_1} = k_c a_L[c_0 - c_z(L_1)] \tag{A3}$$

where $C_z(L_1)$ is the actual concentration at the liquid interface.

When the Laplace transform of eqn. A1 is taken with respect to t_0, a linear second-order differential equation results, and this is solved by using z Laplace transformation, giving

$$C_z = C_z(0)\cosh qz + \frac{C_z'(0)}{q}\sinh qz \tag{A4}$$

where

$$q^2 = p_0/D \tag{A5}$$

and $C_z(0)$ and $C_z'(0)$ are the t_0 Laplace transforms of $c_z(0)$ and $(\partial c_z/\partial z)_{z=0}$, respectively. Using the boundary conditions expressed by eqn. A2, eqn. A4 becomes

$$C_z = C(l', p_0)(\cosh qz + \frac{u}{Dq}\sinh qz) \tag{A6}$$

where $C(l', p_0)$ is the t_0 transformed function $c(l', t_0)$, which we try to express as an analytical function of time.

By means of eqn. A6, $C_z(L_1)$ and $(\partial C_z/\partial z)_{z=L_1}$ can be calculated and then substituted into eqn. A3 after the latter has been transformed with respect to t_0. The result is simplified by making the usual approximation to omit $\sinh qL_1$ compared with $(u/Dq)\cosh qL_1$ and $\cosh qL_1$ compared with $(u/Dq)\sinh qL_1$. These are valid for sufficiently high flow-rates. Subsequently we obtain

$$C(l', p_0) = k \cdot \frac{1}{p_0 \cosh qL_1} \cdot \frac{1}{1 + (k_c'/Dq)\tanh qL_1} \tag{A7}$$

where $k_c' = k_c a_L/a_G$ and k is given by eqn. 6.

Inverse Laplace transformation of this equation to find $c(l', p_0)$ is not easy, but a solution compatible with the experimental data can be found by using certain approximations:

$$\frac{1}{p_0 \cosh qL_1} \approx \frac{1}{p_0} - \frac{4}{\pi} \cdot \frac{1}{p_0 + \alpha} + \frac{4}{3\pi} \cdot \frac{1}{p_0 + 9\alpha} \tag{A8}$$

$$\frac{\tanh qL_1}{Dq} \approx \frac{2}{L_1} \cdot \frac{1}{p_0 + \alpha} \tag{A9}$$

These approximations are derived by taking [16] the inverse Laplace transforms of $1/p_0 \cosh qL_1$ and $\tanh qL_1/Dq$ in the form of elliptical theta functions θ_1 and θ_2, respectively, giving a series of exponential functions of time, $\exp(-\alpha t_0)$, $\exp(-9\alpha t_0)$, $\exp(-25\alpha t_0)$, etc., in both instances. Of these, we retain only the first few terms, as the other with the larger exponential coefficients very soon become negligible. Finally, the retained terms are transformed back to give the approximations A8 and A9.

Using these approximations in eqn. A7, and after some rearrangement, this becomes

$$C(l', p_0) = k\left[\frac{p_0 + \alpha}{p_0(p_0 + \alpha + \omega)} - \frac{4}{\pi} \cdot \frac{1}{p_0 + \alpha + \omega} + \frac{4}{3\pi} \cdot \frac{p_0 + \alpha}{(p_0 + 9\alpha)(p_0 + \alpha + \omega)}\right] \tag{A10}$$

where

$$\omega = 2k_c'/L_1 = 2k_c a_L/a_G L_1 \qquad \text{(A11)}$$

The inverse transformation of eqn. A10 now gives, after collecting terms of the same exponential function,

$$c(l', t_0) = k\left[\frac{\alpha}{\alpha+\omega} - \left(\frac{4}{\pi} - 1 + \frac{\alpha}{\alpha+\omega} + \frac{4}{3\pi}\cdot\frac{\omega}{8\alpha-\omega}\right)\right.$$
$$\left.\exp[-(\alpha+\omega)t_0] + \frac{4}{3\pi}\cdot\frac{8\alpha}{8\alpha-\omega}\exp(-9\alpha t_0)\right] \qquad \text{(A12)}$$

Combining this with eqn. 1 (for $m = 1$), one obtains

$$h = h_\infty - A_1\exp[-(\alpha+\omega)t_0] + A_2\exp(-9\alpha t_0) \qquad \text{(A13)}$$

which is the same as eqn. 2.

REFERENCES

1 N. A. Katsanos and G. Karaiskakis, *Adv. Chromatogr.*, 24 (1984) 125.
2 N. A. Katsanos and G. Karaiskakis, *Analyst (London)*, 112 (1987) 809.
3 N. A. Katsanos, *J. Chromatogr.*, 445 (1988) 39.
4 N. A. Katsanos, *Flow Perturbation Gas Chromatography*, Marcel Dekker, New York, Basle, 1988.
5 N. A. Karsanos and J. Kapolos, *Anal. Chem.*, 61 (1989) 2231.
6 N. A. Katsanos, G. Karaiskakis and P. Agathonos, *J. Chromatogr.*, 349 (1986) 369.
7 P. Agathonos and G. Karaiskakis, *Chromatographia*, 25 (1988) 453.
8 P. Agathonos and G. Karaiskakis, *J. Chem. Soc., Faraday Trans. 1*, 85 (1989) 1357.
9 G. Karaiskakis and N. A. Katsanos, *J. Phys. Chem.*, 88 (1984) 3674.
10 M. L. McGlashan and A. G. Williamson, *J. Chem. Soc., Faraday Trans. 1*, 57 (1961) 588.
11 E. Fuller, P. Schettler and J. C. Giddings, *Ind. Eng. Chem.*, 58 (1966) 19.
12 I. M. Elshayal and B. C. Lu, *J. Appl. Chem.*, 18 (1968) 277.
13 J. Gmehling, U. Onken and W. Artl, *Vapor–Liquid Equilibrium Data Collection, Aliphatic Hydrocarbons C7–C18 (Chemistry Data Series*, Vol. I, Part 6b), University of Dortmund, Dortmund, 1980, p. 246.
14 J. H. Dymond and E. B. Smith, *The Virial Coefficients of Pure Gases and Mixtures —A Critical Compilation*, Clarendon Press, Oxford, 1980.
15 C. Tsonopoulos, *AIChE J.*, 20 (1974) 263.
16 F. Obberhettinger and L. Badii, *Tables of Laplace Transforms*, Springer, Berlin, 1973, pp. 294 and 421.

Journal of Chromatography, 595 (1992) 247–258
Elsevier Science Publishers B.V., Amsterdam

CHROM. 23 918

Gas chromatographic analysis of high-molecular-weight polynuclear aromatic hydrocarbons

I. Molecular weight 328

Agneta Bemgård, Anders Colmsjö and Bengt-Ove Lundmark

Department of Analytical Chemistry, National Institute of Occupational Health, S-171 84, Solna (Sweden)

(First received October 2nd, 1991; revised manuscript received November 27th, 1991)

ABSTRACT

Various columns were investigated with respect to the gas chromatographic analysis of polynuclear aromatic hydrocarbons (PAHs) having molecular weights that exceed 300. Among the columns tested, four columns differing in stationary phase composition were carefully evaluated. Three of these columns were commercially available. The evaluation was focused on cata-condensed PAHs of molecular weight 328. Temperature-programmed retention indices with PAHs as reference markers were calculated and compared.

INTRODUCTION

Polynuclear aromatic hydrocarbons (PAHs) are hazardous environmental chemicals. They are formed primarily during incomplete combustion or pyrolysis of organic materials. The PAH group contains the largest number of mutagenic and/or carcinogenic substances [1,2]. High-molecular-weight PAHs, with six or more rings, are not a well studied group, but their carcinogenic properties are anticipated [3]. Some of these PAHs have been confirmed to be inactive, whereas others have shown weak or moderate activity [4]. Owing to difficulties in the analysis of these compounds, little information on their ambient levels is available. However, some studies have been made. For example, Fetzer and co-workers [5,6] analysed a sample of diesel engine particulate matter and confirmed the existence of naphtho[8,1,2-*abc*]coronene with a molecular weight (M_W) of 374. All PAHs having six or more rings were found to be highly fused types, *i.e.*, no linear or non-alternant PAHs were seen in that sample. The same results were obtained by Peaden *et al.* [7], who separated a carbon black extract by high-performance liquid chromatography (HPLC) and made molecular weight assessments by use of mass spectrometry (MS). They did not find any PAHs of MW = 328 (cata-condensed types) within that sample. However, some sompounds with five-membered rings were found. Romanowski *et al.* [8] reported the existence of PAHs with molecular weights exceeding 300 in an airborne particulate matter. No identifications were made but the sample was analysed by gas chromatography (GC)–MS, showing some compounds with a molecular weight of 328.

For the separation of complex mixtures, capillary GC is a powerful technique owing to its high resolving power. However, for the chromatography of high-molecular-weight compounds, the elution temperature may exceed the temperature limit of the capillary column. The maximum allowable temperature for a capillary column is determined by the temperature stability of the stationary phase and the capillary material.

In recent years, interest in producing heat-stable

0021-9673/92/$05.00

stationary phases has increased. Both the common phases, *i.e.*, methylsilicone and methylphenylsilicone types, and newer modified phases such as the siloxane/silarylene phases [9,10], carborane-modified types [11,12] and polysulphone-modified silicone stationary phases [13,14], have been refined to meet the increased demands on thermal stability.

The temperature limit of a capillary column is also determined by the capillary material. Polyimide-clad fused-silica columns have become commonly used. A serious drawback, however, is the temperature limit of the polyimide, *viz.*, *ca.* 370°C. Even though the column could be used for a short time above this temperature, the lifetime will drastically decrease. To overcome this problem, Lipsky and Duffy [15,16], introduced alumina-clad fused-silica capillaries which were claimed to withstand temperatures far above the polyimide-clad capillary limit. Good elution of, *e.g.*, triglycerides on these columns has been reported [15–17]. The maximum temperature was 440°C. However, in our experience, columns prepared with this type of capillary material become even more brittle than the polyimide-clad columns after high-temperature exposure for an extended period of time.

Another type of high-temperature columns evaluated are the metal capillaries [18,19] recently reintroduced by Chrompack. The material can withstand temperatures above 500°C. In 1987, Termonia *et al.* [20] described high-temperature GC by use of a stainless-steel-armoured polyimide-clad fused-silica column (Rescom, Belgium). Restek have developed stainless-steel columns to which is bound a layer of fused silica a few micrometres thick (Silcosteel) [21].

Inexpensive and durable columns can be made from borosilicate glass. Columns prepared from this material were suggested by Rohwer and Pretorius [22]. It has also successfully been used by Blum and co-workers in the preparation of high-temperature stable, medium-polarity columns used for the analysis of antioxidants, UV stabilizers [23] and metalloporphyrins [24,25].

For the analysis of high-molecular-weight PAHs, the method of choice has been reversed-phase LC [5–7, 26–28], in some instances with the use of packed capillary LC columns [26,27]. The main reason for not analysing these substances by GC lies in their low vapour pressure and low stationary phase solubility. However, a few attempts have been made to chromatograph PAHs of molecular weight exceeding 300 by GC. In 1974, Grob [29] presented a method to chromatograph rubrene (MW 532). The column was only 5.5 m long and the oven temperature was programmed up to 260°C. However, such short columns cannot be used for the separation of complex mixtures. Carbon black samples have been analysed by GC using non-polar, commercially available capillary columns [8,26] and on a laboratory-made medium-polarity column [30] (methylphenylpolysiloxane having 70% phenyl substitution). Peak asymmetry of late-eluting components was reported [26], which was claimed to be attributed to the low solubility to the high-molecular-weight PAHs in the methylpolysiloxane stationary phase. This conclusion indicates the need for columns having stationary phases with higher polarizability to facilitate dissolution of these particular compounds. However, better dissolution means increased retention, requiring increased oven temperatures.

The aim of this work was to evaluate columns with respect to the GC analysis of PAHs of molecular weight 328.

EXPERIMENTAL

Columns

Four different columns were evaluated. The first column was a thin-film (0.12 μm) CP-Sil 8 (having 5% phenyl substitution) polyimide-protected fused-silica column (25 m × 0.32 mm I.D.) from Chrompack (Middelburg, Netherlands). Further, two stainless-steel columns (15 m × 0.28 mm I.D. with a film a few micrometres thick of fused-silica bound to the metal, obtained from Restek (Bellefonte, PA, USA) were tested. One was coated with a methyltrifluoropropylpolysiloxane stationary phase, Rtx-200, and the other with a methyldiphenylpolysiloxane having 5% diphenyl substitution, XTI-5. Both had a film thickness of 0.25 μm and were immobilized. Finally, one laboratory made column was evaluated. The stationary phase was a silarylene/siloxane copolymer having 25% biphenyl substitution, synthesized at the University of Neuchatel, Switzerland. The polymer was coated on polyimide-protected fused-silica tubing (Chrompack) which was flushed with nitrogen prior to the static

coating. The coating procedure was described in a previous paper [10].

Apparatus

GC was performed on a Carlo Erba (Milan, Italy) Model 4160 gas chromatograph equipped with a flame ionization detector. The chromatograph was connected to a laboratory data system (ELDS 900; Chromatography Data Systems, Kungshög, Stenhamra, Sweden). All recording and calculations of chromatographic data were performed with this system. Hydrogen, passed through an oxygen trap, was used as the carrier gas.

For comparison, som experiments were made on a Hewlett-Packard (Avondale, PA, USA) Model 5790 gas chromatograph equipped with a flame ionization detector and connected to the same laboratory data system as above. The carrier gas was oxygen-free helium.

Solutes

The PAHs studied were either commercially available (Promochem, Wessel, Germany) or obtained from other laboratories (see Acknowledgements). There are 39 possible PAH isomers with a molecular weight of 328 containing six fused benzene rings. In this work 14 of these isomers were studied (Fig. 1). The compounds were dissolved in chlorobenzene (BDH, Poole, UK).

To be able to compare the retention indices obtained on the columns evaluated with those published by Lee *et al.* [31], a standard mixture containing seventeen lower molecular weight PAHs, ranging from phenanthrene to coronene, dissolved in cyclohexane–acetone (1:1) was analysed. The larger standard compounds, *viz.*, benzo[*c*]picene, dinaphtho[2,1-*a*:2,1-*h*]anthracene and benzo[*a*]coronene, were also included in this mixture.

As an application of the utility of the columns, an HPLC fraction NBS Standard Reference Material (SRM) 1597, a coal tar extract, [32] containing PAHs with molecular weight 328, dissolved in chlorobenzene, was analysed.

Test conditions

All injections were performed in the on-column mode, except for determinations of capacity factors (k') and column efficieny [measured as height equivalent to a theoretical plate (HETP)], where the split

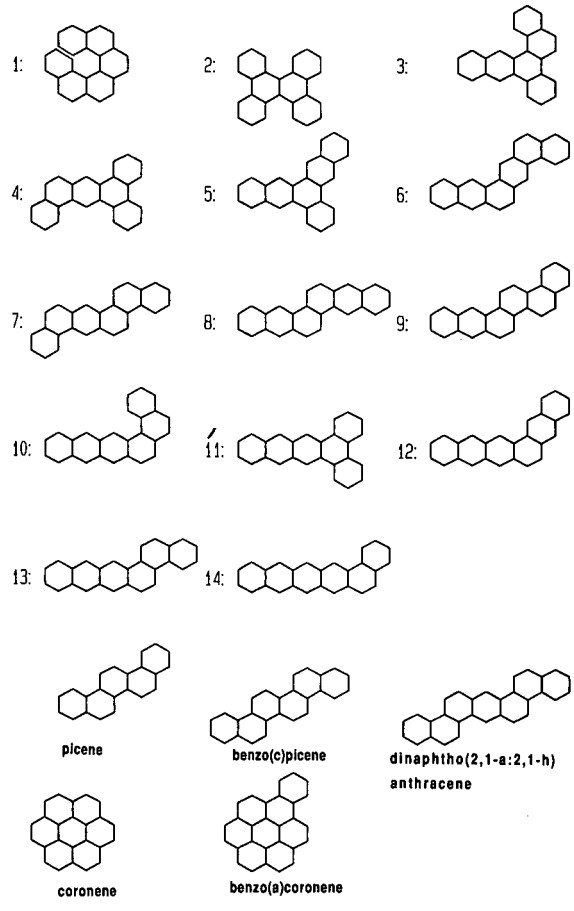

Fig. 1. Structures of the cata-condensed PAHs of molecular weight 328 used in these experiments and the structures of the compounds in the two standard series. All rings are aromatic.

mode was used. In the split mode, the injector temperature was kept at 320°C and the oven temperature was 300°C. The detector temperature was held at 400°C during all runs, except with the Rtx-200 column, where it was 370°C. In the split mode, 1.0 μl of coronene in chlorobenzene was injected with a spliting ratio of 1:200.

For the PAHs in Fig. 1 (MW 328), introduced in the on-column mode, the oven temperature was held at 140°C during the injection. After a 2-min isothermal period, the oven was rapidly heated to 200°C, and after 4 min from injection the temperature programming was started at a rate of 5°C min to 350 or 370°C. The inlet pressure was set to give a slightly higher gas velocity than the optimum (mea-

sured at 300°C). The inlet overpressure ranged from 0.5 to 0.7 atm depending on the length and I.D. of the columns. The injection volume ranged from 0.2 to 1.0 μl per injection.

The PAH mixture containing lower-molecular-weight compounds was also introduced in the on-column mode. The injection volume was 1.0 μl injected at 70°C; after a 2-min isothermal period the oven was programmed at a rate of 5 or 7°C min to 350 or 370°C.

Retention index determinations

The temperature-programmed retention indices (RI) were determined according to the model described by Lee *et al.* [31], where phenanthrene, chrysene, picene and benzo[*c*]picene were used as standard compounds. We found it necessary to extend this standard series by introduction of dinaphtho[2,1-*a*:2,1-*h*]anthracene as the last-eluting standard compound. The addition of this compound is not consistent with the remainder of the series. This is a compromise owing to a lack of the correct standard substance. For the retention index determinations, the value for phenanthrene was set at 300, chrysene at 400, picene at 500, benzo[*c*]picene at 600 and dinaphtho[2,1-*a*:2,1-*h*]anthracene at 700. As an alternative series, a standard series with coronene and benzo[*a*]coronene was used, where coronene was given the value of 100 and benzo[*a*]coronene 200. Molecular structures of the standard series of compounds are shown in Fig. 1. The retention index values for the PAHs investigated were obtained by linear interpolation between the standard compounds eluting just before and after the compound to be determined.

RESULTS AND DISCUSSION

This work was focused on temperature-programmed retention index assessments of some catacondensed PAH isomers consisting of six fused benzene rings (MW 328) (Fig. 1). The indices were measured in two different standard systems and calculated according to ref. 31. One series consisted of phenanthrene, chrysene, picene, benzo[*c*]picene and dinaphtho[2,1-*a*:2,1-*h*]anthracene and the other series coronene and benzo[*a*]coronene. Ten commercially available columns from five different manufacturers were tested, but only a few were sufficiently stable with regard to both the capillary material and the stationary phase stability.

Owing to the low vapour pressure and high boiling points for the high-molecular-weight PAHs, a column intended for the GC analysis of these compounds must be stable at high temperatures, hence a stable stationary phase and a stable protecting layer are required. However, the stationary phase must not only be heat stable, it must also maintain good chromatographic properties at elevated temperatures. When high-molecular-weight compounds are considered in GC, columns having thin stationary phase films are preferred from the viewpoint of elution temperature. The drawback with such columns is a low solute capacity. Moreover, it is favourable if the stationary phase interacts only weakly with the compounds to be chromatographed, giving a comparatively lower elution temperature. Considering the latter fact, a pure methylsilicone stationary phase should be a good choice. However, the solubility of the high-molecular-weight PAHs in these phases is low [26]. The optimum column for the GC of high-molecular-weight PAHs should exhibit solute solubility combined with good thermal stability with low bleeding profiles. As will be discussed, all these criteria are difficult to fulfil, but compromises are possible.

Columns

Among the columns examined, the stainless-steel fused-silica capillary column coated with a methyltrifluoropropyl stationary phase, Rtx-200, was the most non-polar or exhibited the lowest interaction between the stationary phase and the solutes. In Table I are listed the column properties, including the k' values at 300°C for coronene, the corresponding HETP values, the β-value (gas to liquid volume ratio) and the partition coefficient, K, at 300°C (calculated as $\beta\ k'$), which describes the solute solubility or the magnitude of interaction between the stationary phase and the solute. As shown in Table I, the Rtx-200 column has the lowest K value but also a low column efficiency. According to the peak shapes observed for the high-molecular-weight PAHs on this column, the low efficiency seems to depend mainly on a low compatibility between, *e.g.*, coronene and the non-polar stationary phase. On the other hand, the low retention on this stationary phase made it possible to elute the highest molec-

TABLE I

COLUMN CHARACTERISTICS AND CHROMATOGRAPHIC PROPERTIES OF CORONENE AT 300°C

Column	Length (m)	I.D. (mm)	k' (300°C)	HETP (mm)	β	K (300°C)
Rtx-200	15	0.28	5.88	0.43	280	1646
CP-Sil 8	25	0.32	3.40	0.32	667	2268
XTI-5	15	0.28	8.83	0.35	280	2472
Silabiphenyl	20	0.32	6.93	0.34	1600	11086

ular weight compound examined below 330°C, *i.e.*, dinaphtho[2,1-*a*:2,1-*h*]anthracene (MW 378).

Next in order of polarity are the polyimide-covered fused-silica column, CP-Si 8, with a chemical composition of 5% phenyl and 95% methyl substitution, and the stainless-steel fused-silica column, XTI-5, with 5% diphenyl substitution. Owing to the similarity of their stationary phases they exhibit similar retention properties. These columns had K values that were *ca.* 33% higher than that for the Rtx-200 column, indicating increased interactions between the stationary phases and the solute.

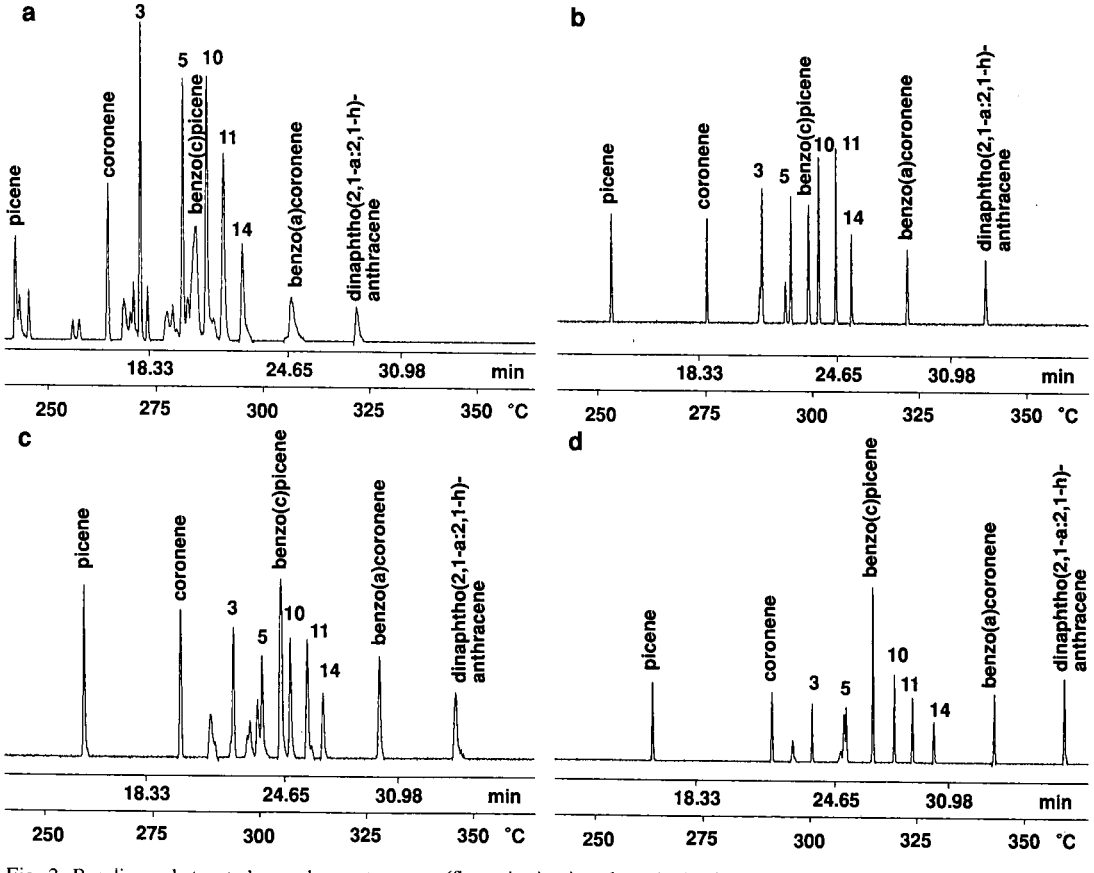

Fig. 2. Baseline-substracted gas chromatograms (flame ionization detection) of a PAH mixture on (a) the Rtx-200 column, (b) the CP-Sil 8 column, (c) the XTI-5 column and (d) the silabiphenyl column. Conditions: on-column injection at 140°C, after 2 min rapidly heated to 200°C and after 4 min from time of injection programmed at 5°C/min to (a) 350°C and (b–d) 370°C. Peak numbers refer to the compounds in Fig. 1.

For the silabiphenyl column, comparison of the partition coefficient in Table I shows very high interactions between the stationary phase and coronene. This non-commercially available column cannot be used for chromatography below 150°C.

In Fig. 2 are shown some chromatograms obtained with these columns. The peak numbers refer to the compounds in Fig. 1. All the chromatograms are baseline subtracted, making it easier to compare the peak shapes and resolution. The CP-Sil 8 and silabiphenyl columns show the best eluition patterns. These two columns were coated with the thinnest stationary phase films, *i.e.*, 0.12 and 0.05 μm. Owing to increased resistance to mass transfer in the liquid phase, it is not completely possible to compare columns with thick and thin stationary phase films with regard to the column efficieny.

In Fig. 3 are shown runs made with the same temperature programmmes to show the bleeding profile on these columns. A high bleeding rate was observed for the CP-Sil 8 column at increased temperatures, whereas the XTI-5 and silabiphenyl columns exhibited only a small increase in bleeding rate at 370°C. The Rtx-200 column (not included in Fig. 3) was only used up to 350°C with a bleeding rate comparable to that of the XTI-5 column.

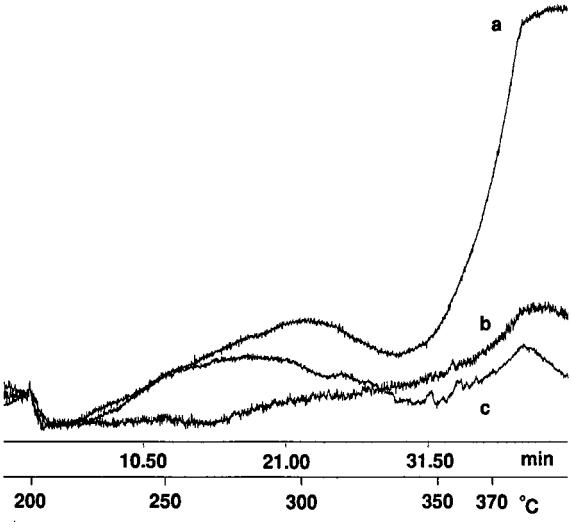

Fig. 3. Bleeding rates from (a) the CP-Sil 8 column, (b) the silabiphenyl column and (c) the XTI-5 column. Temperature programming as in Fig. 2.

Retention indices

If retention indices are calculated according to Kováts [33], using *n*-alkanes as standard compounds, dramatic changes in retention indices between columns of different polarities can be observed. Changes in retention indices with temperature have also often been reported (*e.g.*, [34]). In this work where the solutes and standards are of the same types, such differences should be very small. In order to confirm this assumption, different programming rates (5 or 7°C/min) and different column head pressures (0.5 or 0.7 atm) were employed on the Rtx-200 column. With a test mixture composed of lower-molecular-weight PAHs, the retention index dependence on these parameters could be studied. For example, benzo[*a*]pyrene showed a retention index of 455.70 when the head pressure was held at 0.5 atm at a programming rate of 7°C/min. The elution temperature was 237°C. On the other hand, with a head pressure of 0.7 atm and a programming rate of 5°C min, the elution temperature of benzo[*a*]pyrene was 218°C and the corresponding retention index was 455.20. The same column was further evaluated in a different chromatograph (HP 5790) with helium as carrier gas. This change of chromatograph did not have a significant influence the retention indices of the PAHs. However, a more polarizable column could be expected to be more sensitive to temperature changes. Surprisingly, the retention index for benzo[*c*]picene on the silabiphenyl column, determined with the coronene–benzo[*a*]coronene system, was 145.68 for an elution temperature of 308°C and 145.10 at 319°C. Hence changes in elution temperature of up to 20°C have small effects on the retention indices for the two PAH systems evaluated.

Finally, retention indices for the standard mixture consisting of lower molecular weight PAHs were determined for the four columns and compared with the values reported in ref. 31. The results from these tests are given in Table II, where the precision (standard deviation) is also presented. All the columns showed higher retention index values for the solutes than the values in ref. 31. The differences were smallest for the CP-Sil 8 column. This was as expected, because the retention indices in ref. 31 were obtained on an SE-52 column (having 5% phenyl substitution). Both the non-polar and the most polar columns showed substantially different

TABLE II

TEMPERATURE-PROGRAMMED AVERAGE RETENTION INDICES (I) OF SOME LOWER-MOLECULAR-WEIGHT PAHs ON THE FOUR DIFFERENT COLUMNS

Compound	$I \pm$ S.D.				
	Rtx-200	CP-Sil 8	XTI-5	Silabiphenyl	Ref. 31
Pyrene	352.46 ± 0.14^b	351.47 ± 0.07^a	351.88 ± 0.04^c	352.19 ± 0.04^a	351.22 ± 0.08^c
Benzo[*e*]pyrene	454.22 ± 0.14^b	452.14 ± 0.09^a	452.71 ± 0.05^c	454.33 ± 0.09^a	450.73 ± 0.17^b
Benzo[*a*]pyrene	455.61 ± 0.18^b	453.74 ± 0.09^a	454.38 ± 0.05^c	455.72 ± 0.09^a	$453.44 \pm -^a$

[a] Two determinations.
[b] Three determinations.
[c] Four determinations.

values. The retention indices for benzo[*e*]pyrene on these columns were 3.5 and 3.6 index units (i.u.) higher than on the SE-52 column [31].

In Tables III and IV are given the retention indices of PAHs with MW 328 in the picene and coronene standard system, respectively. The precision is better with the coronene standard. Further, the precision is lower for the higher-molecular-weight PAHs than for the smaller PAHs listed in Table II. However, the calculated standard deviations in Ta-

TABLE III

TEMPERATURE-PROGRAMMED AVERAGE RETENTION INDICES OF SOME PAHs MEASURED WITH THE PICENE STANDARD SERIES COMPOUNDS

The numbers refer to compounds in Fig. 1.

Compound	$I \pm$ S.D.			
	Rtx-200	CP-Sil 8	XTI-5	Silabiphenyl
Picene	500	500	500	500
1	492.60	509.79	509.74	502.45
Coronene	551.67 ± 0.70^a	548.36 ± 0.25^b	549.10 ± 0.59^a	553.94 ± 0.39^b
2	552.65	567.47	566.87	563.05
3	570.10	567.36	575.96	572.16
4	590.92	588.45	588.03	585.61
5	593.70	591.00	590.43	587.47
6	596.12	594.13	593.04	591.90
7	597.47	596.20	595.80	594.50
8	598.44	597.49	597.51	596.24
9	600	599.06	599.03	597.88
Benzo[*c*]picene	600	600	600	600
10	607.31	605.73	605.47	611.03
11	617.81	615.51	615.18	620.51
12	625.31	620.00	618.78	626.24
13	628.67	622.78	622.70	630.25
14	629.34	624.28	624.03	631.54
Benzo[*a*]coronene	659.18 ± 1.52^c	655.84 ± 0.23^b	656.34 ± 1.09^a	663.24 ± 0.56^b
Dinaphtho[2,1-*a*:2,1-*h*]anthrancene	700	700	700	700

[a] Twenty determinations.
[b] Ten determinations.
[c] Seventeen determinations.

TABLE IV

TEMPERATURE-PROGRAMMED AVERAGE RETENTION INDICES OF SOME PAHs MEASURED WITH THE CORONENE STANDARD SERIES COMPOUNDS

The numbers refer to compounds in Fig. 1.

Compound	$I \pm$ S.D.			
	Rtx-200	CP-Sil 8	XTI-5	Silabiphenyl
Picene[a]	49.33	52.49	51.45	46.42
1[a]	40.63	62.13	60.93	48.75
Coronene	100	100	100	100
2	100	118.67	117.63	109.18
3	118.03	127.45	126.52	118.04
4	138.33	139.50	138.48	132.67
5	141.19	141.83	140.81	133.31
6	143.46	144.93	143.89	137.67
7	144.46	147.15	146.32	140.18
8	145.44	148.32	147.55	141.63
9	146.47	149.90	149.19	143.61
Benzo[*c*]picene	147.38 ± 0.49[b]	150.69 ± 0.12[c]	150.31 ± 0.39[d]	145.68 ± 0.13[c]
10	154.08	155.72	155.11	155.15
11	163.19	164.36	163.70	163.29
12	170.53	168.37	167.47	168.12
13	172.70	170.87	170.25	171.58
14	173.48	172.12	171.53	172.77
Benzo[*a*]coronene	200	200	200	200
Dinaphtho[2,1-*a*:2,1-*h*]antracene[a]	235.70	239.07	238.27	231.63

[a] Extrapolated values from coronene–benzo[*a*]coronene.
[b] Sixteen determinations.
[c] Ten determinations.
[d] Twenty determinations.

ble II are based on a smaller number of observations.

The results obtained on the CP-Sil 8 and XTI-5 columns are similar, which is reasonable according to the results for the smaller PAHs. The ΔI values (measured as I on one column minus I on the CP-Sil 8 column) for the compounds in Tables III and IV are listed in Tables V and VI, respectively. By comparing the change in retention index of the reference compounds in the two standard systems, it can be concluded that the Rtx-200 column (the least polar) follows the same trend as the CP-Sil 8 column. The differences in retention indices for coronene and benzo[*a*]coronene in the picene standard system (Table V) are 3.31 and 3.34 i.u. higher than those on the CP-Sil 8 column. This implies that both coronene and benzo[*a*]coronene are influenced to the same extent. The ΔI values for the XTI-5 column are smaller, but also different for the standard compounds, *i.e.*, a difference of 0.74 and 0.50 i.u. for coronene and benzo[*a*]coronene, implying different retention mechanisms acting on the solutes at different temperatures. The column coated with the most polarizable stationary phase, silabiphenyl, shows different ΔI values for coronene and benzo[*a*]coronene, which were 5.58 and 7.40 i.u. higher than those on CP-Sil 8, respectively. From this it can be concluded that the forces that influence the solute retention are different at different temperatures also on this column.

Among the compounds studied, a few showed great differences in retention indices between columns. Most significant were the values for compound **1** (Fig. 1), which eluted prior to picene on the Rtx-200 column (Table III). This solute is non-planar and thereby probably more sensitive to the stationary phase composition. Further, compounds **2**, also non-planar, and **3** show large differences in re-

TABLE V

ΔI-VALUES IN THE PICENE STANDARD SERIES COMPARED WITH CP-Sil 8

The number refer to compounds in Fig. 1.

Compound	*ΔI*		
	Rtx-200	XTI-5	Silabiphenyl
Picene	0	0	0
1	−17.19	−0.05	−7.34
Coronene	3.31	0.74	5.58
2	−14.82	−0.60	−4.42
3	−6.26	−0.40	−4.20
4	2.47	−0.42	−2.84
5	2.70	−0.57	−3.53
6	1.99	−1.09	−2.23
7	1.27	−0.40	−1.70
8	0.95	0.02	−1.25
9	0.94	−0.03	−1.18
Benzo[*c*]picene	0	0	0
10	1.58	−0.26	5.30
11	2.08	−0.33	5.00
12	5.31	−1.22	6.24
13	5.89	−0.08	7.47
14	5.06	−0.25	7.26
Benzo[*a*]coronene	3.34	0.50	7.40
Dinaphtho[2,1-*a*:2,1-*h*]anthracene	0	0	0

TABLE VI

ΔI-VALUES IN THE CORONENE STANDARD SERIES COMPARED TO CP-Sil 8

The number refer to compounds in Fig. 1.

Compound	*ΔI*		
	Rtx-200	XTI-5	Silabiphenyl
Picene	−3.16	−1.04	−6.07
1	−21.5	−1.20	−13.38
Coronene	0	0	0
2	−18.67	−1.04	−9.49
3	−9.42	−0.93	−9.41
4	−1.17	−1.02	−6.83
5	−0.64	−1.02	−6.19
6	−1.47	−1.04	−7.26
7	−2.69	−0.83	−6.97
8	−2.88	−0.77	−6.69
9	−3.43	−0.71	−6.29
Benzo[*c*]picene	−3.31	−0.38	−5.01
10	−1.64	−0.61	−0.57
11	−1.17	−0.66	−1.24
12	2.16	−0.90	−0.25
13	1.83	−0.62	0.71
14	1.36	−0.59	0.65
Benzo[*a*]corone	0	0	0
Dinaphtho[2,1-*a*:2,1-*h*]anthracene	−3.37	−0.80	−7.44

tention index between columns. Owing to their non-planar properties, compounds **1** and **2** have been used in LC for the evaluation of the retention characteristics of stationary phases [35]. Decreased retention was attributed to structural difficulties with fitting the compound geometrically in the stationary phase.

Applications

As an application of the utility of these columns (the Rtx-200 column was not included), a previously separated HPLC fraction of an SRM 1597 sample containing PAHs with MW 328 was chromatographed. The injection mode and temperature programme were the same as described for the high-

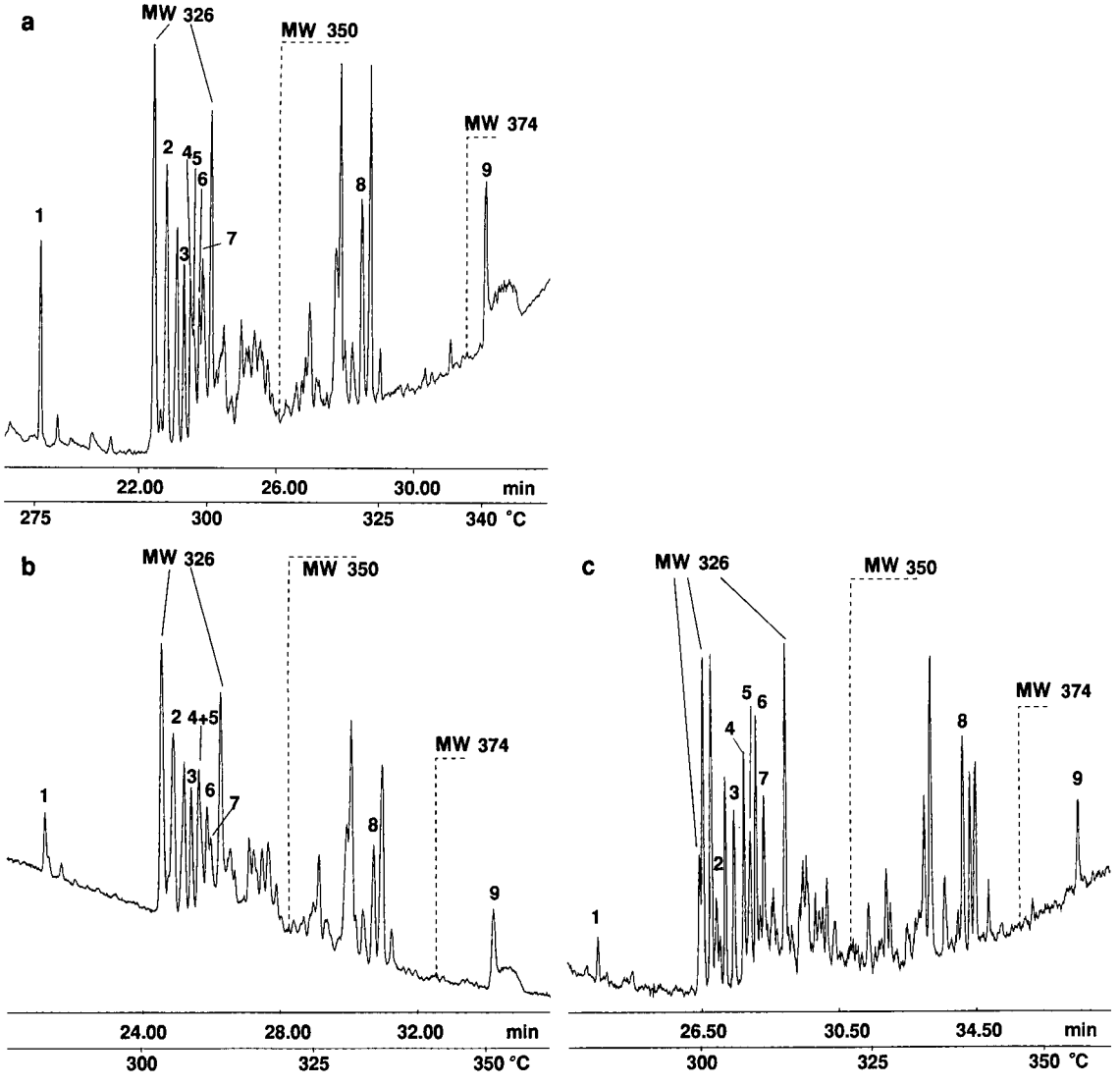

Fig. 4. Gas chromatograms (flame ionization detection) of SRM 1597 sample, previously fractionated by HPLC, injected together with the two standard series compounds on (a) the CP-Sil 8 column, (b) the XTI-5 column and (c) the silabiphenyl column. Temperature programming as in Fig. 2. Peaks: 1 = coronene; 2 = **4**; 3 = **6**; 4 = **7**; 5 = 8; 6 = **9**; 7 = benzo[*c*]picene; 8 = benzo[*a*]coronene; 9 = dinaphtho[2,1-*a*:2,1-*h*]anthrancene. The bold numbers refer to the compounds in Fig. 1.

molecular-weight PAHs under Experimental. After GC with flame ionization detection, the columns were mounted in a Finnigan MAT Incos 50 mass spectrometer and run in the electron impact mode at 70 eV with a transfer line temperature of 350°C. The molecular weights were determined by means of the molecular ions. As is demonstrated in Fig. 4, this sample contained not only PAHs with MW 328 but also at least three with MW 326 and at least nine compounds with MW 350. Traces of the ions having *m/z* 340, 352 and 354 could also be observed. The mass spectra indicated seven isomers having MW 328. Thus, in Fig. 4c, eight peaks of MW 328 were found, of which one was the standard compound benzo[*c*]picene, peak 7 in Fig. 4. By comparing peak resolution it can be seen that the silabiphenyl column has the possibility of resolving more peaks than the CP-Sil 8 and XTI-5 columns for this sample.

The retention indices were calculated and compared with those in Tables III and IV. Five possible isomers having MW 328 were suggested. These are numbered and listed in the caption of Fig. 4.

CONCLUSIONS

High-temperature GC offers the possibility of analysing a variety of PAHs with molecular weights up to at least 400. There are a number of capillary columns available that are suitable for the task, although we have shown that further developments can give columns with better compatibility/solubility and efficiency for high-molecular-weight PAHs. Use of the retention index systems presented in this paper together with mass spectral data offers a good possibility of identifying and determining PAHs in the mass range discussed. The method is a preferred alternative to ordinary HPLC owing to its higher chromatographic efficiency and to micro-LC from the viewpoint of analysis time. Further, the different retention properties for columns with different stationary phase compositions can make GC suitable for studies of compound-specific properties such as polarizability.

ACKNOWLEDGEMENTS

The authors gratefully acknowledge the donation of the Rtx-200 and XTI-5 metal capillary columns by Dr. A. Schuyler (Restek, Bellefonte, PA, USA). Dr. S. Claude (University of Neuchatel) is thanked for supporting us with the silabiphenyl stationary phase. Dr. J. Fetzer (Chevron Research, Richmond, CA, USA) and Dr. S. Wise (National Institute of Standards and Technology, Gaithersburg, MD, USA) are thanked for supplying the standard compounds. Dr. S. Wise is further thanked for the donation of the HPLC fraction of the SRM 1597 sample. Finally, thanks are due to Mrs. B. Holm for reviewing the manuscript.

REFERENCES

1 A. Björseth (Editor), *Handbook of Polycyclic Aromatic Hydrocarbons*, Marcel Dekker, New York, 1983.
2 *Polynuclear Aromatic Compounds, Part 1, Chemical, Environmental, and Experimental Data*, IARC Monogr. Eval. Carcinog. Risk Man, 32 (1983).
3 A. Winterstein and K. Schön, *Hoppe-Seyler's Z. Physiol. Chem.*, 230 (1934) 146.
4 A. Lacassagne, N. P. Buu-Hoi, F. Zadjela and G. Saint-Ruf, *C.R. Acad. Sci., Ser. D*, 266 (1968) 301.
5 K. Jinno, J. C. Fetzer and W. R. Biggs, *Chromatographia*, 21 (1986) 274.
6 J. C. Fetzer, W. R. Biggs and K. Jinno, *Chromatographia*, 21 (1986) 439.
7 P. A. Peaden, M. L. Lee, Y. Hirata and M. Novotny, *Anal. Chem.*, 52 (1980) 2268.
8 T. Romanowski, W. Funcke, J. König and E. Balfanz, *J. High. Resolut. Chromatogr. Chromatogr. Commun.*, 4 (1981) 209.
9 A. Bemgård, L. Blomberg, M. Lymann, S. Claude and R. Tabacchi, *J. High. Resolut. Chromatogr. Chromatogr. Commun.*, 10 (1987) 302.
10 A. Bemgård, L. Blomberg, M. Lymann, S. Claude and R. Tabacchi, *J. High. Resolut. Chromatogr. Chromatogr. Commun.*, 11 (1988) 881.
11 T. R. Lynn, J. W. Churchill and T. B. Lynn, *Brochure: High temperature gas chromatographic phases*, Dexsil, Hamden, CT, 1982.
12 P. Dawes and M. Cumbers, *Int. Lab.*, 19 (1989) 34.
13 R. G. Mathews, *J. Chromatogr. Sci.*, 27 (1989) 47.
14 *General Catalogue, 89–91*, Rescom, Wevelgem, Belgium.
15 S. R. Lipsky and M. L. Duffy, *J. High. Resolut. Chromatogr. Chromatogr. Commun.*, 9 (1986) 376.
16 S. R. Lipsky and M. L. Duffy, *J. High. Resolut. Chromatogr. Chromatogr. Commun.*, 9 (1986) 725.
17 J. V. Hinshaw and L. S. Ettre, *J. High. Resolut. Chromatogr.*, 12 (1989) 251.
18 Y. Takayama, T. Takeichi and S. Kawai, *J. High. Resolut. Chromatogr. Chromatogr. Commun.*, 11 (1988) 732.
19 J. Buyten, C. Duvekot, J. Peene, J. Lips and M. Mohnke, in P. Sandra and G. Redant (Editors), *Proceedings of the 11th International Symposium on Capillary Chromatography, Monterey, May 1990*, Hüthig, Heidelberg, 1990, p. 91.

20 M. Termonia, F. Munari and P. Sandra, *J. High. Resolut. Chromatogr. Chromatogr. Commun.*, 10 (1987) 263.
21 A. Schuyler and J. W. Stauffer, in press.
22 E. R. Rohwer and V. Pretorius *J. High. Resolut. Chromatogr. Chromatogr. Commun.*, 10 (1987) 145.
23 W. Blum and L. Damasceno, *J. High. Resolut. Chromatogr. Chromatogr. Commun.*, 10 (1987) 472.
24 W. Blum, W. J. Richter and G. Eglinton, *J. High. Resolut. Chromatogr. Chromatogr. Commun.*, 11 (1988) 148.
25 W. Blum and G. Eglinton, *J. High. Resolut. Chromatogr.*, 12 (1989) 290.
26 Y. Hirata, M. Novotny, P. E. Peaden and M. L. Lee, *Anal. Chim. Acta*, 127 (1981) 55.
27 A. Hirose, D. Wiesler and M. Novotny, *Chromatographia*, 18 (1984) 239.
28 A. L. Colmsjö and C. E. Östman, *Anal. Chim. Acta*, 208 (1988) 183.
29 K. Grob, *Chromatographia*, 7 (1974) 94.
30 W. J. Simonsick, Jr. and R. A. Hites, *Anal. Chem.*, 58 (1986) 2114.
31 M. L. Lee, D. L. Vassilaros, C. M. White and M. Novotny, *Anal. Chem.*, 51 (1979) 768.
32 *Certificate of Analysis, Standard Reference Material 1597, Complex Mixture of Polycyclic Aromatic Hydrocarbons from Coal Tar*, National Bureau of Standards, Gaithersburg, MD, 1987.
33 E. Sz. Kováts, *Helv. Chim. Acta*, 41 (1958) 1915.
34 M. V. Budahegyi, E. R. Lombosi, T. S. Lombosi, S. Y. Mészáros, Sz. Nyriredy, G. Tarján, I. Timár and J. M. Takács, *J. Chromatogr.*, 271 (1983) 213.
35 L. C. Sander and S. A. Wise, *Adv. Chromatogr.*, 25 (1986) 139.

Journal of Chromatography, 595 (1992) 259–267
Elsevier Science Publishers B.V., Amsterdam

CHROM. 23 925

Determination of α- and β-zearalenol and zearalenone in cereals by gas chromatography with ion-trap detection

K. Schwadorf and H.-M. Müller*

Institute of Animal Nutrition, University of Hohenheim, Emil-Wolff-Strasse 10, W-7000 Stuttgart 70 (Germany)

(Received September 5th, 1991)

ABSTRACT

A method for determination of the estrogenic mycotoxins, α- and β-zearalenol and zearalenone, in cereals (wheat, barley, oats, corn) is described. After extraction with ethylacetate, clean-up involved a base treatment and partition with water; derivatization was by trimethylsilylation. For quantitation and confirmation a capillary gas chromatograph combined with a selective mass detector (ion trap), working in the electron impact-mode was used. The detection limit for the complete method is 1 μg/kg for each of the three mycotoxins in full scan. Recoveries from spiked cereals were 82–86%.

INTRODUCTION

trans-Zearalenone (ZON) [6-(10)-hydroxy-6-oxo-trans-1-undecenyl)-β-resorcylic acid lactone] is a secondary metabolite synthesized by several species of the fungal genus *Fusarium* [1]. It possesses strong estrogenic activity and has been implicated as a causative factor in hyperestrogenism, infertility and other health problems in livestock (swine, cattle, poultry) [1,2]. Numerous reports have demonstrated its worldwide occurrence in cereals and other agricultural commodities [1,3–5].

A variety of other estrogenic substances have been found along with ZON in pure cultures of *Fusarium* isolates on cereals [2,6]. *trans*-α-Zearalenol (α-ZOL) and *trans*-β-zearalenol (β-ZOL) are two of these metabolites which may occur as a diastereomeric mixture [1,6–12]. Experiments with labelled α- and β-ZOL and ZON have suggested that zearalenol is a precursor in the biosynthetic pathway leading to ZON [13]. The presence of α- and β-ZOL in feedstuffs might be of more importance than currently realized. α-ZOL is 3–4 times more estrogenic than ZON, and β-ZOL has the same or slightly less activity as ZON [8]. Both substances therefore could contribute to the total estrogenic activity of *Fusarium*-infested cereal grains, and their presence could explain why feedstuffs without detectable ZON content can be associated with hyperestrogenism in animals. This has been observed repeatedly in our laboratory.

So far the presence of zearalenols in feedstuffs has been investigated to a limited extent. α-ZOL has been detected along with ZON in three cereal samples [14], α- and β-ZOL have been extracted along with ZON from some *Fusarium*-infected stems of corn [9,10], and zearalenol (not specified whether α- or β-ZOL) has been found in one out of 248 German grain samples [15]. This scarce information creates an urgent need to determine the two zearalenols in addition to ZON in a large number of grain samples from several harvest years.

Methods used for the determination of zearalenols and ZON in cereals and animal feed include thin-layer chromatography (TLC) [9,11,12,15,16], high-performance liquid chromatography (HPLC) [8,9,17–19], gas–liquid chromatography (GC), [8,11] and/or GC-mass spectroscopy (MS) [6,8,9,20,21]. Confirmation of ZON in cereals and other commodities by GC–MS has been described in numerous other studies [1,3,4,22–24]. GC–MS has also been used for the confirmation of the two

0021-9673/92/$05.00

zearalenols and of ZON in animal tissues, biological fluids, excreta and pig and cow milk [25–29]. The advantage of GC–MS lies in the precise identification of even minute quantities without the risk of interference by substances that have identical R_f values (TLC) or retention times (HPLC, GC).

The use of large mass spectrometers in GC–MS, particularly in routine monitoring of a large number of samples, is limited by expense and problems in handling and personnel training. Instruments of the new generation of mass-selective detectors, such as the ion-trap detector which can be used as common GC detectors are easier to handle and less expensive than larger mass spectrometers. In the present study we describe the quantification and confirmation of α- and β-ZOL and ZON in cereals by GC with ion-trap detection (ITD).

EXPERIMENTAL

Chemicals and reagents

ZON, α- and β-ZOL were from Makor Chemicals (Jerusalem, Israel). N,O-Bis(trimethylsilyl)trifluoroacetamide (BSTFA) (derivatization reagent) was from Pierce (Oud-Beijerland, Netherlands). All other chemicals and solvents were of reagent grade and obtained from Merck (Darmstadt, Germany).

Cereal samples

All cereal samples (wheat, barley, oats, corn) were obtained either from farms in different districts of Baden-Württemberg (Germany) or from a feed factory, and exhibited various mycological qualities.

Extraction

A base clean-up procedure described in the literature [30] was modified. A 30-g sample of finely ground food was extracted with 200 ml of ethylacetate in a 500-ml screw-cap bottle for 2 h on a rotary shaker. The extract was filtered through two folded filters and evaporated nearly to dryness on a rotary evaporator (water bath 40°C). The residue was dissolved in 20 ml of chloroform and quantitatively transferred to a 100-ml separatory funnel (rinse flask with another 5–10 ml of chloroform followed by a brief sonication). A 10-ml aliquot of saturated sodium chloride solution was added to the separatory funnel. The chloroform solution was extracted twice with 10 ml of 1–2 *M* sodium hydroxide. Both alkali extracts were collected and the chloroform layer was discarded. The alkali phase was purified twice with 5 ml of chloroform; the chloroform layers were discarded. The pH of the alkaline phase was adjusted to 9.4–9.5 (pH meter) by 2 *M* phosphoric acid. Then the solution was extracted three times each with 15 ml of chloroform. The chloroform phases were filtered over anhydrous sodium sulphate into a round-bottomed flask (rinse with additional chloroform). The combined chloroform extracts were evaporated to dryness (up to 40°C bath temperature). Extracts which cannot be derivatized and analysed immediately should be stored in a freezer.

Derivatization

Derivatization was achieved by trimethylsilylation with BSTFA. The complete residue of the extraction was transferred quantitatively to a 1-ml autosampler vial. To the dry residue 100 μl of BSTFA reagent were added. After closing the vial with a crimping cap, the mixture was held at 60°C for 15 min. Thereafter the sample was cooled. In the splitless mode 1–4 μl and in the on-column mode 1 μl were injected into the gas chromatograph.

Apparatus

A Carlo Erba HRGC 5160 Mega Series gas chromatograph (Carlo Erba, Hofheim, Germany) equipped with the fused-silica column Permabond SE-54-DF-0.25 (25 m × 0.25 mm I.D., film thickness 0.28 μm; article no. 723056; Macherey-Nagel, Düren, Germany) was used. The carrier gas was helium (80–90 kPa). Splitless (valve 45 s closed) and on-column (autosampler; secondary cooling 45 s) modes of injection were used. The temperature of the splitless injection port was 260°C; the column temperature programme, following an initial period of 180°C for 2 min, was 4.5°C/min to 270°C, hold for 15 min, 15°C/min to 285°C and hold for 10 min. As a mass spectrometry data system, a Finnigan MAT ITD 800 ion-trap detector (Finnigan MAT, Bremen, Germany) was interfaced to the gas chromatograph. The detector was applied in the electron impact (EI) mode, being equivalent to an electron energy of 70 eV. The temperature of the transfer line was adjusted to 285°C. Only full-scan data were monitored; the selected scan range was 300/400 to 540 a.m.u.

Recovery experiments

Known amounts of ZON, α- and β-ZOL (in methanolic solution) were added to a screw-cap bottle containing 30 g of finely blended cereal samples without detectable amounts of α- and β-ZOL and ZON. After 30 min of vigorous shaking on a rotary shaker the sample was stored for 2 days in a refrigerator and then extracted.

RESULTS AND DISCUSSION

We describe for the first time the quantitation and confirmation of α- and β-ZOL and ZON in cereals by the combination of capillary GC with ITD in the EI mode.

Extracts obtained by the method of Tanaka *et al.* [31] were not pure enough for GC–MS according to our experience, even after application of Sep-Pak silica cartridges (Part No. 51900, Waters Assoc., Milford, MA, USA). This clean-up step also leads to some loss of ZON, α- and β-ZOL. For GC–MS we therefore used the base clean-up procedure described by Mirocha *et al.* [30]. This takes advantage of the solubility of ZON, α and β-ZOL in diluted alkali.

Derivatization was achieved by treating extracts with BSTFA to obtain the corresponding trimethylsilyl ethers (TMS) of ZON (di-TMS-ZON), α-ZOL (tri-TMS-α-ZOL) and β-ZOL (tri-TMS-β-ZOL). These TMS derivatives are stable in the refrigerator for several weeks.

By using other derivatization reagents, such as trifluoroacetic acid anhydride (TFAA), or by operating the ion-trap detector in the chemical ionization (CI) mode, no significant improvement, *e.g.* no intensity gain of the molecular peak, was obtained.

A total ion chromatogram for a standard solution of the three mycotoxins is given in Fig. 1. The specific mass spectra can be seen in Fig. 2, and the GC–MS characteristics are shown in Table I. As has been shown for the TMS ether of ZON, the ratio of intensities in the higher mass region is very consistent and can be used as a diagnostic characteristic [30]. According to our experience this is true also for α- and β-ZOL (Table I). For diagnostic purpose the ions at *m/z* 536 [M^+], 446, 429, 333, 307 (α- and β-ZOL) and *m/z* 462 [M^+], 444, 429, 333, 307 (ZON) can be monitored. There is no significant difference between the mass spectra of both TMS derivatives isomers. The relative intensity of the molecular ion (536) for the β isomer appears to be higher than that for the α isomer (Fig. 2).

The recoveries of the complete method are between 82 and 86% (Table II). The limit of detection of the complete method (ion trap operated in the EI mode, full scan 400–540 a.m.u., signal-to-noise

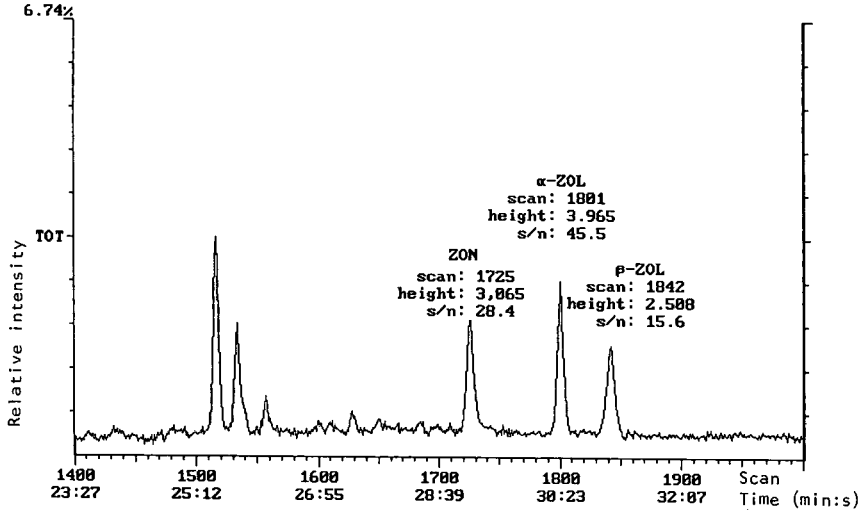

Fig. 1. Total ion chromatograms for α- and β-ZOL and ZON (standard, 2.5 ng each, trimethylsilyl derivatives, EI mode). s/n = signal-to-noise ratio.

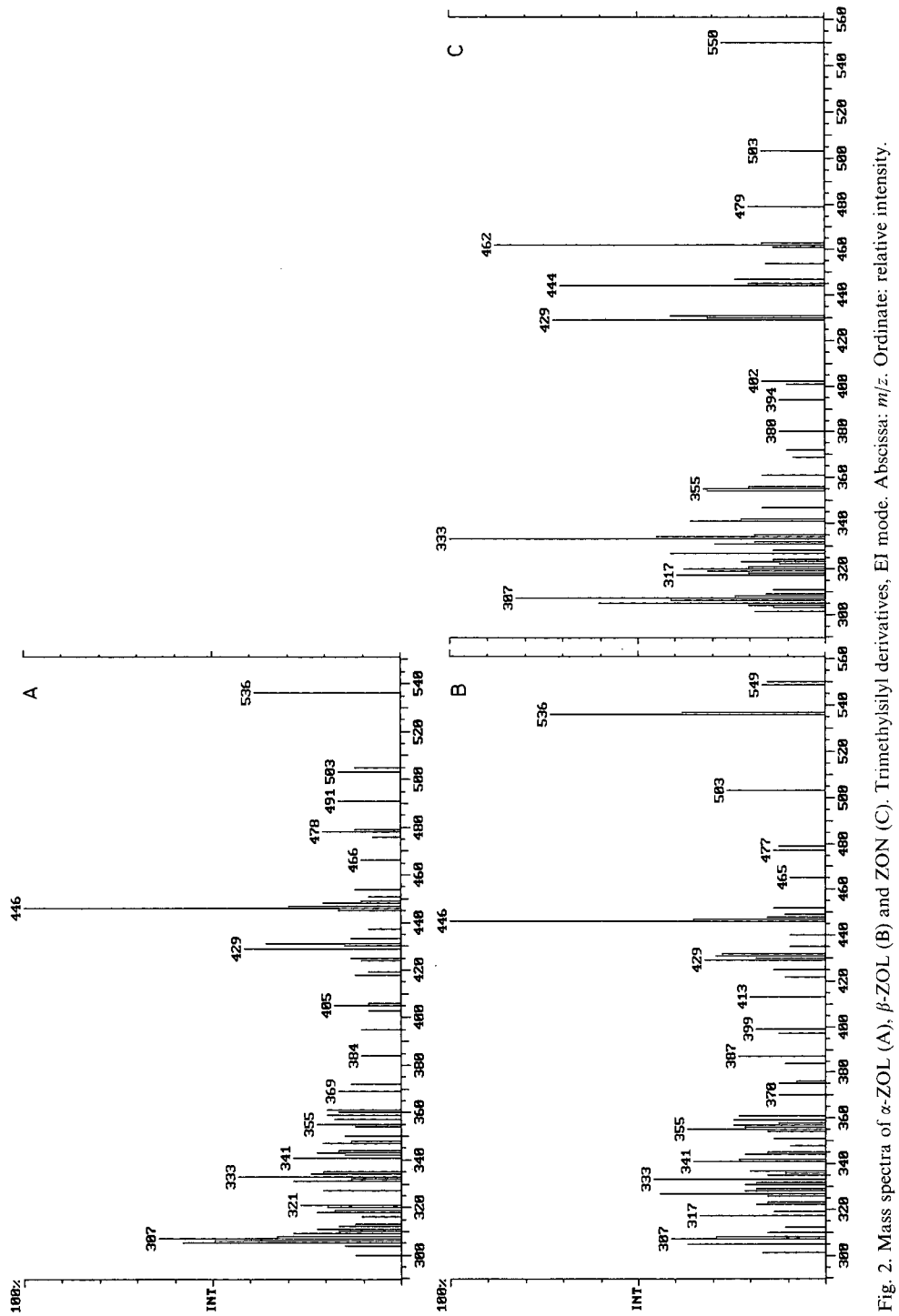

Fig. 2. Mass spectra of α-ZOL (A), β-ZOL (B) and ZON (C). Trimethylsilyl derivatives, EI mode. Abscissa: *m/z*. Ordinate: relative intensity.

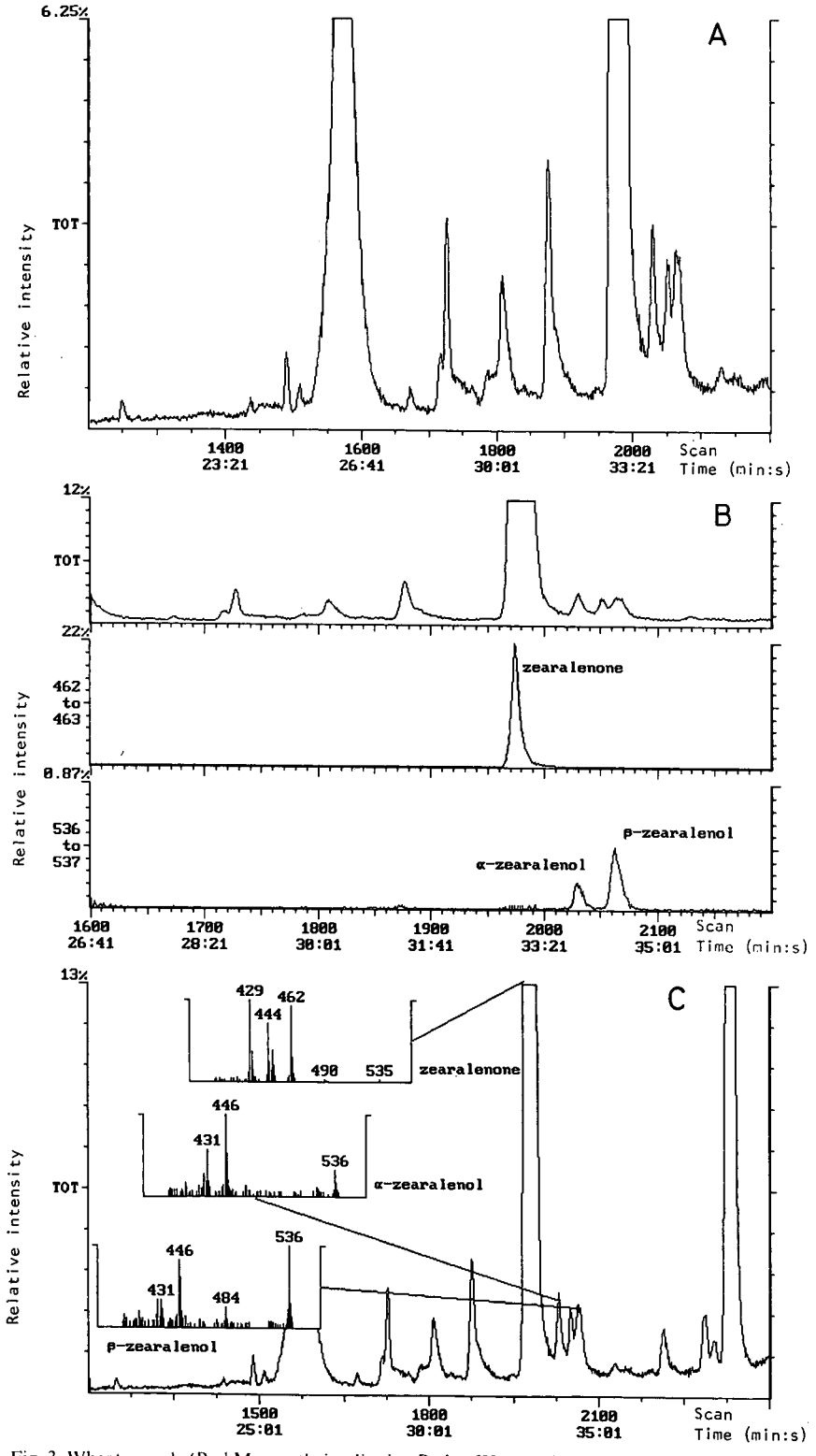

Fig. 3. Wheat sample (Bad Mergentheim district, Baden-Württemberg, 1987 harvest) containing 71 μg/kg α-ZOL, 12 μg/kg β-ZOL and 8036 μg/kg ZON. Total ion chromatogram (A), mass chromatograms of α- and β-ZOL and ZON (B), zoomed total ion chromatogram and mass spectra at retention time of α- and β-ZOL and ZON (C).

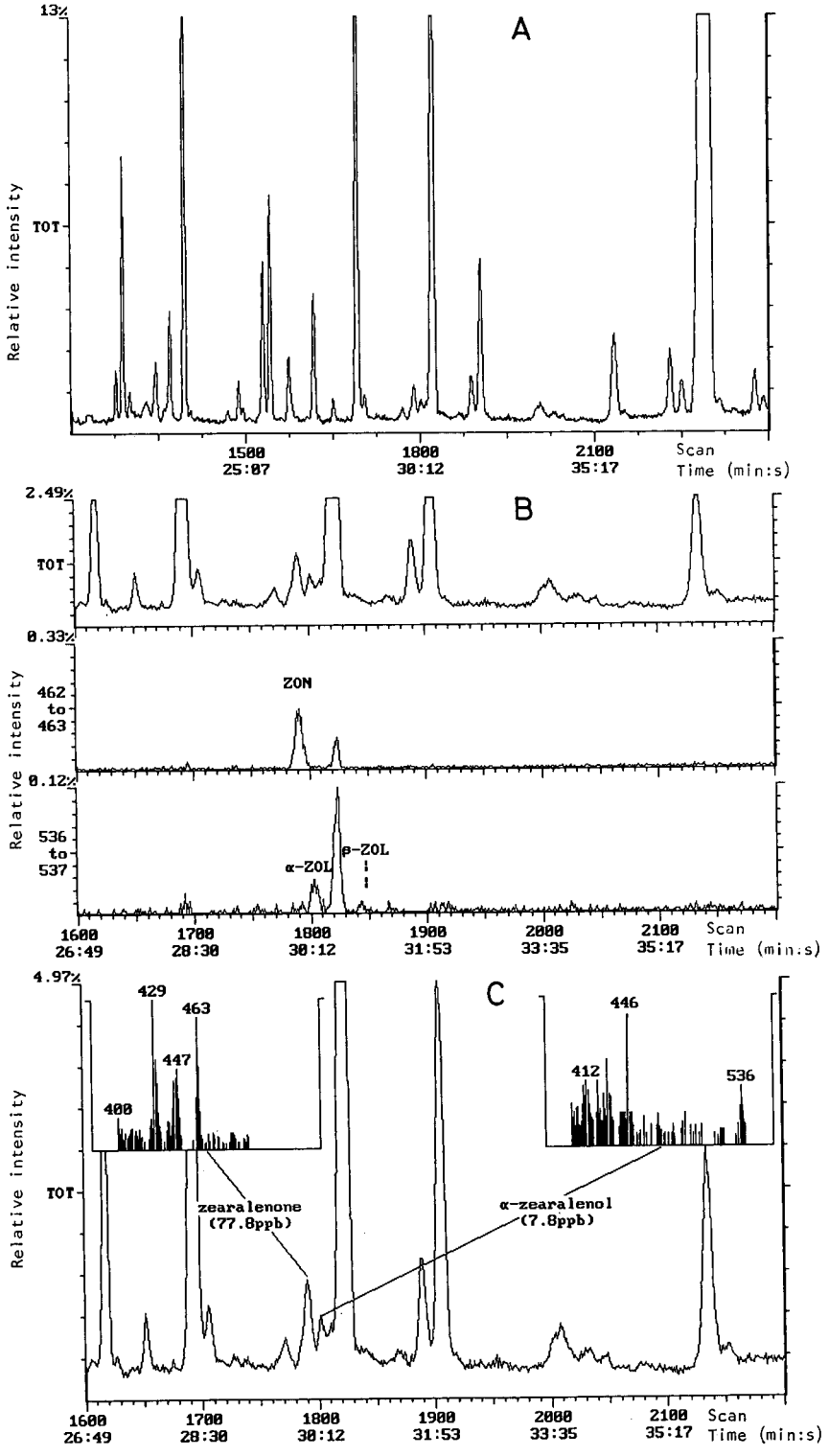

Fig. 4. Wheat sample (Göppingen district, Baden-Württemberg, 1987 harvest) containing 8 μg/kg α-ZOL and 78 μg/kg ZON, β-ZOL not detectable. Total ion chromatogram (A), mass chromatograms of ZON and α-ZOL (B), zoomed total ion chromatogram and mass spectra at retention time of α-ZOL and ZON (C). In ppb, the American billion (10^9) is meant.

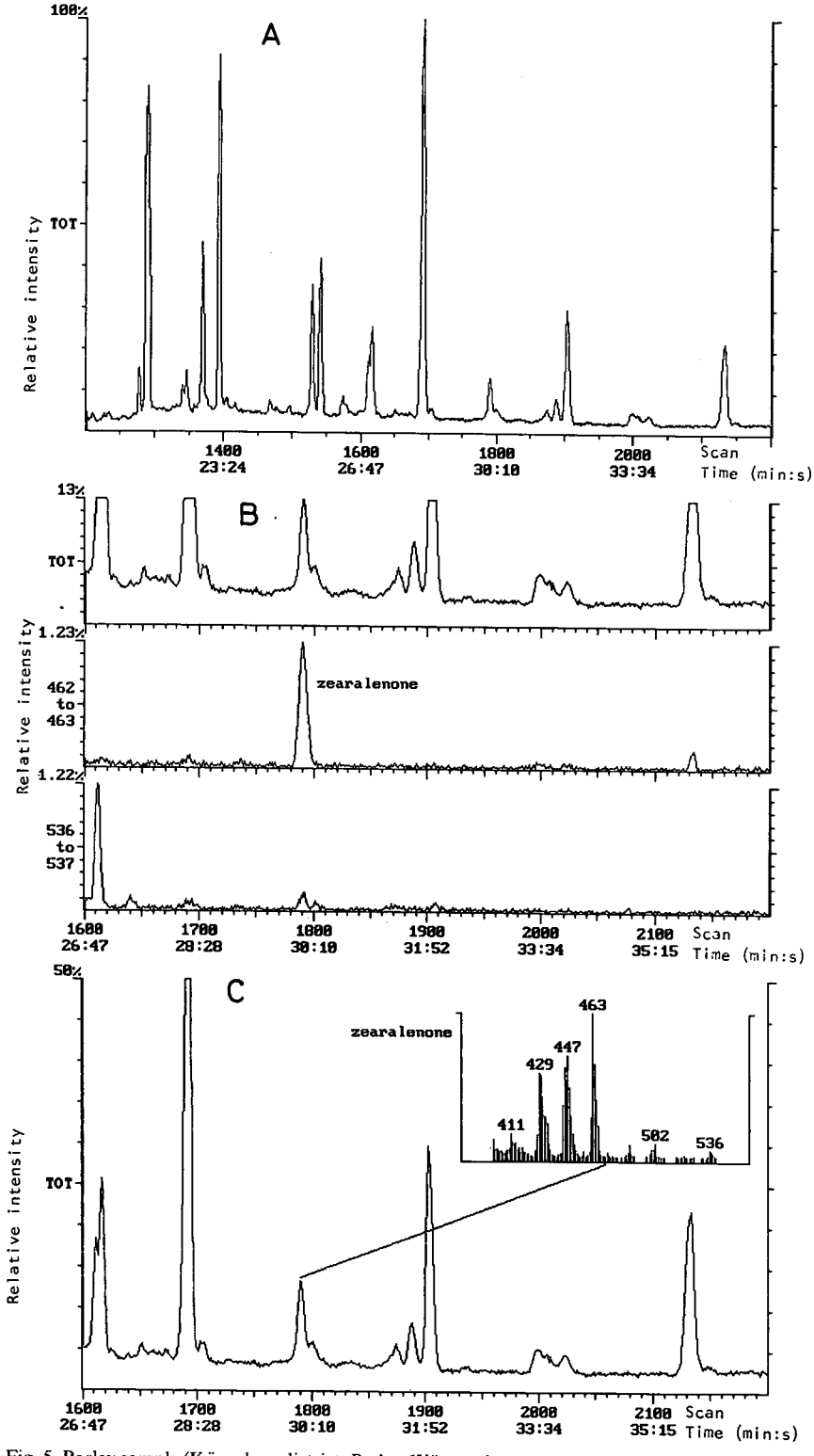

Fig. 5. Barley sample (Künzelsau district, Baden-Württemberg, 1987 harvest) containing 310 μg/kg ZON, α and β-ZOL not detectable). Total ion chromatogram (A), mass chromatogram of ZON (B), zoomed total ion chromatogram and mass spectrum at retention time of ZON (C).

TABLE I

GC–MS OF α- AND β-ZOL AND ZON (AS TRIMETHYLSILYL DERIVATIVES, BSTFA DERIVATIZATION, EI MODE)

[M^+]: molecular ion

Toxin	Retention time[a] (min)	Mass fragments (a.m.u.)	Ratio of intensities	Quantitation mass window (a.m.u.)
α-ZOL	About 31	536 [M^+] 446 429 (333/307)	1 2 1	536–537
β-ZOL	About 32	536 [M^+] 446 429 (333/307)	2 2 1	536–537
ZON	About 30	426 [M^+] 444 429 (333/307)	1 1 1	461–463

[a] Depending on the pressure of carrier gas helium.

ratio 3:1) is 0.5 ng per injection, *i.e.* about 1 μg/kg for α- and β-ZOL and ZON.

Using the described method cereal samples from farms were investigated. The identities of α- and β-ZOL and ZON were determined by comparing the retention times, mass spectra, and ratio of intensities of various mass fragments and ions with those of standards. In a wheat sample both α- and β-ZOL were detected along with ZON (Fig. 3); in another wheat sample α-ZOL and ZON were determined (Fig. 4). The simultaneous occurrence of all three mycotoxins as well as the occurrence of only α-ZOL together with ZON has been reported in literature [6,8,9,14].

By the method described α- and β-ZOL can be quantified and identified together with low and high concentrations of ZON (Figs. 3 and 4). The absence of α- and β-ZOL (detection limit: 1 μg/kg) has been demonstrated in a barley sample containing 310 μg/kg ZON (Fig. 5). There was no interference by other ingredients of wheat and bearley.

TABLE II

RECOVERY OF α- AND β-ZOL AND ZON FROM CEREALS (WHEAT, BARLEY, OATS, CORN)

Samples spiked with 100, 300 and 500 ng of each toxin.

Toxin	Recovery (%)
α-ZOL	82.9 ± 1.2
β-ZOL	86.1 ± 1.3
ZON	85.2 ± 1.5

REFERENCES

1 T. Kuiper-Goodman, P. M. Scott and H. Watanabe, *Regulat. Toxicol. Pharmacol.*, 7 (1987) 253.
2 C. J. Mirocha and C. M. Christensen, in I. F. H. Purchase (Editor), *Mycotoxins* , Elsevier, Amsterdam, Oxford, New York, 1974, p. 129.
3 T. Tanaka, A. Hasegawa, S. Yamamoto, U.-S. Lee, Y. Sugiura and Y. Ueno, *J. Agric. Food Chem.*, 36 (1988) 979.
4 T. Tanaka, S. Yamamoto, A. Hasegawa, N. Aoki, J. R. Besling, Y. Sugiura and Y. Ueno, *Mycopathologia*, 110 (1990) 19.
5 E. W. Sydenham, P. G. Thiel, W. F. O. Marasas, G. S. Shepard, D. J. Van Schalkwyk and K. R. Koch, *J. Agric. Food Chem.*, 38 (1990) 1900.
6 K. E. Richardson, W. M. Hagler, Jr. and C. J. Mirocha, *Agric. Food Chem.*, 33 (1985) 862.
7 D. Stipanovic and H. W. Schroeder, *Mycopathologia*, 57 (1975) 77.
8 W. M. Hagler, C. J. Mirocha, S. V. Pathre and J. C. Behrens, *Appl. Environ. Microbiol.*, 37 (1979) 849.
9 A. Bottalico, A. Visconti, A. Logrieco, M. Solfrizzo and C. J. Mirocha, *Appl. Environ. Micobiol.*, 49 (1985) 547.
10 A. Bottalico, A. Logrieco and A. Visconti, *Mycopathologia*, 107 (1989) 85.

11 K. E. Richardson, W. M. Hagler, Jr. and P. B. Hamilton, *Appl. Environ. Microbiol.*, 47 (1984) 643.
12 A. Badawey, J. Sawinsky and A. Halász, *Acta Aliment.*, 16 (1987) 45.
13 K. E. Richardson, W. M. Hagler, Jr. and P. B. Hamilton, *Appl. Environ. Microbiol.*, 47 (1984) 1206.
14 C. J. Mirocha, B. Schauerhamer, C. M. Christensen, M. L. Niku-Paavola and M. Nummi, *Appl. Environ. Microbiol.*, 38 (1979) 749.
15 A. Thalmann, S. Matzenauer and S. Gruber-Schley, *Ber. Landwirtsch.*, 63 (1985) 257.
16 S. P. Swanson, R. A. Corley, D. G. White and W. B. Buck, *J. Assoc. Off. Anal. Chem.*, 67 (1984) 580.
17 H. L. Trenholm, R. M. Warner and D. W. Fitzpatrick, *J. Assoc. Off. Anal. Chem.*, 67 (1984) 968.
18 G. A. Bennett, O. L. Shotwell and W. F. Kwolek, *J. Assoc. Off. Anal. Chem.*, 68 (1985) 958.
19 R. W. Bagneris, J. A. Gaul and G. M. Ware, *J. Assoc. Off. Anal. Chem.*, 69 (1986) 894.
20 R. F. Vesonder and W. K. Rohwedder, in R. J. Cole (Editor), *Modern Methods in the Analysis and Structural Elucidation of Mycotoxins*, Academic Press, New York, 1986, p. 335.
21 P. F. Ross, in J. L. Richard and J. R. Thurston (Editors), *Diagnosis of Mycotoxicoses*, Martinus Nijhoff, Dordrecht, Boston, Lancaster, 1986, p. 323.
22 W. M. Hagler, Jr., K. Tyczkowska and P. B. Hamilton, *Appl. Environ. Microbiol.*, 47 (1984) 151.
23 W. M. Hagler, Jr., D. T. Bowman, M. Babadoost, C. A. Haney and S. P. Swanson, *Crop Sci.*, 27 (1987) 1273.
24 H. M. Hussein, R. A. Franich, M. Baxter and I. G. Andrew, *Food Add. Contam.*, 6 (1989) 49.
25 C. J. Mirocha, S. V. Pathre and T. S. Robison, *Food Cosmet. Toxicol.*, 19 (1981) 25.
26 J. E. Roybal, R. K. Munns, W. J. Morris, J. A. Hurlbut and W. Shimoda, *J. Assoc. Off. Anal. Chem.*, 71 (1988) 263.
27 M. Palyusik, B. Harrach, C. J. Mirocha and S. V. Pathre, *Acta Vet. Acad. Scient. Hungar.*, 28 (1980) 217.
28 M. Olsen, C. J. Mirocha, H. K. Abbas and B. Johansson, *Poultry Sci.*, 65 (1986) 1905.
29 M. Olsen, H. Petterson, K. Sandholm, A. Visconti, and K.-H. Kiessling, *Food Chem. Toxic.*, 25 (1987) 681.
30 C. J. Mirocha, B. Schauerhamer and S. V. Pathre, *J. Assoc. Off. Anal. Chem.*, 57 (1974) 1104.
31 T. Tanaka, A. Hasegawa, Y. Matsuki, U.-S. Lee and Y. Ueno, *J. Chromatogr.*, 328 (1985) 271.

Journal of Chromatography, 595 (1992) 269–281
Elsevier Science Publishers B.V., Amsterdam

CHROM. 23 872

Analytical methods for monoterpene glycosides in grape and wine

II. Qualitative and quantitative determination of monoterpene glycosides in grape☆

Stéphane G. Voirin☆☆, Raymond L. Baumes*, Jean-Claude Sapis and Claude L. Bayonove

INRA, Institut des Produits de la Vigne, Laboratoire des Arômes et des Substances Naturelles, 2 Place Viala, 34060, Montpellier Cédex 01 (France)

(First received July 29th, 1991; revised manuscript received November 5th, 1991)

ABSTRACT

Free and glycosidically bound terpenes of five *Vitis vinifera* grape cultivars (muscat of Alexandria, muscat of Frontignan, muscat of Hamburg, muscat Ottonel and Gewürztraminer) were investigated. The free and bound fractions were separated by selective retention on Amberlite XAD-2 resin. The glycosidic fractions were analysed by gas chromatography and gas chromatography–mass spectrometry using either enzymic hydrolysis and subsequent analysis of the released aglycones or trimethylsilyl (TMS) and trifluoroacetyl derivatives. The known monoterpenyl, benzyl and 2-phenylethyl β-D-glucopyranosides, β-rutinosides, 6-O-α-L-arabinofuranosyl-β-D-glucopyranosides and 6-O-β-D-apiofuranosyl-β-D-glucopyranosides were determined. A number of other glycosides were detected and the structures of some of them, mainly apiosylglucosides and glucosides with aglycones in higher oxidation state than linalol, were tentatively identified using the mass spectra of their TMS and TFA derivatives and the results obtained from the analysis of their aglycones.

INTRODUCTION

The composition of glycosidically bound volatiles from *Vitis vinifera* grape has been extensively studied. These bound forms consist of β-D-glucopyranosides and, mostly, of 6-O-α-L-arabinofuranosyl-β-D-glycopyranosides, 6-O-α-L-rhamnopyranosyl-β-D-glucopyranosides (rutinosides) [1,2] and 6-O-β-D-apiofuranosyl-β-D-glucopyranosides [3] with monoterpenyl, benzyl and 2-phenylethyl aglycones. Other aglycones have also been identified as monoterpenoids with various oxidation states, carotenoid-related and shikimate-related compounds [4–7]. As many of these aglycones have interesting sensory properties, their flavourless glycosides make up a potential aroma reserve more abundant than the free one [8–10].

Using a procedure involving enzymic hydrolysis, Günata *et al.* [11] showed that grape glycosides are far more abundant in aromatic varieties (muscats and aromatic varieties from the Alsace region) than in non-aromatic varieties. However, as these glycosides have proved difficult to analyse directly [8], no quantitative data have been reported concerning these glycosides individually. The development of a

☆ Part of the Doctoral Thesis of S. Voirin presented to the University of Montpellier.

☆☆ Present address: DOMRECQ, B.P. 47, Aubigny, 80800 Corbie, France.

0021-9673/92/$05.00

method permitting the direct analysis of these glycosides [12] allowed the further investigation of the qualitative and quantitative composition of some *Vitis vinifera* grape cultivars. The results obtained for four muscat cultivars (Alexandria, Frontignan, Hamburg and Ottonel) and Gewürztraminer are reported in this paper.

EXPERIMENTAL

Reagents and reference samples

Analytical-reagent grade solvents (pentane from Labosi and dichloromethane, ethyl acetate and pyridine from Merck) were further purified by redistillation before use. Pektolase 3PA was purchased from Grinsted. All other chemicals were obtained as described in Part I [12].

Plant material

Mature, sound grapes (cultivars Muscat of Frontignan, Muscat of Alexandria, Muscat Ottonel, Muscat of Hamburg and Gewürztraminer) were collected in 1988 at the vineyard of the vine experimental station in Montpellier, France. The grapes were frozen in liquid nitrogen and kept at −18°C until extracted.

Fractionation of free and bound compounds

The clear juice from the grapes was obtained according to the method of Günata *et al.* [11] using 4-nonanol and phenyl β-D-glucopyranoside as internal standards for the free and the bound fractions; 0.28 and 2.5 mg, respectively, were added to 1 kg of berries just before crushing. The juice (50 ml) was fractionated on XAD-2 resin as described in Part I [12]; free compounds were eluted with 50 ml of pentane–dichloromethane (2:1) and glycosides with 50 ml ethyl acetate. The free extract was dried over sodium sulphate and concentrated to a final volume of about 500 μl for gas chromatographic (GC) analysis. The bound extract was concentrated to 1 ml under vacuum at 40°C, then to dryness at 60°C under nitrogen.

GC analysis of the free fractions

The free extracts obtained from 50 ml of grape juice were analysed by GC on a CP-Wax 52 CB fused-silica capillary column (Chrompack) (25 m × 0.32 mm I.D.; 1.2 μm bonded phase) as described in Part I [12].

Enzymic hydrolysis of the bound fractions and GC analysis of the aglycones released

Each enzymic hydrolysis was performed on a glycoside sample obtained from 50 ml of grape juice. The sample was dissolved in 100 μl of 0.2 *M* citrate–phosphate buffer (pH 5.0) and washed four times using 100 μl of pentane–dichloromethane (2:1), 100 μl of Pektolase 3PA solution were added [1.2 mg of Pektolase 3PA in 100 μl of 0.2 *M* citrate–phosphate buffer (pH 5.0)], then the mixure was incubated at 40°C for 12 h. After cooling to room temperature, 28 μg of 4-nonanol were added as internal standard and the mixture was extracted four times with 200 μl of pentane–dichloromethane (2:1). This aglycone extract was concentrated to a final volume of about 50 μl by rectification (Dufton column) at 35°C, then analysed by GC as above for the free fractions.

GC analysis of trimethylsilyl (TMS)-derivatives of the bound fractions

To a glycoside sample obtained from 10 or 15 ml of grape juice were added 20 μl of anhydrous pyridine and 20 μl of trimethylsilylating reagent [N,O-bis(trimethylsilyl)trifluoroacetamide–chlorotrimethylsilane (99:1)]. The mixture was stirred (vortex mixed), heated for 20 min at 60°C and then cooled to room temperature. Injections of about 0.8 μl of these derivatives on to an OV-1 fused-silica capillary column (Delsi Instruments) (50 m × 0.32 mm I.D.; 0.2 μm bonded phase) were made on-column. The equipment consisted of a Varian Model 3300 gas chromatograph fitted with an on-column injector and a flame ionization detector. The injector temperature was programmed at 60°C min^{-1} from 90 to 150°C and then at 10°C min^{-1} to 300°C. The column temperature was programmed at 3°C min^{-1} from 125 to 300°C with hydrogen as carrier gas at 2 ml min^{-1}. The detector temperature was 320°C.

GC analysis of trifluoroacetyl (TFA) derivatives of the bound fractions

A glycoside sample obtained from 15 ml of grape juice as described above was treated as above by using 20 ml of anhydrous pyridine and 20 μl of N-methylbis(trifluoroacetamide) instead of the above trimethylsilylating reagent. Injections of about 0.8 μl of these derivatives on to a CP-Sil 8 CB fused-silica capillary column (Chrompack) (25 m × 0.32

mm I.D.; 1.2 μm bonded phase) were made on-column. The equipment used was the same as above. The injector temperature was programmed at 60°C min^{-1} from 90 to 150°C and then at 10°C min^{-1} to 300°C. The column temperature was programmed at 3°C min^{-1} from 125 to 300°C with hydrogen as carrier gas at 1.3 ml min^{-1}. The detector temperature was 300°C.

Direct GC–MS analysis of the bound fractions

Glycoside samples obtained from 10 or 15 ml of grape juice were subjected to TMS or TFA derivatization, respectively, as reported above, then analysed by gas chromatography–mass spectrometry (GC–MS).

Electron impact mass spectrometry (EI-MS) was applied to the TMS and the TFA derivatives by coupling a Girdel 31 gas chromatograph equipped with the same fused-silica capillary colums as described above to a Nermag R 10-10 mass spectrometer. The transfer line was a platinum capillary tube heated at 260°C. The source temperature was 200°C. Mass spectra were scanned at 70 eV in the range *m/z* 60–1050 at 2.87-s intervals.

For GC, 2-μl volumes of glycoside derivatives were injected with a splitting ratio of 10:1 into an injector held at 320°C. The helium carrier gas head pressure was 90 kPa for TMS derivatives and 10 kPa for TFA derivatives. For TMS derivatives the column was programmed at 3°C min^{-1} from 130 to 300°C and for TFA derivatives at 4°C min^{-1} from 120 to 280°C.

Chemical ionization mass spectrometry (CI-MS) was applied using the same GC and transfer line conditions as for EI-MS. The source temperature was 90°C and ammonia was used as the reactant gas. Mass spectra were scanned at 70 eV in the range *m/z* 60–1050 at 2.87-s intervals.

GC–ion trap detection (ITD) of the free fractions and of the aglycones released from the bound fractions

Electron impact mass spectra were recorded for the free fractions and the aglycones enzymatically hydrolysed from the glycosides by coupling the CP-Wax 52 CB fused-silica capillary column (see conditions above) to a Finnigan MAT ITD 700. The transfer line, heated at 240°C, consisted of an open-split GC–ITD interface at atmospheric pressure and a flow restrictor which was a DB-5 fused-silica capillary column (1.2 m × 0.32 mm I.D.; bonded phase). The source temperature was 220°C. Mass spectra were scanned between 50 and 80 eV in the range *m/z* 31–250 at 2-s intervals.

RESULTS AND DISCUSSION

The technique used in this study involved XAD-2 resin extraction of the grape glycosides, TFA and TMS derivatization followed by GC and GC–MS analysis [12]. Moreover, the aglycones released after enzymic hydrolysis of the five natural glycosidic extracts were analysed by GC and GC–MS in order to obtain further information [11]. Pektolase 3PA, which possessed the glycosidase activity necessary to hydrolyse the four classes of grape glycosides [13,14], was used.

Qualitative analysis

The gas chromatograms of the TMS and TFA derivatives of the grape glycosides studied showed many peaks, most of them arising at retention times higher than that of phenyl β-D-glucopyranoside, as shown for muscat of Alexandria in Figs. 1 and 2. Comparisons with the TFA and TMS derivatives of the synthetic compounds described in Part I [12] and of geranyl 6-O-β-D-apiofuranosyl-β-D-glucopyranoside [3] permitted a positive identification of the corresponding natural glycosides and a tentative identification of the 6-O-β-D-apiofuranosyl-β-D-glucopyranosides with the same aglycones [3] (Table I). However, no glycoside of citronellol was detected in the natural extracts, reinforcing the hypothesis reported by Wilson *et al.* [15] on its enzymic production. Likewise, no 2,6-dimethyl-3-hydroxy-1,7-octadien-6-yl-β-D-glycopyranoside could be positively identified, suggesting that the natural compound might be 3-glycosylated or diglycosylated.

Concerning the absolute configuration of the linalyl glycosides, it was interesting that in the chromatograms of the TFA derivatives of the grape glycoside extracts, only one isomer was found for each glycoside. The synthetic diastereoisomeric (*R*) and (*S*)-linalyl glycosides were shown to be well resolved in Part I [12], which allowed the assignment of the *S* configuration to the linalyl moiety in linalyl β-D-glucopyranoside, linalyl β-rutinoside and linalyl 6-

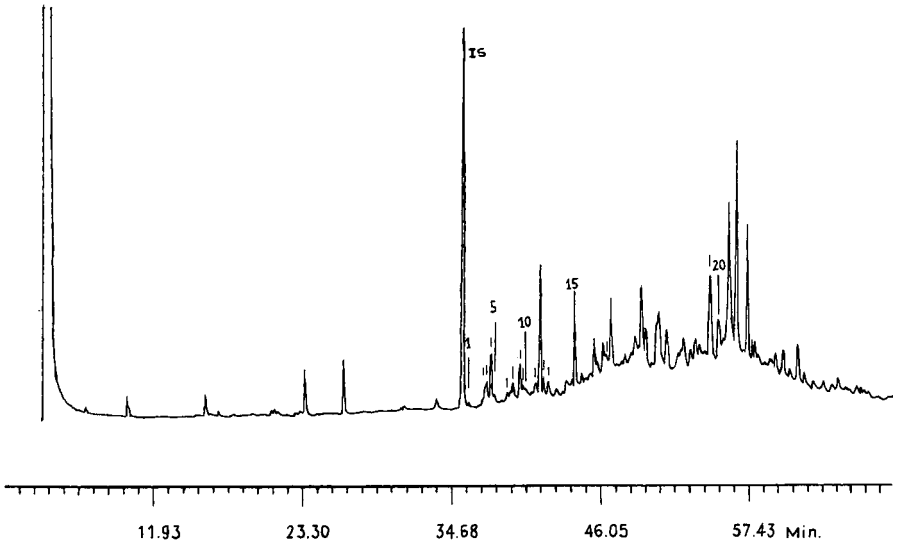

Fig. 1. GC of TMS derivatives of muscat of Alexandria glycosides. For conditions, see Experimental. Dashes are shown over the peaks corresponding to compounds reported in this paper: glycosides of (1) 3,7-dimethyl-1,5,7-octatrien-3-ol (hotrienol), (2) benzyl alcohol, (3) (*S*)-linalool, (4,5,6) linalyl oxides, (9) 2-phenylethanol, (10) nerol, (13) geraniol, (7,8,11,12,14–18) unknown monoterpendiols 1–9 reported in Table IV, (19) apiosylglycosides of benzyl alcohol and of linalyl oxides, (20) arabinosylglycoside of nerol, (21) apiosylglycosides of nerol and linalyl oxides, (22) arabinosylglycoside of geraniol and apiosylglycoside of 2-phenylethanol and (23) apiosyl glycoside of geraniol and rutinoside of geraniol.

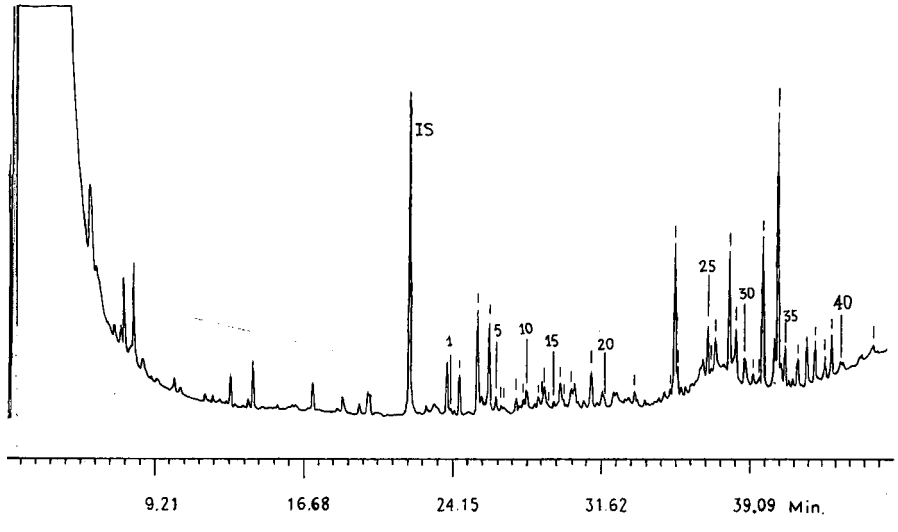

Fig. 2. GC of TFA derivatives of muscat of Alexandria glycosides. For conditions, see Experimental. Dashes are shown over the peaks corresponding to compounds reported in this paper: glycosides of (1) hotrienol, (2) benzyl alcohol, (3,4) furanic linalol oxides, (4) (*S*)-linalool, (8) 2-phenylethanol, (9) nerol, (10) pyranic linalol oxide, (13) geraniol, (19) 3,7-dimethyl-2,6-octadienoic acid, (4–7,11,12,14–21) unknown monoterpendiols 1–14 reported in Table VI, (23) rutinosides of (*S*)-linalool, (28) geraniol, (33) 3,7-dimethyl-2,6-dienoic acid, (25) arabinosylglycosides of (*S*)-linalool, (29) nerol, (33) geraniol, (35,36) 3,7-dimethyl-2,6-octadienoic acids, (26) apiosylglycosides of benzyl alcohol, (27) (*S*)-linalool, (30) nerol, (31) 2-phenylethanol, (32) pyranic linalool oxide, (34) geraniol, (35) α-terpineol, (38,39) 3,7-dimethyl-2,6-octadienoic acids, (37,40,41) apiosylglycosides partially trifluoroacetylated and (22,24) shikimic acid derivatives.

TABLE I

CONCENTRATIONS OF GLYCOSIDES OF TERPENOLS AND AROMATIC ALCOHOLS IN SOME AROMATIC GRAPE VARIETIES (μg PER LITRE OF JUICE)

Glycosides	Muscat of Alexandria	Muscat of Frontignan	Muscat of Hamburg	Muscat Ottonel	Gewürz-traminer
Glucosides					
Geranyl	50	89	–	207	43
Neryl	22	69	–	147	–
(*S*)-Linalyl	[a]	[a]	–	–	–
Terpenic aglycones in higher oxidation state[b]	3424	7427	1208	14 181	1254
Benzyl	360	122	282	417	262
2-Phenylethyl	203	130	–	277	513
Rutinosides					
Geranyl	323	330	257	372	613
Neryl		288[c]	222	227[c]	284[c]
(*S*)-Linalyl	589	478	27	948	–
Terpenic aglycones in higher oxidation state[d]	[d]	–	–	–	–
Benzyl	–	–	[e]	–	–
Arabinosylglycosides					
Geranyl	1315	2169	794	3758	5474
Neryl	461	2448	1110	1577	824
(*S*)-Linalyl	395	297	–	569	–
Terpenic aglycones in higher oxidation state[f]	268	322	342	160	420
Benzyl	–	1555[c]	–	1229[c]	1534[c]
Apiosylglycosides					
Geranyl	2085	1143	625	2554	4136
Neryl	366	1536	786	845	508
(*S*)-Linalyl	406	64	133	–	–
α-Terpineyl	[g]	–	[g]	–	–
Terpenic aglycones in higher oxidation state[h]	257	3843	364	409	343
Benzyl	64	376	241	385	656
2-Phenylethyl	242	–	183	726	–

[a] Minor compound coeluted with unknown glycoside 1 (Table VI).
[b] Glucosides of hotrienol, furanic and pyranic linalol oxides, terpenediols (MW = 170 and 172) and 3,7-dimethyl-2,6-octadienoic acids were tentatively identified. Their total amount was determined without calibration factor.
[c] Co-eluted compounds quantitatively determined using either the calibration factor of the first or that of the second.
[d] A rutinoside of a 3,7-dimethyl-2,6-octadienoic acid was the only compound tentatively identified in this class (as trace compound co-eluted with geranyl arabinosylglucoside in muscat of Alexandria).
[e] Minor compound co-eluted with a ferulic acid glycoside.
[f] Arabinosylglycosides of 3,7-dimethyl-2,6-octadienoic acid were the only compounds tentatively identified in this class. Their total amount was determined without calibration factor.
[g] Minor compound co-eluted with a 3,7-dimethyl-2,6-octadienoyl arabinosylglycoside and a ferulic acid glycoside.
[h] Apiosylglycosides of furanic and pyranic linalol oxides and of 3,7-dimethyl-2,6-octadienoic acids were tentatively identified. Their total amount was determined without calibration factor.

O-α-L-arabinofuranosyl-β-D-glucopyranoside in the grape cultivars studied. This identification was confirmed for the last two linalyl diglycosides [14] by comparison of synthetic (*S*)-linalyl β-D-glucopyranoside with the corresponding compound released by specific hydrolysis of the natural glycoside extracts with either a pure β-L- arabinofuranosidase or a pure α-L-rhamnopyranosidase [10,16,17]; however, as a pure β-D-apiofuranosidase or synthetic (*R*)- or (*S*)-linalyl 6-O-β-D-apiofuranosyl-β-D-glucopyranoside was not available, the configuration of the linalyl apiosylglucoside was not determined.

These results are in good agreement with those obtained by Salles [18] for the linalyl glycosides in muscat of Alexandria grapes.

Many more peaks were detected in the chromatograms of the grape TMS and TFA glycosides; EI-MS showed for most of them osidic fragment ions

TABLE II

CONCENTRATIONS OF BOUND AND FREE TERPENOLS AND AROMATIC ALCOHOLS IN SOME AROMATIC GRAPE VARIETIES (μg PER LITRE OF JUICE)

Compound	Ref.	Muscat of Alexandria		Muscat of Frontignan		Muscat of Hamburg		Muscat Ottonel		Gewürz-traminer	
		Free	Bound	Free	Bound	Free	Bound	Free	Bound	Free	Bound
Geraniol	[a]	606	980	416	928	281	427	425	1780	698	2458
Nerol	[a]	147	284	320	1350	191	452	160	876	133	617
Linalol	[a]	712	201	385	152	451	28	296	231	–	12
α-terpineol	[a]	24	5	27	21	24	14	26	25	10	24
Total		1489	1470	1148	2451	947	921	907	2922	841	3111
Hotrienol	[b]	8	5	5	14	5	–	9	8	–	–
cis + *trans*-Furanic linalol oxides	[b]	20	27	53	40	45	11	191	56	–	–
cis + *trans*-pyranic linalol oxides	[b]	298	29	352	60	198	14	685	61	–	7
2,6-Dimethyl-3,7-octadiene-2,6-diol	[b]	1279	1184	1099	1194	666	54	1777	1250	–	45
2,6-Dimethyl-1,7-octa diene-3,6-diol	[c]	175	54	300	83	160	134	1227	162	–	12
(*E,Z*)-8-Hydroxy linalols + (E)-3,7-dimethyl-2-octene-1,7-diol	[d]	141	454	261	1410	184	251	383	1901	88[j]	439[j]
2,6-Dimethyl-7-octene-2,6-diol	[e]	–	10	14	41	15	6	13	20	–	–
3,7-Dimethyl-1,7-octanediol + 2,6-dimethyl-7-octene-1,6-diol	[f,g]	21	52	76	226	32	55	29	75	33[k]	56[k]
(*Z*)-3,7-Dimethyl-2-octene-1,7-diol	[h]	7	6	23	20	12	9	20	20	32	11
(*E,Z*)3,7-Dimethyl-2,6-octa dienoic acids	[c]	620	429	398	324	937	121	253	125	178	183
Total		2569	2250	2581	3412	2254	655	4587	3678	331	753
Citronellol	[a]	15	24	22	84	30	80	18	42	27	113
Unknown terpene	[i]	–	–	–	–	–	–	–	–	–	221
Benzyl alcohol	[a]	101	184	221	423	130	192	209	464	224	527
2-Phenylethanol	[a]	125	160	106	220	56	54	195	423	141	222

[a] NBS Library.
[b] Rapp and Knipser [24].
[c] Rapp *et al.* [25].
[d] Bock *et al.* [26].
[e] Williams *et al.* [27].
[f] Rapp *et al.* [28].
[g] Versini *et al.* [29].
[h] Ohloff *et al.* [30].
[i] EI-MS: *m/z* (relative intensity, %) 41(100), 69(70), 39(35), 81(33), 67(21), 53(13), 93(13), 95(11), 55(10), 43(10), 121(7), 107(6).
[j] 8-Hydroxylinalols as trace component.
[k] 3,7-Dimethyl-1,7-octanediol only detected.

characteristic of the four classes of grape glycosides. Their tentative identifications relied on the fragmentation rules observed in the EI-MS of synthetic glycosides and on their corresponding CI-MS, as reported previously [3,12]; further, they were facilitated by the qualitative determination of the aglycones released after enzymic hydrolysis of the natural glycoside extracts (Table II).

All the major aglycone compounds analysed have already been positively identified (see references in Table II), except for an unknown compound detected only in Gewürztraminer, the mass spectrum of which showed fragments characteristic of terpene (see footnote *i* in Table II). Those which could not be identified were minor compounds and are not reported in Table II, in addition to C_6 compounds, arising from lipidic precursors [19] and C_{13} norisoprenoids, the results of which will be reported in a future paper.

Among the aglycones released by enzymic hydrolysis, terpenoids with higher oxidation states than linalool (linalool oxides, monoterpendiols, hotrienol, monoterpenic acids) were quantitatively important. As synthetic glycosides of such compounds were not available for most of them, they were tentatively identified in the chromatograms of the grape TMS and TFA glycosides.

Glycosides of linalol oxides and monoterpendiols tentatively identified

Most of the unknown peaks in the chromatograms of the TMS and TFA grape glycosides showed fragment ions characteristic of glycosides with terpenic aglycones. As the structure of the sugar residue was easily deduced by EI-MS [3,12], CI-MS of their TMS derivatives gave for the derivatized aglycones molecular weights of 152, 170, 242 and 244, corresponding respectively to hotrienol, linalol oxides (Table III) and monoterpenediols with two or one double bonds (Table IV).

As shown in Table III for the TMS derivatives of glycosides with aglycones with molecular weights of 152 and 170, one peak corresponding to a glycoside of Ho-trienol and three peaks corresponding to glycosides of linalool oxides were detected in the chromatograms of the grape TMS glycosides together with three peaks corresponding to apiosyl glycosides of linalool oxides reported previously [3]. However, it was not possible by EI-MS to establish further the complete structures of their aglycones among the different possible isomers.

As regards the TFA derivatives, GC–CI-MS coupling gave unsatisfactory results, as reported previously for synthetic glycosides [3,12], but allowed the location of one peak corresponding to a glycoside of Ho-trienol (pseudo-molecular ion at $m/z = 716$) and one peak corresponding to a glycoside of a linalool oxide (pseudo-molecular ion at $m/z = 734$). Using EI-MS data, two more peaks corresponding to glycosides of linalool oxides were detected in the chromatograms of the TFA derivatives of the grape extracts together with four peaks corresponding to apiosylglycosides of linalool oxides reported previously [3].

EI-MS (Table V) showed two types of fragmentation for the aglycone residue, as reported previously for furanic (characteristic fragment ions at m/z 111 and 93) and pyranic (m/z 94 and 68) linalol oxide acetates [20] and peracetylated 6-O-α-L-arabinofuranosyl-β-D-glucopyranosides previously isolated from grape [6], thus allowing them to be distinguished.

As regards monoterpenediol glycosides, nine peaks corresponding to monoterpendiol glycosides (molecular weight of derivatized aglycone = 242 or 244) were identified in the chromatograms of the TMS derivatives of the five grape extracts. EI-MS (Table III) exhibited characteristic fragmentations, similar to those obtained from the synthetic diastereoisomeric 2,6-dimethyl-3-hydroxy-1,7-octadien-6-yl-β-D-glucopyranosides [12], and CI-MS provided the expected molecular weights (see above).

Similarly, fourteen unknown peaks exhibiting fragment ions characteristic of glycosides with terpenoid aglycones were located in the chromatograms of the TFA derivatives of the five grape extracts (Table VI). For most of them these fragment ions were similar to those reported for the synthetic diastereoisomeric 2,6-dimethyl-3-hydroxy-1,7-octadien-6-yl-β-D-glucopyranosides [12]. These peaks were thus tentatively identified as monoterpendiols glycosides; their formal identification will be difficult owing to the numerous isomers of these compounds.

At the end of the gas chromatograms of the TMS and TFA glycosides, unknown peaks with low intensities showed EI-MS characteristics of terpenoid

TABLE III

MASS SPECTRA OF TMS DERIVATIVES OF GLYCOSIDES WITH AGLYCONES TENTATIVELY IDENTIFIED AS HOTRIENOL AND LINALOL OXIDES IN *VITIS VINIFERA* GRAPES

Aglycone residue	RRT[a]	EI-MS, characteristic fragment ions [*m/z* (relative intensity, %)] of			MW[b] (MW_s)	MW of aglycone[c] (MW_a)
		Sugar moiety	Aglycone moiety	Sugar and aglycone-moiety		
Glucosides						
Hotrienyl	1.007	217(100), 361(16), 191(8), 204(7), 242(3)	153(33), 71(27), 81(11), 133(4)		601	152
Linalyl oxide	1.067	204(60), 217(35), 361(26), 271(6), 331(5), 191(5), 233(4), 243(3.5), 319(2), 263(2), 305(1.5), 451(0.5)	153(100), 71(44), 81(14), 135(9.7), 154(5.5), 93(5), 69(5)	271(6)	620	170
Linalyl oxide	1.076	204(76), 361(53), 217(48), 271(13), 243(7), 191(7), 331(7), 319(4), 233(4), 263(3), 305(2), 451(0.4)	153(100), 71(53), 81(20), 135(13), 93(8), 69(5)	271(13)	620	170
Linalyl oxide	1.119	204(100), 217(21), 361(20), 271(7), 191(5), 243(3), 305(2), 233(2), 319(2), 263(2), 451(0.5)	81(11), 153(11), 135(9), 71(7), 93(2)	271(7)	620	170
Apiosylglucosides[d]						

[a] Retention time relative to phenyl β-D-glucopyranoside.
[b] From CI-MS with ammonia as reactant gas.
[c] Obtained as $MW_a = MW_s - 451$ (molecular weight of the sugar moiety) + 1.
[d] Data reported previously [3].

TABLE IV

MASS SPECTRA OF TMS DERIVATIVES OF GLUCOPYRANOSIDES WITH UNKNOWN MONOTERPENEDIOL AGLYCONE TENTATIVELY IDENTIFIED IN *VITIS VINIFERA* GRAPES

Aglycone residue	RRT[a]	EI-MS, characteristic fragment ions [*m/z* (relative intensity, %)] of		MW[b] (MW_s)	MW of underivatized aglycon[c] (MW_a)
		Sugar moiety	Aglycon moiety		
Unknown 1	1.128	331(76), 263(38), 204(35), 191(32), 233(27), 217(21), 361(9.2), 243(3.8), 305(3.4), 319(1.7), 271(1.6)	143(100), 82(12)	692	170
Unknown 2	1.143	331(100), 263(46), 204(45), 191(30), 233(27), 217(25), 361(16), 305(4.1), 243(2.7), 271(2.4), 319(1.9)	143(83), 82(8.3), 241(2.5)	692	170
Unknown 3	1.180	204(100), 331(64), 217(54), 191(36), 263(31), 233(27), 361(19), 305(4.6), 243(4)	143(37), 135(36), 225(26), 93(25), 107(24), 75(15), 81(4.5), 131(2.9), 241(1.9)	692	170
Unknown 4	1.190	331(49), 263(27), 191(25), 204(23), 217(21), 233(19), 361(15), 243(2.7), 305(2.5), 271(1.6), 319(0.8)	143(100), 82(15), 135(3.2), 225(2.8), 93(2.6), 81(2.4), 131(2.3), 107(1.5), 141(1.5)	692	170
Unknown 5	1.210	217(100), 204(37), 331(34), 361(20), 263(17), 233(14), 191(9.9), 243(6.3), 271(2.5), 319(1.9)	143(32), 81(20), 69(16), 75(8.3)	694	172
Unknown 6	1.274	204(100), 217(60), 331(36), 361(31), 191(22), 263(17), 233(17), 243(4.1), 305(3.9), 319(3.3), 271(2.9)	135(25), 225(25), 143(21), 93(18), 107(15)	692	170
Unknown 7	1.322	204(74), 331(71), 217(62), 361(35), 263(34), 191(33), 233(30), 243(5.6), 305(4.3), 319(3.6), 271(3.1)	135(47), 225(34), 93(31), 107(30), 143(28), 67 (11), 81(6.3)	692	170
Unknown 8	1.347	331(76), 217(54), 253(46), 204(40), 191 (20)	81(100), 131(76)	694	172
Unknown 9	1.363	217(100), 204(29), 331(22), 361(18), 263(12), 191(7.8), 271(7), 233(6.9), 243(3.7), 319(3.4), 305(2.5)	121(25), 143(18), 75(9.8), 93(8.1)	692	170

[a,b] See footnotes *a* and *b* in Table III.

[c] Obtained as $MW_a = MW_s - 451$ (molecular weight of the glucose moiety) $- 73$ (TMS) $+ 2$ ($2 \times H$).

TABLE V

MASS SPECTRA OF TFA DERIVATIVES OF GLYCOSIDES WITH AGLYCONES TENTATIVELY IDENTIFIED AS HOTRIENOL, LINALOL OXIDES AND MONOTERPENIC ACIDS IN *VITIS VINIFERA* GRAPES

Aglycone residue	RRT[a]	EI-MS, Characteristic fragment ions [*m/z* (relative intensity, %)] of		CI-MS, characteristic fragment ions [*m/z* (relative intensity, %)] of[c]
		Sugar moiety	Aglycone moiety[b]	
Glucosides				
Ho-trienyl	1.081	319(100), 193(17), 205(6), 177(6)	93(82), 134(68), 69(66), 79(63), 135(60), 119(50), 91(47), 107(45), 92(36), 109(29), 81(26), 77(23)	603(20), 716(16), 490(4)
A furanic linalyl oxide	1.160	319(17), 193(2.5), 177(1.5), 205(1.5), 265(0.7), 547(0.3), 291(0.1)	111(100), 93(44), 69(22), 71(21), 153(11), 94(5)	734(13), 508(5)
A furanic linalyl oxide	1.174	319(36), 193(5), 205(4), 177(4), 265(1.3)	111(100), 71(60), 93(54), 69(35), 153(9), 94(6.5)	
A pyranic linalyl oxide	1.279	319(29), 205(2.5), 177(2.5), 193(2), 265(0.7)	68(100), 94(92), 81(46), 71(33), 111(17), 69(11)	
A' 3,7-dimethyl-2,6-octadienoic acid	1.427	319(8), 193(1.5), 177(1.5), 205(1.5)	69(100), 123(20), 151(18), 168(12), 82(10)	
Rutinosides				
A 3,7-dimethyl-2,6-octadienoic acid[d]	1.822	193(11), 207(3), 265(1), 206(0.6), 278(0.4), 179(0.4), 177(0.4), 319(0.3), 435(0.3), 292(0.2)	69(100), 123(15.3), 82(7), 151(5), 168(4)	
Arabinosylglycosides				
(*E*) and (*Z*)-3,7-dimethyl-2,6	1.894	193(25), 265(2), 278(1.5), 319(0.8), 177(0.3), 279(0.3)	69(100), 123(24), 151(19), 82(17), 168(10)	
Octadienoic acid	1.921	193(8), 421(3), 279(2.5), 265(0.2), 278(0.1)	69(100), 123(18), 151(18), 82(14), 168(7)	
Apiosylglycosides[e]				

[a] Retention time relative to phenyl β-D-glucopyranoside.
[b] A small portion of *m/z* 69 can be accounted for by CF_3^+.
[c] From CI-MS with ammonia as reactant gas.
[d] Co-eluted with geranyl arabinosylglycoside.
[e] Data reported previously [3].

TABLE VI

MASS SPECTRA OF TFA DERIVATIVES OF GLUCOPYRANOSIDES WITH UNKNOWN MONOTERPENEDIOL AGLYCONE TENTATIVELY IDENTIFIED IN *VITIS VINIFERA*

Aglycone residue	RRT[a]	EI-MS, characteristic fragment ions [*m/z* (relative intensity, %)] of	
		Sugar moiety	Aglycone moiety[b]
Unknown 1	1.182	319(6.5), 193(1.7), 177(0.8), 205(0.7), 265(0.5), 547(0.1)	71(100), 82(75), 83(36), 69(18), 93(11), 81(10)
Unknown 2	1.196	319(100), 193(6.7), 205(6.1), 547(5.4), 177(3.7), 291(0.6)	71(53), 93(21), 69(20), 81(19), 109(12), 107(11)
Unknown 3	1.208	319(8.1), 193(3), 205(2.4), 177(1.6)	71(100), 83(74), 85(66), 82(60), 94(21), 69(19), 109(18), 84(10)
Unknown 4	1.214	319(39.4), 205(2.6), 177(0.5), 193(0.3)	81(100), 69(71), 80(71), 95(58), 68(49), 93(48), 79(41), 121(39), 67(29), 136(18)
Unknown 5	1.296	319(18), 205(2.8), 177(2.1), 193(1.9), 265(0.6), 547(0.2), 291(0.2)	93(100), 71(42), 94(14), 67(12), 79(12), 134(11), 81(11)
Unknown 6	1.302	319(19), 205(2), 177(0.8), 193(0.7)	71(100), 82(19), 93(14), 109(13), 67(11), 72(9), 94(8)
Unknown 7	1.315	205(3), 177(1.9), 319(1.9)	96(100), 93(86), 68(79), 81(78), 95(64), 67(57), 69(42), 110(32), 71(22), 80(21), 109(21), 108(19), 92(18), 135(17)
Unknown 8	1.332	319(62), 193(11), 205(9.1), 177(3.8), 547(3.2), 265(2)	93 (100), 69(93), 71(42), 81(32), 109(22), 91(20), 92(14), 77(12), 70(12) 97(12), 83(12), 121(10), 119(10)
Unknown 9	1.340	319(4.6), 193(2.9), 265(0.3)	69(100), 109(38), 93(28), 121(15)
Unknown 10	1.353	319(17), 177(4.2), 193(2.1), 205(1.6)	93(100), 80(81), 94(41), 71(32), 121(25), 81(25), 79(24), 119(17), 107(17), 97(16), 91(14), 109(14), 105(13), 92(13)
Unknown 11	1.362	319(17), 193(4), 205(2.3), 177(2), 265(0.5), 547(0.5)	71(100), 93(38), 109(31), 69(30), 94(20), 68(19), 84(19), 81(18), 80(16), 82(15), 119(14), 121(12), 95(12), 107(11)
Unknown 12	1.413	319(20), 193(4.5), 205(2.8), 177(2.5), 265(1)	71(100), 69(54), 93(35), 109(29), 80(27), 82(22), 68(19), 81(19), 94(16), 85(13), 107(13), 84(12), 95(11), 97(10)
Unknown 13	1.445	319(16), 193(4.8), 205(4.3), 177(4.3)	80(100), 69(45), 111(44), 147(44), 93(23), 166(22), 165(21), 98(19), 91(18), 97(16), 105(15), 107(15), 119(13), 77(12)
Unknown 14	1.519	319(45), 193(3.6), 205(3.5), 177(3.4), 265(2.1), 547(0.3)	71(100), 93(21), 121(20), 69(20), 114(16), 96(15), 82(13), 97(12), 95(12)

[a,b] See footnotes *a* and *b* in Table V.

diglycosides. CI-MS of their TMS derivatives gave results consistent with diglycosides of monoterpendiols (molecular weights of 242 and 244 for the aglycones), but EI-MS of both TMS and TFA derivatives gave different spectra to those observed above for the glycosides of monoterpendiols. As no synthetic representatives of monoterpendiol diglycosides were available, we could not draw a conclusion, but it was interesting that (*E*)-2,6-dimethyl-6-hydroxy-2,7-octadien-1-yl (unknown configuration of C-6) β-D-glucopyranoside and 6-O-α-L-arabinofuranosyl-β-D-glucopyranoside were previously positively identified in grape [6,7].

Glycosides of monoterpenic acids

In the chromatograms of the TFA derivatives of the five grape extracts, some peaks were tentatively identified from their EI-MS data (Table V) as (*E,Z*)-3,7-dimethyl-2,6-octadienoyl glycosides, rutinosides, arabinosylglycosides and apiosylglycosides. The fragment ions assigned to the aglycones were similar to those reported for (*E,Z*)-3,7-dimethyl-2,6-octadienoic acids [21]; the ions at *m/z* 151 and 123 represented the cleavage of bonds next to C=O and the other diagnostic peaks were found at *m/z* 168, 82 and 69. It is interesting that these glycosides were absent in the gas chromatograms of the corre-

sponding TMS glycoside extracts, as they were probably deglycosylated by the chlorotrimethylsilane present in the silylating reagent, as already reported for other 1-O-acyl glycosides [22].

Other glycosides

The gas chromatograms of the TFA derivatives of the grape glycoside extracts showed few peaks of compounds different from terpenoid derivatives. The more important of them were tentatively identified as glycosides of ferulic, coumaric, vanillic and syringic acids, and have been reported elsewhere [14].

Quantitative analysis

The concentrations reported in Table I were determined using TFA derivatives of the glycoside extracts with phenyl β-D-glucopyranoside as internal standard according to the method developed in Part I [12]; the global calibration factors used were those described previously for the available reference compounds [12], but the concentrations of the tentatively identified apiosylglycosides were determined using the global calibration factors for the 6-O-β-L-arabinofuranosyl-β-D-glucopyranosides with the corresponding aglycone. The other glycosides, tentatively identified as monoglycosides and diglycosides of linalool oxides, monoterpenediols and 3,7-dimethyl-octa-2,6-dienoic acids, could not be determined individually owing to a lack of reference compounds; their total amount, determined using no calibration factor, was reported in Table I as indicative of the relative amounts of glycosides with aglycones in higher oxidation states than linalool in the four different classes of glycosides.

As regards apiosylglycosides, small peaks corresponding to partially trifluoroacetylated apiosylglycosides were found in the range of high retention times, as reported previously [3], and were not taken into the quantitative determination of the apiosylglycosides reported, as they were much smaller than the fully trifluoroacetylated compounds and as no calibration factors were available. Synthesis of these apiosylglycosides is in progress to investigate how to overcome this major drawback for their quantitative determination.

Table I showed a similar general glycoside distribution to that reported previously for muscat of Alexandria and Rhine Riesling grapes [1]. The proportion of disaccharides compared with monoglycosides was generally high, but only for those glycosides with aglycones in the linalol oxidation state. Indeed, glycosides with aglycones in higher oxidation states than linalol were found to be abundant in muscat Ottonel but also in muscat of Frontignan and muscat of Alexandria. In fact, such glycosides were more abundant than those with aglycones in the linalol oxidation state in the five cultivars, but the reverse was true for the diglycosides, except for the apiosylglycosides in muscat of Frontignan. Further, the proportion of rutinosides compared with the two other pentosylglycosides was generally low.

As regards aglycones in the linalol oxidation state, glycosides of geraniol were generally the most abundant (particularly in Gewürztraminer), except for the two pentosylglycosides in muscat of Frontignan and Hamburg; glycosides of α-terpineol appeared as minor components only.

The total amounts of bound aroma components were higher in Gewürztraminer, muscat of Frontignan and Ottonel than in muscat of Alexandria and muscat of Hamburg, the last containing the lowest levels of each class of glycosides, consistent with the results reported by Günata [9] using enzymic hydrolysis.

We then compared the concentrations thus determined for the glycosides with those determined using the known procedure involving enzymic hydrolysis of their aglycones [11]. The volatiles released were analysed by GC and quantitatively determined without calibration factors (Table II).

Comparison of the results in Table I with those in Table II showed that the conclusions deduced from Table I concerning the aglycones (see above) are consistent with thosed which could be obtained from Table II, taking into consideration the properties of the glycosidase activities of Pektolase 3PA [13,23].

Finally the free fractions obtained in these experiments were analysed by GC and the concentrations of the compounds, also reported as bound compounds, were quantitatively determined using the global calibration factors given in the Part I [12] for the available reference compounds. These results are reported in Table II together with those obtained on the bound forms.

CONCLUSIONS

This work showed that direct GC and GC–MS analysis of TFA-derivatized non-volatile glycosides allowed their qualitative and quantitative determinations in some aromatic grape cultivars. This method appeared to be the best suited for the direct analysis of monoterpene glycosides, the most abundant of grape glycosides.

Combination of direct analysis after TMS and TFA derivatization or after enzymic hydrolysis of the glycosidic fractions allowed a breakthrough in the qualitative determination of monoterpene glycosides. It confirmed the complexity and heterogeneous nature of grape glycosides and the high proportions of bound monoterpenes compared with free monoterpenes.

ACKNOWLEDGEMENTS

We thank Dr J. L. Le Quere and E. Semon, Laboratoire des Arômes, Dijon, France, for recording the mass spectra.

REFERENCES

1 P. J. Williams, C. R. Strauss, B. Wilson and R. A. Massy-Westropp, *Phytochemistry,* 21 (1982) 2013.
2 P. J. Williams, C. R. Strauss, B. Wilson and R. A. Massy-Westropp, *Phytochemistry,* 22 (1983) 2039.
3 S. G. Voirin, R. L. Baumes, S. M. Bitteur, Z. Y. Günata and C. L. Bayonove, *J. Agric. Food Chem.,* 38 (1990) 1373.
4 P. J. Williams, C. R. Strauss and B. Wilson, *J. Chromatogr.,* 235 (1982)471.
5 C. R. Strauss, B. Wilson and P. J. Williams, *Phytochemistry,* 26 (1987) 1995.
6 C. R. Strauss, P. R. Gooley, B. Wilson and P. J. Williams, *J. Agric. Food Chem.,* 35 (1987) 519.
7 C. R. Strauss, B. Wilson and P. J. Williams, *J. Agric. Food Chem.,* 36 (1988) 569.
8 C. R. Strauss, B. Wilson, P. R. Gooley and P. J. Williams, in T. H. Parliment and R. Croteau (Editors), *Biogeneration of Aromas (ACS Symposium Series,* Vol. 317), American Chemical Society, Washington, DC, 1986, p. 222.
9 Z. Günata, *Doctoral Thesis,* Montpellier University, 1984.
10 Z. Günata, S. Bitteur, R. Baumes, J. M. Brillouet, C. Tapiero, C. Bayonove and R. Cordonnier, *Fr. Pat. Appl.,* 8802961, 1989.
11 Z., Günata, C. Bayonove, R. Baumes and R. Cordonnier, *J. Chromatogr.,* 331 (1985) 83.
12 S. G. Voirin, R. L. Baumes, Z. Y. Günata, S. M. Bitteur, C. L. Bayonove and C. Tapiero, *J. Chromatogr.,* 590 (1992) 313.
13 R. Cordonnier, Z. Günata, R. Baumes and C. Bayonove, *J. Int. Sci. Vigne Vin,* 23 (1989) 7.
14 S. Voirin, *Doctoral Thesis,* Montpellier University, 1990.
15 B. Wilson, C. R. Strauss and P. J. Wilson, *J. Agric. Food Chem.,* 32 (1984) 919.
16 Z. Günata, S. Bitteur, J. M. Brillouet, C. Bayonove and R. Cordonnier, *Carbohydr. Res.,* 184 (1988) 139.
17 Z. Günata, J. M. Brillouet, S. Voirin, R. Baumes and R. Cordonnier, *J. Agric. Food Chem.,* 38 (1990) 772.
18 C. Salles, *Doctoral Thesis,* Montpellier University, 1989.
19 R. Cordonnier and C. Bayonove, *Connaiss. Vigne Vin,* 15 (1981) 269.
20 G. Ohloff, K. H. Schulte-Elte and B. Willhalm, *Helv. Chim. Acta,* 47 (1964) 602.
21 W. Renold, R. Naf-Muller, U. Keller, P. Willhalm and G. Ohloff, *Helv. Chim. Acta,* 57 (1974) 1301.
22 G. M. Martinelli, *Eur. J. Mass Spectrom. Biochem. Med. Environ. Res.,* 1 (1980) 33.
23 Y. Z. Günata, C. L. Bayonove, C. Tapiero and R. E. Cordonnier, *J. Agric. Food Chem.,* 38 (1990) 1232.
24 A. Rapp and W. Knipser, *Vitis,* 18 (1979) 229.
25 A. Rapp, W. Knipser and L. Engel, *Vitis,* 19 (1980) 226.
26 G. Bock, I. Benda and P. Schreier, *J. Food Sci.,* 51 (1986) 659.
27 P. J. Williams, C. R. Strauss and B. Wilson, *Phytochemistry,* 19 (1980) 1137.
28 A. Rapp, H. Mandery and H. Ullemeyer, *Vitis,* 22 (1983) 225.
29 G. Versini, A. Scienza, A. Dalla Serra, M. Dell'Eva and A. Rapp, in P. Schreier (Editor), *Bioflavour '87, Analysis Biochemistry Biotechnology,* Walter de Gruyter, Berlin, New York, 1988, p. 161.
30 G. Ohloff, K. H. Schulte-Elte and B. Willhalm, *Helv. Chim. Acta,* 47 (1964) 602.

Journal of Chromatography, 595 (1992) 283–287
Elsevier Science Publishers B.V., Amsterdam

CHROM. 23 885

Degradation of polysulphones by alkali fusion

J. K. Haken* and M. Camamo☆

Department of Polymer Science, University of New South Wales, P.O. Box 1, Kensington, NSW 2033 (Australia)

(First received September 4th, 1991; revised manuscript received November 14th, 1991)

ABSTRACT

The degradation of both aliphatic and aromatic polysulphones was carried out using alkaline fusion with chromatographic and spectrophotometric determination of the reaction products. The results are compared with those achieved with other functional classes of condensation polymers.

INTRODUCTION

The degradation of polymers of various functional classes as a preliminary to analysis of the reaction fragments has been carried out using hydrolytic cleavage. Many of the polymers, because of their inherent stability, require more stringent conditions than are possible using solution reaction and solid alkali has been used. The potassium hydroxide fusion reagent approximates the hemihydrate and consists of *ca.* 85% alkali.

Functional classes of polymers examined using alkali fusion include polyamides [1], polyimides [2], polyhydrazides [3], polyesters [4,5] and polyurethanes [6]. Although the analyses have largely been qualitative, the quantitative nature of the reactions has been discussed [7] and several studies concerning silicone polyesters have been reported [8,9].

The alkaline fusion procedure used is an extension of that developed by Siggia and co-workers [10], who described their procedure as fusion reaction gas chromatography (GC) [11], it being restricted to the detection of materials amenable to GC while the current procedure is applicable to all cleavage products.

The polysulphones represent a further functional class of polymers and studies are reported using both aliphatic and aromatic homologues with the results being compared with those achieved with other functional classes of condensation polymers. The chemical cleavage of these polymers has not previously been reported and, as the structures are theoretically amenable to cleavage, the possibility of reaction as an analytical procedure is considered.

Alkyl sulphones react with alkali to produce olefins, α-bromodiethyl sulphone [12], α-bromopropyl ethyl sulphone [13] and bis(α-chloroethyl) sulphone [14] yielding *cis*-2-butene, *cis*-2-pentene and potassium 2-butene-2-sulphonate, respectively.

Rearrangement of olefinic sulphones occurs with alkali such that the position of the double bond is moved and ultimately cleavage occurs at the new site of the double bond with the formation of a saturated hydrocarbon fragment and an aldehyde. Propylene sulphone reacted with hot aqueous sodium hydroxide to produce acetaldehyde and sodium 2-methylsulphonyl-1-propanesulphonate [15–16].

Simple aromatic sulphones cleave at the sulphone link. Ingold and Jessop [17] and others [18,19] found that benzene and benzenesulphonic acid were the products of the alkaline cleavage of diphenylsulphone. Phenol was also a significant product at temperatures below the decomposition point of benzenesulphonic acid. Phenylbenzylsulphone yielded phenol and sulphur dioxide whereas ben-

☆ Present address: Stephenson & Associates Pty. Ltd., P.O. Box 88, Chatswood, NSW 2057, Australia.

0021-9673/92/$05.00

zylmethyl sulphone yielded similar products with the addition of methanesulphonic acid. Commercially available aromatic polysulphones are reported to be insoluble and not attached by alkali. Samples were immersed at room temperature for 180 days in 10% and saturated sodium hydroxide without effect [20].

EXPERIMENTAL

Samples

Three samples of polyolefinic sulphones, *viz.*, poly-1-(butene sulphone), poly(1-hexene sulphone) and poly 1-(cyclohexene sulphone) were used. The samples were provided by Professor J. O'Donnell of the University of Queensland.

Two commercially available types of aromatic polysulphones were used, namely the polyether sulphone Ultrason E2000 (BASF) or the ICI product Vitrex and the bisphenol A derivative of the polyether sulphone Udel P1700 (BASF) or PSOME (Amoco).

Ultrason E2000 or Vitex

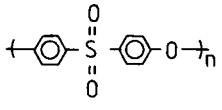

Udel P1700 or PSOME

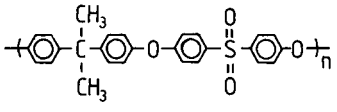

Alkali fusion procedure

Alkali fusion was carried out using 200–300 mg of polymer and 1–3 g of a prefused mixture of potassium hydroxide and 5% sodium acetate. The reaction was carried out by heating the polymer-reagent mixture in a stainless-steel, screw-capped pressure tube at various temperatures and for various times.

The reaction vessel was then allowed to cool and the reactants were placed in a 50-ml conical flask with water (30 ml). Chloroform (10 ml) was added and the mixture placed in a 100-ml separating funnel. The organic layer was separated using two aliquots of 10 ml of chloroform and then heated to evaporate the chloroform. The chloroform/organic layer was evaporated to 2–3 ml. Gas chromatography–mass spectrometry (GC–MS) was used for analysis. The aqueous phase was evaporated to dryness and the solid also examined by infrared spectrometry. The analytical scheme is shown in Fig. 1.

Gas chromatography

For GC a Perkin-Elmer Model 8410 gas chromatograph was used. The carrier gas was helium at a flow-rate of 1000 ml min^{-1}. The column was 12 ft. × 0.25 in. O.D. aluminium packed with 10% OV-1, temperature programmed from 35°C at a rate of 15°C/min to 200°C.

Confirmatory analyses

Infrared spectrometry. Infrared spectrometry was performed with a Hitachi Model 270-30 infrared spectrometer in the region 400–4000 cm^{-1} with the sample on a silver bromide plate.

Mass spectrometry. Chemical ionization mass spectrometry was conducted on the aqueous layer using a Finnigan Model 3200 quadrupole GC–MS system interfaced with an Incos Model 2300 data system. The ion source was maintained at 100°C by filament emission (100 mA) with source pressure of

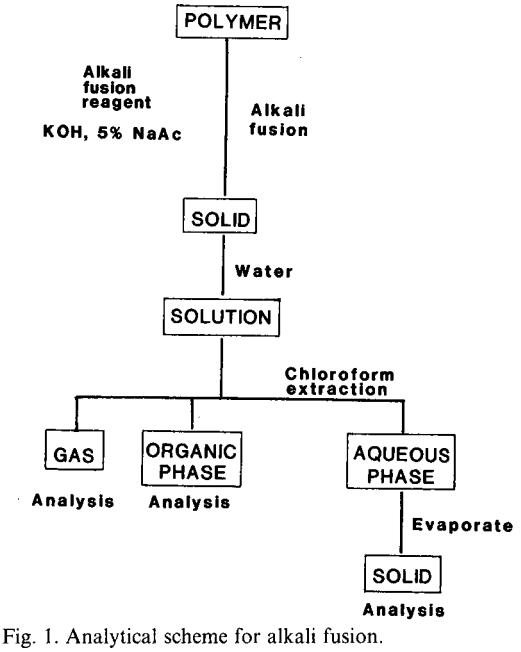

Fig. 1. Analytical scheme for alkali fusion.

0.8 Torr. A 1.5 m × 4 mm I.D. open tubular-glass column was used with methane as carrier/reagent gas at a flow-rate of 20 ml/min. The column (1.8 m × 2 mm I.D.) was packed with 2% OV-17 on Chromosorb G (100–120 mesh). The column was temperature programmed from 40°C at 10°C/min to 150°C.

NMR spectrometry. ^{1}H and $C^{13}NMR$ were carried out on Bruker AC300 F spectrometer operating at 300 MHz.

RESULTS AND DISCUSSION

The olefinic polysulphones were readily cleaved by reaction at 200°C for 1 h. Poly 1-(butene sulphone) and poly(1-hexene sulphone) produced 1-methyl 1,3-propanediol and 1-methyl-1,3-pentanediol, respectively, while poly(1-cyclohexene sulphone) produced ethanol and *n*-octanol, the former predominating. The saturated ring structure of the sulphone was opened and cleavage occurred. The liberation of sulphur dioxide was apparent immediately on opening the reactors. Measurement of the gas liberated is not suitable for determination of the sulphones, however, as some reaction occurs with the potassium hydroxide with the formation of potassium hydrogensulphite. Fig. 2 shows chromatograms of the alcohols produced by cleavage of the three olefinic polysulphones.

The simpler aromatic polymer was fused at temperatures between 250 and 300°C for times up to 24 h, as shown in Table I. No cleavage occurred at short reaction times and a minimum reaction time of 6 was necessary for degradation to occur. The polymer was cleaved at the S–C bond with liberation of sulphur dioxide. The reactions are shown in Fig. 3.

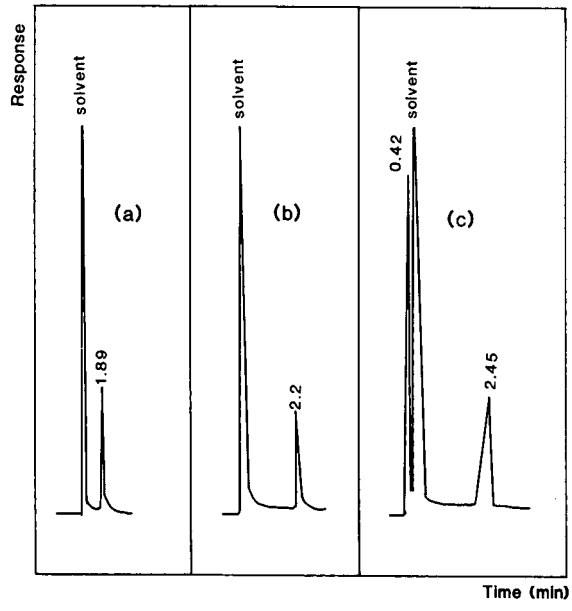

Fig. 2. Chromatograms showing reaction products of olefinic sulphones: (a) 1-methyl-1,3-propanediol from poly(1-butene sulphone); (b) 1-methyl-1,3-pentanediol from poly(1-hexene sulphone); (c) ethanol and *n*-octanol from poly(1-cyclohexene sulphone).

After 6 h of reaction a small amount of phenol

TABLE I

ALKALI FUSION CONDITIONS FOR SIMPLE AROMATIC POLYSULPHONES

Expt. No.	Polymer	Temperature (°C)	Time (h)	Observation
1	Ultrason E2000	300	2	Polymer did not dissolve
2	Ultrason E2000	250	4	As above
3	Ultrason E2000	350	4	As above
4	Ultrason E2000	300	6	White powder resulted, soluble in water
5	Ultrason E2000	300	12	As above
6	Ultrason E2000	280	24	As above
7	Udel P1700	280	4	White powder resulted, soluble in water to form a yellow solution
8	Udel P1700	400	4	Polymer did not dissolve
9	Udel P1700	280	12	As above
10	Udel P1700	280	24	As above

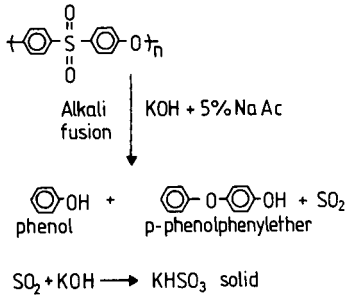

Fig. 3. Alkaline cleavage of simple aromatic polysulphone. NaAc = Sodium acetate.

was present, but on further reaction the phenol concentration increased. Fig. 4 shows chromatograms of the two reaction products at 6 and 24 h, where it was apparent that the *p*-phenol phenyl ether is degraded with further reaction. After 6 h of reaction

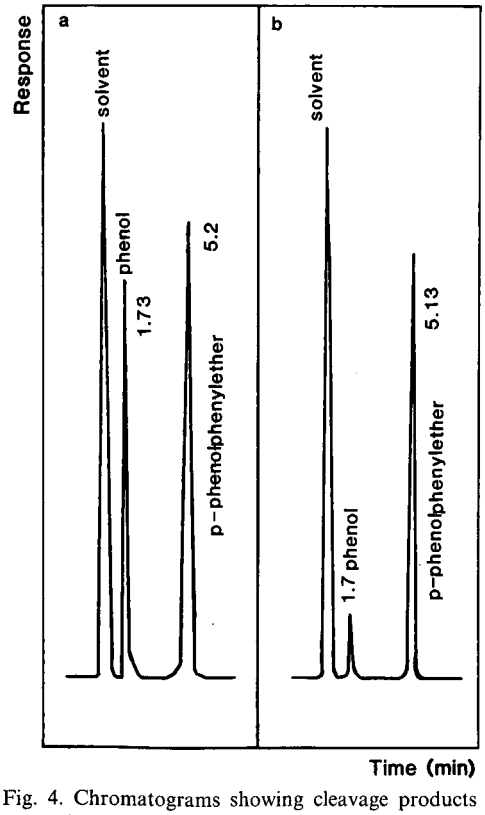

Fig. 4. Chromatograms showing cleavage products of simple aromatic polyether sulphone after (a) 6 h and (b) 24 h of reaction.

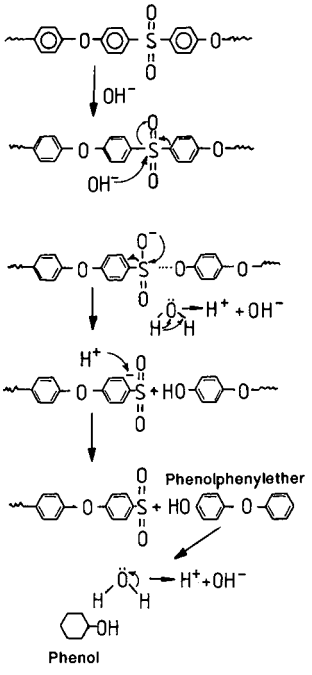

Fig. 5. Proposed degradation scheme for aromatic polyether sulphone.

sulphur dioxide could be detected on opening the reactor but with longer reaction times reaction with the alkali occurred to form potassium hydrogensulphite. The reaction scheme proposed for the degradation is shown in Fig. 5.

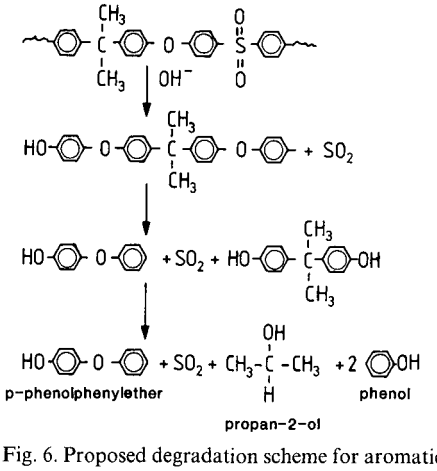

Fig. 6. Proposed degradation scheme for aromatic polyether sulphone copolymer with bisphenol A.

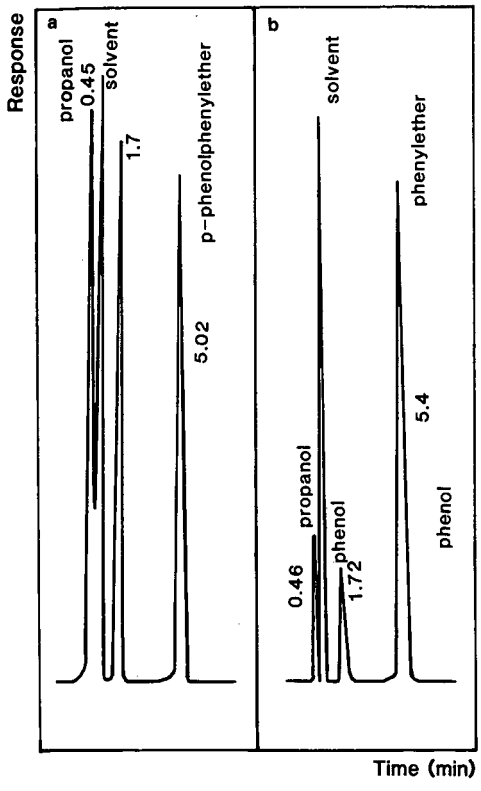

Fig. 7. Chromatogram showing cleavage products of aromatic polyether sulphone copolymer with bisphenol A after (a) 6 h and (b) 24 h of reaction.

The polysulphone copolymer with bisphenol A was examined as shown in Table I. The same constraints as with the simple polymer concerning degradation were apparent, the presence of the bisphenol A apparently not further reducing the reactivity of the volatile products were present, two as expected being common with the simple polymer, the third was 2-propanol.

The predominance of phenol at shorter reaction times was also observed. The presence of bisphenol A was also confirmed by NMR. The possible cleavage mechanism is shown in Fig. 6, which shows a chromatogram of the reaction products of the bisphenol A copolymer at 6 and 24 h, the results being in agreement with those for the simple polymer shown in Fig. 7.

The alkaline cleavage of sulphones shows that the olefinic materials are readily cleaved under the same or milder conditions thatn appllied to other condensation polymers. The aromatic materials, however, are much more resistant to cleavage than the other polymer systems examined and the conditions necessary are not compatible with those used in earlier studies. It is evident that the susceptibility of the two polymers to cleavage is very similar; the presence of bisphenol A in the copolymer does not further increase the resistance to cleavage as has been observed with other polymers containing bisphenol A [21].

In all of the analyses the identities of the compounds shown were confirmed by the various spectroscopic techniques. The spectra obtained are in agreement with those in available reference collections.

REFERENCES

1 J. K. Haken and J. A. Obita, *J. Chromatogr.*, 244 (1982) 265.
2 J. K. Haken and J. A. Obita, *J. Chromatogr.*, 244 (1982) 259.
3 J. K. Haken and J. A. Obita, *J. Chromatogr.*, 239 (1982) 377.
4 J. K. Haken and M. A. Rohanna, *J. Chromatogr.*, 349 (1985) 349.
5 J. K. Haken, N. Harahap and R. P. Burford, *J. Chromatogr.*, 387 (1987) 223.
6 P. A. D. T. Vimalasiri, R. P. Burford and J. K. Haken, *Rubber Chem Technol.*, 60 (1987) 555.
7 J. K. Haken, *J. Chromatogr.*, 406 (1987) 167.
8 J. K. Haken, N. Harahap and R. P. Burford, *J. Coatings Technol.*, 60 (1988) 759, 53.
9 J. K. Haken, N. Harahap and R. P. Burford, *Prog. Org. Coat.*, 17 (1989) 277.
10 S. P. Frankoski and S. Siggia, *Anal. Chem.*, 44 (1972) 507.
11 L. R. Whitlock and S. Siggia, *Sep. Purif. Methods*, 3 (1974) 299.
12 C. C. Price and S. Oae (Editors), *Sulphur Bonding*, Ronald Press, New York, 1962.
13 F. G. Bordwell and G. D. Cooper, *J. Am. Chem. Soc.*, 73 (1951) 5187.
14 F. G. Bordwell and G. D. Cooper, *J. Am. Chem. Soc.*, 73 (1951) 5184.
15 C. S. Marvel and E. D. Weil, *J. Am. Chem. Soc.*, 76 (1954) 61.
16 S. Sugden, J. B. Reed and H. Wilkins, *J. Chem. Soc.*, (1925) 1525.
17 C. K. Ingold and J. A. Jessop, *J. Chem. Soc.*, (1930) 708.
18 A. Button and V. A. Welch, *J. Chem. Soc.*, 31 (1956) 3240.
19 B. M. Trost and M. R. Ghadirij, *J. Am. Chem. Soc.*, 108 (1986) 1098.
20 ICI Advanced Materials Vitrex PES High Temperature Thermoplastic Data Sheet, ICI, London.
21 J. K. Haken, N. Harahap and R. P. Burford, *J. Coat. Technol.*, 62 (1990) 780, 109.

Journal of Chromatography, 595 (1992) 289–299
Elsevier Science Publishers B.V., Amsterdam

CHROM. 23 912

Automated clean-up procedure for the gas chromatographic–high-resolution mass spectrometric determination of polychlorinated dibenzo-*p*-dioxins and dibenzofurans in milk

J. A. van Rhijn, W. A. Traag, W. Kulik and L. G. M. Th. Tuinstra*

State Institute for Quality Control of Agricultural Products, Bornesteeg 45, 6708 PD Wageningen (Netherlands)

(First received September 12th, 1991; revised manuscript received November 21st, 1991)

ABSTRACT

A highly automated extraction and clean-up method for polychlorinated dibenzodioxins and polychlorinated dibenzofurans is described. The method includes the use of gel permeation chromatography, alumina clean-up and porous graphitized carbon chromatography, followed by analysis by gas chromatography–high-resolution mass spectrometry. The procedure allows for the analysis of six milk samples per day in addition to two quality control samples and a blank. Detection limits on a fat basis for the individual congeners in milk samples are in the sub-ppt range. Long-term performance was investigated and data are given for reproducibility, precision and accuracy.

INTRODUCTION

Since the detection of polychlorinated dibenzodioxins (PCDDs) and polychlorinated dibenzofurans (PCDFs) in biological samples, analysis of these compounds has been subject of intense research [1–10]. The toxicological behaviour of these compounds has been reviewed by, *e.g.*, Van Zorge *et al.* [11]. Of the total of 75 possible PCDD congeners and 135 possible PCDF congeners, only the seventeen 2,3,7,8-chlorine-substituted compounds are of toxicological interest. Therefore, the development of methods of analysis has been focused on these most toxic congeners.

For convenience, the toxicity of all 2,3,7,8-chlorine-substituted congeners is expressed in toxic equivalents to the most toxic compound; 2,3,7,8-TCDD, by multipyling the amount of each congener with the toxic equivalence factors (TEF) published by Van Zorge *et al.* [11]. The total toxicity of all congeners can then be expressed as a single figure with the dimensions of toxic equivalent to 2,3,7,8-TCDD (TEQ).

The low concentration levels of these compounds in biological samples, typically in the low pg/g range, requires a highly sensitive and highly specific method of analysis. A combination of several different clean-up techniques must be used to obtain a sufficiently clean sample extract. Commonly used extraction and clean-up techniques include liquid–liquid partitioning [2–6,12,13], solid sorbent extraction [7], gel permeation chromatography [2–4,13], column chromatography using a variety of sorbents, *e.g.*, basic, acid or neutral alumina [2,4–6,8–10,12,13], silica [8,10], acid- or base-impregnated silica [5,8–10,13], Florisil [2–4], potassium silicate [8,10], caesium silicate [8,10] and carbon chromatography [2,5,6,8–10,13].

Carbon chromatography may be used for both the isolation and clean-up of the dioxins [5,6,12] or just for the separation of dioxins from interfering compounds [2,8–10,13]. Saponification for removal

0021-9673/92/$05.00

of the fat cannot be used as chemical modification of the dioxins may occur [14]. Even though extensive and selective clean-up is applied, some workers prefer to increase the selectivity even further by using tandem mass spectrometric methods [12].

Smith *et al.* [1] developed an analytical method employing several multilayer columns and carbon chromatography. This method has been adapted by several researchers [5,8,10] and, although the working procedure is laborious, it is probably one of the most often used methods of analysis. Recently, Liem *et al.* [6] developed an elegant method of analysis based on the use of a carbon sorbent for the isolation and clean-up of the dioxins and furans from milkfat.

In the Netherlands, the dioxin exhaust from municipal incinerators was recently found to be the main cause of unacceptably high dioxin levels in cows' milk in the locality. The large-scale inspection of cows' milk made the development of a method with a high capacity for clean-up and analysis necessary.

A common feature of all the methods described previously is the low sample throughput owing to laborious manual procedures. Therefore, these methods are not very suitable for routine analyses of large numbers of samples.

This paper describes a highly automated extraction and clean-up method based on gel permeation chromatography (GPC), alumina clean-up and carbon chromatography using a graphitized carbon high-performance liquid chromatographic (HPLC) column as described by Creaser and Al-Haddad [15]. Automated gas chromatographic–high-resolution mass spectrometric (GC–MS) measurement in combination with fully automated data processing is used for quantification.

The procedure allows for the clean-up and analysis of six milk samples per day in addition to two quality control samples and a procedural blank. The performance of the method with regard to repeatability and accuracy was tested by analysing samples of known content. The long-term performance was monitored using a set of two quality control samples which were analysed within each series of samples.

EXPERIMENTAL

Reagents and samples

All solvents were obtained from Merck (Darmstadt, Germany), except toluene, which was obtained from Promochem (Wesel, Germany). All solvents except toluene were distilled in glass prior to use. The toluene used was of nanograde quality and dit not introduce any interferences. BioBeads SX-3 were obtained from Bio-Rad Labs. (Veenendaal, Netherlands). Basic alumina, activity I, was obtained from Woelm (Eschwege, Germany). Prior to use, the alumina was deactivated with 7% demineralized water to achieve a quantitative recovery of the analytes.

Cows' milk samples were stored at −20°C until fat extraction. After fat extraction, the milk samples and the quality control samples were stored at room temperature.

Native and ^{13}C-labelled PCDD and PCDF standard mixtures were obtained from Cambridge Isotope Labs. (Woburn, MA, USA). All other reagents were of analytical-reagent grade.

Control samples

One quality control sample was a batch of milkfat originating from an industrial area in the Netherlands. The sample contained 2.62 pg of TEQ (toxicity equivalent to 2,3,7,8-TCDD) per gram of fat as revealed by repeated analysis. The other quality control sample was milkfat accurately spiked with PCDDs/PCDFs. Milkfat was first decontaminated using active carbon. Complete absence of PCDDs/PCDFs was confirmed by analysis. Thereafter, amounts of 2 pg per gram per compound of native PCDDs/PCDFs were added, the octachlorinated compounds were added at a level of 4 pg per gram of fat by addition of a dilute solution of the dioxin and furan congeners. This resulted in an artificially contaminated batch of milkfat containing 5.85 pg TEQ per gram.

Equipment

All glassware was successively washed with a detergent and flushed with hot water, acetone and demineralized water. The glassware was dried in an oven at 120°C and subsequently silanized using a 4% solution of dimethylchlorosilane (DMCS) in

toluene. Immediately before use, the glassware was rinsed with the organic solvent to be used.

The gel permeation chromatographic system consisted of a (Gilson Villiers le Bel, France) Model 305 HPLC pump, a Gilson Model 231-401 autosampler equipped to inject 12.5 ml of sample solution [16] and a Gilson Model 202 fraction collector adapted to collect fractions of 300 ml using 500-ml flasks as collection vessels. The GPC column, obtained from Spectrum (Los Angeles, CA, USA), was glass (60 cm × 2.5 cm I.D.), packed with BioBeads-SX_3 and equipped with adjustable plunger.

The basic alumina clean-up was performed with an instrument for automatic sample preparation with extraction columns (ASPEC, Gilson) for use with 3-ml disposable solid-phase extraction columns. Empty columns were purchased from Baker (Phillipsburg, NJ, USA). The columns were packed with 1.00 g of deactivated basic alumina shortly before use.

Carbon clean-up was performed with a HPLC system consisting of a Gilson Model 305 pump, a MUST column-switching device, including timer and solvent-select valve (Spark Holland, Emmen, Netherlands), a Gilson Model 231-401 autosampler, equipped with a 5-ml sample loop, and a Gilson Model 202 fraction collector adapted to take 100-ml flasks as collection vessels to collect fractions of 30 ml. A Hypercarb, porous graphitized carbon (PGC) column obtained from Shandon (Runcorn, UK) was used to separate the dioxins from non-planar co-extracted organic contaminants.

The GC–MS system consisted of an HP 5890 gas chromatograph (Hewlett Packard, Avondale, PA, USA), equipped with an HP 7673A autosampler, coupled to a VG Autospec-Q trisector (EBE) double-focusing mass spectrometer (VG Analytical, Manchester, UK) operated in the selected ion monitoring (SIM) mode at 10 000 mass resolution. Within each window, SIM was performed by adjusting the accelerating voltage. A dwell time of 50 ms per ion was used. Electron impact ionization was used with an electron energy of 35 V and a trap current of 500 μA.

Separation of the PCDDs and PCDFs was achieved on a 60 m × 0.25 mm I.D. DB5 column (film thickness 0.25 μm) obtained from J & W Scientific (Folsom, CA, USA).

Sample extraction and clean-up

Sample extraction. Milk samples were extracted using a quantitative liquid–liquid extraction method as described by Helrich [17]. To 150 ml of milk, sodium oxalate and ethanol were added. The fat was isolated by liquid–liquid extraction with diethyl ether and light petroleum (b.p. 40–60°C). The resulting fat-containing organic layer was dried over sodium sulphate and evaporated to dryness. The amount of fat remaining was determined by weight.

Gel permeation chromatography. An amount of 6 g of fat was dissolved in ethyl acetate–cyclohexane (1:1, v/v). This solution was fortified with 60 pg each of the ^{13}C-labelled PCDDs and PCDFs, resulting in a fortification level of 10 pg per compound per gram of fat. The solution was made up to 30 ml with ethyl acetate–cyclohexane (1:1, v/v) and mixed thoroughly. Two sample bottles were each filled with 15 ml of this solution. From the first bottle an aliquot of 12.5 ml, corresponding to 2.5 g of fat, was applied to the GPC column. The column was eluted at a flow-rate of 1 ml/min during sample transfer. After the sample had been applied, the flow-rate was increased to 5 ml/min. The dioxin-containing fraction was collected between 51 and 88 min. After 88.5 min, the flow-rate was reduced from 5 to 1 ml/min and from the second bottle again 12.5 ml were injected and the procedure was repeated. A second injection cycle is necessary to clean a total amount of 5 g of fat.

The dioxin-containing fractions were combined and 50 μl of dodecane were added. The solvent was evaporated at 40°C on a rotary evaporator to a volume of about 1 ml. The residue was quantitatively transferred into a sample tube using hexane as washing solvent and, using a gentle stream of nitrogen, evaporation was continued until only the dodecane was left. To the resulting residue 0.5 ml of hexane was added and the contents of the tube were mixed thoroughly using a vortex mixer.

Alumina clean-up. Using the ASPEC instrument, the alumina column was washed with 5 ml of hexane and the fraction of 0.5 ml resulting from the GPC clean-up was quantitatively transferred to the column. All solvent eluting from the column was collected starting from the moment of sample application. Then the dioxins were eluted with 3 ml of hexane and the eluate was collected. The resulting 3.5 ml of eluate were transferred to a sample bottle.

Graphitized carbon chromatography. The 3.5-ml hexane fraction resulting from the alumina clean-up was quantitatively transferred to the 5-ml sample loop of the autosampler. By switching the valve the sample was injected on to the PGC column. The column was successively eluted with cyclohexane–dichloromethane (1:1, v/v) and toluene, both at a flow-rate of 2 ml/min. When the column was eluted with cyclohexane–dichloromethane (1:1, v/v), the dioxins were retained whereas non-planar organic contaminants were eluted and discarded. After 30 min, the solvent was changed to toluene. After another 30 min the PGC column was eluted in the back-flush mode and the eluate was collected. The collection vessel was a 100-ml flat-bottomed flask which can be attached to the rotary evaporator. Collection took place during the first 15 min of the back-flush. Next the column was eluted in the back-flush mode with toluene for a further 15 min. The direction of the flow and the solvent was changed again and the column was regenerated with cyclohexane–dichloromethane (1:1, v/v) for 30 min. After this period the system was ready for injection of the next sample.

Preparation of the sample for GC–MS. The 30-ml toluene fraction resulting from the carbon chromatographic separation, was evaporated on a rotary evaporator to *ca.* 1 ml and quantitatively transferred to a tapered tube using hexane as washing solvent. The remaining solvent was evaporated under a stream of nitrogen. The walls of the tapered tube were flushed thoroughly with small volumes of hexane, typically decreasing from 200 to 50 μl. After complete evaporation of the solvent, the residue was dissolved in a 10-μl aliquot of the syringe standard solution containing 10 pg/μl of the syringe standard 1,2,3,4-[^{13}C]TCDD using a vortex mixer at low speed. The resulting sample extract was transferred to the insert of a GC autosampler vial using a syringe. A 50-μl insert was used (LC-Service, Emmen, Netherlands).

Gas chromatography–mass spectrometry

In order to perform GC–MS analyses continuously, the gas chromatograph was equipped with an autosampler. Aliquots of 2 μl of the samples were injected splitless on to a non-polar column and, using helium as the carrier gas, group separation of tetra-, penta-, hexa-, hepta- and octachlorinated congeners was achieved.

During sample injection the oven temperature of the gas chromatograph was set at 100°C and the injector temperature was kep at 280°C. After 3 min the temperature of the oven was increased to 200°C at 15°C/min and from 200 to 280°C at 4°C/min, the final temperature being maintained for 25 min. The interface between the GC and MS instruments was kept at 280°C. Injection by the autosampler, ramping of the GC oven temperature and acquisition of the MS data were synchronized by the use of the VG Sios interface.

The MS data acquisition is based on SIM. For each group of congeners with the same degree of chlorination, up to ten ions were monitored (see Table I). In general, the two largest peaks in the chlorine isotope cluster of the molecular ion were measured, except for [^{13}C]HxCDF and [^{13}C]HpCDF, because for these compounds MS interferences of the M + 4 peak from high levels of native HxCDD and HxCDF would be expected owing to a possible lack of GC resolution. Instead, for these two compounds the M^+ and $[M+2]^+$ ions were measured, these being the third largest and the largest peaks, respectively. An ion of perfluorkerosene (PFK) was used as lock-mass channel to correct for "magnet drift".

Relative response factors were determined from a calibration graph consisting of seven different levels of native congeners in the concentration range 100 fg/μl–10 pg/μl.

In Table I, for each level of chlorination of dioxins and furans, the monitored ions and the limits of their isotope ratios are given. The complete process from sequential injections up to and including quantification is fully automated.

RESULTS AND DISCUSSION

For positive identification of the congeners, the following criteria are adopted: the relative retention time of the unknown and the labelled compound must match, *i.e.*, the ratio of the retention time of the analyte (B) to that of the internal standard (A) should be equal to the relative retention time of the analyte in a calibration mixture within a margin of ± 5 s/A; and the isotope ratios, measured within the cluster of ions monitored, should be equal to the theoretical value within a margin of 15% (see Table I). If these criteria are satisfied, the recorded data

TABLE I

SOME ACQUISITION AND IDENTIFICATION PARAMETERS FOR SEVENTEEN 2,3,7,8-CHLORINE-SUBSTITUTED DIOXINS AND DIBENZOFURANS INCLUDING THEIR ^{13}C-LABELLED ANALOGUES

T = Tetra; Pe = penta; Hx = hexa; Hp = hepta; O = octa.

Compound	Selected ion ratio A/B[a]	*m/z*		Theoretical abundance, A/B
		A	B	
TCDF	M/M+2	303.90	305.90	0.77
TCDD	M/M+2	319.90	321.89	0.77
[^{13}C]TCDF	M/M+2	315.94	317.94	0.77
[^{13}C]TCDD	M/M+2	331.94	333.93	0.77
PeCDF	M+2/M+4	339.86	341.86	1.55
PeCDD	M+2/M+4	355.85	357.85	1.55
[^{13}C]PeCDF	M+2/M+4	351.90	353.90	1.55
[^{13}C]PeCDD	M+2/M+4	367.89	369.89	1.55
HxCDF	M+2/M+4	373.82	375.82	1.24
HxCDD	M+2/M+4	389.82	391.82	1.24
[^{13}C]HxCDF	M/M+2	383.86	385.86	0.51
[^{13}C]HxCDD	M+2/M+4	401.86	403.85	1.24
HpCDF	M+2/M+4	407.78	409.78	1.03
HpCDD	M+2/M+4	423.78	425.77	1.03
[^{13}C]HpCDF	M/M+2	417.83	419.82	0.44
[^{13}C]HpCDD	M+2/M+4	435.82	437.81	1.03
OCDF	M+2/M+4	441.74	443.74	0.89
OCDD	M+2/M+4	457.74	459.73	0.89
[^{13}C]OCDD	M+2/M+4	469.78	471.78	0.89

[a] M = Molecular ion, containing ^{35}Cl exclusively.

are used for quantification. The quantification was performed using the isotope dilution method [13], thus correcting for possible losses of compounds during the extraction and clean-up procedure.

The described method was initially tested for accuracy and repeatability by analysing six samples of an artificially contaminated milkfat containing 2 pg of each compound per gram of fat, except for the octachlorinated congeners, which were present at 4 pg/g. Expressed in 2,3,7,8-TCDD equivalents (TEQ), the sample contains 5.85 pg TEQ per gram of fat.

The mean concentration of the individual congeners (pg/g fat), as determined for these six samples, are given in Table II. From these data, it follows that both the accuracy and repeatability are good: the mean accuracy expressed in pg TEQ per gram of milkfat as compared with the content known from the addition of dioxins was 106%; the accuracy ranged from 97% to 131%, except for OCDD, which showed an accuracy of 158%, indicating too high results. In general, the results of analysis for a few compounds are systematically high. Analysis of the contaminated fat does not show any background contribution for these compounds. Until now the reason for these high results is unknown. Especially for OCDD several other groups seem to have had the same problem concerning high results.

The determination of the TEQ value of the sample, *i.e.*, the sum of TEQ values of the individual congeners, shows a relative standard deviation (R.S.D.) of 6.8%. The mean R.S.D. is 11.8% for the determination of the individual congeners. Obviously, to some extent, random fluctuations in the amounts of the individual congeners are ruled out by calculation of the TEQ value for the seventeen congeners.

TABLE II

RESULTS OF THE ANALYSIS OF ARTIFICIALLY CONTAMINATED MILKFAT (QCS 2), USED TO ESTABLISH THE INITIAL PERFORMANCE OF THE DESCRIBED METHOD OF ANALYSIS ($n=6$)

Compound	TEF	Mean (pg/g)	S.D. (pg/g)	R.S.D. (%)	Accuracy (%)
2,3,7,8-TCDF	0.1	2.05	0.28	13.6	97.4
2,3,7,8-TCDD	1	2.22	0.26	11.7	99.3
1,2,3,7,8-PeCDF	0.05	2.03	0.16	7.8	104.5
2,3,4,7,8-PeCDF	0.5	2.04	0.16	7.8	106.2
1,2,3,7,8-PeCDD	0.5	1.96	0.21	10.5	99.2
1,2,3,4,7,8-HxCDF	0.1	2.20	0.18	8.3	114.4
1,2,3,6,7,8-HxCDF	0.1	2.25	0.18	8.1	108.9
2,3,4,6,7,8-HxCDF	0.1	2.51	0.29	11.4	120.7
1,2,3,7,8,9-HxCDF	0.1	2.22	0.19	8.5	125.3
1,2,3,4,7,8-HxCDD	0.1	2.34	0.43	18.4	109.8
1,2,3,6,7,8-HxCDD	0.1	2.46	0.25	10.1	109.0
1,2,3,7,8,9-HxCDD	0.1	2.13	0.31	14.7	98.7
1,2,3,4,6,7,8-HpCDF	0.01	2.55	0.38	15.0	120.9
1,2,3,4,7,8,9-HpCDF	0.01	2.27	0.30	13.3	115.7
1,2,3,4,6,7,8-HpCDD	0.01	2.83	0.56	19.9	130.9
OCDF	0.001	4.42	0.47	10.7	106.7
OCDD	0.001	5.77	0.69	11.9	157.6
Total TEQ (pg/g)		6.23	0.43	6.8	98.6

The analyses of the other quality control sample originating from an industrial area in the Netherlands showed similar results on repeatability; the mean R.S.D. is 9.6% ($n=4$) for the determination of individual congeners; the R.S.D. of the TEQ value of this sample is 6.3%. The accuracy cannot be estimated for this sample as its true value is unknown.

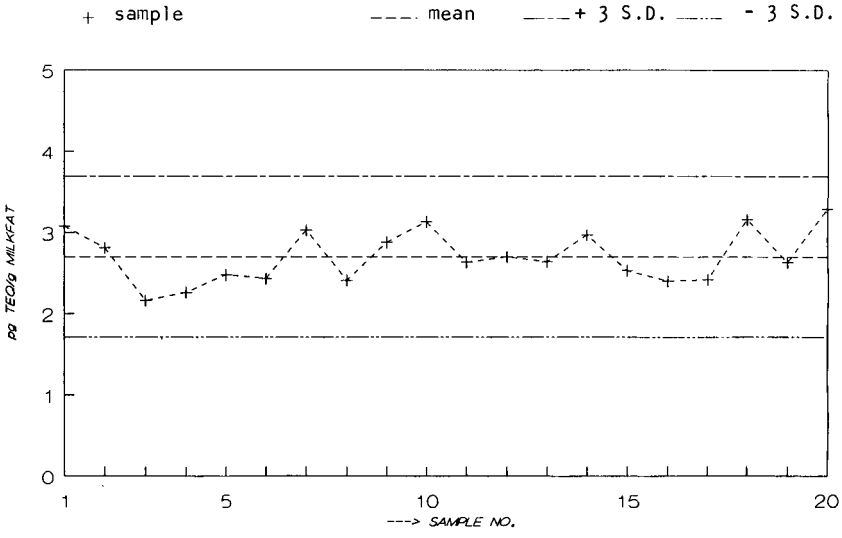

Fig. 1. Quality control chart based on data resulting from the analysis of quality control sample 1 (QCS 1) (see text) during a period of 3 months.

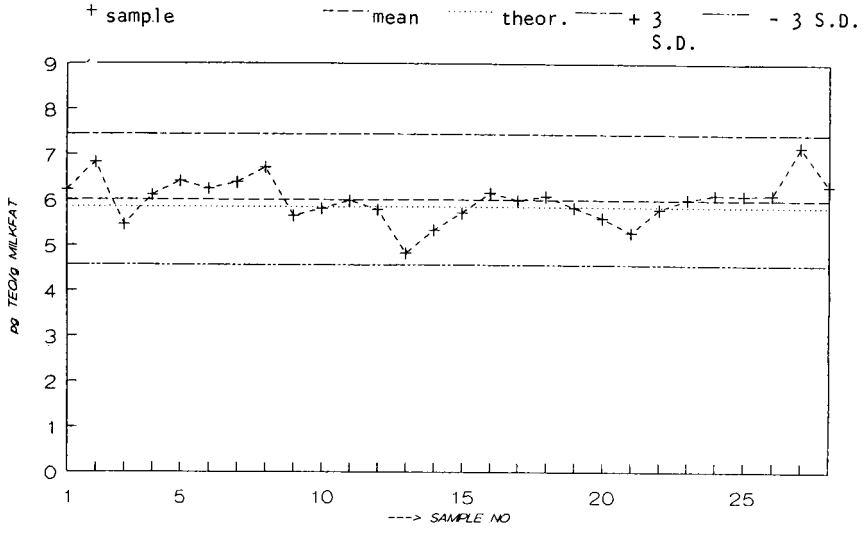

Fig. 2. Quality control chart based on data resulting from the analysis of quality control sample 2 (QCS 2) (see text) during a period of 3 months.

The method has been applied over a period of 3 months to the analyses of 180 samples of cows' milk in an excretion experiment with lactating cows [18]. In each series of twelve unknown samples, a set of at least three quality control samples (QCS) is analyzed, *i.e.*, one aliquot of the milk fat from a contaminated area (QCS 1), one aliquot of the artificially contaminated milkfat (QCS 2) and a blank (QCS 3) that is taken through the entire procedure. The blank is processed after quality control samples 1 and 2. From these data, the long-term reproducibility of the results is found to be good. The mean result for QCS 1 from twenty measurements (over a 3-month period) was 2.62 pg TEQ/g milkfat with R.S.D. = 11.5% (Fig. 1). The mean result for QCS 2 from 28 measurements (within the same period) was 6.04 pg TEQ/g milkfat with R.S.D. = 9.0% (Fig. 2).

The blanks did not contain any dioxins above the limit of determination. These results show that the long-term reproducibility, even with the low TEQ values occurring in biological samples, can be very good. The mean recovery, as calculated from all 228 samples that were analysed during the 3-month period (*i.e.*, including both unknown samples and quality control samples), ranged from 54.7 ± 26.5% for 2,3,7,8-TCDD to 76.9 ± 54.2% for OCDD. It should be noted that with isotope dilution, the percentage is of limited importance as the calculation of the amounts should not be a function of the recovery. A low recovery, however, results in a high limit of determination. For this reason, we require minimum recovery of about 25% for the three most important congeners, *viz.*, 2,3,7,8-TCDD, 1,2,3,7,8-PeCDD and 2,3,4,7,8-PeCDF, which together contribute about 75% to the total TEQ value of Dutch cows' milk.

Fig. 3 and 4 show parts of chromatograms of a calibration standard and a milk sample, respectively. Only the tetra- and pentachlorinated congeners are shown as these are the most important compounds with respect to their TEF values. The chromatograms reveal that milk samples (Fig. 4) are effectively cleaned by the described method; no major interferences are present. The total TEQ value for the milk sample shown is 2.65 pg TEQ per gram of fat. Therefore, it is obvious that the method is sufficiently sensitive to analyse even low-contaminated biological samples.

The limit of determination (LOD) is estimated to be about 0.5 pg TEQ per gram of milkfat. Environmental contamination may have its own specific pattern of congeners depending on the local sources of pollution. As the LOD is dependent on the relative amounts of the seventeen congeners, it is therefore also dependent on the type of sample and on

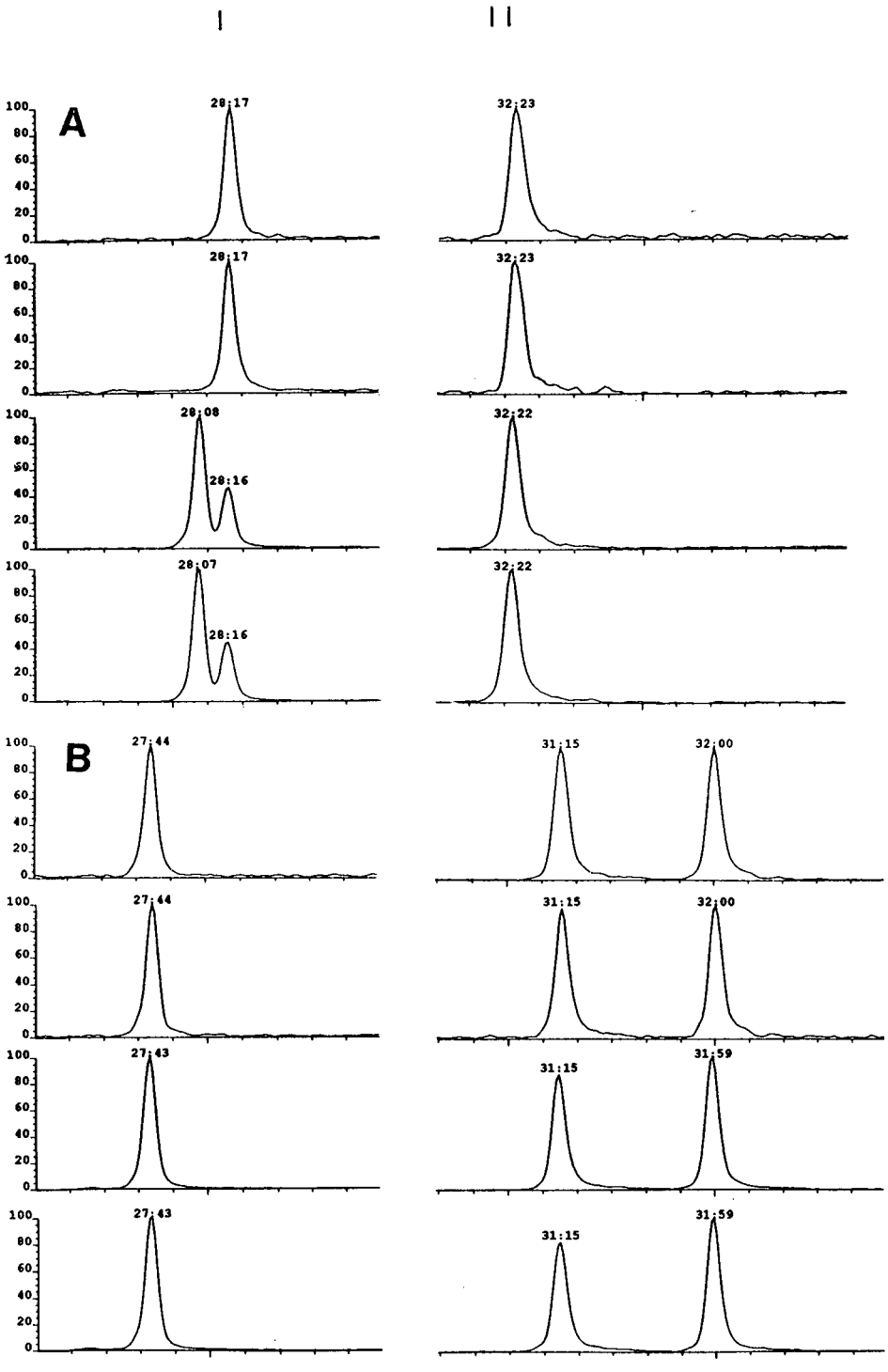

Fig. 3. Parts of a chromatogram of a calibration standard at a level of 1 pg/μl showing 2,3,7,8-TCDD and 1,2,3,4-[^{13}C]TCDD (internal standard) (A, I), 1,2,3,7,8-PeCDD (A, II), 2,3,7,8-TCDF (B, I) and 1,2,3,7,8-PeCDF and 2,3,4,7,8-PeCDF (B, II). The two upper traces show the ions of the native compounds and the lower traces show the ^{13}C-labelled analogues. Ions monitored according to Table I. From top to bottom, ions are of increasing *m/z* value. Peaks are labelled with retention time (min)

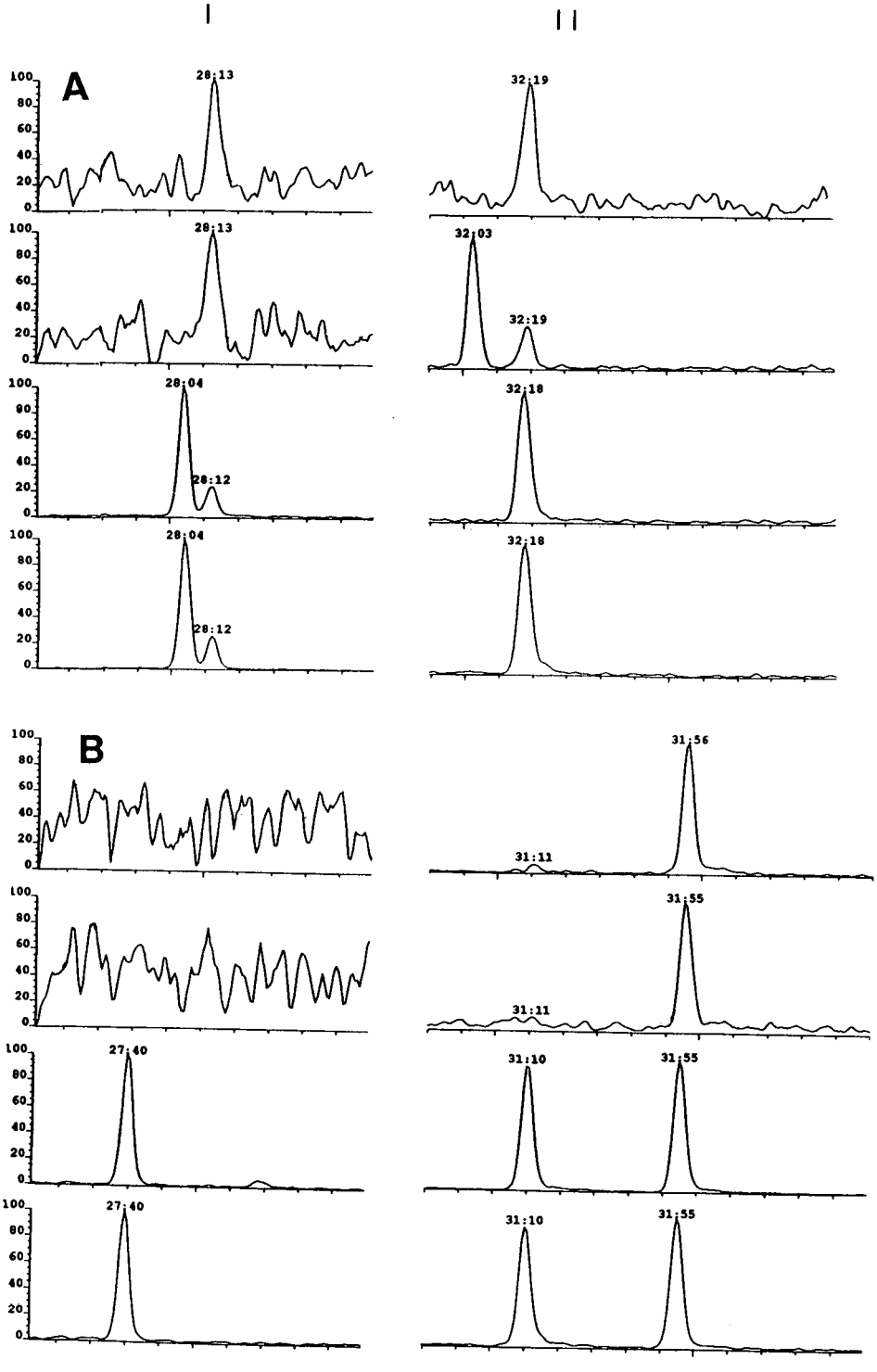

Fig. 4. Parts of a chromatogram of an extract of milkfat showing the acquisition windows of tetra- and pentachlorinated congeners as in Fig. 3. The two upper traces show the ions of the native compounds and the lower traces show the ^{13}C-labelled analogues. Ions monitored according to Table I. From top to bottom, ions are of increasing m/z value. Peaks are labelled with retention time (min). It can be seen that 2,3,7,8-TCDF and 1,2,3,7,8-PeCDF are absent in milkfat.

the area from which it originates. Further, the LOD is dependent on the presence of interferences which may be matrix dependent. As mentioned before, there are no significant interferences caused by extracts of milkfat, which may be partly due to the fact that milkfat is relatively clean in comparison with other matrices, but it is also a result of the highly selective method used.

One problem involving interfering compounds was the occurrence of large amounts of phthalates in the part of the chromatogram where the pentachlorinated congeners elute. These amounts were large enough to disturb the ionization conditions in the ion source of the mass spectrometer. The phthalates are suspected to be present in solvents and packing material. We reduced this problem to such an extent by introducing the alumina clean-up that the analysis was not hindered by the presence of the phthalates.

The graphitized carbon column shows some tailing on the elution profile of the dioxins. When samples with widely differing contents are analysed, some cross-contamination may occur. This cross-contamination is of the order of 1–4% of the preceding sample, but may be decreased by eluting with toluene in the back-flush mode for a longer period, at the expense of a lower sample throughput.

CONCLUSIONS

The proposed method gave reproducible and accurate results for milkfat samples. When the results are expressed in pg TEQ per gram of fat, the mean accuracy was 103% ($n=28$) for a sample that was artificially contaminated at the Dutch tolerance level. The repeatability was good, with R.S.D. of 8.6% for the determination of TEQ values and 11.8% for the determination of individual congeners. The long-term performance was evaluated using two different quality control samples and was excellent. QCS 1 gave a mean result of analysis of 2.65 pg TEQ/g with R.S.D. = 11.5% ($n=20$). The mean result of analysis of QCS 2 was 6.04 pg TEQ/g with R.S.D. = 9.0% ($n=28$).

The chromatograms show efficient clean-up of the sample extracts, as no interferences are present. By applying a high degree of automation and organization, high sample throughputs can be achieved which cannot be matched by other methods at the same level of contamination. The described clean-up method is highly automated using Gilson x–y–z robots for injection, fraction collection and solid-phase extraction. This results in a high sample throughput as compared with other methods [10]. With three skilled technicians, the clean-up and MS analysis of six unknown samples per day are possible. In each series of twelve unknown samples, a set of three quality control samples can be handled at the same time by the same technicians. To achieve this, strict organization of the procedure is necessary.

ACKNOWLEDGEMENTS

The authors thank Mr. P. W. J. Kolkman and R. J. van Mazijk for their assistance.

REFERENCES

1 L. M. Smith, D. L. Stalling and J. L. Johnson, *Anal. Chem.*, 56 (1984) 1830–1824.
2 P. Fürst, Chr. Fürst, H. A. Meemken and W. Groebel, *Z. Lebensm.-Unters.-Forsch.*, 189 (1989) 338–345.
3 P. Fürst, H. A. Meemken and W. Groebel, *Chemosphere*, 15 (1986) 1977–1980.
4 P. Fürst, H. A. Meemken, Chr. Krüger and W. Groebel, *Chemosphere*, 16 (1987) 1983–1988.
5 A. K. D. Liem, G. S. Groenemeijer, G. A. L. de Korte, A. van Laar, J. A. Marsman, A. P. J. M. de Jong and R. C. C. Wegman, *Water Pollution Research Report Series No. 5*, EUR 11355, Commission of the European Communities, 1988, pp. 76–89.
6 A. K. D. Liem, A. P. J. M. de Jong, J. A. Marsman, A. C. den Boer, G. S. Groenemeijer, R. S. den Hartog, G. A. L. de Korte, R. Hoogerbrugge, P. R. Kootstra and H. A. van 't Klooster, *Chemosphere*, 20 (1990) 843–850.
7 K. Norén and A. Lundén, in O. Hutzinger and H. Fieldler, (Editors), *Proceedings, 10th International Meeting on Dioxins, Bayreuth, 10–14 September 1990*, Ecoinforma Press, Bayreuth, Vol. 1, 1991, pp. 263–266.
8 P. Schmid, M. E. Suter-Hofmann and Ch. Schlatter, *Chemosphere*, 18 (1989) 1741–1748.
9 Y. Tondeur, W. F. Beckert, S. Billets and R. K. Mitchum, *Chemosphere*, 18 (1989) 119–131.
10 S. G. Isaacs, W. E. Turner and D. G. Patterson, Jr., in O. Hutzinger and H. Fieldler (Editors), *Proceedings, 10th International Meeting on Dioxins, Bayreuth, 10–14 September 1990*, Ecoinforma Press, Bayreuth, Vol. 2, 1991, pp. 149–152.
11 J. A. van Zorge, J. H. van Wijnen, R. M. C. Theelen, K. Olie and M. van den Berg, *Chemosphere*, 19 (1989) 1881–1895.
12 A. P. J. M. de Jong, A. K. D. Liem, A. C. den Boer, E. van der Heeft, J. A. Marsman, G. van de Werken and R. C. C. Wegman, *Chemosphere*, 19 (1989) 59–66.

13 W. A. Teilliard, H. B. McCarty and J. R. King, in O. Hutzinger and H. Fieldler (Editors), *Proceedings, 10th International Meeting on Dioxins, Bayreuth, 10–14 September 1990*, Ecoinforma Press, Bayreuth, Vol. 2, 1991, pp. 303–306.
14 J. Ryan, R. Lizotte, L. G. Panopio and B. P. Y. Lan, *Chemosphere*, 18 (1989) 149–154.
15 C. S. Creaser and A. Al-Haddad, *Anal. Chem.*, 61 (1989) 1300–1302.
16 L. G. M. Th. Tuinstra, J. A. van Rhijn, A. H. Roos, W. A. Traag, R. J. van Mazijk and P. J. W. Kolkman, *J. High Resolut. Chromatogr.*, 13, (1990) 797–801.
17 K. Helrich, (Editor), *Official Methods of Analysis of the Association of Official Analytical Chemists*, Vol. 1, Association of official Analytical Chemists, Arlington, VA, 15th ed., 1990, Section 970.52.
18 A. H. Roos, P. L. M. Berende, W. A. Traag, J. A. van Rhijn, M. J. B. Mengelers and L. G. M. Th. Tuinstra, *Excretion of Polychlorinated Dibenzo-p-dioxins and -furans in Milk of Cows fed on Dioxins in the Dry Period (in Dutch) Report 91.01*, State Institute for Quality Control of Agricultural Products (RIKILT-DLO), Wageningen, 1991.

Journal of Chromatography, 595 (1992) 301–311
Elsevier Science Publishers B.V., Amsterdam

CHROM. 23 887

Quantitative hydrocarbon group analysis of gasoline and diesel fuel by supercritical fluid chromatography

Per E. Andersson, Mustafa Demirbüker and Lars G. Blomberg*

Department of Analytical Chemistry, University of Stockholm, Arrhenius Laboratory, 106 91, Stockholm (Sweden)

(First received September 10th, 1991; revised manuscript received November 20th, 1991)

ABSTRACT

A two-dimensional supercritical fluid chromatographic system is described for the determination of saturates, alkenes and mono-, di- and tri-aromatics in gasoline and diesel fuel. Aromatics were isolated from saturates/alkenes and group separated according to the number of aromatic rings on a capillary column packed with silica of particle size 4 μm. The alkenes were separated from saturates on a 38-mm capillary column packed with a silica-based cation exchanger which had been modified *in situ* with silver nitrate. Elution of alkenes was facilitated by the use of a relatively high column temperature, 65°C, and operation in the back-flush mode. Carbon dioxide was used as the mobile phase. Relative standard deviations were generally in the range 0.4–20.0%. At a low content of alkenes, 0.5%, a relative standard deviation of 8.4% was achieved. The analysis time was under 8 min. The utility of the method is demonstrated by the analysis of feedstock before and after hydration.

INTRODUCTION

The determination of saturates, alkenes and aromatics in petroleum products has for many years been performed by the fluorescent indicator adsorption (FLIA) method [1]. However, this method suffers from the problems [2] that manual detection leads to low precision, the applicability is limited for samples containing significant amounts of pentane or lighter fractions, or materials with an end-point above 315°C, and the analysis times are relatively long.

In recent years, appreciable efforts have been made to develop procedures that could replace the FLIA method [3]. Mass spectrometry and nuclear magnetic resonance have been applied [4–6]. Recently, a method utilizing near-infrared spectrometry was presented [7]. It is evident that greater opportunities for improvement are offered by introducing greater instrumentation, making use of high-performance liquid chromatography (HPLC). Various types of separation columns have been used. Suatoni *et al.* [8,9] achieved the separation of saturates, alkenes and aromatics from a heavy gasoline distillate by the use of a silica column and a low-polarity perfluorocarbon mobile phase. This method was further investigated by Miller *et al.* [10]. Separation of saturates and alkenes was obtained also by Matsushita *et al.* [11] using a dual-column system consisting of a silica column followed by a silica column impregnated with silver nitrate. The latter column type is unstable, silver nitrate gradually being rinsed from the column. A much higher stability is achieved when a silica-based cation exchanger is used as the support for the silver ions. Such columns have been used in more recent work [12,13]. Further, in an IP method, amino columns are recommended for the separation of aromatic hydrocarbons in diesel fuel [14]. In this method, separation takes *ca.* 30 min. An amino-bonded silica column followed by a silica column was used in an HPLC–capillary gas chromatographic (GC) system for the characterization of diesel fuels [15]. Separation of the saturates into the acyclic and cyclic alkane groups on columns packed with polystyrene–divinylbenzene copolymer particles in LC [13,16] and molecular sieve 13X in GC [17,18] has been demonstrated. Further, an HPLC–

0021-9673/92/$05.00

GC system containing a molecular sieve 13X GC column for paraffins, olefins, naphthenes and aromatics (PONA) analysis has recently been introduced by Chrompack (Middelburg, Netherlands).

Separation of the different hydrocarbon groups is generally obtained by HPLC, the analysis greatly hampered, however, by the lack of suitable universal detectors. Refractive index (RI) and UV detectors have been used, but extensive calibration of these detectors is required owing to their specificity to certain types of compounds. Use of RI and UV detectors in tandem has also been reported [16,19]. The IR detector has also been employed [10,11]; the relative response factors of this detector spanned a wide range, thus limiting the methods to a particular distillate product. Dielectric constant detection (DCD) has been used in the HPLC analysis of fuels [12–13,20–22). DCD was reported to have a uniform response when used in connection with mobile phases having high dielectric constants. However, the Freon mobile phase is expensive.

Flame ionization detection (FID) gives an almost equal response for a wide range of hydrocarbons, and is therefore ideal for the analysis of petroleum products. However, FID is not suitable for HPLC of lighter fractions, but can readily be used in connection with compressed fluids, *e.g.*, when carbon dioxide, in a supercritical or subcritical state, is employed as the mobile phase. A number of papers on the analysis of fuels by means of supercritical fluid chromatography (SFC)–FID have appeared [2,3,6, 23–32]. The columns used for SFC have largely been of the same type as those employed in HPLC. Column types and conditions have been selected according to the aim of the analysis. Separation on a silica column has been shown to be sufficient for the determination of alkanes and mono-, di- and triaromatics. When it is of interest to determine alkenes, *e.g.*, in gasoline, diesel and jet fuel, silica–silver-loaded cation exchangers have been employed [29]. For group separation of crude oils, a system consisting of two cyano columns and one silver-loaded cation exchanger has been used [3]. Asphaltenes and resins were eluted from the first column by back-flushing.

There is a clear connection between the composition of the fuel and the exhaust gas of automobiles. Currently, there is interest in developing new fuels which on combustion will emit compounds that are less toxic. Alkenes may cause coating of injection nozzles and valves, which leads to impaired combustion and more toxic exhaust gases. It is therefore of interest that the content of alkenes in the fuels is low. In this connection, analytical methods for the determination of low levels ($< 2\%$) of alkenes in fuels would be needed. Few methods for the determination of alkenes in gasoline and diesel fuels at these concentration levels have appeared [29,33].

The aim of this work was to develop a method, based on packed capillary SFC using neat carbon dioxide as the mobile phase, for the quantitative analysis of petroleum distillation fractions used for fuels.

EXPERIMENTAL

Analyses were performed on a Lee Scientific (Salt Lake City, UT, USA) 600 Series SFC system connected to an ELDS (Kungshög, Sweden) data system. The columns were connected to the injector, two Valco (Houston, TX, USA) N6W six-port switching valves and detector by means of fused-silica capillary tubing (50 μm I.D.). Transfer lines were connected to the columns and to the restrictor by capillary mini-unions with MVSU/004 and MDGF/005 ferrules (SGE, Ringwood, Victoria, Australia). The tops of the FS.25 polyimide ferrules (Valco) that were used in these unions were filed flat. A frit restrictor (Lee Scientific) (50 μm I.D.), adjusted to give a linear flow-rate of *ca.* 5.5 mm/s, was used. A diagram of the column-switching system is shown in Fig. 1. Carbon dioxide of SFC grade, (Scott Specialty Gases, Plumsteadville, PA, USA) was used as the mobile phase. Samples were introduced without dilution using a 60-nl internal sample loop valve (Valco). A splitting ratio of 1:1 and a timed split of 0.2 s were used.

Columns were prepared from fused-silica capillary tubing of 250 μm I.D. and 430 μm O.D. (Polymicro Technology, Phoenix, AZ, USA). The packed bed was supported by a glass-fibre filter [34].

All columns were prepared using a slurry packing technique as described previously [34]. Superspher Si 60 (4 μm) (Merck, Darmstadt, Germany) and Nucleosil 5 SA (Macherey–Nagel, Düren, Germany) were used as packing materials. Impregnation with Ag^+ was carried out as described previously [35].

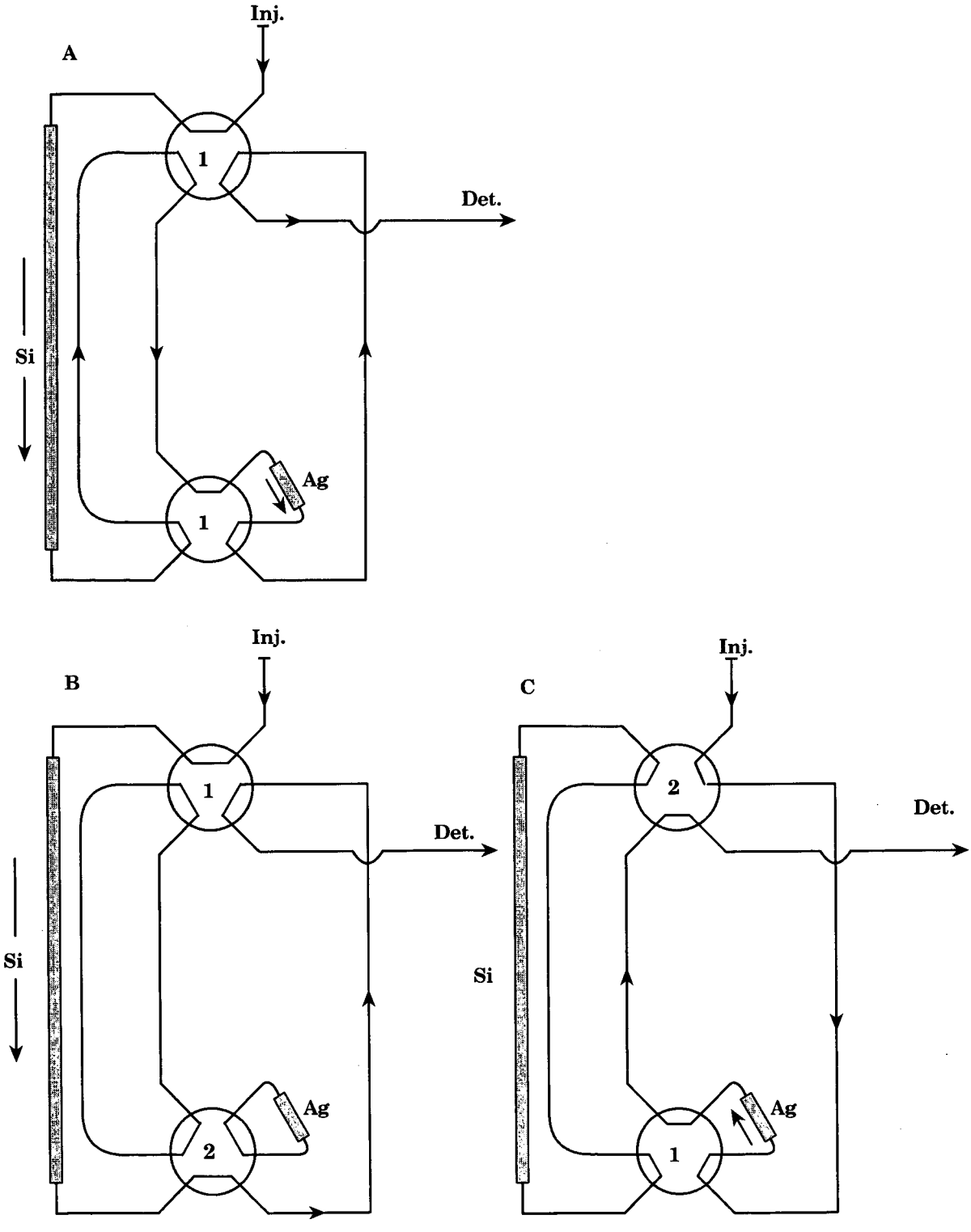

Fig. 1. Schematic diagram of the column-switching system. (A) Separation on the Si column, saturates and alkenes transferred to the Ag column; (B) aromatics transferred from Si column to flame ionization detector; (A) saturates eluted from the Ag column; (C) alkenes back-flushed from the Ag column.

A series of fuels was analysed. The compositions of the lead-free gasolines F1–F4 and the diesel fuels D1, D2 and D4–D9 have been described elsewhere [36,37]. Samples of feedstock were obtained from Neste (Porvoo, Finland).

Separations were performed at 300 atm and 65°C. Injection of the sample was made on the silica column, where the aromatics were retained. The saturates and alkenes were transferred to the silver-loaded cation-exchange column. This column was then switched out of the system and the aromatics were eluted from the silica column directly to the flame ionization detector. The saturates were then eluted from the argentation column and detected by FID. Finally, the alkenes were back-flushed from the argentation column and detected. In addition, the system allows back-flushing of the silica column.

RESULTS AND DISCUSSION

Separation on the silica column

Performance under different conditions was investigated. First, it was found that the retention of alkanes was influenced to a much greater extent than that of aromatics by the mobile phase density. At a density of 0.67 g/cm^3, tetracosane and benzene co-eluted. This was observed at 100°C and 300 atm and also at 65°C and 184 atm. At 130°C and 200 atm, density 0.38 g/cm^3, benzene was eluted before heptadecane. At higher densities, 0.82 g/cm^3, which here was obtained at 65°C and 300 atm, the alkanes and alkenes eluted as a single peak. Lee *et al.* [24] found that in the range 0.88–0.93 g/cm^3, at 35°C, the retention was only slightly influenced by mobile phase density. However, at a density of 0.58 g/cm^3, which was obtained at 90°C and 221 atm, severe overlap between saturates and aromatics was observed.

The second factor to be considered concerns the pressure drop over the column. Such a pressure drop creates a density gradient over the column, which can be significant at temperatures close to critical, where density is highly pressure dependent. Further, the pressure drop will, of course, increase with increasing column length and decreasing particle size. Finally, the restriction over the column would be so high that, in order to maintain a sufficiently high mobile phase flow-rate, only a small restriction can be attached to the column end. Further, the degree of restriction applied is decreased with decreased inlet pressures and increased mobile phase flow-rates. Adverse combination of the above-mentioned factors resulted in decreased performance; the mobile phase density was too low for elution of solutes that have low mobile phase solubility. The conditions used were 30°C and 115 atm with a mobile phase velocity of 5.5 mm/s, using a 320-mm column, packed with 4-μm silica particles. The performance was, however, much improved when a restrictor giving a mobile phase velocity of 1.8 mm/s was used. Low temperatures for separation of fuels on silica columns were used by Di Sanzo and Yoder [32] and Lee *et al.* [24], *viz.*, 30°C and 115 atm and 35°C and 245 atm, respectively. No adverse effect of pressure drop was observed with the columns and flow-rates applied; the columns were 250 mm long, packed with 5-μm particles, and the mobile phase velocity was 0.6 mm/s [32] and 1.3 mm/s [24].

The use of low column temperatures may lead to some complications. Relatively long equilibration times are required to attain stable conditions at 30°C. Moreover, heat from the detector may destabilize the conditions. Further, in the region close to the critical temperature, the density, and thereby retention, changes drastically with temperature. In this work, separation was performed at 65°C and 300 atm, density 0.82 g/cm^3, on a 320-mm microcolumn packed with 4-μm silica particles. The mobile phase velocity was 5.5 mm/s. An optimum velocity of *ca.* 5 mm/s has been reported for a similar column system [38]. The conditions have thus been traded to advantage to give separations of the groups of interest and a high speed of analysis. In comparison with previous work [24,32], our method results in better resolution and shorter analysis times.

The requirements on the silica column are more stringent for the separation of diesel fuel samples than for gasoline samples as shown by the separation of commercial fuels shown in Figs. 2 and 3. Separation of saturates and alkenes from aromatics can be difficult for heavy commercial diesel fuels. Highly alkylated aromatics have relatively short retention times, *e.g.*, triethylbenzene is eluted before benzene (Table I). Such aromatics may elute relative close to peak 1. The improved separation

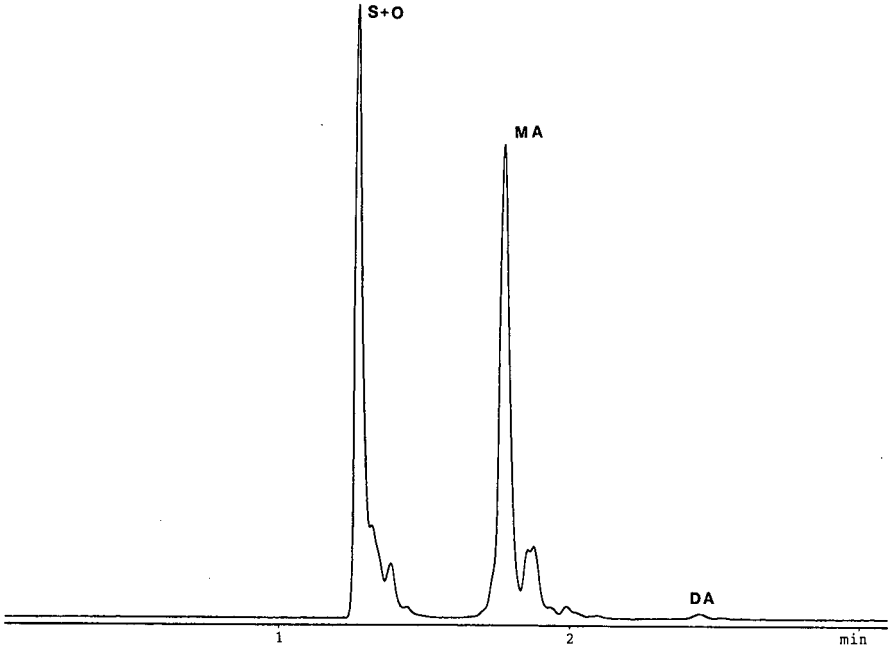

Fig. 2. Supercritical fluid chromatogram (FID) of gasoline F4 on a fused-silica column (320 mm × 0.25 mm I.D.), packed with Superspher Si 60, 4 μm. Mobile phase, carbon dioxide; 65°C and 300 atm. Peaks: S = saturates; O = alkenes; MA = monoaromatics; DA = diaromatics.

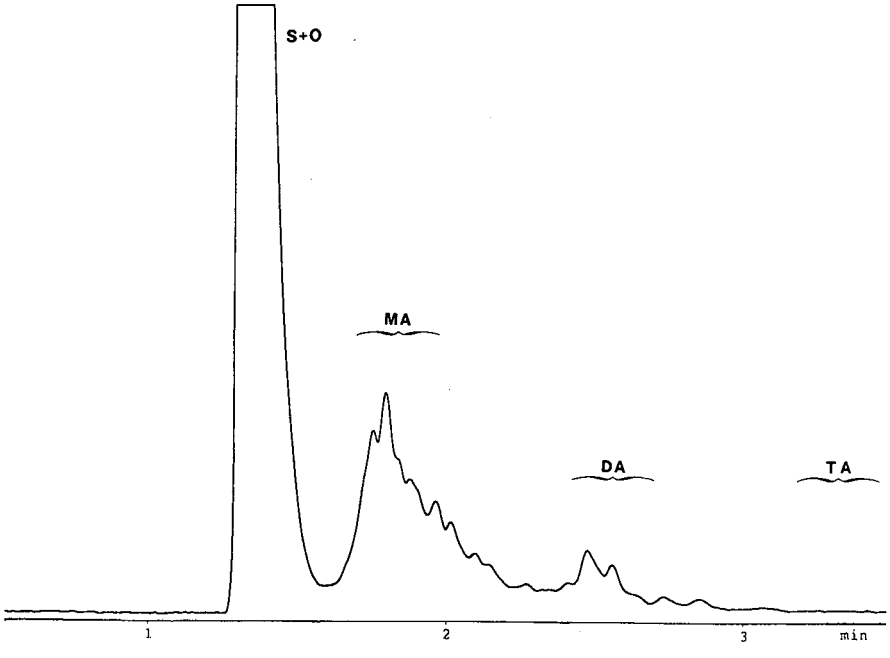

Fig. 3. Supercritical fluid chromatogram (FID) of diesel fuel D6. Column, conditions and peaks as in Fig. 2, TA = triaromatics.

TABLE I

RETENTION OF STANDARD COMPOUNDS ON A MICROCOLUMN PACKED WITH SILICA PARTICLES

Compound	Retention time (min)
Hexane	1.03
Decane	1.03
Tetracosane	1.07
Cyclohexane	1.07
2-Methyl-2-butene	1.08
1-Hexadecene	1.08
Decahydronaphthalene	1.13
Triethylbenzene	1.35
Benzene	1.39
Propylbenzene	1.39
Naphthalene	1.88
Anthracene	2.80

achieved in this work is due mainly to the use of small spherical silica particles having a high surface area; some improvement was obtained by increasing the column length. The chromatographic performance of the silica column was maintained throughout this investigation.

In the present system, it is possible to reverse the mobile phase flow on the silica column. The elution of triaromatics and polar compounds is thereby improved.

Separation on the silver-loaded cation-exchange column

The group separation of petroleum liquids by SFC and a dual-column system consisting of a silica column and a silica column impregnated with silver nitrate was first reported by Norris and Rawdon [2].

TABLE II

RETENTION OF STANDARD COMPOUNDS ON A MICROCOLUMN PACKED WITH A SILVER-MODIFIED CATION EXCHANGER

Compound	Retention time (min)
Hexane	0.38
Decane	0.38
Tetracosane	0.38
Benzene	0.64
2-Methyl-2-butene	0.84
1-Hexadecene	4.0

Later, Campbell *et al.* [29] reported that they were unable to reproduce this work. The observed irreproducibility may be explained by the fact that silver nitrate is successively leached out from the impregnated column. The chromatograms presented by Norris and Rawdon [2] therefore ought to have been produced on partially impregnated silica.

Fused-silica capillaries, packed with a silica-based cation exchanger, and modified *in situ* with Ag^+, have been used for the separation of triacylglycerols [34,35]. These columns were highly stable under SFC conditions, and maintained their retention properties even after heat treatment to 130°C. The strength of the silver–alkene complexes formed in silver-loaded columns decreases with increasing temperature, and excessive retention times can easily be avoided by the use of increased column temperatures.

Alkenes and aromatics are selectively retained on an Ag^+-containing argentation column (Table II). In our system, the aromatics will however, never enter this column, but are switched directly to the flame ionization detector from column 1. Further, an argentation column is farily sensitive towards non-elutable compounds, and is therefore protected by column 1. With such protection, the chromatographic properties of the silver column did not change even after more than 100 fuel injections.

Branched alkenes are much less retained than linear alkenes [39], and co-elution of long *n*-alkanes and short isoalkenes may occur in gasoline analyses. Such co-elution was not observed with the columns used here (Table II). Diesel fuels consist of more high-boiling fractions, and it seems that the separation of saturates and alkenes can be achieved relatively easily in this instance. A large difference in retention was, for example, observed for *n*-tetracosane and 1-hexadecene (Table II).

Alkenes present in diesel fuels have, in general, a relatively high molecular weight and often occur in concentrations less than 2 vol.% [22]. It may therefore be difficult to elute them from the silver column as measurable peaks. Two steps were taken to make elution feasible. First, a relatively high column temperature, 65°C, was applied, the strength of the olefin–silver complex thereby becoming weakened. Second, alkenes were eluted from the silver column in the back-flush mode immediately after the straight elution of the saturates. Further, the length of the silver column is only 38 mm.

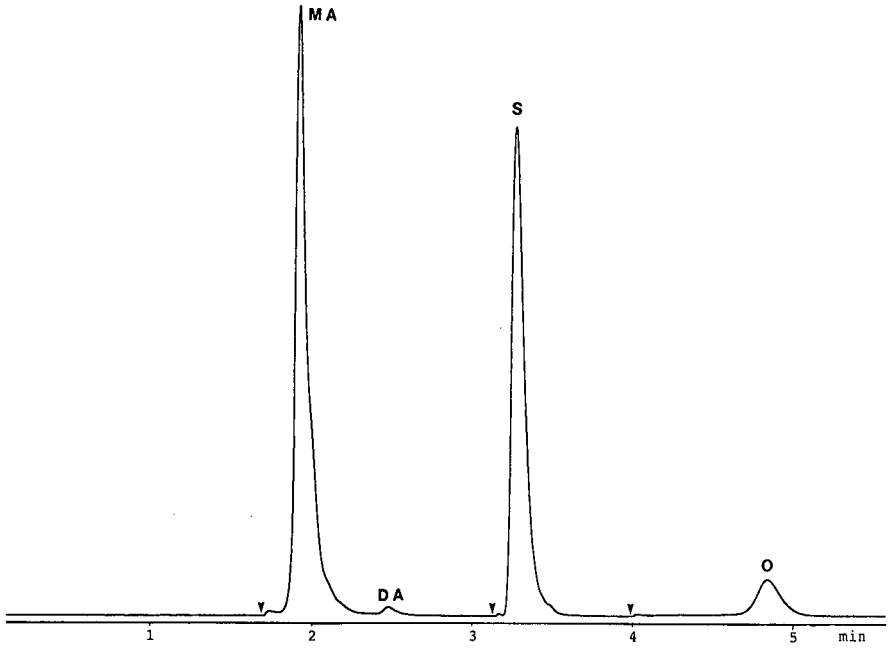

Fig. 4. Supercritical fluid chromatogram (FID) of gasoline F4 on the dual-column system. Columns: silica column as in Fig. 2 and a fused-silica column (38 mm × 0.25 mm I.D.) packed with Nucleosil 5 SA cation exchanger and modified *in situ* with silver nitrate. Conditions: 65°C and 300 atm. Switching points indicated with arrows.

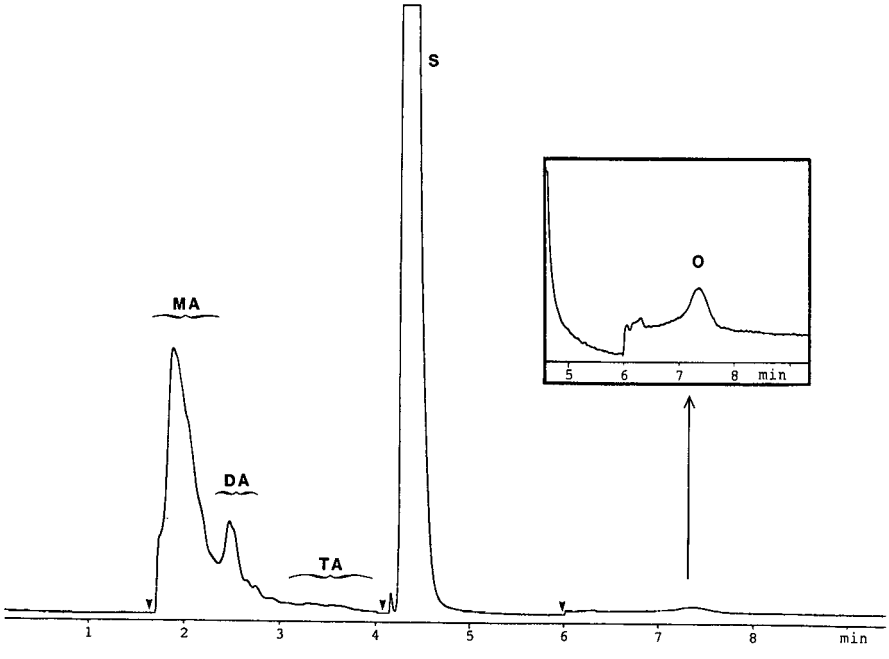

Fig. 5. Supercritical fluid chromatogram (FID) of diesel fuel D6. Columns and conditions as in Fig. 4. Switching points indicated with arrows. Inset magnified 17-fold.

Separation on the dual-column system

A quantitative determination of mono-, di- and triaromatics and the sum of aliphatics and alkenes was obtained on running the sample through the silica column. In addition, information concerning the appropriate switching times was achieved. It was necessary to take into consideration, however, that the linear flow-rate was lower when the argentation column was connected to the system.

Using the dual-column system, peak 1 (Figs. 2 and 3) was transferred to the argentation column for separation of saturates and alkenes. The resulting chromatograms from a gasoline and a diesel fuel are shown in Figs. 4 and 5.

When using 0.25 mm I.D. fused-silica micropacked columns, Skaar *et al.* [31] noted that the stability of the packed bed was inadequate for use with alternating flow directions. No such instability was experienced with the connectors used in this work. Further, columns of this type often broke when high pressure were applied [34], although this problem was overcome when we changed to thick-walled, fused-silica tubing. The flow of mobile phase is low in this type of column and this places stringent demands on the dead volumes of the connections, especially in systems where many connections are being applied.

Quantitative analysis

Quantitative data obtained with FLIA, HPLC and SFC–FID system used in this work are compared in Table III. The gasoline composition data obtained by FLIA are taken from ref. 36 and the diesel composition analysed by FLIA and HPLC–RI detection from ref. 37. The HPLC–RI analysis was performed according to ref. 14. An exact com-

TABLE III

COMPARISON OF SFC–FID WITH HPLC AND FLIA RESULTS FOR GASOLINE (F) AND DIESEL FUEL (D) SAMPLES

Fuel	Components[a]	FLIA (vol.%)	HPLC (vol.%)	SFC–FID (wt.%)
F1	S	71.3		64.1
	A	27.2		34.8
	O	1.5		0.7
F4	S	52.7		41.2
	A	42.6		53.3
	O	4.7		5.5
D1	S	95.6		97.3
	A	2.7	1.8	2.4
	O	1.4		0.1
D2	S	83.3		81.0
	A	14.7	16.9	18.7
	O	2.0		0.3
D6	S	71.2		69.1
	A	27.7	26.1	28.8
	O	1.0		0.5
D7	S	79.6		76.0
	A	19.8	20.0	23.8
	O	0.9		0.2
D8	S	80.4		77.3
	A	19.4	20.5	22.4
	O	0.2		0.3
D9	S	83.3		80.7
	A	16.0	17.3	19.0
	O	0.7		0.3

[a] S = saturates; A = aromatics; O = alkenes.

TABLE IV

SFC–FID REPEATABILITY STUDY WITH RELATIVE STANDARD DEVIATIONS (R.S.D.) (n = 8)

Fuel	S[a] (%)	R.S.D. (%)	MA[a] (%)	R.S.D. (%)	DA[a]+ TA[a](%)	R.S.D. (%)	O[a] (%)	R.S.D. (%)
D6	69.1	0.4	22.6	1.0	6.2	6.2	0.5	8.4
F4	41.2	2.5	52.3	2.0	1.0	9.4	5.5	1.4

[a] MA = Monoaromatics; DA = diaromatics; TA = Triaromatics; S = saturates; O = alkenes.

parison of the results is difficult to make as FLIA and HPLC–RI results are reported in volume % and SFC–FID results in weight %. The results obtained with the different methods are, however, in relatively good agreement. A comparison made by Lee *et al.* [6] of the quantitative analysis of aromatics in diesel fuels by FIA and SFC–FID using a silica column showed much greater differences. The supercritical fluid chromatograms presented showed considerable overlap between saturates and monoaromatics, and that explains the observed differences.

The repeatability of the quantitative analysis is shown in Table IV.

Diesel fuels are often prepared from heavier distillates that have been cracked and hydrated. Using the method presented in this work, the hydration step can be monitored (Figs. 6 and 7).

Instrumental methods for quantitative analysis of fuels by means of HPLC or SFC are currently being developed. HPLC methods suffer from the lack of universal detectors. Further, they often give incomplete separations and long analysis times. The combination of a silica and a silver-loaded cation-exchange column in connection with a supercritical mobile phase and FID as described by Campbell *et al.* [29] is a promising approach. Their methodology, however, involves some drawbacks. First, it is

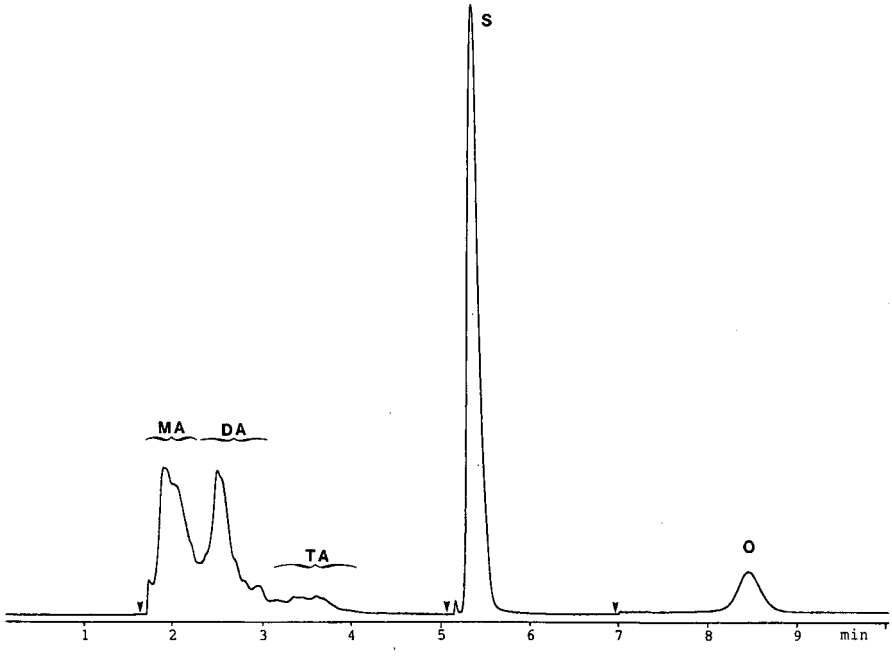

Fig. 6. Supercritical fluid chromatogram (FID) of feedstock. Columns and conditions as in Fig. 4.

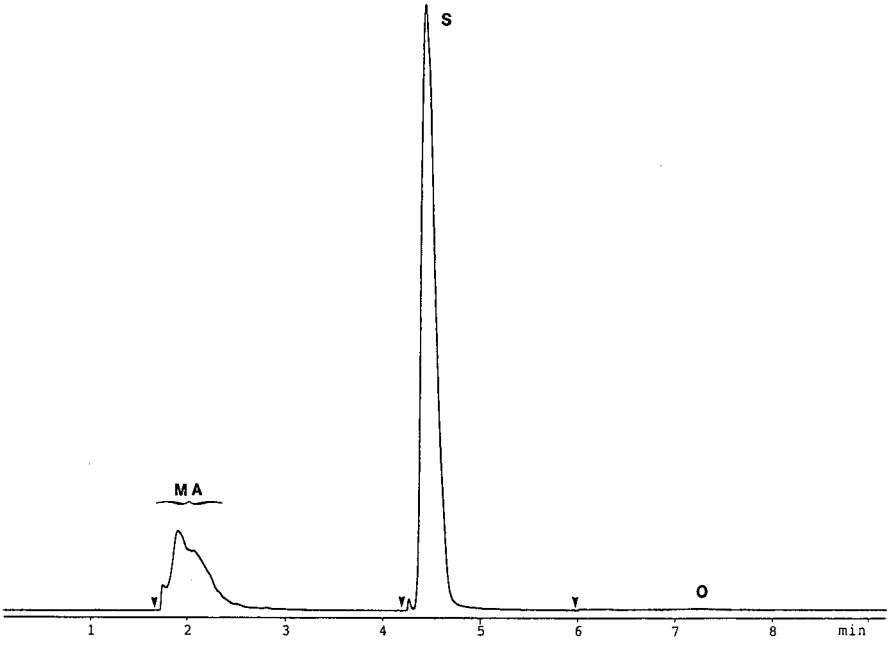

Fig. 7. Supercritical fluid chromatogram (FID) of feedstock after hydration. Columns and conditions as in Fig. 4.

complicated by the use of a mixed mobile phase, of 10% carbon dioxide in sulphur hexafluoride (SF_6). Second, the use of SF_6 as mobile phase necessitates the use of a gold-plated flame ionization detector. Third, even though the alkenes were back-flushed from the silver-impregnated column, long residence times were experienced. This resulted in broad peaks and long analysis times. Further, elution as such broad peaks makes the quantification of minor amounts of alkenes impossible. The silver column was kept at a low temperature, 40°C, and that, in combination with a weak mobile phase, is the reason for the broad peaks. The difficulties therefore increased when higher boiling distillates were analysed. It was erroneously thought that it was best to avoid heating the column in order to prevent degradation.

In this work, it has been demonstrated that saturates and alkenes can be separated from aromatics in SFC using neat carbon dioxide as mobile phase when capillary columns packed with small particles (4 μm) are being used. Moreover, the application of a relatively high temperature of the silver column, 65°C, resulted in short analysis time and minor amounts of alkenes in gasoline and diesel fuels could be quantified.

ACKNOWLEDGEMENTS

This work was supported by Neste (Porvoo, Finland) and the OK Environmental Fund. Fuel samples were kindly given by R. Westerholm.

REFERENCES

1 *Annual Book of ASTM Standards*, ASTM D1319, Part 23, American Society for Testing and Materials, Philadelphia, PA, 1984.
2 T. A. Norris and M. G. Rawdon, *Anal. Chem.*, 56 (1984) 1767–1769.
3 H. E. Schwartz, J. M. Levy and J. P. Guzowski, in C. M. Wright (Editor), *Modern Supercritical Fluid Chromatography*, Hüthig, Heidelberg, 1988, pp. 135–154.
4 R. S. Ozubko, D. M. Clugston and E. Furimsky, *Anal. Chem.*, 53 (1981) 183–187.
5 L. Petrakis, D. T. Allen, G. R. Gavalas and B. C. Gates, *Anal. Chem.*, 55 (1983) 1557–1564.
6 S. W. Lee, B. J. Fuhr and B. Glavinevski, *SAE Technical Paper Series 872142*, SAE, Warrendale, PA, 1987.
7 J. J. Kelly and J. B. Callis, *Anal. Chem.*, 62 (1990) 1444–1451.
8 J. C. Suatoni, H. R. Garber and B. E. Davis, *J. Chromatogr. Sci.*, 13 (1975) 367–371.
9 J. C. Suatoni, in K. H. Altgelt and T. H. Gouw (Editors), *Chromatography in Petroleum Analysis*, Marcel Dekker, New York, 1979, pp. 121–155.
10 R. L. Miller, L. S. Ettre and N. G. Johansen, *J. Chromatogr.*, 259 (1983) 393–412.

11 S. Matsushita, Y. Tada and T. Ikushige, *J. Chromatogr.*, 208 (1981) 429–432.
12 P. C. Hayes, Jr. and S. D. Anderson, *Anal. Chem.*, 58 (1986) 2384–2388.
13 P. C. Hayes, Jr. and S. D. Anderson, *J. Chromatogr.*, 387 (1987) 333–346.
14 *IP Standard Methods for Analysis and Testing of Petroleum Products*, Designation IP 391/90, Institute of Petroleum, London, 1990.
15 I. L. Davies, K. D. Bartle, G. E. Andrews and P. T. Williams, *J. Chromatogr. Sci.*, 26 (1988) 125–130.
16 T. V. Alfredson, *J. Chromatogr.*, 218 (1981) 715–728.
17 L. H. Henrich, *J. Chromatogr. Sci.*, 26 (1988) 198–205.
18 J. J. Szakasits and R. E. Robinson, *Anal. Chem.*, 63 (1991) 114–120.
19 S. V. Rose, J. P. Crombeen and D. L. G. Lammerts van Bueren, presented at the *Pittsburgh Conference on Analytical Chemistry and Applied Spectroscopy, New York, 1990*, abstract 1109.
20 P. C. Hayes, Jr. and S. D. Anderson, *Anal. Chem.*, 57 (1985) 2094–2098.
21 P. C. Hayes, Jr. and S. D. Anderson, *J. Chromatogr. Sci.*, 26 (1988) 210–217.
22 P. C. Hayes, Jr. and S. D. Anderson, *J. Chromatogr. Sci.*, 26 (1988) 250–257.
23 B. J. Fuhr, L. L. Klein, C. Reichert and S. W. Lee, *LC · GC Int.*, 4, No. 1 (1991) 36–39.
24 S. W. Lee, B. J. Fuhr, L. R. Holloway and C. Reichert, *Energy Fuels*, 3 (1989) 80–84.
25 E. Lundanes and T. Greibrokk, *J. Chromatogr.*, 349 (1985) 439–446.
26 H. E. Schwartz and R. G. Brownlee, *J. Chromatogr.*, 353 (1986) 77–93.
27 E. Lundanes, B. Iversen and T. Greibrokk, *J. Chromatogr.*, 366 (1986) 391–395.
28 J. M. Levy and J. P. Guzowski, *Fresenius' Z. Anal. Chem.*, 330 (1988) 207–210.
29 R. M. Campbell, N. M. Djordjevic, K. E. Markides and M. L. Lee, *Anal. Chem.*, 60 (1988) 356–362.
30 B. W. Wright, H. R. Udseth, E. K. Chess and R. D. Smith, *J. Chromatogr. Sci.*, 26 (1988) 228–235.
31 H. Skaar, H. R. Norli, E. Lundanes and T. Greibrokk, *J. Microcol. Sep.*, 2 (1990) 222–228.
32 F. P. Di Sanzo and R. E. Yoder, *J. Chromatogr. Sci.*, 29 (1991) 4–7.
33 P. C. Hayes, Jr., and S. D. Anderson, J. Chromatogr., 437 (1988) 365–377.
34 M. Demirbüker and L. G. Blomberg, *J. Chromatogr. Sci.*, 28 (1990) 67–72.
35 M. Demirbüker and L. G. Blomberg, *J. Chromatogr.*, 550 (1991) 765–774.
36 R. N. Westerholm, T. E. Alsberg, Å. B. Frommelin, M. E. Strandell, U. Rannug, L. Winquist, V. Grigoriadis and K.-E. Egebäck, *Environ. Sci. Technol.*, 22 (1988) 925–930.
37 R. N. Westerholm and K.-E. Egebäck, *National Swedish Environmental Protection Agency Report Series, Report 3968*, SNV, Solna, Sweden.
38 K. M. Payne, I. L. Davies, K. D. Bartle, K. E. Markides and M. L. Lee, *J. Chromatogr.*, 477 (1989) 161–168.
39 B. Smith and R. Ohlson, *Acta Chem. Scand.*, 16 (1962) 351–358.

Journal of Chromatography, 595 (1992) 313–318
Elsevier Science Publishers B.V., Amsterdam

CHROM. 23 888

Peak dispersion and separation efficiency in high-performance zone electrophoresis with gel-filled capillaries

Ernst Kenndler* and Christine Schwer

Institute for Analytical Chemistry, University of Vienna, Währingerstr. 38, A-1090 Vienna (Austria)

(First received August 8th, 1991; revised manuscript received November 13th, 1991)

ABSTRACT

The Einstein–Nernst equation for the relationship between diffusion coefficient, D, and ionic mobility, u, was applied to describe the peak dispersion in zone electrophoresis with gel-filled capillaries. It follows that the effective charge number is the only analyte-specific parameter that influences the plate height or the plate number. Peak broadening is thus independent of D and u, because these parameters can be substituted by physical and instrumental constants. The plate number depends linearly on the effective charge number of the separands. Plate numbers in the range of several millions are predicted for highly charged molecules. This theoretical approach is discussed on the basis of electropherograms of oligonucleotides.

INTRODUCTION

Capillary zone electrophoresis in gel-filled tubes is a separation technique of very high efficiency. Especially for oligo- and polynucleotides, extremely high plate numbers in the range of several millions have been achieved. These high plate numbers are usually attributed to the reduced diffusion coefficients, D_i, of the molecules in the gel matrix, apparently leading to large values for the plate number, N_i, according to the expression [1–4].

$$N_i = u_i \, U / 2 \, D_i \qquad (1)$$

where U is the applied voltage and u_i is the effective ionic mobility of the separand, i. This equation was derived for conditions where only diffusion, and no additional effects on band broadening, such as Joule heating, hydrodynamic or electroosmotic flow, migration dispersion or extra-column contributions, take place.

It must be taken into account, however, that the electrophoretic migration caused by the gradient of the electric potential is influenced by the gel matrix in a way similar to the corresponding migration caused by the gradient of the chemical potential, the diffusion. The diffusion coefficient and the mobility are in fact related according to the Einstein–Nernst equation [*e.g.*, 5,6]:

$$D_i = u_i \, k \, T / z_i \, e_0 \qquad (2)$$

where k is the Boltzmann constant, T is the absolute temperature, e_0 is the electronic charge and z_i is the effective charge number of the ion, i. In principle, this equation is valid only for infinite dilution. For finite concentrations, it has two main limitations. One is based on the different concentration dependence of the ionic mobility and the diffusion coefficient: the mobility is normally more strongly decreased than the diffusion coefficient by increasing concentration. The second limitation arises for weak electrolytes when the diffusion coefficient of the ionic species, which is migrating by electrophoresis as well as by diffusion, differs from that of the uncharged molecule, which does not undergo electromigration.

In previous papers [7–10], the consequences of the replacement of the ratio u/D in the expression for the plate number in capillary zone electrophoresis (eqn. 1) by the Nernst–Einstein equation, leading to

0021-9673/92/$05.00

TABLE I

DIFFUSION COEFFICIENTS, D, AND ELECTROPHORETIC MOBILITIES, u, OF NUCLEOTIDES WITH DIFFERENT BASE NUMBERS, n

z is the charge number of the separand; under the given electrophoretic conditions, z is assumed to be $n+1$.

n	D (10^{-6} cm^2/s)	u (10^{-5} cm^2/V · s)	u/z (10^{-5} cm^2/V · s)	$D/(u/z)$ (10^{-2} V)
1	1.42	11.52	5.76	2.47
6	0.490	11.48	1.64	2.99
8	0.415	11.44	1.27	3.27
10	0.351	11.38	1.03	3.39
12	0.310	11.30	0.869	3.57
14	0.287	11.07	0.738	3.89
16	0.269	10.85	0.638	4.21
18	0.239	10.57	0.556	4.30
20	0.218	10.34	0.492	4.43
22	0.201	10.08	0.438	4.59
24	0.188	9.87	0.395	4.76
26	0.166	9.65	0.357	4.61
28	0.163	9.44	0.326	5.01
30	0.146	9.22	0.297	4.91
32	0.146	9.03	0.274	5.34

$$N_i = z_i e_0 U / 2 k T \quad (3)$$

for systems without electroosmosis, was discussed. The same equation was derived by Giddings [1–3], setting equal the friction coefficients occurring in the transport equations for diffusion and electromigration such as in the derivatization of the Nernst–Einstein equation.

It can be seen from eqn. 3 that (within the limitations mentioned above) the plate number is dependent on the effective charge number as the only analyte-specific parameter, and not on diffusion coefficient and mobility. The validity of this transformation was demonstrated experimentally with ions with different charges in free capillary zone electrophoresis, carried out without electroosmotic flow [10]. In this work, this theoretical approach was applied to zone electrophoresis in gel-filled capillaries. Its validity is discussed based on diffusion coefficients of oligonucleotides, published by Yin *et al.* [11], and the corresponding mobilities, and also by comparison of the actual plate numbers with the maximum obtainable value.

EXPERIMENTAL

Ionic mobilities were calculated from published electropherograms [11]. These electropherograms were obtained with oligonucleotides as separands [the 8-, 10-, 12-, 14-, 16-, 18-, 20-, 22-, 24-, 26-, 28-, 30- and 32-mers of a size marker mixture of the sequence d(GACT)$_n$ and d(GACT)$_n$GT]. Separation was carried out in a gel-filled capillary (100 μm I.D., 69 cm total length, 46 cm length to the detector; polyacrylamide gel made from 6% T, 5% C[a]; buffer 0.1 *M* Tris–0.25 *M* boric acid–7 *M* urea). The mobilities of adenosine-5′-monophosphate and pd $(A)_6$ were determined by extrapolation from the observed relationship between the mobility and the base number. Diffusion coefficients determined by the stopped-flow method were taken from the literature [11].

The second moments (variances), σ^2, caused by the finite volumes of injection and the detector cell were calculated from the corresponding rectangular functions with the width, w, by $\sigma^2 = w^2/12$. For the injection zone of the electropherogram under consideration, a length of about 0.25 mm was calculated from the given injection voltage and time [11]. For the length of the detector cell, a value of 0.7 mm was taken [12]. Based on the additivity of the variances, a value of 0.22 mm was derived in this in-

[a] C = g N,N′-methylbisacrylamide (Bis)/%T; T = g acrylamide + g Bis per 100 m of solution.

stance for the standard deviation, $\sigma_{z,ex}$, caused by both extra-column effects.

The peak widths based on time, σ_t, of the oligonucleotides were measured from the published electropherogram. [11]. From these values, the corresponding standard deviations based on length, σ_z, were calculated taking into account the different migration velocities, also derived from the electropherogram.

RESULTS AND DISCUSSION

Relationship between diffusion coefficient and ionic mobility

The ionic mobilities and the diffusion coefficients of the solutes under discussion are given in Table I. The diffusion coefficient and the normalized mobilities (u_i/z_i, the mobility of the ion with unit charge number) exhibit a similar dependence on the base number, n, namely an almost linear relationship between log D and log (u/z), respectively, and log n, as shown in Fig. 1.

According to the Nernst–Einstein equation, the ratio of the diffusion coefficient and the normalized mobility should be constant, as eqn. 2 can be transformed into

$$D_i/(u_i/z_i) = kT/e_0U \quad (4)$$

At 20°C, this ratio has the value 0.0255 V. It can be seen from Table I (assuming that z equals $n + 1$) that this theoretical value is in fact observed for the 1- and 6-mers. Values for the other separands are in the same range, but they increase with increasing base number. The higher oligonucleotides show a deviation from the theoretically predicted value up to a factor of 2.

These deviations of the ratio $D_i/(u_i/z_i)$ of the separands with higher base numbers can be caused, besides a systematic error in the determination of the diffusion coefficients (the changes in peak widths, observed by the stopped-flow method, become very small for the higher oligomers), by the limitations of the Nernst–Einstein equation. For dilute aqueous solutions and simple electrolytes these deviations are, however, much lower, of the order of only about 10% [5,6].

On the other hand, the different experimental conditions in determining the diffusion coefficients

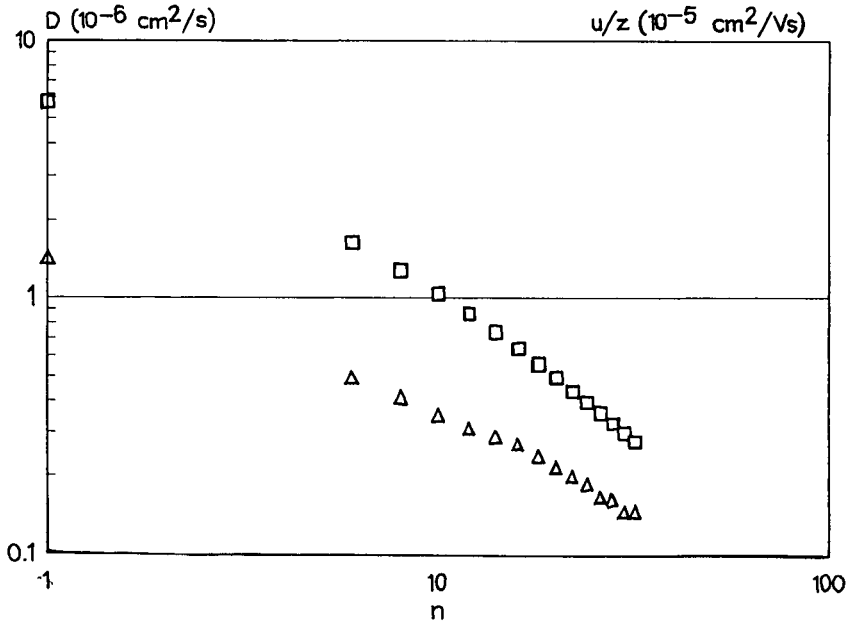

Fig. 1. Logarithmic plots of the dependence of (△) diffusion coefficient, D, and (□) normalized ionic mobility, u/z, on the base number, n, of the oligonucleotides. The normalized mobility is the mobility of the ion with unit charge. The charge number, z, is assumed to be $n+1$.

compared with mobilities may also be responsible for this deviation, briefly discussed as follows. The migration of a charged polymer in a gel is explained in the short-chain limit by a theory introduced by Ogston [13], where a sieving mechanism is assumed. The movement of large polymer chains, on the other hand, is best described by the so-called reptation theory [14–17]. This theory was modified, as additional stretching of the large polymer chain must be considered, resulting in field-dependent mobilities [15].

As in capillary zone electrophoresis high electric fields are applied (several hundred V/cm), possibly the conformation also of small fragments (even several-ten-mers) is influenced by the electric field. Hence it may be assumed that diffusion coefficients determined by the stopped-flow method, where no electric potential is applied along the capillary, will differ from the diffusion coefficients established under separation conditions, at least for higher oligomers, where this deviation was in fact observed.

Another reason for the observed deviation may be the fact that the effective charge number differs from the nominal charge number, as calculated from the base number, especially when large polymers are considered.

However, as diffusion and electrophoretic migration are influenced by the gel matrix in a similar way, the Einstein–Nernst relationship (which is generally applied in reptation theory) is also applied for the given conditions.

Dependence of plate number on electrical charge

It was discussed above that the substitution of the ratio of mobility and diffusion coefficient (eqn. 2) in eqn. 1 for the plate number leads to an expression that depends on, besides non-specific parameters such as voltage and temperature, only the effective charge number as an analyte-specific parameter (eqn. 3). At 20°C and with an effective voltage of 12 000 V (used in the experiments), the plate number may thus be calculated from $N_i = 237\,700 z_i$.

In the derivation of this expression, contributions to the peak width other than diffusion, namely temperature gradients or extra-column effects due to injection and detection, are ignored, in addition to the limited validity of the Nernst–Einstein relationship at higher concentrations, and the possible de-

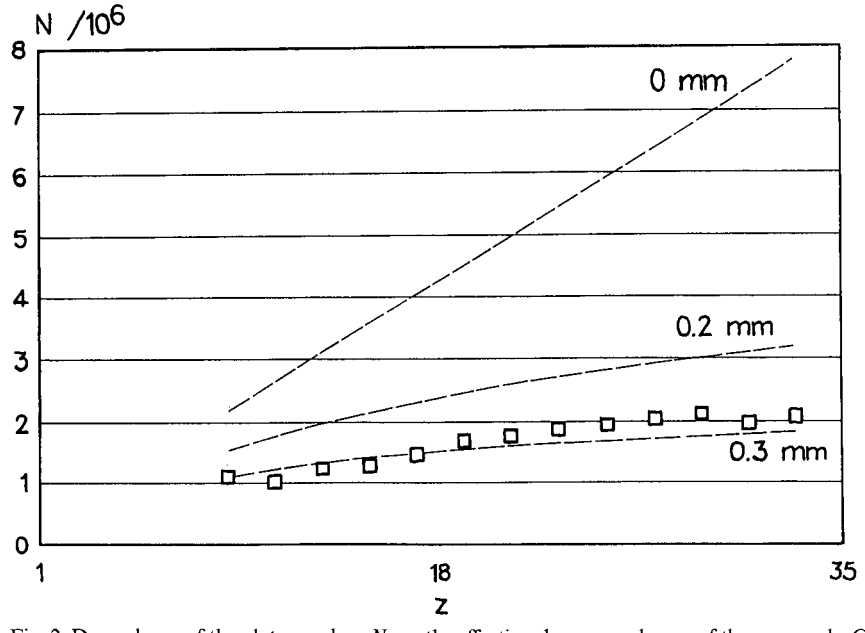

Fig. 2. Dependence of the plate number, N, on the effective charge number, z, of the separands. Conditions: effective voltage, 12 000 V; temperature, 20°C. Broken lines: theoretical dependence according to eqn. 3, for different extra-column contributions, expressed by the standard deviation, $\sigma_{z,ex}$ = 0 mm (without extra-column effects), 0.2 mm and 0.3 mm. □ = Experimental values obtained from the electropherogram of the oligonucleotides; z is assumed to be $n + 1$.

viation of the effective from the nominal charge number. Therefore, this plate number represents the maximum obtainable value. It is shown in Fig. 2 as a function of the charge number of the separands, assuming that the charge originates from the dissociation of the phosphate groups only. In this instance, z is connected to the base number, n, by $z = n + 1$. This maximum plate number is, *e.g.*, 2 140 000 for the 8-mer and increases linearly to 7 840 000 for the 32-mer.

Owing to the finite injection volume and the volume of the detector cell, extra-column band broadening occurs, this effect being the greater the higher is the efficiency of the separation capillary. The theoretical dependence of the plate number was calculated for different extra-column contributions, namely for realistic values of 0.2 and 0.3 mm for $\sigma_{z,ex}$, the particular standard deviation based on length. The result of this calculation is shown in Fig. 2: the plate number increases with increasing charge number in both instances, but this increase is not as steep as for $\sigma_{z,ex} = 0$, and it is not linear. For the 32-mer, for example, only $2 \cdot 10^6$–$3 \cdot 10^6$ plates can be reached theoretically for an extra-column contribution corresponding to about 0.2–0.3 mm for $\sigma_{z,ex}$. This value for $\sigma_{z,ex}$ is realistic, taking into account the experimental conditions as discussed above.

The experimentally observed peak widths $\sigma_{z,i}$ (based on length) of the oligonucleotides are presented in Table II. They decrease with increasing base number. This means that the plate heights in fact decrease with increasing n, as was predicted from theory (eqn. 3).

TABLE II

PEAK STANDARD DEVIATIONS, σ_z, BASED ON LENGTH, OF THE OLIGONUCLEOTIDES WITH DIFFERENT BASE NUMBERS, n

The values were calculated from published electropherogram [11].

n	σ_z (mm)	n	σ_z (mm)
8	0.437	22	0.335
10	0.454	24	0.329
12	0.413	26	0.321
14	0.405	28	0.315
16	0.379	30	0.326
18	0.352	32	0.318
20	0.344		

The decrease in the peak width with increase in base number cannot be attributed to the decrease in the diffusion coefficients, an argument which often occurs in the literature, because the resulting diffusion must not be considered independently from electromigration, and therefore from the ionic mobility, as discussed above. Taking the case that the ions of a species have identical diffusion coefficients, but different charges, and hence different electrophoretic velocities, they will then exhibit different migration times, t, in a column with (effective) length, l, resulting in different plate heights, H, according to $2\,Dt = Hl$. The ions with the higher charge are migrating faster, and therefore have a shorter time available for diffusion, which leads to a smaller plate height, despite the identical diffusion coefficients. This example demonstrates clearly that a discussion on plate numbers that is focused on diffusion coefficients alone must lead to a misinterpretation of the electrophoretic results.

From the standard deviations given in Table II, the plate numbers for the particular analytes were calculated according to the equation $N_i = l^2/\sigma^2_{z,i}$, for an effective length of 460 mm. The values are shown in Fig. 2, assuming that the charge number, z, is correlated with the base number, n, by $z = n + 1$. The plate numbers in fact increase with increasing charge number, from about $1.1 \cdot 10^6$ for the 8-mer ($z = 9$) to $2.1 \cdot 10^6$ for the 32-mer ($z = 33$). It can be seen that the experimental values are in good agreement with those predicted from theory, taking a value of 0.22 mm for the extra-column contribution to σ_z as derived under Experimental.

Further confirmation of the theory discussed here will be obtained by reducing the extra-column peak broadening, which should lead to higher plate numbers, approaching closer the maximum obtainable values, as expected by theory. This goal should be reached by decreasing the aperture of the detector cell, because this cell width has the most pronounced extra-column contribution on the total variance; this work is in progress in cooperation with Schomburg's group.

SYMBOLS

D diffusion coefficient (cm^2/s)
e_0 electronic charge
E electric field strength (V/cm)

H plate height
k Boltzmann constant
L total length of the separation capillary
l effective length; electrophoretic migration distance; distance from injector to detector
n base number of oligonucleotide
N plate number
σ_{ex} peak standard deviation caused by extra-column effects
σ_t peak standard deviation based on time
σ_z peak standard deviation based on length; $\sigma_z = \sigma_t v$
t migration or retention time
T absolute temperature (K)
u effective ionic mobility ($cm^2/V \cdot s$) of a charged particle, given by $u = vE$
u/z reduced ionic mobility; mobility of the particle with unit charge number
U effective voltage (V); potential drop from injector to detector across effective length
v electrophoretic velocity (cm/s), given by l/t
z effective charge number (z also indicates the axis of migration)

REFERENCES

1 J. C. Giddings, *Sep. Sci.*, 4 (1969) 181.
2 J. C. Giddings, in I. M. Kolthoff and P. J. Elving (Editors), *Treatise on Analytical Chemistry*, Part I, Vol. 5, Wiley, New York, 1981, pp. 63–164.
3 J. C. Giddings, *J. Chromatogr.*, 480 (1989) 21.
4 J. W. Jorgenson and K. D. Lucas, *J. High Resolut. Chromatogr. Chromatogr. Commun.*, 4 (1981) 230.
5 R. A. Robinson and R. H. Stokes, *Electrolyte Solutions*, Butterworths, London, 1959.
6 J. O'M. Bockris and A. K. Reddy, *Modern Electrochemistry*, Plenum Press, New York, 1970.
7 E. Kenndler, *Österr Chem.-Ztg.*, 12 (1988) 353.
8 E. Kenndler, *Chromatographia*, 30 (1990) 713.
9 C. Schwer and E. Kenndler, *Chromatographia*, 30 (1990) 546.
10 E. Kenndler and C. Schwer, *Anal. Chem.*, 63 (1991) 2499.
11 H.-F. Yin, M. H. Kleemiss, J. A. Lux and G. Schomburg, *J. Microcol. Sep.*, 3 (1991) 331.
12 J. A. Lux, H.-F. Yin and G. Schomburg, *J. High-Resolut. Chromatogr. Chromatogr. Commun.*, 13 (1990) 436.
13 A. G. Ogston, *Trans. Faraday Soc.*, 54 (1958) 1754.
14 G. W. Slater and J. Noolandi, *Phys. Rev. Lett.*, 55 (1985) 1579.
15 G. W. Slater and J. Noolandi, *Biopolymers*, 25 (1986) 431.
16 G. W. Slater, J. Rousseau and J. Noolandi, *Biopolymers*, 26 (1987) 863.
17 G. W. Slater, J. Rousseau, J. Noolandi, C. Turmel and M. Lalande, *Biopolymers*, 27 (1988) 409.

Journal of Chromatography, 595 (1992) 319–325
Elsevier Science Publishers B.V., Amsterdam

CHROM. 23 941

High-sensitivity laser-induced fluorescence detection of native proteins in capillary electrophoresis

Thomas T. Lee and Edward S. Yeung*

Department of Chemistry and Ames Laboratory of USDOE, Iowa State University, Ames, IA 50011 (USA)

(First received September 16th, 1991; revised manuscript received December 3rd, 1991)

ABSTRACT

A highly sensitive laser-induced (LIF) detection scheme for native, tryptophan- or tyrosine-containing proteins in capillary electrophoresis (CE) has been demonstrated. The 275.4 nm line from an argon-ion laser is used to excite native protein fluorescence. A limit of detection (LOD) ($S/N = 2$) of $1 \cdot 10^{-10}$ M for conalbumin represents a 140-fold improvement over earlier reports. With stacking at injection, the LOD is $3 \cdot 10^{-12}$ M. Linear dynamic ranges of at least 5 and 4 orders of magnitude for, respectively, tryptophan and bovine serum albumin are found. The practical performance and blueprint of an easily constructed, rugged, compact and user-friendly LIF detector for CE are shown.

INTRODUCTION

The high efficiency and speed of capillary electrophoresis (CE) in the resolution of biomolecules have attracted much attention [1]. However, efficient separation is not sufficient unless coupled to adequate detection. In this regard, CE presents a challenge as the nl cell volume and on-column arrangement render traditional detectors designed for high-performance liquid chromatography (HPLC) unsuitable.

The analysis of biological materials and the determination of biomolecules are of indispensable importance to the field of biotechnology. Despite the prominent role of proteins in biotechnology, the detection of proteins in CE is far from satisfactory. So far, amperometric detection [2] is hampered by electrode fouling while conductometric [3] and mass spectrometric detection [4] are unreliable and insensitive. Radiochemical detection [5], though quite sensitive, requires labeling as well as handling and disposing of hazardous materials with short shelf-lives. Although widely used and convenient, the best ultraviolet-visible absorption detectors with the cross-beam arrangement [6] offer a limit of detection (LOD) in the μM range because of the inherently short pathlength provided by the capillary tubing. This represents a major drawback for CE in the analysis of proteins in biological matrices where the demand for concentration detection sensitivity is far more stringent [7]. Besides, it excludes CE from the realm of trace analysis where HPLC is still the method of choice in spite of the poor separation efficiency of the latter.

In general, fluorescence detection in CE exhibits the best performance in sensitivity, linearity and selectivity. Even though conventional excitation sources have been used [8], the achievable sensitivity is offset by the inherent difficulty in focusing a large amount of light from a divergent light source into the nl detection region while minimizing light scattering. Utilization of the laser as a fluorescence excitation source reduces such problems and defines the state-of-the-art in CE detectors today [9]. Unfortunately, implementation of this approach to the detection of proteins is by no means straight-forward because usually it is necessary to label the analytes with fluorescent tags. Because of differences in the extent of incorporation of the tags into each protein molecule, pre-column labeling gives rise to multiple

0021-9673/92/$05.00

peaks for each type of protein in the electropherogram [10,11]. On-column labeling of proteins with laser-induced fluorescence (LIF) detection offers slightly better sensitivity than absorbance, but at the expense of separation efficiency due to the slow kinetics of inter-species conversion [11,12]. The advantages gained in the 100-fold improvement in sensitivity over absorbance afforded by a post-column labeling scheme with LIF are largely offset by instrumental complexity as well as the dependence of peak efficiency upon reagent flow rate and reaction distance [10]. A technique retaining the sensitivity of post-column labeling with LIF while avoiding derivatization is indirect fluorescence detection [13]. However, the need to work at low buffer concentrations renders practical applications difficult.

Swaile and Sepaniak [11] have demonstrated LIF detection of native, underivatized proteins in CE based on the fluorescence of tryptophan and tyrosine residues. In their study, an argon-ion laser operating at 514 nm was frequency-doubled to 257 nm with a harmonic generator. But instrumental instability and poor match between the excitation wavelength and excitation maxima of the fluorophores limited the sensitivity of the technique to no better than post-column labeling with LIF [10].

Nevertheless, the ability to detect proteins at trace levels remains attractive and, in the case of assuring the purity of biopharmaceticals, essential. According to a 'Points to Consider' draft issued by the US Food and Drug Administration (FDA) on biopharmaceuticals [14], the analytical goal for protein impurities and contaminants are in the 1 to 100 ppm range. However, it is possible that a highly immunogenic protein impurity present at the ppm level can elicit an allergic response in a high percentage of human recipients [15,16]. Hence, the current analytical goals set forth by the FDA merely reflect the sensitivity limits of existing technologies. This is supported by a more recent draft in which the term "analytical goals" was remplaced by phases such as "as free as possible" [17].On this note, the impact realized through coupling the high separation efficiency of CE to n*M*-detection sensitivity for proteins would be dramatic in the development and proliferation of biopharmaceuticals.

Despite the unparalleled performance of LIF detection in CE [9–11,13,18,19], there have only been a limited number of applications reported. The need for the separation scientist to acquire the expertise in designing, assembling, operating and/or maintaining an LIF detector may be a deterrent. Hence, there is a need for an easily constructed, user-friendly and rugged LIF detector which the non-specialist can build and use without having to expend too much effort or resources. In the present work, a highly sensitive LIF detection scheme for CE based on native protein fluorescence is reported and various aspects of it are discussed. In addition, a compact, rugged and user-friendly instrumental arrangement is described.

EXPERIMENTAL

The experimental setup used in the present work resembles the one described previously [18] with several modifications. First, a Model 2045 argon-ion laser (Spectra-Physics, Mountain View, CA) was optimized for deep UV operation. A prism was used to isolate the 275.4 nm line (utilized to excite protein fluorescence) from the total output. Secondly, 2 UG-1 band pass filters (Schott Glass Technologies, Duryea, PA, USA) were used to selectively pass the fluorescence. Thirdly, a compact, rugged LIF detector housed in a light-tight Plexiglas box (25 cm × 35 cm × 10 cm) was constructed. A diagram of the detector arrangement is shown in Fig. 1.

As depicted in Fig. 1, the device represents a simple and rugged design for LIF detection. It consists of 8 main components: a quartz 1-cm focal length lens (L), capillary holder (CH), 20× microscope objective (MO), microscope objective holder (MOH), mirror (M) and mirror mount (MM), photomultiplier tube (PMT) with filter (F), plexiglas box (PB) and 2 light shields (LS). The laser beam enters the otherwise light-tight box PB through a 3-mm hole. L is rigidly mounted to PB so that the focal point of the excitation beam is uniquely defined and used as the reference point for all the other components. The capillary with a small section of its coating removed is mounted on a 2-dimensional stage (CH) capable of 10-μm resolution. Two short pieces of quartz capillary 350 μm O.D. × 250 μm I.D. glued to CH serve to guide the separation capillary through the optical region. This can hold the common 150 μm O.D. capillary tubing. Alterna-

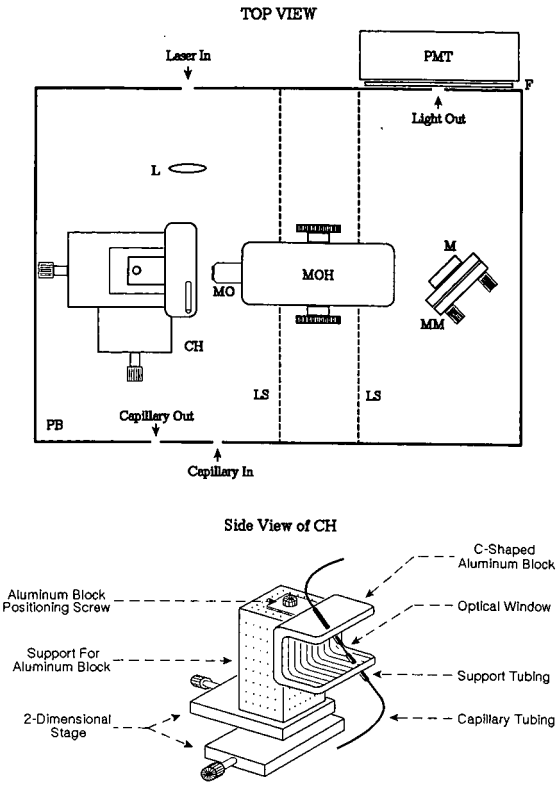

Fig. 1. Experimental arrangement of LIF detector for CE.

tively, 350 μm O.D. separation capillaries can be inserted directly into CH. The mounted capillary is at an angle of about 20° with respect to the incident laser beam to minimize scattering off the capillary walls. We find that this configuration is rigid enough with regard to noise from mechanical vibrations. With this design, capillary change can be accomplished in less than 5 min.

By examining the diffraction image of the transmitted light while translating CH, the incident light can easily be focused tightly into the center of the capillary. With a fluorophore (*e.g.* 10^{-5} *M* fluorescein solution at pH 8) running through the capillary, MO, positioned roughly such that its focal point is at the same height as the capillary window and pointing toward the excitation region, is translated with MOH so that the fluorescence image can be focused onto the exit plane of PB. By judging the sharpness of the image on the wall behind which the PMT is located, the optimal location of MO is determined. Finally, the angle of M relative to PMT and MO is adjusted with MM such that the fluorescence image clears the hole on the wall of PB that is just large enough to allow passage of the fluorescence spot while excluding light scattered off the capillary walls. F can then be used to selectively pass light of the appropriate wavelengths onto the PMT. The LSs are effective in excluding stray light from passage from the region around CH into the PMT. With this arrangement, we are able to routinely obtain detection limits within an order of magnitude of the state-of-the-art [9]. With the top of PB in place, one can generally work in moderate room light without additional shielding.

In other studies in our laboratory, an air-cooled Ar ion laser was used. The laser and the rest of the optical components can then be bolted together on a 3/4-in. Plexiglas base plate. A single 488 nm interference filter is mounted at the entrance to PB to eliminate room light. The components shown in Fig. 1 only cost a total of US$ 2000.

All separations were performed using a 5 m*M* sodium phosphate buffer at pH 10.2; the analytes were dissolved in the same buffer just before use unless specified otherwise. An electric field strength of 286 V/cm and a 77-cm long 50 μm I.D., 150 μm O.D. untreated fused-silica capillary were used throughout.

RESULTS AND DISCUSSION

The high sensitivity of LIF detection of native proteins is shown in Fig. 2 where the peak results

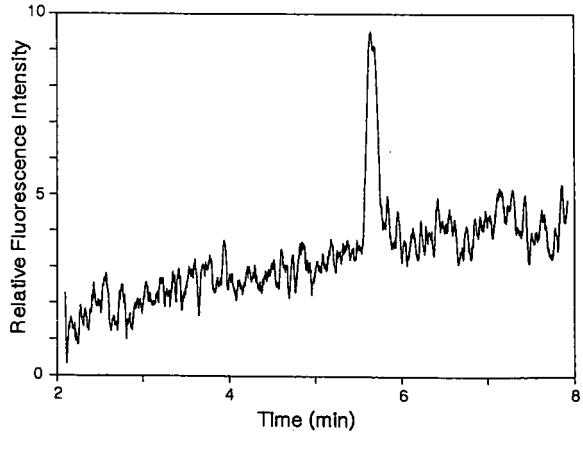

Fig. 2. Electropherogram of $5 \cdot 10^{-10}$ *M* conalbumin injected.

from the injection of conalbumin present at $5 \cdot 10^{-10}$ M in the sample. The LOD ($S/N = 2$) of $1 \cdot 10^{-10}$ M here represents a 140-fold improvement over the one reported for the same analyte previously [11]. The major reason for this is the simplicity and ruggedness of the present optical setup. Frequency-doubling is instrumentally elegant and requires a smaller argon ion laser, but produces light which is inherently noisy because of the quadratic dependence in the intensity of the frequency-doubled light on the intensity of the source. Temperature stability of the doubling crystal is also a problem. Besides, the excitation wavelength of 275.4 nm in the present system is a much better match with the fluorescence-excitation maxima of most proteins [20] than the 257 nm in ref. 11. Moreover, the high power used there prescribes long warm-up times. Since practical LIF detection is flicker noise limited, a frequency-doubled light source directly restricts the performance of the detector. However, the factors discussed above are not a concern in the present optical arrangement and, as a result of the much smaller source flicker, a drastic improvement in performance is realized. It is interesting to note that the fused-silica of the capillary tubing exhibits luminescence that can be visually discerned upon excitation at 275.4 nm. Even with 2 UG-1 band pass filters in place, this background luminescence cannot be totally eliminated, thereby providing an indication of the large spectral width of the luminescence. Consequently, the LOD of the present detector is limited by source-induced background luminescence flicker noise. Accordingly, increasing the dynamic reserve of the laser light or reducing the quantity of luminescent impurities in the fused-silica of the capillary tubing would further lower the LOD attainable with the present detector. We note that 10^{-10} M is an actual injected LOD and not one extrapolated from runs at high concentrations. This is important since adsorption of analytes onto the capillary walls can prevent one from taking advantage of the high sensitivity of LIF for studying small samples at low concentrations. The actual mass LOD (injection volume = a few nl) is around 10^{-14} g, which is quite impressive. As shown in Figs. 3 and 4, the present detector shows a linear dynamic range of at least 5 and 4 orders of magnitude for tryptophan and BSA, respectively. The correlation coefficient for each set in linear plots is better than 0.999. This is the first time that good quantitation is shown for LIF over a large concentration range. This highlights the stability of the present optical system over a series of runs. The linearity of the data in Fig. 4 also shows that adsorption of BSA is not a problem even at these low concentrations. Although the high cost of argon-ion lasers that can produce deep UV light is a disadvantage of the present detection scheme, it will eventually gain popularity as laser technology advances in the future.

Table I is a summary of the reported limits of detection for proteins in CE using various LIF techniques. Indirect fluorescence, native fluorescence excited at 257 nm, on-column and post-column labeling with LIF all offer higher LODs than native fluorescence exited at 275 nm. The LOD achievable with indirect fluorescence detection is limited by the

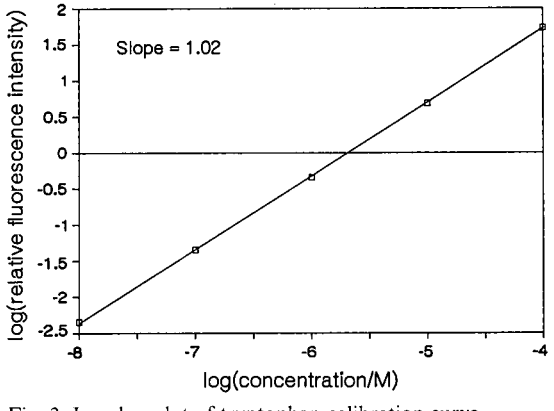

Fig. 3. Log–log plot of tryptophan calibration curve.

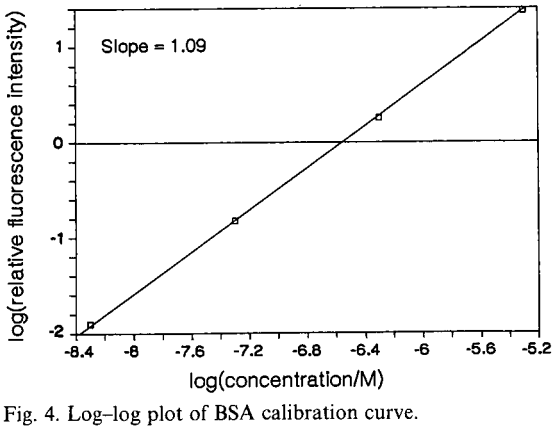

Fig. 4. Log–log plot of BSA calibration curve.

TABLE I

LIMITS OF DETECTION FOR PROTEINS IN CE BY LIF

Calculated from a signal-to-noise (S/N) ratio of 2.

Detection scheme	LOD (M)				Ref.
	Conalbumin	Horse heart myoglobin	Bovine serum albumin (BSA)	Lyoszyme	
Native fluorescence (257 nm excitation)	$1 \cdot 10^{-8}$	–	–	–	11
Indirect fluorescence	–	–	–	$5 \cdot 10^{-6}$	13
Pre-column labeling with FITC[a]	$1 \cdot 10^{-10}$	–	–	–	11
On-column labeling with TNS[b]	$3 \cdot 10^{-7}$	–	–	–	11
Post-column labeling with OPA[c]	–	$1 \cdot 10^{-8}$	–	–	10
Native fluorescence (275 nm excitation)	$1 \cdot 10^{-10}$	–	$2 \cdot 10^{-10}$	–	This work
Native fluorescence with stacking (275 nm excitation)	$3 \cdot 10^{-12}$	–	$1 \cdot 10^{-11}$	–	This work

[a] Fluorescein isothiocyanate.
[b] 2-*p*-Toluidinonapthalene-6-sulfonate.
[c] *o*-Phthalaldehyde.

dynamic reserve of the laser light [13] and the difficulty in selecting a well-behaved fluorophore with an electrophoretic mobility close to that of the analyte [21]. On-column labeling LIF detection is hampered by the large flicker noise on the fluorescence background resulting from the presence of unbound fluorophores in the eluent [11]. The performance of post-column labeling LIF is compromised by the short reaction time at the optimal reagent flow rate and flow distance [10]. Rather surprisingly, pre-column labeling LIF with FITC for conalbumin, which contains 102 side chain amine groups [22], offers an LOD no better than native fluorescence detection excited at 275 nm. This is in contrast to reports that FITC-derivatized amino acids can be detected in the 10^{-12} M range [9]. The probable reason for this is the formation of multiple peaks on the electropherogram with pre-column labeling, which increases the magnitude of background fluctuations close to the migration time of the major peak and decreases the size of the major peak [11]. Consequently, the use of native fluorescence as a detection principle for proteins in CE surrenders little in detection sensitivity. One gains in the simplicity and speed of analysis compared to fluorescence derivatization, which may not even be feasible at these low concentrations and small amounts. The sample is also preserved for further studies or use. One may even be able to implement fluorescence-detected circular dichroism [23] to study protein conformations. A drawback of the present detection scheme is that only tryptophan- or tyrosine-containing proteins are amenable to detection. Therefore, some peptides and small proteins may escape detection.

The LODs of $1 \cdot 10^{-10}$ and $2 \cdot 10^{-10}$ M for conalbumin and BSA, respectively, were obtained with the analytes dissolved in buffers identical in composition to the running buffer (5 mM sodium phosphate at pH 10.2). Interestingly, when a 5 mM sodi-

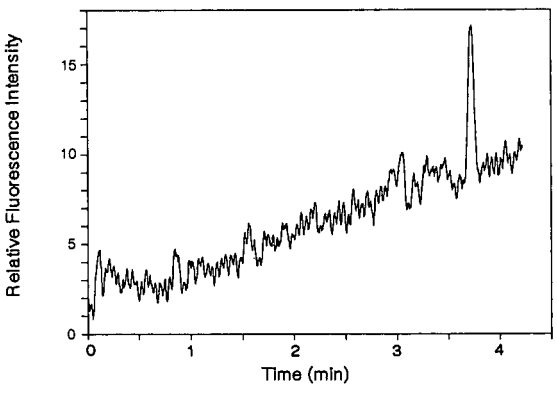

Fig. 5. Electropherogram of $1 \cdot 10^{-8}$ *M* tryptophan injected.

um phosphate solution at pH 6.68 was used as the sample buffer, the LODs for the same analytes decreased to $3 \cdot 10^{-12}$ and $1 \cdot 10^{-11}$ *M* respectively, with a small loss of separation efficiency. The phenomenon bears some similarity to electrophoretic concentration (or stacking). The lower ionic strength of the pH 6.68 sample buffer also increases the effective injection potential. Electrophoretic concentration has been applied to the analysis of dilute peptide samples with CE where the pH of the sample buffer is higher than that of the running buffer and with that, it has been claimed the LOD can be lowered by at least 5 times [24]. Therefore, electrophoretic concentration, when optimized and coupled to LIF detection of native proteins, possesses tremendous potential in protein determination at the trace level. The present enhancement should be applicable to physiological samples, which are near neutral pH. Further work on this is now under way.

Fig. 5 depicts an electropherogram showing tryptophan present at $1 \cdot 10^{-8}$ *M* in the sample. The estimated LOD (at *S/N* of 2) for tryptophan is $2 \cdot 10^{-9}$ *M*. Conalbumin, which contains 15 tryptophan and 21 tyrosine residues [22], does not show a linear increase in detection sensitivity as expected from the number of tryptophan residues. There are several explanations for this. First, the quantum yield of fluorescence of tryptophan residues in a hydrophobic microenvironment is about 3 times smaller than that for residues in a hydrophilic microenvironment [25]. Hence, it is possible that most or all of the tryptophan residues in conalbumin are located in the hydrophobic core of the protein. Secondly, a variety of functional groups such as peptide bonds [26] and protonated amine groups [27] are effective in quenching the fluorescence of tryptophan residues in proteins. Thirdly, the fluorescence and fluorescence-excitation spectra of tryptophan and proteins differ [20]. The present optical arrangement might favor tryptophan fluorescence over conalbumin fluorescence. However, the LOD of BSA ($2 \cdot 10^{-10}$ *M*) is only twice that for conalbumin, even though the former possesses only 1 tryptophan and 16 tyrosine residues [28]. The hydrophilic microenvironment of the tryptophan residue in BSA might serve as an explanation. Another reason is that energy-transfer from the tyrosine and phenylalanine residues to the tryptophan residue in BSA might increase the effective fluorescence quantum yield of the tryptophan residue [20]. Why this energy-transfer phenomenon occurs selectively in BSA but not in conalbumin is unclear.

ACKNOWLEDGEMENTS

Ames Laboratory is operated for the US Department of Energy by Iowa State University under contract No. W-7405-Eng-82. This work was supported by the Director of Energy Research, Office of Basic Energy Sciences and Office of Health and Environmental Research.

REFERENCES

1 W. G. Kuhr, *Anal. Chem.*, 62 (1990) 403R.
2 R. A. Wallingford and A. G. Ewing, *Anal. Chem.*, 60 (1988) 258.
3 X. Huang, J. Luckey, M. Gordon and R. Zare, *Anal. Chem.*, 61 (1989) 766.
4 R. Caprioli, W. Moore, M. Martin, B. Dague, K. Wilson and S. Moring, *J. Chromatogr.*, 480 (1989) 247.
5 S. Pentoney, R. Zare and J. Quint, *Anal. Chem.*, 61 (1989) 1642.
6 J. W. Jorgenson and Y. Wahlbroehl, *J. Chromatogr.*, 315 (1984) 135.
7 J. Briggs and P. R. Panfili, *Anal. Chem.*, 63 (1991) 850.
8 J. Green and J. Jorgenson, *J. Chromatogr.*, 352 (1986) 337.
9 Y.-F. Cheng and N. J. Dovichi, *Science (Washington, D.C.)*, 242 (1989) 562.
10 B. Nickerson and J. W. Jorgenson, *J. Chromatogr.*, 480 (1989) 157.
11 D. F. Swaile and M. J. Sepaniak, *J. Liq. Chromatogr.*, 14 (1991) 869.
12 D. F. Swaile and M. J. Sepaniak, *Anal. Chem.*, 63 (1991) 179.
13 W. G. Kuhr and E. S. Yeung, *Anal. Chem.*, 60 (1988) 2642.

14 *Points to Consider in the Production and Testing of New Drugs and Biologicals Produced by Recombinant DNA Technology (draft)*, Office of Biologics Research and Review, Food and Drug Administration, Bethesda, MD, 1983.
15 F. Tron, F. Degos, C. Brechot, A.-M. Courouce, A. Goudeau, F.-N. Marie, Adamowicz, P. Saliou, A. Laplanche, J.-P. Benhamon and M. J. Girard, *J. Infect. Dis.*, 160 (1989) 199.
16 D. C. Powers, S. D. Sears, B. R. Murphy, B. Thumar and M. L. Clements, *J. Clin. Microbiol.*, 27 (1989) 2666.
17 *Points to Consider in the Manufacture and Testing and Monoclonal Antibody Products for Human Use (draft)*, Office of Biologics Research and Review, Food and Drug Administration, Bethesda, MD, 1987.
18 T. Lee, E. S. Yeung and M. Sharma, *J. Chromatogr.*, 565 (1991) 197.
19 P. Gozel, E. Gassmann, H. Michelsen and R. N. Zare, *Anal. Chem.*, 59 (1987) 44.
20 F. W. J. Teale, *Biochem. J.*, 76 (1960) 381.
21 F. E. P. Mikkers, F. M. Everaerts and Th. P. E. M. Verheggen, *J. Chromatogr.*, 169 (1979) 1.
22 J. Williams, T. Elleman, I. Kingston, A. Wilkens and K. Kuhn, *Eur. J. Biochem.*, 122 (1982) 297.
23 P. L. Christensen and E. S. Yeung, *Anal. Chem.*, 61 (1989) 1344.
24 R. Aebersold and H. D. Morrison, *J. Chromatogr.*, 516 (1990) 79.
25 S. V. Konev, *Fluorescence and Phosphorescence of Proteins and Nucleic Acids*, Plenum Press, New York, 1967, p. 83.
26 R. W. Cowgill, *Biochim. Biophys. Acta*, 75 (1963) 272.
27 F. W. J. Teale, *Photoelec. Spectrometry Group Bull.*, 13 (1961), 346.
28 B. Meloun, L. Moravek and V. Kostka, *FEBS Letters*, 58 (1975) 134.

Journal of Chromatography, 595 (1992) 327–333
Elsevier Science Publishers B.V., Amsterdam

CHROM. 23 874

Relationship between zone length and step height in isotachophoresis

M. T. Ackermans, F. M. Everaerts and J. L. Beckers*

Laboratory of Instrumental Analysis, Eindhoven University of Technology, P.O. Box 513, 5600 MB, Eindhoven (Netherlands)

(Received October 11th, 1991)

ABSTRACT

The relationship between response factor (*RF*) and specific zone resistance at 25°C (SZR_{25}) in isotachophoresis was evaluated and a linear relationship between *RF* and SZR_{25} values could be established for strong ionic components. Working at a constant electric current, the *RF* value is proportional to the zone length (seconds) per mole of component. Because the SZR_{25} values are linearly related to the step heights in the isotachopherograms, the zone lengths per mole of sample component must be linearly related to the step heights of the sample components. If this relationship is measured for a standard mixture with an equimolar composition, all other unknown sample components can be quantified from the step heights in a single experiment. This principle was verified experimentally for several anionic and cationic leading electrolyte systems at different pH values.

INTRODUCTION

Isotachophoresis (ITP) is a well known separation technique for the qualitative and quantitative analysis of ionic components using differences in effective electrophoretic mobilities. The separation mechanism is well defined and can be described by mathematical models [1–3] and over a wide range applications have been reported [4–8]. Further, the method can be used for the determination of several physico-chemical parameters such as absolute mobilities and p*K* values [9,10].

When applying a separation technique in the analysis of an unknown sample, quantitative information cannot be easily obtained. Generally, the sample composition has to be determined first, after which calibration graphs have to be set up, before quantitative analyses are possible. A unique feature of ITP is that, in contrast to most other separation techniques, the step heights in the isotachopherograms contain both qualitative and quantitative information. In this paper, the relationship between response factor (*RF*) and step height is discussed.

THEORY

When the steady state in ITP is reached, all sample zones migrate with equal velocity, v_{ITP} (cm/s):

$$v_{ITP} = m_L E_L = m_i E_i$$

where m_i, m_L, E_i and E_L are the mobilities ($cm^2/V \cdot s$) of a sample ion *i* and the leading ion L and the electric field strengths (V/cm) in the corresponding zones, respectively.

For a not too high applied electric current density, a linear relationship between step height and the specific zone resistance at 25°C (SZR_{25}, Ω m) is obtained, applying an a.c. detector [11]. Hence if for two standard components, with known p*K* values and mobilities at infinite dilution, the SZR_{25} values are calculated using a mathematical model for the steady state in ITP, a linear relationship between step height and SZR_{25} values can be set up. Applying this relationship, the SZR_{25} value of an unknown sample component can be calculated from its step height. If the SZR_{25} values for an unknown sample component are determined for two different electrolyte systems, its mobility and p*K* value can be

0021-9673/92/$05.00

calculated with the concept of the isoconductor [10]. For a known pK value, *e.g.*, for strong ionic species, the mobility can be obtained from a single experiment.

For quantification of sample components, the response factor RF (C/mol) can be used, representing the slope of a calibration graph of the product of the zone length ZL (s) and the applied current I (A) *versus* the amount of the sample component Q (mol):

$$RF = \frac{ZL \cdot I}{Q}$$

Once the mobilities and pK values of sample components are known, the RF values can easily be calculated [11]. This means that if for a given electrolyte system the relationship between step height and SZR_{25} value is established from a single experiment, both quantitative and qualitative parameters can be obtained for strong, monovalent ionic species.

TABLE I

MOBILITIES AT INFINITE DILUTION, m ($cm^2/V \cdot s$), AND pK VALUES FOR IONIC SPECIES USED IN THE CALCULATIONS AND COMPOSITIONS OF SEVERAL ELECTROLYTE SYSTEMS

Ionic species	$m \cdot 10^5$	pK
Acetic acid	−42.4	4.76
β-Alanine	36.7	3.552
ε-Aminocaproic acid	28.8	4.37
Creatinine	37.2	4.828
Histidine	29.6	6.04
Hydrochloric acid	−79.1	−2.0
Imidazole	52.0	7.15
MES[a]	−28.0	6.1
Potassium	76.2	14.0
Tris[b]	29.5	8.1

Anionic electrolyte systems (electrolyte: 0.01 M HCl)

pH	Counter ion	Terminator
3.2	β-Alanine	Propionic acid
4.0	ε-Aminocaproic acid	Pivalic acid
5.0	Creatinine	Pivalic acid
6.0	Histidine	MES[a]
7.0	Imidazole	–

Cationic electrolyte systems (electrolyte: 0.01 M KOH)

pH	Counter ion	Terminator
4.3	Acetic acid	Acetic acid
5.0	Acetic acid	Acetic acid
6.0	MES[a]	Histidine

[a] MES = 2-(N-Morpholino)ethanesulphonic acid.
[b] Tris = Tris(hydroxymethyl)aminomethane.

Relationship between RF and SZR_{25}

In Table I the mobilities at infinite dilution and the pK values of several ionic species and the compositions of several electrolyte systems, used in the calculations and experiments, are given. In order to study the relationship between SZR_{25} values and quantitative parameters, we calculated for monovalent ions with an SZR_{25} value of 50 Ω m, assuming a certain pK value, the mobilities at infinite dilution, the total concentration, the ionic concentration, the zone pH and RF value for a leading electrolyte system of 0.01 M HCl adjusted to pH = 3.2 by adding β-alanine. In Table II, all calculated values are given, and it can be concluded that for components with equal SZR_{25} values (*i.e.*, identical step heights and effective electrophoretic mobilities), the mobility at infinite dilution, the total concentration and the pH increase with increasing pK values, whereas the ionic concentration and the RF values decrease. This means that without further information no quantitative information can be obtained from a single step height in this way.

For strong ionic species, we calculated for the same electrolyte system as used for Table II, for different mobilities at infinite dilution, the SZR_{25} values, the ionic concentration (equal to the c_{tot}),

TABLE II

CALCULATED MOBILITY AT INFINITE DILUTION, m ($cm^2/V \cdot s$), TOTAL CONCENTRATION, c_{tot} (mol/l), IONIC CONCENTRATION, c (mol/l), ZONE pH AND RF VALUES (10^5 C/mol) FOR A COMPONENT WITH A SZR_{25} VALUE OF 50 Ωm IN A LEADING ELECTROLYTE OF 0.01 M HCl AT pH 3.2 FOR DIFFERENT pK VALUES OF THE COMPONENT

pK	$m \cdot 10^5$	c_{tot}	c	pH	RF
−1.0	−13.78	0.0033	0.0033	3.79	5.12
2.0	−13.96	0.0033	0.0033	3.79	5.05
2.5	−14.37	0.0034	0.0033	3.80	4.91
3.0	−15.50	0.0037	0.0032	3.81	4.56
3.5	−18.73	0.0044	0.0031	3.86	3.82
4.0	−26.42	0.0059	0.0029	3.95	2.85
4.5	−41.69	0.0081	0.0024	4.11	2.07
5.0	−69.07	0.0105	0.0019	4.31	1.60

TABLE III

CALCULATED SZR_{25} VALUES (Ω m), IONIC CONCENTRATION, c (mol/l), pH AND RF VALUES (10^5 C/mol) FOR STRONG MONOVALENT IONIC SPECIES WITH DIFFERENT MOBILITIES AT INFINITE DILUTION, m ($cm^2/V \cdot s$), IN A LEADING ELECTROLYTE OF 0.01 M HCl AT pH 3.2

$m \cdot 10^5$	SZR_{25}	c	pH	RF
−70	9.08	0.0095	3.23	1.77
−60	10.64	0.0089	3.28	1.89
−50	12.85	0.0081	3.33	2.08
−40	16.20	0.0071	3.40	2.35
−30	21.89	0.0060	3.50	2.81
−20	33.57	0.0044	3.65	3.77
−10	70.71	0.0025	3.92	6.83

pH and RF values. All calculated values are given in Table III, and indicate that there is a linear relationship between SZR_{25} and RF values. In order to check whether such a linear relationship is valid for all electrolyte systems, we calculated the SZR_{25} and RF values for strong ionic species for several anionic and cationic electrolyte systems at different pHs. The compositions of the electrolyte systems are given in Table I. In Table IV all calculated values are given and in Fig. 1 the relationships between RF and SZR_{25} values are shown for (A) anionic and (B) cationic systems. For cationic systems at a low pH, the contribution of the hydrogen ions to the zone conductivity is large, resulting in an elongation of the zones and higher RF values, especially for components with low effective mobilities. In

TABLE IV

CALCULATED VALUES FOR SZR_{25} (Ω m) AND RF (10^5 C/mol) FOR STRONG IONIC SPECIES IN SEVERAL ELECTROLYTE SYSTEMS AT DIFFERENT pH

$m \cdot 10^5$ ($cm^2/V \cdot s$)	Anions									
	pH 3.2		pH 4		pH 5		pH 6		pH 7	
	SZR_{25}	RF	SZR_{25}	RF	SZR_{25}	RF	SZR_{25}	RF	SZR_{25}	RF
−70	9.08	1.77	11.41	1.39	10.88	1.46	11.72	1.35	9.75	1.65
−60	10.64	1.89	13.38	1.46	12.77	1.55	13.75	1.42	11.43	1.77
−50	12.85	2.08	16.18	1.57	15.43	1.68	16.62	1.52	13.80	1.94
−40	16.20	2.35	20.44	1.73	19.48	1.87	21.00	1.66	17.41	2.20
−30	21.89	2.81	27.68	2.00	26.36	2.19	28.46	1.92	23.52	2.64
−20	33.58	3.77	42.67	2.58	40.55	2.88	43.90	2.46	36.08	3.56
−15	45.65	4.74	58.22	3.18	55.24	3.59	59.94	3.02	49.02	4.52
−10	70.71	6.83	90.77	4.45	85.88	5.09	93.55	4.22	75.91	6.52
	Cations									
	pH 4.3		pH 5		pH 6					
	SZR_{25}	RF	SZR_{25}	RF	SZR_{25}	RF				
70	10.10	1.57	10.26	1.54	11.80	1.33				
60	11.87	1.68	12.01	1.64	13.83	1.39				
50	14.29	1.84	14.52	1.79	16.70	1.48				
40	17.98	2.10	18.36	2.01	21.10	1.62				
30	24.32	2.59	24.74	2.40	28.73	1.86				
25	29.42	3.06	30.03	2.73	34.85	2.06				
20	37.06	3.96	38.07	3.25	44.27	2.37				
15	–	–	51.64	4.21	60.52	2.91				
10	–	–	79.03	7.14	94.53	4.07				

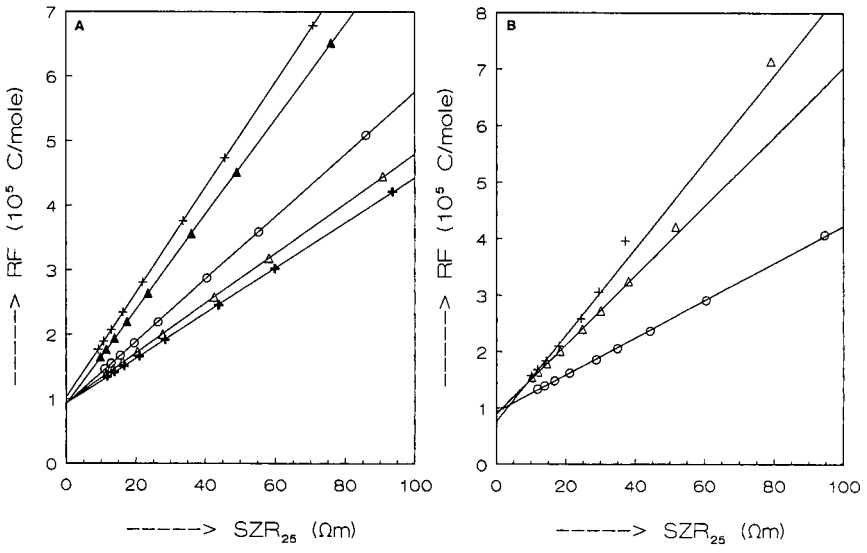

Fig. 1. Calculated relationship between response factor (*RF*, C/mol) and specific zone resistance at 25°C (SZR_{25}, Ω m) for several strong monovalent ions in (A) anionic electrolyte systems at pH (+) 3.2, (△) 4, (○) 5, (+) 6 and (▲) 7 and (B) cationic electrolyte systems at pH (+) 4.3, (△) 5 and (○) 6.

fact, the mathematical model for ITP is not valid because a moving boundary system is present. For the regression lines in Fig. 1, the deviating *RF* values are not taken into account.

From Fig. 1, it is clear that in all electrolyte systems linear relationships are obtained between SZR_{25} and *RF* values. If the mobility of the sample component is very high, the influence of the counter ions on the SZR value is almost zero and hence the *y*-intercept is about $1 \cdot 10^5$ C/mol, the value of the Faraday constant.

Working at a constant electric current, the *RF* value for a sample component will be proportional to the ratio of the zone length (s) to the injected amount of the sample component. Because the *RF* value is linearly related to the SZR_{25} and this parameter is linearly related to the step height, the zone lengths must be linearly related to the step heights for equimolar sample compositions. If this is true in practice, it is a unique advantage of ITP that if the relationship between zone length and step height is measured with a sample of equimolar composition, for all unknown samples (independent of the kind of ionic species) the quantitative composition can be determined directly. For strong divalent ions the same relationship between zone length and step height holds, although the *RF* value and zone length are twice as large because the concentration in its zone is half the concentration of monovalent ions. Under Results and Discussion these relationships are established for different anionic and cationic sample compositions in different leading electrolyte systems.

EXPERIMENTAL

Instrumentation

For all ITP experiments a laboratory-built apparatus [1] with conductivity and UV detectors (254 nm) was used. In this apparatus a closed system is obtained by shielding the separation capillary from the open electrode compartments with semipermeable membranes. A PTFE capillary tube (0.2 mm I.D.) was used. The sample was introduced with a syringe.

Chemicals

All chemicals were of analytical-reagent grade. Before preparing the sample solutions, all chemicals were dried at 105°C.

RESULTS AND DISCUSSION

To check experimentally whether a linear rela-

TABLE V

MEASURED STEP HEIGHTS, H, AND FROM THESE STEP HEIGHTS CALCULATED MOBILITIES AT INFINITE DILUTION, m ($cm^2(V \cdot s)$), SPECIFIC ZONE RESISTANCES AT 25°C, SZR_{25} (Ω m), CALCULATED RESPONSE FACTORS, RF (10^5 C/mol), EXPERIMENTALLY DETERMINED RF VALUES (10^5 C/mol) AND ZONE LENGTHS, ZL (s), FOR SEVERAL COMPONENTS IN AN EQUIMOLAR SAMPLE COMPOSITION IN DIFFERENT ELECTROLYTE SYSTEMS

Component	H	$m \cdot 10^5$	SZR_{25}	RF		ZL
				Calc.	Exptl.	
Leading electrolyte potassium acetate at pH 4.3, electric current 2 μA, injection volume 1 μl for given zone length						
Silver	18.0	61.54	11.55	1.66	1.64	127.6
Barium	19.7	65.01	12.08	3.32	3.34	134.0
Sodium	24.4	52.50	13.56	1.80	1.74	201.0
TMA[a]	32.8	44.37	16.21	1.97	1.91	152.0
TEA[b]	51.8	32.68	22.20	2.43	2.31	179.0
TRIS	59.9	29.50	24.74	2.63	2.49	195.0
TBA[c]	97.4	–	35.42	–	3.27	253.0
Leading electrolyte potassium acetate at pH 5.0, electric current 2 μA, injection volume 1 μl for given zone length						
Silver	14.6	62.24	11.57	1.62	1.59	117.0
Sodium	18.7	53.99	13.43	1.72	1.68	199.0
Lithium	30.3	39.20	18.70	2.04	1.96	150.0
TEA	39.0	32.65	22.65	2.27	2.16	169.0
TRIS	44.7	29.50	25.32	2.43	2.40	182.5
TBA	68.5	21.04	36.03	3.12	3.08	234.0
Leading electrolyte histidine chloride at pH 6.0, electric current 20 μA, injection volume 3 μl for given zone length						
Chlorate	23.0	67.16	12.23	1.37	1.44	35.6
Fluoride	27.8	57.99	14.26	1.43	1.45	36.5
Sulfamate	32.0	51.50	16.12	1.50	1.55	38.8
Chloroacetate	41.2	41.82	20.05	1.63	1.65	43.3
Benzoate	53.2	34.03	25.15	1.80	1.86	47.0
Octylsulfonate	66.1	27.97	30.70	2.00	2.06	52.3

[a] TMA = tetramethyl ammonium bromide.
[b] TEA = tetraethyl ammonium bromide.
[c] TBA = tetrabutyl ammonium bromide.

tionship can be established between RF values and step heights, we determined the RF values by measuring the zone lengths for different amounts of monovalent strong cationic and anionic sample mixtures at an equimolar sample composition for different electrolyte systems. From the step heights we further calculated the mobilities at infinite dilution and the theoretical RF values. In Table V the measured step heights, the calculated mobilities at infinite dilution, the calculated SZR_{25} values, the calculated and measured RF values and the zone lengths of the components in the sample of equimolar composition are given. The concentrations of all monovalent sample components were 0.00154 M for the cations and 0.00167 M for the anions. The RF values were determined by measuring the zone lengths for different injection volumes. In the cationic mixture, the barium concentration was 0.00077 M and the measured zone length fits those of the monovalent cations.

In Fig. 2, the experimentally determined relationships between (A) step heigth H and specific zone resistance SZR_{25}, (B) response factor RF and SZR_{25}, (C) zone length ZL of the equimolar sample composition and the step height H and (D) response factor RF and step height H for cations in a leading electrolyte system at pH 4.3 and 5 and anions at pH 6 are given (see Table V for further conditions). It can be concluded that all relationships are linear. The y-intercepts in Fig. 2B approximate the expected value of the Faraday constant. When choosing the sample composition, special care must be taken to avoid zone elongation due to impurities originating from the electrolyte system.

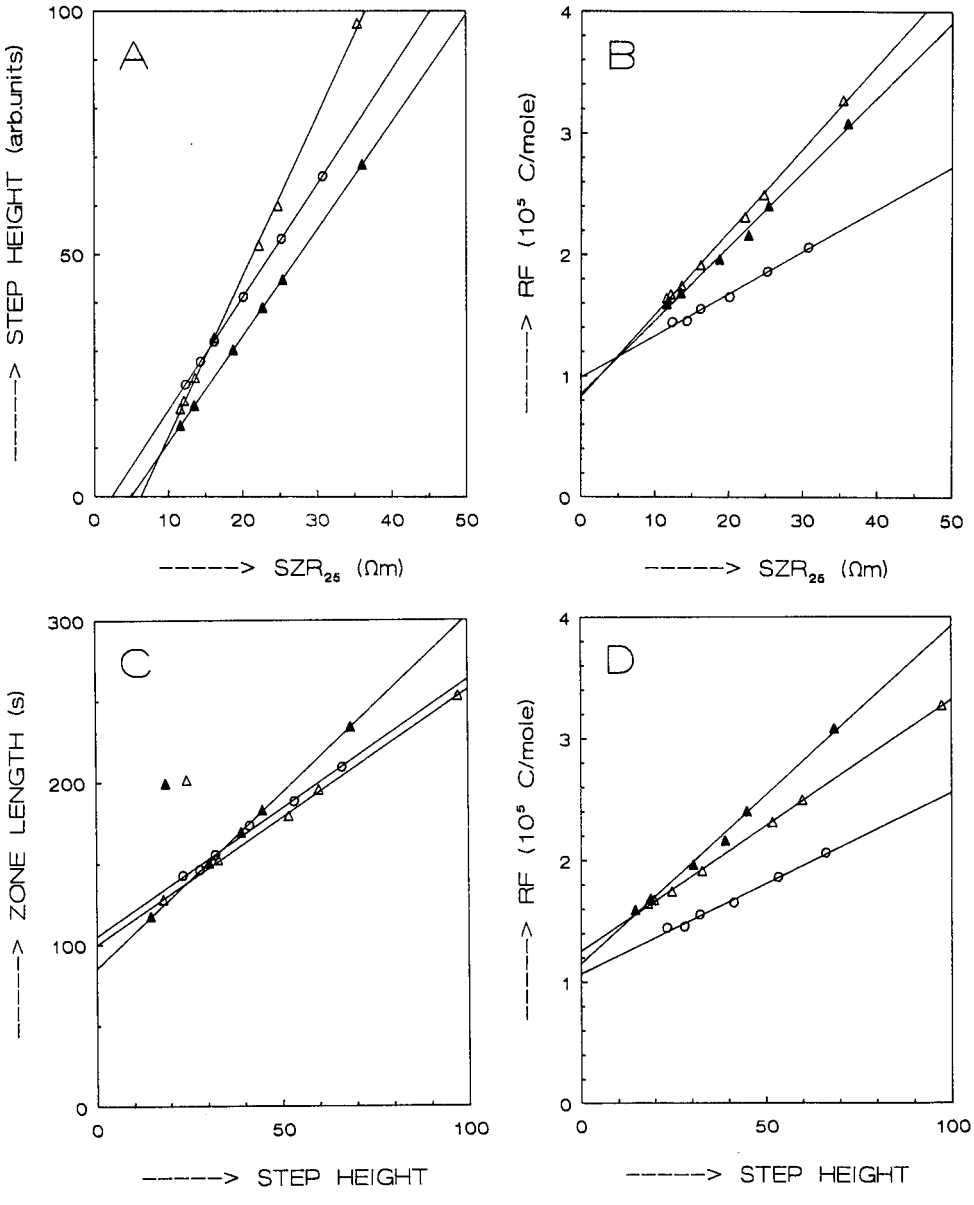

Fig. 2. Experimentally determined relationship between (A) step height H and specific zone resistance SZR_{25}, (B) response factor RF and SZR_{25}, (C) zone length ZL for an equimolar sample composition and H and (D) RF and H for cations in a leading electrolyte system at pH (△) 4.3 and (▲) 5 and anions at pH (○) 6. For further information, see Table V.

For this reason, different sample components are chosen for the different electrolyte systems. Often impurities present in the solvent and the electrolyte systems show a constant zone length, *i.e.*, the component present in the sample mixture with the same step height will have a constant elongation of its zone length. In that case, the zone length of that component does not fit the relationship between zone length and step height, whereas it does fit the relationship between RF value and step height, as the slopes of the calibration graph with and without this impurity are identical. This can be seen in Fig.

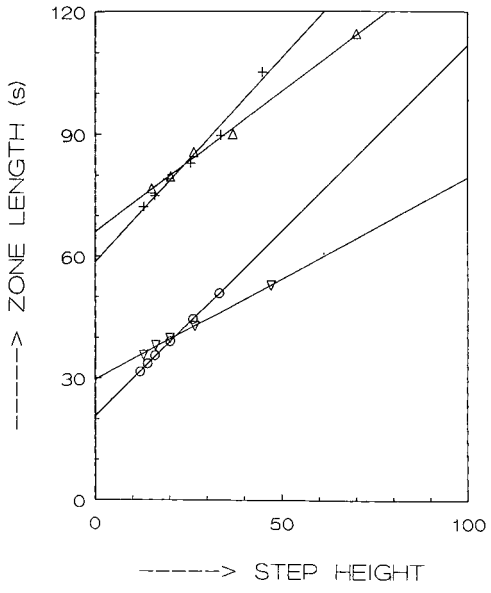

Fig. 3. Experimentally determined relationship between zone length and step height for anionic electrolyte systems at pH (○) 3.2 (10 μA), (+) 4 (10 μA), (△) 5 (10 μA) and (▽) 6 (20 μA). For further information, see text.

2C, where the zone length of sodium (present in the electrolyte system) is much too long, whereas in Fig. 2D the measured *RF* values fit the linear relationship between *RF* and step height.

As a last example, the zone lengths of a mixture with an equimolar composition of 0.00167 *M* chlorate, bromate, sulphamate, iodate, phosphate (only present at pH 3.2 and 4) and octylsulphonate were measured in anionic leading electrolytes at pH 3.2 (concentration of the leading ion 0.005 *M*), 4, 5 and 6. In Fig. 3, the relationships between zone length and step height are given. For all electrolyte systems linear relationships can be observed.

We also repeated several separations at different electric currents. For high electric currents, lower step heights and smaller zone lengths were observed, owing to the higher temperature of the system resulting in higher electrophoretic mobilities. Nevertheless, for all these systems, when applying different electric currents linear relationships were obtained.

CONCLUSIONS

A linear relationship between *RF* and SZR_{25} values was established theoretically for strong anions and cations. The zone lengths per mole of component are proportional to the *RF* values, applying a constant direct current, and the step heights are proportional to the SZR_{25} values. Hence a linear relationship can be expected between the zone lengths for an equimolar sample composition and the step heights of the components. This principle was checked for several anionic and cationic components in different electrolyte systems at different pH values. The results demonstrate that isotachophoresis has the unique advantage that, if the sample components are unknown, for strong ionic species quantitative information can be obtained in a single experiment. This can be of interest in, *e.g.*, the study the kinetics and reaction mechanisms of unknown intermediates.

REFERENCES

1 F. M. Everaerts, J. L. Beckers and Th. P. E. M. Verheggen, *Isotachophoresis —Theory, Instrumentation and Applications*, Elsevier, Amsterdam, 1976.
2 P. Bocek, M. Deml, P. Gebauer and V. Dolnik, *Analytical Isotachophoresis*, VCH, Weinheim, 1988.
3 Z. Deyl (Editor), *Electrophoresis, Part A: Techniques*, Elsevier, Amsterdam, 1979.
4 P. Gebauer, V. Dolnik, M. Deml and P. Bocke, *Adv. Electrophoresis*, 1 (1987) 281.
5 Z. Deyl (Editor), *Electrophoresis, Part B: Applications*, Elsevier, Amsterdam, 1979.
6 J. Akiyama, *Bunseki*, 1 (1979) 49.
7 Z. Prusik, in O. Mikes (Editor), *Laboratory Handbook of Chromatography and Allied Methods*, Horwood, Chicester, 1979, p. 649.
8 C. J. van Oss, *Sep. Purif. Methods*, 8 (1979) 119.
9 T. Hirokawa, M. Nishino, N. Aoki, Y. Kiso, Y. Sawamoto, T. Yagi and J. Akiyama, *J. Chromatogr.*, 271 (1983) D1.
10 J. L. Beckers, *J. Chromatogr.*, 320 (1985) 147.
11 J. L. Beckers and F. M. Everaerts, *J. Chromatogr.*, 470 (1989) 277.

Journal of Chromatography, 595 (1992) 334–336
Elsevier Science Publishers B.V., Amsterdam

CHROM. 23 882

Short Communication

Chromatographic behaviour of dipyridylsulphides

Relationship between log k' values and structure by reversed-phase high-performance liquid chromatography☆

J. Klimeš, V. Klimešová and K. Waisser

Faculty of Pharmacy, Charles University, Heyrovského 1203, 501 65 Hradec Králové (Czechoslovakia)

(First received July 30th, 1991; revised manuscript received November 19th, 1991)

ABSTRACT

Relationships between the structure and retention time in a group of dipyridylsulphides have been investigated. The retention time has been determined by high-performance liquid chromatography on a chemically bonded octadecylsilica column with methanol–13 m*M* phosphate buffer (pH 7) as the mobile phase, using UV detection. From the values of the logarithm of the capacity factor the contributions of the half-molecular fragments have been calculated. The contributions of the fragments can be used to calculate the capacity factors of other dipyridylsulphides. One example of the study of the structure–antituberculous activity relationship from the carbothioamides series is presented.

INTRODUCTION

The hydrophobicity of substances is undoubtedly the most important physical property affecting their biological activity. Since the time when Hansch and Fujita [1] formulated a general equation for the relationships between hydrophobicity, expressed in terms of the logarithm of the partition coefficient for the octanol–water system, and quantitatively expressed biological activity, many systems have been developed for estimation of hydrophobicity. Partition chromatography has played an important role [2–4]. The purpose of this work was to study the relationship between the structure and retention parameter obtained by high-performance liquid chromatography (HPLC) measurement (the logarithm of the capacity factor, log k') on a chemically bonded octadecylsilica column in a series of substituted dipyridylsulphides. The thioamides of this group are potential antituberculous drugs [5,6].

EXPERIMENTAL

Materials

Substances were prepared as described previously [5,6]. Solvents were of analytical reagent quality and were used without further purification.

High-performance liquid chromatography

The chromatographic system consisted of a Varian 8500 pump, a Varian Varichrom UV–VIS detec-

☆ Dedicated to Professor Roland Mayer on the occasion of his 65th birthday.

0021-9673/92/$05.00

TABLE I

LOGARITHM OF THE CAPACITY FACTOR FOR DIPYRIDYLSULPHIDES

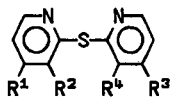

Type I

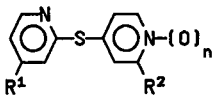

Type II

Compound No.	Type	R^1	R^2	R^3	R^4	n	Log k'
1	I	CN	H	CN	H	–	1.0625
2	I	$CSNH_2$	H	$CSNH_2$	H	–	0.9669
3	I	$CONHNH_2$	H	$CONHNH_2$	H	–	−0.00505
4	I	$CONH_2$	H	$CONH_2$	H	–	0.0964
5	I	H	CN	H	CN	–	0.8230
6	I	H	$CSNH_2$	H	$CSNH_2$	–	0.1493
7	I	CN	H	H	CN	–	0.9609
8	I	$CSNH_2$	H	H	$CSNH_2$	–	0.4952
9	II	CN	CN	–	–	0	1.0641
10	II	$CSNH_2$	$CSNH_2$	–	–	0	0.8819
11	II	CN	CN	–	–	1	0.5291
12	II	$CSNH_2$	$CSNH_2$	–	–	1	1.1180

tor, operated at 254 nm, and a Spectra-Physics SP 4100 integrator. The column (250 × 4 mm I.D.) was packed with Silasorb C_{18} 7.5 μm particle size (Lachema, Brno, Czechoslovakia). The pyridylsulphide solutions in methanol were injected into the column via a 10-μl loop. The mobile phase was methanol–13 m*M* phosphate buffer, pH 7 (30:70, v/v), at a flow-rate of 1 ml/min. The experiments were performed at room temperature. The retention time of potassium iodide was taken as t_0. The capacity factor, k', was evaluated from the t_0 value and the retention time of the solute, t_R, by eqn. 1.

$$k' = (t_R - t_0)/t_0 \quad (1)$$

The results are summarized in Table I.

TABLE II

VALUES OF THE LOGARITHM OF THE CAPACITY FACTOR FOR THE HALF-MOLECULAR FRAGMENTS

$r = 0.994$, $s = 0.002$, $n = 12$.

Fragments R–$S_{1/2}$[a]	Log k'
R	
(a) 4-Cyano-2-pyridyl	0.531
(b) 3-Cyano-2-pyridyl	0.411
(c) 2-Cyano-4-pyridyl	0.533
(d) 4-Thiocarbamoyl-2-pyridyl	0.476
(e) 3-Thiocarbamoyl-2-pyridyl	0.068
(f) 2-Thiocarbamoyl-4-pyridyl	0.406
(g) 4-Carbamoyl-2-pyridyl	0.048
(h) 4-Carbazoyl-2-pyridyl	−0.003
(l) 1-Oxido-2-cyano-4-pyridyl	−0.002
(j) 1-Oxido-2-thiocarbamoyl-4-pyridyl	0.642

[a] $S_{1/2}$ = one half of a sulphur atom.

Calculations

The regression equations were calculated on an IQ-151 personal computer (ZPA Nový Bor, Czechoslovakia) using a Multireg-H program.

The values of log k' for the half-molecular fragments were calculated by the iteration procedure (see Table II). For symmetrical sulphides, the half-molecular fragment value was obtained by dividing the log k' value by two. For unsymmetrical sulphides, *e.g.* Nos. 7, 8, 9, 10, 11 and 12, the values obtained for the symmetrical substituents served as the basis and, furthermore, these values were modified in the whole group to obtain the least standard deviation.

DISCUSSION

Structure–capacity factor relationships

The method used is based on the assumption that the mutual interaction between the pyridine rings is neglibible and therefore the use of the contributions corresponding to the half-molecular fragments is justified. On the basis of these fragment contributions, log k' can be calculated for other dipyridylsulphides not investigated in the present paper, *e.g.* for *bis*(2-thiocarbamoylpyridine-1-oxide-4-yl)sulphide log $k' = 2 \times 0.068 = 0.136$.

Interactions, however, can occur between the substituents on the pyridine ring. For instance, a comparison of the values in Table I for compounds 9 and 11 shows that the presence of 1-oxide results in a decrease in lipophilicity. In contrast, comparison of the values for compounds 10 and 12 shows that the presence of 1-oxide results in an increase in lipophilicity. In this case there is, however, a strong non-binding interaction between the thioamide and oxide groups (a hydrogen bond formation). From the values of half-molecular contributions the values of capacity factors were calculated for some other compounds studied from the standpoint of the structure–antituberculous activity relationships.

Structure–antituberculous activity relationships

The structure–antituberculous activity relationships were investigated only in the group of thioamides.

The values of the minimal inhibitory concentrations (MIC) were taken from the literature [5,6]. For the group of five thioamides, eqn. 2 was found to hold:

$$\text{Log MIC} = -0.5477 \log k' + 1.241 \quad (2)$$

$$n = 5 \quad r = 0.800 \quad s = 0.187$$

The antituberculous activity increases with increasing lipophilicity.

Similar conclusion have been reached when other thioamides of the dipyridylsulphides group have been examined [7].

CONCLUSION

The approach outlined in this paper for calculating the logarithm of the capacity factor from half-molecular contributions has not been employed in the literature hitherto. It can also be useful in other groups of isosteric compounds, such as other diarylsulphides, diarylethers, diarylmethane derivatives, etc. As log k' from chromatography on octadecyl silica columns can be considered a parameter of lipophilicity, the approach can be utilized in the quantitative structure–activity relationship (QSAR) method.

REFERENCES

1 C. Hansch and T. Fujita, *J. Am. Chem. Soc.*, 86 (1964) 1618.
2 R. Kaliszan, *Quantitative Structure–Chromatographic Retention Relationships*, Wiley, New York, 1987.
3 T. Braumann, *J. Chromatogr.*, 373 (1986) 191.
4 D. J. Minick, J. J. Sabatka and D. A. Brant, *J. Liq. Chromatogr.*, 10 (1987) 2565.
5 V. Klimešová, M. Čeladník and Ž. Odlerová, *Česk. Farm.*, 38 (1989) 388.
6 V. Klimešová, J. Vinšová, M. Čeladník and Ž. Odlerová, *Česk. Farm.*, 39 (1990) 104.
7 M. Čeladník, J. Vinšová, V. Klimešová, K. Waisser, K. Palát and Ž. Odlerová, *Česk. Farm.*, 32 (1983) 97.

Journal of Chromatography, 595 (1992) 337–339
Elsevier Science Publishers B.V., Amsterdam

CHROM. 23 935

Short Communication

High-performance liquid chromatography of isopropylphenols

M. Petro*, K. Križanovič and K. Ďulák

Research Institute of Chemical Technology, 836 03 Bratislava (Czechoslovakia)

(First received September 10th, 1991; revised manuscript received December 12th, 1991)

ABSTRACT

This paper presents a method for the direct determination of phenol, monoisopropylphenols (2-, 3- and 4-), diisopropylphenols (2,4-, 2,5-, 2,6- and 3,5-) and triisopropylphenols (2,4,5- and 2,4,6-) in technical alkylates. The possibility of controlling the alkylation reaction of phenol with propylene is shown. The 99% confidence limit is 10 ± 0.2%. The possibility of removing isopropylphenylethers from the alkylate and their determination are also discussed.

INTRODUCTION

The alkylphenols are important intermediates in the production of polymer additives with special applications. The most important of these compounds are the isopropylphenols. High-performance liquid chromatography (HPLC) has been used successfully in the separation of alkylphenols using both normal- [1–6] and reversed-phase [1–3,5,7,8] columns. The relationship between the molecular structure and retention of methylphenols has been studied [9]. Previously reported analytical procedures used UV and electrochemical detection [2,6,10] of alkylphenols.

This paper reports the direct determination of 4-isopropylphenol and other isomers as well as the products of side-reactions. The investigations were undertaken to develop an HPLC procedure capable of resolving and quantitating mixtures of isopropylphenols which would be applicable to the determination of industrially important isomers in technical mixtures [11].

EXPERIMENTAL

Chromatographic equipment

All separations were carried out using a Varian 2210 isocratic system, which includes a Model 2010 pump, a Model 2550 variable-wavelength UV detector, a Model 2081 column/valve mounting module and a Rheodyne injector. Retention data and the peak areas were measured and calculated by a Model SP 4200 computing integrator (Spectra-Physics).

Column

The column was a Separon SGX (Tessek, Czechoslovakia) consisting of 300 × 3.3 mm I.D. glass tubing packed with 5-μm silica.

Reagents

The chemicals were of analytical-reagent grade; *n*-hexane and dioxane were of spectroquality grade. Dioxane was dried and cleared of peroxidies by

0021-9673/92/$05.00

TABLE I
RELATIVE RETENTION TIMES OF ISOPROPYLPHENOLS

Compound	Relative retention time
2,4,6-Triisopropylphenol	0.228
2,6-Diisopropylphenol	0.243
2,4,5-Triisopropylphenol	0.380
2,5-Diisopropylphenol	0.416
2,4-Diisopropylphenol	0.492
2-Isopropylphenol	0.568
3,5-Diisopropylphenol	0.654
3-Isopropylphenol	0.791
4-Isopropylphenol	0.857
Phenol	1.000

passing through a 60 × 2 cm I.D. column filled with activated alumina.

The standards used (Table I) were prepared by the Division of Organic Chemistry in this Institute according to standard procedures; their purities and structures were established by elemental analysis, standard physicochemical techniques (Table II), ^{1}H NMR, ^{13}C NMR and gas chromatography–mass spectrometry.

Mobile phase

The mobile phase consisted of 2% (v/v) dioxane in *n*-hexane. The mobile phase for the separation of ethers was *n*-hexane.

Standard solutions

Standard solutions were prepared in the range 1–30 mg per 50 ml. Stock solutions of isopropylphenols were first prepared by dissolving 200 mg of the appropriate compound in 50 ml of mobile phase, then working standards were prepared by dilution of the stock solutions. The stock solutions were stable for up to 1 week when stored in the refrigerator.

TABLE II
BOILING AND FREEZING POINTS OF ISOPROPYLPHENOLS

Compound	Boiling point (°C)[a]	Freezing point (°C)
2,4,6-Triisopropylphenol	135	28
2,4,5-Triisopropylphenol	145	75
2,6-Diisopropylphenol	121	18
2,5-Diisopropylphenol	131	26
2,4-Diisopropylphenol	127	22
3,5-Diisopropylphenol	134	50
2-Isopropylphenol	94	15
4-Isopropylphenol	108	63

[a] 1.6 kPa.

Sample solution

For the analysis of technical mixtures of isopropylphenols 100–300 mg of sample were accurately weighed into a 50-ml calibrated flask, dissolved and diluted to volume with mobile phase.

Chromatographic procedure

The separations were performed in the isocratic mode at ambient temperature at a flow-rate of 1.0 ml/min (2 ml/min for the separation of ethers). Volumes of 10 μl of the solutions were introduced on to the column with a constant-volume loop injector. The detector was operated at 280 nm (0.32 a.u.f.s.).

Calculation

Calibration graphs were generated by plotting the peak area *versus* the concentration of standard substances in the concentration range 20–600 μg/ml. In all instances the calibration graphs were linear with a correlation coeficient of 0.999. Values of unknown sample concentrations were determined by comparison with the calibration graph.

Separation of ethers

Ethers were first isolated from the technical mixture with *n*-hexane on a 250 × 10 mm I.D. column packed with 100–160 μm Silasorb L (Lachema, Brno, Czechoslovakia). First three 100-ml fractions were concentrated to 10-ml volumes and reinjected onto an analytical column.

RESULTS AND DISCUSSION

To find the optimum chromatographic system the influence of the mobile phase on the retention time was studied. Combinations of methanol, acetonitrile and water were evaluated as mobile phases. Reversed-phase HPLC was found not to provide a satisfactory separation of closely related couples of the compounds 2-isopropylphenol, 3-isopropylphenol, 2,4-diisopropylphenol and 2,5-diisopropylphe-

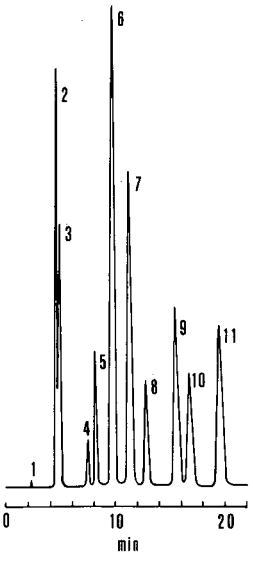

Fig. 1. High-performance liquid chromatogram of a mixture of isopropylphenols. Compact glass column, 300 × 3.3 mm I.D. Separon SGX, 5 μm; eluent, *n*-hexane–dioxane (98/2, v/v); flow-rate, 1 ml/min; UV detector, 280 nm. Peaks: 1 = phenyl isopropyl ether; 2 = 2,4,6-triisopropylphenol; 3 = 2,6-diisopropylphenol; 4 = 2,4,5-triisopropylphenol; 5 = 2,5-diisopropylphenol; 6 = 2,4-diisopropylphenol; 7 = 2-isopropylphenol; 8 = 3,5-diisopropylphenol; 9 = 3-isopropylphenol; 10 = 4-isopropylphenol; 11 = phenol.

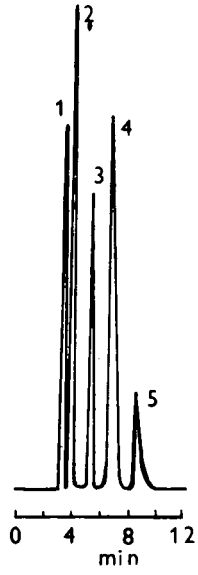

Fig. 2. High-performance liquid chromatogram of a mixture of isopropylphenylethers. Compact glass column, 300 × 3.3 mm I.D. Separon SGX, 5 μm; eluent, *n*-hexane; flow-rate, 2 ml/min; UV detector, 280 nm. Peaks: 1 = 2-isopropylphenyl isopropyl ether; 2 = 2,4-diisopropylphenyl isopropyl ether; 3 = phenyl isopropyl ether; 4 = 4-isopropylphenyl isopropyl ether and 2,6-diisopropylphenyl isopropyl ether; 5 = 2,4,6-triisopropylphenyl isopropyl ether.

nol [12]. Attempts to improve the peak shapes, retention time and resolution by altering the concentrations of the solvent were unsuccessful.

Good separation of isopropylphenols (Fig. 1) and isopropylphenylethers (Fig. 2) was achieved by normal-phase HPLC. As illustrated in Fig. 1, separation of mixtures of isopropylphenols can be obtained by the use of an isocratic solvent system *n*-hexane–dioxane (98:2, v/v). The use of dioxane as the modifier in the mobile phase for the separation of alkylphenols by normal-phase HPLC is in agreement with the principles of solvent selectivity (dioxane, tetrahydrofuran and propan-2-ol, respectively) discussed by Dzido and Soczewiński [13].

REFERENCES

1 J. F. Schabron, R. J. Hurtubise and H. F. Silver, *Anal. Chem.*, 50 (1978) 1911.
2 J. F. Schabron, R. J. Hurtubise and H. F. Silver, *Anal. Chem.*, 51 (1979) 1426.
3 P. Jandera, J. Churáček, J. Čáslavský and D. Szabo, *Chromatographia*, 14 (1981) 100.
4 R. J. Hurtubise, A. Hussain and H. F. Silver, *Anal. Chem.*, 53 (1981) 1993.
5 K. Callmer, L. E. Edholm and B. E. F. Smith, *J. Chromatogr.*, 136 (1977) 45.
6 K. Karch, I. Sebestian, I. Halász and H. Engelhardt, *J. Chromatogr.*, 122 (1976) 171.
7 K. Ogan and E. Katz, *Anal. Chem.*, 53 (1981) 160.
8 Tj. Th. Lub, H. C. Smit and H. Poppe, *J. Chromatogr.*, 149 (1978) 721.
9 V. P. Dimitrikov and V. M. Nabivach, *Zh. Anal. Khim.*, 42 (1987) 1110.
10 R. E. Shoup and G. S. Mayer, *Anal. Chem.*, 54 (1982) 1164.
11 Ł. Bystrický and M. Petro, Cz. Patent 248 490, *C.A.*, 109 (1988) P 243 328 m.
12 M. Petro and Ł. Bystrický, *Chem. Pap.*, 40 (1986) 357.
13 T. Dzido and E. Soczewinski, *J. Chromatogr.*, 395 (1987) 489.

Journal of Chromatography, 595 (1992) 340–345
Elsevier Science Publishers B.V., Amsterdam

CHROM. 23 956

Short Communication

Analyses of isomeric mono-O-methyl-D-glucoses, D-glucobioses and D-glucose monophosphates by high-performance anion-exchange chromatography with pulsed amperometric detection

Kyoko Koizumi*, Yoko Kubota, Hisako Ozaki, Keiko Shigenobu, Masako Fukuda and Toshiko Tanimoto

Faculty of Pharmaceutical Sciences, Mukogawa Women's University, 11-68 Koshien Kyuban-cho, Nishinomiya 663 (Japan)

(First received August 28th, 1991; revised manuscript received December 13th, 1991)

ABSTRACT

To investigate the contribution of each hydroxyl group of D-glucose to retention on pellicular quaternary amine-bonded resins and to the pulsed amperometric detector response, all sets of isomeric mono-O-methyl-D-glucoses and D-glucobioses and three isomeric D-glucose monophosphates were analysed by high-performance anion-exchange chromatography under alkaline conditions with pulsed amperometric detection. The results showed that the reduction of retention time on mono-O-methylation follows the order 2-OH > 3-OH > 6-OH ≥ 4-OH > 1-OH. Although the elution order of 1-, 3- and 6-phosphates was the same as obtained for the corresponding methyl esters, in the case of glucobioses the elution position was somewhat affected by the configurational contribution and hydrophobic interaction. The pulsed amperometric detector response was little affected by the acidity of each hydroxyl group of D-glucose. The suppression of the pulsed amperometric detector response by substitution of hydroxyl group seemed to be due to the inhibitory effect of the substituent group on the vicinal hydroxyl groups and, as a rule, the degree of suppression caused by 6-O-substitution was the smallest.

INTRODUCTION

Recently it has been shown that an accurate and sensitive analysis of carbohydrates can be performed using high-performance anion-exchange chromatography (HPAEC) coupled with triple-pulse amperometric detection (PAD) at a gold electrode, and this method has become a powerful tool in carbohydrate research [1–3]. In HPAEC, strong alkaline solutions are used as eluents and the hydroxyl groups of carbohydrates can be ionized under these conditions. It is known that there are subtle differences in the pK_a of the hydroxyl groups in carbohydrates [4–5].

In this work we analysed all sets of isomeric mono-O-methyl-D-glucoses and D-glucobioses to investigate the contribution of each hydroxyl group of D-glucose to the elution position during HPAEC and to PAD response [6]. In addition, the chromatographic behaviour of three isomeric D-glucose monophosphates on this HPAEC system was examined.

0021-9673/92/$05.00

EXPERIMENTAL

Materials

Methyl β-D-glucoside [7] was prepared by methylation and deacetylation of tetra-O-acetyl-α-D-glucosyl bromide [8]; m.p. 111°C, $[\alpha]_D^{22}$ −32.7° ($c=2$, H_2O).

2-O-Methyl-D-glucose [9] was prepared by methylation and deacetylation of 1,3,4,6-tetra-O-acetyl-α-D-glucose [10] (m.p. 98°C); m.p. 157–158°C.

For the preparation of 3-O-Methyl-D-glucose [9], 3-O-methyl-1,2:5,6-diisopropylidene-D-glucofuranose (prepared by methylation according to Hakomori's method [11] from 1,2:5,6-diisopropylidene-D-glucofuranose [12]) was deisopropyridenated with Amberlite IR-120B (H^+) to give 3-O-methyl-D-glucose; m.p. 166.5–168°C.

4-O-Methyl-D-glucose was prepared by methylation and deacetylation of 1,2,3,6-tetra-O-acetyl-β-D-glucose (m.p. 127–127.5°C, $[\alpha]_D^{22}$ −33.5°) [13]; chromatographically pure syrup.

6-O-Methyl-D-glucose [9] was prepared by methylation and deacetylation of 1,2,3,4-tetra-O-acetyl-β-D-glucose [14] (m.p. 118–119°C, $[\alpha]_D^{22}$ +8.3°); m.p. 146–147°C.

Trehalose (α,α-1,1), maltose (α-1,4), cellobiose (β-1,4), isomaltose (α-1,6) and gentiobiose (β-1,6), were of the highest grade commercially available. Kojibiose (α-1,2), sophorose (β-1,2), nigerose (α-1,3) and laminalibiose (β-1,3) were all gifts. These glucobioses were purified by high-performance liquid chromatography (HPLC) on a YMC-Pack PAMN column (250 × 10 mm I.D.) (YMC, Kyoto, Japan) with 60–75% acetonitrile before use.

Neotrehalose (α,β-1,1) and isotrehalose (β,β-1,1) were synthesized by glucosylation of a mixture of 2,3,4,6-tetra-O-acetyl-α- and β-D-glucopyranoses with tetra-O-acetyl-α-D-glucopyranosyl bromide in the presence of mercuric cyanide according to the procedure of Helferich and Weis [15]. The reaction product was separated by column chromatography on a Lobar prepacked column, LiChroprep Si 60 (40–63 μm), size C (Merck, Darmstadt, Germany) with benzene–acetone (7:1). The peracetylated disaccharide fraction obtained was deacetylated, and two isomeric trehaloses were separated by HPLC on Asahipak NH2P-50 (250 × 10 mm I.D.) (Asahi Kasei, Tokyo, Japan) with acetonitrile–water (75:25) (Fig. 1). HPLC analyses of two fractions, I and II, on a graphitized carbon column, Hypercarb (100 × 4.7 mm I.D.) (Shandon Scientific, Cheshire, UK), with acetonitrile–water (3:97) showed that I was neotrehalose containing traces of trehalose and II was pure isotrehalose (Fig. 2). Fraction I was purified by repeating chromatography under the same conditions as in Fig. 2. Characterization of neotrehalose and isotrehalose was performed by ^{13}C NMR spectroscopy [16].

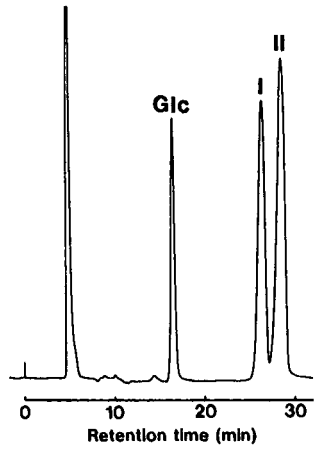

Fig. 1. Separation of two isomeric trehaloses in chemically synthesized products on an Asahipak NH2P-50 column. Peaks: Glc = glucose; I = neotrehalose containing small amounts of trehalose; II = isotrehalose. Chromatographic conditions: eluent, acetonitrile–water (75:25); flow-rate, 2.4 ml/min; temperature, ambient; detector, Shodex RI SE-61.

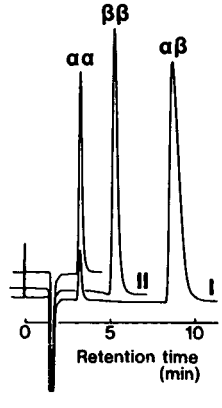

Fig. 2. Analysis of fractions I and II in Fig. 1 on a graphitized carbon column, Hypercarb. Peaks: αα = trehalose; αβ = neotrehalose; ββ = isotrehalose. Chromatographic conditions: eluent, acetonitrile–water (3:97); flow-rate, 1 ml/min; temperature, 35°C; detector, Shodex RI SE-61.

α-D-Glucose 1-phosphate disodium salt hydrate ($C_6H_{11}O_9PNa_2 \cdot 3H_2O$) and D-glucose 6-phosphate disodium salt hydrate ($C_6H_{11}O_9PNa_2 \cdot 3.5H_2O$) were purchased from Nacalai Tesque (Kyoto, Japan) and Sigma (St. Louis, MO, USA), respectively, and were of the highest grade. They were used as such, because they are very labile, decomposed on lyophilization, and lost unsettled water of crystallization on vacuum drying. D-Glucose 3-phosphate was a gift.

Apparatus and column

HPAEC was conducted with a Dionex BioLC Model 4000i system and a Model PAD 2 pulsed amperometric detector. The column used was a Dionex HPIC-AS6 (250 × 4 mm I.D., the same type of column as CarboPac PA-1) equipped with an AG6 guard column (50 × 4 mm I.D.) (all from Dionex, Sunnyvale, CA, USA). A Chromatopac C-R3A digital integrator (Shimadzu, Kyoto, Japan) was used to calculate peak areas.

Chromatographic conditions and measurements

The following pulse potentials (E) and durations (t) were used at range 2 (sampling period, 200 ms): $E_1 = 0.10$ V ($t_1 = 300$ ms); ($E_2 = 0.60$ V ($t_2 = 120$ ms); $E_3 = -0.80$ V ($t_3 = 300$ ms). The response time of the PAD 2 detector was set to 1.0 s. The eluents for monomethyl ethers and monophosphates of D-glucose, and glucobioses were 50 and 200 mM sodium hydroxide solutions, respectively, which were prepared by dilution of carbonate-free 50% sodium hydroxide solution in 18 MΩ cm deionized water, purified using a NANO-pure II (Barnstead, Newton, MA, USA). For control of retention, sodium acetate of analytical reagent grade was added to the eluent. Eluents containing sodium acetate were filtered through a 0.2-μm membrane filter. Eluents prepared daily were degassed by sonication under bubbling of helium gas and kept under a stream of helium. All purified samples of monomethyl-D-glucoses and glucobioses were lyophilized. Samples obtained in the amorphous state were dried as completely as possible in a desiccator over phosphorus pentoxide and were then weighed with the utmost caution to avoid taking up water during weighing. Each sample solution of $5 \cdot 10^{-4}$ M prepared using 18 MΩ cm deonized water was filtered through a 0.2-μm membrane filter. The sample size used for an analysis was 50 μl. All HPAEC analyses were carried out at ambient temperature with a flow-rate of 1 ml/min.

RESULTS AND DISCUSSION

Contribution of each hydroxyl group of D-*glucose to retention*

The retention times (t_R) of five positional isomers of monomethyl-substituted D-glucose with 50 mM sodium hydroxide solution are listed in Table I. Methyl β-D-glucoside, with its most acidic hydroxyl group occupied by a methyl group, was eluted much earlier than the positional isomers. Roberts *et al.* [4] reported the acidities of hydroxyl groups in methyl α- or β-D-glucopyranoside to be 2-OH > 6-OH > 3-OH > 4-OH when the sodium hydroxide concentration is ⩽ 0.1 M. According to Rendleman's review [5], the acidity of hydroxyl groups in methyl D-glucopyranoside decreases in the order 2-OH ≫ 6-OH > 3-OH > 4-OH, and substitution for the hydroxyl group at C-2 should increase the acidities of the 3- and 4-hydroxyl groups. It is easily understandable that masking of the more acidic hydroxyl group by a methyl group should result in a greater reduction in t_R. However, the elution order of mono-O-methyl-glucoses was 4-methyl, 6-methyl, 3-methyl and 2-methyl derivatives, and the differences in their t_R values were small. This result indicates that the presence of a free 1-OH group reduces the effect of differences in acidities of the

TABLE I

RETENTION TIMES (t_R) AND RELATIVE DETECTOR RESPONSES (RDR)/OH OF MONOMETHYL-D-GLUCOSES

The analytical conditions were as described in the text.

Monomethyl-D-glucose	t_R (min)	RDR/OH[a]
1-Methyl	1.7	0.59
2-Methyl	5.4	0.64
3-Methyl	4.8	0.60
4-Methyl	3.9	0.65
6-Methyl	4.0	0.88

[a] The ratio of (molar response of monomethyl-D-glucose)/4 to (molar response of D-glucose)/5 was used as the reference standard.

other hydroxyl groups, and other effects such as hydrophobic interaction might prevail.

The results of the analysis of glucobioses are summarized in Table II. In glucobioses, the linkage positions influence the elution position for the same reason as described above, but the situation is more complicated. Masking of the most acidic 1-OH by a glucosidic linkage should result in the weakest retention and, in fact, 1,1-linked trehaloses were earlier eluted than the other glucobioses, but the t_R values of three trehaloses with different linkage configuration differed from each other. Of the reducing glucobioses, kojibiose (α-1,2), having a masked 2-OH group, whose acidity is said to be the highest of the hydroxyl groups other than 1-OH, eluted with a relatively short t_R, whereas sophorose (β-1,2), which also has a masked 2-OH group had the highest t_R value of all glucobioses. Except for 1,4-linked isomers (maltose and cellobiose), the α-linked isomers generally moved faster than their β-linked counterparts. This tendency is similar to that of their retention on a graphitized carbon column [17], on which planar molecules are generally retained more than non-planar molecules [18]. The elution order of three trehaloses was trehalose (αα), isotrehalose (ββ) and neotrehalose (αβ), and was the same as that on the graphitized carbon column (Fig. 2), while on the octadecylsilane (ODS) column neotrehalose eluted faster than isotrehalose (Fig. 1). Nevertheless, it has previously been indicated on the basis of the retention order of cyclodextrins [19] that there are some hydrophobic interactions on this HPIC column. Honda *et al.* [20] also pointed out that the partition mode should be considered for the separation of neutral sugars on this column. They studied the relationship between capacity factor (k') and partition coefficient (K) for 1-butanol, and concluded that the k' of neutral sugars with a larger K was larger, for example the K of maltose (17.9) was larger than that of cellobiose (10.0), and therefore maltose eluted more slowly than cellobiose. Previously we investigated HPAEC of each homologous series of D-gluco-oligo- and -polysaccharides on an HPIC-AS6 column using a 150 m*M* sodium hydroxide solution containing 100 m*M* sodium acetate as the eluent [21]. Under these conditions the elution order of the smallest member in each series, glucobiose, was the same as that under the present conditions, except that β-1,3 and β-1,2 were eluted at the same time, whereas comparison of the t_R values of glucotrioses showed a change in the elution order of β-1,2, α-1,4 and α-1,3, that is their t_R values increased in that order, and moreover, in the cases of degrees of polymerization ⩾8 (gluco-octaose), β-1,2, eluted faster than β-1,4.

TABLE II

RETENTION TIMES (t_R) AND RELATIVE DETECTOR RESPONSES (RDR)/OH OF D-GLUCOBIOSES

The analytical conditions were as described in the text.

D-Glucobiose	t_R	RDR/OH[a]	
	(min)	1[b]	2[c]
Trehalose (α,α-1,1)	2.9	0.55	0.60
Neotrehalose (α,β-1,1)	4.2	0.59	0.59
Isotrehalose (β,β-1,1)	4.0	0.58	0.58
Kojibiose (α-1,2)	6.4	0.73	0.74
Sophorose (β-1,2)	13.6	0.90	1.03
Nigerose (α-1,3)	10.7	0.72	0.79
Laminalibiose (β-1,3)	12.7	0.68	0.74
Maltose (α-1,4)	11.0	0.66	0.71
Cellobiose (β-1,4)	7.8	0.80	0.83
Isomaltose (α-1,6)	5.7	0.67	0.72
Gentiobiose (β-1,6)	7.7	0.82	0.88

[a] The ratio of (molar response of D-glucobiose)/8 to (molar response of D-glucose)/5.
[b] Eluent: 200 m*M* sodium hydroxide.
[c] Eluent: 200 m*M* sodium hydroxide containing suitable amounts of sodium acetate (40–75 m*M*) for control of t_R to around 4 min.

We next investigated the separation of three positional isomeric monophosphates of D-glucose which are important compounds for biosynthesis and biodegradation of starch and glycogen. Sugar monophosphates are bivalent acidic compounds and, consequently, they are strongly retained on the anion-exchange resin. To elute them from the column, addition of considerable amounts of sodium acetate to the eluent was necessary. Fig. 3 shows an elution profile of three isomeric monophosphates of D-glucose by isocratic elution with 50 m*M* sodium hydroxide solution containing 300 m*M* sodium acetate. Within 7.5 min adequate separation was achieved. When the ionic strength of the eluent was increased and the t_R of the last peak was 5 min, baseline separation of the three isomeric monophosphates of D-glucose was still possible. The elution order of 1-, 3- and 6-phosphates was the same as that of the corresponding methyl ethers. Any

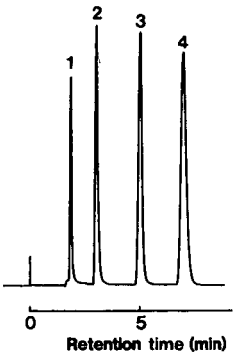

Fig. 3. Elution profile of glucose monophosphates on an HPIC-AS6 column. Peaks: 1 = glucose; 2 = glucose 1-phosphate; 3 = glucose 6-phosphate; 4 = glucose 3-phosphate. Chromatographic conditions: eluent, 50 m*M* sodium hydroxide solution containing 300 m*M* sodium acetate; flow-rate, 1 ml/min; temperature, ambient; detector, PAD 2.

eluent which is strong enough to elute monophosphates caused glucose to elute with or very near the front.

Contribution of each hydroxyl group of D-*glucose to the PAD response*

As PAD detects the electric current produced by the oxidation of oxyanions, transformed from the hydroxyl groups of carbohydrates with strong alkali in the eluent, it is thought that the PAD response is proportional to the number of oxyanions. If all free hydroxyl groups of glucose and glucose derivatives are in the same situation, the responses of PAD for monosubstituted glucose derivatives (four free OH groups) and glucobioses (eight free OH groups) should be 4/5 and 8/5 of that for glucose (five free OH groups), respectively. Consequently, relative detector responses (RDR, relative to glucose) were compared in one OH equivalent.

Table I shows the RDR/OH of monomethyl-D-glucoses. The presence of methyl ether suppressed the PAD response. 6-Methyl had the least effect and the effects of the other methyls were about the same. The results shown in Table I suggest that the PAD response was little affected by the acidity of each hydroxyl group of D-glucose and the presence of a methyl group might hinder the interaction between the vicinal hydroxyl groups and the electrode of the detector. In the way, it was confirmed that the lowest alkali concentration of eluent which gave sufficient detector response for D-glucose derivatives was 50 m*M*.

The relative detector responses of D-glucobioses are summarized in Table II. To correct the difference in peak areas arising from the large difference in t_R values, the t_R values of all glucobioses were adjusted to about 4 min by addition of suitable amounts of sodium acetate to the eluent. Comparison of RDR/OH of eleven D-glucobioses showed that those of the three 1,1-linked trehaloses were almost the same, and masking of the 1-OH with another glucosyl residue resulted in the largest reduction in the PAD response. In other cases, the response was affected by the linkage configuration rather than the linkage position, β-linked isomers generally showing a larger response than α-linked isomers. This phenomenon may be explained on the basis of interaction between hydroxyl groups in the same molecule, for example the 3-OH and 2'-OH groups of maltose (α-1,4), form a hydrogen bond and they are somewhat protected against oxidation, whereas the two glucose residues of cellobiose (β-1,4), are favourably located and all hydroxyl groups of cellobiose are available for oxidation on the electrode.

Glucose 1- and 6-phosphates gave values of 0.72 and 0.99 relative to the response for glucose in one OH equivalent, respectively. Townsend *et al.* [22] reported that the presence of phosphate suppresses the PAD response. However, it is thought that the suppression is a result of masking of hydroxyl group(s), and RDR/OH was actually little affected by phosphate substituted on the 6-OH group of glucose, though 1-phosphate suppressed the PAD response somewhat.

ACKNOWLEDGEMENTS

We are grateful to Professor A. Amemura (Fukuyama University) for gifts of sophorose, nigerose and laminalibiose, and to Professor S. Hizukuri (Kagoshima University) and Dr. T. Nakajima (Tohoku University) for gifts of D-glucose 3-phosphate and kojibiose, respectively.

REFERENCES

1 R. D. Rocklin and C. A. Pohl, *J. Liq. Chromatogr.*, 6 (1983) 1577–1590.

2 M. R. Hardy, R. R. Townsend and Y. C. Lee, *Anal. Biochem.*, 170 (1988) 54–62.
3 Y. C. Lee, *Anal. Biochem.*, 189 (1990) 151–162.
4 E. J. Roberts, C. P. Wade, and S. P. Rowland, *Carbohydr. Res.*, 17 (1971) 393–399.
5 J. A. Rendleman, Jr., *Adv. Chem. Ser.*, 117 (1973) 51–68.
6 K. Koizumi, most of this work was presented at the *Abe Seminar on Glycoscience and Glycotechnology, Osaka, Jan. 8, 1990*, pp. 1–5 (Abstracts).
7 E. Pacus, *Methods in Carbohydrate Chemistry*, Vol. 2, Academic Press, New York, London, 1963, p. 356.
8 R. U. Lemieux, *Method Carbohydr. Chem.*, 2 (1963) 221–222.
9 E. J. Bourne and S. Peat, *Adv. Carbohydr. Chem.*, 5 (1950) 148–151.
10 B. Helferich and J. Zirner, *Chem. Ber.*, 95 (1962) 2604–2611.
11 S. Hakomori, *J. Biochem. (Tokyo)*, 55 (1964) 205–208.
12 J. D. Stevens, *Method Carbohydr. Chem.*, 6 (1972) 124–125.
13 B. H. Koeppen, *Carbohydr. Res.*, 24 (1972) 154–158.
14 D. D. Reynolds and W. L. Evans, *Organic Syntheses*, Coll. Vol. III, John Wiley, New York, 1955, p. 432.
15 B. Helferich and K. Weis, *Chem. Ber.*, 89 (1956) 314–321.
16 T. Usui, N. Yamada, K. Matsuda, K. Tuzimura, H. Sugiyama and S. Seto, *J. Chem. Soc., Perkin Trans. 1*, (1973) 2425–2432.
17 K. Koizumi, Y. Okada and M. Fukuda, *Carbohydr. Res.*, 215 (1991) 67–80.
18 *Application Notes*, Shandon Scientific, Runcorn, UK, 1988.
19 K. Koizumi, Y. Kubota, T. Tanimoto and Y. Okada, *J. Chromatogr.*, 454 (1988) 303–310.
20 S. Honda, S. Suzuki, T. Ueno and K. Kakehi, *Chromatography (Japan)*, 11 (1990) 22–23.
21 K. Koizumi, Y. Kubota, T. Tanimoto and Y. Okada, *J. Chromatogr.*, 464 (1989) 365–373.
22 R. R. Townsend, M. R. Hardy, O. Hindsgaul and Y. C. Lee, *Anal. Biochem.*, 174 (1988) 459–470.

Journal of Chromatography, 595 (1992) 346–350
Elsevier Science Publishers B.V., Amsterdam

CHROM. 23 964

Short Communication

Determination of maleic hydrazide in tobacco by micellar liquid chromatography

S. S. Yang

Research Center, Philip Morris USA, P.O. Box 26583, Richmond, VA 23261-6583 (USA)

(First received November 13th, 1991; revised manuscript received December 18th, 1991)

ABSTRACT

A reversed-phase high-performance liquid chromatographic method with UV detection was developed to determine maleic hydrazide (MH) residues in tobacco. Sample preparation consisted of an initial hydrolysis of MH residues with 12 *M* hydrochloric acid by sonication at an elevated temperature, followed by neutralization with an aqueous sodium hydroxide solution. Chromatographic separation was performed on a C_{18} column with a mobile phase containing 4.0 m*M* cetyltrimethylammonium bromide in 40 m*M* phosphate buffer (pH = 7.0). Other sample preparation procedures were investigated including extraction/digestion with the aid of different energy sources (*e.g.*, conventional heater and microwave oven) and these results are also discussed.

INTRODUCTION

Maleic hydrazide (MH) is a synthetic plant growth regulator widely used in tobacco farming as a suckering control agent. The normal practice is to apply MH to the upper half of tobacco plants shortly after topping. The applied MH then gradually translocates to other parts of the plant. The fate and metabolism of MH in tobacco plants has been investigated using foliar-absorbed ^{14}C-labelled MH [1]. This study showed that MH and its metabolites translocated to actively growing tissues of the whole plant and some of these compounds are extractable with methanol. The major component in the methanol extract was identified as a β-D-glucoside of MH. A review article published in 1987 [2] discussed in detail the absorption, translocation and metabolism of MH in tobacco plants.

A number of analytical procedures for the determination of MH residues in tobacco or tobacco products have been published. The distillation–spectrophotometric method and its various modifications [3–6] have been widely used. In these procedures MH residues are reductively hydrolyzed to hydrazine by zinc in a concentrated alkali solution. The evolved hydrazine is subsequently derivatized with *p*-dimethylaminobenzaldehyde, and measured spectrophotometrically at 455 nm. A gas chromatographic method consisting of hydrolysis of MH residues in 2 *M* hydrochloric acid at 90–95°C and derivatization with N,O-bis(trimethylsilyl)acetamide has also been reported [7]. In addition, an immunoassay method using a monoclonal antibody-based enzyme for the analysis of MH was described in 1989 [8].

We describe here a reversed-phase high-performance liquid chromatographic (HPLC) procedure for the determination of MH residues in tobacco and tobacco products. The sample preparation involves hydrolysis of MH residues in 12 *M* hydrochloric acid, followed by neutralization with a sodium hydroxide solution after cooling the sample in a cold

0021-9673/92/$05.00

water bath. Several other sample preparation procedures were also evaluated.

EXPERIMENTAL

Reagents

Maleic hydrazide and cetyltrimethylammonium bromide (CTAB) were purchased from Aldrich and were used as received. β-D-Glucosidase was obtained from Sigma. All water used was treated by a Milli-Q system to provide organic-free, 18 mΩ grade water.

Apparatus

The instrument used consisted of a Hewlett-Packard 1090L high-performance liquid chromatograph equipped with a UV–VIS photodiode array detector, an autosampler, and a Hewlett-Packard 9000 LC workstation. The wavelength monitored for quantitation was 330 nm. The analytical column used was a Hewlett-Packard Hypersil ODS column (5 μm particle size, 20 cm × 4.6 mm I.D.). The injection volume was 5 μl. The column was maintained at ambient temperature. The mobile phase consisted of two solutions: solution A was 2.5 m*M* CTAB in 40 m*M* phosphate buffer (pH 7.0); solution B was 7.5 m*M* CTAB in 40 m*M* phosphate buffer (pH 7.0). The initial composition was 30% of solution B in A and was maintained for 4 min. Solution B was then raised to 90% in 0.5 min and kept for another 4 min before changing back to the initial 30% composition. The HPLC run was stopped after 20 min.

Sample preparation

A 0.25-g portion of ground tobacco was placed in a 30-ml glass vial with a PTFE-lined cap. After adding 2 ml of 12 *M* hydrochloric acid, the vial was capped, placed in an ultrasonic bath (Branson, Model 3200) containing hot water at a temperature of approximately 60°C or above and sonicated for 40 min (the sonication and the allowing neutralization steps should be performed under a working hood equipped with a sliding glass shield). The sample was then cooled in a cold water bath. Two 1-ml aliquots of 12 *M* sodium hydroxide were sequentially added to the sample which remained in the cold water bath with the vial cap, or a small watch glass, pressed on lightly (to vent pressure) during the whole neutralization process. After the addition of each 1-ml aliquot of sodium hydroxide solution, several minutes were allowed for heat dissipation. An aliquot of approximately 1 ml of the neutralized sample was then filtered through a 0.45-μm disposable filter into an autosampler vial for HPLC analysis.

Other sample preparation procedures

Water extraction. Ground tobacco (1.0 g) was placed in a 50-ml flask and 10 ml of water were added. The mixture was shaken on an orbital shaker for 1 h. An aliquot of approximately 1 ml of the extract was filtered and sealed in a sample vial.

Water extraction/enzyme hydrolysis. Ground tobacco was extracted and filtered as under *Water extraction.* Approximately 2 ml of the filtrate were transferred into a test tube and 10 mg of β-D-glucosidase were added. The test tube was immersed in a 37°C water bath for 4 h with occasional shaking by hand. A portion of the sample was then filtered and used for HPLC analysis.

NaOH digestion/reflux. A 5-g amount of ground tobacco were mixed with 25 ml of 10 *M* sodium hydroxide solution in a 150-ml round-bottom flask and the mixture was refluxed for 3 h. After refluxing, the condensor was removed and the round-bottom flask was placed in a cold water bath under a working hood equipped with a glass shield. A total volume of 50 ml of 5 *M* hydrochloric acid solution was slowly added to the sample flask, which remained in the cold water bath and was covered with a watch glass during the neutralization process. Approximately 1 ml of the neutralized sample solution was filtered and sealed into a sample vial.

NaOH digestion/microwave irradiation. A ground tobacco sample of 0.1 g was weighed into a PTFE-lined microwave digestion vessel equipped with a safety disk for high pressure venting (CEM, Matthews, NC, USA) and 3 ml of 10 *M* sodium hydroxide solution were added. After the vessel cap was hand-tightened, the whole assembly was placed in a MDS-81 microwave oven. The sample mixture was subjected to three 6-min cycles, each consisting of 3 min of microwave irradiation at 15% power followed by 3 min fan-cooling, for a total treatment time of 18 min. After the sample cooled and the internal pressure was released, the vessel was carefully opened and 3 ml of 10 *M* hydrochloric acid

solution were slowly added following the procedures described under *Sample preparation*. An aliquot of neutralized sample solution was filtered and sealed into an HPLC autosampler vial.

Standards and addition plot

A stock solution of MH was prepared by weighing 100 mg of MH into a 100-ml volumetric flask and diluting to volume with water (nominally 1 mg MH/g of solution). This stock solution was used for both preparation of calibration standards and recovery studies.

Spiked samples were prepared by weighing 0.25 g of ground, MH-free tobacco into each of five 25-ml glass vials and weighing 50, 37.5, 25, 12.5 and 5 mg of the stock solution into each vial (nominally 200, 150, 100, 50 and 20 μg of MH per g of tobacco), respectively. After waiting for 1 h, each spiked sample was treated by the procedure described under *Sample preparation*. Data obtained from HPLC analysis were used to establish an addition plot using peak area *vs.* amounts of MH in tobacco (ppm). Calculation was based on external standards using the addition plot.

RESULTS AND DISCUSSION

Due to the high solubility of MH in water and alcohol, an initial attempt using water and/or methanol as an extracting solution was made. However, only a small amount of MH, *e.g.*, 40–50 ppm, was observed in a sample (No. 9), which contained 210 ppm of MH as previously determined by a method [6] from the International Organization for Standardization (ISO) (see Table I). The MH determined from a water/methanol extraction would account only for the free form of MH and not for any conjugated MH. It has been known that MH, after being sprayed on crops, can be metabolized to glucosides, *e.g.*, mostly β-D-MH-glucoside in potato [9]. As such, an enzyme-catalyzed hydrolysis using β-D-glucosidase was performed on the extract after the tobacco sample was extracted with water. The amount of MH measured increased to 80–90 ppm, which obviously was a combined contribution from free MH and hydrolyzed β-D-MH-glucoside.

In the published methods, total MH was obtained using strong acid or base to hydrolyze the bound or conjugate form of MH. MH residues were first hydrolyzed in concentrated sodium hydroxide or hydrochloric acid solutions with heating. MH was then either converted into hydrazine [3–6] in the presence of a catalyst or derivatized for subsequent chromatographic analysis [7], except in one case where MH was directly quantitated using ion chromatography [10]. In our study, a 3-h reflux with 10 *M* sodium hydroxide was required for the hydrolysis of MH residues. Although such a procedure produced data comparable to the ISO method, other less time-consuming sample preparation techniques were investigated.

TABLE I

COMPARISON OF DIFFERENT METHODS FOR DETERMINING MH RESIDUES

Samples are Bright tobacco.

Sample	MH residues (ppm)		
	ISO[a]	LC-1[b]	LC-2[c]
1	110	118	105
2	78	75	90
3	97	105	96
4	158	144	145
5	112	107	117
6	49	54	38
7	104	97	97
8	97	93	87
9	210	220	209
10	29	22	18

[a] ISO = International Organization for Standardization (ISO) official method.
[b] LC-1 = NaOH digestion with 3 h reflux + HPLC.
[c] LC-2 = HCl digestion with sonication + HPLC.

One means for reducing sample preparation time involved the use of microwave digestion with closed vessels. Microwave irradiation has been used in elemental analysis to aid acid digestion. In our study, however, digestion of organic material (*e.g.*, ground tobacco) mixed with a concentrated sodium hydroxide solution was cautiously attempted. Small samples, generally less than 0.1 g tobacco mixed with 3 ml of 10 *M* sodium hydroxide solution, were irradiated at low power levels. The results obtained using this method were similar to those obtained from the ISO method. However, sparks and arcing were observed during the irradiation process and as a result, corrosion-like, damaged areas were found

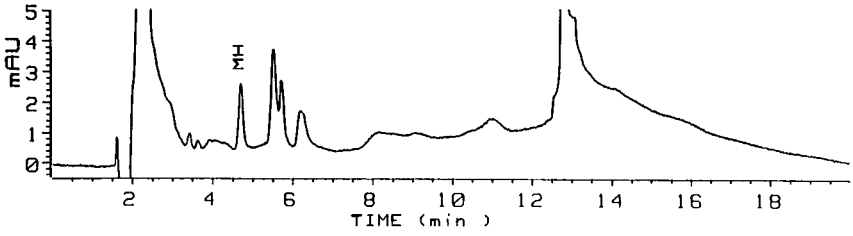

Fig. 1. Chromatogram of a Bright tobacco sample at a 80 ppm level of maleic hydrazide. Column, Hewlett-Packard Hypersil ODS, 200 mm × 4.6 mm I.D.; detection, UV 330 nm; injection volume, 5 μl; column temperature, ambient; mobile phase, cetyltrimethylammonium bromide in phosphate buffer (pH 7.0); flow-rate, 0.8 ml/min. Details in text.

on the inner wall of the PTFE-lined vessels. A possible explanation is that the large quantity of energy from microwave irradiation causes rapid evaporation of water molecules and leads to the desolvation of some sodium hydroxide, especially those around the edge of solution surface. These sodium hydroxide crystals interacted with microwave energy and created "hot spots", where damage occurred.

Another approach to reduce sample preparation time was the use of sonication as an external energy source. Ground tobacco samples mixed with concentrated hydrochloric acid were sonicated in a water bath at or above 60°C. Although more than 70% of the MH residues can be extracted in the first 20 min, a sonication time of 40 min is necessary to obtain a satisfactory recovery. After sonication, the yellow-brown tobacco sample had turned into a dark slurry. The slurry solution was neutralized by slow addition of sodium hydroxide solution. Vapor loss during acid–base reaction was minimized by using a cold water bath and a watch glass to enhance vapor condensation. The total sample loss from vaporization was usually less than 1% (w/w). As shown in Table I, the results obtained using this sample preparation procedure were consistent with those from the ISO method and the more rigorous basic reflux sample preparation.

Fig. 1 is a representative chromatogram obtained from a tobacco sample containing 80 ppm MH. Chromatographic separation was performed on a C_{18} column. MH was eluted isocratically from the column at 4.7 min by a mobile phase containing (CTAB) in phosphate buffer (pH 7.0). The concentration of CTAB was initially 4.0 m*M* for the elution of MH and was then increased to 7.0 m*M* to speed the elution of strongly retained compounds. As the concentration of the surfactant in the mobile phase is well above its critical micellar concentration (cmc = 1.3 m*M* for CTAB), there is no change in the amount of surfactants adsorbed on the stationary phase regardless of the change in the total surfactant concentration [11]. This makes it possible to change mobile phase composition or even perform gradient elutions without time-consuming column re-equilibration between injections.

Adequate buffer strength is important for peak shape and sensitivity. Initially a buffer of 10 m*M* phosphate was used. This buffer gave reasonable peak shape for a small volume of standard compound (Fig. 2a), but distorted peaks and hence poor detection limits were observed for tobacco samples

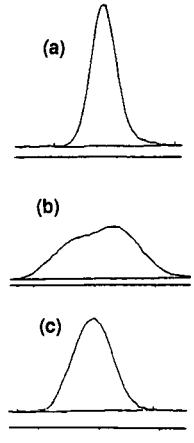

Fig. 2. Peak shape of MH in chromatograms. Chromatographic conditions as in Fig. 1 except buffer strength in the mobile phase. (a) Standard solution of MH, 10 m*M* phosphate buffer; (b) tobacco sample, 10 m*M* phosphate buffer; (c) tobacco sample, 40 m*M* phosphate buffer.

TABLE II

REPLICATE ANALYSES OF TWO BRIGHT TOBACCO SAMPLES

Run No.	MH residues (ppm)	
	Sample 4	Sample 9
1	148	210
2	150	203
3	150	215
4	141	207
5	149	210
Average	144	209
R.S.D. (%)	4	2

TABLE III

RECOVERIES OF MALEIC HYDRAZIDE SPIKED INTO TOBACCO SAMPLES

Amount added (μg/g)	Amount found (μg/g)	Recovery (%)
29	27	92
66	68	103
103	98	95
194	180	93
241	228	95
249	238	95
Average recovery		95

as shown in Fig. 2b. A possible source for this peak distortion could be the presence of a high concentration of sodium chloride (*e.g.*, approximately 5–6 *M*), produced from the acid–base neutralization, which caused slower solute diffusion in the injected sample solution than in the bulk mobile phase. This was further confirmed by obtaining a similarly distorted peak from a standard solution of MH which was 6 *M* in NaCl. The peak shape of MH in tobacco samples was improved by using a stronger buffer of 40 m*M* phosphate solution (Fig. 2c). This stronger buffer capacity also greatly reduced other possible causes of peak distortion, one of which may be that the pH of the 'neutralized' tobacco solution may not be neutral, pH 7 ± 0.5.

This procedure proved to provide the degree of precision and accuracy needed for the routine determination of MH in tobacco. The relative standard deviation from five replicate analyses of two samples, Nos. 4 and 9, were 4% and 2%, respectively (Table II). Recoveries of MH from tobacco samples are listed in Table III and the average recovery was 95%. The detection limit was 20 μg/g for tobacco samples. The standard addition plot in the range 29–249 ppm gives a slope of 0.189 with an intercept of 0.827 and a correlation coefficient of 0.998.

CONCLUSIONS

The reported procedure provides a method for the determination of MH in tobacco. Sample preparation is straightforward and the use of a micellar mobile phase for the HPLC analysis gives good reproducibility. This method has been tested on a variety of tobacco samples including Burley, Bright and Oriental tobaccos and their products, with satisfactory results.

ACKNOWLEDGEMENTS

The author would like to thank his senior colleagues, Mr. D. Davis, Dr. D. Ingraham, Mr. W. Ryan and Mr. D. Watson for their helpful discussion.

REFERENCES

1 D. S. Frear and H. R. Swanson, *J. Agric. Food Chem*, 26 (1978) 660.
2 S. A. Meyer, T. J. Sheets and H. Seltmann, *Rev. Environ. Contam. Toxicol.*, 98 (1987) 43.
3 J. R. Lane, D. K. Gullstrom and J. E. Newell, *J. Agric. Food Chem.*, 6 (1958) 671.
4 M. Ihnat, R. J. Westerby and I. Hoffmann, *J. Assoc. Off. Anal. Chem.*, 56 (1973) 1164.
5 *Official Methods of Analysis*, Vol. 13, Association of Official Analytical Chemists, Arlington, VA, 1980, p. 1018.
6 *ISO Method No. 4867*, Internation Organization for Standardization, Paris, 1980.
7 A. F. Haeberer and O. T. Chortyk, *J. Assoc. Off. Anal. Chem.*, 62 (1979) 171.
8 R. O. Harrison, A. A. Brimfield and J. O. Nelson, *J. Agric. Food Chem.*, 37 (1989) 958.
9 W. H. Newsome, *J. Agric. Food Chem.*, 28 (1980) 1312–1313.
10 W. H. Newsome, *J. Agric. Food Chem.*, 28 (1980) 270–272.
11 J. G. Dorsey, M. G. Khaledi, J. S. Landy and J. L. Lin, *J. Chromatogr.*, 316 (1984) 183–191.

Journal of Chromatography, 595 (1992) 351–354
Elsevier Science Publishers B.V., Amsterdam

CHROM. 23 959

Short Communication

Endogenous alkaloids in man

XI.☆ Analysis of glyoxylate-derived 1,3-thiazolidines by ion-pair-assisted reversed-phase chromatography

Gerhard Bringmann*, Christiana Hesselmann and Doris Feineis

Institute of Organic Chemistry, University of Würzburg, Am Hubland, 8700 Würzburg (Germany)

(First received September 24th, 1991; revised manuscript received December 16th, 1991)

ABSTRACT

Reversed-phase ion-pair chromatography, using cetyltrimethyl ammonium hydrogensulphate as detergent, has been applied to the analysis of the highly polar glyoxylate-derived 1,3-thiazolidines **1**, **2** and **3**. On the base of this high-performance liquid chromatographic separation of the diastereomeric compounds **1a/b** and **3a/b** was achieved. Removal of the hydrophobic couterion by precipitation as its insoluble iodide, followed by an extraction with chloroform, seems to be a promising first step to establish ion-pair-assisted chromatography as a preparative high-performance liquid chromatographic method for the isolation of polar compounds.

INTRODUCTION

Binucleophilic amino acids, such as L-cysteine and D(−)-penicillamine, as well as their biogenic amines, such as cysteamine, rapidly undergo a cyclo-condensation reaction with glyoxylic acid, leading to the 1,3-thiazolidines **1a/b**, **2** and **3a/b** (Fig. 1), respectively, without formation of side-products [1,2].

The deliberate formation of such extremely polar, alkaloid-type heterocycles by a spontaneous, *i.e.* non-enzymatic, reaction is part of our therapeutic concept for the treatment of glyoxylate-induced oxalurias, with the aim of achieving chemical and thus physiological deactivation of toxic glyoxylic acid [2,3]. A drastic reduction in the glyoxylate level of the organism is necessary, especially for the treatment of the inherited metabolic disease hyperoxaluria [4], which is characterized by a fatal overproduction of oxalic acid and thus calcium oxalate. Also for ethylene glycol intoxications [5] and metabolic problems resulting from transurethral prostatectomy [6], the harmless scavenging of glyoxylic acid must be the goal of a specific therapy, since in both cases symptoms can be observed that indicate a direct action of glyoxylic acid on the central nervous system [7].

In this paper, we describe an analytical device that is not only suitable for the separation of the structurally similar thiazolidines **1**, **2** and **3**, but also allows the resolution of diastereomeric pairs of 2,4-thiazolidine-dicarboxylic acids **1a** and **1b** as well as **3a** and **3b** (see Fig. 2). With the assistance of ion-pair-forming detergent cetyltrimathyl ammonium

☆ For Part X, see ref. 4.

0021-9673/92/$05.00

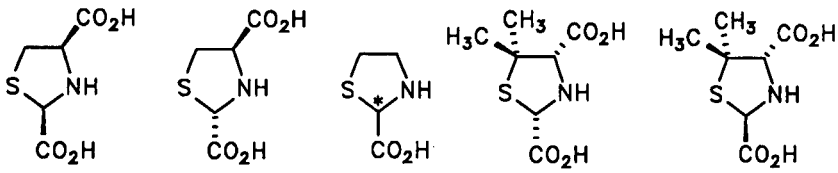

Fig. 1. Structures of glyoxylate-derived 1,3-thiazolidines.

hydrogensulphate, sufficient interaction between the hydrophobic substrate/counterion pair and the non-polar stationary C_{18} phase can be achieved. Using a coupled procedure, consisting of precipitation of the lipophilic cation (with iodide) and subsequent extraction (into chloroform), the detergent may furthermore be removed nearly quantitatively — an important precondition for a possible application of this method to preparative high-performance liquid chromatography (HPLC).

Ion-pair-assisted reversed-phase chromatography proved to be superior not only to thin-layer chromatography, but also to the method of ion suppression by the choice of the pH. Although classical chromatography of disubstituted thiazolidines on silica gel or on paper with special eluent systems adopted from amino acid analysis is possible and has been described for **1** [8], separation of the diastereomers could not be attained. Undesired effects on both the stationary phase and the dissolved molecule, caused by pH changes in ion-suppression chromatography, are limited in ion-pair chromatography, since it can be performed under neutral pH conditions.

EXPERIMENTAL

Chemicals

High-purity Milli-Q water (Millipore, Bedford, MA, USA) and chloroform of analytical-grade quality were used. Sodium dihydrogenphosphate dihydrate and disodium hydrogenphosphate monohydrate were obtained from Merck (Darmstadt, Germany). Cetyltrimethyl ammonium bromide was purchased from Fluka (Buchs, Switzerland) and converted into the hydrogensulphate by recrystallization from 0.5 *M* aqueous sulphuric acid. The aqueous mobile phase (pH 7.4) was prepared by dissolving 3.52 g (9.2 mmol) of cetyltrimethyl ammonium hydrogensulphate, 7.14 g (40 mmol) of disodium hydrogenphosphate dihydrate and 2.07 g (15 mmol) of sodium dihydrogenphosphate monohydrate in 1 l of HPLC-grade water. The organic mobile phase was HPLC-grade methanol. The mobile phase components were filtered through an HV 0.45-μm pore membrane filter (Millipore) and deaerated by sonication.

Synthesis

The thiazolidines **1** and **2** were prepared by dissolving a 1:1 molar ratio of glyoxylate (Merck) and of the aminothiols cysteamine or L-cysteine (Fluka) in ethanol. The solutions were adjusted to pH 6.5–7 with 2 *M* sodium hydroxide. The resulting crystalline heterocycles **1** and **2**, respectively, were isolated according to the procedure described by Fourneau *et al.* [9]. Compound **3** was synthesized by adding an equimolar amount of D-penicillamine (Degussa, Germany) to an aqueous solution of glyoxylic acid and isolated by freeze-drying. In principle, these syntheses have already been published in the literature [9–12], but without a full characterization of the diastereomeric products. Complete elucidation of the structure of the thiazolidines **1a/b**, **2** and **3a/b** by spectroscopy and by X-ray crystallography will be reported in a separate paper.

High-performance liquid chromatography

All experiments were carried out on a modular HPLC system, consisting of two M 510 pumps (Waters), a U6K injection valve (Waters) and a Lambda-Max Model 481 spectrophotometer (Waters). Chromatographic analyses were performed on a reversed-phase C_{18} column (Waters μBondapak C_{18}, 30 cm × 3.9 mm I.D., particle size 10 μm) using various mixtures of an isocratic mobile phase of methanol–phosphate buffer (pH 7.4) with 0.35% cetyltrimethyl ammonium hydrogensulphate as ion-

pair reagent. The UV absorption wavelength was set at 265 nm. The flow-rate was maintained at 2 ml/min. An HPLC manager PC control system (Waters, Maxima System with Interface I-200) in combination with Maxima evaluation software 820 was used for data acquisition and processing.

Calibration graphs and detection limits

Stock solutions of the thiazolidines **1**, **2** and **3** were prepared by dissolving 9.71 mg of **1**, 9.18 mg of **2** and 13.99 mg od **3** in 1 ml of Milli-Q water. Various aliquots of the undiluted (40, 20 μl) and of the ten-fold diluted stock solution (80, 60, 40, 20 μl) were subjected to HPLC in the system mentioned above to obtain data for calibration graphs and for detection limits. In each instance, calibration curves were constructed by plotting the integrated peak area against the corresponding thiazolidine standard concentration.

Detergent extraction procedure

A 166-mg aliquot (10 mmol) of potassium iodide was added to 100 ml of a solution of 3.52 g (9.2 mmol) of cetyltrimethyl ammonium hydrogensulphate in 1 l of Milli-Q water. After extraction with chloroform (3 × 33 ml), the organic layer was made up to 100 ml. Three aliquots of 10 ml were evaporated to dryness. The amount of detergent extracted was obtained by weighing the residue and calculating the average recovery.

RESULTS AND DISCUSSION

Choice of a suitable detergent

Sufficient interaction between highly polar substrate molecules and non-polar stationary phase can be achieved only by using distinctly lipophilic counterions dissolved in the mobile phase. Because of the presence of only one amino group, but two carboxyl functions, the amphoteric thiazolidines **1**, **2** and **3** were chromatographed in an anionic form, under addition of a positively charged detergent. In this way, up to two detergent molecules can be bound to the dicarboxylic acids at appropriate pH values.

Because of the very high polarity of the examined heterocycles **1**, **2** and **3**, an important factor in the selection of an appropriate eluent is the choice of the ion-pair reagent. The first, orientating experiments aimed at finding a suitable detergent were performed under pH conditions (pH 9.4) that allow the complete double deprotonation of the substrate molecules, thus maintaining the pH value near to the point of destruction of a C_{18} phase for a short time. Initially, we tested tetrabutyl ammonium chloride under these pH conditions, using a water–acetonitrile-containing solvent — a system that has already been described in the literature — for the ion-pair chromatography of an *N*-formylated 1,3-thiazolidine from penicillin degradation [13]. However, for the highly polar 2,4-thiazolidine-dicarboxylic acids, sufficient retention could not be achieved. In contrast, the long-chain, distinctly more lipohilic cetyltrimethylammonium ion could be used far more successfully under identical analytical conditions.

Optimization of the eluent

For the elaboration of optimum chromatographic conditions, maximum ionization of the substrate molecules was required. However, the extreme pH sensitivity of the column material, particularly towards quaternary ammonium salts in alkaline media, had to be taken into account [14]. Fortunately, using cetyltrimethyl ammonium salts in water–methanol mixtures at pH 7.4, sufficient ionization of the substrate molecules could be achieved. As Fig. 2 shows, separation of the 1,3-thiazolidine **2** and the diastereomers **1a** and **1b**, as well as **3a** and **3b**, could be achieved in a single analytical step, using this column-preserving eluent system.

Reproducibility and linearity

For an examination of the reproducibility and linearity of the described analytical procedure, and for an estimation of the detection limit, as obtained by UV recording at the absorption maximum of the compounds at 265 nm, analysis functions $m = f(R)$, with m = mass of the analyte and R = detector response, were determined for **1**, **2** and **3**. For all these compounds, a linear correlation between the injected mass and the detector response was found over the whole concentration range (see Experimental section), with a correlation coefficient $r > 0.99$.

The detection limits for **1a** ($3.4 \cdot 10^{-6}$ g), **1b** ($1.3 \cdot 10^{-5}$ g), **2** ($1.6 \cdot 10^{-5}$ g), **3a** ($3.9 \cdot 10^{-6}$ g), and **3b** ($2.4 \cdot 10^{-5}$ g), which are in the microgram range for UV spectroscopic detection (265 nm), reflect the

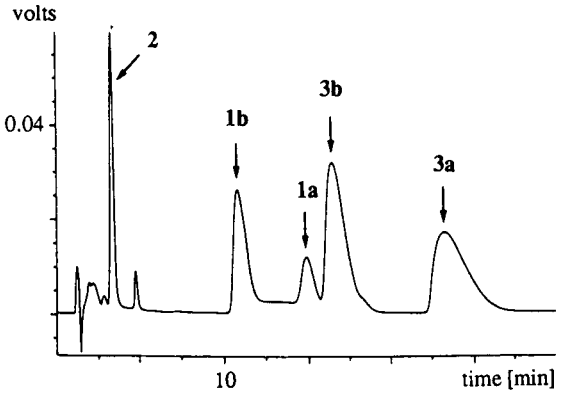

Fig. 2. Ion pair-assisted reversed-phase HPLC separation of the diastereomeric 1,3-thiazolidines **1a/b**, **2** and **3a/b**. Eluting solvent: aqueous mobile phase–methanol (50:50). Chromatographic conditions: see Experimental section.

low-intensity UV maximum of the small thiazolidine heterocycles, which moreover is located almost exactly at the UV cut-off of the utilized solvents. In consequence, although the practicability of the analytical procedure is restricted to samples whose content of **1**, **2** and **3** are not in the trace range, the possibility of a complete removal of the detergent hints at novel fields of application.

Removal of the detergent

The special problems of the extraction of aqueous, detergent-containing solutions with organic solvents (*i.e.* the formation of emulsions) and the problems of precipitation (*i.e.* adsorption effects) could be solved by a promising coupled procedure, by extracting the initially precipitated iodide and its aqueous mother liquor with chloroform. In this way, not only could substance inclusions eventually formed in the precipitation step be released, but also, astonishingly, practically no problems of emulsion formation occurred. Recovery of cetyltrimethyl ammonium hydrogensulphate was calculated to be 103%.

CONCLUSION

The method presented in this paper is a novel approach to the solution of the presented chromatographic problems. Not only is it applicable to analytical samples, but it also seems to be of value for exploitation even on a preparative scale. In this way, ion-pair-assisted reversed-phase chromatography, with its great chromatographic potential, might be admitted to the arsenal of preparative HPLC methods for the first time. This work is in progress.

ACKNOWLEDGEMENT

We gratefully acknowledge the financial support of this work by the Fonds der Chemischen Industrie.

REFERENCES

1 G. Bringmann, S. Schneider and A. Hille, *Nachr. Chem. Techn. Lab.*, 34 (1986) 222.
2 G. Bringmann, D. Feineis, H. Friedrich and A. Hille, *Planta Med.*, 57 (Suppl. 1) (1991) 73.
3 G. Bringmann, D. Feineis, Ch. Hesselmann, S. Schneider, M. Koob and D. Henschler, *Life Sci.*, submitted for publication.
4 H. E. Williams and L. H. Smith, Jr. in J. B. Stanbury, J. B. Wyngaarden, D. S. Fredrickson, J. L. Goldstein and M. S. Brown (Editors), *The Metabolic Basis of Inherited Disease*, McGraw-Hill, New York, Hamburg, 5th ed., 1983, pp. 204–228.
5 C. L. Winek, D. P. Shingleton and S. P. Shanor, *Clin. Toxicol.*, 13 (1978) 297.
6 C. Perier, J. Frey, C. Auboyer, A. Richard, G. Aulagnier, P. Heritier and A. Gilloz, *Clin. Chem.*, (Winston-Salem, N.C.) 34 (1988) 1471.
7 M. F. Parry and R. Wallach, *Am. J. Med.*, 57 (1974) 143.
8 A. J. L. Cooper, M. T. Haber and A. Meister, *J. Biol. Chem.*, 257 (1981) 816.
9 J. C. Fourneau, O. Efimovsky, J. C. Gaignault, R. Jacquier and C. LeRidant, *C. R. Acad. Sci. Ser. C*, 272 (1971) 1515.
10 C. De Marco, C. Cini, R. Coccia and C. Blarzino, *Ital. J. Biochem.*, 28 (1979) 104.
11 R. Bentley, A. H. Cook and J. A. Elvidge, *J. Chem. Soc.*, (1949) 3216.
12 I. McMillian and R. J. Stoodley, *Chem. Commun.*, (1968) 11.
13 I. Ghebre-Selassie, S. L. Hem and A. M. Knevel, *J. Pharm. Sci.*, 71 (1982) 351.
14 V. B. Meyer, *Praxis der Hochleistungsflüssigchromatographie*, Diesterweg, Sauerländer, Frankfurt, Aarau, Salzburg, 5th ed., 1988, p. 154.

Journal of Chromatography, 595 (1992) 355–358
Elsevier Science Publishers B.V., Amsterdam

CHROM. 23 979

Short Communication

Separation and purification of azetidinyl methyl sulfinates using preparative high-performance liquid chromatography

Frank Brown, Jr. and Perry C. Heath

Lilly Research Laboratories, Chemical Process Research and Development Division, Eli Lilly & Company, Indianapolis, IN 46285 (USA)

(First received November 27th, 1991; revised manuscript received December 30th, 1991)

ABSTRACT

An improved method for the separation and purification of azetidinyl methyl sulfinates is described. This method utilizes a Waters preparative high-performance liquid chromatographic set-up. The methyl sulfinate isomers are isolated in high purity and no double bond isomerization is observed to occur. The diastereomers eluted from both the analytical and preparative columns at approximately the same retention times under the conditions used in the method.

INTRODUCTION

In our laboratories a method for determining the purity of azetidinyl sulfinyl chloride (**1**) involves quenching it with methyl alcohol to yield ($\alpha\beta$,2β,3β)-2-(methoxysulfinyl)-α(1-methylethenyl)-4-oxo-3-(phenoxyacetylamino)-1-azetidineacetic acid, (4-nitrophenyl)methyl esters **2** and **3**[a] which are then quantitated by high-performance liquid chromatography (HPLC). The success of this method depends on having azetidinyl methyl sulfinates **2,3** of known purity for use as reference standards. Being able to separate and purify each diastereomer is also desirable so that the UV response of each isomer can be measured and compared.

Previous workers have attemped to purify **2,3** using flash chromatography [1] and preparative HPLC [2]. However these procedures did not separate the isomers or completely remove all of the impurities. Furthermore both of these methods utilized columns containing normal-phase silica, which caused partial isomerization of the isopropenyl bond of **2,3** to give **4,5** (refer to Fig. 1). To further complicate matters the double bond isomers were found to coelute with **2,3** under their separation conditions. These results prompted us to investigate the application of a preparative HPLC method utilizing a reversed-phase column for separating and purifying **2,3**.

EXPERIMENTAL

Materials

The acetonitrile, methyl alcohol, and tetrahydrofuran were HPLC grade. The water was deionized and all other chemicals were reagent grade.

[a] Azetidinyl sulfinyl chloride **1** is a single diastereomer whose configuration about the sulfur atom is unknown. The methyl sulfinates **2,3** are a pair of diastereomers that are epimeric at the sulfur atom.

0021-9673/92/$05.00

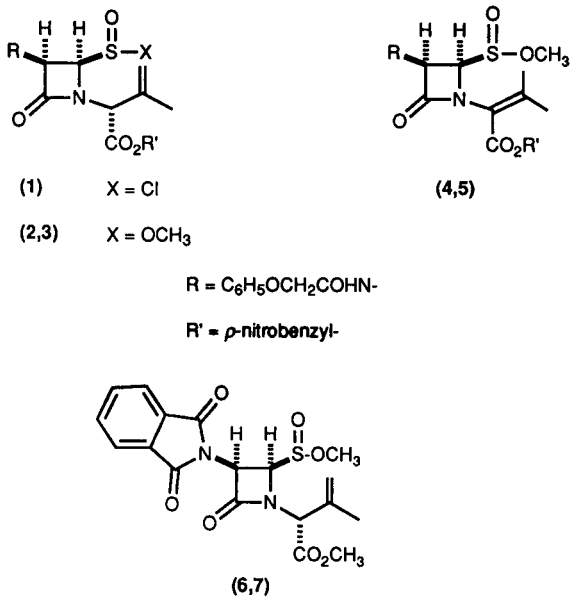

Fig. 1. Structures of azetidinyl sulfinyl chloride and azetidinyl methyl sulfinates.

Analytical HPLC

The analytical HPLC system was composed of a Waters 600 multi-solvent delivery system (with 225-μl pump heads), a Rheodyne Model 7125 valve, a Kratos Spectroflow 757 absorbance detector, and a Hitachi Model D-2000 chromato-integrator. The system was operated at room temperature at a flow-rate of 3 ml/min and the peaks were monitored at 300 nm. The mobile phase was a mixture of acetonitrile–0.2% (v/v) glacial acetic acid in water (45:55). A Prep Nova-Pak HR C_{18} cartridge column (100 mm × 8 mm I.D., 6 μm particle size) was used.

The following system was used to determine the purity of the azetidinyl methyl sulfinates after purification: Waters 600 multi-solvent delivery system, Rheodyne Model 7125 valve, Kratos Spectroflow 757 absorbance detector, and Hitachi Model D-2000 chromato-integrator. The mobile phase was a mixture of methyl alcohol–tetrahydrofuran–0.02 % trifluoroacetic acid in water (50:5:45). The flow-rate was 1.0 ml/min and the column temperature was 50°C. The peaks were monitored at 260 nm.

Preparative HPLC

The same Waters 600 multi-solvent delivery system as described above was used except that all sections of tubing between the pump and the detector outflow were replaced with 16 mm O.D., 1.02 mm I.D. stainless-steel tubing. The L-Series flowcell, 12-μl volume in the Kratos Spectroflow 757, was replaced with an L-Series flowcell of 2.5 μl and 3 mm pathlength. A Prep Nova-Pak HR C_{18} cartridge column (100 mm × 25 mm I.D., 6 μm particle size) was used. The flow-rate was 30 ml/min. A 10.0-ml sample loop (16 mm O.D., 1.02 mm I.D. stainless-steel tubing) was used. The mobile phase and detector wavelength were the same as those for the analytical set-up.

Purification procedure

Methyl alcohol was added to a toluene solution of the azetidinyl sulfinyl chloride [3] and the solvent was evaporated under reduced pressure to afford an orange, gummy solid. This solid was then dissolved in the mobile phase and injected into the preparative HPLC system at a 50 to 100-mg loading level. The collected fractions were concentrated under reduced pressure to remove acetonitrile and then extracted with methylene chloride. The methylene chloride extracts were washed with saturated brine and then dried by stirring over magnesium sulfate. The fractions were then evaporated under reduced pressure to afford colorless, amorphous solids.

RESULTS AND DISCUSSION

*Purification of **2,3** via preparative HPLC*

After failing to purify and separate **2,3** *via* flash chromatography or a Waters Prep 500, we turned our attention to an alternative means of purification. An analytical HPLC method was developed for separating **2,3** *via* a Waters Prep Nova-Pak HR C_{18} column. This method provided good peak shapes and allowed for a good separation of **2** from **3** and from the other impurities present in the sample. However, our main interest in this method was to employ it as a basis for developing a preparative-scale method for separating and isolating **2,3**.

The preparative-scale method was easily accomplished by making some minor modifications of the equipment and substituting a larger, preparative-scale column for the analytical one. Thus, the original pump and detector could be utilized for both analytical and preparative purposes. In this method

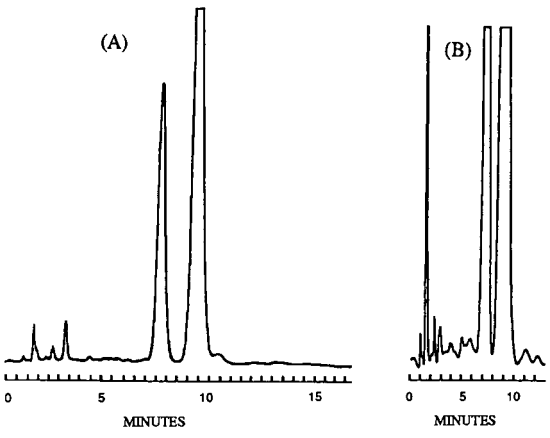

Fig. 2. HPLC of crude methyl sulfinates **2,3** on the analytical column (A) and the preparative column (B). The diastereomers **2,3** eluted at 7.68 and 9.45 min on the analytical column (column: 100 mm × 8 mm I.D., Prep Nova-Pak HR C_{18}; sample: 1 mg/ml, 20-μl injection; flow-rate: 3 ml/min) and 7.19 and 8.91 min on the preparative column (column: 100 mm × 25 mm I.D., Prep Nova-Pak HR C_{18}; sample: 100 mg/ml, 1-ml injection; flow-rate: 30 ml/min).

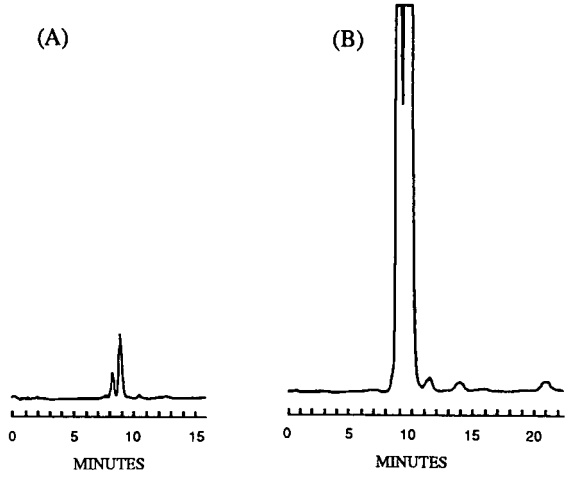

Fig. 3. HPLC of crude methyl sulfinates **6,7** on the analytical column (A) and the preparative column (B). The diastereomers **6,7** eluted at 8.14 and 8.79 min on the analytical column (column: 100 mm × 8 mm I.D., Prep Nova-Pak HR C_{18}; sample: 1mg/ml, 20-μl injection; flow-rate: 3 ml/min) and 8.62 and 9.91 min on the preparative column (column: 100 mm × 25 mm I.D., Prep Nova-Pak HR C_{18}; sample: 50 mg/ml, 1-ml injection; flow-rate: 30 ml/min).

the larger column allowed for a ten-fold increase in the flow-rate. At this higher flow-rate the sample components eluted at 7.19 and 8.91 min on the preparative column and 7.68 and 9.45 min on the analytical column (see Fig. 2). Another advantage of this method was that it utilized a column containing reversed-phase silica that was less likely to cause double bond isomerization of **2,3**, because of the non-polar nature of this stationary phase.

In a typical preparative run, 50–100 mg of the **2,3** reaction mixture was loaded onto the column. At this loading rate excellent separation of the desired components was effected. As can be seen in Table I, the methyl sulfinates **2,3** were separated and recovered in purities exceeding 94%. We saw no evidence of double bond isomerization occurring during the run. Also, HPLC showed that the purified methyl sulfinates did not contain the double bond isomers **4,5**.

No attempt was made to optimize the loading rate of **2,3** on the column. Our interest was in obtaining highly purified methyl sulfinates for use as analytical reference standards. However, because a

TABLE I

PURIFICATION OF METHYL SULFINATES

Substrate	Amount purified[a] (g)	Amount recovered (mg)		Total recovery (%)	Purity[b] (%)	
		4 or **8**[c]	**5** or **9**		**4** or **8**[c]	**5** or **9**
4,5	1.0	195	570	76.5	97.6	97.6
4,5	1.5	220	620	56.0	94.9	95.1
8,9	1.2	320	523	70.2	95.6	95.5

[a] Weights are pooled amounts from 50–100-mg injections.
[b] Determined by HPLC.
[c] Early-eluting component arbitrarily assigned as **4** or **8**.

typical preparative run lasted only 10–15 min, it was possible to accumulate quantities of material in a reasonable amount of time by making multiple injections of the reaction mixture.

The purified diastereomers were successfully employed as reference standards in an HPLC procedure developed to quantitate the yield of azetidinyl sulfinyl chloride **1**.

Purification of ***6,7***

The Waters preparative method was extended to the separation and purification of methyl sulfinates **6,7** [3]. Because **6,7** are less lipophilic than **2,3** the solvent composition had to be modified so that a good separation of the components could be effected[a]. Even though the two components were only slightly separated (see Fig. 3) purified samples of each component were obtained (see Table I). As with the purification of **2,3** no evidence of double bond isomerization was observed during the purification of **6,7** when the column containing reversed-phase silica was utilized.

[a] The mobile phase used in this separation was acetonitrile–0.2% (v/v) glacial acetic acid in water (30:70).

CONCLUSIONS

An improved method for the separation and purification of azetidinyl methyl sulfinates has been developed. This method utilizes a Waters 600 multisolvent delivery system that can be easily modified to perform both analytical and preparative-scale HPLC runs. The methyl sulfinate distereomers can be separated with good resolution in a single run using the method. No double bond isomerization is observed to occur and the diastereomers are isolated in high purity. The components of the crude mixture have approximately the same retention time on both the analytical and preparative columns.

ACKNOWLEDGEMENTS

The authors gratefully acknowledge Mr. Leonard Winneroski for his help with the HPLC preparative runs. Mr. David Robbins is thanked for his help in determining the purity of the methyl sulfinate diastereomers.

REFERENCES

1 W. C. Still, M. Kahn and A. Mitra, *J. Org. Chem.*, 43 (1978) 2923–2925.
2 F. Ginah, personal communication.
3 S. Kukolja, S. R. Lammert, M. R. B. Gleisner and A. I. Ellis, *J. Am. Chem. Soc.*, 98 (1976) 5040–5041.

Journal of Chromatography, 595 (1992) 359–363
Elsevier Science Publishers B.V., Amsterdam

CHROM. 23 965

Short Communication

Wide dynamic range electron-capture detection using the electron-capture detector pulse frequency signal

Raymond J. Lagomarsino* and Norman Latner

Environmental Measurements Laboratory, US Department of Energy, 376 Hudson Street, New York, NY 10014-3621 (USA)

(First received July 2nd, 1991; revised manuscript received December 18th, 1991)

ABSTRACT

A method has been developed that extends the dynamic range of the Varian constant-current, pulse-modulated detector by employing pulse frequency as the chromatographic output signal. A description of the technique of acquiring and utilizing the pulse frequency signal for gas chromatography–electron capture detection analysis is presented. Application of the system for the measurement of perfluorocarbon tracer compounds in ambient air samples is demonstrated.

INTRODUCTION

A constant-current, pulse-modulated electron-capture detector (ECD) provides a linear response for concentrations extending over four orders of magnitude [1–3]. However, chromatographic peak voltage outputs for the entire linear response range cannot be obtained with the Varian ^{63}Ni electron-capture detector system because of range limits imposed by the electrometer circuitry. Two switches divide the detector response into lower (ECD-1) and upper (ECD-10) output voltage ranges. In the high sensitivity ECD-1 range, chromatographic peaks greater than 1 V cannot be accurately quantified because of amplifier saturation. At ECD-10, detection sensitivity is compromised because the circuit is designed to attenuate the output voltage to one-tenth (0.1) that of ECD-1 so as to accommodate those peaks with intensities greater than 1 V.

These limitations in the detector output voltage were expected to severely affect the quality and output of the analytical results of samples collected during a series of atmospheric tracer experiments. The field experiments, designed to provide empirical tracer data to evaluate mathematical models of atmospheric transport and dispersion of pollutants, involve the release of measured and controlled quantities of perfluorocarbon tracers into the atmosphere. The tracers are collected in adsorbent tubes contained in air samplers located along the anticipated plume trajectory. The tracer quantities in each sample are then measured by gas chromatography (GC)–ECD. Details of this tracer technology have been previously published [4–6].

Highly variable ranges of tracer concentrations were expected, which would require output voltage range changes during the analysis to accommodate the different peak intensities. Because of the difficulty of establishing the expected atmospheric concentration of each tracer, the peak voltage could not be predicted, which prevented setting of the appropriate output voltage range. Since the entire sample is analyzed to obtain maximum sensitivity, the appropriate range setting could not be determined by pre-

liminary analysis. It was therefore desirable to develop a method to obtain a chromatographic output encompassing the entire linear range of the detector.

The operation of the constant-current, pulse-modulated ECD is based on the principle of applying varying frequency pulses to maintain a cell current that is equal to a a reference current as molecules with electron-capture properties enter the detector cell. These frequency signals are proportional to the output voltage but are not channeled through the output circuitry. This paper describes the method of extracting and utilizing the ECD pulse frequency signals for wide dynamic range gas chromatographic analyses.

EXPERIMENTAL

Sample collection

The samples were collected during the Atmospheric Studies in Complex Terrain (ASCOT) program, a series of tracer experiments in a valley located in western Colorade, USA [7]. These field experiments involved the atmospheric release of three perfluorocycloalkane compounds: perfluoromethylcyclopentane (PMCP), perfluoromethylcyclohexane (PMCH) and perfluorodimethylcyclohexane (PDCH). The sampling systems employed for these studies have been described elsewhere [8].

Gas chromatographic analysis

The sample tubes containing the adsorbed tracers were analyzed by a Varian 3700 gas chromatographic system (Varian Assoc., Palo Alto, CA, USA) that was modified for perfluorocarbon tracer analyses [9]. Details of the analysis system has been given elsewhere [8]. The detector reference current and base frequency were 567 pA and 4.10 kHz, respectively. No adjustments or modifications were made to the detector or the associated electronics to improve the linear range [10–13].

Accessing and processing the ECD pulse frequency signals

The method by which the ECD responds to a sample with electron-capture properties is via injected negative pulses which sweep out the free electrons and produce a cell current. The frequency of these negative pulses is varied to maintain a constant value equal to the reference current. In response to the different sample concentrations in the cell, the frequency can change from its base value of 4.10 kHz to approximately 1.4 MHz (*ca.* 250 to 1). However, the output amplifier stages of the electrometer system limit the dynamic range of the analog signal to about 100 to 1. While appropriate for most analytical work, it was clearly not suitable for the wide and variable range of concentrations that were expected for the ASCOT samples. No significant improvement could be made to the amplifier stages, which appeared to be well designed. Measurements made at our Laboratory confirm that the pulse frequencies are linear and proportional to the voltage over a wide range of concentrations [14].

Utilizing the frequency pulses introduces a coupling and interface problem. The 50-V negative pulses being fed to the detector are too high to be used by most conventional circuitry. In addition, the high impedance and sensitive nature of the detector circuitry permits only minimal disturbance of the shielding. A practical solution to these problems

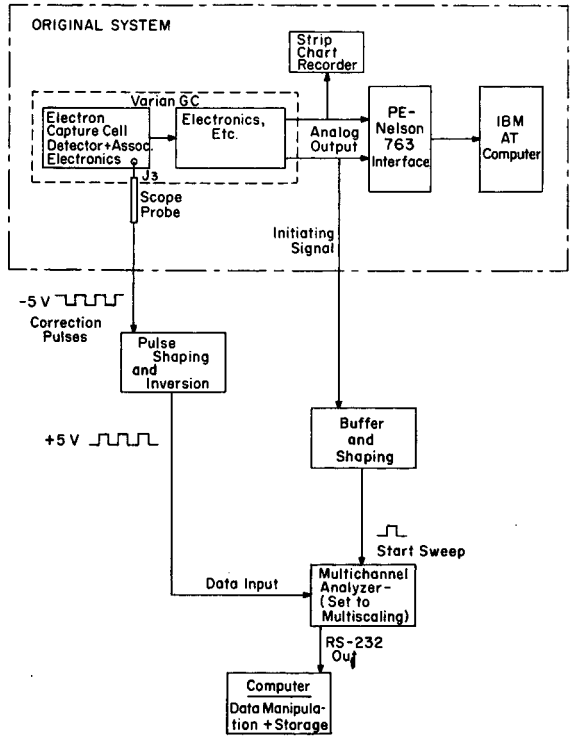

Fig. 1. Block diagram of the ECD pulse frequency system.

was to couple the signal via a 10:1 HP Model 10041A oscilloscope probe (Hewlett-Packard, Palo Alto, CA, USA) the high impedance and low capacitance of which offer isolation while reducing the signal level to 5 V. The shape and size of the probe necessitated only a small opening in the shield to access the injected pulses. The negative pulses were inverted and widened by a Canberra Model 1455 logic shaper/delay circuit (Canberra Industries, Meriden, CT, USA; in order to be accepted by a Tracer Northern Model TN1760 multichannel analyzer (MCA) (Northern Scientific, Middleton, WI, USA) set to operate in the multiscaling mode. A block diagram of this system is shown in Fig. 1. The dwell time of the MCA, *i.e.*, the fixed time at which each channel accepts pulses, was set at 500 ms, along with a 1000-channel scan setting to accommodate the maximum time required for the chromatographic analysis.

An initiating signal from the gas chromatograph, after buffering and shaping, was used to start the multichannel sweep. The resulting chromatographic scan, which is completed in 8.3 min, was transferred via the MCA's RS-232 port to an Hewlett-Packard 85 computer for data manipulation and permanent storage.

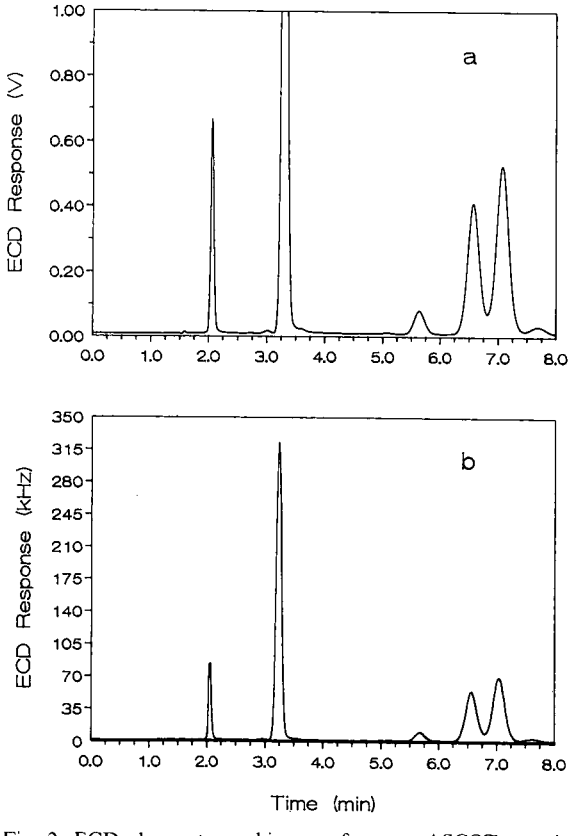

Fig. 2. ECD chromatographic scan from an ASCOT sample analysis: (a) voltage output; (b) pulse frequency output. Chromatographic conditions: 6 ft (1.8 m) × 1/8 in O.D. (3.2 mm, stainless steel) 0.1% SP-1000 on Carbopack C column (Supelco, Bellefonte, PA, USA); detector temperature at 180°C; column temperature at 135°C (isothermal); carrier gas 5% hydrogen in nitrogen at a flow-rate of 22 ml min^{-1}.

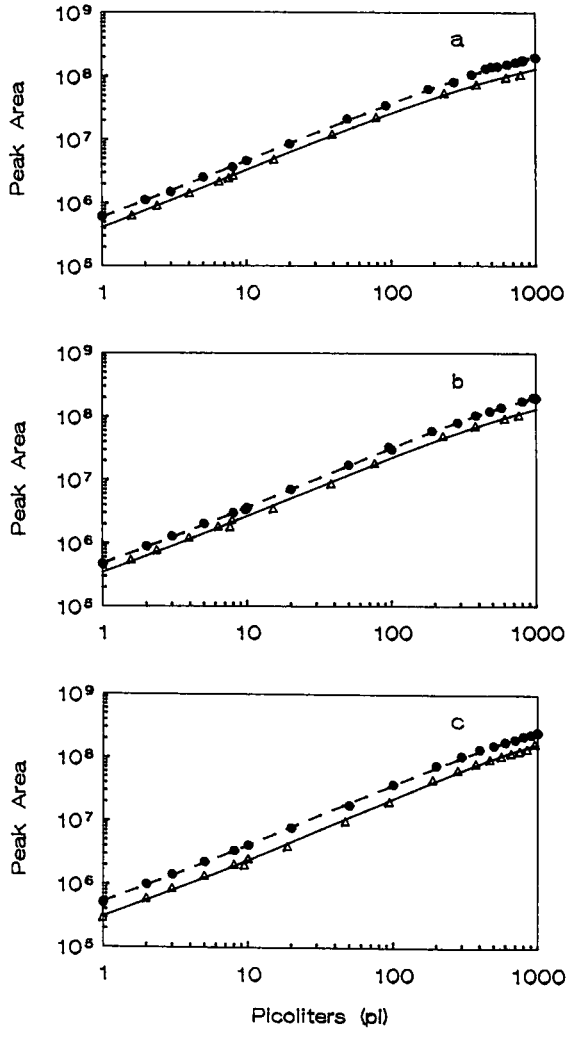

Fig. 3. ECD voltage and pulse frequency calibration curves: (a) perfluoromethylcyclopentane (PMCP); (b) perfluoromethylcyclohexane (PMCH); (c) perfluorodimethylcyclohexane (PDCH). ECD-10 voltage peak areas normalized (× 10) to ECD-1. △ = Frequency; ● = voltage.

RESULTS

The voltage and pulse frequency chromatographic signals were simultaneously recorded for each sample analysis. Electrometer gain was maintained at ECD-1 for maximum sensitivity of detection ($5 \cdot 10^{-3}$ pl or 5 fl) for those tracer peaks representing ambient background concentrations (<1 fl l^{-1}). The analog output voltage (ECD-1) was fed to a PE-Nelson Model 763 (Cupertino, CA, USA) analog-to-digital (A/D) interface and the digitized chromatographic signal recorded in an IBM PC/AT for subsequent quantitative determination of each tracer with PE-Nelson Model 2600 software. The initiating signal used to start the pulse frequency multichannel sweep was also used to simultaneously start the A/D interface at sample injection in order to synchronize the peak retention times. Each sample tracer quantity was first determined from the voltage output recording. Voltage system results in excess of 35 pl for PMCP, 85 pl for PMCH and 200 pl for PDCH were rejected because these volumes represent peak heights of 1 V, which is the upper limit before amplifier saturation at ECD-1. Those tracers exceeding these values were quantitatively determined from the corresponding pulse frequency recording. Fig. 2a shows a typical chromatographic scan of the voltage output from an ASCOT sample analysis, illustrating amplifier saturation by PMCH. The corresponding pulse frequency scan illustrating no PMCH saturation and from which the PMCH was quantitatively determined is shown in Fig. 2b.

The ECD pulse frequency, MCA system and the voltage system were separately calibrated for each tracer. Voltage calibrations were obtained at the two voltage output settings, ECD-1 and ECD-10. The results of voltage and pulse frequency system calibrations for each of the tracer compounds are shown in Fig. 3. These calibrations curves illustrate

TABLE I

COMPARISON OF RESULTS: VOLTAGE *VERSUS* PULSE FREQUENCY SIGNALS

PMCP				PMCH				PDCH[a]			
Sample type[b]	V[c]	PF[d]	% dif[e]	Sample type	V	PF	% dif	Sample type	V	PF	% dif
A	0.32	0.32	0.0	A	0.36	0.37	−2.8	A	0.31	0.34	−9.7
A	0.42	0.42	0.0	A	0.78	0.80	−2.6	A	0.41	0.42	−2.4
A	2.98	3.00	−0.7	A	1.83	1.85	−1.1	A	2.05	2.00	2.4
A	4.28	4.39	−2.6	A	6.15	6.20	−0.8	A	4.40	4.20	4.5
A	8.12	8.16	−0.5	A	9.31	9.40	−1.0	A	9.82	9.72	1.0
A	18.1	18.5	−2.2	A	13.4	12.8	4.5	A	13.9	13.0	6.5
A	27.2	28.7	−5.5	A	27.6	29.2	−5.8	A	26.9	26.4	1.9
A	31.9	33.2	−4.1	A	43.0	43.8	−1.9	A	46.1	47.1	−2.2
S	44.9	45.8	−2.2	A	78.2	76.5	2.1	A	61.0	63.9	−4.8
S	87.0	88.0	−1.1	S	87.2	86.4	0.9	A	89.4	91.0	−1.8
S	145	152	−4.8	S	145	141	2.8	A	149	156	−4.7
S	240	250	−4.2	S	241	235	2.5	S	247	256	−3.6
S	450	465	−3.3	S	451	465	−3.1	S	463	453	2.2
S	715	724	−1.3	S	717	705	1.7	S	735	728	1.0
S	822	839	−2.1	S	825	810	1.8	S	845	831	1.7
Average			−2.3				−0.2				−0.5
R.S.D.			1.8				2.8				4.2

[a] Values based on the sum of the three peaks of the PDCH isomers in the 5.30–7.35 min range.
[b] A = ASCOT (V = ECD-1); S = Spiked (V = ECD-10).
[c] V = Tracer volume (pl) obtained from the voltage signal.
[d] PF = Tracer volume (pl) obtained from the pulse frequency signal.
[e] % dif = (V − PF)/V × 100.

the wide dynamic range of the pulse frequency system and confirm the proportionality of the voltage with the pulse frequency.

Comparisons of the voltage and pulse frequency results for each tracer over the linear response range (0.3–850 pl) are shown in Table I. Those results below the saturation volumes at ECD-1 were obtained from ASCOT sample analyses because both outputs were routinely recorded. To provide comparison results above the ECD-1 saturation, volumes adsorbent-collected air samples were spiked with tracers and the samples analyzed with the electrometer gain at ECD-10.

The distribution of the percent differences between the results from the pulse frequency and voltage methods of analyses for PMCH and PDCH, and the mean percent difference for each tracer illustrate that these measurements do not reveal any statistically significant differences between the two methods. For PMCP there appears to be a slight negative bias for the pulse frequency method relative to the voltage method, but the mean percent difference between the two methods is zero within two standard deviations.

CONCLUSIONS

We have demonstrated the viability of quantitative GC–ECD analyses using the detector pulse frequency signals as chromatographic output. We expect to provide a pulse frequency system for a recently acquired Varian 6000 GC–ECD perfluorocarbon tracer analyzer by substituting an IBM-AT compatible, MCA plug-in card for the the standalone MCA.

REFERENCES

1 R. J. Maggs, P. L. Joynes, A. J. Davies and J. E. Lovelock, *Anal. Chem.*, 43 (1971) 1966.
2 J. E. Lovelock and A. J. Watson, *J. Chromatogr.*, 158 (1978) 123.
3 P. L. Patterson, *J. Chromatogr.*, 134 (1977) 25.
4 J. E. Lovelock and G. J. Ferber, *Atm. Environ.*, 16 (1982) 1467.
5 G. J. Ferber, J. L. Heffter, R. R. Draxler, R. J. Lagomarsino, R. Dietz, F. L. Thomas and C. L. Benkowitz, *Cross-Appalachian Tracer Experiment (CAPTEX'83) Final Report*, ERL ARL-142 NOAA Technical Memorandum, Air Resources Laboratory, US Department of Commerce, Silver Spring, MD, 1986.
6 R. R. Draxler and J. L. Heffter (Editors), *Across North America Tracer Experiment (ANATEX), Volume 1: Description, Primary Site Ground-Level Sampling and Meteorology*, ERL ARL-167 NOAA Technical Memorandum, Air Resources Laboratory, US Department of Commerce, Silver Spring, MD, 1989.
7 W. E. Clements, J. A. Archuleta and P. H. Gudiksen, *J. Applied Meteorol.*, 28 (1989) 405.
8 R. J. Lagomarsino, F. L. Thomas, T. J. Weber and L. R. Greenfield, *Cross-Appalachian Tracer Experiment (CAPTEX'83) Quality Assurance of Surface Samples, Report EML-462*, US Department of Energy, New York, NY, 1987.
9 R. Dietz, Department of Applied Science, Brookhaven National Laboratory, Upton, NY, 1980, personal communication.
10 J. J. Sullivan and C. A. Burgett, *Chromatographia*, 8 (1975) 176.
11 G. Wells, *J. Chromatogr.*, 346 (1985) 1.
12 W. B. Knighton and E. P. Grimsrud, *J. Chromatogr.*, 288 (1984) 237.
13 P. Rotocki and B. Drozdowicz, *Chromatographia*, 27 (1989) 71.
14 N. Latner and R. J. Lagomarsino, *Improved Gas Chromatographic Electron-Capture Analysis Using a Pulse Frequency Method, Report EML-532*, US Department of Energy, New York, NY, 1991.

Journal of Chromatography, 595 (1992) 364–367
Elsevier Science Publishers B.V., Amsterdam

CHROM. 23 955

Short Communication

Identification of ochratoxin A in food samples by chemical derivatization and gas chromatography–mass spectrometry

Yuying Jiao☆, Werner Blaas, Christian Rühl* and Rudolf Weber

Max von Pettenkofer-Institut des Bundesgesundheitsamtes, P.O. Box 330013, 1000 Berlin 33 (Germany)

(First received October 2nd, 1991; revised manuscript received December 9th, 1991)

ABSTRACT

The contamination of foods with ochratoxin A can be determined very sensitively by high-performance liquid chromatography (HPLC) with fluorescence detection. A novel procedure is described to confirm OA-positive results quantitatively down to the HPLC detection limit of 0.1 ppb. For this, ochratoxin A in the sample extract is converted into its O-methylochratoxin A methyl ester derivative, which is identified subsequently by gas chromatography–mass spectrometry negative-ion chemical ionization and multiple ion detection modes using the hexadeuterated O-methyl-d_3-ochratoxin A methyl-d_3 ester derivative as internal standard for quantification. In the analysis of more than 60 contaminated samples, the procedure was found to be very accurate.

INTRODUCTION

The contamination of foods and feeding stuffs by the mycotoxin ochratoxin A (OA) {(*R*)-N-[5-chloro-3,4-dihydro-8-hydroxy-3-methyl-1-oxo-1*H*-2-benzopyran-7-yl)carbonyl]-L-phenylalanine, $C_{20}H_{18}ClNO_6$, [303-47-9]} is a problem of international concern [1–3]. It has been reported that OA is implicated in Balkan endemic nephropathy, a chronic renal diseasec in man [4,5]. Recently, the Joint FAO/WHO Expert Committee on Food Additives proposed a provisional tolerable weekly intake (PTWI) of 112 ng/kg body weight [6].

For the determination of OA in foods, high-performance liquid chromatography (HPLC) with fluorescence detection has often been used. Positive results have been confirmed by different techniques, *e.g.*, by changing the fluorescence excitation wavelength [7] or scanning the fluorescence spectrum [8], by thin-layer chromatography [9], direct-inlet mass spectrometry (MS) [10], HPLC–MS [11], enzyme-linked immunoassay [12] or methylation of OA to OA methyl ester (OA-Me) or O-methyl-OA methyl ester ($OA\text{-}Me_2$), followed by identification of these derivatives by HPLC [13–15] or gas chromatography–electron impact MS (GC–EI-MS) [16]. However, only immunoassay was suitable for confirming positive OA results in the detection limit range 0.1–0.3 ppb (μg/kg).

This paper describes a sensitive and accurate procedure for the confirmation of OA in foods by its conversion to $OA\text{-}Me_2$, which is detected subsequently by means of GC–negative-ion chemical ion-

☆ Permanent address: Research Centre for Eco-Environmental Sciences, Academica Sinica, Beijing, China.

0021-9673/92/$05.00

ization (NICI) MS in the multiple ion detection (MID) mode using hexadeuterated OA-Me_2-d_6 as internal standard.

EXPERIMENTAL

Chemicals

OA was obtained from Sigma. A stock solution (100 μg/ml) was prepared in methanol. For the generation of diazomethane and deuterated diazomethane, Diazald and Deutero-Diazald Prep Set, respectively, from Aldrich were used.

Instrumentation

HPLC was performed using a Varian Model 5000 liquid chromatograph equipped with a Hewlett-Packard Model 1046 A programmable fluorescence detector. The analytical conditions were as follows: column, Merck LiChrospher 100 RP-18, 5 μm (250 mm × 4 mm I.D.); mobile phase, water–acetonitrile–acetic acid (525:450:25); flow-rate, 1.0 ml/min; injection volume, 20 μl; excitation wavelength, 330 nm; and emission wavelength, 460 nm.

The GC–MS equipment consisted of a Finnigan Model 4500 quadrupole mass spectrometer with an Incos data system interfaced by direct coupling with a Hewlett-Packard Model 5890 gas chromatograph with on-column injector. The GC column used for the analysis was a 10 m × 0.25 mm I.D. Supelco PTE-5 fused-silica capillary column (film thickness 0.25 μm) coupled with a 2 m × 0.53 mm I.D. deactivated J&W Scientific retention gap. Initially the column was held at 60°C for 2 min and then programmed at 25°C/min to the final temperature of 310°C with a hydrogen carrier gas flow-rate of *ca.* 70 cm/s. Samples were injected with a Hamilton on-column syringe with a 0.17 mm O.D. fused-silica needle. When after a few injections the GC peak became broad, about 20 cm of the retention gap were cut off.

The MS conditions were as follows: NICI–MID mode, reagent gas, methane; pre-pressure, 0.45 Torr; operating pressure, $3 \cdot 10^{-5}$ Torr; electron energy, 70 eV; emission current, 0.30 mA; multiplier voltage, 1.45 kV; ion source temperature, 120°C; interface temperature, 270°C; scan time for *m/z* 416, 417, 419, 431 and 437 ions, 0.2 s each.

Sample preparation

The described clean-up procedure is a modification of the method of Hadlok *et al.* [17]. A 30-g aliquot of the finely ground sample was mixed with 50 ml of 0.4 *M* magnesium chloride solution, 30 ml of 2 *M* hydrochloric acid and 100 ml of toluene in a 500-ml centrifuge tube. The tube was shaken automatically for 60 min and then clarified by centrifugation at 15 900 *g* (9000 rpm) for 40 min. A 50-ml volume of the supernatant toluene layer was run through a Sep-Pak silica cartridge, prewetted with 5 ml of toluene. The cartridge was washed with 10 ml of *n*-hexane, 20 ml of *n*-hexane–diisopropyl ether (1:1), 20 ml of toluene–acetone (95:5) and 10 ml of toluene. Thereafter OA was eluted with 10 ml of toluene–acetic acid (9:1). The eluate was evaporated to dryness on a rotary evaporator and the residue dissolved in 0.50 ml of methanol. A 20-μl volume of this extract was injected on to the HPLC column. For calculation the external standard method was used.

Preparation of the internal standard OA-Me_2-d_6

An excess of an ethereal solution of deuterated diazomethane, freshly prepared from Diazald-N-methyl-d_3 [18], was added dropwise to a solution of 100 μg of OA in 5 ml of deuterium oxide and 2 ml of 2-(2-ethoxyethoxy)ethan(ol-*d*) in a brown 250-ml flask. The mixture was stirred overnight and then concentrated using a gentle stream of nitrogen. After transferring the residue by means of 2 ml of water–methanol (3:1) to a Sep-Pak C_{18} cartridge, prewetted with 2 ml of methanol and 5 ml of water, the cartridge was washed with 10 ml of water–methanol (3:1) and OA-Me_2-d_6 was eluted with 10 ml of methanol–water (3:1). The eluate was evaporated to dryness and the residue dissolved in 10 ml of acetone. The absence of OA and OA-Me-d_3 in the HPLC trace confirmed the quantitative reaction of OA to its OA-Me_2-d_6 derivative. The standard remains stable for at least 4 months.

Derivatization of the sample extract

To 400 μl of the methanolic sample extract an amount of OA-Me_2-d_6 was added that was comparable to the amount of OA in the sample determined. Subsequently an excess of an ethereal solution of diazomethane, freshly prepared from Diazald [18], was added. After automatic shaking over-

night, the solvents were removed, the residue transferred by means of 0.2 ml of methanol to a Sep-Pak C_{18} cartridge, prewetted with 2 ml of methanol and 5 ml of water, and the cartridge was washed with 5 ml of water–methanol (3:1). Subsequently, OA-Me_2 was eluted with 5 ml of methanol–water (3:1) and the eluate evaporated to dryness. The residue was dissolved in 50–80 μl of methanol and injected on to the HPLC column. The fraction eluting between 22 and 29 min was collected, evaporated to dryness and again cleaned, as described above, using a Sep-Pack C_{18} cartridge. Finally, the OA-Me_2-containing residue was dissolved in 50 or 100 μl of acetone and a 1-μl aliquot was injected into the GC–MS system. Comparing the areas of the base peaks at *m/z* 416 and 419, the internal standard method was used for calculation. The small amount of *m/z* 419 ion derived from OA-Me_2 (due to the chlorine isotope abundance, 32% of the area of the *m/z* 417 peak) was taken into consideration.

RESULTS AND DISCUSSION

Analytical procedure

Over 400 food samples were analysed for contamination with OA; the results will be published elsewhere on completion of the study. The analytical procedure given proved to be very rapid and reliable. On spiking OA-free samples with 0.3–5.0 ppb of OA, the recovery was 74–113%. The detection limit was about 0.1 ppb. To confirm positive results, OA can be determined very sensitively, as described here, at levels down to the HPLC detection limit by its derivatization to OA-Me_2 and subsequent GC–MS analysis in the NICI and MID modes. Hexadeuterated OA-Me_2-d_6 served as an internal standard for quantification.

The NICI mass spectra of OA-Me_2 and OA-Me_2-d_6 are shown in Fig. 1a and b, respectively. The base peaks at *m/z* 416 and 419 are assigned to the $[M-CH_3]^-$ and $[M-CD_3]^-$ ions, respectively, and the peaks at *m/z* 431 and 437 to the molecular ions M^-. Separated by 2 mass units and corresponding to the natural abundance, the chlorine isotope peaks are recognizable in each instance. To increase the sensitivity of the GC–MS analysis, the MID mode using the *m/z* 416, 417, 419, 431 and 437 ions was applied. The fragment ion of *m/z* 418 was not chosen because of occasional interferences from unknown compounds eluting close to OA-Me_2.

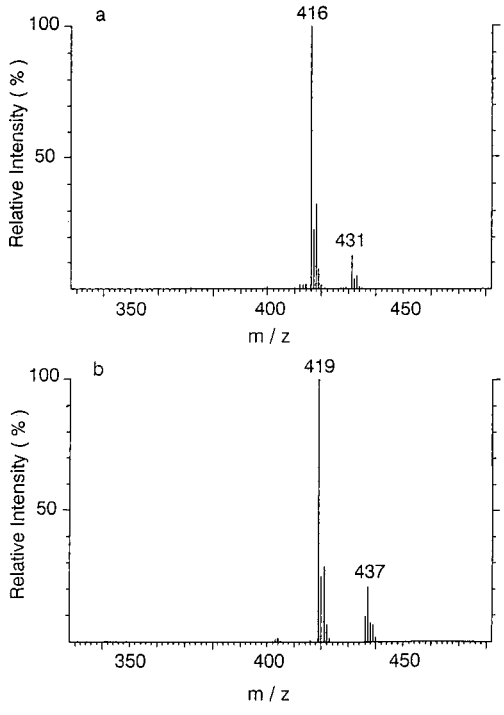

Fig. 1. NICI mass spectra of (a) OA-Me_2 and (b) hexadeuterated OA-Me_2-d_6.

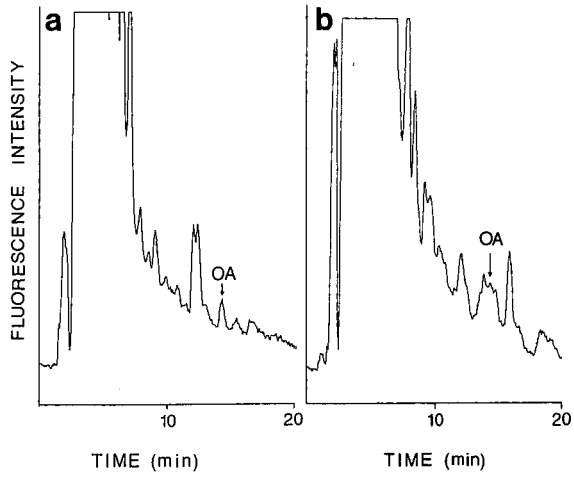

Fig. 2. HPLC determination of OA in (a) a sample of a maize–peanut snack containing 0.13 ppb of OA and (b) a bran sample containing less than 0.17 ppb of OA.

Analysis of samples

Sixty-seven of the samples that according to the HPLC analysis were contaminated with OA were analysed by the GC–MS method. In one sample OA was not detected. Although the HPLC retention time of one peak in this sample was very close to the retention time of OA and there was no shoulder on the HPLC trace after addition of OA, according to the GC–MS data we believe that an unknown compound co-eluted here.

For the other 66 samples, the agreement of the results of HPLC and GC–MS analyses was very good. If the samples were contaminated with more than 0.5 ppb, 99.0% of the value estimated by HPLC was found by GC–MS analysis on average (n = 22, S.D. = 13.1); for less contaminated samples (0.07–0.50 ppb OA) the value was 89.1% (n = 44, S.D. = 33.2).

Fig. 2a and b shows the HPLC of a maize–peanut snack and a wheat bran sample, respectively. The appropriate GC–MS results are shown in Fig. 3a and b. For the snack the contamination with OA was estimated to be 0.13 ppb by both HPLC and GC–MS. Owing to the overlapping peaks, the OA contamination of the bran sample could not be determined accurately by HPLC, but was calculated to be less than 0.17 ppb; using GC–MS, 0.13 ppb of OA was determined.

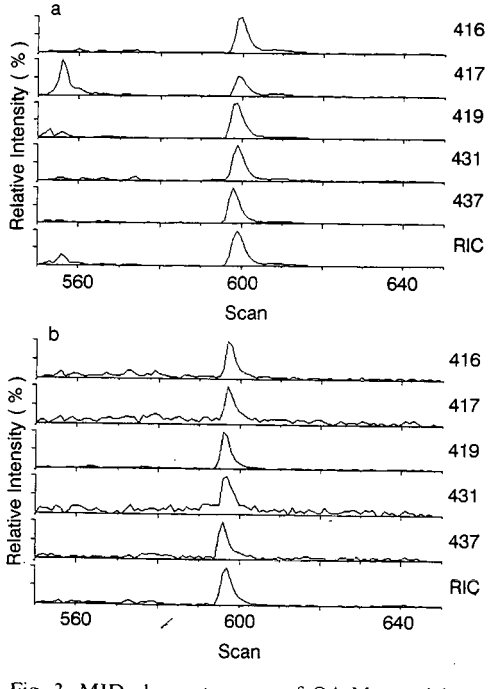

Fig. 3. MID chromatograms of OA-Me_2 and hexadeuterated OA-Me_2-d_6 in the same samples as illustrated in Fig. 2: (a) maize–peanut snack; (b) bran sample.

REFERENCES

1 *Environmental Health Criteria 105, Selected Mycotoxins: Ochratoxins, Trichothecenes, Ergot*, World Health Organization, Geneva, 1990.
2 Deutsche Forschungsgemeinschaft, *Ochratoxin A: Vorkommen und toxikologische Bewertung*, VCH, Weinheim, 1990.
3 C. F. Jelinek, A. E. Pohland and G. E. Wood, *J. Assoc. Off. Anal. Chem.*, 72 (1989) 223.
4 P. Krogh, B. Hald, R. Plestina and S. Ceovic, *Acta Pathol. Microbiol. Scand., Sect. B*, 85 (1977) 238.
5 T. Petkova-Bocharova, I. N. Chernozemsky and M. Castegnaro, *Food Addit. Contam.*, 5 (1988) 299.
6 Joint FAO/WHO Expert Committee on Food Additives, Document PCS/90.43, 37th Meeting, Geneva, 5 14 June, 1990.
7 M. V. Howell and P. W. Taylor, *J. Asssoc. Off. Anal. Chem.*, 64 (1981) 1356.
8 K. Ranfft, R. Gerstl and G. Mayer, *Agribiol. Res.*, 43 (1990) 44.
9 P. Nowotny, W. Baltes, W. Krönert and R. Weber, *Chem. Mikrobiol. Technol. Lebensm.*, 8 (1983) 29.
10 J. Bauer and M. Gareis, *J. Vet. Med. B*, 34 (1987) 613.
11 D. Abramson, *J. Chromatogr.*, 391 (1987) 315.
12 M. Gareis, E. Märtlbauer, J. Bauer and B. Gedek, *Z. Lebensm.-Unters.-Forsch.*, 186 (1988) 114.
13 H. Cohen and M. Lapointe, *J. Assoc. Off. Anal. Chem.*, 69 (1986) 957.
14 H. Tsubouchi, H. Terada, K. Yamamoto, K. Hisada and Y. Sakabe, *J. Agric. Food Chem.*, 36 (1988) 540.
15 T. D. Phillips, A. F. Stein, G. W. Ivie, L. F. Kubena, A. W. Hayes and N. D. Heidelbaugh, *J. Assoc. Off. Anal. Chem.*, 66 (1983) 570.
16 R. Scheuer, G. Hofmann and L. Leistner, *Jahresbericht der Bundesanstalt für Fleischforschung, Kulmbach*, 1984, p. C19.
17 R. M. Hadlok, U. Christen, S. Wiedmann, A. Moritz and G. Wagner, *Mykotoxine in vom Tier stammenden Nahrungsmitteln: Ochratoxin A und Sterigmatocystin in der Nahrungsmittelkette*, Justus-Liebig-Universität, Giessen, 1989.
18 Aldrich *Technical Information Bulletin*, No. AL-180, February 1989.

Journal of Chromatography, 595 (1992) 368–374
Elsevier Science Publishers B.V., Amsterdam

CHROM. 23 994

Short Communication

Comparison of commercially available thin-layer chromatography plates with mixtures of dyes, analgesics and phenols

Donald L. Gumprecht

Department of Chemistry, University of Alabama, Box 870336, Tuscaloosa, AL 35487-0336 (USA)

(First received October 23rd, 1991; revised manuscript received January 3rd, 1992)

ABSTRACT

A series of five commercially available thin-layer chromatography plates has been compared using three different mixtures. The plates examined were Analtech, Baker, Merck, Whatman and Eastman Kodak silica gel plates. The first four are layers on glass while the last is a layer on a polyester sheet. All have a F_{254} fluorescent indicator. The Kodak plate is not strictly comparable to the others but was included since it is quite widely used. Some very significant differences were noted in R_F values as well as in the relative order in which the components were eluted. The highest R_F values on glass plates were generally obtained either using Analtech or Whatman plates depending on the solvent. The lowest R_F values were nearly always obtained using Merck plates. Screening of chromatographic plates is particularly important when analyzing unknown mixtures.

INTRODUCTION

Thin-layer chromatography (TLC) as an analytical tool has been in use for many years. Although it can be used as a method of quantitative analysis, the major uses are for qualitative purposes. Identification of the components of a mixture is a primary use. Another practical use is in screening reaction mixtures for both major and minor products – either known or unknown.

Industrial as well as academic laboratories frequently have on hand several types of commercially available TLC plates. However, it has been our experience that screening of the plates themselves is seldom done. Many investigators use a "favorite" plate or one that has worked well on a previous project or has been recommended by a colleague. The purpose of the present work was to analyze several mixtures in order to compare commercially available TLC plates under identical conditions and solvent systems to determine whether differences in the plates would give varying results.

A number of references have been found comparing reversed-phase TLC plates under various conditions [1–6]. Work has been done on toxicologically interesting substances comparing silica gel coated films and sheets with silica gel coated glass plates [7]. Work has also been done with varying solvent systems since these play a major role in analyses by TLC. It is believed, however, that the majority of investigators tend to screen solvent systems much more extensively than the plates themselves [8–11].

0021-9673/92/$05.00

EXPERIMENTAL

Mixtures analyzed

Three different mixtures have been analyzed in order to determine if differences exist between various commercial TLC plates. The first mixture examined was a solution of six major dyes in toluene and is available as Test Dye Mixture IV (30-04) from Analtech. A number of minor unknown dyes were present. The major dyes are listed in Table I with the color and a "typical" R_F value on silica gel with toluene as the mobile phase as reported by Analtech in an unnumbered bulletin accompanying the dye mixture. No details are given on plate or experimental conditions.

The second mixture examined consisted of four compounds found in various commercial analgesic products such as Advil, Tylenol, Anacin and Excedrin. The compounds are acetaminophen, ibuprofen, acetylsalicylic acid and caffeine and were dissolved in chloroform–ethanol (1:1).

The third mixture tested was composed of phenol, *o*-hydroxymethylphenol (o-MP), *p*-hydroxymethylphenol (p-MP), *o,o'*-dihydroxydiphenylmethane (o,o'-DHDPM) and *p,p'*-dihydroxydiphenylmethane (p,p'-DHDPM) dissolved in methanol. This mixture is typical of those found in commercial water soluble phenol-formaldehyde resins [12].

Each of the three mixtures was run on the five TLC plates with different solvents. The R_F values reported are the average of three separate runs.

TLC plates

Five commercially available TLC plates were used in obtaining data. These plates are identified as Analtech 47511 (Newark, DE, USA), Baker 7001-04 (Phillipsburg, NJ, USA), Eastman Kodak 13181 (Rochester, NY, USA), Merck 5715-7 (Darmstadt, Germany) and Whatman 4500-105 (Maidstone, UK). With the exception of the Kodak plate all were 250-μm silica gel layers on glass with a fluorescent indicator. The Kodak plate is a 100-μm layer on a polyester sheet and although not directly comparable was included in the study because it is widely used in academic and industrial laboratories. All plates have an average pore diameter of 60 nm. The Baker plate contains an inorganic binder while all others have an organic binder. This information was obtained from technical bulletins or direct contact with the manufacturer.

Before use, the plates were cut to *ca.* 5 cm wide by 10 cm long. The test mixtures were applied from a microliter syringe and allowed to dry. The sample volume was 4 μl and the spot diameter was 4–5 mm. The plates were not pre-dried but used directly so that temperature and humidity conditions would be equal.

TABLE I

COMPOSITION OF ANALTECH DYE MIXTURE (MAJOR DYES ONLY)

From Analtech Bulletin.

Dye	Color	Typical R_F
Fat Red 7B	Purple	0.64
Solvent Green 3	Green	0.38
Sudan II	Peach	0.34
Sudan II	Orange	0.28
Sudan Blue	Blue	0.16
Sudan Orange G	Yellow	0.03

Procedure

The solvent to be used was placed in a chromatography tank (28 × 25 × 7.5 cm) and allowed to stand 1 h at room temperature (23–24°C). The spotted plates were all placed in the solvent at the same time and the solvent allowed to rise about 9 cm before removing and drying. The plates run with the dye mixture were examined directly. The plates run with the analgesic mixture and the phenols were examined under a 254 nm ultraviolet lamp and the spots marked. As a secondary detection method the phenol plates were sprayed with a ceric ammonium nitrate solution since any overlapping or unknown spots can often be identified by the color [12].

RESULTS AND DISCUSSION

Dye mixture

There is an obvious difference in the R_F values reported by Analtech in Table I using toluene with a silica gel plate and those obtained in our data. Even using a commercially available Analtech plate our data were from 44 to 81% higher for the various major spots. All of the other layers on glass showed similar but smaller differences. The Kodak plate showed differences even larger – from 53 to 243%.

Another difference observed was the relative lo-

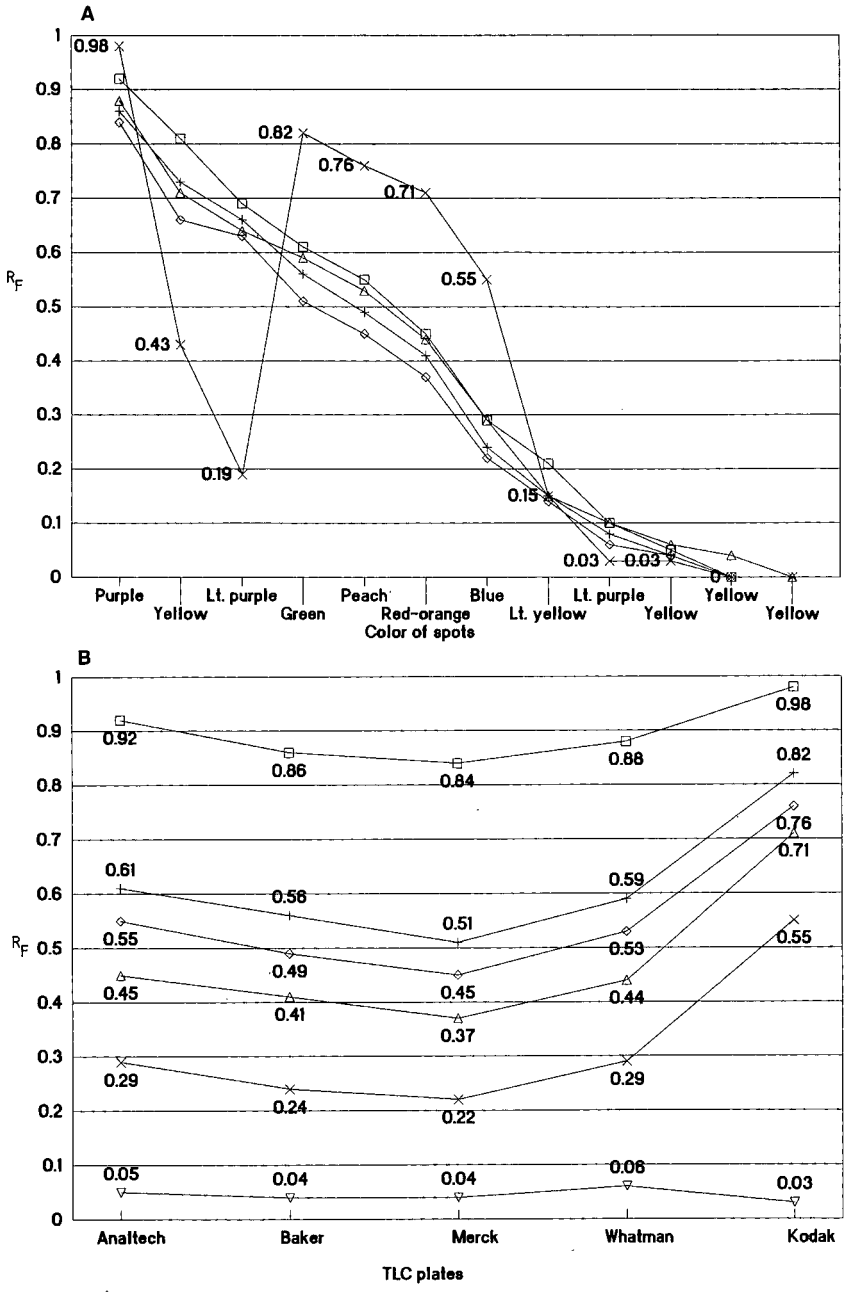

Fig. 1. (A) R_F values of dye mixture with toluene mobile phase; □ = Analtech; + = Baker; ◇ = Merck; △ = Whatman; × = Kodak. (B) R_F values of major dyes only with toluene mobile phase; □ = purple; + = green; ◇ = peach; △ = red-orange; × = blue; ▽ = yellow; Lt. = light.

cation of various spots obtained with the Kodak plate as compared to the layers on glass. On the Kodak plate as shown in Fig. 1A, two minor spots (yellow and light purple) which had the second and third highest R_F value on glass plates with toluene were displaced to sixth and seventh place. A second light purple spot appeared to overlap with the major yellow spot at R_F 0.03. For the major spots the

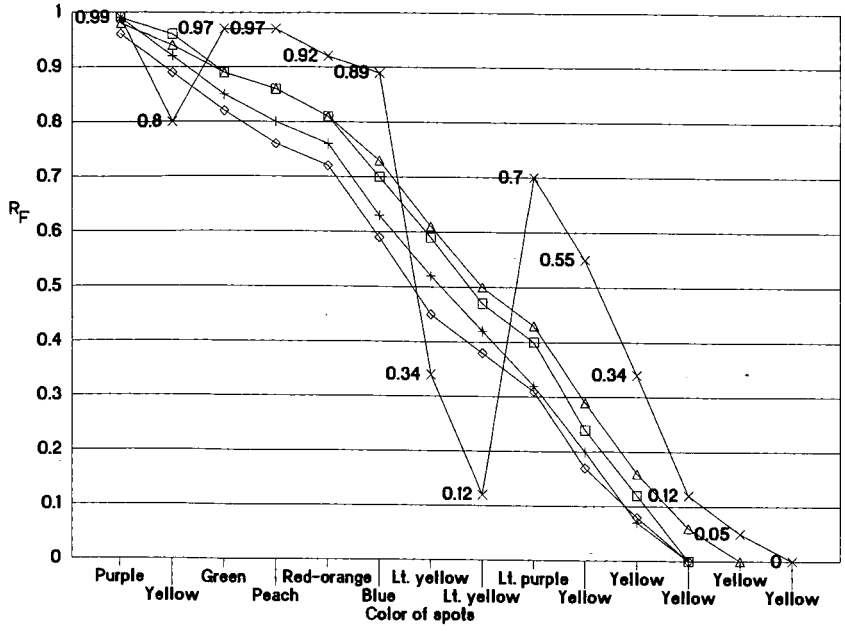

Fig. 2. R_F values of dye mixture with methylene chloride mobile phase. □ = Analtech; + = Baker; ◇ = Merck; △ = Whatman; × = Kodak.

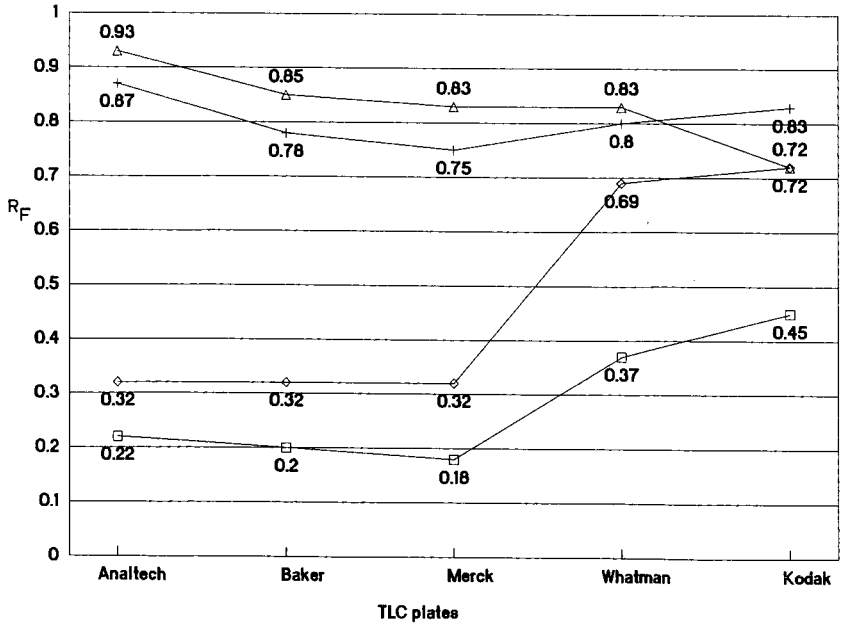

Fig. 3. R_F values of analgesic mixture. Mobile phase 1,2-dichloroethane–acetic acid (12:1); □ = Acetaminophen; + = acetylsalicylic acid; ◇ = caffeine; △ = ibuprofen.

R_F values were much higher on the Kodak plate than on the glass plates as shown in Fig. 1B with the exception of the yellow dye. Fig. 1B shows values plotted for the six major dyes only, with spot separations being nearly equal on all glass plates. The R_F values follow a pattern with Analtech and Whatman having the highest values and Merck the lowest.

With methylene chloride as the mobile phase the order in decreasing R_F values was somewhat different as shown in Fig. 2. With the glass plates the yellow minor spot had the second highest R_F and the light purple spot was ninth. With the Kodak plate the yellow minor spot was fifth and the light purple was sixth. On this plate the major peach-colored spot was not detected, possibly due to overlapping with the major green spot at R_F 0.97. The Whatman plate with toluene gave the best separation of twelve spots observed. Some overlapping of spots occurred with methylene chloride.

Analgesic mixture

The mixture of analgesics also showed some wide variations in R_F values for a given compound in a mixture. With glass plates only, caffeine with 1,2-dichloroethane–acetic acid as the mobile phase had R_F values ranging from 0.32 to 0.69; with acetaminophen the values ranged from 0.18 to 0.37 [13]. With ethyl acetate the values for acetylsalicylic acid ranged from 0.43 to 0.85. The R_F values for 1,2-dichloroethane–acetic acid were on average highest with Analtech, followed by Whatman, Baker and Merck with exceptions being caffeine and acetaminophen with the Whatman plate as shown in Fig. 3.

With ethyl acetate Analtech and Whatman gave the highest values for glass plates while Merck was lowest with the exception of acetylsalicylic acid. The best separation of analgesics as shown by the data in Fig. 4 was on the Whatman plate with ethyl acetate as the solvent. Actually all four glass plates gave good separations with differences being slight when ethyl acetate was the solvent. The Kodak plates in both solvent systems gave good separation of two components but overlapping of spots resulted in poor overall separation of all four components.

An interesting difference was also noted in the relative spot locations on the glass plates with ethyl acetate. The Analtech, Baker and Merck plates gave ibuprofen, acetylsalicylic acid, acetaminophen and caffeine in descending order of R_F values. On the Whatman plate acetaminophen and acetylsalicylic acid were reversed.

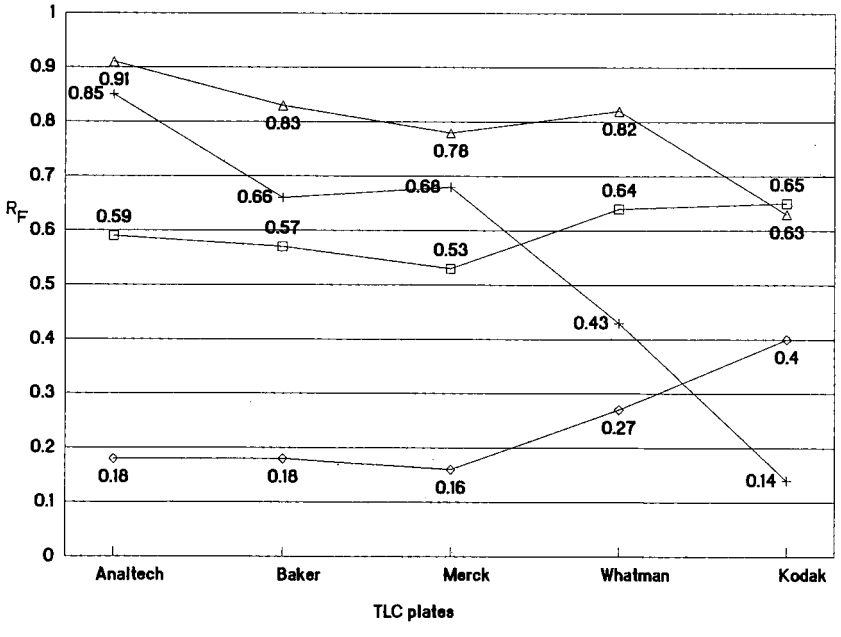

Fig. 4. R_F values of analgesic mixture. Mobile phase ethyl acetate. Symbols as in Fig. 3.

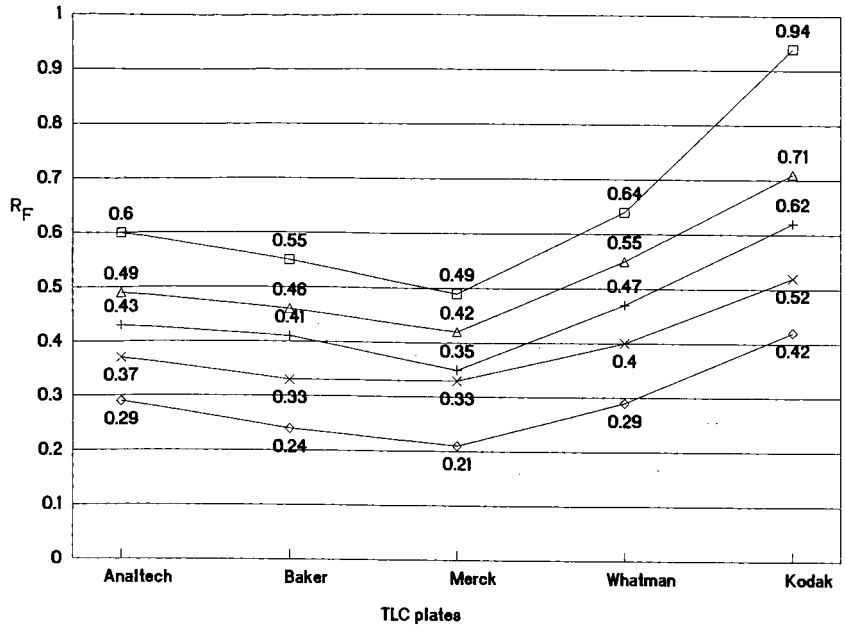

Fig. 5. R_F values of mixture of phenols. Mobile phase cyclohexane–acetone (7:3). □ = Phenol; + = o-MP; ◇ = p-MP; △ = o,o'-DHDPM; × = p,p'-DHDPM.

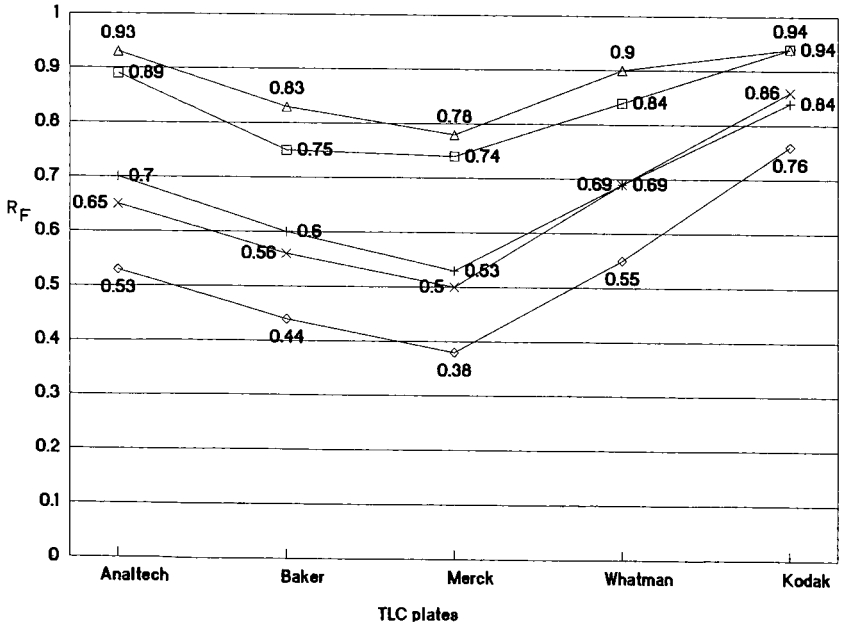

Fig. 6. R_F values of mixture of phenols. Mobile phase chloroform–methanol (92:8). Symbols as in Fig. 5.

TABLE II

RELATIVE EFFECTIVENESS OF SEPARATION

Relative separation effectiveness	Dye mixture		Analgesic mixture		Phenol mixture	
	Toluene	Methylene chloride	Dichloroethane–acetic acid	Ethyl acetate	Cyclohexane–acetone	Chloroform–methanol
Best	Analtech	Merck	Merck	Analtech	Kodak	Analtech
	Baker	Baker	Baker	Baker	Whatman	Baker
	Kodak	Analtech	Analtech	Whatman	Merck	Merck
	Merck	Whatman	Whatman	Merck	Analtech	Whatman
	Whatman	Kodak	Kodak	Kodak[b]	Baker	Kodak[b]
Worst	Analtech[a]					

[a] From Table I (Analtech data).
[b] Spots overlapped.

Phenol mixture

Data for the mixture of phenols are shown in Figs. 5 and 6. Although there were some R_F variations between the glass plates, the range of variations was not as great as with the dyes and analgesics. However, the range of R_F values was in nearly the same order as with previous mixtures. Either the Analtech or Whatman plates gave the highest values depending on the solvent used, followed by Baker and then Merck with the lowest values. The maximum range between high and low R_F values for the glass plates was 45%. It is of interest that using the two different solvent systems the relative positions of phenol and o,o'-DHDPM were reversed. With cyclohexane–acetone, phenol had the highest R_F value on all five plates while o,o'-DHDPM was second. With the chloroform–methanol solvent the positions were reversed on all the glass plates and the two spots coincided on the Kodak plate. This was determined by observation of the spot colors obtained on spraying the chromatograms with ceric ammonium nitrate after the examination under UV light.

General

(1) Several factors common to all solvents and plates have been observed. Table II shows the relative effectiveness of separation based on distances between spots on each plate.

(2) Highest R_F values on glass plates are consistently found with either Analtech or Whatman with Merck being lowest.

(3) With a few exceptions reasonable separations are obtained on all of the glass plates in spite of large variations in R_F values or reversal of relative spot locations.

(4) In comparing the Kodak flexible plate with the glass plates, the Kodak plate generally has higher R_F values probably because of the smaller layer thickness. The exception is the analgesics where acetaminophen and caffeine have lower values.

(5) Run times on the Kodak plate are 2–3 times longer than on the glass plates, all of which are consistent within 1–2 min.

REFERENCES

1 G. Grassani-Strezza and M. Cristalli, *J. Chromatogr.*, 214 (1981) 209–216.
2 U. A. Th. Brinkman and G. de Vries, *J. Chromatogr.*, 258 (1983) 43–55.
3 I. D. Wilson, *J. Chromatogr.*, 291 (1984) 241–247.
4 I. D. Wilson, *J. Chromatogr.*, 438 (1988) 419–422.
5 U. A. Th. Brinkman and G. de Vries, in J. C. Touchstone and J. Sherma (Editors), *Tech. Appl. Thin Layer Chromatogr. [Proc.-Bienn. Symp. Thin Layer Chromatogr.], 3rd 1982*, (1985) 87–107.
6 U. A. Th. Brinkman and G. de Vries, *J. Chromatogr.*, 265 (1983) 105–110.
7 P. Schweda, *J. Chromatogr.*, 63 (1971) 67–72.
8 A. J. Scism, *J. Chem. Educ.*, 62 (1985) 361.
9 F. Bobbio, P. Bobbio and S. C. de Souza, *J. Chem. Educ.*, 64 (1987) 182.
10 B. De Spiegeleer, B. M. De Moerloose, P. H. Slegers and A. S. Guido, *Anal. Chem.*, 59 (1987) 62–64.
11 C. F. Poole and S. K. Poole, *Anal. Chem.*, 61 (1989) 1257A–1262A.
12 D. L. Gumprecht, *For. Prod. J.*, 19 (1969) 38–40.
13 R. F. Roswell and N. M. Zacyzek, *J. Chem. Educ.*, 56 (1979) 834.

Journal of Chromatography, 595 (1992) 375–376
Elsevier Science Publishers B.V., Amsterdam

CHROM. 23 974

Book Review

Chiral separations by liquid chromatography (*ACS Symposium Series*, No. 471), edited by S. Ahuja, American Chemical Society, Washington, DC, 1991, 239 pp., price US$ 59.95, ISBN 0-8412-2116-2.

The importance of stereochemistry in the various fields of life sciences cannot be over-emphasized and the significance of stereoisomerism in relation to the biological activity of pharmaceutical or, *e.g.*, agricultural chemical entities has become a serious issue. Frequently observed large differences in the physiological effects between stereoisomers and enantiomers clearly demonstrate the need to isolate the individual compounds and examine each one separately. However, this also takes for granted that there are methods available for analysing the stereochemical composition (optical purity, enantiomeric excess) accurately and reliably. The range of separation techniques dealing with enantioseparation is wide, but all share in a way the same general principle, that the chiral analytes [mixtures of enantiomers, selectands (SA)], have to interact with a chiral source, the chiral selector (SO), via intermolecular contacts in combination with spatial orientation of the SA guest molecules and the chiral SO host molecule; the resulting quasi-diastereomeric SO–SA_R and SO–SA_S molecular associates are unequal in physico-chemical terms. The stereodiscrimination is largely determined by spatial parameters, the conformation of the SO and SA molecules and the spatial arrangement and size of the substituents on the centres of chirality.

This is a simplified view of the complex multiple binding procedures involved in pronounced stereodiscrimination and the field has been extensively discussed during a number of dedicated symposia and also in symposia dealing with separation techniques such as gas, thin-layer, liquid and supercritical fluid chromatography and electrophoresis. Several books on the subject of "chiral chromatography" have been published in recent years and document the rapidly growing knowledge base in this research area.

However, this book, which is a multi-author volume, is composed of papers which have in part been presented and discussed at a dedicated symposium in Washington, DC, in August 1990. In thirteen chapters a relatively broad range of stereoselective liquid chromatographic techniques is covered and treated variably in depth. However, as expected particularly in a symposium volume, chapters on certain aspects are missing and the style and content of the chapters appear inhomogeneous and/or vary in their adequacy of reviewing similar types of work.

In Chapter 1, "Chiral separations; an overview" by S. Ahuja, also the Editor of this book, "it has been tried to cover in a brief form the whole field by also listing a great number of (scientifically slangily termed "chiral columns") commercially available (more than 170) chiral stationary phases in a Table". Such a list is impressive, but what is the benefit of it to either a specialist or a beginner in the field when it seems rather confusing?

T. Doyl in Chapter 2, "Analytical criteria for chiral HPLC", stresses particularly some aspects of optical trace analysis. This is a very important subject but the chapter does not give complete coverage, as the applications cited are limited and do not reflect the real world, in, *e.g.*, drug chemistry.

Chapter 3, "Commercially available brush-type chiral selectors for the direct resolution of enantiomers" by S. Perrin and W. Pirkle, describes very clearly the chemical structures of the prominent chiral selector molecules which predominantly involve charge-transfer interactions in addition to others between SO and SA. As stated, to use the so-called Pirkle-type chiral stationary phases (CSPs) most successfully it is frequently necessary to derivatize the analytes in order to achieve a more pronounced π–π interaction between SO and SA

and to stress stereodifferentiation phenomena. Generally, adequate chemical manipulation of the chiral analyte can often lead to an improved enantioseparation.

Chapter 4, by R. Menges and D. Armstrong, deals with some covalently immobilized β-cyclodextrin-type CSPs (including derivatized types) and lists many applications in table form. The reader obtains a good impression of which chemical structure features the SA molecule should have for a good chance of being separated on a cyclodextrin-type CSP. However, developments in this area are very rapid and therefore such a book chapter can never be complete.

This is true also for the very brief Chapter 5, "Chromatographic optical resolution on polysaccharide carbamate phases" by Y. Okamoto *et al.*, as judged by the impressive original work by Okamoto published elsewhere.

Chapters, 6, 7 and 8 give adequate credit to the impressive stereoselectivity of so-called protein-type (biopolymer-type) CSPs, cover their availability and pinpoint the possibilities of tuning the stereoselectivity by varying the aqueous mobile phase parameters, such as pH, ionic strength, temperature, type and amount of organic modifier and addition of ion-pair reagents.

The brief Chapter 9, by E. Gil-Av, and Chapter 10, by S. Hara and co-workers, concentrate on chiral separations involving predominantly SO–SA hydrogen bonding association. The potential of this approach is clearly demonstrated, although the chapters are more like selective reviews.

An interesting research paper is presented in Chapter 11, "High pressure liquid chromatographic resolution of optical isomers; influence of mobile and π-donor stationary phases" by S. Dhanesar. This chapter deals with the influence of mobile phase characteristics and composition (non-aqueous solvents) on the observed enantioseparation on certain brush-type CSPs. However, its relevance to non-specialists in the field is questionable.

Chapter 12 is a too-specific paper for such a book and describes an application for "separating aminoglutethimide and its major metabolite". Such a specific application belongs in a journal and not in a book intended to cover the field more broadly.

Chapter 13, "Amino acid racemization; a tool for dating?" by V. Meyer, is interesting to read and gives some additional ideas about the input of "chiral separations" in very diversified fields of science.

Summarizing, this multi-author book is a typical symposium volume composed of review-type chapters on various aspects and methods of *Chiral separations by liquid chromatography*, but also containing pure research papers. Most of the chapters are written by leading authorities in this rapidly evolving field and guarantee a good inside view of this research area. However, some successful chiral separation techniques are not covered at all or only poorly, *e.g.*, chiral ligand exchange chromatography, electrophoresis and indirect enantioseparation methods, which is a shortcoming.

The slight inhomogeneity of the book is highlighted by the camera-ready printing of the chapters, which differ in layout and typeface. The indexing is not very detailed.

An attempt has been made to cover the theory and practice of chiral separations, and this has largely succeeded. Despite the shortcomings of a symposium volume covering only partially a particular research field and therefore being different in style and direction compared with a comprehensive text book, it will certainly be of value in laboratories involved with enantioseparations.

Graz (Austria) W. Lindner

Author Index

Errata

corrected 31 Oct 95

J. Chromatogr., 587 (1991) 338–342 /
Page 342, ref. 1 should read "P. Werkhoff and W. Bretschneider, *J. Chromatogr.*, 405 (1987) 87".

J. Chromatogr., 589 (1992) 31–43 /
Page 31, name of third author should read "H. Piryns".

J. Chromatogr., 590 (1992) 263–270 /
Page 264, *Standard metal solutions* section, 5th line: "(II) chloride" should read "managanese(II) chloride".

Announcing...

International Ion Chromatography Symposium 1992

September 21-24, 1992
Johannes-Kepler-University
Linz, Austria

PROGRAM CHAIRMAN:

Günther K. Bonn
Johannes-Kepler-University
Analytical Chemistry Dept.
Altenbergerstrasse 69
A-4040 Linz, Austria
Telephone: (+43-732)2468 723
Fax: (+43-732)2468 679

SESSION TOPICS:

Fundamental Principles and General Aspects of IC
Sample Handling and Pretreatment
General Novel Applications
Environmental Applications
Industrial Applications
Applications in the Nuclear and Power Generation Industry
Capillary Electrophoresis for Inorganic Ions

PLENARY LECTURERS:

J.F.K. Huber, University of Vienna, Vienna, Austria
P.R. Danesi, International Atomic Energy Agency (IAEA), Seiberdorf, Austria
Petr Bocek, Czechoslovak Academy of Sciences, Brno, Czechoslovakia
M.D.H. Amey, Winfrith Technology Centre, Dorchester, U.K.

For program details and registration information, write or call:

Century International, Inc.
P.O. Box 493
Medfield, MA 02052 USA
508/359-8777 • 508/359-8778 (FAX)

Journal of Chromatography Library, 50

Liquid Chromatography in Biomedical Analysis

edited by **T. Hanai,** *International Institute of Technological Analysis, Health Research Foundation, Kyoto, Japan*

This book presents a guide for the analysis of biomedically important compounds using modern liquid chromatographic techniques. After a brief summary of basic liquid chromatographic methods and optimization strategies, the main part of the book focuses on the various classes of biomedically important compounds: amino acids, catecholamines, carbohydrates, fatty acids, nucleotides, porphyrins, prostaglandins and steroid hormones. The different chapters discuss specialized techniques pertaining to each class of compounds, such as sample pretreatment, pre- and post-column derivatization, detection and quantification.

1991 xii + 296 pages
Price: US $ 138.50 / Dfl. 270.00
ISBN 0-444-87451-8

Contents:

Elsevier Science Publishers

P.O. Box 211, 1000 AE Amsterdam, The Netherlands
P.O. Box 882, Madison Square Station, New York, NY 10159, USA

Laboratory information management

new!

An International Journal
Section of Chemometrics and Intelligent Laboratory Systems

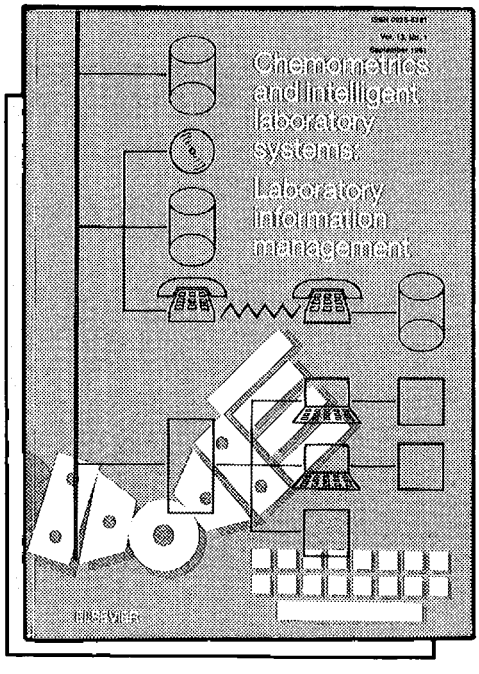

Editor:
R.D. McDowall, Beckenham, Kent, UK
Editor for North America:
R.R. Mahaffey, Eastman Chemicals Division, Kingsport, TN, USA

The journal covers all aspects of information management in a laboratory environment, such as information technology, storage, processing and flow of data. The following topics are covered:

- **Laboratory Information Management Systems (LIMS)**
- **Means of integrating and merging laboratory information**
- **Networks**
- **Regulatory Aspects**
- **Electronic Laboratory Notebooks**
- **Human aspects of laboratory automation**

Subscription Information:
1992: Vol. 17 (3 issues)
Dfl. 406.00 / US$ 201.00
(including postage)
ISSN 0925-5281

A Free Sample Copy is Available on Request

Elsevier Science Publishers
P.O. Box 330
1000 AH Amsterdam
The Netherlands
Tel: (31-20) 5862 873
Fax: (31-20) 5862 845

in the USA and Canada
P.O. Box 882
Madison Square Station
New York, NY 10159, USA
Tel: (212) 633 3750
Fax: (212) 633 3764

ELSEVIER SCIENCE PUBLISHERS

Chromatography, 5th edition

Fundamentals and Applications of Chromatography and Related Differential Migration Methods

edited by **E. Heftmann**, *Orinda, CA, USA*

These are completely new books, organized according to the successful plan of the previous four editions. While avoiding repetition of material covered in the previous editions, the authors have succeeded in presenting a coherent and comprehensive picture of the state of each topic. The books provide beginners as well as experienced researchers with a key to understanding current activities in various separation methods. They will also serve as textbooks for graduate courses in technical, medical and engineering schools as well as all universities offering science courses.

Part A: Fundamentals and Techniques

Journal of Chromatography Library Volume 51A

Part A covers the theory and fundamentals of such methods as column and planar chromatography, countercurrent chromatography, field-flow fractionation, and electrophoresis. Affinity chromatography and supercritical-fluid chromatography are covered for the first time. Each topic is treated by one of the most eminent authorities in the field.

Contents Part A: 1. Theory of chromatography *(L.R. Snyder)*. 2. Countercurrent chromatography *(Y. Ito)*. 3. Planar chromatography *(S. Nyiredy)*. 4. Column liquid chromatography *(H. Poppe)*. 5. Ion-exchange chromatography *(H.F. Walton)*. 6. Size-exclusion chromatography *(L. Hagel and J.-C. Janson)*. 7. Affinity chromatography *(T.M. Phillips)*. 8. Supercritical-fluid chromatography *(P.J. Schoenmakers and L.G.M. Uunk)*. 9. Gas chromatography *(C.F. Poole and S.K. Poole)*. 10. Field-flow fractionation *(J. Janca)*. 11. Electrophoresis *(P.G. Righetti)*. Manufacturers and dealers of chromatography and electrophoresis supplies. Subject Index.

1992 xxxvi + 552 pages
Price: US $ 179.50 / Dfl. 350.00
ISBN 0-444-88236-7

Parts A & B Set
Set price: US $ 333.50 / Dfl. 650.00
ISBN 0-444-88404-1

Part B: Applications

Journal of Chromatography Library Volume 51B

Part B presents various applications of these methods. New developments are reviewed and summarized. Important topics such as environmental analysis and the determination of synthetic polymers and fossil fuels, are covered for the first time.

Contents Part B: 12. Inorganic species *(P.R. Haddad and E. Patsalides)*. 13. Amino acids and peptides *(C.T. Mant, N.E. Zhou and R.S. Hodges)*. 14. Proteins *(F.E. Regnier and K.M. Gooding)*. 15. Lipids *(A. Kuksis)*. 16. Carbohydrates *(S.C. Churms)*. 17. Nucleic acids, their constituents and analogs *(N-I Jang and P.R. Brown)*. 18. Porphyrins *(K. Jacob)*. 19. Phenolic compounds *(J.B. Harborne)*. 20. Drugs *(K. Macek and J. Macek)*. 21. Fossil fuels *(R.P. Philp and F.X. de las Heras)*. 22. Synthetic polymers *(T.H. Moury and T.C. Schunk)*. 23. Pesticides *(J. Sherma)*. 24. Environmental analysis *(K.P. Naikwadi and F.W. Karasek)*. 25. Amines from environmental sources *(H.A.H. Billiet)*. Manufacturers and dealers of chromatography and electrophoresis supplies. Subject Index.

1992 xxxii + 630 pages
Price: US $ 189.50 / Dfl. 370.00
ISBN 0-444-88237-5

Elsevier Science Publishers

P.O. Box 211, 1000 AE Amsterdam, The Netherlands
P.O. Box 882, Madison Square Station, New York, NY 10159, USA

PUBLICATION SCHEDULE FOR 1992

Journal of Chromatography and *Journal of Chromatography, Biomedical Applications*

MONTH	O 1991	N 1991	D 1991	J	F	M	A	
Journal of Chromatography	585/1	585/2 586/1 586/2 587/1	587/2 588/1 + 2	589/1 + 2 590/1 590/2	591/1 + 2 592/1 + 2 593/1 + 2	594/1 + 2 595/1 + 2	596/1 596/2 597/1 + 2	The publication schedule for further issues will be published later.
Cumulative Indexes, Vols. 551–600								
Bibliography Section						610/1		
Biomedical Applications				573/1 573/2	574/1 574/2	575/1 575/2	576/1	

INFORMATION FOR AUTHORS

(Detailed *Instructions to Authors* were published in Vol. 558, pp. 469–472. A free reprint can be obtained by application to the publisher, Elsevier Science Publishers B.V., P.O. Box 330, 1000 AH Amsterdam, The Netherlands.)

Types of Contributions. The following types of papers are published in the *Journal of Chromatography* and the section on *Biomedical Applications:* Regular research papers (Full-length papers), Review articles and Short Communications. Short Communications are usually descriptions of short investigations, or they can report minor technical improvements of previously published procedures; they reflect the same quality of research as Full-length papers, but should preferably not exceed five printed pages. For Review articles, see inside front cover under Submission of Papers.

Submission. Every paper must be accompanied by a letter from the senior author, stating that he/she is submitting the paper for publication in the *Journal of Chromatography*.

Manuscripts. Manuscripts should be typed in double spacing on consecutively numbered pages of uniform size. The manuscript should be preceded by a sheet of manuscript paper carrying the title of the paper and the name and full postal address of the person to whom the proofs are to be sent. As a rule, papers should be divided into sections, headed by a caption (*e.g.*, Abstract, Introduction, Experimental, Results, Discussion, etc.). All illustrations, photographs, tables, etc., should be on separate sheets.

Introduction. Every paper must have a concise introduction mentioning what has been done before on the topic described, and stating clearly what is new in the paper now submitted.

Abstract. All articles should have an abstract of 50–100 words which clearly and briefly indicates what is new, different and significant.

Illustrations. The figures should be submitted in a form suitable for reproduction, drawn in Indian ink on drawing or tracing paper. Each illustration should have a legend, all the *legends* being typed (with double spacing) together on a *separate sheet.* If structures are given in the text, the original drawings should be supplied. Coloured illustrations are reproduced at the author's expense, the cost being determined by the number of pages and by the number of colours needed. The written permission of the author and publisher must be obtained for the use of any figure already published. Its source must be indicated in the legend.

References. References should be numbered in the order in which they are cited in the text, and listed in numerical sequence on a separate sheet at the end of the article. Please check a recent issue for the layout of the reference list. Abbreviations for the titles of journals should follow the system used by *Chemical Abstracts.* Articles not yet published should be given as "in press" (journal should be specified), "submitted for publication" (journal should be specified), "in preparation" or "personal communication".

Dispatch. Before sending the manuscript to the Editor please check that the envelope contains four copies of the paper complete with references, legends and figures. One of the sets of figures must be the originals suitable for direct reproduction. Please also ensure that permission to publish has been obtained from your institute.

Proofs. One set of proofs will be sent to the author to be carefully checked for printer's errors. Corrections must be restricted to instances in which the proof is at variance with the manuscript. "Extra corrections" will be inserted at the author's expense.

Reprints. Fifty reprints of Full-length papers and Short Communications will be supplied free of charge. Additional reprints can be ordered by the authors. An order form containing price quotations will be sent to the authors together with the proofs of their article.

The most useful chiral separation column, ULTRON ES-OVM, for enantiomeric drugs.

Substance	Rs	Substance	Rs	Substance	Rs
Acetylpheneturide	2.74	Disopyramid	2.04	Nisoldipine	2.36
Alimemazine	6.06	Eperisone	1.15	Nitrendipine	1.80
Alprenolol	1.09[1]	Ethiazide	1.42	Oxazepan	2.65[2]
Arotinolol	1.95	Fenoprofen	0.80	Oxprenolol	1.38
Bay K 8644	5.92	Flurbiprofen	1.27	Pindolol	2.04
Benproperine	3.27	Glutethimide	1.36	2-Phenylpropionic acid	0.80
Benzoin	8.41	Glycopyrronium	1.73	Pranoprofen	0.63
Biperiden	3.17	Hexobarbital	1.70	Prenylamine	0.86
Bunitrolol	3.08	Homochlorcyclizine	3.04	Profenamine	3.31
Bupivacaine	1.26	Hydroxyzine	2.15	Promethazine	1.42
Chlormezanone	6.48	Ibuprofen	1.72	Propranolol	1.24
Chlorphenesin	2.23	Ketoprofen	1.37	Terfenadine	2.22
Chlorpheniramine	2.36	Lorazepam	2.55[2]	Thioridazine	0.72
Chlorprenaline	2.34	Meclizine	3.71	Tolperisone	1.50
Cloperastin	2.85	Mepenzolate	1.40	Trihexyphenidyl	5.16
Dimethindene	4.33	Mephobarbital	1.70	Trimipramine	3.69
1,2-Diphenylethylamine	1.74	Methylphenidate	1.13[1]	Verapamil	1.49

NOTE: 4.6×150mm column at room temp. except[1] 6.0×150mm at room temp. and[2] 6.0×150mm at 10°C

From trace analysis for metabolites

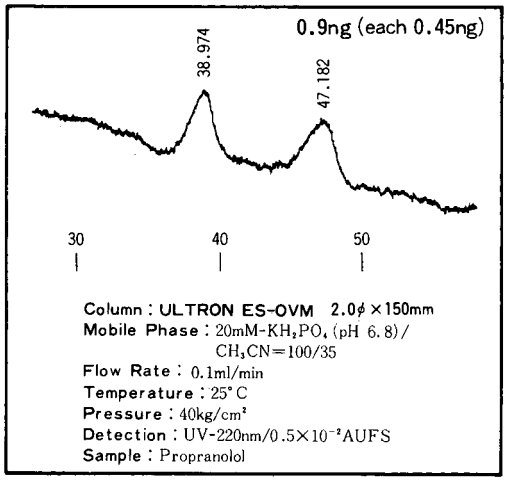

Column : ULTRON ES-OVM 2.0φ×150mm
Mobile Phase : 20mM-KH_2PO_4 (pH 6.8)/CH_3CN=100/35
Flow Rate : 0.1ml/min
Temperature : 25°C
Pressure : 40kg/cm²
Detection : UV-220nm/0.5×10⁻²AUFS
Sample : Propranolol

to preparative scale

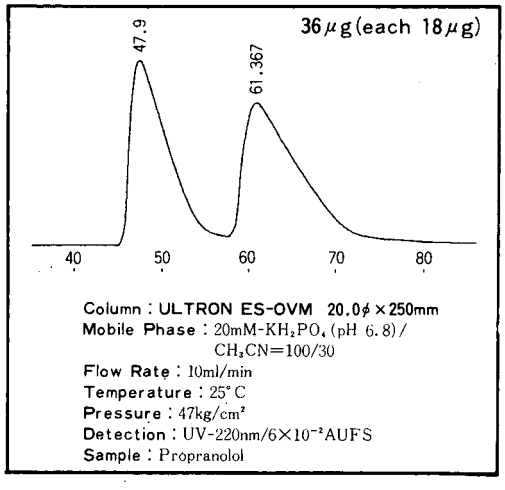

Column : ULTRON ES-OVM 20.0φ×250mm
Mobile Phase : 20mM-KH_2PO_4 (pH 6.8)/CH_3CN=100/30
Flow Rate : 10ml/min
Temperature : 25°C
Pressure : 47kg/cm²
Detection : UV-220nm/6×10⁻²AUFS
Sample : Propranolol

SHINWA CHEMICAL INDUSTRIES, LTD

50 Kagekatsu-cho, Fushimi-ku, Kyoto 612, JAPAN
Phone: 80-75-621-2360 Fax : 80-75-602-2660

Please contact in United States of America and Europe to :

Rockland Technologies, Inc. 538 First State Boulevard, Newport, DE 19804, U.S.A.
Phone : 302-633-5880, Fax : 302-633-5893

This product is licenced by Eisai Co., Ltd.